

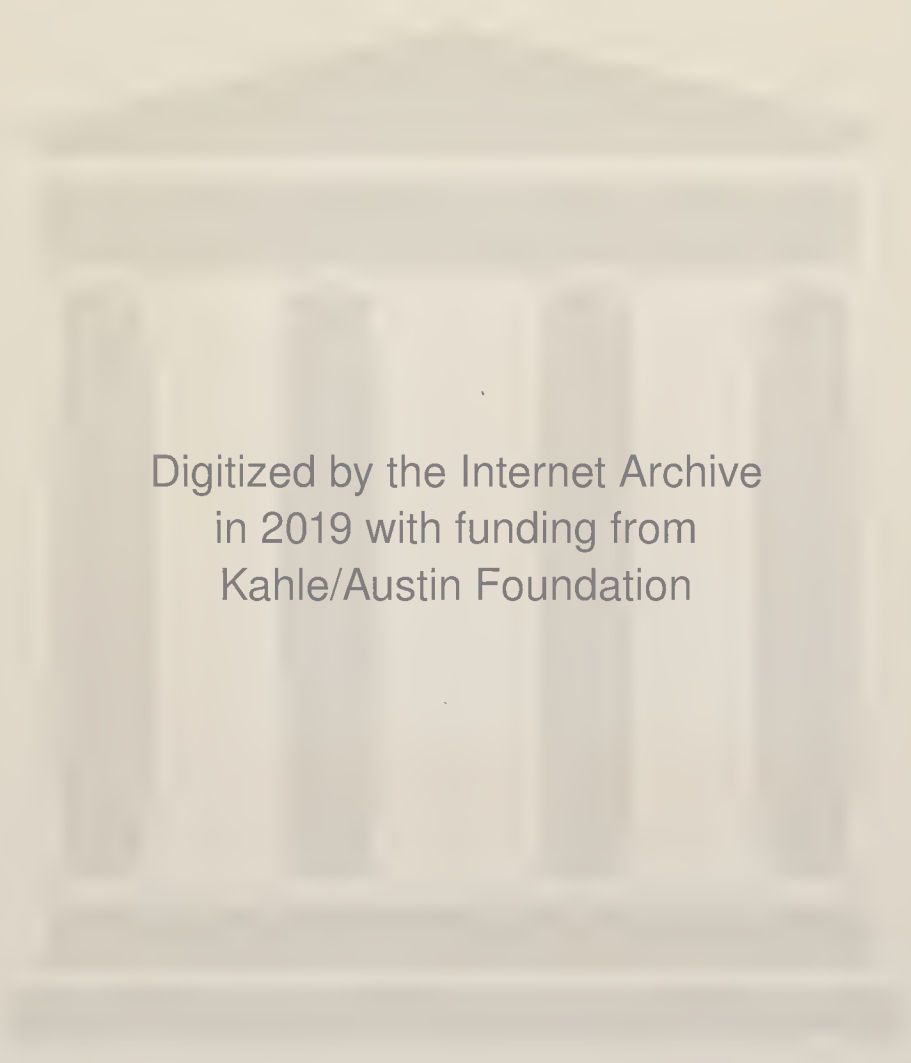
SPACE PROBES AND  
PLANETARY EXPLORATION

---

NUNC COGNOSCO EX PARTE



TRENT UNIVERSITY  
LIBRARY



Digitized by the Internet Archive  
in 2019 with funding from  
Kahle/Austin Foundation



SPACE PROBES  
AND PLANETARY  
EXPLORATION



# SPACE PROBES AND PLANETARY EXPLORATION

---

*by*

WILLIAM R. CORLISS



WRITTEN UNDER THE SPONSORSHIP OF THE  
NATIONAL AERONAUTICS AND  
SPACE ADMINISTRATION

D. VAN NOSTRAND COMPANY, INC.  
PRINCETON, NEW JERSEY

TORONTO

NEW YORK

LONDON

D. VAN NOSTRAND COMPANY, INC.  
120 Alexander St., Princeton, New Jersey (*Principal office*)  
24 West 40 Street, New York 18, New York

D. VAN NOSTRAND COMPANY, LTD.  
358 Kensington High Street, London, W.14, England

D. VAN NOSTRAND COMPANY (Canada), LTD.  
25 Hollinger Road, Toronto 16, Canada

COPYRIGHT © 1965, BY  
D. VAN NOSTRAND COMPANY, INC.

Copyright assigned to the Administrator of the National Aeronautics and Space Administration. All royalties from the sale of this book accrue to the United States Government

Published simultaneously in Canada by  
D. VAN NOSTRAND COMPANY (Canada), LTD.

*No reproduction in any form of this book, in whole or in part  
(except for brief quotation in critical articles or reviews), may  
be made without written authorization from the publishers.*

PRINTED IN THE UNITED STATES OF AMERICA



## FOREWORD

---

---

Within a few short years everyone on Earth will have had an opportunity to visit the Moon, our neighboring planets, and the far reaches of our Solar System—not physically, but through the television eyes and other sensors of unmanned spacecraft. Already the Ranger pictures have been viewed with interest throughout the world. Countless thousands have followed the Mariners on their long journeys, with some of the anticipation that accompanies a personal visit to a new place.

Advances in space science and technology during recent years are best characterized as explosive. The dynamic nature of developments in space probes, rocket vehicles, data handling, and communication systems make the task of capturing a candid view very difficult. However, that is just what William R. Corliss has done in this book.

The aspect of space probe design that continually haunts the engineer is compromise. One of the best features of this book is the treatment of tradeoffs that confront the space scientist and engineer in the planning and implementation of a mission.

This book is written for those engaged in the business of exploring space, and for those on the fringes who want to appreciate better the breadth and depth of the subject. The material presented, and the format of presentation, will make this especially interesting and useful to the engineer. It is a current effort, coming directly from Mr. Corliss' contact with engineers and scientists in the field. His visits with most of the NASA laboratories, the Jet Propulsion Laboratory, aerospace companies, and universities, plus his assimilation of large quantities of published and unpublished data, have equipped him with an up-to-the-minute view.

In spite of its technical nature, the organization of this book and its link with the exciting, history-making projects of our space age make it enjoyable as well as informative reading. I am pleased to recommend "Space Probes and Planetary Exploration" as an addition to the library of everyone interested in the mysteries of space exploration.

ORAN W. NICKS, *Director*  
Lunar and Planetary Programs  
National Aeronautics and Space Administration



## PREFACE

---

---

Beyond the realm of the satellite and outside the volume circumscribed by the Moon's orbit stretches the domain of the deep-space probe. The targets of these unmanned, instrumented spacecraft are the Sun, planets, comets, asteroids, and space itself. Ultimately they will go to the stars.

The complete space probe is more than a few hundred kilograms of intricate machinery hundreds of millions of kilometers from Earth. It is a radio-knit system of many parts, with a spacecraft at one end and man at the other. In between are tracking stations, immense paraboloid antennas, and data reduction equipment. From man to spacecraft sensor; that is the scope of the book.

Emphasis is on equipment and technique rather than results and their interpretations. Except for four general chapters at the beginning, the reader is assumed to have a scientific or engineering background.

The author wishes to acknowledge the help of many individuals in the National Aeronautics and Space Administration, the Jet Propulsion Laboratory, the Department of Defense, industry, and the universities.

WILLIAM R. CORLISS



# TABLE OF CONTENTS

---

---

## *Part I. The Interplanetary Challenge*

CHAPTER 1	Interplanetary Scientific Objectives	3
CHAPTER 2	History of Interplanetary Inquiry and Exploration	7
CHAPTER 3	The Status of Interplanetary Exploration	19
CHAPTER 4	Integrating the Spacecraft, Earth-Based Facilities, and Instrumentation	36

## *Part II. Missions, Spacecraft, and Techniques*

CHAPTER 5	Interplanetary Transportation and Space Dynamics	43
CHAPTER 6	Space Communications and Data Handling	79
CHAPTER 7	Navigation, Guidance, and Control of Interplanetary Spacecraft	105
CHAPTER 8	Earth-based Facilities and Operations	127
CHAPTER 9	Launch Vehicles	154
CHAPTER 10	Spacecraft Design	176
CHAPTER 11	Characteristics of Specific Space Probes	244

## *Part III. Scientific Instruments*

CHAPTER 12	Scientific Experimentation in Space	281
CHAPTER 13	Instruments for Measuring the Interplanetary Medium	296
CHAPTER 14	Instruments for Measuring Planetary Atmospheres	381
CHAPTER 15	Instruments for Analyzing a Planet's Crust	427
CHAPTER 16	Instruments for Detecting Life	477
CHAPTER 17	Instruments used on Solar, Cometary, and Asteroidal Probes	503
	Bibliography	508
	Index	533



*Part I*

THE INTERPLANETARY CHALLENGE

---





# *Chapter 1*

---

## INTERPLANETARY SCIENTIFIC OBJECTIVES

---

---

The solar system is a magnificent frontier for exploration. There is an inexhaustible supply of research problems, ranging from Jupiter's red spot and the "canals" of Mars to the turbulent fluxes of particles and force fields that fill interplanetary space. Perhaps somewhere in the solar system's  $10^{30}$  cubic kilometers of space there is even a clue to the origin of life and man himself.

Space probes are highly instrumented, unmanned machines capable of performing a great variety of scientific and engineering research in outer space by remote control. Not only do space probes provide science with a new research tool but they also help chart the way for the eventual manned flights to the Moon and planets. In this sense, space probes are the precursors of man throughout the solar system.

As space probes radiate outward from the Earth, at first along the plane of the ecliptic toward Mars and Venus, later to the other planets and to the asteroids and comets, two primary objectives shape astronomical planning:

1. The flight of man himself to the planets,
2. The increase of scientific knowledge and understanding.

It is fashionable to emphasize the divergence of philosophy inherent in these two objectives. On one hand, there is knowledge for the sake of knowledge; on the other, knowledge promoting subjective human goals. The conflict is best seen in the assertion that man is non-essential out in space; that instruments can make all necessary measurements. Such an attitude undermines human involvement in space flight. In direct opposition is the claim that space exploration must be a human adventure, where man himself treads the surface of the Moon and Mars. The latter con-

tention dates back to the birth of astronautics and, though it is assailed by some logic, molds our present interplanetary efforts. Space probes actually serve both philosophies by telemetering back to Earth the scientific data needed for planning manned space voyages.

The proper question to ask about any particular astronomical experiment is whether the task can be carried out effectively *without* man's presence. If the answer is "yes," the unmanned vehicle is the correct instrument to use. Often, however, the space phenomenon being investigated is so unfamiliar that intriguing facets might be missed entirely by a narrowly planned experiment. Man, an adaptive component par excellence, might do a better job in such cases. But let no one underrate the ultimate versatility of those self-adapting machines, the automata, their sensors, and their artificial brains. Sophisticated machines are logical companions for man in the exploration of space.

Three basic ground rules and constraints shape the planning of space probe experiments:

1. Experiments must be designed to minimize perturbations to extraterrestrial biological and chemical populations. One consequence of this constraint is that equipment must be sterilized on trips to and from extraterrestrial biological provinces.
2. Experiments supporting manned lunar and interplanetary exploration should be given preference. This is not a serious restriction today, since almost any new knowledge of interplanetary space promotes manned ventures. Priority should also be given to proving out equipment and operating techniques vital to manned space flight.
3. National budgetary limitations.

The *technical* problems of space exploration are solvable. Certainly the mesmerism of the Moon and planets and man's ebullient nature will overcome the other obstacles.

What legitimate tasks can be set for space probes? A few of the more important scientific questions within space-probe capabilities are noted below. Some are of recent origin; some have dogged science ever since the planets were first seen. Not unexpectedly, many questions are concerned with the accurate mapping of the physical phenomena in outer space. *Active* experiments, involving intentional cause and effect, soon to be added to the more common *passive*, listening experiments, significantly extend a probe's ability to find the answers to the questions.

#### *Questions of Interplanetary Physics:*

1. Do Earth-verified physical laws hold throughout the solar system?
2. How did the solar system originate and evolve?

3. What is the nature of gravity?
4. Are the Earth-based scales of time and distance valid over solar-system distances?
5. What are the magnitudes and distributions of the particle fluxes, electromagnetic radiations, magnetic fields, and particulate matter throughout the solar system?

*Questions Concerning Planetary Atmospheres:*

1. What are the origins, compositions, and physical characteristics of the planetary and satellite atmospheres?
2. What meteorological processes occur on other planets and satellites?
3. Do other planets have radiation belts?
4. What use can be made of planetary atmospheres during manned space missions?

*Questions about Planetary Surfaces and Interiors:*

1. What are the temperatures, compositions, and physical properties of the planetary and satellite surfaces?
2. How will these properties affect manned exploration?
3. What are the "geologies" of the other planets?
4. What are the accurate masses and shapes of the planets?
5. Are there unnatural surface or subsurface features on the planets and satellites?

*Questions Concerning Extraterrestrial Life:*

1. Does extraterrestrial life exist now? In the past?
2. If so, what is (was) it like? How did it begin and evolve?
3. Is the panspermia hypothesis\* valid?
4. Are there any other bases for the origin and evolution of life than that which we now know?

*Questions about the Sun, the Comets, and the Asteroids:*

1. How did the asteroid belt originate?
2. How are comets created? What are their compositions?
3. How are solar flares generated? Can they be predicted?

*Questions about Interstellar Space:*

1. What fields and fluxes of particles exist between the stars?
2. Is our interstellar distance scale accurate?
3. What is the origin of galactic cosmic rays?
4. Does life exist outside the solar system?

\* See discussion below, page 33.

*Unaskable Questions:* The exploration of outer space should have the unpredictability of an honest slot machine. If startling, totally unexpected phenomena are not discovered, it will be a disappointing universe indeed.

The plan of this book is first to show how space probes function and carry scientific instruments to distant points, then to describe the instruments that ferret out the answers to the questions posed above. The actual data obtained from probes and its interpretation are subjects left for other texts. This book concentrates on probe equipment and methodology.

Space probes are mechanical pathfinders for man's expansion into space. They scout the way and prove out the equipment. As the stars themselves become attainable, unmanned automata will again spearhead the assault.

## *Chapter 2*

---

### HISTORY OF INTERPLANETARY INQUIRY AND EXPLORATION

---

---

#### **2-1. Approaches to Astronautical History**

The usual history of astronautics begins with the Babylonian scripts of 4000 B.C. that depict a man ascending skyward aided by an eagle. Another well-worn tale is that of the Chinese Mandarin Wan-Hoo and his suicidal rocket-propelled car of 1500-A.D. vintage. All astronautical histories introduce the space age with the German V-2 war rocket and the Viking high altitude rockets fired from White Sands following World War II.

Rocket development has been well-documented in this way; but astronautics is more than just a recapitulation of rocketry. Modern rockets would be useless without parallel advances in tracking, communications, and launching facilities. For example, without refined communication equipment a Venus probe could not bridge 80,000,000 kilometers. Accurate attitude control systems, reliable power supplies, and good tracking facilities are all essential to good spacecraft performance. A complete history of space probes must describe almost all elements in that complex intermingling of technologies called astronautics.

The history of instrumented space probes is still, however, only a fractional part of the general history of astronautics. The discipline of bioastronautics may be safely omitted, for example, since space probes are controlled by internal electronic organs and the distant hand of man. Because man is not aboard, space-probe history is distinct from, though not completely independent of, the history of manned vehicles.

## 2-2. From Passive Terrestrial Observer to Active Space Probe

The concept of the unmanned space probe ranging the solar system, telemetering scientific data back to Earth, is comparatively modern. In fact, the history of interplanetary inquiry has been rather sharply channeled into just two categories:

1. Passive observation from the Earth's surface,
2. Plans for *manned* space flight to the Moon and beyond.

Unmanned scientific satellites received little attention until 1951, when a key paper with the diminutive title *Minimum Satellite Vehicles* (Ref. 2-14) was presented at the Second Congress of the International Astronautical Federation (IAF), by Gatland, Kunesch, and Dixon. Even though by 1946 the V-2 had shown small satellite vehicles to be feasible, astronautics has been historically synonymous with manned space flight. It is also notable that the early thinkers in astronautics placed little emphasis on the acquisition of scientific data in outer space.

The first scientific studies of the heavens began with the systematic astronomical observations of the Babylonians and Egyptians, thirty centuries before Christ. Great precision and impressive instrumentation have developed over the years. With the advent of modern physics and its spectrosopes, particle counters, and radio telescopes, data on the solar

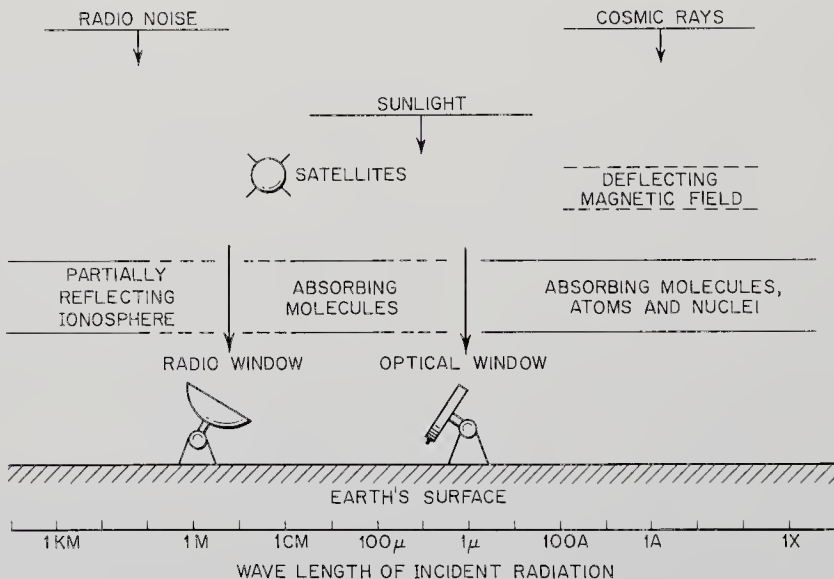


Fig. 2-1. Schematic showing atmospheric-absorption mechanisms. Spectral windows permit only small portions of the electromagnetic spectrum to reach the Earth's surface, limiting man's view of the universe.

system have piled up rapidly. Our knowledge of outer space is really remarkable, considering the opaqueness of our atmosphere to the photons, particles, and meteorites that bring us our only extraterrestrial information (Fig. 2-1). The summary of our current knowledge of outer space presented in Chapter 3 is largely the result of centuries of passive listening.

The blind spots forced on the terrestrial observer by the Earth's atmosphere and magnetic field were recognized long ago when scientists began to locate telescopes on high mountains and to send instruments aloft in balloons. In 1928, the American rocket pioneer, Robert H. Goddard, first demonstrated the practicality of high altitude research rockets, though a Frenchman named Dencesse had designed a camera-equipped rocket for military reconnaissance as far back as 1895. After the Viking shots and Aerobee successes in the late 1940's, high altitude research became commonplace. In the light of history, the logical sequence of unmanned scientific vehicles has been:

1. The high altitude sounding rocket.
2. The unmanned, instrumented satellite.
3. The space probe.

Unmanned satellites and space probes both had difficult births. Logic and scientific need were not enough to divert attention from the more dramatic plans for manned space conquest.

Hermann Oberth, the great German aeronautical thinker, originated the research satellite concept in his 1923 book, *Rocket to Outer Space* (Ref. 2-26). Although Oberth proposed a manned space station, one of its major functions was the acquisition of scientific data, an unusual concept for a spacecraft in those days. Actually, Oberth was preceded in the space station idea by Kurd Lasswitz, who employed a space station in his novel *Of Two Planets* published in 1897 (Ref. 2-21). Lasswitz, however, used antigravity rather than centrifugal force to position his station over the North Pole. Scientific research was not mentioned in the Lasswitz novel.

The flood of satellite literature did not start until 1951. Many proposals began circulating when the technical community realized that rockets large enough to place small instrument packages in orbit were just around the corner. A typical suggestion was MOUSE, a 1953 acronym for Minimum Orbital Unmanned Satellite of the Earth. The scientific interest aroused by the forthcoming International Geophysical Year stimulated the United States Government to announce the Vanguard Program on July 29, 1955. After decades of neglect, the instrumented satellite suddenly became technically feasible, scientifically desirable,

financially possible, and politically astute. It was not far from this point to unmanned space probes.

The first mention of an unmanned research probe appeared in Goddard's 1919 classic, *A Method of Reaching Extreme Altitudes* (Ref. 2-15). Goddard suggested using a rocket to explode a couple of pounds of flash-powder on the Moon's surface. He calculated that the flash could be seen from Earth with a telescope having a twelve-inch aperture. The scientific value of exploding flashpowder is questionable, but nevertheless it is the first recorded concept of a space probe. Willy Ley later improved on Goddard's idea by proposing a Moon rocket loaded with powdered glass and an explosive charge that would spread it over a wide area that could be permanently seen from Earth. The next landmark occurred on September 20, 1952, when Burgess and Cross presented a short paper entitled *The Martian Probe* to a meeting of the British Interplanetary Society (Ref. 2-2). The term "probe" had its origin with this article. Despite the technical merit of the probe concept, interest lagged behind the upsurge in satellite thinking. Five years later, sparked by papers such as Singer's *Interplanetary Ballistic Missiles, A New Astrophysical Research Tool*, space probe enthusiasm increased rapidly (Ref. 2-32).<sup>\*</sup> Hardware projects, like the Pioneer probes, began to materialize.

### 2-3. History of the Space Probe

So far, space-probe history has been discussed only in terms of the spacecraft alone. Since space probes are the products of merging several convergent technologies, a convenient approach to their developmental history consists of singling out the important technical elements and sketching each briefly. These are listed below with references to subsequent technical chapters in this book in which they are discussed:

<i>Element of Probe Technology</i>	<i>Technical Chapter</i>
Aerodynamic theory and attitude control	5
Space communications and data handling	6
Navigation, guidance, and control	7
Testing, checkout and Earth-based facilities	8
Rockets	9
Space-probe systems	10 and 11

From this list it is clear that today's probes did not appear full blown. They depend upon developments in many fields, only one of which is rocketry.

<sup>\*</sup>Singer's paper was read at the Eighth IAF meeting, in Barcelona, just a few days after Sputnik I was successfully launched, on October 4, 1957.



*Astrodynamic Theory and Attitude Control.* Astrodynamics has often been called an engineering extension of celestial mechanics. In this limited sense, it dates back to the early Egyptians and Babylonians who first tried to explain the regular features of the stellar motion. Tycho Brahe's careful observations in the late sixteenth century laid the experimental foundations for Kepler's three laws. Newton followed with his universal law of gravitation, published in 1687. The powerful mathematical methods of celestial mechanics sprang from the eighteenth- and nineteenth-century masters like Clairaut, Lagrange, Laplace, and Gauss. The crowning achievements of celestial mechanics were the predictions and subsequent discoveries of Neptune, by Galle, in 1846, and Pluto, by Tombaugh, in 1930.

Despite this distinguished background, many modifications and extensions of celestial mechanics were necessary before precision space probe trajectories could be calculated. Celestial mechanics had not needed and had not generated mathematical techniques for dealing with strong applied thrusts.

The first real astrodynamical computations were done in the 1920's and 1930's by foresighted amateurs such as Hohmann, Goddard, von Pirquet, and Oberth (see Bibliography). The goals of these pioneers were to determine energy requirements and rocket sizes. They were happy enough to show space flight to be feasible, and had little incentive to work out new methods of high precision. Most of this early astrodynamical work appeared in the then rather obscure monographs and periodicals, like the *Journal of the British Interplanetary Society*. Such literature was not accepted by members of the scientific community at that time. As astronautics became more respectable and recognized as a fertile field for study, some astronomers began devoting effort to the stimulating problems of trajectory optimization, orbital dynamics, and the adaptation of celestial mechanics techniques. Still, even in 1955, though many hundreds of feasibility calculations had been made, astrodynamics was still at such a primitive level that it could not accurately fly a probe to another planet.\*

Even the first Earth satellites strained the meager resources of astrodynamics. High-speed, precision techniques to deal with the perturbing forces of the Earth's bulge and atmospheric drag were wanting. At this point, the finesse of celestial mechanics and the vigor of its young offshoot, astrodynamics, were finally welded together.

Three subareas of astrodynamics are of special interest in interplanetary exploration:

\*It was *fashionable* in this period of astronautical history to calculate lunar and Martian voyages.

1. Low thrust-to-weight-ratio trajectories typical of electrical propulsion.
2. Trajectory optimization with respect to parameters like energy, time, and launch vehicle weight.
3. Attitude control.

Classical celestial mechanics is silent concerning these problems. The significance of such studies was pointed out by the advanced thinkers like Oberth, Goddard, and Esnault-Pelterie, but little work was done before 1955.

Another facet of astrodynamics, still critical today, is the acquisition of more precise astrodynamic constants, such as better values for the masses of the planets and the ratio of the Astronomical Unit to the kilometer. Interplanetary radar experiments and data from probes like Mariner 2 are rapidly improving the accuracy of our model of the solar system. Hand in hand with the appearance of better physical data has been the introduction of better digital computers and more sophisticated trajectory programs. Today, no one would think of launching a space probe without extensive machine calculations taking into account all known perturbing forces. In short, astrodynamics is maturing and is already a powerful, productive tool of space flight.

*Space Communications and Data Handling.* Historically, space communications resembles astrodynamics. Both spring from parent disciplines with long, distinguished backgrounds. Communication by electromagnetic radiation can be traced back to Hertz' induction experiments in 1887. It is true that radio communication does not stretch back into antiquity like celestial mechanics; but certainly Hertz, Maxwell, and Ampère can hold their places in history beside Laplace, Newton, and Clairaut.

Marconi demonstrated long distant radio communication in a series of experiments commencing in 1895, but remote control and telemetering developed much more slowly. In the 1920's and 1930's, radio control was demonstrated for boats and aircraft. Radiosondes were shown feasible during the same period. World War II stimulated developments in everything electronic, but even at the end of the war the miniaturized telemetering equipment typical of space probes like Surveyor, Mariner, and Ranger would have been considered fantastic. The slow growth of telemetering was a significant factor in the delayed development of instrumented satellites and space probes.

As the early pioneers were contemplating manned rockets and voyages to the Moon and planets during the first half of this century, they paid scant attention to the special problems of space communication. Some of the neglect was undoubtedly due to the almost universal belief that

man would ride along as an observer and data memory device. This point is consistent with the parallel given concerning the slighting of instrumented probes and satellites. Another factor was the common thought, still not completely dispelled, that space communication should be easier than terrestrial communication because the sender and receiver are almost always in sight of one another in space and the fickle atmosphere of the Earth is replaced by the more dependable near-vacuum of outer space.

Satellite command and telemetering are not particularly difficult because distances are still small. In fact, radio amateurs can listen to satellite transmissions with ease. Lunar-probe communication is more difficult, but easily within the 1950 state of the art. To converse effectively with a space probe 100,000,000 km away, however, new technical developments were needed despite the line-of-sight and transmission medium advantages cited above. Most of these inventions appeared after 1940.

Small, compact electronic payloads with low power drains and high reliabilities were made possible by the invention of the transistor by Bardeen and Brattain in 1943. The discovery of the maser reduced receiver thermal noise temperatures to less than 20°K, permitting an increase of more than an order of magnitude in the signal-to-noise ratio. Coupled with these unpredictable breakthroughs was the gift from radio astronomy of immense, steerable antennas. In 1953, a 15-meter diameter dish went operational at the Naval Research Laboratory. The 26-meter Goldstone antenna and the 76-meter giant at Jodrell Bank, in England, followed in 1958 and 1959. The sheer size of these installations has proven to be just as important as electronic finesse in space communications. Improvements came from still another quarter: communication theory. The quantization of information and the formulation of laws governing its transmission and reception, by Shannon and Weaver, in 1948, led to improvements in data-processing by reducing data redundancy and permitting more information to flow over a given channel.

Even more important than these technical factors has been the shift away from the black-box approach, in which radio equipment is "hung on" the spacecraft with little regard for other subsystems, to the system approach, where all components are subservient to over-all mission goals. No definite date can be assigned to this transition in thinking. No press announcements were made. The systems approach is an obvious necessity when viewing sensitive probe interfaces like those between solar cell and radio antenna orientation, antenna beam width and attitude-control-system accuracy, and power supply weight versus transmitter weight. System thinking is exemplified by the NASA Deep Space Instrumentation

Facility (DSIF), a carefully engineered Earth-based communications terminal subsystem which is meticulously matched to the interplanetary spacecraft and overall mission objectives.

*Guidance, Navigation, and Control.* Space probes, like primitive man, will use the stars and other natural landmarks for navigation. Supplementing this time-honored approach are a number of technical aids that have been developed over the last several hundred years:

*Terrestrial Instrument*

Accurate chronometer	John Harrison, 1729
Sextant	U.S. and England, 1731
Reliable ephemerides	England, 1767
Gyroscope	Foucault, 1852
Schuler pendulum	Schuler, 1923
Radar	U.S., England, France, Germany, about 1935

Since these basic devices were invented, there have been a great many technical improvements. The early marine chronometers, for example, have been superseded by precision electronic clocks for space flight. Modern gyroscopes, using air bearings and force-field suspensions, are orders of magnitude more accurate than Foucault's first models.

Most of the early navigational aids owe their births to sea commerce and the search for colonies. World War II triggered an intense burst of development. By its end, the German V-2 boasted commendable gyros and accelerometers. The cold war aftermath saw gyro development continued with emphasis on unmanned, guided weapons. By 1953, MIT scientists were able to fly a B-29 from Boston to Los Angeles with only an inertial guidance system at the helm. Further development of guidance equipment for the ICBM's made accurately aimed interplanetary probes reasonable technical targets.

It is interesting to look back and discover that precision inertial guidance was actually discounted by the early planners of space flight due to seemingly unsolvable technical problems. Early astronautics therefore concentrated on stellar navigation, just as terrestrial navigators did. The remarkable developments in inertial navigation have reinstated this technique. Interplanetary space vehicles will probably use some combination of inertial guidance, stellar navigation, and radio tracking from Earth.

Parallel to engineering advances, theoretical work should have been moving ahead in astronavigation; but as in the other "auxiliary" disciplines, deep-space navigation and guidance suffered from disinterest.

The first paper of real significance to the navigation of space probes was presented by Herrick in 1950 (Ref. 2-17). The avalanche of literature began with the onset of the space age in 1957. As in space communication, a most significant trend has been the integration of the navigation and guidance equipment into the joint probe-Earth-facility system.

Almost ignored amid the flood of new gyroscopes and accelerometers has been the progress of computers and adaptive automata. Space vehicles, like the Mariners, are now commanded by the DSIF to perform various functions, like scanning a planetary disk or changing the vehicle's attitude in space. In future probes that will range to the limits of the solar system, it will probably be desirable to provide greater autonomy. Norbert Wiener's 1948 book *Cybernetics* set many people to thinking about such "intelligent" machines. During the 1950's, many checker- and chess-playing computers were demonstrated. More recent have been the mechanical rats that "learn" to run mazes to perfection. Today's Earth-guided space vehicle, which was preceded by remotely controlled ships and aircraft, may in turn be supplanted by machines that can make their own way in space.

*Testing, Checkout, and Earth-Based Facilities.* Before a space probe leaves its launch pad, it is subjected to thousands of tests. When it finally lifts off, it is followed on its flight by strategically placed telescopic and electronic eyes all over the world. This mighty complex of launch ranges, test sites, and tracking stations is the least publicized facet of all astronautics. Even though the largest fraction of the space dollar is spent on facilities and ground support equipment, literature on the subject was almost non-existent until 1960, when a few papers began to appear.

The first rockets in history, using solid propellants, did not demand extensive ground facilities for testing and launching. The military and Fourth-of-July rockets were fired from simple racks or were just stuck into the ground at improvised sites. Probably the first rocket range with any technical sophistication was the artillery range of the Royal Laboratory at Woolwich, England, where Congreve experimented with his war rockets in 1802. Even Goddard was at a loss for a test site and flew his first liquid-fueled models from empty fields near Auburn, Massachusetts, in 1926. In 1930, Goddard moved his tests to Mescalero Ranch near Roswell, New Mexico, where he experimented with larger rockets. In the same year, the German amateur rocket organization, the *Verein für Raumschiffahrt* (VfR), obtained permission to use some government-owned concrete barracks on the northern outskirts of Berlin for rocket tests. The installation was christened the *Raketenflugplatz* (rocket flight place). Although barely instrumented at all by modern standards, many farsighted experiments were carried out at "ranges" such as these in the

1930's. Meanwhile, rocket amateurs the world over were testing home-made devices in deserted fields and lots, incurring the wrath of fire department officials and local property owners wherever they went.

Peenemunde, located on the Baltic coast, was the first modern launch range. As the German war rocket facilities were built up, from 1937 on, Peenemunde acquired rocket test stands, tracking radar, a liquid-oxygen plant, and many of the trappings of a modern range.

The White Sands Proving Grounds, in New Mexico, constituted the first American launch site of any size. Here, captured German V-2's, Private A's, WAC Corporals, and other military and high altitude rockets were fired from 1946 on. Strangely enough, Goddard's New Mexico test site of the 1930's was only a hundred miles east of White Sands. Another strange geographical coincidence occurred when the Eastern Test Range (ETR) was activated at Cape Canaveral (now Cape Kennedy) in 1950, just a few tens of miles from where Jules Verne had his Baltimore Gun Club fire a manned projectile to the Moon.

The first nonfictional flight from ETR took place on July 24, 1950, when a Project Bumper shot, using a V-2 first stage and a WAC Corporal upper stage, was successfully fired. The ETR is now a multi-billion dollar facility, extending over 8000 km along an arc of islands and deployed ships terminating near Ascension Island.

Another major U.S. launch facility is the Western Test Range (WTR), at Point Mugu, in California, which was opened in 1958 and is used primarily for military space programs.

Missile ranges like the ETR and WTR must be supplemented by other ground facilities, since successful deep space shots quickly pass beyond the limits of the equipment on the ranges. Several worldwide tracking and communications networks have sprung up since 1957. The Vanguard program began the Minitrack network of tracking stations in 1957. It consisted of interferometer stations sprinkled along the 75th Meridian and in a few other selected spots. Similar, but more advanced, networks since installed include the Microlock Doppler tracking equipment for Earth satellites, the Project Mercury tracking net (1960), and the Deep Space Instrumentation Facility (DSIF).

Another important segment of space technology is preflight testing and checkout. These activities are essential to the establishment of reliable equipment, especially space probes that must function for many months during the long journey around the Sun to the target planet.

Ground checkout and reliability tests have always been performed before committing components and vehicles to a mission, but it took the ICBM program to evolve the massive launch-simulation equipment duplicating the shock and vibration of an actual launch. The scientific satellite

and space probe efforts stimulated the construction of large environmental simulation chambers, where the Sun's effects, the vacuum of space, and other phenomena are manufactured on the ground before any flight takes place. Today, every major government and industrial space laboratory possesses large environmental test facilities.

*Rockets.* The long and fascinating evolution of rockets has been well-documented (Refs. 2-1, 2-10, 2-13, 2-23, 2-25). With so much readily available rocket history, only a short table of key events seems necessary here:

<i>Date</i>	<i>Event</i>
1919	Goddard publishes his rocket test results (Ref. 2-15).
1926	Goddard launches first liquid-fuel rocket intended for high-altitude probes.
1936	Guggenheim Aeronautical Laboratory, forerunner of JPL, founded at California Institute of Technology to study sounding rockets.
1938	First flight of A-2, precursor to German V-2.
1953	First Redstone Flight.
1957	First successful Atlas ICBM Launch.
1958	Pioneer 1, first successful probe launched.
1962	Mariner 2 Venus probe successfully launched.
1964	Mariner 4 Mars probe successfully launched.

*Space Probe Systems.* The Pioneer space probes were the first U.S. space vehicles to leave the gravitational field of the earth. This series of vehicles used the World Tracking Net, the early version of the DSIF, which had stations at Cape Canaveral, Jodrell Bank, Singapore, and Hawaii, and a portable station set up at Salisbury, Southern Rhodesia. With this integrated ground support and space vehicle system, the Pioneers were already immeasurably more complex in terms of equipment, facilities, and people than any visionary had ever foreseen.

The Pioneer Program originated in early 1956, when the Army Ballistic Missile Agency and JPL were asked to launch two lunar probes during the International Geophysical Year. The probe objectives were to be:

1. Measure cosmic rays in deep space.
2. Verify the design of the tracking and communications systems.
3. Obtain a better value for the mass of the Moon by observing probe perturbations in the Moon's vicinity.

The booster used for the first two Pioneer shots was the Thor-Able-I. The Juno-II vehicle was used for the remainder of the shots. Pioneers 1, 2,

and 3 reached very high altitudes, but fell back to Earth before reaching the neighborhood of the Moon. Pioneers 4 and 5 were injected into orbits around the Sun, where they still remain. Even the probes that fell short of their target transmitted useful information about the geomagnetic field and radiation belts back to the Earth.

Like the first Pioneers, the Rangers and Surveyors are lunar probes and have historical and technological relevance to this book. The first true planetary probes are the Mariners, which will probably be followed by the Voyager series. Concurrent with the Mariner program, the national lunar effort is providing pertinent technology through the Ranger and Surveyor programs. Just as the manned landings on the lunar surface require extensive probe exploration beforehand, the manned voyages to Mars—the next celestial target for manned spacecraft after the Moon—also demand detailed knowledge of the planet's surface and environment. All of these programs just mentioned are too young to have developed much history.

Before leaving the subject of space probe evolution, consider what comes next. What technical developments will trigger new generations of space probes? There will certainly be a trend toward *active* probes that carry out cause-and-effect experiments in addition to *passive* listening. The advances in computers and cybernetics will certainly be adopted by probe designers, continuing the trend toward self-adapting machines and internal control.

If history has said little about the conventional concept of the space probe, it has said even less about possible extrapolations to automata. What man thinks of himself as replaceable by a machine? It is not too surprising that astronautics has been preoccupied with manned space flight to the near exclusion of the somewhat distasteful automata. The conflict between man and machine is just beginning. Although human involvement in space flight was confidently asserted in Chapter 1, there is always that seed of doubt, that small voice warning against the superior machine that might usurp man's role in space.

Machines may never completely replace man in space, but the start of the competition has been signaled. Already there are many who say that man is not needed in space. There are many others who say that machines will always have extremely limited capabilities and that man is essential for reliability and serendipity. History will probably prove both groups to be shortsighted.



# *Chapter 3*

---

## THE STATUS OF INTERPLANETARY EXPLORATION

---

---

### 3-1. Introduction

Once a space probe has penetrated a distance of twenty Earth radii into interplanetary space, it enters a new realm for scientific research. Behind are the Earth's atmosphere and magnetosphere; beyond, deep space with eight unexplored planets, swarms of asteroids, and the mysterious comets. It is hard to avoid a parallel with the early explorers of the seas, when they left behind the vicissitudes of coastal waters and set forth on broad unknown oceans. In sharp contrast, however, the first interplanetary ships are unmanned, and their goal is scientific knowledge rather than new trade routes.

It is not feasible to summarize all that is known about interplanetary space and the planets in a single chapter. What is possible is a short status report on those parts of astronomical science where space probes are helping to expand our knowledge. Stellar astronomy and geophysical research can be carried out better and more cheaply by satellite observatories and will not be covered here, but no Earth- or satellite-based instruments can substitute for the simplest probe under the clouds of Venus. Consequently, this chapter concentrates on the middle ground, the space between the effective termination of the Earth's magnetic field and the beginning of interstellar space.

### 3-2. Between the Planets: Interplanetary Physics

Continuing the ocean analogy drawn in the last section, few of the physical events occurring out on the interplanetary sea ever reach instruments in our sheltered harbor beneath the Earth's atmosphere and

magnetic field. Most satellites only partially penetrate these shields. Far-ranging space vehicles are needed to chart the force fields, particle fluxes, and bits of matter that crisscross the depths of outer space.

*Astronomical Data.* Even if the atmosphere were completely transparent, the Earth-based astronomer could not accurately measure the absolute masses and distances of the planets.

*Relative planetary distances* are measured with high precision in terms of the Astronomical Unit (A.U.), but what is the ratio of the A.U. to the kilometer? Conventional astronomical measurements, involving analysis of the perturbations of the planets and asteroids, have led to an adopted value of  $1.495 \times 10^8$  km for the A.U. Accuracy is limited because of the uncertainty of the planetary masses. Radar astronomy measurements at JPL, MIT, Jodrell Bank, and other facilities have increased the precision considerably. The average of several radar determinations made in 1961 was  $1.495983 \times 10^8$  km (Ref. 3-40). But the accuracy of radar measurements depends upon the velocity of light, which is affected by the electron density of the interplanetary medium.\* Space probes can provide direct measurements of the interplanetary gas density, permitting precise corrections of radar data. Careful tracking of probes from Earth and the analysis of their trajectory perturbations by the planets can lead to better mass values for the planets and, indirectly, to a better value for the A.U.

The seven significant figures just quoted for the radar-measured value of the A.U. might seem precise enough. Unfortunately, small uncertainties in the A.U. can lead to large probe miss distances in trajectory analysis, possibly causing a future manned space vehicle to miss its planetary target.

*Gravitational Fields and Relativity.* Newton's Law of Gravitation and Einstein's General Theory of Relativity, despite their elegance, do not represent complete descriptions of gravity. In addition, the General Theory of Relativity has not been adequately tested by experiment. One of the important checks of the General Theory, the measurement of the rotation of the perihelion of Mercury, depends upon accurate planetary masses. Here again, scientists are caught in a box of relative measurements, where planetary masses are measured in terms of the Earth's. The box cannot be escaped until probes obtain absolute mass data.

Emphasizing the complexity of the universe (and to scuttle any thoughts concerning the patness of science), some cosmologists now believe that the value of the gravitational constant in Newton's Law varies with time. To compound this crime against the simplicity of nature, the

\* An electron density of  $10^9/\text{cm}^3$  would delay Venus echoes by 0.03 sec, corresponding to a range error of almost 5000 km.

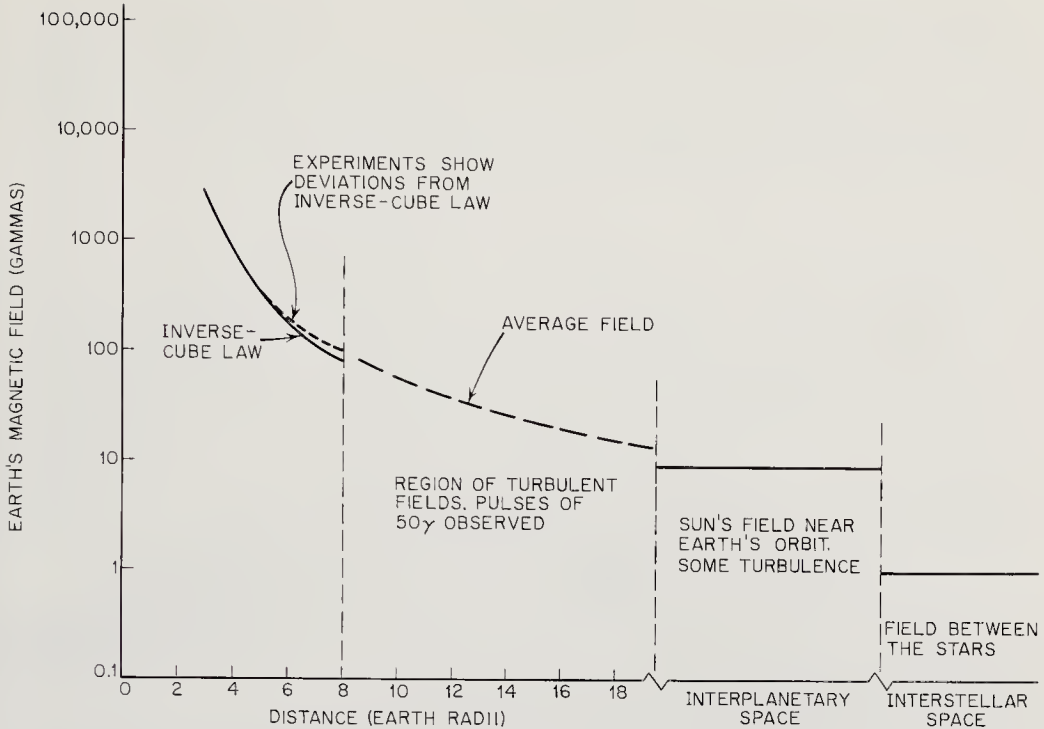


Fig. 3-1. Current measurements of magnetic fields in space show the Earth's field dropping off rapidly out to about eight Earth radii. Between eight and twenty Earth radii, there exists a variable, turbulent, highly asymmetric region marking the transition zone between the Earth's field and that of the Sun.

velocity of light may also exhibit secular changes. Possibilities like these can be checked by space experiments.

Space probes can aid cosmology and relativity theory in several other ways. A space probe carrying a high-frequency transponder could give continuous, highly accurate distance measurements\* between the probe and the Earth, helping to tie down the interplanetary distance scale. More advanced concepts involve placing an atomic clock on a probe to measure relativistic time dilation effects. It might also be possible to confirm the gravitational red shift predicted by the General Theory of Relativity by stationing identical atomic clocks on the Earth and far out in space. Any changes in frequency between clocks would be due to the change in gravitational field strength (Ref. 3-7).

*Magnetic Fields.* The other important action-at-a-distance field besides gravity in outer space is the magnetic field. At the surface of the Earth, the total magnetic field is some 50,000 gammas (one gamma =  $10^{-5}$  gauss). As a space vehicle moves away from the sunlit side of the Earth, the strength of the dipole magnetic field first drops according to an in-

\* More properly, time of transmission multiplied by the velocity of light.

verse cube law (Fig. 3-1). Between eight and twenty Earth radii away, a probe's magnetometer would indicate passage through the transition zone between the Earth's field and the interplanetary field that is derived mainly from the Sun (Fig. 3-2). In this zone, shock waves and transients

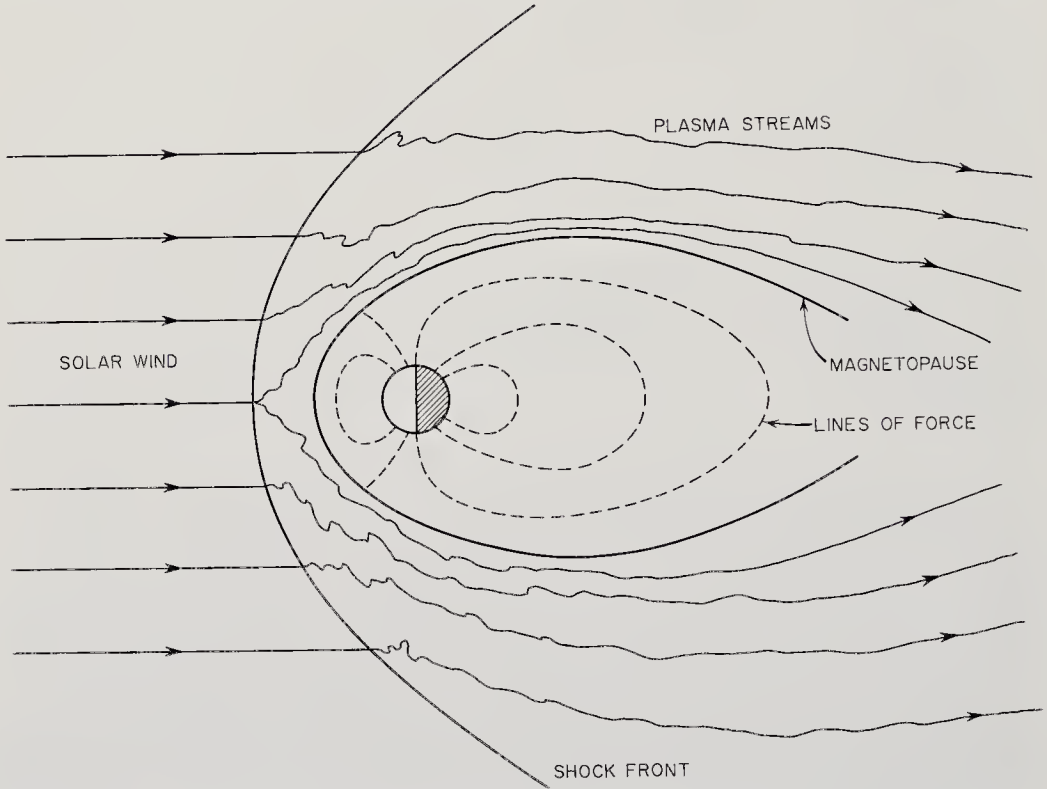


Fig. 3-2. Conceptual sketch showing the flow of solar plasma around the Earth's magnetopause. The Earth's magnetic field is distorted into a teardrop shape by the solar wind.

would cause magnetometer readings to fluctuate wildly. Probes like Pioneer 5 and Mariner 2 have recorded fluctuations of 50 gammas. The transition region is not symmetric but is drawn out into a teardrop shape with the tail blown away from the Sun by the solar wind. Surrounded by this irregular magnetic cavity, the Earth swings around the Sun partially insulated from physical events occurring outside the magnetosphere.

Complete magnetic isolation from interplanetary magnetic effects does not occur on the Earth's surface. Tongues of plasma frequently shoot off the Sun's surface and, dragging their magnetic lines of force with them, engulf the Earth and inject current carriers into the Earth's radiation belts.

Three scientific tasks can be set for space probes as they move toward their planetary destinations:

1. Record the vagaries of the transition zone between the Earth and the rest of the solar system.
2. Survey synoptically the interplanetary magnetic field.
3. Record the fine structure of the interplanetary field fluctuations.

Once a space probe approaches Venus, Mars, or any other object in space, its magnetometer will start searching for indigenous magnetic fields. There is no fundamental reason to believe that a planet must have a magnetic field. Although the Earth possesses one, Russian and U.S. probes have indicated that the Moon and Venus have small fields, perhaps none at all. The synchrotron radiation emanating from Jupiter indicates that that planet may have radiation belts and a surface field of perhaps  $10^4$  gauss. The magnetic splitting of the solar spectral lines (Zeeman effect) implies strong, though perhaps localized, magnetic fields on the solar surface. Clearly, space probes could help unravel some of these problems.

Moving still farther away from the Sun, a probe should encounter another transition zone, between the solar system and interplanetary space. The polarization of starlight indicates that an interstellar magnetic field of about one gamma exists. But what is the origin of the interstellar field, and where is the boundary between it and the solar-system magnetic cavity?

*Interplanetary Plasma and Particle Fluxes.* Matter throughout the universe is usually found in the plasma state. Since a plasma contains charged particles, it interacts with magnetic fields, and plasma in motion can, in turn, generate magnetic fields.

Space probes can carry instruments beyond the Earth's magnetosphere into the stormy plasma seas dominated by the steady solar wind, solar flares, and the galactic cosmic ray flux. Satellites with greatly elongated orbits, like the Interplanetary Monitoring Platform (IMP), can strike a short distance out into interplanetary space, but are primarily reserved for studying geophysical phenomena.

A guide to the particle fluxes measured in space is shown in Fig. 3-3. Ultimately, particle fluxes, measured as functions of energy and position, will be available for the solar system. Such a solar-system weather map would be considerably more sophisticated than the morphological chart of Fig. 3-3.

In deep space, the solar wind seems to be the most dependable solar phenomenon. E. N. Parker coined the term "solar wind" during studies of the interplanetary medium. Instead of assuming a solar corona in hydrostatic equilibrium, he postulated a continuous efflux of mass from the Sun's surface in the form of a fluid with an ion density of about

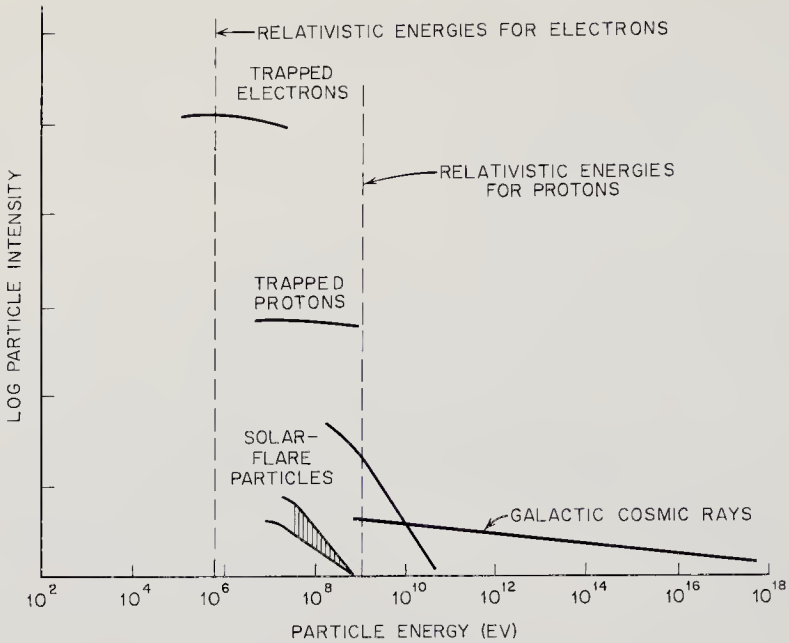


Fig. 3-3. The intensities and energies of nuclear particle radiations in space. The "trapped" particles are those in the Earth's radiation belts. (Adapted from Ref. 3-43.)

100/cm<sup>3</sup>, traveling at about 500 km/sec. Substantiation of this hypothesis comes from the blowing of comet tails away from the Sun like wind-socks; and, more directly, from probe plasma measurements. Plasma detectors aboard Mariner 2 showed that the solar wind has a particle density between 0.5 and 30/cm<sup>3</sup> and a plasma velocity of from 200 to 1200 km/sec. Additional data are needed to determine how the wind varies with position and time.

Superimposed on the solar wind are irregular disturbances called solar flares. Flares are immense tongues of plasma that erupt from the Sun's surface. Flinging themselves across interplanetary space, they engulf planets that happen to be in their paths. The plasma in the flares and the magnetic fields they drag along with them create magnetic storms on the Earth. Once the Earth is immersed in a plasma tongue, the magnetic fields on the outside of the tongue deflect galactic cosmic rays away from the Earth, causing the characteristic Forbush decrease of cosmic-ray intensity (Fig. 3-4). Large flares bring enough ionizing radiation with them to pose serious threats to manned space flight. Space probes can help define flare details. More knowledge might lead to flare-prediction techniques that would hold manned spacecraft on their launch pads when flares are threatened.

The last important component of the interplanetary corpuscular population is the cosmic ray flux. Some cosmic rays are born on the Sun,

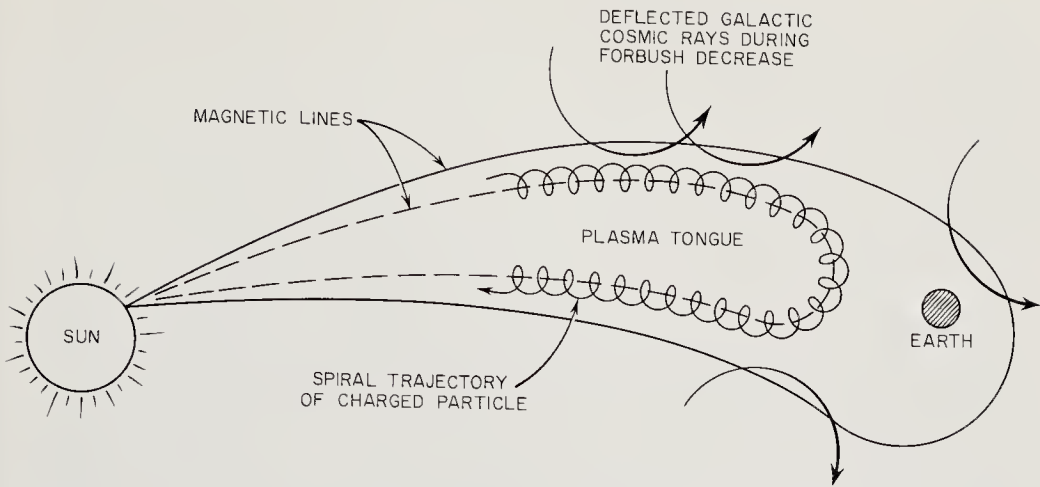


Fig. 3-4. Schematic drawing of a solar flare engulfing the Earth, causing a Forbush decrease of cosmic-ray flux.

along with solar flares. Compared to cosmic rays of galactic origin, which may have energies per nucleon as high as  $10^{19}$  ev, the solar cosmic rays are low-energy phenomena, with maximum energies of just a few billion electron volts per particle. The different compositions of the two cosmic ray populations shown in Table 3-1 indicate that stars like the Sun may inject significant quantities of matter into the galactic cosmic-ray accelerating mechanism (whatever that may be). Solar-generated cosmic rays obviously vary in position and intensity, depending upon solar flare activity. In large flares, the proton flux over 20 Mev may exceed 1000 protons/cm<sup>2</sup>-sec-steradian for more than a day. The galactic cosmic ray flux drops off rapidly as the particle energy increases (Fig. 3-3). Energies are higher and fluxes lower than those of solar cosmic rays. The integrated, galactic cosmic-ray flux over 500 Mev is only about 0.18 particles/cm<sup>2</sup>-sec-steradian.

TABLE 3-1. RELATIVE ABUNDANCES OF COSMIC RAY PARTICLES\*

<i>Element</i>	<i>Galactic</i>	<i>Solar</i>
Hydrogen	2500	varies
Helium	360	1250
Lithium, beryllium, boron	11	0.3
Carbon	18	6
Nitrogen	8	2
Oxygen	10	10
Fluorine	1	0.4
Neon	3	1.5
$11 \leq Z \leq 18$	9	1.3

\* Ref. 3-25

Space probes will provide synoptic measurements of both cosmic ray populations well away from the Earth's magnetic field. Active experiments involving particle injection, possibly using nuclear explosions, might be used if the man-made effects were sure to be short-lived. Undoubtedly, space probes will find unexpected radiations in space, just as the Earth's radiation belts surprised the first satellite experimenters.

*Electromagnetic Radiation.* Space-probe sensors fixed on the Sun see a rich and broad electromagnetic spectrum. Even the narrow band of wavelengths seen on the ground (3000A to 13,000A) has more than 26,000 absorption lines originating in the Sun's cooler upper layers. Above the Earth's atmosphere, the spectrum opens up at both ends (Fig. 2-1, page 8). Below 3000A, a complex, time-varying spectral picture is seen by high altitude rockets and satellites. Our knowledge of the spectrum over 13,000A is limited since few experiments in that spectral region have been carried out above the atmosphere. Large terrestrial radio telescope dishes peer out into interstellar space through the radio windows in the atmosphere, but they are too large for present space vehicles. Looking away from the Sun, starlight and galactic radio noise bathe space probes with very low fluxes of noise from radio stars, also the 1420-Mc signal from interstellar hydrogen.

A space probe would be inefficiently used if assigned solely to the visual observation of the Sun and stars. The electromagnetic radiation from these objects can be studied more effectively from Earth satellites like the Orbiting Astronomical Observatory (OAO) and Orbiting Solar Observatory (OSO). Probes could supplement orbital data with information gathered far away from the Earth's influence.

*Particulate Matter.* Variouslly called cosmic dust, interplanetary matter, and micrometeoroids, these small bits of matter seem to have a higher concentration around the Earth than those other areas in the solar system penetrated by space probes. Some micrometeoroids have an asteroidal origin and densities of from 3 to 8 g/cm<sup>3</sup>; most, however, are light and fluffy (densities less than 1 g/cm<sup>3</sup>), possibly indicating a cometary origin.

Mariner-2 measurements show that the interplanetary dust concentration is at least 10,000 times lower than it is in the vicinity of the Earth. This is fortunate for space-vehicle designers, who must protect manned cabins and liquid-filled radiators against these projectiles, which have velocities relative to the Earth of between 28 and 72 km/sec.

The data in Fig. 3-5 come from satellite-mounted detectors, Earth-based visual measurements of meteors, and studies of the zodiacal light. Probes, of course, will carry instruments to measure the possible presence of dust clouds around other planets as well as the detailed dust distribution in space. Since much of the dust probably originates from



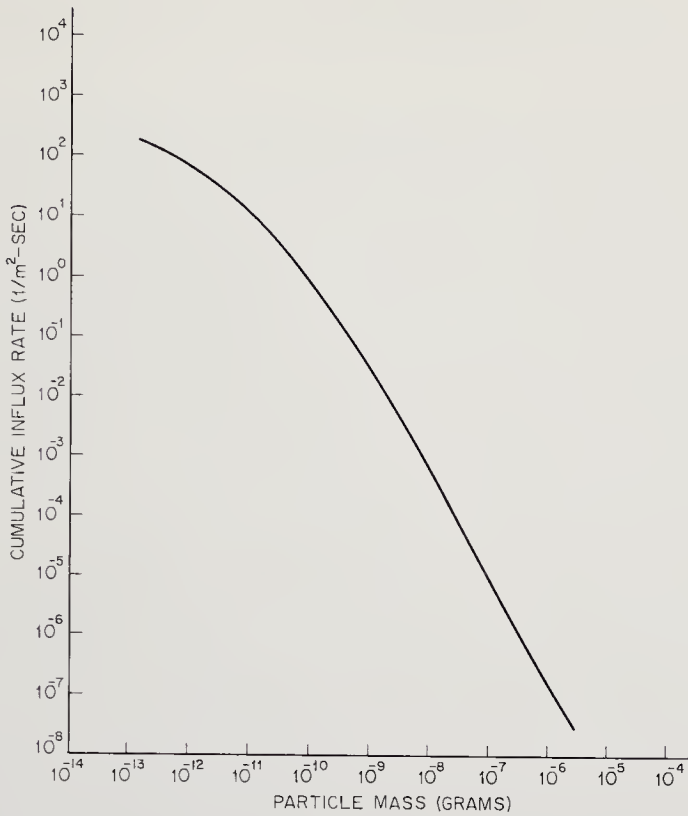


Fig. 3-5. Average mass distribution curve for micrometeoroids in the vicinity of the Earth. Ordinate is cumulative; i.e., any point includes all heavier particles. In deep space away from the Earth, the micrometeoroid flux apparently drops three or four orders of magnitude.

the disintegration of comets and asteroids and from lunar material ejected during meteoroid collisions, it will be intriguing to search for dust streams and irregularities in its distribution.

*Role of the Space Probe in Interplanetary Physics.* The interplanetary fields and particle fluxes undergo large distortions in the neighborhood of the Earth. Probes, then, are valuable for measuring unperturbed distributions and fluxes in deep space. Stellar astronomy and physical phenomena not significantly disturbed by the Earth's atmosphere and magnetic field can be studied more easily from the ground and Earth satellites.

### 3-3. Exploration of the Planets

Human curiosity dictates that most space probes be aimed at planetary targets, for on these bodies, some similar to the Earth, there may be other life forms and hints about man's own beginnings. The objective of this section is to sketch some of the planetary characteristics and suggest how

probes might expand our knowledge, thereby paving the way for manned expeditions.

*General Characteristics of the Planets.* The solar system offers the space explorer nine planets, thirty-one natural satellites, and innumerable asteroids and comets as astronomical targets. The planets all move around the Sun in the same direction, in ellipses of low eccentricity, with their orbital planes slightly inclined to one another. The four inner, minor planets (sometimes called "terrestrial") and Pluto have average densities of four or five times that of water. The four major planets have average densities between 0.7 and 2.5. While the following planetary vignettes suggest that the four major planets are inhospitable to life, there are still many mysteries for probes to unravel beneath their swirling methane and ammonia clouds. The greatest discoveries in science have often been found where least expected. With this homily in mind, the space-probe designer should incorporate enough flexibility into his vehicle to take advantage of unforeseen opportunities.

*Mercury.* This planet stays so close to the Sun that it is difficult to observe. Scattered sunlight during the day and the thick layers of the Earth's atmosphere after sunset frustrate terrestrial observers. The planet's orbit is well known, but its diameter and mass have less precision than desired. Probes could be orbited around Mercury to pinpoint its mass. Better visual measurements could be made from astronomical satellites above the Earth's atmosphere.

The surface temperature of Mercury apparently reaches about 600°K on the hot side, but, because one side of the planet always faces away from the Sun, the temperature of the perpetually dark side cannot be much above absolute zero. Some atmosphere probably exists, but it would be frozen on the cold side. The atmosphere's composition and extent are the subject of considerable debate. Some scientists predict that Mercury also has a cloud of dust around it, much like that of the Earth. On-the-spot vehicles can resolve these questions.

Estimates of Mercury's density vary from 3.7 to 6.2, with the high side favored. A high concentration of iron, possibly indicating a core, and perhaps a magnetic field are inferred from the high density. Besides checking on such suppositions, surface instruments could make heat-flow measurements and record seismic data on a planet whose proximity to the Sun should create large thermal gradients as well as distorting core hydrodynamics and surface geology.

*Venus.* Like Mercury, Venus is so close to the Sun that astronomers see it fully lighted only when it is across the solar system from the Earth. When it is close, it reveals only a frustrating thin crescent. No natural satellite helps fix its mass accurately. To make matters more difficult,

it is perpetually covered by thick clouds. The utility of a probe is manifest.

Spectroscopic observations indicate a high concentration of carbon dioxide in the Venusian atmosphere. This discovery, by Dunham, in 1933, disappointed many who looked for an Earth-like atmosphere that would reinforce the then-common intuition that Venus was a primitive model of the Earth. This hoped-for resemblance became even more remote after Mariner 2 scanned the planet's heavy cloud banks with radiometers, on December 14, 1962. A cold cloud cover 24 km thick, with its base about 72 km above the surface, has been inferred from the Mariner-2 data. The surface atmospheric pressure might be twenty times that on Earth. Surface temperature seems to be about 600°K, a fact supporting the so-called "Greenhouse Model" of the Venusian atmosphere in which solar energy penetrates the atmosphere but cannot be reradiated through the cloud cover at long wavelengths.

Radar roughness measurements of the surface of Venus show enough relief to dispel thoughts of a liquid surface. There may, however, be lakes of liquid metals or other fluids at 700°K. Surface observations from the Earth are impossible, except for fleeting, perhaps illusory, impressions gained as the clouds shift.

An artificial satellite of Venus would reveal a great deal about its atmosphere as well as permitting a more accurate calculation of its mass. A sample-taking probe flying through the atmosphere or descending to the surface would be of even more value to the planetologist.

*Mars.* Since Venus seems unlikely to harbor life, much astronomical attention has shifted to Mars, where a transparent atmosphere has long allowed close observation of its surface. The data available do not preclude the existence of some form of life, but the same data have posed even more questions: What are the strange markings called canals? How did the two tiny moons originate? Why are they so close to the surface (9400 km and 23,500 km)? Does Mars have a core? What creates the so-called blue haze?

The Martian atmosphere is mostly nitrogen with some carbon dioxide, water vapor, and oxygen. Atmospheric phenomena that look like dust storms and clouds are occasionally noted, making a meteorological satellite of Mars a useful tool. The atmospheric pressure on Mars is considerably less than that on Earth (only 10 millibars, according to some scientists). It may not be feasible to deploy balloons, parachutes, and maneuverable reentry bodies.

The surface of Mars seems to have little relief when compared to Earth's mountains. Well-marked features include the polar caps, the dark maria, and deserts. An instrumented observational satellite would

pick out more detail, as well as provide some answers to the controversial canal question. A remote television camera might indicate whether the canals are long continuous cracks in the crust, lines of separated points, or engineering works. The surface of Mars has a mean temperature of about  $-70^{\circ}\text{C}$ , but at the equator the average rises to a little over  $0^{\circ}\text{C}$ , making life at least possible.

Better mapping of the surface from geological and thermal standpoints would tell much concerning the origin and history of the planet.

Mars has a mean density of 4.0. It also shows a decided equatorial bulge about 34 km in radius. The origin of the bulge and the existence of a core are important in probe studies. Unmanned probes must also complete topographical and chemical analyses of the surface before manned vehicles can be designed.

The two tiny satellites (Phobos is 8 km in diameter, Deimos is 16 km) are mysterious because of their small size and apparent low density. Some astronomers have speculated that they might be artificial. Rendezvous with these strange objects by probes should clear up their origin.

*The Major Planets.* Beyond the asteroid belt, four huge planets (Jupiter, Saturn, Uranus, Neptune), all with similar characteristics, revolve around the Sun. Their diameters range from 50,000 km to 140,000 km. Densities are low, falling between 0.7 and 2.5. Their atmospheres are dense and optically impenetrable. The gases detected above the unseen surfaces are mainly hydrogen, helium, methane, and ammonia, in strong contrast to the nitrogen, oxygen, and carbon dioxide of the terrestrial planets. Space probes must search out the reasons for the remarkable differences between the minor and major planets. Did they have different origins? Some scientists have proposed that the major planets were once even larger and have since "evaporated" away. The propulsion requirements needed to reach these huge, low-density spheres and the (perhaps erroneous) low likelihood of finding life, make them secondary astronomical objectives for probes. There is no discounting, however, the tantalizing physical and chemical problems that must exist beneath the imposing layers of gases.

In the face of the general similarities just mentioned, each of the four major planets has peculiar, specific features that call for special explanations. The  $13,000 \times 40,000$  km red spot on Jupiter is a prime example. What is it and why does it wander erratically? Is it an island of light-gas ices floating on denser gases, like ice cream in a soda? Frequent, inexplicable bursts of radio signals also emanate from sources near Jupiter's surface. Jupiter's twelve natural satellites pose new questions about planetary evolution. The more distant and irregular of the moons may be captured asteroids. Conversely, some of the asteroids, like the Trojans

group, may be lost Jovian satellites. In fact, the dynamics and histories of all major-planet satellites need considerable study. Comparison of chemical samples from the moons with those from the planets and asteroids might unravel the puzzle.

Saturn has a spectacular system of rings, but otherwise seems a small version of Jupiter. The rings, most investigators agree, are composed of fine particles, probably bits of ordinary ice. The axis of the next major planet, Uranus, is tilted so far that its rotation is actually retrograde with respect to all other planets, excepting perhaps Venus. Does the tilt infer a near collision with another planet in the past? No one knows. Circling the last major planet, Neptune, is a very dense moon, even larger in size than our own. Triton's density of nearly five, its 4000-km diameter, and perfect circular orbit seem incongruous. Triton is unlike the other satellite of Neptune and has twice the density of its parent planet.

The outer planets are logical targets for advanced space probes, possessing adaptive control characteristics. With vastly improved sensors and small computers aboard, automata should have the flexibility and learning abilities necessary to investigate the complex and unpredictable planetary phenomena prevailing beyond the asteroid belt.

*Pluto.* Pluto is small and dense, like the inner terrestrial planets. Yet, it is on the outer limits of the solar system. Possibly it is a lost moon of Neptune. A probe to Pluto might radio back some of the answers to questions about its origin, but the closer planets and satellites must be explored first.

### 3-4. Asteroids, Comets, and the Sun

There is no shortage of scientific missions for instrumented probes within the solar system. Although Mars and Venus are first-priority targets, the Sun, the asteroids, and some of the comets may yield more important astronomical data than space-vehicle studies of the major planets.

Between Mars and Jupiter lie the orbits of tens of thousands of small objects, ranging from dust grains to 768-km planetoids, like Ceres. Sizes, orbits, and albedoes are the only real data available for the asteroids. Their creation is a matter of surmise. Certainly mutual collisions have caused some fragmentation. Gravitational interactions with other bodies in the solar system have probably modified the geometry of the asteroid belt. If space probes could discover the chemical composition of a typical asteroid, it would be a clue to the belt's origin and perhaps the formation of the entire solar system. Unfortunately, individual asteroids will be difficult to catch. They are many in number but occupy an awesome volume of space. Rendezvous with a specific asteroid would probably

be controlled by the probe itself, since an observer on Earth would be ineffectual because of distance and the smallness of the asteroid. Suggestions have also been made by many that instruments be landed on asteroids and carried piggy-back for a "free" ride around the solar system.

Comets seem to be conglomerates of ices and dust that move in highly elongated orbits around the Sun. Some astronomers believe that the whole solar system is surrounded by a halo of comets and that the comets themselves are made of the primordial stuff of the universe. When comets approach the Sun, they usually flare up under the influence of the solar wind, producing a long tail, blown in the direction of the solar wind. The tails disappear as the comets recede from the Sun, leaving only the customary nucleus and nebulous coma. Many suggestions have been made for probe flights through comets. Since a comet's nucleus is only a few kilometers in extent, it presents a difficult target. The much larger tail offers a more sporting chance.

The Sun is by far the largest object in our system, as well as its main-spring of energy. The Earth itself is a fair solar probe. With Orbiting Solar Observatories (OSO's) in operation, supplemented by many observers on the ground, careful watch is continuously kept on the Sun with all manner of instruments. In general, unmanned probes would be most useful only if they could be sent to within a few tenths of an A.U. of the Sun and thus be out of the influence of the geomagnetic field that distorts solar plasma. They would also be in a good spot to observe transitory solar events at close range.

### 3-5. Extraterrestrial Life

No matter how much is said about the importance and manifest value of physical science in space, the major driving force behind astronautics has always been the search for life outside our planet and transportation of Earthmen to the Moon and planets. In support of this strong assertion, consider the intense excitement and speculation generated by the least clue to extraterrestrial life: the Martian canals, the "organized" matter in some meteorites, even the creation of amino acids in terrestrial experiments.

There are in reality no data from astronomy, biology, or astronautics that conclusively declare the existence or nonexistence of life in the universe outside the Earth. The present widespread belief in the existence of extraterrestrial life stems from the slightest of hints and a great deal of enthusiasm.

One important exobiological hypothesis states that, given the right conditions, life is spontaneously born and evolved. Consequently, atten-

tion has been focused upon determining just what these right conditions might be and where they exist in the universe. The right conditions for "life as we know it" (that ubiquitous qualifying phrase) include the presence of water, carbon, oxygen, a source of radiant energy, and temperatures between 200°K and 500°K. Of course, once life arises it may be transported or kept dormant under much more severe conditions. Simple terrestrial life forms can apparently survive the rigors of outer space. Life "as we do not know it" may be based on radically different chemical processes and environmental conditions. The generality of the preceding statements typifies the speculation about extraterrestrial life. In the absence of conclusive data, the searching role of space probes becomes obvious.

When the terrestrial planets are examined for the right conditions for life as we know it, only Mars survives the screening. It is warm enough and has some oxygen and water. The dark areas (maria) can apparently regenerate themselves after being covered by Martian dust storms, a most life-like characteristic. The infrared reflection spectrum of the dark areas has some similarity to that of certain terrestrial vegetation. These are suggestive but not conclusive facts.

With such possibilities, a Martian probe must first of all be sterile to preclude contaminating Mars with terrestrial organisms. Secondly, life-detection experiments should have high priority. Thirdly and most important, equipment returned to Earth, such as sampling devices, must be rigorously sterilized to prevent back-contamination by possible Martian life forms.

Our knowledge of life-sustaining conditions on planets other than Mars is even less precise. Life may be hidden by clouds, by geological and other planetary features. Even our own Moon may have residual or transported forms of life in sheltered spots on or beneath the surface. The possibilities of life developing and existing outside the narrow limits of earthly life are unknown but may be many in number.

Another old and still useful exobiological hypothesis is that of *panspermia*, which states that life may have been (and may still be) transported through space as simple life forms (spores) by natural phenomena such as meteoroids. Over the immense age of the universe, life may have become as common and widespread as it is on Earth today, where every breath of air and clump of soil are laden with it. Artificial panspermia has also been considered by many science fiction novelists and by some scientists with impeccable reputations. Such accidental or intentional propagation of life through space should not be difficult for an advanced civilization; we, as a case in point, feel obliged to sterilize our space probes to prevent such dispersion. A major objective of any space program

should be the substantiation or refutation of the panspermia hypothesis.

In addition to the direct detection of extraterrestrial life, long range communication with other intelligent life forms is considered by some to be a reasonable and practical goal. Some terrestrial experiments (Project Ozma) have already started. Interstellar communication by radio waves seems best left to Earth-based equipment, where ample power and large antennas are readily available. This subject, except for elements of communication theory, will be bypassed.

Setting aside interstellar conversation and the analysis of organic materials in recovered meteorites, the biological tasks confronting interplanetary probe designers are still imposing. Experimental biology of completely unknown organisms cannot be carried out across tens of millions of miles without astute experimental planning and clever invention.

### 3-6. Interstellar Probes

Beyond Pluto stretch 4.3 light years of "empty" space before the nearest stellar system is encountered. This great void is populated by perhaps one proton per cubic centimeter, a weak magnetic field of about one gamma, and maybe a few pieces of meteoric or cometary dust that have escaped from stellar systems. The first interstellar probes will penetrate only short distances into this unexplored space, because of their limited lifetimes. They will still, however, be able to gather a great deal of data useful to the astronomers and cosmologists. Perhaps they will be able to detect the postulated cometary halo about solar system. What, for instance, is the acceleration mechanism for galactic cosmic rays? How much matter really resides between the stars? The scale measuring the universe depends upon the proper correction for the reddening of starlight by such interstellar matter.

Before the nearest stellar systems can be probed, one of two technological breakthroughs must take place. Either probe equipment, including electronics and power supplies, must be given lifetimes on the order of ten years, or self-diagnosing, self-repairing automata must be developed. Both avenues will certainly be attempted.

Pursuing the subject of automata further, the most valuable space probe will probably be the most adaptable one, that is, a device that can recognize new situations and alter its actions accordingly. For although life will probably be uncovered elsewhere in space and bizarre physical phenomena recorded, the most revolutionary discoveries will be the unexpected ones. No matter how many brainstorm sessions are held on earth and despite our richly prophetic science fiction, there is an infinite reservoir of unknown, unpredictable knowledge to be tapped in outer space.



Only manned vehicles or machines with man-like qualities will be versatile enough to reap the full harvest. It would be a travesty of science to explore the universe with equipment tailored to detect only the expected event and anticipated datum.

## *Chapter 4*

---

### INTEGRATING THE SPACE VEHICLE, EARTH-BASED FACILITIES, AND INSTRUMENTATION

---

---

#### 4-1. Defining the Generalized Interplanetary Exploratory System

Not so many years ago, even as late as World War II, complex vehicles and weapons were assemblies of separately designed components (black boxes) rather than thoughtfully integrated systems. Often the interfaces between components failed to match properly, reducing the overall system performance level. The design and manufacture of the B-58 supersonic bomber during the 1950's typified the upsurge of systems analysis, in which each component is made subservient to system needs. This approach produces highly tuned equipment, but it has disadvantages when applied to scientific spacecraft. The trouble arises when widely separated researchers design different items of scientific equipment for a satellite or space probe. In addition, scientists are generally unaware of the delicate interfaces present in space vehicles. They are inclined to supply instruments and experiments that are not precisely adjusted to the system as a whole.

With the advent of the streetcar-satellite concept, typified by the Orbiting Geophysical Observatory (OGO) series, the pendulum has started to swing back ever so slightly toward reasonably tolerant spacecraft frames in which interface matching are not so critical. By supplying standardized mounting racks and busbars, satellites like OGO make it easy for experiment designers. At the same time, however, overall system performance is reduced. A satellite of a given weight, for example, could return more useful data if its components were better integrated

and each experiment designed with the others in mind. The pendulum will not swing back very far in the case of space probes, where weight is far more important than it is on satellites. Probe experimenters must provide more systems-oriented engineering than they would for an equivalent satellite experiment. The tradeoffs are sharper and interfaces more sensitive.

A space-probe system is more than just a vehicle. It includes all Earth-based facilities and the rocket booster as well. Furthermore, the vehicle is subdivided into several subsystems, such as the power supply, the communications equipment, and so forth. The interfaces between the components or subsystems are characterized by spatial, mechanical, electrical, thermal, and radiative links. Fortunately, not all interfaces are sensitive. Every system with  $n$  subsystems will have  $n(n-1)/2$  interfaces, with proper matching of many critical to good performance.

A generalized interplanetary probe may be defined in terms of its subsystems and their interfaces as it is in Fig. 4-1. The figure might represent a Mariner, Voyager, or IMP. The type of interface and its general importance to space probes are discussed in the blocks of the figure. Even

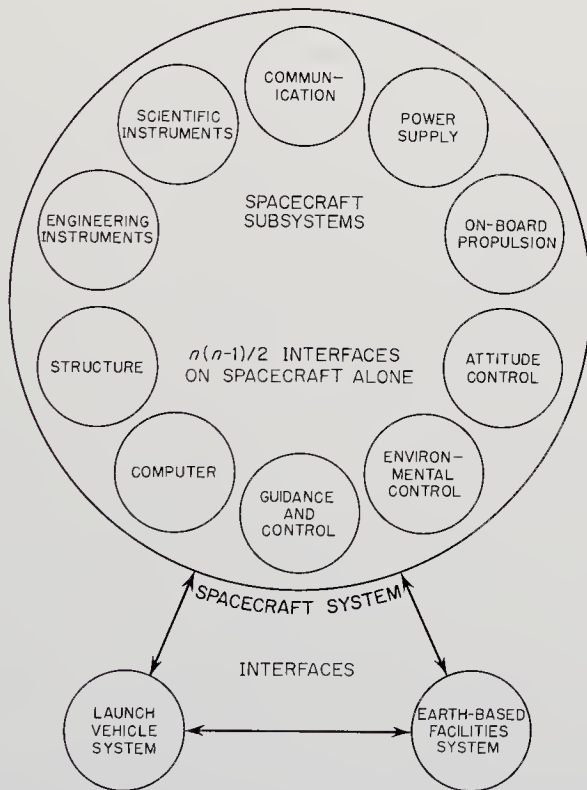


Fig. 4-1. Interface diagram for the spacecraft, Earth-based facilities, and the launch vehicle. Individual subsystems are shown only for the spacecraft.

in the generalized model there are 45 interfaces, a number which must be multiplied by perhaps an order of magnitude when the wide variety of experiments and the various types of interfaces are considered. A space probe integrator must keep a careful eye on each interface and maximize the return relative to the investment, or, in other words, optimize system performance.

#### 4-2. Measures of System Performance

In systems analysis, it is desirable to have a single figure of merit that integrates all performance factors into a single number, like a cost-effectiveness parameter. This tack is difficult in the case of space probes because no one can really put a value on the scientific information which is the real product of the operation. Furthermore, the probe might uncover unexpected physical phenomena that negate any prior assessment of an experiment's value. Data from space experiments also tend to be highly redundant so that a figure of merit like *bits of data received per dollar invested* is not particularly significant. Space probes are more of a gamble than an ICBM. The data that are returned may not be at all commensurate with the investment.

There are several important performance factors that cut across the system interfaces and have important meaning in performance analysis. Vehicle weight, system reliability, and system cost are the most important of these. During the preliminary planning of a probe mission, targets are set for each of these three factors with an eye toward maximizing the scientific value of the mission. Since scientific value cannot be quantified, the establishment of reliability budgets, weight targets, and cost limitations becomes highly subjective and in the end the designer depends upon experience and intuition. Cost limitations may be dictated by political considerations, though fortunately these do not loom large in the design of space probes.

The space probe systems analyst breaks his system down into physi-

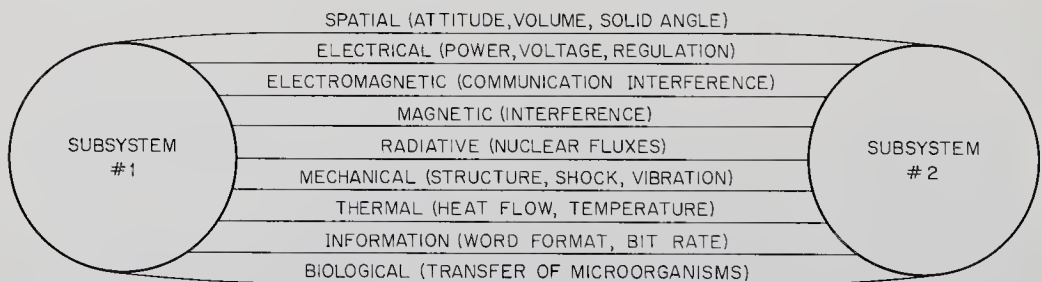


Fig. 4-2. Nine different kinds of interfaces may connect any two subsystems or systems. The importance of each kind of interface depends upon the subsystems involved.

cally meaningful parameters and varies them to achieve or, if possible, surpass the targets that have been set for weight, reliability, cost, or other secondary figure of merit. If it turns out to be easy to surpass a specific performance objective, the target may be raised, or there may be a tradeoff that improves one of the other secondary figures of merit; for they cannot be mutually independent.

Any spacecraft optimization focuses attention on the many interfaces present in a spacecraft system. Each of the  $n(n-1)/2$  interfaces will

TABLE 4-1. DEFINITION OF THE GENERALIZED SPACE-PROBE SYSTEM

<i>Systems and Subsystems</i>	<i>Functions</i>
Spacecraft system	Carry instruments to planetary targets and relay information back to Earth.
Communications subsystem	Relay information (data and commands) between Earth and spacecraft, and between spacecraft and landing capsules, etc.
Power-supply subsystem	Provide electrical power to spacecraft.
On-board propulsion subsystem	Execute mid-course and terminal maneuvers.
Attitude-control subsystem	Stabilize spacecraft attitude and modify attitude upon command.
Environmental-control subsystem	Maintain specified temperatures, radiation levels, etc.
Guidance-and-control subsystem	Receive commands from memory or from Earth and relay them to appropriate subsystems. Establish status of spacecraft (including spatial coordinates), transmit critical data to Earth, and act to reduce deviations from desired performance.
Computer subsystem	Carry out mathematical computations and store information.
Structure subsystem	Support and maintain spacecraft configuration under design loads.
Engineering-instrument subsystem	Measure status of spacecraft.
Scientific-instrument subsystem	Measure scientific phenomena.
Launch-vehicle system	Launch spacecraft from Earth's surface and place it into desired trajectory.
Earth-based facility system	Provide all necessary services for launch vehicle and spacecraft; viz., testing, tracking, communication, data reduction, computation, decision making, etc.

consist of several interlocking parameters which tie the system together physically and mathematically. A thermal interface will involve parameters like temperature and rate of heat flow. An electrical interface is bridged by voltage and current parameters (see Fig. 4-2). Finally, as already pointed out, all subsystems are tied together at a still higher level by weight, cost, and reliability. Thus, each parameter helps to bind the system into a well-performing whole. Each experiment, each component, and their interfaces must be carefully scrutinized to insure not only that the experiment or component will work when immersed in the system but that the over-all system performance is not degraded by poor design or unmatched interfaces.

Interfaces can be split into two categories. The first group deals only with the proper functioning of the spacecraft itself; that is, the attainment of the target trajectory, proper orientation in space, adequate power production, and so on. As Fig. 4-1 indicates, some of these interfaces are quite sensitive and must be handled with care. Part II of this book is devoted to this phase of space probe engineering. Part III concerns itself with the second group of interfaces, those between the scientific instruments and the rest of the space-probe system. Every experiment must be designed so that it doesn't harm other experiments.

The age of the black box has passed. On a space probe on which where every pound destined for Mars may cost \$100,000 and where every hour of reliable operation is wrung from perverse equipment by painstaking development, there is no room for unmatched interfaces.

*Part II*

MISSIONS, SPACECRAFT, AND TECHNIQUES

---

---





# Chapter 5

---

## INTERPLANETARY TRANSPORTATION AND SPACE MECHANICS

---

---

### 5-1. Prologue

The most obvious and fundamental property of a space-probe system is its ability to transport scientific instruments accurately from the surface of the Earth to an astronomical target—planet, asteroid, comet, or just deep space—where measurements may be made. Whether in free flight through space or impelled by a reaction engine, the spacecraft's motion is described by physical laws that dictate the duration and cost of the mission and influence the size and shape of the spacecraft. A short but sharply focused review of space mechanics is in order before spacecraft design is discussed.

This review concentrates upon such critical facets of space mechanics as launch windows and the tradeoffs between propulsive requirements, mission duration, and spacecraft payload. The considerations listed in Table 5-1 point out the strong influence that space mechanics has upon the character and magnitude of space probe interfaces.

The discipline of space mechanics (also called space dynamics) includes astrodynamics. Astrodynamics is narrower in scope and does not encompass rocket launch-vehicle dynamics or space-vehicle attitude control. Several good textbooks and collections of papers are available for detailed study of these technical provinces (Refs. 5-1, 5-15, 5-38, and 5-42).

Chapter 2 claimed astrodynamics to be a fusion of classical celestial mechanics and astronautics. A striking feature of astrodynamics and space mechanics today is the slow emergence of elegant, mathematical generalizations so typical of the older celestial mechanics. The advent of the high-speed digital computer diverted the attention of the theorists

TABLE 5-1. INTERFACE IMPLICATIONS FOR SPACE MECHANICS

<i>Systems and Subsystems</i>	<i>Implications for Space Mechanics</i>
Spacecraft System:	
Communication subsystem	Spacecraft distance to Earth must be held to reasonable values. Should not transit Sun.
Power-supply subsystem	No Sun shadowing. Spacecraft must be kept at reasonable distance from Sun.
Propulsion subsystem	Minimize midcourse and terminal maneuvers.
Attitude-control subsystem	Avoid frequent reorientation of spacecraft units.
Environmental-control subsystem	Keep spacecraft at a reasonable distance from the Sun. Avoid planet shadows and other low-temperature regions.
Guidance-and-control subsystem	Maneuvers should be simple and few.
Computer subsystem	Minimize on-board computations.
Structure subsystem	Avoid high accelerations during launch and reentry.
Engineering-instrument subsystem	None.
Scientific-instrument subsystem	Pass close enough to and on the proper side of the target to enable instruments to function properly; viz., the sunlit side is usually preferred.
Launch-vehicle System:	Reduce energy requirements to keep booster size and cost low.
Ground-support System:	Trajectory must pass over established stations during launch and operational phases.

from broad generalizations to the intricacies of computer programming. Practical problems in space mechanics are most often solved by the repeated application of simple physical laws (like Newton's Law of Motion) in differential form and their subsequent integration by machine over the spacecraft trajectory. More general laws in integral form are now being constructed, so that perhaps a decade from now there will be powerful generalizations in space dynamics equivalent to Kepler's Laws. During this gestation of analytical techniques, however, differential, machine-aided techniques (such as dynamic programming) dominate the scene.

The step-wise integration of simple force equations over a trajectory by a machine, which also keeps track of the precise positions and effects of all perturbing celestial bodies in its memory, cannot be easily described in terms of readily assimilated mathematical and graphical

models. Consequently, this chapter will rely on a few readily comprehended space-mechanical models, particularly those of Vertregt (Ref. 5-42). It will conclude with the now-common time-date-energy maps of propulsive requirements that are the children of the less general but more precise differential techniques that are easily programmed on machines.

## 5-2. Description of Interplanetary Exploratory Missions

The basic problem of space exploration can be facetiously described as that of getting from one place to another despite, or with the help of, inverse-square-law gravitational fields. The only known mechanism for producing the necessary thrusts in outer space is the reaction engine. Perhaps it is deceptively simple to say that there are really only two elementary equations in space dynamics:

$$F = \frac{GmM}{r^2} \qquad F = \frac{d(mv)}{dt}$$

where:  $F$  = force (newtons)

$m$  = spacecraft mass (kg)

$M$  = mass of the gravitating body (kg)

$r$  = distance from spacecraft to center of body (m)

$v$  = spacecraft velocity (m/sec)

$t$  = time (sec)

$G$  = the universal gravitational constant.

The force on the right, controllable by man, is used to offset and overcome the force on the left, which is produced by nature. But outer space is full of gravitating bodies moving along complex paths at high speeds, and the production of reaction forces is costly in terms of human resources. The superficial simplicity of the equations yields in practice to complicated tradeoffs and performance optimization.

To appreciate the actual complexity of space-probe trajectory design, consider the following mutually conflicting ground rules that are applied to space-probe trajectory calculations:

1. Payload should be maximized.
2. Cost should be minimized.
3. The spacecraft must be kept within range of the communication system.
4. Mission duration should be minimized because of the finite lifetimes of the subsystems.
5. Meteoroid swarms, radiation belts, and solar flares should be avoided.
6. The Sun must not be crossed because of its interference with the communication system.

7. The probability of planetary biological contamination by the spacecraft should be small ( $< 10^{-4}$ ).
8. The trajectory should be accurate enough so that designing instrumentation with large dynamic ranges will be unnecessary.
9. U.S. launchings are restricted to the Eastern and Western Test Ranges. Only certain launch azimuths are permitted if land masses are to be avoided.

There are also limiting physical laws that will act as constraints upon the more advanced missions of the future. For example, spacecraft cannot equal or exceed the velocity of light. The energy content of fuel is limited by  $E = mc^2$ . Of course, neither of these limits is approached at present.

TABLE 5-2. SPACE-PROBE MISSIONS

<i>Mission Type</i>	<i>Required Propulsive Functions*</i>	<i>Extant Programs</i>
Planetary Missions:		
Simple flyby	BXM, BOXM	Mariner
Crocco or resonance flyby	BXM, BOXM	
Planetary orbital injection	BXMO, BOXM	
Hard or soft landing	BXXM(R or P)	Voyager
Sample return	BXXMRBXXMR **	
Solar Missions:		
Flyby at 0.1 to 0.3 A. U.	BXMO	
Impact	BXM	
Out-of-Elliptic Missions	BXMO	
Asteroidal Missions:		
Fly-through belt	BXM	
Rendezvous with asteroid	BXXMZ	
Sample return	BXXMZXXMR	
Cometary Missions (same as for asteroids)		
Interplanetary Space Missions:		
Solar orbit	BXO	Pioneer
Eccentric Earth orbit	BO	IMP
Interstellar Missions	BX	

- \* B = boost from Earth's surface
- X = escape or capture maneuver
- M = midcourse correction
- O = orbital injection
- R = reentry or entry
- P = powered descent
- Z = rendezvous

\*\* Note the complexity of a sample-return mission

Space-probe missions can be defined by exclusion: they comprise all space missions excluding Earth-satellite and manned missions. Even though the bulk of the national space program is discarded by such a definition, a great variety of stimulating scientific missions remains. Restricting the field further, this book does not deal with lunar probes.

The number and variety of the missions listed in Table 5-2 make it obvious that space-probe design will be difficult to generalize. The scientific payoff of any one of the missions, however, is likely to be worth considerable effort.

### 5-3. Review of Some Techniques of Space Mechanics

In the early days of astronautics, crude trajectory *feasibility* studies were the rule. Even today (and probably tomorrow too), new space missions are planned or "scoped," using simplified techniques based upon coplanar, circular planetary orbits, and instantaneous applications of thrust at various points along the trajectory. In such calculations, the spacecraft is first boosted into an Earth-satellite orbit or an escape trajectory. Then, an instantaneous impulse is applied and the craft is

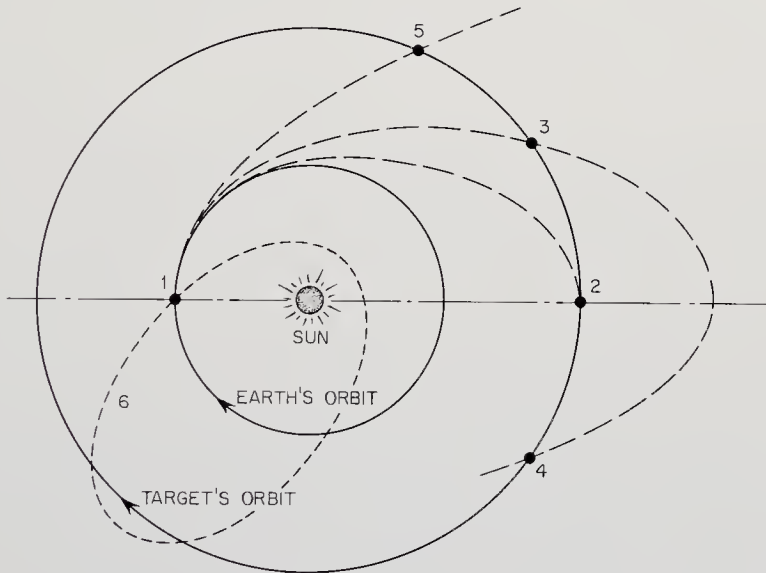


Fig. 5-1. Various types of interplanetary ballistic trajectories. (1) Impulse applied to leave Earth orbit. (2) Impulse applied to leave Hohmann cotangential transfer orbit and enter orbit of target planet. (3) Impulse to terminate short-path elliptical transfer orbit. (4) Impulse to terminate long-path elliptical transfer orbit. (5) Impulse to terminate fast hyperbolic transfer orbit. (6) Crocco or resonance orbit with a period such that the spacecraft meets the Earth after an integral number of revolutions. Planet flybys do not require impulses at (2), (3), or (4).

injected into a ballistic, elliptical orbit around the Sun (Fig. 5-1). This impulse also signals the change from geocentric to heliocentric coordinates. It is typical of feasibility studies that the gravitational effects of the Sun are ignored during the boost phase and those of the Earth neglected during the vehicle's swing around the Sun to the target planet. When the target planet is approached, another impulse is applied and the spacecraft is captured. Either injection into satellite orbit or landing maneuvers follow. The first planetary probes, like the Mariners, do not execute the capture maneuver, but rather *fly by* the planet of interest. Feasibility calculations are simple, depending only on Newton's Law of Gravitation and the properties of the conic sections (Ref. 5-42). Because such calculations can be put into appealing graphical form, they form the foundation of the space mechanics discussions in Sect. 5-4.

The simplifying assumptions of feasibility calculations make them unsuitable for computing precision trajectories for actual probe flights. The orbits of the planets *are* elliptical and *not* coplanar. The gravitational effects of the Sun and other bodies must be accounted for. So must drag forces, the pressure of sunlight, and other perturbations. Finally, precision techniques have to be readily adaptable to digital computers. Under such conditions, the differential approach portrayed in Fig. 5-2 is

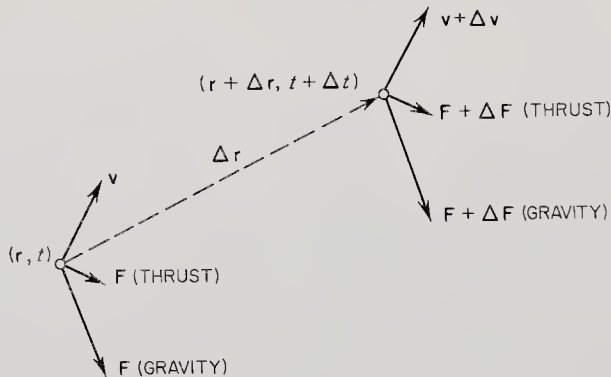


Fig. 5-2. Differential approach to trajectory calculations. Integration of the trajectory is usually performed on a digital computer. Note:  $\mathbf{r} + \Delta\mathbf{r} = \mathbf{r}(t + \Delta t) = \mathbf{r}(t) + \dot{\mathbf{r}}(t)\Delta t + \dots$  and  $\mathbf{v} + \Delta\mathbf{v} = \mathbf{v}(t + \Delta t) = \mathbf{v}(t) + \dot{\mathbf{v}}(t)\Delta t + \dots$ .

appropriate. With ephemerides stored in the computer, all applied forces acting on the spacecraft can be estimated and its acceleration can be computed over a short span of time  $\Delta t$ . Referring to Fig. 5-2, the spacecraft position at the time  $t + \Delta t$  will be  $\mathbf{r} + \Delta\mathbf{r}$ , and the new velocity  $\mathbf{v} + \Delta\mathbf{v}$ . At  $t + \Delta t$ , the applied forces will be slightly different and new positional and velocity vectors must be calculated for  $t + 2\Delta t$ . In this stepwise fashion the whole vehicle trajectory can be computed.

The geometrically appealing but approximate feasibility techniques and the precise though formless differential approaches provide some general rules for the trajectory designer:

1. Impulsive thrusts near planets should be delivered quickly (theoretically in zero time) so that their effect will not be compromised by the negative term due to gravitational acceleration in the classical rocket equation:

$$\Delta v = g_0 I_{sp} \ln \frac{m_0}{m_f} - v_D - g_0 t \sin \theta \quad (5-1)$$

where:

- $\Delta v$  = velocity increment (m/sec)
- $g_0$  = acceleration due to gravity (m/sec<sup>2</sup>)
- $I_{sp}$  = propulsion system specific impulse (sec)
- $m_0, m_f$  = initial and final spacecraft masses (kg)
- $v_D$  = drag velocity penalty (m/sec)
- $\theta$  = angle with horizontal.

2. In general, impulsive thrusts should be applied close to the launching planet so that propellant will not have to be carried needlessly to high levels of gravitational potential energy.

3. The different periods of the planets lead to launch windows—short periods of time in which interplanetary transfer is particularly easy in terms of energy.

4. Lack of precision in the Earth-launch operation make midcourse trajectory correction essential if a specific celestial target is to be intercepted. Such considerations do not apply to solar probes, vehicles flying through the asteroid belt, or those just sent into deep space for scientific monitoring purposes.

*Low-Thrust Propulsion.* So far, only ballistic trajectories in which the space vehicle travels without thrust along a conic section have been mentioned. Before considering the intricacies of ballistic space travel, let us examine the simpler case of continuous thrust. Advanced probe propulsion systems, like the ion and plasma engines contemplated for trips beyond Mars will provide small propulsive thrusts over long periods of time. Continuously applied forces in effect modify the inverse-square-law force applied by gravity. Thus, the trajectories of electrically propelled ships will not be conic sections. A special segment of astrodynamics has been built up around these low-thrust space vehicles (Refs. 5-24, 5-27, and 5-32).

The mathematical formulation for low-thrust trajectories is straightforward and must, of course, reduce to the proper conic section when the applied force is reduced to zero. For an interplanetary spacecraft escap-

ing a planet, the planar differential equations in polar coordinates are:

$$\frac{d^2r}{dt^2} - \frac{v_c^2}{r} + \frac{GM}{r^2} = a_f \cos \phi \quad (5-2)$$

$$\frac{1}{r} \frac{d(rv_c)}{dt} = a_f \sin \phi \quad (5-3)$$

where:  $v_c$  = the circumferential velocity (m/sec)

$a_f$  = accelerating force applied by engine (newtons)

$\phi$  = angle between thrust vector and local vertical.

Equation (5-2) balances thrust, gravitational force, centrifugal force, and radial acceleration. If  $a_f = 0$ , Eq. (5-2) will yield a conic section. Equation (5-3) relates the circumferential component of applied thrust to the rate of change of angular momentum. The latter quantity is conserved in conic sections.

It is customary to introduce four dimensionless parameters at this point:

$$\begin{aligned} a_f &= \alpha \left( \frac{GM}{r_0^2} \right) & v_c &= v \sqrt{\frac{GM}{r_0}} \\ \rho &= \frac{r}{r_0} & t &= (\tau - \tau_0) \sqrt{\frac{r_0^3}{GM}} \end{aligned} \quad (5-4)$$

The parameter  $\alpha$  is the ratio of the applied thrust to the initial gravitational force. For electrical propulsion systems,  $10^{-2} > \alpha > 10^{-5}$ . In terms of the dimensionless parameters, the equations of motion become particularly simple:

$$\frac{d^2\rho}{d\tau^2} - \frac{v^2}{\rho} + \frac{1}{\rho^2} = \alpha \cos \phi \quad (5-5)$$

$$\frac{1}{\rho} \frac{d(\rho v)}{d\tau} = \alpha \sin \phi \quad (5-6)$$

In applying Eqs. (5-5) and (5-6) to low-thrust planetary probes, departure usually begins from a circular Earth orbit where  $\rho_0 = 1$ ,  $\dot{\rho}_0 = 0$ , and  $v_0 = 1$ . Energy is added until the spacecraft's energy equals or exceeds zero. By definition, planetary escape occurs when the sum of an object's kinetic and potential energies equals zero. A zero-energy trajectory is parabolic, while a hyperbolic path possesses positive total energy. When escape takes place, the vehicle coordinates are shifted to a heliocentric set. Escape has occurred only relative to the planet of origin, not the solar system as a whole.

The shape of the escape trajectory will depend upon the angle  $\phi$ . Under radial acceleration, where  $\phi = 0$  and  $\rho v = \text{constant}$ , Eq. (5-5) becomes:



$$\ddot{\rho} - \frac{\rho_0^2 \nu_0^2}{\rho^3} + \frac{1}{\rho^2} = \alpha \quad (5-7)$$

Integration of Eq. (5-7) shows that escape can occur with constant radial thrust only when  $\alpha > 1/8$ . In circumferential acceleration,  $\phi = \pi/2$  and  $\alpha = \text{constant}$ . In tangential acceleration  $\phi = \tan^{-1} \nu/\rho$ .

In all cases of constant application of low thrust, the space vehicle spirals out to planetary escape from the initial circular orbit. Once the field of the Sun becomes dominant, the vehicle spirals heliocentrically inward or outward to its destination. The equations of motion are then put in heliocentric terms, otherwise the calculations are similar to those made for the planetary case.

Studies have shown that the most efficient thrust programs vary both the magnitude and orientation of the thrust vector. In general, however, the most efficient thrust program lies between tangential and circumferential conditions. Low-thrust propulsion always requires more total energy than an equivalent ballistic program because the engine is continuously fighting against gravity. By applying low thrusts only when passing through perigee, the energy requirements can be reduced to nearly those of the ideal instantaneous impulse. Instead of the usual spiral orbit, this approach produces a series of ever-larger ellipses. A pulsed-thrust program also permits escape with radial thrust even when  $\alpha < 1/8$ .

The great advantage of low-thrust propulsion comes from the higher specific impulses of electrical engines (5000-10,000 sec, compared to 200-400 sec for chemical rockets). Higher payload-to-gross-weight ratios are possible. However, the problem of building electrical power plants that can operate reliably for several years seems a major obstacle.

*Propulsion-System Comparison Techniques.* Chemical propulsion seems likely to reign supreme for boosters and spacecraft until well after 1970. Nuclear heat transfer rockets and electrical propulsion systems (ion and plasma engines) are under intensive development, but their operational use must await major advances in nuclear powerplant engineering. Keeping this time scale in the back of the mind, a common astrodynamics exercise compares the overall performance of such advanced engines with the ubiquitous chemical rocket. Here, the role of space mechanics is twofold. First, the characteristic velocity or energy requirement for flight from the Earth to the target must be specified. Second, mass ratios are computed using relationships like Eq. (5-1). No specific comparisons of systems will be made in this book. In general, such comparisons show large payload advantages for nuclear and electrical propulsion only when very ambitious missions are considered. The real challenge in comparing propulsion systems transcends space mechanics and mass ratios, since it in-

volves estimation of cost, reliability, and nuclear safety. Many of these factors are still judged on an intuitive basis.

*Optimization Techniques.* Hand in hand with propulsion system comparison comes trajectory optimization. Special techniques are employed to find the best trajectory compatible with the system constraints listed in Table 5-1. The following questions are typical of those answered with the help of space mechanics optimization techniques (Refs. 5-24, 5-27, and 5-33).

1. What is the optimum staging for a given rocket?
2. What is the optimum thrust program for a low-thrust space vehicle?
3. What is the maximum payload-to-gross-weight ratio for a power-limited vehicle; i.e., an electrically propelled spacecraft?

In solving astrodynamic optimization or extremal problems, three techniques find favor today (Ref. 5-27):

1. The calculus of variations (Ref. 5-33)
2. The direct method of gradients (a numerical technique used in the calculus of variations)
3. Dynamic programming (Ref. 5-2)

All three methods are adaptable to digital computers, a property most appropriate to current trajectory analysis techniques.

*The Problem of Trajectory Accuracy.* A space probe may miss its target because of five kinds of "inaccuracies":

1. Ignorance concerning the true distances and masses of objects in the solar system in absolute terms; i.e., kilograms and meters
2. Approximations made in trajectory calculations
3. Lack of precision performance by probe-system hardware. Trajectory dispersion may arise from booster deviations, guidance-equipment errors, deviations in midcourse propulsion system functioning, and so on.
4. Uncertainty in the initial conditions
5. Post-injection perturbations (solar wind, etc.)

The effects of each assumed error can be found mathematically in terms of trajectory dispersion or the target miss distance (Ref. 5-1). Present-day errors in all categories are large enough to make midcourse corrections mandatory for space probes. Otherwise, planetary targets might be missed by many radii. This guidance problem will be covered more thoroughly later. The role of space mechanics here is the identification of the ultimate consequences in terms of trajectory dispersion.

*Relativistic Space Mechanics.* Einstein's Special Theory of Relativity affects space probes in three ways:

1. If the engine's propellant leaves the spacecraft at a velocity close to that of light, the specific impulse will be modified by the relativistic increase in propellant mass (Ref. 5-20).
2. If the vehicle itself is traveling close to the speed of light relative to some external reference frame, time dilation will be apparent to an observer in the reference frame.
3. Immense quantities of energy are needed to accelerate a spaceship close to the velocity of light. Using nuclear fuel and reasonable mass ratios (about 1000), it is impossible to reach 20% of the velocity of light (Ref. 5-16).

Such relativistic effects are not likely to be important to probe technology over the next twenty years, probably much longer. Interstellar probes, when they become practical, will have to travel close to the speed of light if data are to be acquired during the life of the experimenter.

*The Use of Gravity and Asteroids.* Opportunities exist for "free" rides within the solar system. Perhaps the most daring of the suggestions is that of Cole (Ref. 5-12). He suggests propulsively diverting a small asteroid so that its orbit approaches Mars closely enough so that the gravitational perturbation of Mars will cause the asteroid to make a close approach to Earth. Many have also suggested just hitchhiking a ride around the solar system on an asteroid without deflecting its orbit. While such free rides are possible in theory, and though a small, permanent asteroidal instrument platform would have many advantages, the realization of the idea is several decades away.

Several scientists have recommended using celestial bodies for gravitationally changing the velocity vector of a spacecraft in order to save fuel (Refs. 5-18 and 5-40). In a sense, this effect is already used on planetary missions, since the spacecraft velocity is increased after it enters a planet's sphere of influence. If a resonance or Crocco trajectory passing close to two planets in one solar orbit is planned, planetary fields are useful in shaping the trajectory. When the fringes of the solar system are explored in the distant future, the gravitational fields of the major planets may be very helpful. To illustrate, astronomers postulate that Pluto was ejected from the satellite system of Neptune by interplanetary perturbations. A spacecraft could be flung outward in like fashion.

#### 5-4. Propulsive Functions

Although some energy advantages may be gained by gravitational interactions with the planets, the great bulk of a space vehicle's energy

must be produced by a rocket engine. The propelling of a payload from the surface of the Earth to the surface of Mars might be done with one or two well-aimed impulses. In actuality, an interplanetary mission is usually broken down into several basic propulsive functions (Table 5-2, page 46):

1. Boost to orbit or escape from the originating planet.
2. Orbit-to-orbit transfer between planets.
3. Midcourse and terminal maneuvers for purposes of accuracy.
4. Reentry propulsion.
5. Powered descent to a planetary surface.
6. Rendezvous propulsion

The Earth-orbit-to-planetary-orbit trip is critical in mission planning for it requires a great deal of energy and takes the most time. Rendezvous maneuvers occur only when homing on an asteroid or comet nucleus. The six functions will be discussed in the above order.

*Boost to Orbit or Escape.* The first task of any launch vehicle is propelling the vehicle out of the gravitational well created by the Earth's gravitational field. The depth of this potential well is  $-GmM/r$ . In the case of the Earth, this corresponds to  $6.25 \times 10^7$  joules/kg of payload, which translates to an escape velocity of 11.2 km/sec. A rocket ascent trajectory is more complex than this simple concept suggests. Complicating factors include the drag forces of the atmosphere, the variation of  $g_0$  with altitude, centrifugal forces, the curvature of the Earth, and the need for carrying propellant to high levels of potential energy because

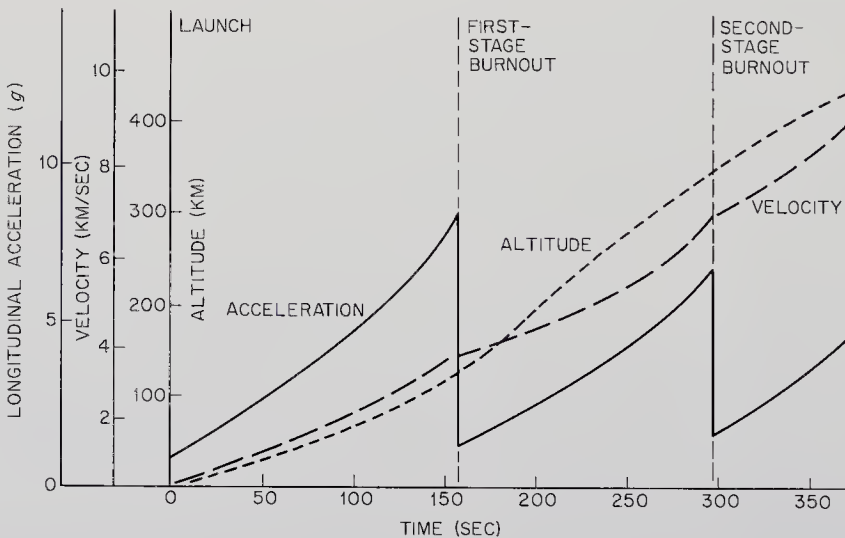


Fig. 5-3. Major launch-vehicle trajectory parameters as functions of time after launch.

of the finite burning time of the rocket. Considering only drag, propellant acceleration, and gravitational losses, the approximate velocity change acquired by an ascending rocket was given by Eq. (5-1).

Most launch vehicles have several stages. Equation (5-1) must be applied separately for each stage, accumulating the velocity additions as the rocket rises. The usual stepwise ascent is shown in Fig. 5-3, especially in the acceleration parameter.

The major consequences of propelling the space vehicle out of any potential-energy well is the price paid in terms of the mass ratio: the quotient of the launch-vehicle mass and the final payload mass. That this ratio is high even for Earth-satellite launching is obvious in Fig. 5-4. Other space missions have been marked on Fig. 5-4 to show the exponential relationship between velocity additions and mass ratio. Every kilogram of probe payload saved has great leverage on the booster mass. The advantages of staging, where portions of the launch vehicle that are no longer needed are discarded, are also clearcut from Fig. 5-4.

The ascent trajectory may include the injection of the space vehicle

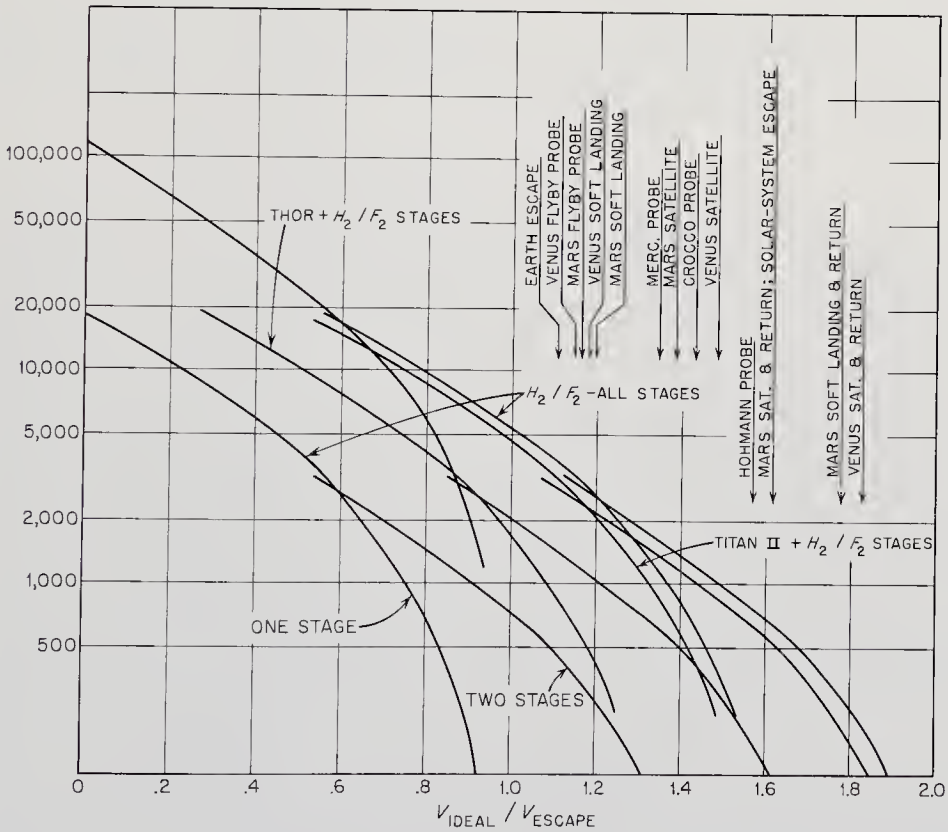


Fig. 5-4. Rocket mass ratio plotted for different mission velocity requirements. Note the powerful influence of specific impulse and staging.

into an Earth-satellite orbit or carry it directly into an interplanetary trajectory with the last thrust application. Since a 500-km Earth orbit is well up toward the top of the Earth's potential energy well, little additional velocity is needed for escape.

A continuous range of mass ratios is implied by Fig. 5-4, while in actuality the United States possesses a "stable" of launch vehicles with well-defined thrust levels. This limited number of boosters and combinations of upper stages means that only certain curves in Fig. 5-4 have practical significance.

*Orbit-to-Orbit Transfers.* Once a space probe is in a parking orbit around the Earth or coasting parabolically at high altitudes, one final impulse must be applied to send the vehicle off on a ballistic trajectory that will intersect the orbit of the selected astronomical target. The classical way to effect this transfer from the Earth's orbit to the target planet's orbit is by the Hohmann transfer ellipse. All ballistic trajectories are conic sections, but the Hohmann ellipse has the special property of requiring the least energy for a two-impulse transfer between planetary orbits. The Hohmann ellipse is cotangential to both planetary orbits as shown in Fig. 5-1. Contrary to popular belief, it has been shown that other trajectories requiring less energy than the Hohmann ellipse exist if more than two impulses are permitted (Ref. 5-14).

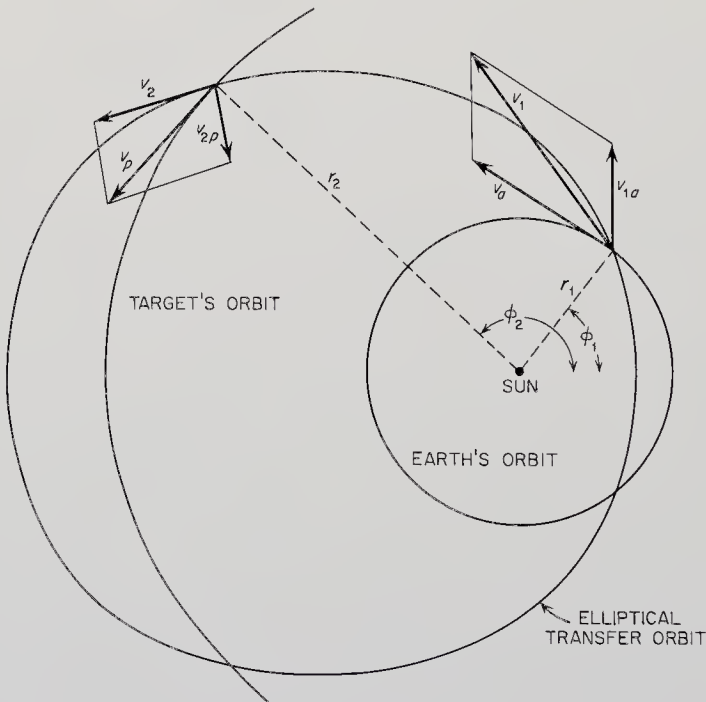


Fig. 5-5. Definition of velocities for a trip to an outer planet. (After Vertregt, Ref. 5-42.)

Accurate, three-dimensional trajectory calculations must always be made by a computer before any probe launching, but with a few simplifying assumptions a particularly appealing geometrical picture of interplanetary trajectories can be drawn.

Assume that:

1. Thrusting times are short compared to the length of the interplanetary transfer.
2. Only the Sun's attraction is important during the coasting phase between satellite orbits about the terminal planets.
3. Planetary orbits are circular and coplanar.

Following Vertregt's approach (Ref. 5-42), two new quantities are defined in terms of conic-section parameters (Fig. 5-5):

$$\frac{r_2}{r_1} = n \qquad \frac{a(1 - e^2)}{r_1} = p$$

- where
- $r_2$  = the radius from the Sun to the planet or spacecraft (km)
  - $r_1$  = the radius from the Sun to the Earth (km)
  - $n$  = the radial distance expressed in A. U. (dimensionless)
  - $a$  = the major semi-axis of the transfer ellipse (km)
  - $e$  = the eccentricity of the ellipse, which is the ratio of the minor and major axes
  - $p$  = a dimensionless parameter.

All possible two-impulse interplanetary ballistic trajectories may be represented as points on a graph of  $e$  vs.  $p$ . On Fig. 5-6, the four different conic sections are confined to mutually exclusive areas on the  $e$ - $p$  graph. The hyperbolas all have  $e > 1$  and they are unbounded on the graph. The line  $e = 1$  represents parabolic trajectories. The ellipses are confined to the triangular area; here, of course,  $e < 1$ . A little juggling of conic section parameters will confirm the equations given for the sides of the triangles. Circular orbits, where  $e = 0$ , are impossible for orbital transfer. The transfer ellipse with the least eccentricity is the cotangential Hohmann ellipse represented by the lower vertex of the triangle.

Carrying this geometric portrayal a step further, simple equations for the transit times and energies can be derived. On Fig. 5-5, the following velocities are defined:

$$\left. \begin{aligned} v_a^2 &= \frac{GM}{v_1} & v_b^2 &= \frac{GM}{v_2} \\ v_1^2 &= GM \left( \frac{2}{r_1} - \frac{1}{a} \right) & v_p^2 &= GM \left( \frac{2}{r_2} - \frac{1}{a} \right) \end{aligned} \right\} (5-8)$$

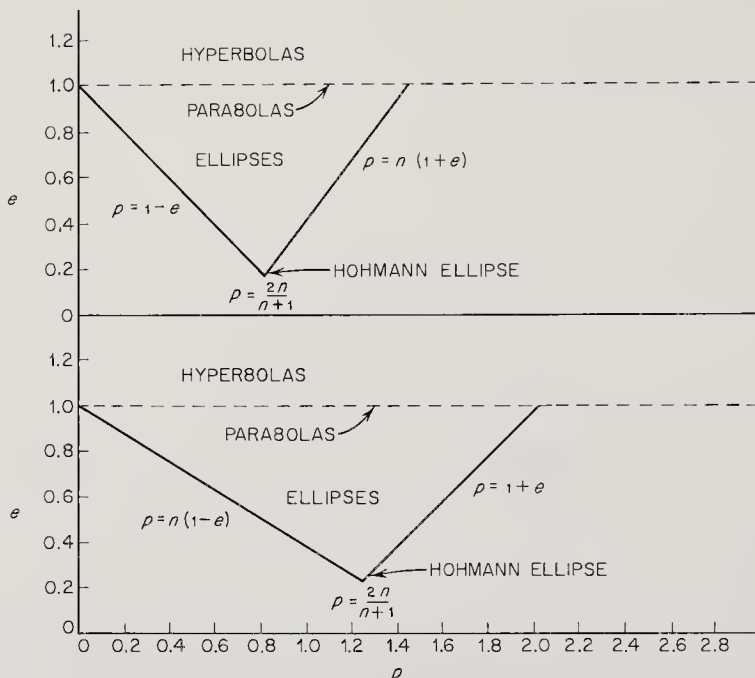


Fig. 5-6. Regions of permissible conic-section transfer orbits for one-way trips to the inner planets (above) and outer planets (below). (After Vertregt, Ref. 5-42.)

- where:  $v_a$  = the orbital velocity of planet  $a$
- $v_b$  = the orbital velocity of planet  $b$
- $v_1$  = the velocity of an object in the transfer ellipse at its intersection with planet  $a$ .
- $v_2$  = the velocity of an object in the transfer ellipse at its intersection with planet  $b$ .

If a new dimensionless quantity  $q = a/r_1$  is introduced:

$$\left. \begin{aligned}
 v_p^2 &= v_a^2/n \\
 v_1^2 &= v_a^2 \cdot \frac{2q - 1}{q} \\
 v_2^2 &= v_a^2 \cdot \frac{2q - n}{qn}
 \end{aligned} \right\} (5-9)$$

In order to change the velocity of the space probe,  $v_a$ , to the velocity needed for entry into the transfer ellipse,  $v_1$ , the cosine law must be used

$$v_{1a}^2 = v_a^2 + v_1^2 - v_a v_1 \cos \left( \theta_1 - \frac{\pi}{2} \right) \tag{5-10}$$



Now the angle  $\theta$  must be found from the equation:

$$\tan \theta = -r \frac{d\phi}{dr}$$

Since  $\phi$  and  $r$  are related by

$$r = \frac{a(1 - e^2)}{1 + e \cos \phi},$$

an equation for  $\theta$  can be found

$$\tan \theta = -\frac{1 + e \cos \phi}{e \sin \phi}.$$

Using trigonometric identities, eliminating  $\phi$ , and substituting into Eq. (5-10)

$$v_{1a}^2 = v_a^2 + v_a^2 \frac{2q - 1}{q} - v_a^2 \cdot 2q \sqrt{\frac{2q - 1}{q}} \sqrt{\frac{1 - e^2}{2q - 1}}$$

which leads to

$$\frac{v_{1a}}{v_a} = \left[ 3 - 2 \sqrt{q(1 - e^2)} - \frac{1}{q} \right]^{1/2}$$

and in terms of  $p$ , recalling that  $p = a(1 - e^2)/r_1 = q(1 - e^2)$

$$\frac{v_{1a}}{v_a} = \left[ 3 - 2 \sqrt{p} - \frac{1 - e^2}{p} \right]^{1/2}$$

In a similar fashion an analogous equation for  $v_{2p}$  can be derived

$$\frac{v_{2p}}{v_a} = \left[ \frac{3 - 2 \sqrt{p/n}}{n} - \frac{1 - e^2}{p} \right]^{1/2}$$

Now the quantity that is of most interest in establishing the difficulty of an interplanetary voyage is the sum  $v_{1a} + v_{2p}$ . The sum is frequently called the characteristic velocity for the mission. Vertregt defines a dimensionless number  $E$  to measure the difficulty of the mission:

$$E = \frac{v_{1a} + v_{2p}}{v_a}$$

which, of course, is just the total velocity increment expressed in units of the Earth's orbital speed around the Sun. The final equation for  $E$  is not particularly simple, though it is only algebraic and is derived using relatively straightforward techniques:

$$E = \left[ 3 - 2 \sqrt{p} - \frac{1 - e^2}{p} \right]^{1/2} + \left[ \frac{3 - 2 \sqrt{p/n}}{n} - \frac{1 - e^2}{p} \right]^{1/2} \quad (5-11)$$

Equation (5-11) is the key to the so-called isoerg diagrams. The equation

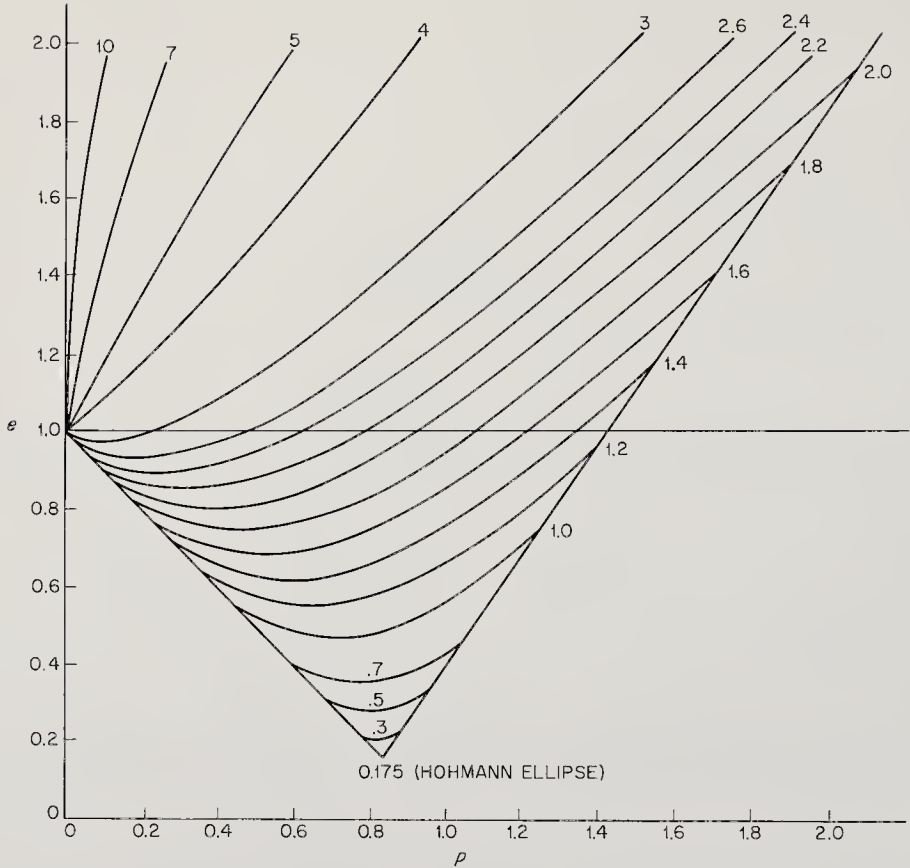


Fig. 5-7. Isoerg diagram for a one-way trip to Venus, using two impulses. "Energy units" that are multiples of the Earth's velocity. Launch to Earth orbit is not included. (Adapted from Vertregt, Ref. 5-42.)

is applicable to inner and outer planets and any of the conic-section trajectories. A typical isoerg diagram from Ref. 5-42 is shown in Fig. 5-7 for the Earth-Venus trajectories. For any given  $E$  and  $e$ , there are two possible elliptical trajectories, each with a different value of  $p$ . Since  $p$  is proportional to the major semi-axis, there should be some additional figure of merit that will separate the two possible ellipses. This figure of merit is time, which is not surprising, since a larger value of  $p$  infers a more lengthy journey.

Vertregt also derives an equation for the duration of the voyage by appealing to the same trigonometric arguments used to find  $E$ . Measuring the duration of the mission in units of the Earth's orbital period,  $T$ , he finds

$$T = \frac{q^{3/2}}{2\pi} [(\tau_1 - \tau_2) - e(\sin \tau_1 - \sin \tau_2)] \quad (5-12)$$

where  $\tau_1 = \cos^{-1} \frac{1 - 1/q}{e}$  and  $\tau_2 = \cos^{-1} \frac{1 - n/q}{e}$ .

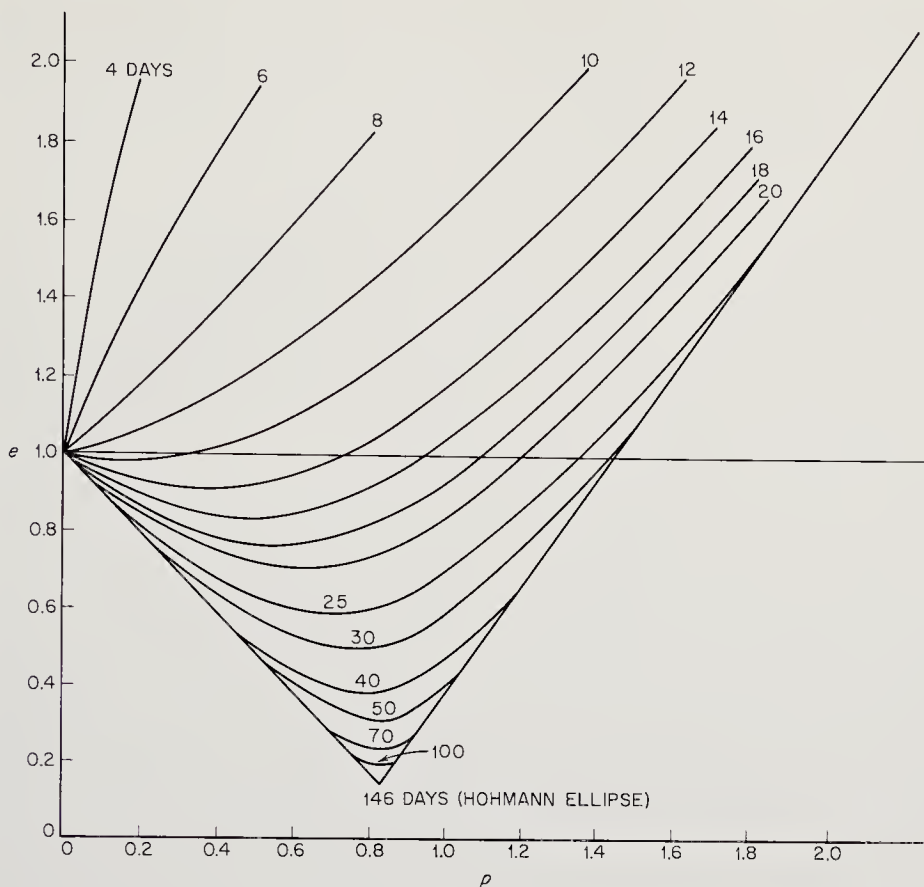


Fig. 5-8. Isochrone diagram for a one-way trip to Venus, using two impulses. Short trips are energetic and hyperbolic. (Adapted from Vertregt, Ref. 5-42.)

The results are plotted on an isochrone (equal time) diagram, Fig. 5-8. The curves are also double-valued for elliptical transfers. The very short trips are hyperbolic in nature, as expected, and a cross reference to Fig. 5-7 shows them to be more energetic also.

The preceding arguments assume that the target planet, asteroid, or comet will be in the right place at the right time; i.e., when the space probe orbit intersects the planet's orbit. Unhappily, the planets are not that cooperative, and low-energy launchings must await firing windows, periods when the two terminal planets are in favorable positions. Although these synchronizations can also be handled with the geometrical techniques just described, it seems appropriate to jump right to the propulsive requirement "maps" presented in Sec. 5-5. Maps such as these (Figs. 5-14 through 5-22, pages 68-74) are the common currency of space technology. They are computer-constructed for elliptical, non-coplanar planetary orbits and are more precise than the simplified curves shown in Figs. 5-7 and 5-8.

*Midcourse Maneuvers.* At one or more points along a spacecraft's trajectory it will be necessary to apply corrective thrusts to assure hitting the desired celestial target. Minor thrust adjustments are made by an onboard propulsion system, which carefully controls the impulse delivered and the direction of the thrust vector.

Chapter 7, which covers vehicle guidance and trajectory correction in more detail, will show how really small the planetary targets are, particularly if narrow flyby or reentry corridors must be hit.

The amounts of fuel and oxidizer needed for a midcourse or terminal maneuver depend upon how much velocity change is needed. Equation 5-1 can be used to determine the mass ratio, but drag and gravitational losses must be subtracted in deep space.

*Reentry.* If the target planet has an atmosphere of adequate density or if a space probe is returning to Earth from a sample-collecting mission, the braking forces of atmospheric reentry may be used to slow the spacecraft's descent to a speed where wings or parachutes may be used. Accuracy requirements are high, but the fuel-mass savings over powered descent by retrorocket are great. The probe reentry corridor portrayed in Fig. 5-9 is much larger than it would be for manned spacecraft, which are less tolerant of reentry deceleration and heating. As the reentering vehicle plunges into a dense atmosphere, deceleration forces and aerodynamic heating narrow the reentry corridor shown in Fig. 5-10.

For trajectory-calculating purposes, the path of the reentering space vehicle is usually broken up into three segments. In the first segment, the spacecraft has penetrated far enough into the atmosphere so that the drag is no longer negligible. In the second regime, the aerodynamic drag

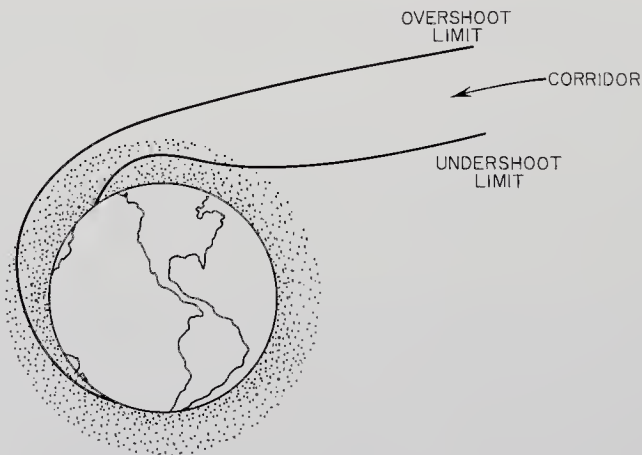


Fig. 5-9. Earth-atmosphere reentry overshoot and undershoot limits. The reentry corridor may be further narrowed by deceleration and aerodynamic-heating limitations.

forces are dominant and gravity may now be ignored. This is the region where deceleration and heating are highest. The differential equation of motion is quite simple in this case:

$$m \frac{dv}{dt} = -C_D A \rho(r) v^2 / 2. \tag{5-13}$$

An atmospheric model must be adopted in order to specify the mass density,  $\rho(r)$ . The model usually takes the form  $\rho = \rho_0 \exp(-Br)$ , where  $r =$  altitude and  $B$  and  $\rho_0$  are constants. When Eq. (5-13) is integrated and plotted, curves like those shown in Fig. 5-10 result. The third, and final, reentry regime occurs when the space vehicle has been slowed to a point when drag forces are comparable to gravitational forces. If the spacecraft can survive to this point, success is usually assured, because thermal forces have subsided and the vehicle begins to cool. Wings and parachutes can take over for the actual landing maneuver.

So far, reentry has been assumed to occur during the first penetration of the atmosphere. It is quite feasible to cause the craft to skip out of the atmosphere after losing some of its velocity and then reenter on the second, third, or some later pass. The extreme case is that of *braking ellipses*, where the vehicle just brushes the atmosphere at each perigee pass. It is slowed step-wise and finally captured after much of its velocity

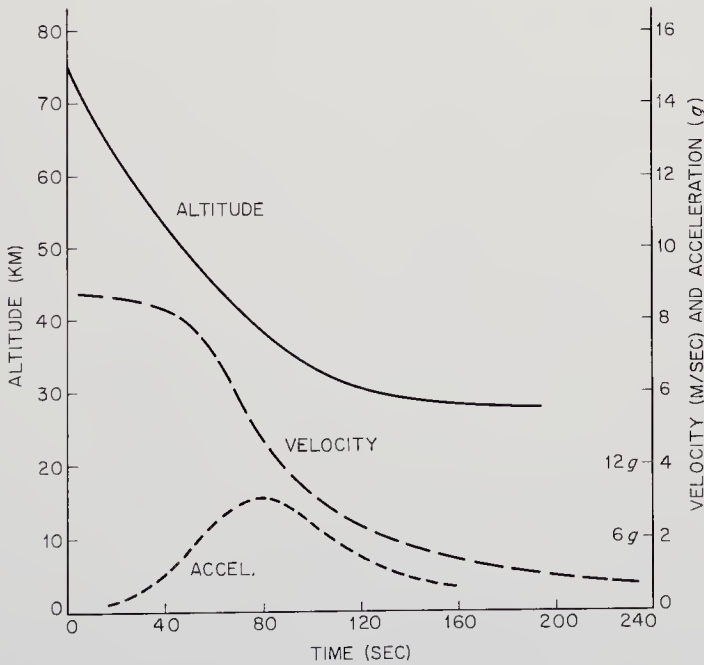


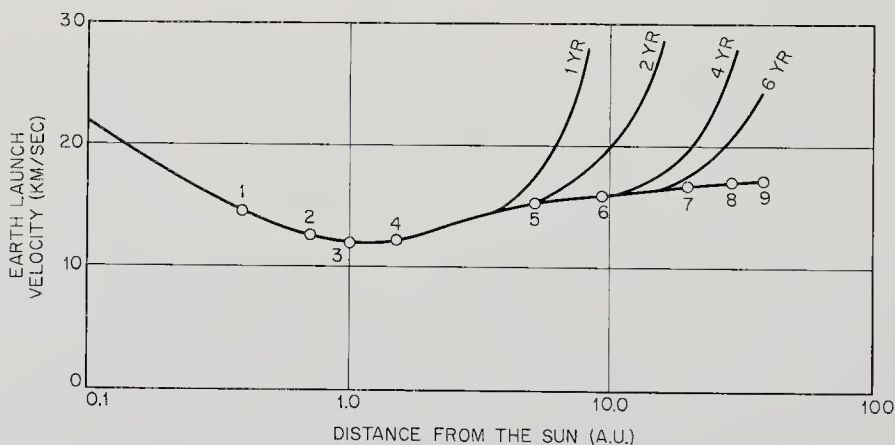
Fig. 5-10. Typical reentry parameters for a space vehicle using atmospheric braking on approach to the Earth.

has been lost. Braking ellipses are useful in hyperbolic encounters when relative velocities are high.

*Powered Descent.* Many of the astronomical targets of space probes do not boast atmospheres dense enough to brake high-velocity vehicles, yet they still have strong gravitational fields. The Earth's Moon and Mercury are typical of such bodies. The only way to softly land a probe on such an object is through the use of retrorockets. Directed opposite to the velocity vector, retrorocket thrust eases the spacecraft to the target's surface without damaging equipment. During soft landings, the vehicle may touch down at between 0 and 10 m/sec. Hard landings may range from 10 to 100 m/sec. Both hard and soft landings require retrorockets, because the approach velocities of an unimpeded spacecraft are usually measured in thousands of meters per second.

*Rendezvous.* If a space vehicle is to examine an asteroid or comet, velocity matching will be necessary. The rendezvous maneuver is somewhat simpler than planetary intercept, because the weaker gravitational fields of asteroids and comets will have much smaller effects upon the trajectory.

In essence the rendezvous maneuver consists first of rough matching of both velocity and trajectory by a series of thrusts. Docking, the final phase of the maneuver, would be achieved by small impulses generated by the on-board propulsion system followed by a physical link, such as a



MINIMUM-ENERGY FLIGHT TIMES:

- |                       |                       |
|-----------------------|-----------------------|
| 1. MERCURY (0.29 YR)  | 6. SATURN (5.95 YRS)  |
| 2. VENUS (0.41 YR)    | 7. URANUS (16.1 YRS)  |
| 3. EARTH              | 8. NEPTUNE (30.6 YRS) |
| 4. MARS (0.70 YR)     | 9. PLUTO (46.7 YRS)   |
| 5. JUPITER (2.69 YRS) |                       |

Fig. 5-11. Velocity requirements for flyby probes within the solar system. Solar probes would be at extreme left, interstellar probes at the far right. Faster trips require more energy as shown by the steeply rising flight-time curves. Energy for launching from Earth's surface is included. (Ref. 5-19)

cable, to ease the vehicle to the surface. Velocity matching would be adequate in many cases since unmanned space probes could easily withstand a residual impact velocity of several meters/sec.

*Other Space-Probe Missions.* Many space probes are aimed at the planets in the solar system, but future plans call for flights to the comets, the asteroids, the Sun, or just into deep space. The space mechanical problems are somewhat different for each case.

To put a space probe into orbit around the Sun, the launch vehicle merely boosts the probe out of the potential-energy well of the Earth. The probe will swing around the Sun in an orbit similar to that of the Earth. If an orbit close to the Sun is desired, an extra impulse must be applied that either places the probe in a highly elliptical orbit with a perihelion near the Sun or carries the probe in toward the Sun to where another impulse will place it in a tight orbit around the Sun. The closer the solar probe is placed to the Sun, the larger the energy requirements (Fig. 5-11). The orbiting of a solar probe at 0.1 A. U. from the Sun is, in fact, one of the most difficult missions within the solar system.

All of the probe missions mentioned so far have been confined to the plane of the ecliptic; but scientists are most interested in the space radiation levels and micrometeoroid fluxes well away from the ecliptic. To inject a probe into a plane that is tilted with respect to the ecliptic takes thrust; the greater the change in plane angle, the higher the impulse requirements (Fig. 5-7). Of course, the total energy of a probe circling the Sun in a plane inclined  $90^\circ$  to the ecliptic is equal to the energy of a probe in the plane of the ecliptic if the orbital radii are the same. Although there is no net change in probe energy, the probe propulsion system must first apply power to change the plane of rotation and second to bring the orbit radius back to its original value.

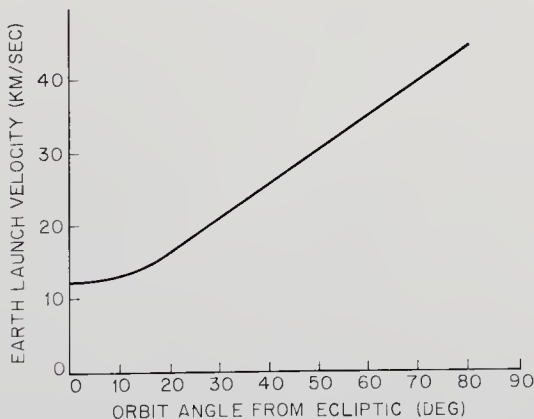


Fig. 5-12. Velocity requirements for out-of-the-ecliptic probes. Probes are positioned 1 A.U. from the Sun after plane change. (Ref. 5-19)

The comets and asteroids move in eccentric ellipses about the Sun. The space mechanical techniques for reaching them are the same as for the planets. Comets and asteroids are relatively easy to fly by, but matching their velocities for prolonged inspection demands a great deal from the propulsion system. The higher the eccentricity of the target's orbit, the greater the energy requirements. A mission to any specific asteroid or comet is planned like a planetary mission. Maps of the propulsion requirements have been prepared for some of these interesting celestial objects. (See Fig. 5-21, page 75.)

The ultimate mission now conceived is interstellar flight. The pro-

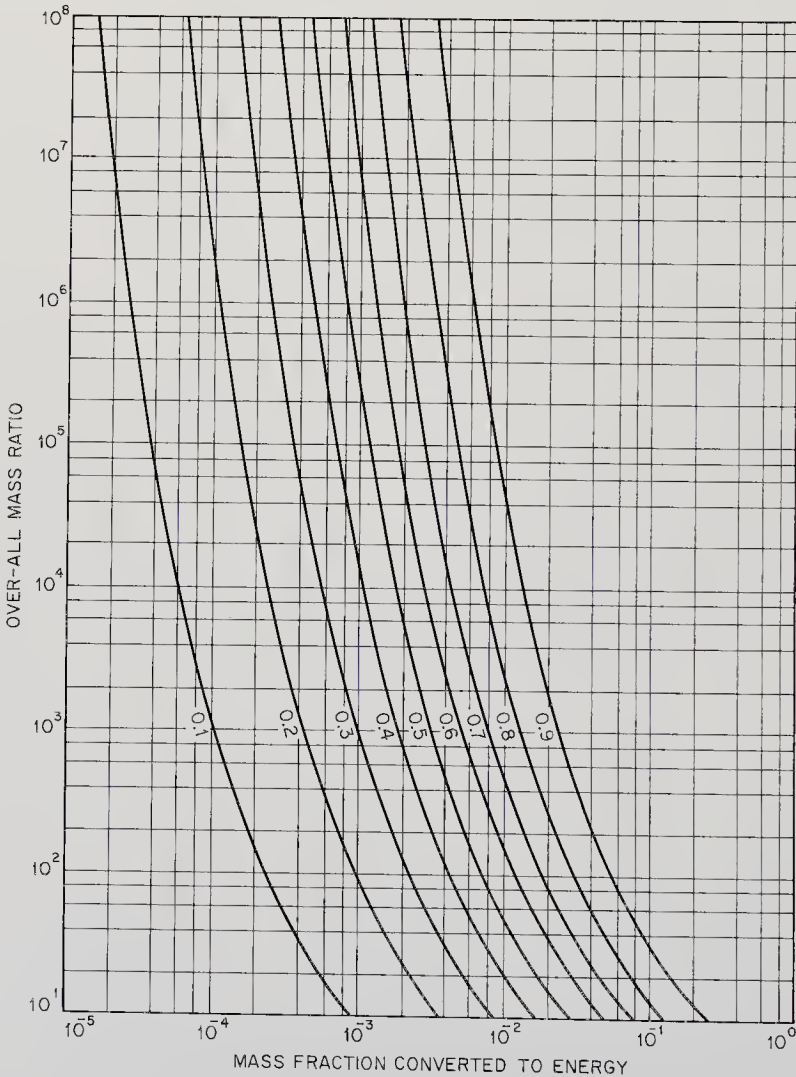


Fig. 5-13. Mass ratios for interstellar flights approaching the velocity of light. Curves assume a many-staged nuclear rocket where the fuel is all converted into exhaust kinetic energy. (Ref. 5-37)



pulsive functions are simple: escape the Earth's field and then that of the Sun. The factor of time enters the picture here, because a minimum-energy interstellar probe would just drift to the edge of the Sun's field and then slowly fall into toward the target star. Such a low-velocity maneuver would take thousands of years in view of the immense distances that must be covered. All interstellar mission planners contemplate flying the probe close to the velocity of light in order to cut down the travel time. A simple calculation shows that the energy needed to attain a velocity just one tenth that of light is several orders of magnitude greater than that for solar-system escape starting from the Earth's orbit. Energy, then, is used mainly for accelerating the interstellar probe to near-optic velocities and then slowing it down as it nears its stellar destination. The top speed desired determines the energy requirement (Fig. 5-13).

### 5-5. Flight Maps

When the computer-calculated flight maps (Figs. 5-14 through 5-21) are examined, several points become apparent:

1. There are launch windows of varying sizes for all planets and heliocentric objects. The windows are more pronounced for the closer planets,

TABLE 5-3. MINIMUM-ENERGY ONE-WAY INTERPLANETARY FLYBY FLIGHTS\*

<i>Planet</i>	<i>Launch Date</i>	<i>Flight Time (days)</i>	<i>Kinetic Energy (joules/kg <math>\times 10^8</math>)</i>
Venus	11-12-65	108	0.066
	6-11-67	142	0.032
	1-13-69	126	0.038
	8-19-70	116	0.042
Mars	11-19-64	244	0.045
	1-5-67	202	0.046
	3-2-69	178	0.044
	5-24-71	210	0.039
	7-30-73	192	0.073
	9-15-75	206	0.093
	10-19-77	224	0.085
Mercury	11-23-67	107	0.206
	4-4-68	92	0.416
	7-30-68	89	0.522
	11-12-68	103	0.224
Jupiter	1-3-70	985	0.376

\* Adapted from Ref. 5-9. Only trajectories requiring less than half a revolution around the Sun have been included. Firing windows are approximately 19 and 26 months apart for Venus and Mars respectively. The period of recurrence for minimum-energy conditions is approximately eight years for Venus and fifteen years for Mars. The series of Venus launch windows listed above would begin to repeat after 1973, for example.

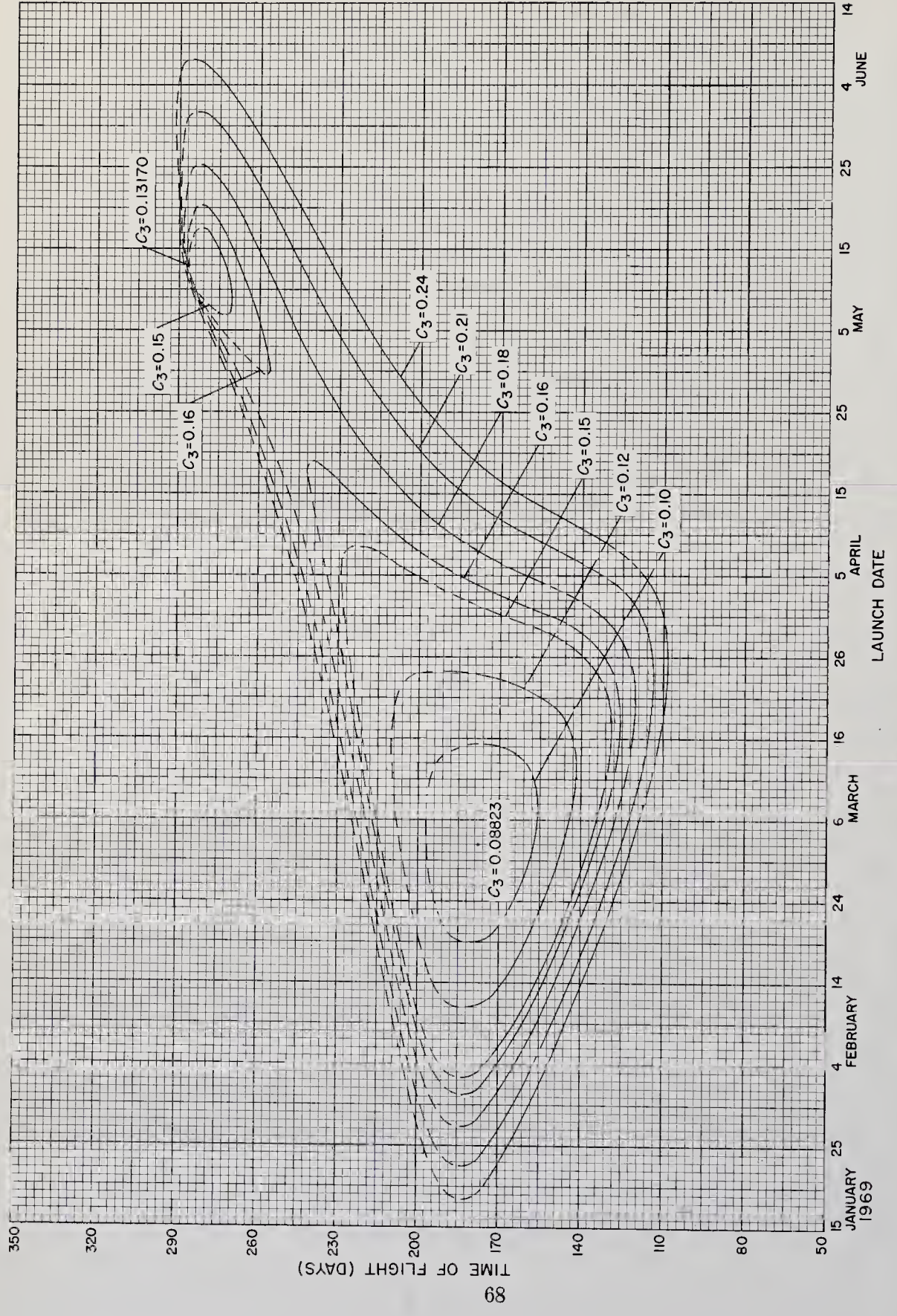


Fig. 5-14. Time-of-flight and launch-date map for a 1969 Mars-flyby probe.  $C_3$  is twice the total geocentric injection energy per unit mass. Units =  $m^2/sec^2 \times 10^8$ . (JPL data)

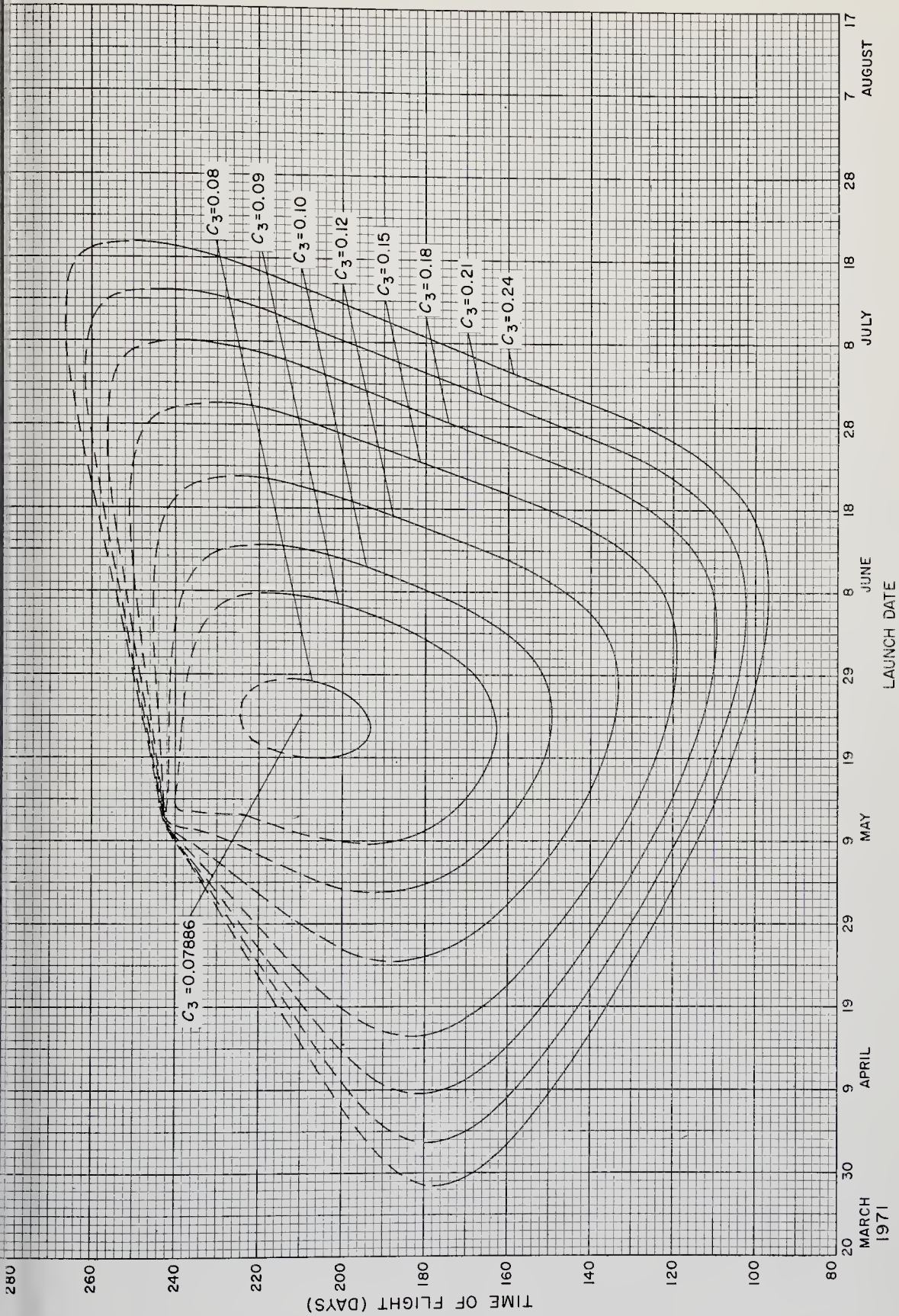


Fig. 5-15. Time-of-flight and launch-date map for a 1971 Mars-flyby probe.  $C_3$  is twice the total geocentric injection energy per unit mass. Units =  $m^2/sec^2 \times 10^8$ . (JPL data)

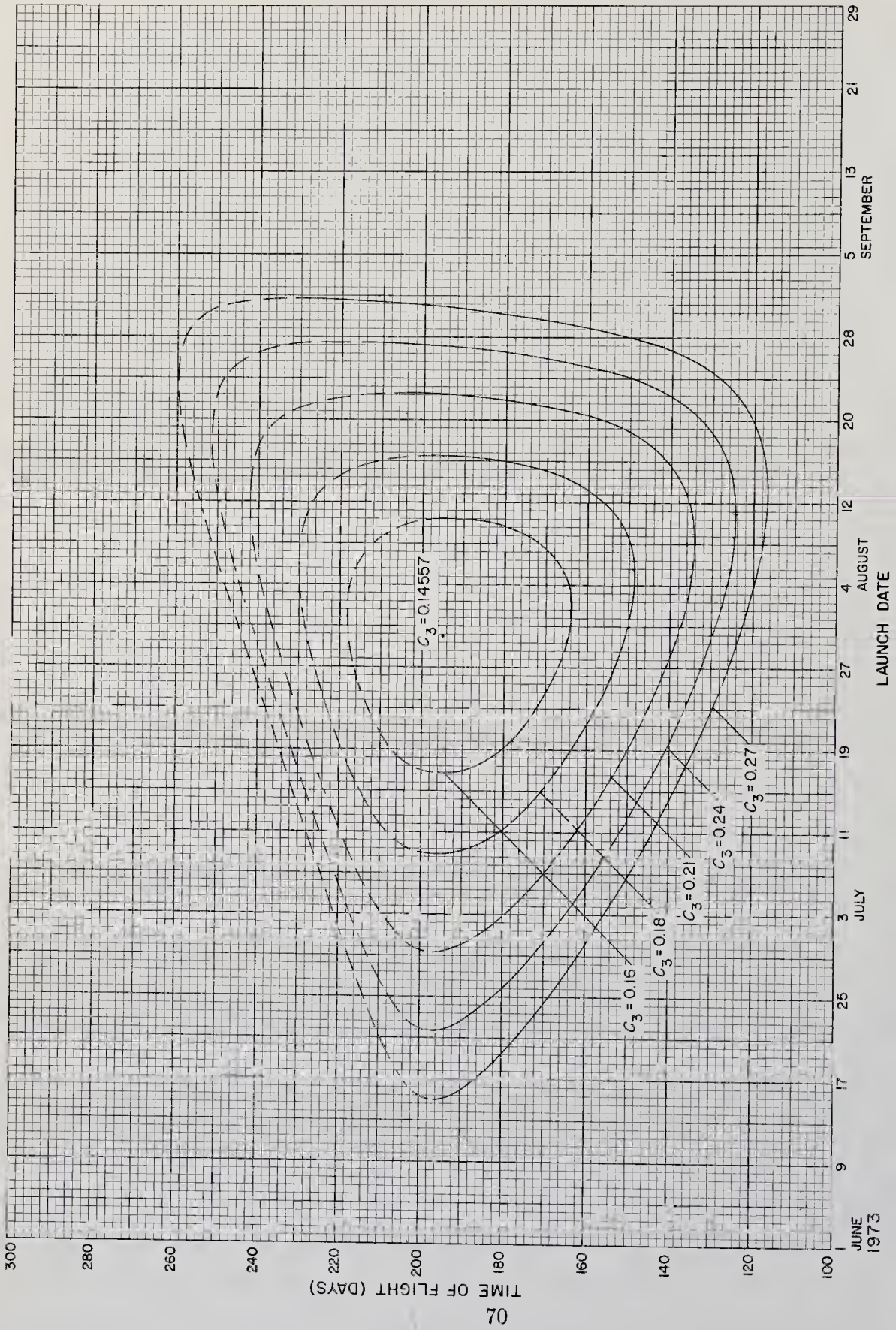


Fig. 5-16. Time-of-flight and launch-date map for a 1973 Mars-flyby probe.  $C_3$  is twice the total geocentric injection energy per unit mass. Units =  $m^2/sec^2 \times 10^8$ . (JPL data)

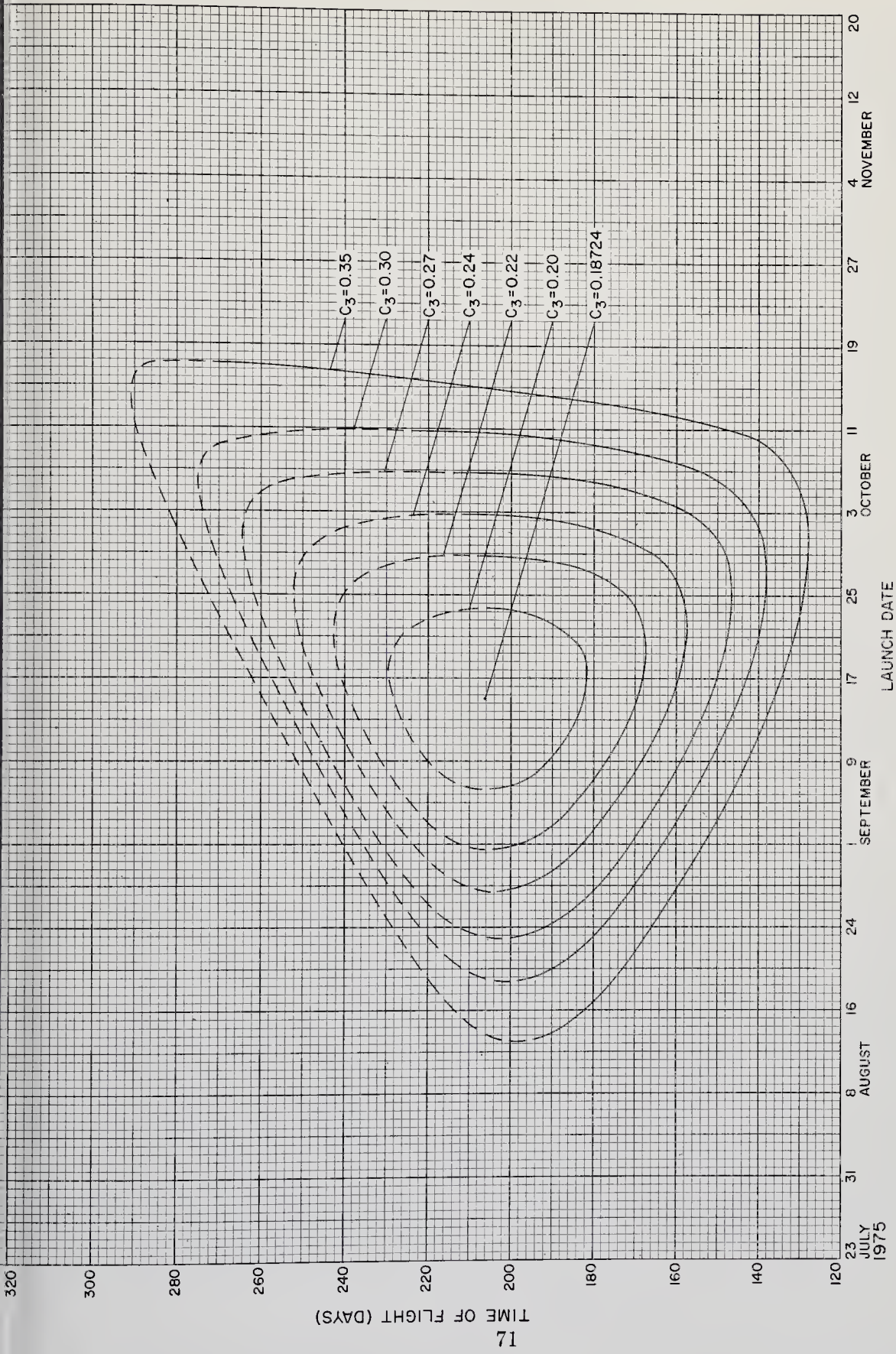


Fig. 5-17. Time-of-flight and launch-date map for a 1975 Mars-flyby probe.  $C_3$  is twice the total geocentric injection energy per unit mass. Units =  $m^2/sec^2 \times 10^8$ . (JPL data)

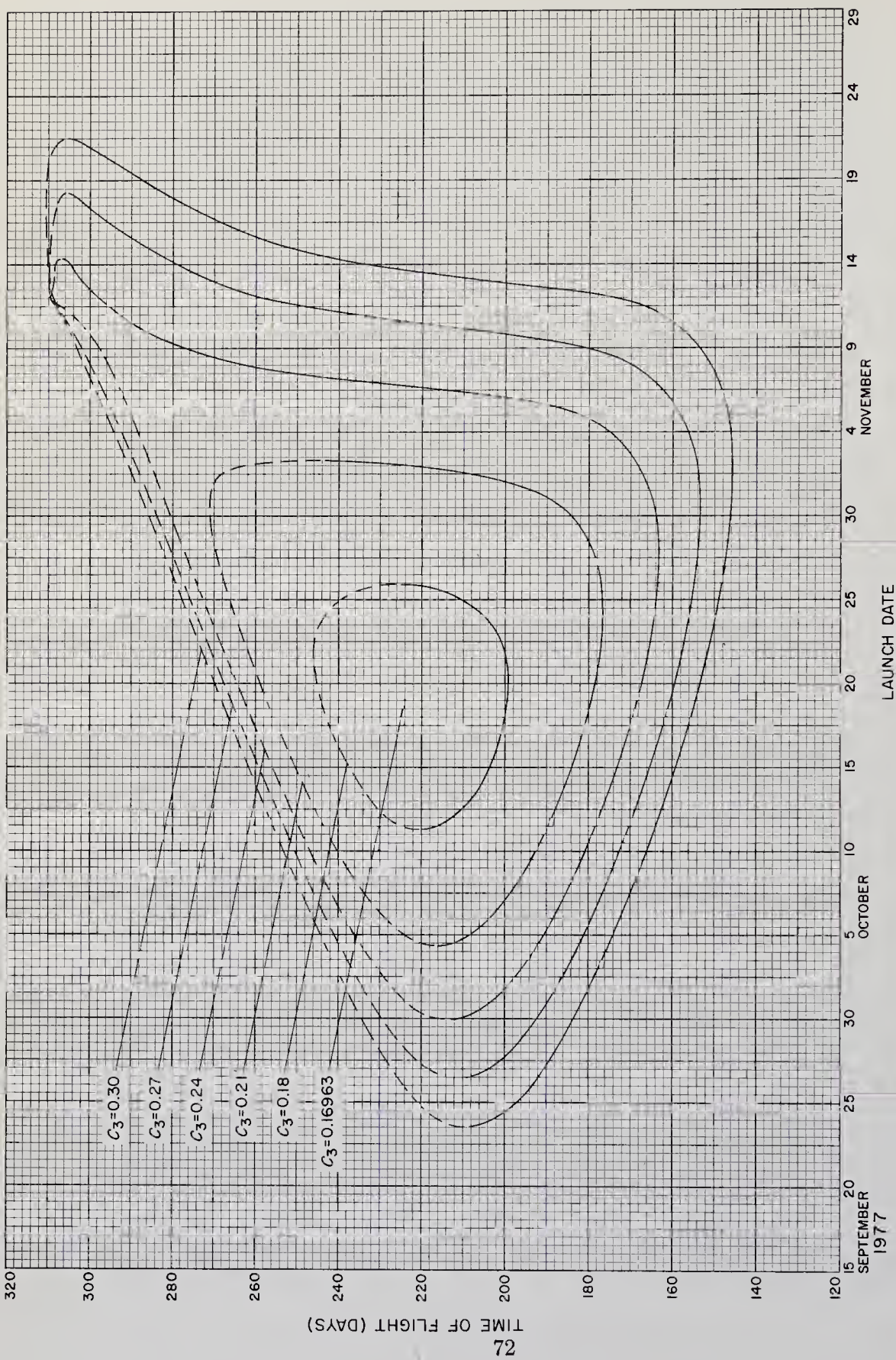


Fig. 5-18. Time-of-flight and launch-date map for a 1977 Mars-flyby probe.  $C_3$  is twice the total geocentric injection energy per unit mass. Units =  $m^2/sec^2 \times 10^8$ . (JPL data)

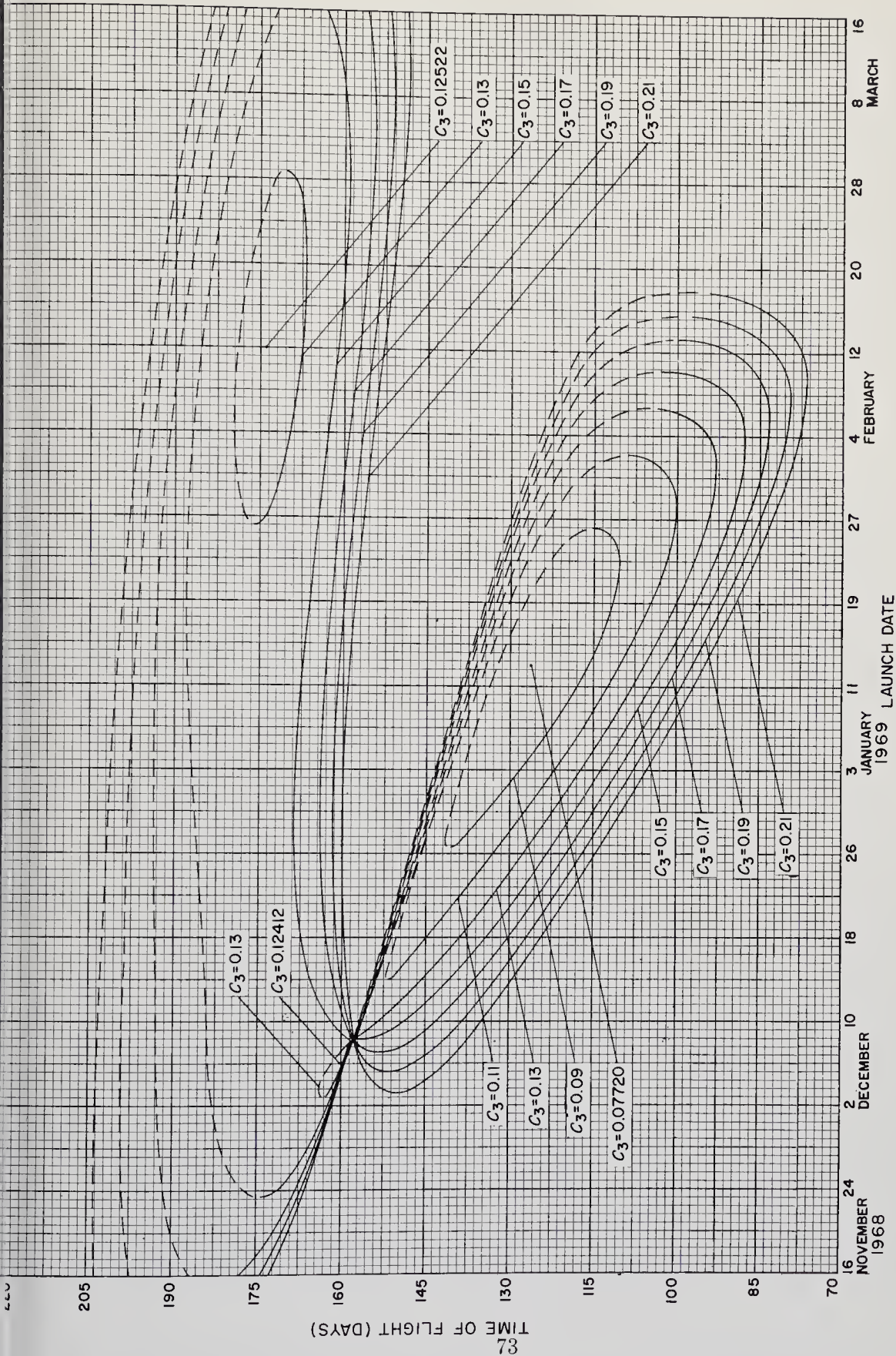


Fig. 5-19. Time-of-flight and launch-date map for a 1968-1969 Venus-flyby probe.  $C_3$  is twice the total geocentric injection energy per unit mass. Units =  $m^2/sec^2 \times 10^8$ . (JPL data)

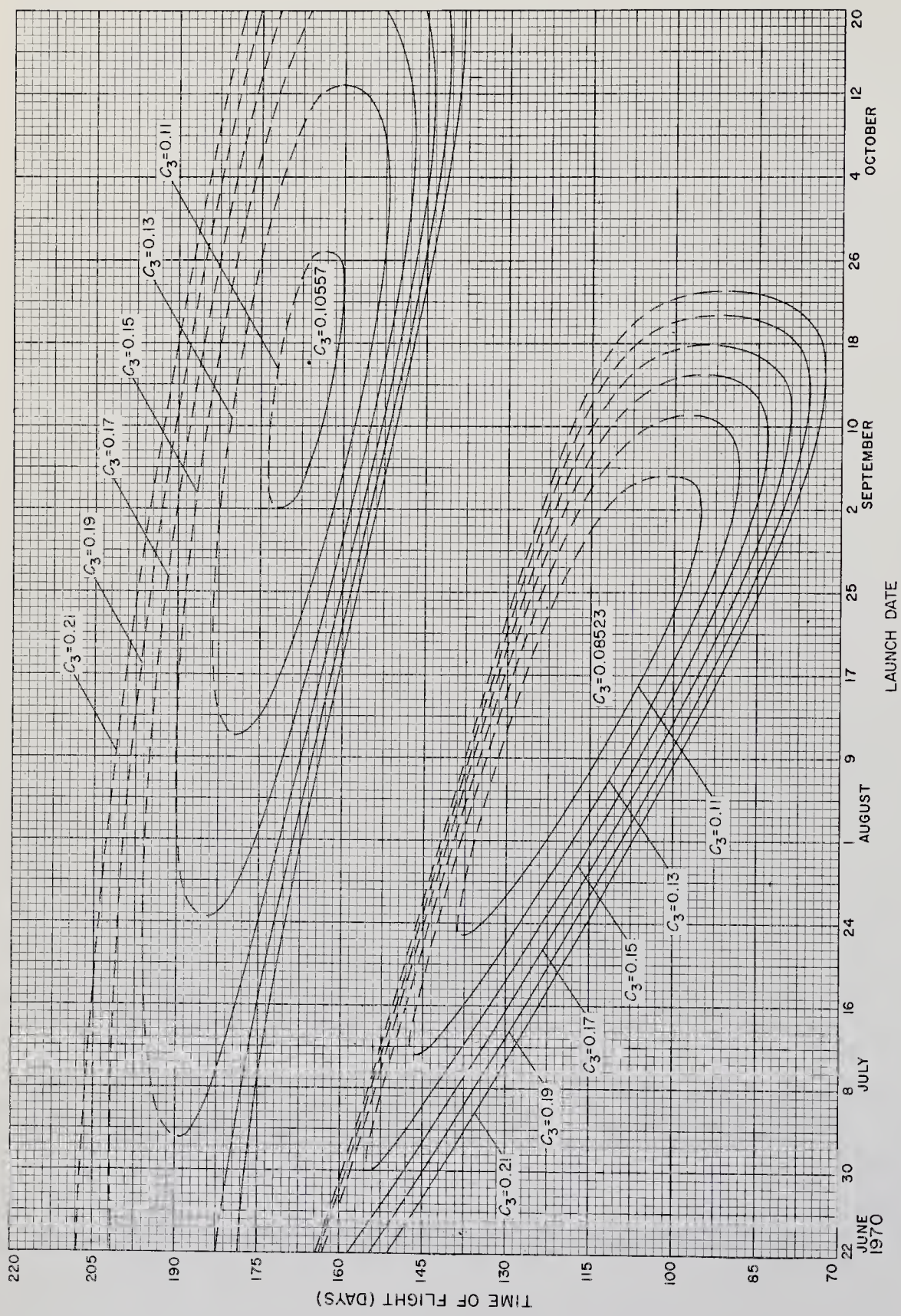


Fig. 5-20. Time-of-flight and launch-date map for a 1970 Venus-flyby probe.  $C_3$  is twice the total geocentric injection energy per unit mass. Units =  $m^2/sec^2 \times 10^8$ . (JPL data)



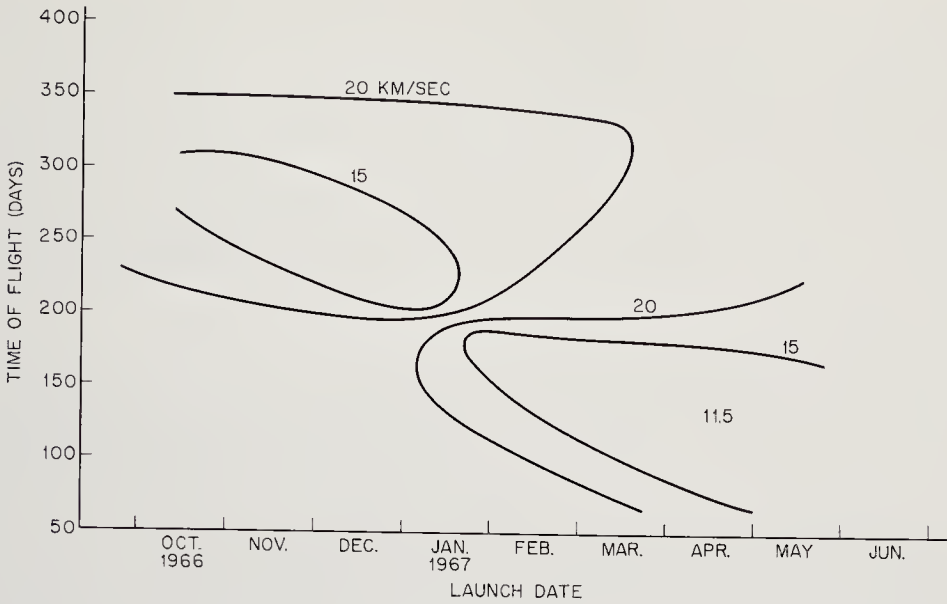


Fig. 5-21. Time-of-flight and launch-date map for a 1966-1967 probe to the comet Tempel. Contours are measured in terms of geocentric injection velocity. (Ref. 5-31)

especially Mars. Windows must be used as long as propulsion capabilities are severely restricted.

2. Velocity and energy requirements vary from launch window to launch window. Table 5-3 summarizes the more important windows that will be available over the next few decades.

3. The contours of the maps are not simple, owing to the ellipticity and

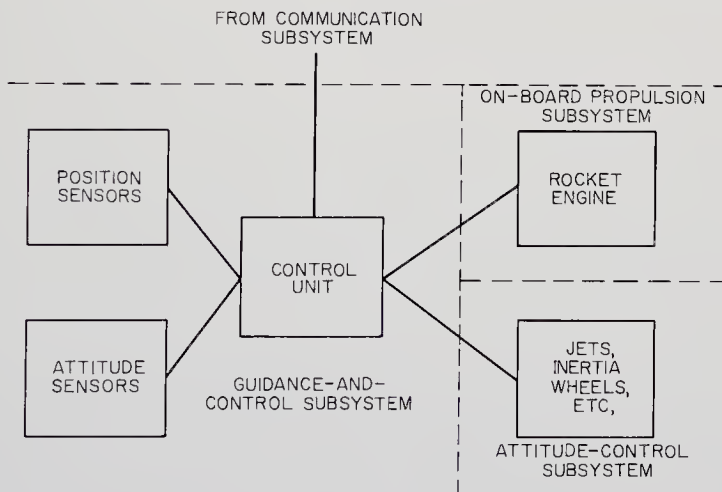


Fig. 5-22. Schematic showing the relationships between the attitude-control subsystem and other spacecraft subsystems.

three-dimensionality of the planetary orbits and the synodic effects, which tend to repeat themselves over long periods of time.

4. The maps themselves are not complete estimates of the difficulty of interplanetary flight. Takeoff and landing energy increments must be added.

Since the solar system never repeats itself exactly, the maps are only guides to estimate-making. Every mission must be preceded by detailed studies.

### 5-6. Attitude Control

A rigid spacecraft moving freely through space has at least six degrees of freedom. The three position variables and the methods of manipulating them were discussed in the preceding sections. The remaining three degrees of freedom concern the attitude or orientation of the vehicle in space with respect to some selected reference frame.

Most space vehicles control at least one of these degrees of freedom. The picture is complicated in the more advanced space probes, which are often jointed or hinged, a fact which adds degrees of freedom. For example, the highly directional communication antenna of a planetary probe must point at the Earth during transmission and reception. At the same time the scientific instrumentation and solar-cell array may have to point in other directions. The spacecraft must be jointed to accomplish these pointing feats simultaneously. Each joint adds one more degree of freedom that must be controlled. Joints also cause the principal moments of inertia of the vehicle to vary with time; this further complicates the situation.

The complete attitude-control subsystem consists of:

1. Spacecraft sensors (star trackers, gyros, etc.) that inform the guidance-and-control subsystem of the craft's orientation with respect to some set of reference axes.

2. A small computer and control system for translating sensor-derived information and positioning commands into signals that actuate the inertia wheels or other devices used to change the spacecraft attitude.

3. Inertia wheels, attitude-control jets, magnetic bars, and other attitude-control devices that act upon commands coming from the control unit.

The purpose of this part of the book is the presentation of the general physical concepts that apply to the attitude control of spacecraft. The actual hardware necessary to perform the function is described later.

The attitude control of Earth satellites and space probes differs in several ways. First, much satellite instrumentation is Earth-directed and must be continuously reoriented as the satellite moves around the planet. Second, disturbing torques are larger in the neighborhood of the Earth.

Disturbances include atmospheric drag, gravity gradients, and magnetic fields. In contrast, the probe is affected mainly by changes in its internal angular momentum, solar radiation pressure, and meteoroid hits. Lastly, the Earth satellite can be designed to make use of the Earth's fields and atmosphere in stabilizing its own attitude. The space probe has little recourse but to provide internal torque generators, with perhaps a modicum of help from solar pressure.

*Coordinate Systems.* The reference axes in space may be fixed in the framework of the fixed stars. They might be geocentric, planetocentric, heliocentric, or another of the many available possibilities (Ref. 5-34).

In establishing its attitude, the space probe usually locks one attitude-control sensor and one spacecraft axis on the Sun. This is convenient for keeping the solar-cell panels pointed at the Sun. Earth lock is employed by interplanetary spacecraft to provide signals for aiming the parabolic antennas used in communication. Even with two degrees of freedom thus fixed, others remain unspecified with a jointed structure. During most of an interplanetary voyage, however, it may be possible to let the other degrees of freedom drift until the target is approached. In the case of Mariner 2, Venus lock was attained just prior to scanning the planet with radiometers.

*Equations of Motion.* In the simplest meaningful case, there will be a set of axes  $X, Y, Z$ , which also coincide with the principal moments of inertia of the vehicle,  $I_x, I_y, I_z$ , which are assumed constant in time for this example. The  $x, y, z$  are a set of external reference axes to which  $X, Y, Z$  are compared. When the spacecraft is properly aligned, the two sets of axes are coincident (Fig. 5-23). The angles  $\omega_x, \omega_y, \omega_z$ , indicate roll, pitch, and yaw respectively in the figure.

If  $\Omega$  is the angular velocity of the vehicle relative to the external reference frame, and  $\omega$  is the angular velocity of the reference frame with respect to inertial space, the angular momentum of the vehicle,  $\mathbf{H}$  is:

$$\mathbf{H} = I_x(\Omega_x + \omega_x)\mathbf{e}_x + I_y(\Omega_y + \omega_y)\mathbf{e}_y + I_z(\Omega_z + \omega_z)\mathbf{e}_z \quad (5-14)$$

where the  $\mathbf{e}$ 's are unit vectors.

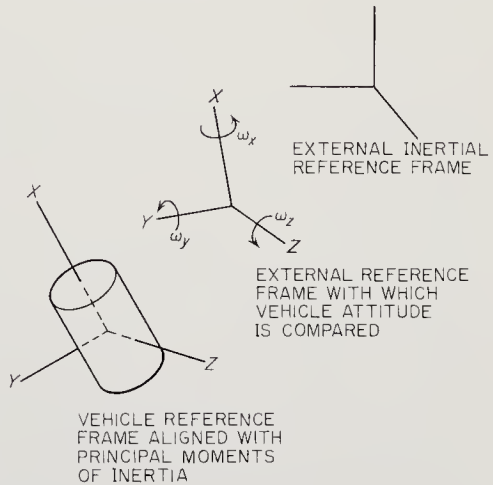


Fig. 5-23. Reference systems for attitude control  $\Omega$  is the angular velocity of the  $X, Y, Z$  axes relative to the  $x, y, z$ , axes.  $\omega$  is the angular velocity of the  $x, y, z$ , axes relative to inertial space.

The fundamental equation of attitude control is written by simply equating the external torque,  $\mathbf{L}$ , to the rate of change of angular momentum:

$$\dot{\mathbf{H}} + \boldsymbol{\omega} \times \mathbf{H} = \mathbf{L} \quad (5-15)$$

The mathematical formulation of attitude dynamics has been carried much further by Roberson (Ref. 5-34) and others. Complicating factors are introduced by the changing moments of inertia arising from jointed structures, the loss of propellant, and the ejection of instrument capsules from the vehicle.

The external torques that are applied to space probes, say from solar pressure, are slight, and practical considerations concentrate upon the gross motions that occur when the spacecraft must acquire the Earth, Sun and target objects. Another difficulty that is sometimes encountered on the vehicle concerns the calculational load on the spacecraft computer. In handling the attitude-command and sensor signals, large matrices of trigonometric terms must be processed when analyzing the different axes and reference frames.

# Chapter 6

---

## SPACE COMMUNICATIONS AND DATA HANDLING

---

---

### 6-1. Prologue

Space probes are fundamentally information gatherers. As extrapolations of man's senses, probes transmit data back to man across millions of kilometers of empty space. The most obvious communication link across this near vacuum employs electromagnetic waves—radio. Eventually, probes will return actual samples of the environment through which they fly, as well as geological and biological specimens from the planets they explore. Until that day, electromagnetic waves are the only communication threads linking the distant sensors with Earth-bound man.

First, distinguish between space-probe and Earth-satellite communications. There is immediately a distance ratio of about 100,000 : 1. As a further distinction, space probes are almost always within the line of sight of one of the Earth-based DSIF\* stations, while the horizon quickly cuts off radio contact between a fast-moving Earth satellite and any single ground station. As a result, satellites frequently store data for later transmission to Earth in a burst when they are over a ground station. Space probes, in contrast, often transmit scientific and engineering data\*\* continuously. Another shadowing effect occurs when solar-cell power supplies are cut off from sunlight when the satellite swings behind the Earth. Space probes are in the Sun all the time, except when they pass behind a planet or land under an opaque atmosphere. This greater availability of energy is fortunate for the space probes because their

\* DSIF—Deep Space Instrumentation Facility, a NASA-JPL facility forming the basis for all U.S. space-probe communication.

\*\* Engineering data comes from sensors monitoring the status of the spacecraft. Examples: temperature of the electronics equipment, solar cell current.

power supplies are harder to design than those of satellites due to more stringent weight restrictions.

Communication is a two-way affair, even for space probes. In addition to transmitting engineering and scientific data back to Earth, the communication subsystem must also carry commands from the mission director to the spacecraft. A third demand is imposed on the communication link: it must be compatible with the tracking and guidance subsystem (Fig. 6-1). The use of a spacecraft radio transponder—an elec-

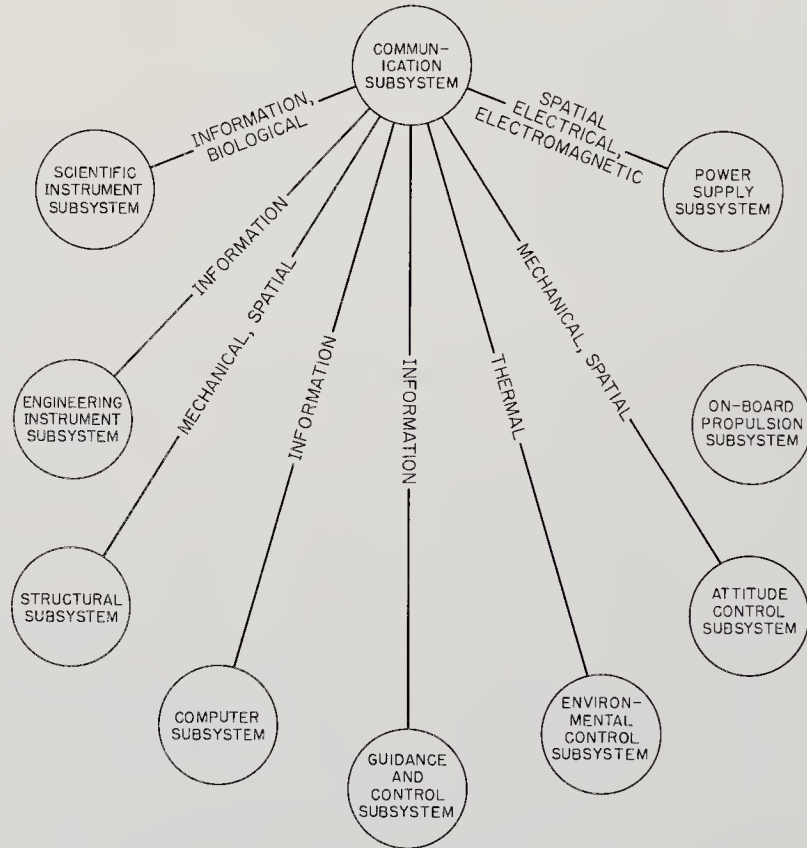


Fig. 6-1. Interface diagram showing the more important relationships between the communication subsystem and the rest of the subsystems.

tronic device that automatically responds to Earth interrogation for tracking purposes—illustrates the interweaving of space-probe subsystems. Also, the choice of an automatic phase-control communication subsystem for the Jet Propulsion Laboratory (JPL) space probes stemmed from tracking requirements, further binding these two subsystems.

From the preceding observations, the communication subsystem manifestly has very strong system ties; that is, the interfaces are complex and sensitive (Fig. 6-1). The more difficult areas will be discussed later in

this chapter, particularly in Sec. 6-5, where the communication-subsystem constraints are analyzed.

Data processing deserves more attention than it enjoys. It is critical in conveying intelligence from distant sensors to the human brain. Data processing is sometimes viewed with suspicion by scientists because it introduces additional machinery between the experimenter and his apparatus. Without mechanized data processing, however, the tremendous deluge of data from space vehicles could overwhelm scientists. The complete communication subsystem encompasses data selectors, which ultimately must have some degree of adaptability and judgment, the data storage equipment, and the data-formating devices that present the

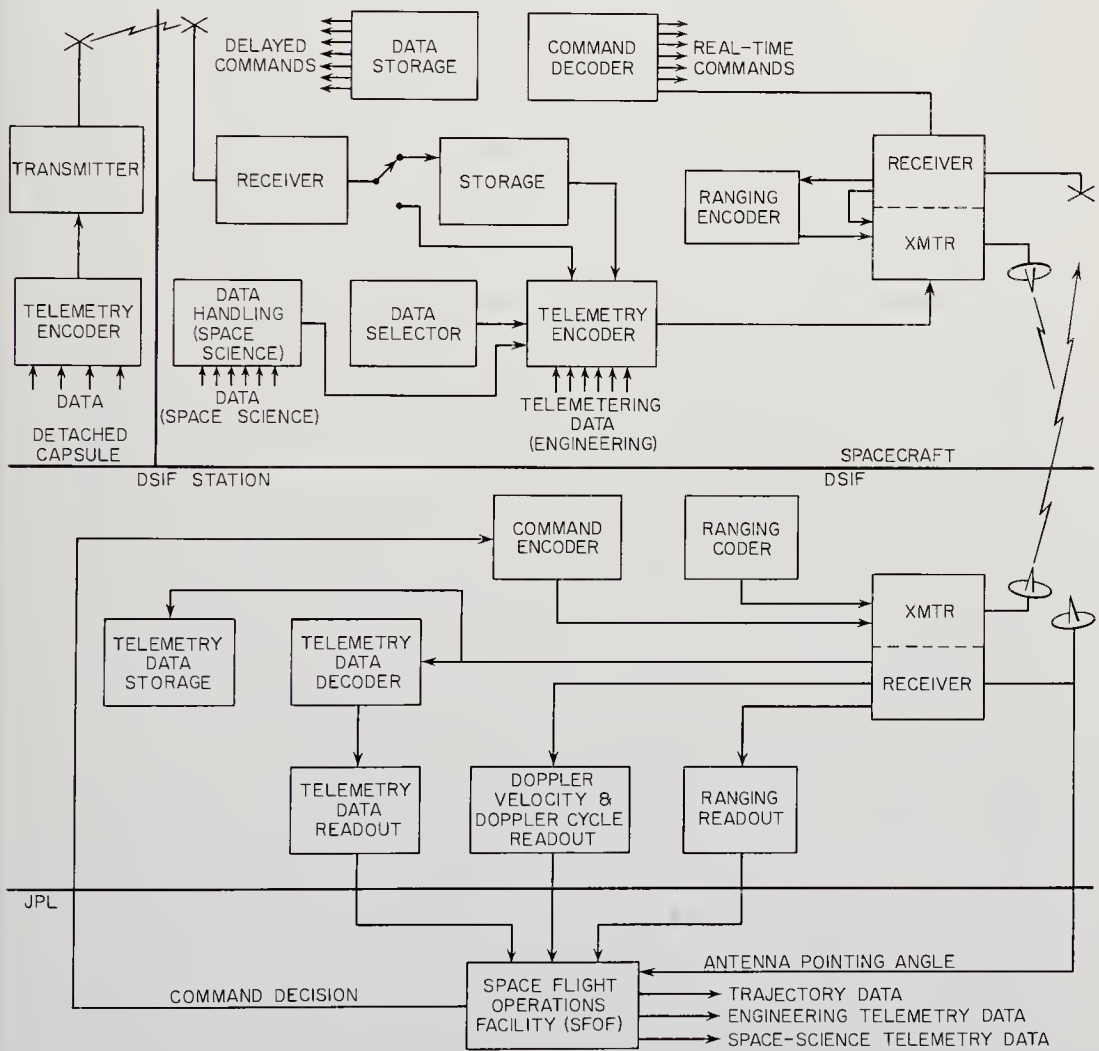


Fig. 6-2. Simplified block diagram of a typical space-probe communication subsystem, including ground-based equipment. (JPL drawing)

experimenter and mission director with information in easily digested forms. The block diagrams in Fig. 6-2 show typical data-processing equipment and in addition the real extent of a complete probe communication subsystem. Most of the equipment shown is actually located on the ground, not in the spacecraft.

With such a complex subsystem, engineering tradeoffs are difficult to discern. The all-important range equation, Eq. (6-8), for example, involves six controllable variables and still does not deal with such pertinent factors as cost and reliability. No amount of manipulation of the basic range equation alone will yield a good communication subsystem.

By way of illustration, if more weight were allotted to the power supply, the result would be a more powerful radio transmitter and a higher rate of information transfer. But with a fixed payload, experiments would have to be sacrificed to provide this additional power. The over-all scientific value of the probe might actually be reduced by this kind of tradeoff. Or perhaps money might be better spent in building larger terrestrial antennas rather than in developing a bigger spacecraft transmitter. In the end, the many interlocking parameters must be expressed in terms of a single payoff function, a figure of merit, which evaluates the mission as a whole.

In attempting to solve these complex, interlocked problems, various groups of engineers have come up with different kinds of space-probe communication systems; some good, some less so. A typical high-performance space communication subsystem is that used for the JPL Mariner probes. Much of the experience going into the final subsystem design was derived from the successful Pioneer lunar-probe program (Ref. 6-9). Figure 6-2 shows the major features of the basic JPL communication subsystem. Further description is embodied in the initials PCM/PSK/PM, short for Pulse-Code Modulation, Phase-Shift Keying, Phase Modulation. Though the letters apply ostensibly only to the method of modulation, they also contain the essential germ of the communication-subsystem design philosophy. PCM (pulse-code modulation) indicates a digital system rather than one that transmits continuously varying data. PSK (phase-shift-keying) is one of several techniques for impressing a one or a zero in binary language on a radio carrier or sub-carrier. PSK was selected because it is compatible with the phase-lock receivers, in which the phase of the carrier signal is "locked onto," enabling precise Doppler tracking of the probe.

The success of the PCM/PSK/PM phase-lock approach is evident in the excellent performance of Mariner 2, which transmitted 8.33 bits of data per second from a distance of 60,000,000 km with a radiated power of only three watts. In another several years, the state of the art will



allow satisfactory communications with a probe at the edge of the solar system. The most important problems are no longer those of conquering distance, but rather of insuring equipment reliability for years at a time, increasing the rate of data transmission, and handling intelligently the huge masses of data that converge on the Earth from successful space vehicles.

## 6-2. Information and Languages

The basic commodity of communication is information. To evaluate the performance of a communication subsystem, information must be quantified and made measurable. The unit of currency is the bit: a one or a zero, a yes or a no, a pulse or a lack of a pulse, or, in the case of the JPL probes using phase-shift keying, a phase difference of  $0^\circ$  or  $180^\circ$  with respect to some reference point. Two bits provide four possibilities: 00, 01, 10, and 11. These four binary numbers are the equivalents of 0, 1, 2, and 3 in the decimal system. The binary system of numbers based on the bit is convenient to mechanize in terms of lights, pulses, and many other two-valued electromechanical devices. The whole digital computer industry is based upon the binary system.

Information is much like heat energy in the sense that it cannot be transferred from one place to another without being degraded to some extent. In fact, the laws of information theory have some of the trap-pings of thermodynamics. Information possesses entropy, for example. An important equation relates the rate of information transfer,  $H$ , measured in bits/sec, to the bandwidth of the communication channel,  $B$ , measured in cycles/sec. Nature introduces noise into all communication equipment, making the reception and interpretation of transmitted information more difficult. The relationship between  $H$  and  $B$ , taking noise into account is:

$$H = B \log_2 (1 + S/N) \quad (6-1)$$

where:

$$S/N = \text{the signal-to-noise power ratio.}$$

The larger the signal-to-noise ratio, the more information one can send over a given channel.  $S/N = 1$  for threshold reception, but in practice  $S/N = 10$  is needed for fair readability.

A word of data is made up of several bits. In the Mariner-2 experiments, the basic data words were seven and eight bits long, depending upon whether scientific or engineering instruments were being read. Experimental parameters could thus take on 128 and 256 quantized levels. This range of possible values was more than adequate for the dynamic ranges of most of the Mariner-2 experiments. Data words for scientific

measurements were also organized into a format consisting of 168 bits made up from 21 eight-bit words. Every other word of data was only seven bits long, accounting for the two different word lengths. The eighth bit on each second word was a parity bit (Fig. 6-3). The parity bit

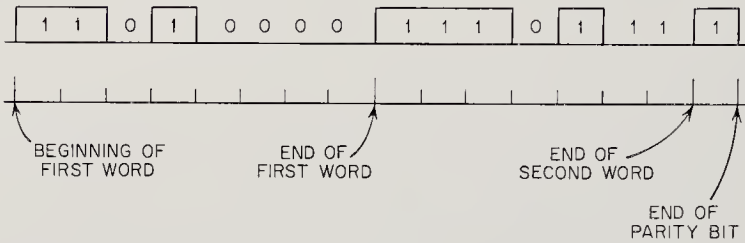


Fig. 6-3. Two-word sequence of scientific data from Mariner 2. The eight-bit word 11010000 is followed by the seven-bit word 1110100 and the parity bit, which must be 1 in this case. The pulses indicated in the diagram actually represent changes in phase rather than changes in amplitude. Engineering (spacecraft-status) data were encoded in seven-bit words on Mariner 2.

enables those analyzing the data to determine whether a bit was somehow lost in the transmission process. The parity bit is a one if an odd number of ones precede it; otherwise it is a zero. The value of the parity bit can be calculated aboard the spacecraft and then checked during data reduction on the ground. Parity bits are commonly used in digital computations. Of course, if an even number of bits are somehow lost, the parity bit will not reveal this fact, but this event is less likely than the loss of a single bit.

In a sense, the addition of the parity bit to a word is a simple form of redundancy, since the parity bit would be superfluous if data transmission were perfect. Redundancy occurs whenever data is repeated or its information content is wholly or partially reiterated. Spoken languages are always partially redundant, because missing words in a passage can frequently be reconstructed from the context. Like a missing word, the parity bit indicates that an error has been made in transmission.

Data points can always be repeated to help insure correct reception. This is a more extreme, but still not foolproof, form of redundancy. No finite amount of redundancy will ever guarantee perfect transmission of information. In practice, fortunately, spacecraft sensor readings are radioed back to Earth so frequently that badly distorted words are usually easy to spot—a technique equivalent to correcting a message by context.

Because so much data from space experiments represent physical parameters that change little with the passage of time, those who analyze data are often faced with miles of magnetic tape and reams of printed

data points that vary slowly or not at all. Many have thought to ease the burdens on the communication subsystem and the data processors by either automatically selecting the data to be sent or compressing it (Table 6-1).

In automatic data selection, physical measurements might be sent at a rate depending upon how fast they vary. If, for example, magnetic-field sensors indicated a sudden change, the spacecraft circuits would recognize the altered situation and send data points more frequently. Less but more important information is sent with data selection. In the case of data compression, the same amount of information is sent but in a more compact form; that is, fewer bits. Take a string of fifty constant eight-bit data points. The number 50 and the value of the constant data point could be sent in just two eight-bit words, leaving 48 words available for other uses. Many organizations are working on concepts such as these to try to reduce the tremendous masses of data that flow to the Earth each day from space experiments without compromising the scientific content of the data.

TABLE 6-1. TYPICAL INFORMATION RATES\*

<i>Type of Message</i>	<i>Straight Transmission</i>	<i>With Compression</i>
Color TV (commercial)	$7 \times 10^7$ bits/sec	$10^6$ bits/sec
Black and white TV (commercial)	$4 \times 10^7$	$10^5$ to $10^6$
Speech	$7 \times 10^4$	$10^2$
Facsimile	$2.4 \times 10^3$	$10^2$
Coded English text (20 words/min)	10	2

\* Adapted from Ref. 6-12.

Another possibility is the use of a *matched receiver*, where the transmission of a single code word signifies a whole message, much like the low-cost Happy Birthday telegrams.

The information received from space probes is restricted by the limited power available for communication and the immense transmission distances. Such factors tend to lower  $H$ , the bit rate. Of course, even one bit/sec from the surface of Mars for a few days could completely revolutionize our concept of the planet.

### 6-3. Information Carriers in Outer Space

There are two ways to transmit information across interplanetary space:

1. Impress signals upon (modulate) action-at-a-distance fields. Examples: radio and optical communication.

2. Impress information upon physical particles and hurl them across space. Examples: recoverable data capsules, communication by beams of atomic particles.

Although radio methods are now used very successfully for interplanetary communication, the search for better techniques continues. There are good, practical reasons for keeping an open mind. New technological developments might increase our ability to communicate many-fold, but perhaps most important is the ever-increasing pressure from commerce and government that forces science to higher radio frequencies and smaller portions of the usable electromagnetic spectrum. There is also an attendant increase in artificial interference in the spectrum. Fortunately, methods of generating, transmitting, and detecting extremely high frequency electromagnetic waves are developing rapidly. A late and startling example of this trend is the laser.

There is a broad frequency range, 400 to 10,000 Mc, in which interplanetary radio communication is fairly easy. The invention of the laser has suddenly shifted much advanced development effort by orders of magnitude in frequency to the optical region ( $10^{14}$  cycles/sec). The high directivity of the laser beam, the coherence of its radiation, and its power transmission capabilities make it a possible replacement for conventional radio communication in interplanetary exploration (Ref. 6-1). Furthermore, the high frequency of the laser would easily permit many wide bandwidth channels without crowding. At present, short-range laser communication systems have been demonstrated terrestrially on an experimental basis, but many advances in modulation, detection, and aiming must be made before they can be applied to space-probe communications. Atmospheric absorption of laser radiation is also a problem.

Even higher in the frequency spectrum are X-rays and gamma rays. In fact, the elementary atomic particles may also be considered to be high-frequency wave packets if the philosophy of waves mechanics is applied. For particles, the pertinent relationship is:

$$f = cp/h \tag{6-2}$$

where:  $c$  = the velocity of light (m/sec)

$p$  = the momentum of the particle (kg-m/sec)

$h$  = Planck's constant ( $6.62 \times 10^{-34}$  joule-sec).

Most investigators have agreed that these energetic photons and particles, though high in information-carrying ability, would be quickly scattered by interplanetary matter and magnetic fields. Absorption in the Earth's atmosphere would also be prohibitive.

### 6-4. Carrier Modulation

Once an information carrier has been selected—in all probability a high frequency electromagnetic wave—a method for impressing information upon it must be found. Primitive telegraphy had a simple approach: turn the carrier on and off. This was a special case of amplitude modulation. Obviously, the amplitude of a carrier could be varied in a more complex manner, such as is shown in Fig. 6-4. Besides the property of amplitude, a sine-wave carrier also has a frequency and a phase, both of which can be varied in response to modulating information.

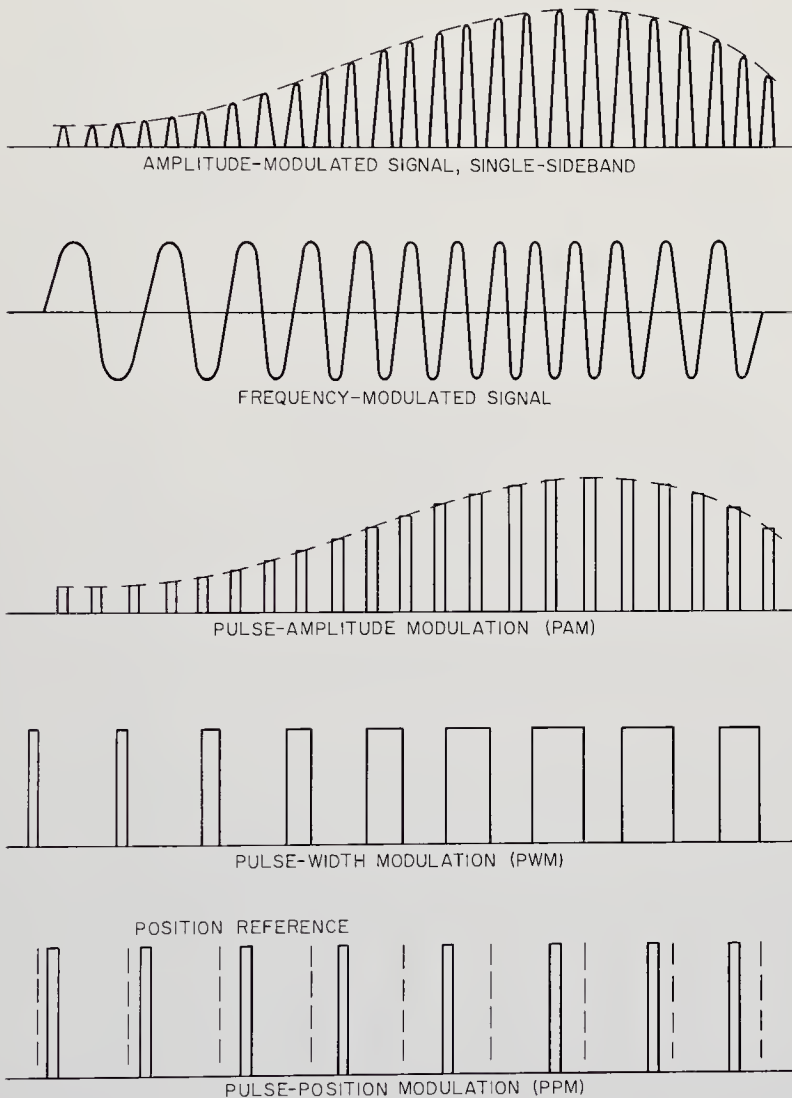


Fig. 6-4. Different kinds of carrier modulation. Each pulse in the last three examples consists of a short train of carrier sine waves. See Fig. 6-5 for pulse-code modulation (PCM).

In searching for better ways to extract information from weak signals in the presence of noise, the trend has been toward pulse-type modulation. Here some property of the carrier is either on or off, in phase or out, or some other two-valued characteristic is switched. The reduction in the number of levels of modulation to two makes detection simpler and more certain. Digital modulation is also amenable to internal verification using the parity bit. Finally, it is more easily manipulated by today's computing machines. The different kinds of pulse modulation are shown in Fig. 6-4. The most important type for space-probe data transmission is Pulse Code Modulation (PCM) (Fig. 6-5).

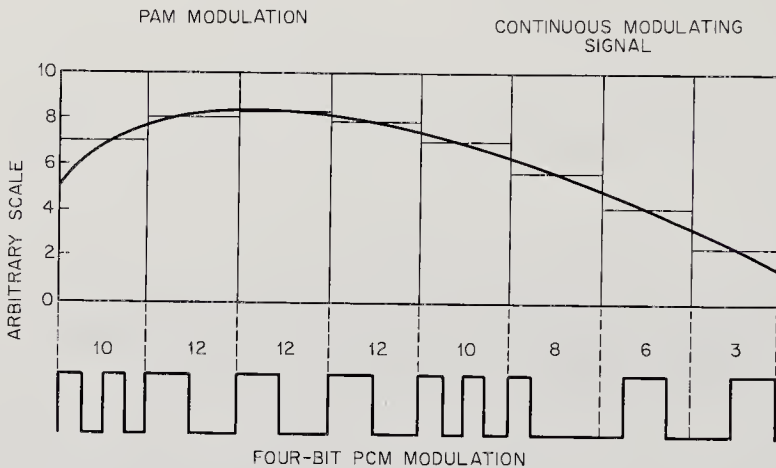


Fig. 6-5. Comparison of PAM and PCM modulation. The PCM pulses are based on a four-bit word. The decimal equivalent is indicated above the word. The full 16-level range of the four-bit words is used here.

With such a variety of modulation techniques, how is a choice finally made for space-probe systems? The correctness of the choice is all the more important when the economic implications are recognized. Although there is always some degree of interchangeability and some technological overlap between different modulation schemes, once a choice has been made and millions of dollars spent in building up equipment and facilities, there is little turning back. Many United States space probes use the PCM/PSK/PM system of modulation developed at JPL. Inherent in this approach is the phase-control feature, an automatic feedback electronic technique that locks the receiver onto the incoming signal. Why was the phase-lock PCM/PSK/PM system of modulation chosen?

1. PCM/PSK systems have very low bit error probabilities in the presence of noise (Fig. 6-6).
2. PCM systems are compatible with standard digital data processing equipment.

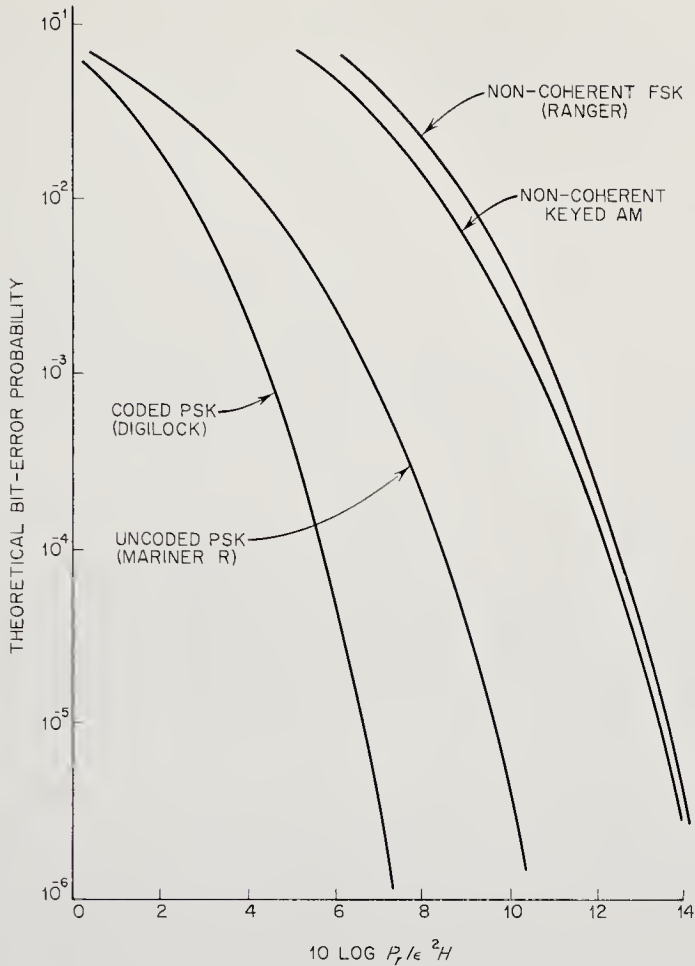


Fig. 6-6. Bit-error rates for various types of coding. The superiority of PSK is evident. On the abscissa:  $P_r$  = received power,  $\epsilon^2$  = Gaussian-noise spectral density, and  $H$  = information rate.

3. A phase-lock system is desirable for proper tracking of the spacecraft. Tracking depends upon the precise measurement of the Doppler frequency changes in the spacecraft signals due to vehicle motion and Earth rotation.
4. The translation into spacecraft equipment is relatively simple.

The phase-lock feature of the JPL system is achieved by a feedback circuit of the type shown schematically in Fig. 6-7. The two voltage inputs to the frequency multiplier are the input signal,  $e_i = \sqrt{2} A \sin(\omega_0 t + \theta_1)$  and the initially arbitrary output of the voltage-controlled oscillator (VCO),  $e_0 = \sqrt{2} K \cos(\omega_0 t + \theta_2)$ . The output of the multiplier is:

$$e_d = e_0 e_i = AK [\sin(\theta_1 - \theta_2) + \sin(2\omega_0 t + \theta_1 + \theta_2)] \quad (6-3)$$

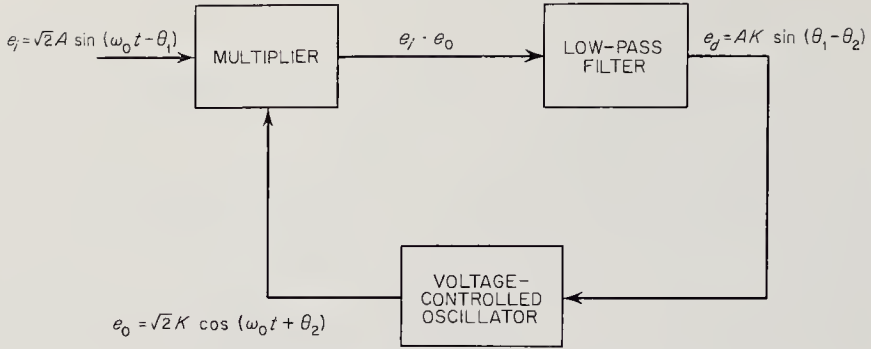


Fig. 6-7. Automatic phase-control loop. The voltage-controlled oscillator varies its frequency until  $\theta_1 - \theta_2 = 0$ .

where:  $A, K =$  amplitudes

$\omega = 2\pi$  times the frequency

$\theta_1, \theta_2 =$  the phases relative to some reference point.

A low-pass filter following the multiplier discards the high frequency component in Eq. (6-3). The frequency of the oscillator is then controlled by the phase difference term. The VCO will track the incoming signal and vary its own frequency until it has locked on and  $(\theta_1 - \theta_2) = 0$  (Ref. 6-25).

One other aspect of carrier signal modulation is multiplexing. All scientific and engineering instruments cannot be monitored simultaneously on today's complex probes and satellites. The bandwidth and power requirements would be too high. Instead, each sensor is sampled periodically by a commutating or multiplexing device such as that shown in Fig. 6-8.

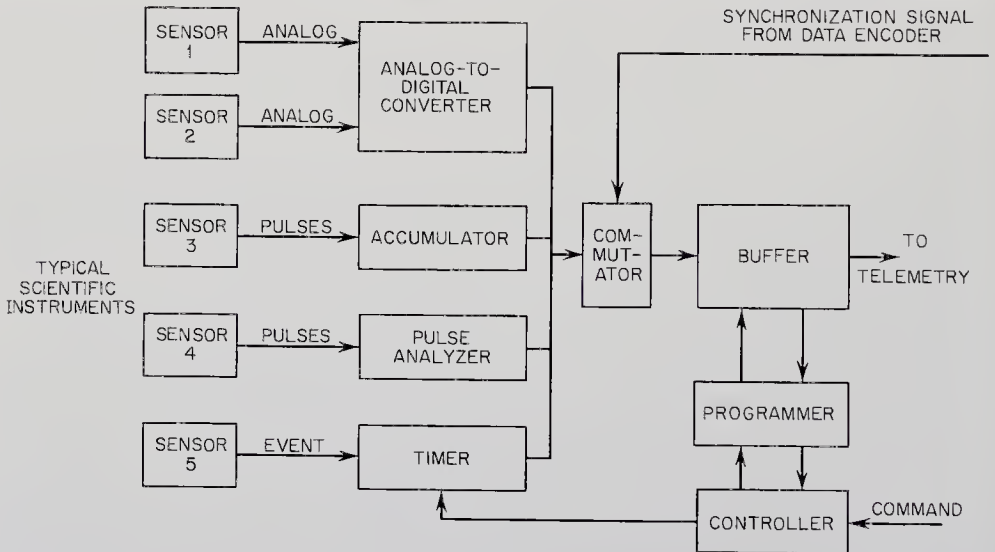


Fig. 6-8. Typical scientific data automation system (Mariner-2 DAS). Engineering data could be handled in the same fashion.



Since most parameters being measured change very slowly, samples may be taken every few seconds or even minutes apart without compromising the experiment. The multiplexer may intermix the engineering and scientific data in various proportions, depending upon what is needed most for the success of the mission at any particular time. Each complete revolution of the commutator or scan of data is called a frame. When the frames are received at the Earth, they must be decommutated, in a process which is the reverse of that occurring on the spacecraft.

In summary, the high frequency radio signals directed toward the earth from a JPL space probe are modulated by a train of phase shifted signals, each shift or lack of it representing a data bit. The bits are organized into words, and the words into frames. Decommutation and detection take place on Earth to reveal the output of the scientific sensors and the engineering status of the spacecraft.

### 6-5. Communication System Design

Many, but not all, parameters affecting the design of a space communication system are related by a single equation. The reasoning leading to this simple equation follows.

The signal power density available at a distance  $R$  from a directional spacecraft antenna is:

$$S = G_t P_t / 4\pi R^2 \quad (6-4)$$

where:  $S$  = power density (watts/m<sup>2</sup>)

$P_t$  = power radiated by transmitter (watts)

$G_t$  = transmitter antenna gain, a dimensionless parameter reflecting the focusing capability of the antenna relative to an isotropic antenna

$R$  = distance or range of transmitter (m).

The power intercepted by the receiving antenna is:

$$P_r = SA_r = G_t P_t A_r / 4\pi R^2 \quad (6-5)$$

where:  $A_r$  = the effective area of the receiving antenna (m<sup>2</sup>).

$A_r$  is related to other antenna parameters by:

$$A_r \equiv \lambda^2 G_r / 4 \quad (6-6)$$

where:  $\lambda$  = the wavelength (m)

$G_r$  = the gain of the receiving antenna.

Substituting Eq. (6-5) into Eq. (6-4):

$$P_r = G_t P_t^2 G_r / (4\pi R)^2 \quad (6-7)$$

The noise power interfering with the reception of the desired signal is

derived from the random thermal energy emitted by all objects within the lobes of the receiving antenna and components of the receiver. Noise power depends upon the temperature of the radiating body. For the purposes of this discussion, the noise power from such sources may be written as:

$$P_n = kTB$$

where:  $P_n$  = noise power (watts)

$k$  = the Boltzmann constant ( $1.38 \times 10^{-23}$  joules/°K).

$T$  = the effective noise temperature of the source (°K)\*

More will be said about noise sources later. Meanwhile, if threshold reception is defined by  $P_r/P_n = 1$ , a range equation may be derived from Eqs. (6-6 and 6-7):

$$R = \left[ \frac{P_t G_t \lambda^2 G_r}{16\pi^2 k T_{sys} B} \right]^{1/2} \quad (6-8)$$

where:  $T_{sys}$  = the total receiver system noise temperature from all sources.

In space communication, the practical range is about one third that indicated in Eq. (6-8). Present state of the art limits  $R$  to about  $5 \times 10^{10}$  km (Ref. 6-17).

*Constraints and Tradeoffs.* In attempting to minimize the denominator and maximize the numerator in the range equation, the fundamental problems in communication-subsystem design stand out vividly.

Radio noise is perhaps the most ubiquitous, unirradicable source of communication-subsystem degradation. Noise is generated by random thermal motion within the electronic equipment itself, in the surrounding environment by lightning and the warm Earth itself, and in the skies by the stars, the Sun, and the planets. The avoidance of external noise and the reduction of internal noise strongly influence over-all subsystem design.

External noise sources begin with the Earth, which radiates noise like a black body at between 200 and 300°K. If the lobe of the receiving antenna intercepts any part of the Earth, the random noise received will overwhelm any signals from the spacecraft. To prevent this occurrence, highly directional antennas must be used. The lobes must be pointed sharply forward, as they are in parabolic and horn antennas. Such directional antennas also have high gains (high  $G_r$ ) and improve the transmission link in this way. They are, however, bulky and must be pointed with high accuracy (Fig. 6-15).

Man-made terrestrial noises, arising from automobile ignition systems and power-transmission lines, force system designers to build their an-

\* In the case of a black body, this is the true surface temperature of the body.

tennas in remote localities. The Deep Space Instrumentation Facility (DSIF) parabolic dishes (actually paraboloids of revolution) are placed in remote, radio-quiet spots near Goldstone, California; Woomera, Australia; and Johannesburg, South Africa.

Some astronomical objects generate large quantities of radio noise. The Sun is a very localized source, radiating prodigious amounts of random noise (Fig. 6-9). Other stars are also strong sources, but they are less important because of their great distances. As long as astronomical sources are localized, like the Sun, the antennas and even the spacecraft trajectories can be programmed to avoid them. The Milky Way, however, contains most of the radio stars in our galaxy and lies

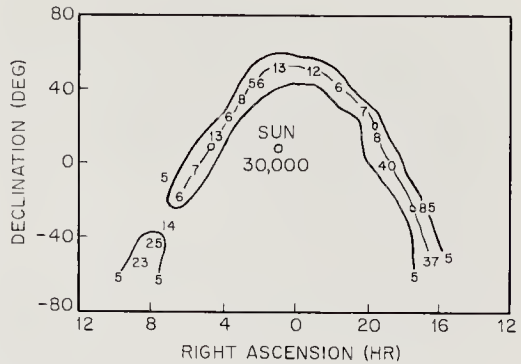


Fig. 6-9. Sky-temperature map at 960 Mc taken with a 26-meter antenna. Noise sources are concentrated along the Milky Way.

in the plane of the ecliptic, just like the trajectories of most space probes. Cosmic noise from these stellar sources is unavoidable and affects the choice of frequency. Figure 6-10 indicates that cosmic noise drops off sharply with frequency, a fact that pushes space communication frequencies towards 1000 Mc and above.\*

The effects of atmospheric attenuation can be accounted for in terms of effective temperatures, just like noise sources. Radio waves arriving from outer space are partially absorbed in the Earth's atmosphere primarily by water vapor and oxygen. The degree of attenua-

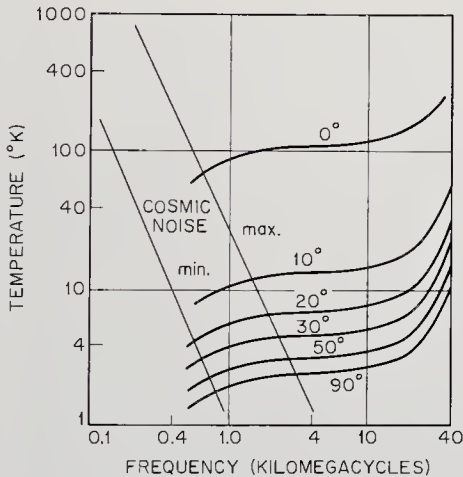


Fig. 6-10. Temperature due to cosmic noise and atmospheric absorption for various elevation angles of the antenna.

tion is a function of the antenna's elevation angle—or equivalently the amount of atmosphere the signal must penetrate. The attenuation is expressed in terms of equivalent temperature in Fig. 6-10. A sharp rise in equivalent temperature around 40,000 Mc indicates that the opaque edge

\* The DSIF, which has operated at 890 and 900 Mc has shifted to 2100 and 2300 Mc.

of one of the radio windows in the atmosphere is being approached (Fig. 2-1, page 8).

Internal receiver noise comes from the random motion of electrons in the circuitry. Major advances have been made in the anti-noise program by replacing hot, noisy vacuum tubes with parametric amplifiers and masers. The maser operating at cryogenic temperatures is generally recognized to be the best present-day solution of the problem of receiver noise. A liquid-helium-cooled maser amplifier—like those used at the focus of the DSIF receiver—has a noise temperature of just a few degrees above absolute zero. On missions where low noise is not critical, signals from the antenna can be fed directly into parametric amplifiers which have noise temperatures around 200°K.

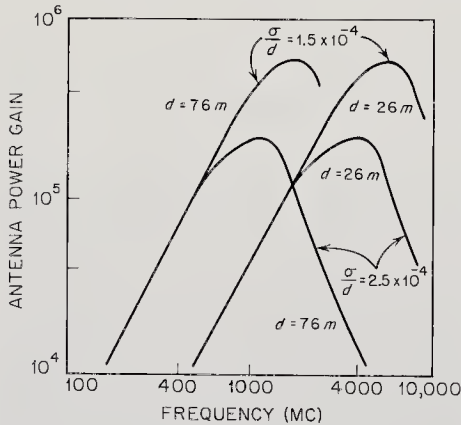


Fig. 6-11. Representative effect of antenna distortions on performance ( $d$  = antenna diameter,  $\sigma$  = deformation).

In comparing Figs. 6-10 and 6-11, the broad minimum in external noise and the maxima in practical antenna gains coincide fairly well. Interplanetary space communications will, at least until lasers prove themselves, take place through the wide window between 400 and 10,000 Mc.

Several other constraints are placed upon communication-subsystem design by the launching vehicles and spacecraft. The maximum physical size of the booster shroud will limit rigid spacecraft antenna diameters to less than three meters during the next ten years. Deployable spacecraft antennas will, like their terrestrial counterparts, be restricted by manufacturing tolerances. The upper limit for unfurlable space-vehicle antennas appears to be about ten meters in diameter.

Spacecraft interfaces again come into play when the beamwidth of the onboard transmitting antenna is being chosen. The sharper the beam, the more precise the attitude-control system will have to be to keep the

In attaining the large antenna areas required by Eq. (6-8), extremely large, steerable, parabolic dishes have been erected around the world, mostly for radio astronomy. Antenna construction is hampered by distortions caused by manufacturing inaccuracies, wind and gravity deformation, and thermal effects. The results of these distortions are expressed in terms of gain reduction in Fig. 6-11. The gains of today's large antennas peak between 1000 and 10,000 Mc, another force operating on frequency selection.

antenna pointed properly at the Earth. As a general rule, pointing accuracy or attitude stability must be about one tenth the antenna beamwidth angle, otherwise excessive signal power will be lost. Many satellites use omnidirectional (isotropic) antennas. Even Mariner 2 used such an antenna while it was close to Earth and while its attitude was being established. Later Mariner 2 switched to a high-gain parabolic dish. The tradeoff between antenna gain and beamwidth is illustrated in Fig. 6-12. The high-gain parabolic dishes are extremely sensitive to attitude

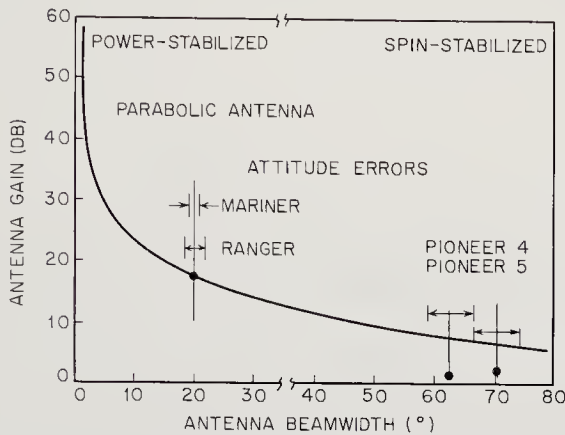


Fig. 6-12. Spacecraft antenna gain vs. antenna beamwidth, showing the effects of attitude errors. (Ref. 6-17)

perturbations, but the performance improvement obtained by their use may be well worth the extra effort in designing a precision attitude-control subsystem.

Electrical power is a scarce commodity on spacecraft, creating a bottleneck that reduces the performance of all vehicle components including the communications subsystem. Larger boosters can inject larger payloads into interplanetary trajectories. In turn, larger power supplies will be built for such craft. But weight is only part of the problem. As power levels mount above 1000 watts, solar-cell panels become huge and increasingly unmanageable. Solar-cell performance also varies during a mission. Toward Mars, the solar flux drops from 1400 watts/m<sup>2</sup> at the Earth's orbit according to the inverse square law. In the direction of Venus, the flux and performance first increase, but eventually the solar cells get so hot that efficiency drops sharply. The advent of compact nuclear power supplies will solve some of the problems. Unhappily, reliable, operational reactor space power plants are several years away. Furthermore, their fluxes of nuclear particles often interfere with space-probe measurements. Space probes are thus power-limited for the next

decade. The next major improvements in bit rate and communication range will stem from increases in available power.

The final major constraint is imposed by the long-lifetime requirements of space probes. The key word here is "reliability," a word often used to describe all the ills that can befall space hardware. The lifetime requirements for space-probe missions are portrayed in Fig. 6-13. For

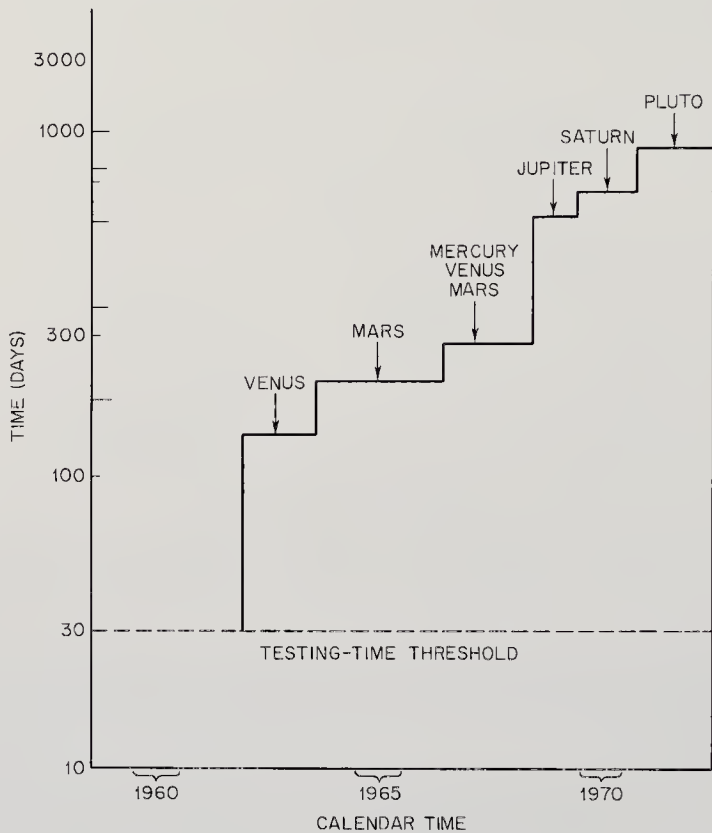


Fig. 6-13. Estimated spacecraft lifetime requirements. (JPL graph)

missions to the nearer planets, lifetimes of six months are adequate; but for exploration of the major planets and the edges of the solar system, several years of successful operation will be demanded from the communication subsystem. For instance, lifetime increases of a factor of five or more over contemporary equipment will have to be demonstrated before Pluto becomes a reasonable target. The rigors of heat sterilization of equipment makes the goal all the more difficult to attain (Chap. 10). Some important steps forward have been made with the introduction of transistors and printed circuits. Further developments in the fields of molecular and solid-state electronics may eventually bridge the lifetime bottleneck.

*The Deep Space Instrumentation Facility (DSIF)*. Data radioed back from a distant spacecraft are first picked up by one or more of the parabolic dish antennas in the DSIF network. From these stations in California, Australia, and South Africa,\* the data are relayed back to the Jet Propulsion Laboratory via commercial teletype circuits and a microwave link between the Goldstone, California, site and JPL. At JPL, the data are fed into the Space Flight Operations Facility (SFOF) shown schematically in Fig. 6-2, where data processing occurs (Sec. 6-6).

The most impressive external feature of a DSIF station is, of course, the huge dish antenna (Fig. 6-15). Paraboloids were chosen over horn

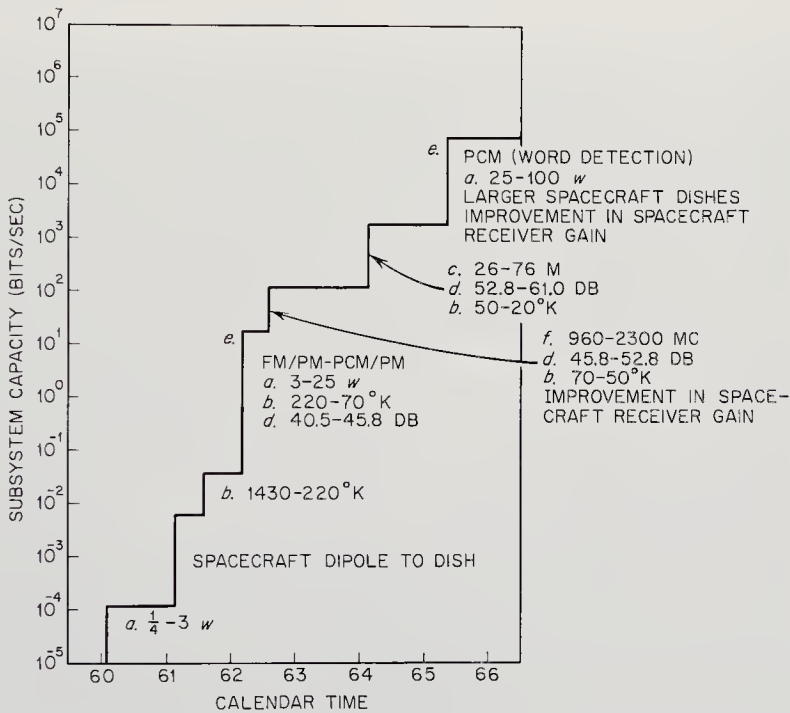


Fig. 6-14. Origin of improvements in interplanetary telemetry capacity: a. increase in spacecraft power capabilities; b. reduction in ground antenna temperature; c. increase in ground antenna size; d. increase in ground equipment gain; e. improvement in coding technique; f. change in frequency. (JPL graph)

antennas for space-probe applications because of their lower cost. Without the large DSIF antennas, with their associated cryogenic masers and parametric amplifiers, the micromicrowatt spacecraft signals would be lost amid the noise. The technical proficiency embodied in the DSIF stations makes interplanetary communications possible.

*Improving the Communication Subsystem.* Except for the reliability

\* Additional DSIF stations will be operational at Canberra and Madrid in 1965.

TABLE 6-2. TYPICAL VALUES FOR PRESENTLY ATTAINABLE DEEP SPACE COMMUNICATION SYSTEMS\*

	<i>Spacecraft-to-Earth Link</i>				<i>Earth-to-Spacecraft Link</i>			
	Moon	Venus	Mars	Edge of Solar System	Moon	Venus	Mars	Edge of Solar System
Distance from Earth (km)	$4.0 \times 10^5$	$5.9 \times 10^7$	$2.2 \times 10^8$	$7.1 \times 10^9$	$4.0 \times 10^5$	$5.9 \times 10^7$	$2.2 \times 10^8$	$7.1 \times 10^9$
Space loss (db)	212	255	267	297	212	255	267	297
Modulation loss (db)	4	4	4	4	8	8	8	8
Miscellaneous system loss (db)	4	4	4	4	4	4	4	4
Spacecraft antenna gain (db)	26	26	23	34	0	0	19	31
Ground antenna gain (db)	53	53	53(61) <sup>b</sup>	61	51	51	51	51
Transmitting power (watts)	10	3	10	50	10,000	100,000	10,000	100,000
Receiver noise spectral density (dbm/cps)	-174	-181	-181	-181	-164	-164	-164	-169
Performance margin (db)	6	6	6	6	43	12	9	6
Data rate (bits/sec) <sup>a</sup>	$7.1 \times 10^5$	56	5.6 <sup>c</sup>	2.2	1	1	1	1

\* Adapted from Ref. 6-24.

<sup>a</sup> Bit error rate  $5 \times 10^{-3}$  for spacecraft-to-Earth link,  $1 \times 10^{-5}$  for Earth-to-spacecraft link.

<sup>b</sup> 61-db antenna will be available for later Mars probes.

<sup>c</sup> Data rate will be 35 bits per sec for later Mars probes when 61-db antenna is available.



barrier, space probes with modest information rates could range the solar system almost at will, so far as the capabilities of the communication subsystem are concerned. This position, so enviable from the standpoints of those concerned with booster and power supply, was not achieved without a number of engineering developments. The most important of these accomplishments are recapitulated in Fig. 6-14. The upward steps, the improvements in performance, came from five basic sources:

1. More spacecraft power available
2. Bigger Earth-based receiving antennas (a 64-meter dish is being installed at Goldstone)
3. Reductions in receiver noise temperatures with the introduction of



Fig. 6-15. The 26-meter (85-ft) paraboloid antenna at the JPL Goldstone station. (Courtesy of the Jet Propulsion Laboratory)

low-noise antenna feeds and cryogenically cooled masers and parametric amplifiers

4. Use of higher frequencies
5. Better coding methods available (PCM/PSK/PM)

Further upward steps in Fig. 6-15 will be accomplished mainly through the employment of more powerful transmitters on the space probe. Reliability does not show on Fig. 6-15, but it could easily be added as a third axis. Improvements along the reliability axis would be achieved mainly by improvements in component design.

### 6-6. Data Processing

An extremely important but often unrecognized link in the communication chain stretching from the spacecraft sensor to the human being who finally evaluates the data is the final piece in the chain, the data processing and display equipment.

An impressive feature of the data arriving from outer space is its quantity. Mariner 2 produced some 90,000,000 bits during its four months of operation. And space probes are niggardly with data compared to the much closer Earth satellites. Satellites may produce millions of bits per day apiece. The longer-lived satellites and probes of the future may number twenty or more active vehicles at any one moment. Some sort of automatic data processing is obviously necessary if proper use is to be made of these new tools of space exploration.

Data automation is the manipulation and partial reduction of data by machinery, notably digital computers. The central idea is to divert the torrent of data into computers directly as it arrives from space vehicles, thereby eliminating the human from the first part of the chain. The computers would separate (decommutate) the channels, add time information, and calculate and insert spacecraft position and attitude data on the record. The machines would finally present tapes, cards, plotted data, or other visual displays to the experimenter.

This machine-made aspect of the final data package worries many scientists, particularly those with long laboratory experience, during which they personally took and reduced many measurements. It is hard enough for the scientist to be separated from his apparatus by millions of kilometers, but harder to be kept from the raw data when it does arrive. The interposition of computers, especially those which may compress data or exert judgment over it, is contrary to the spirit of conventional laboratory research. The fear is, of course, that some unknowing circuit will somehow distort the data—perhaps by discarding data points that are out of line but really highly significant because they represent un-

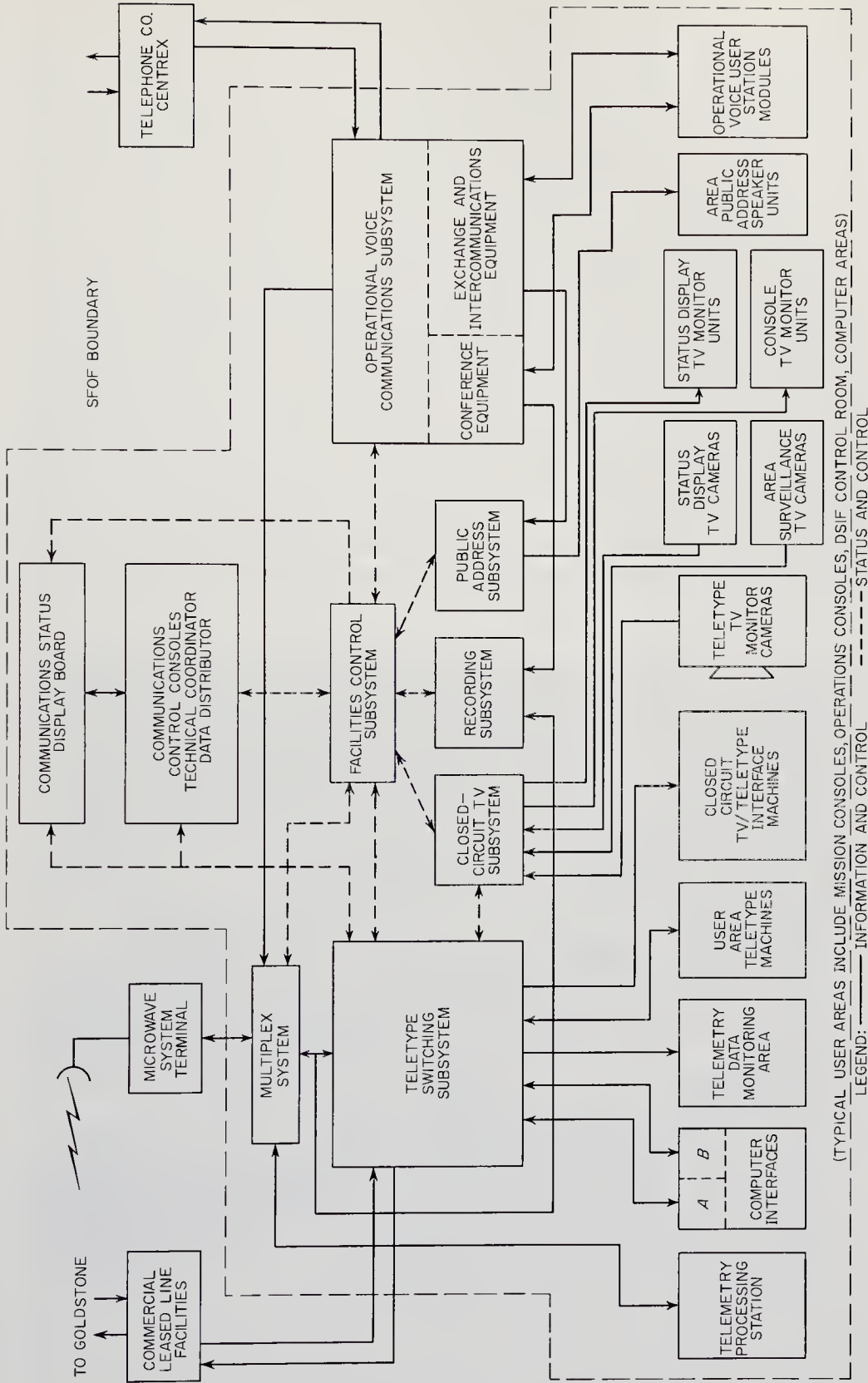


Fig. 6-16. The Space Flight Operations Facility (SFOF) communication lines. The computer interfaces are shown in Fig. 6-18. (JPL diagram)

expected events. This argument goes to the heart of a later subject: automata. Just how far can machines be trusted? The only answer in the case of data handling is that there is no other choice. Space research is out of necessity mechanized, more so than most of Earth-based science. The machines must be designed so that they do not indiscriminately discard valuable data.

Experimenters using interplanetary space probes are in somewhat more relaxed position than those with sensors aboard satellites. There are far fewer bits per second, and launchings are infrequent, because the low-energy launch windows are spaced by many months. There is some time for relatively leisurely data reduction. Furthermore, rarely will there be more than a few probes operating in interplanetary space at any one time. In fact, the large DSIF antennas can track and receive data from only one probe at a time unless the probe employs data storage and programmed transmissions, or unless two probes are within the ground antenna beam and two separate receiver channels are used.

The data deluge may be reduced to manageable proportions in the



Fig. 6-17. Some of the consoles at the Space Flight Operations Facility (SFOF). Mission data are displayed for the operators on the screens and boards. (Courtesy of the Jet Propulsion Laboratory)

case of space probes, but the functions of engineering data analysis and spacecraft command become more difficult than they are for satellites. Such spacecraft actions as midcourse maneuvering, Earth-lock, Sun-lock, and planetary acquisition are all events which must be precisely timed and consummated with a high degree of accuracy. The terrestrial segment of the communication subsystem must therefore provide timely data on the spacecraft status and effective means for directing the mission. The handling of scientific data is not subservient to mission control, but there is a definite shift in emphasis when satellites are compared to probes.

*SFOF Communications.* The JPL Space Flight Operations Facility is linked to the DSIF ground stations around the world by commercial teletype circuits and the Goldstone microwave radio link. The SFOF is that part of the total probe system that takes the scientific and engineering data from the DSIF stations and processes it, records it, and displays portions of it for purpose of mission control and scientific evaluation. The complexity of the SFOF communications block diagram, Fig. 6-16, plus the SFOF consoles and display equipment shown in Fig. 6-17, make it evident that more command and control displays are needed for properly managing a space-probe mission.

The SFOF is used here as a prime example of a data processing facility. Although the SFOF differs somewhat from another NASA system, STARS (Satellite Telemetry Automatic Reduction System, Ref. 6-2), the SFOF is more pertinent, because it has been tailored specifically to

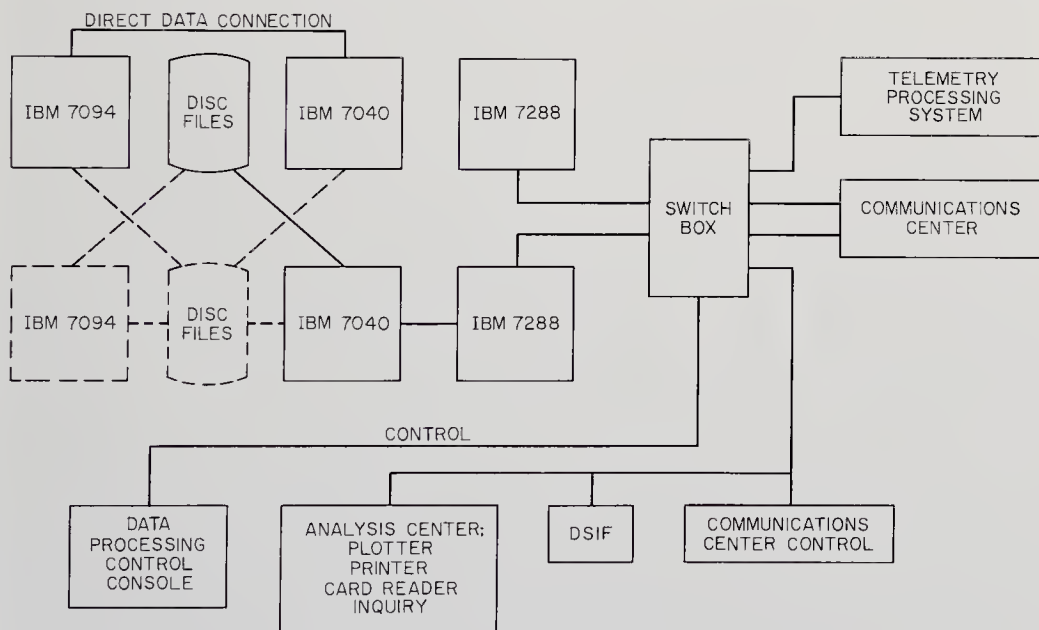


Fig. 6-18. SFOF computer facility block diagram. (JPL diagram)

space-probe systems. Like the DSIF, it is a system-in-being that must be factored into the design of all space probes. Compatibility is essential since no one would countenance the expensive construction of a second set of facilities.

In Fig. 6-16, the two blocks at lower left are pertinent according to their labels, but their functions must be elaborated. The job of the Telemetry Processing System is the conversion of the data received in analog, digital, or composite form to a 36-bit format compatible with standard IBM processing equipment. Both stored information and data flowing into the SFOF in real time can be handled. The Central Computing Complex, Fig. 6-18, is an impressive array of inter-connected digital equipment and data storage facilities. Data arriving from the DSIF can be stored on the two IBM 1301 Disc Files, which have a total capacity of 108,000,000 characters. Two IBM 7040 computers, each with 32,000-word memories, are employed. One is kept in backup status, should there be a failure of the prime computer. An IBM 7094 is the main data processor. After the addition of time, spacecraft position, and spacecraft attitude to the data, the processed data go to the experimenter for further analysis, or it is sent along with engineering data of importance to the several display devices shown in Figs. 6-16 and 6-17. The mission director is kept continuously informed to the probe status by these displays. Side by side with the displays are the command functions permitting rapid and effective control of the spacecraft. In many ways, the SFOF is similar to a military command post—say a SAGE center—in both purpose and layout. There is little choice except to automate a spacecraft control center in this fashion when data arrive in such torrents from successful space vehicles and when commands must be astutely timed.

# Chapter 7

---

## NAVIGATION, GUIDANCE, AND CONTROL OF INTERPLANETARY SPACECRAFT

---

---

### 7-1. Prologue

Every machine requires a control system. It may be only a simple on-off switch, it may incorporate a human operator, or there may be complex electromechanical controls similar in logical makeup to an animal's nervous system. The first satellites were little more than passive, instrumented projectiles. In contrast, the advanced space probes now being studied take on many of the properties of self-controlled automata.

It is a philosophical error, however, to think only in terms of spacecraft control, for a space probe depends upon extensive ground support facilities for accurate launching, guidance to its target, and communication of commands. Continuing the biological analogy, the nerve fibers (wires) carrying command and control information to and from the various subsystems permeate all space-probe system components, even though some of the subsystems may be circling Jupiter while others remain back on Earth. A study of the guidance-and-control subsystem on the interface diagram, Fig. 7-1, shows that almost every subsystem interface is penetrated by an information link across which command and control words flow. In fact, the guidance-and-control subsystem is so intimately embedded in all portions of the space-probe system that it is difficult to dissect it for proper inspection.

The guidance-and-control subsystem is defined by Fig. 7-2. There are two separate paths leading into this subsystem. The communication subsystem relays spacecraft status information, such as environmental-temperature data from thermocouples. The guidance-and-control subsystem responds by making decisions based on this information and passing the internally generated commands on to the proper actuators. Commands

from the Earth and the spacecraft programmer are also brought in by the communication subsystem. In this case, the guidance-and-control subsystem merely interprets and encodes the instructions and then transmits them to the actuators.

In many respects the guidance-and-control subsystem acts like the human brain. The human brain is, in fact, a part of the control subsystem, since it stores commands in the on-board programmer and makes active decisions via the communication subsystem. The midcourse maneuver of contemporary space probes, for example, is directed from the Earth after suitable deliberation.

One of the most important control functions is the accurate guidance of the space probe to its ultimate destination. There is some confusion in the literature regarding terminology. Here, the term *navigation* will be applied only to the measurement of the spacecraft position and velocity relative to the desired trajectory. Navigation includes tracking, inertial measurements, and other position-finding operations. *Guidance* will be used to describe that portion of the control function that deals

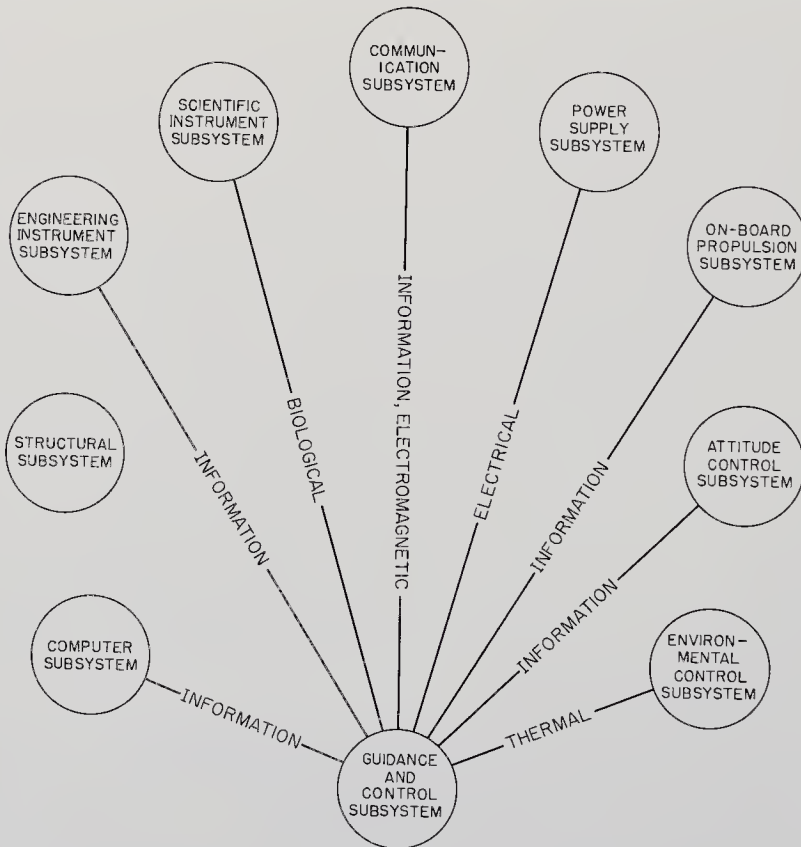


Fig. 7-1. Interface diagram showing the more important relationships between the guidance-and-control subsystem and the rest of the subsystems.



with modifying the trajectory in response to navigational error information.

Trajectory control assumes importance in space flight because small errors early in the launch and injection operations cause large trajectory dispersions in the vicinity of the target. A launch velocity error of just 30 cm/sec (1 ft/sec) at the Earth would cause a probe to miss Venus by 16,000 km! The detection and correction of these small errors by mid-course- and terminal-guidance operations are essential to successful interplanetary exploration. Of course, the proper operation of other control equipment is just as vital to success. Spacecraft attitude control, temperature stabilization, and initiation of planetary scanning are also critical to the space-probe system.

Spacecraft control can draw on the wealth of control theory and device development accumulated over the past century. Probe guidance-and-control subsystems draw most heavily upon advances that have been made in aeronautics and ballistic missile technology. That spacecraft control is already highly developed is shown by the precision of the Mariner-2 Venus fly-by in 1962, the photographic reconnaissance of the other side of the Moon by the Russian probe, Lunik 3, in 1959, and the Ranger-6 and Ranger-7 lunar impacts.

The frontier of control subsystem development now deals mainly with cognitive and adaptive devices; that is, controls that can sense events, make judgments based on this data and its own stored fund of experi-

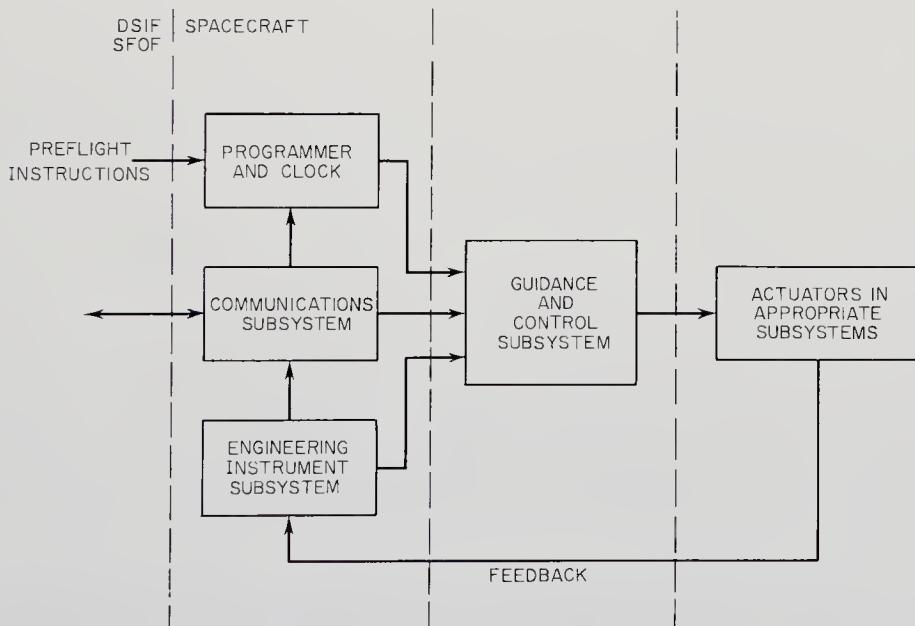


Fig. 7-2. Flow of guidance-and-control data in a space-probe system.

ence, and finally provide the appropriate signals necessary to carry out its decisions. In a span of time probably measured in decades, efforts in this field will lead to space-probe automata which will minimize and perhaps completely eliminate long-distance control of spacecraft from the Earth.

## 7-2. Directable Functions of a Space-Probe System

The essence of control is the detection of a performance deviation and the subsequent correction of the error. Even simple switch functions, such as the turning on of scientific equipment as a fly-by probe approaches the target, can be embraced by this generalization. A good control subsystem always acts in such a way as to reduce the error between actual performance and some established standard. The control subsystem must know what perfect performance is beforehand. Such knowledge is either built into its memory or communicated to it from the ground.

Control functions, like switching, highlight the existence of two different kinds of control. Switching is often an *open-loop* control function; that is, after the switch has been thrown there is no feedback of corrective information to the control subsystem and no further adjustments, as in solar-cell deployment. In *closed-loop* control, feedback of corrective information is provided and the control subsystem will continue to adjust parameters until performance errors have been reduced to within specified minimum values. The thermostatic control of the spacecraft temperature is typical of closed-loop control.

Control functions can also be classified as either *internal* or *external* to the spacecraft. The thermostatically controlled louvers on a spacecraft environmental-control system typify internal, closed-loop control. No directions from Earth are necessary. Present-day space-probe trajectory control, on the other hand, is an external, closed-loop function, because many of the decisions are made on the Earth.

Closed-loop functions incorporating feedback are complicated because the output modifies the input. The phase-lock circuit illustrated in Fig. 6-7 is typical. In this circuit, the amplitude of the output signal was proportional to the phase difference between the incoming signal and the output of the voltage-controlled oscillator. The output signal, however, controlled the frequency of the oscillator, forcing it to lock onto the incoming signal. The mathematical description of circuits with feedback is complicated, and the reader is referred to Mishkin and Braun (Ref. 7-17) and Truxal (Ref. 7-32).

It is easy to make an extensive list showing dozens of spacecraft functions that must be controlled. A few of the most important are listed in Table 7-1.

TABLE 7-1. SOME IMPORTANT SPACE-PROBE CONTROL FUNCTIONS

<i>Function</i>	<i>Classification</i>
Launch initiation	Open, external
Launch trajectory control	Closed, internal
Booster thrust termination	Open, internal
Deployment of solar-cell panels	Open, internal
Midcourse maneuver	Closed, external
Increase fraction of engineering data transmitted to Earth	Open, external
Acquisition of Sun	Closed, internal
Selection of best data for transmission	Closed, internal
Attitude stabilization	Closed, internal
Spacecraft temperature control	Closed, internal
Acquisition of planet	Closed, internal
Scan of planet	Open, internal
Deployment of instrument capsule	Open, external
Sampling of planetary surface	Open, internal*
Change in search mode on planetary surface because of unexpected conditions	Closed, internal *

\* Internal with automata, external if directed from the earth.

The classifications shown in Table 7-1 are not inviolate. As probes become better automated, there will be more closed, internal control functions. The eventual presence of man on the spacecraft will further the shift toward closed, internal control. Although it seems unlikely at the moment, there is always the possibility that unmanned probes might develop more external controls in defiance of the above prediction. This reversal could occur if internal control subsystems prove to be unreliable during the long interplanetary flights. In this case, more of the control subsystem would be left behind on Earth and the burden on the communication subsystem would increase correspondingly. The reliability hurdle for autonomy is a high one; one which cannot be scaled at present.

### 7-3. Space-Probe Guidance

For most space probes, the most important control function is that which insures the interception of a specific target. Before any corrective maneuvers are undertaken, some form of instrumentation must indicate whether the spacecraft is off course and, if so, by how much. For guidance purposes, the trajectory is usually broken up into three distinct parts:

1. *Launch guidance*: from booster lift-off until an Earth satellite orbit or escape velocity is achieved.
2. *Midcourse guidance*: from the launch phase until the target is approached.

3. *Terminal guidance:* in the vicinity of the target. If the launch trajectory could be made accurate enough, it would be possible to dispense with midcourse and terminal guidance, but such accuracy\* is far beyond our present and projected capabilities. On planetary-fly-by missions, however, midcourse guidance is often precise enough so that terminal maneuvers are unnecessary. The cross-sectional target is also quite large for some fly-bys; viz., Mariner 2 (Fig. 7-10). Even though propulsive correction of the trajectory near the planet may not be needed in all three categories, tracking and position finding are always required, otherwise the scientific measurements would have little meaning.

*Launch Guidance.* The launch function is common to all spacecraft. Launch guidance has been under intense development ever since Goddard stabilized his liquid rockets with gyroscopes in 1935. Deviations from the planned launch trajectories can be sensed externally by tracking radar (Chap. 8), or internally by inertial guidance instrumentation (Chap. 10). Both techniques are highly developed and are sometimes used jointly in space-vehicle launchings.

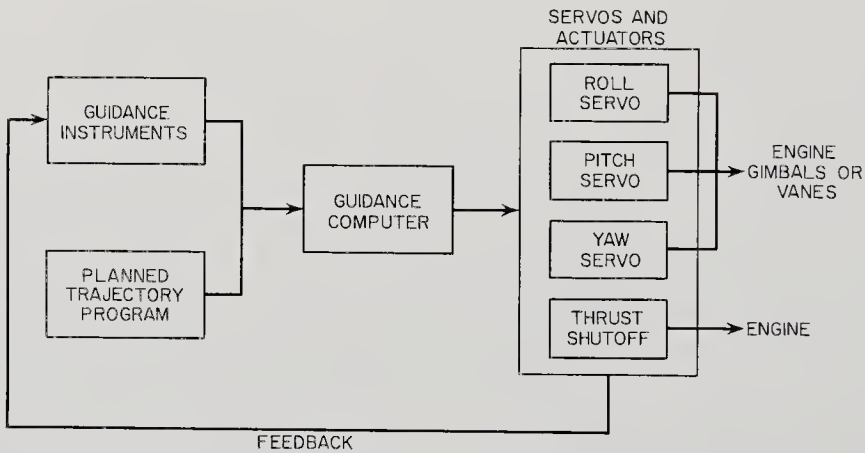


Fig. 7-3. Block diagram of typical rocket ascent guidance-and-control sub-system.

The nominal specifications of the ascent trajectory includes position and attitude coordinates plus vehicle velocity and the flight-path angle (Fig. 7-3). Expressing these coordinates,  $x_i$ , in a generalized fashion, the actual state of the ascending space vehicle at any time is given by:

$$S(x_1, x_2, \dots \dots x_n).$$

\*For a Venus fly-by, the miss distance is about 500 km for every cm/sec velocity error at launch.

The planned, or nominal, trajectory may be different in one or all of the  $x_i$ :

$$S^*(x^*_1, x^*_2, \dots, x^*_n),$$

where:  $x_i$  = the actual coordinates of the space vehicle

$x^*_i$  = the desired coordinates of the space vehicle.

$S$  and  $S^*$  are related by the following equation, which ignores second order coupling terms. Such linear dependence is, in fact, a very common assumption in guidance calculations (Ref. 7-31).

$$S(x_i) = S^*(x^*_i) - \sum_i \frac{\partial S^*}{\partial x_i} \Delta x^*_i \tag{7-1}$$

In the booster control circuits, the coordinate errors are sensed by a combination of inertial instruments and tracking radars and are fed into a guidance computer as shown in Fig. 7-3. The computer signals the booster autopilot to make appropriate changes in course, attitude, and thrust termination time. After the corrections have been made, new and, hopefully, smaller errors are sensed and sent back around the closed loop to the computer for further action. Ascent guidance has been refined to the point where space-vehicle velocities and headings at thrust termination are within a few meters per second and tenths of a degree of the planned values (Fig. 7-4).

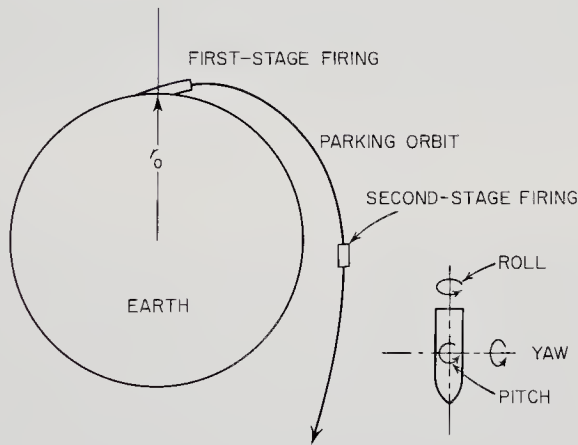


Fig. 7-4. Typical space-probe launch.

*Midcourse Guidance.* As a space probe moves out beyond the Earth's gravitational field, onboard inertial instruments and radar tracking stations become less precise. Inertial devices, like gyroscopes, tend to drift and lose their accuracies over the long periods of time typical of interplanetary flight. It is also difficult to compensate the gyros for the gravitational fields of the disappearing Earth, the gravitationally ascendant

Sun, and other astronomical bodies. Even though radar can be used to measure the distances between the planets, spacecraft are many orders of magnitude smaller and cannot be skin tracked at distances of millions of kilometers with Earth-based radars of reasonable size. With the failure of tracking radars and inertial equipment, spacecraft position finding becomes the job of three other techniques of astronomical navigation (Fig. 7-5).

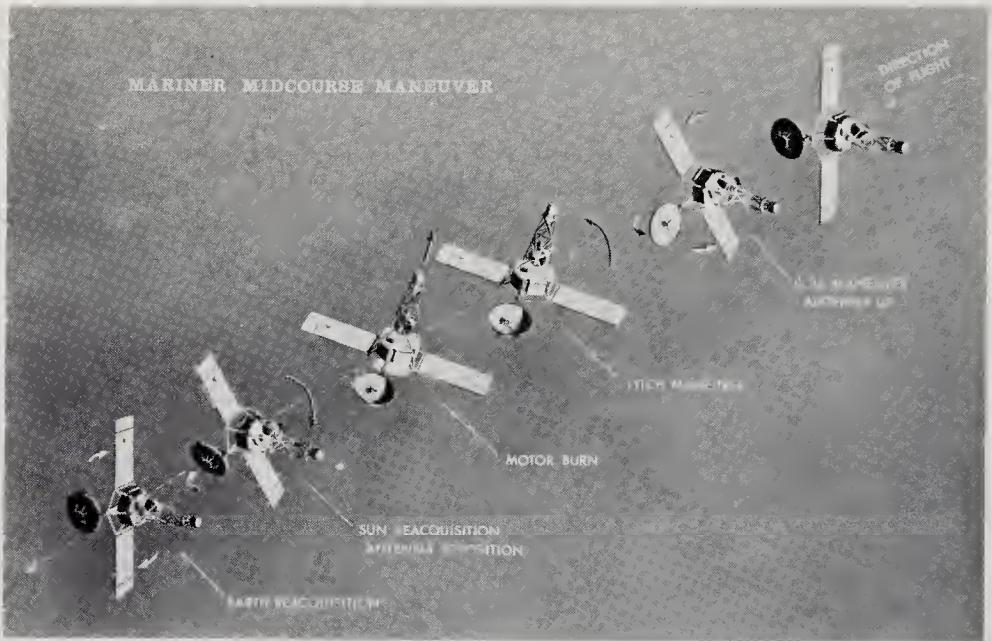


Fig. 7-5. Typical sequence in a space-probe midcourse maneuver (Mariner 2). (Courtesy of NASA)

1. *The radio interferometer*, in which a radio transponder aboard the spacecraft is triggered to transmit an accurately timed and phased signal in the direction of the waiting antennas on the Earth. By measuring the time required for signal transmission, the signal phases at two stations, and the Doppler frequency shift, very accurate measurements of distance, angular position, and radial velocity respectively can be obtained.

2. *DSIF tracking*, in which two angles and a range rate are derived from each DSIF station. Range can also be measured by time-of-transmission calculations.

3. *Celestial navigation*, in which onboard sensors measure the angles between three astronomical objects (usually the Sun is one of these) and the computer calculates the position from these data.

Before any of these three position-finding techniques are brought into play, the launch-phase tracking radars and onboard gyros have already

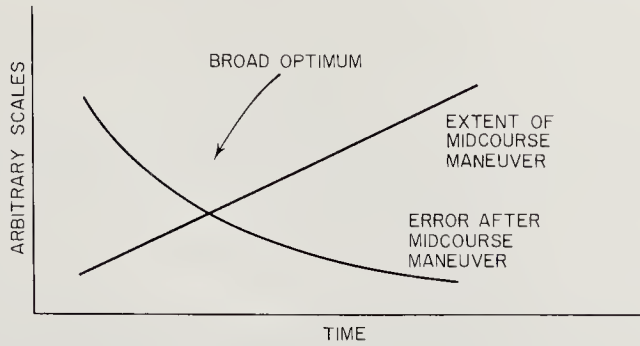


Fig. 7-6. Factors affecting the timing of the midcourse maneuver for interplanetary spacecraft. The longer the maneuver is delayed, the more difficult it is to make.

made fairly accurate estimates of the burden of residual errors carried over from the launch operation. These inherited errors and deep-space forces, especially those due to solar pressure and the solar wind, cause the trajectory to deviate from the planned one. The error estimates must be verified by the navigation techniques listed above before midcourse maneuvering can begin. Dispersion is harder to eliminate late in the mission because of the greater propellant requirements, yet an early correction leaves more time for errors to build up again. In addition, the trajectory is not known with as much precision early in the mission. There are, in fact, optimum times to apply midcourse corrections (Fig. 7-6). The best time to initiate midcourse maneuvers for a planetary-flyby probe is usually between two and ten days after launch.

Before calculating the magnitude and direction of the midcourse im-

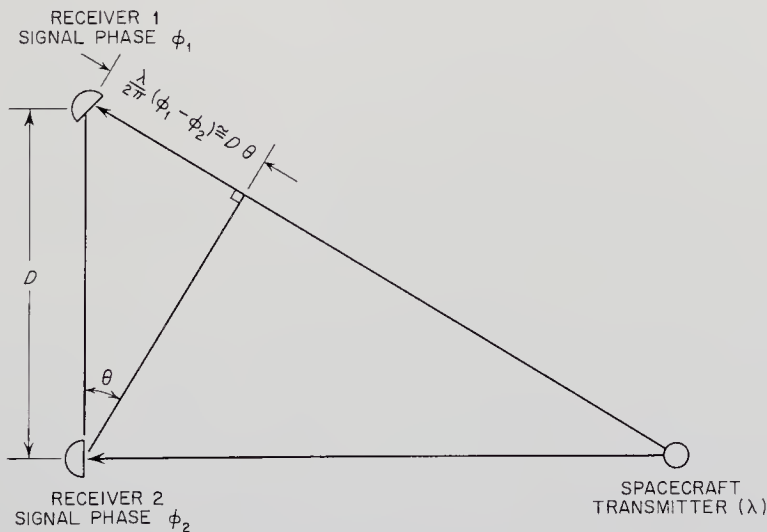


Fig. 7-7. Interferometer principle as used in measuring angular bearing.

pulse, let us examine the different methods of deep-space navigation in more detail.

The interferometer principle is illustrated in Fig. 7-7. Two Earth-based antennas are shown receiving the same spacecraft signal but with different phases. The bearing of the spacecraft is given by:

$$\theta = \lambda(\phi_1 - \phi_2)/2\pi D \quad (7-2)$$

where:  $\theta$  = the bearing angle

$\lambda$  = the wavelength of the electromagnetic signal transmitted by the spacecraft transponder (m)

$D$  = the length of the baseline (m)

$\phi_1$  = the phase of the signal at station 1

$\phi_2$  = the phase of the signal at station 2.

Range data can be derived just by measuring the round trip time of radio signals. The radial range rate may be calculated from the Doppler effect:

$$V_r = \Delta f/c$$

where:  $V_r$  = radial velocity (range rate) (m/sec)

$\Delta f$  = the change in transponder signal frequency due to the Doppler effect

$c$  = the velocity of light.

The Minitrack system is based on interferometry and has been very successful in tracking Earth satellites. Minitrack is accurate to about two minutes of arc for satellites.

The DSIF tracking equipment does not use interferometry to determine the probe's bearing. A transponder on the spacecraft sends signals back to DSIF stations when they are within view. Stations make two angular measurements with their highly accurate 26-meter dishes, plus one Doppler range-rate measurement. These data are sent back to the SFOF by teletype. The SFOF computing facility at JPL continuously refines its estimate of the actual probe trajectory from this information. With a large number of data points and sufficient smoothing time, extremely accurate position estimates can be made; the more data received, the more accurate is the estimate of the probe trajectory. The DSIF pointing angles for the 26-meter antennas are accurate to about 0.1 degree for strong signals. Doppler range-rate measurements are good to  $\pm 0.2$  m/sec. Using the time-of-transmission approach, the range from the Earth's surface can be measured to  $\pm 30$  meters for a strong signal. Range and range-rate accuracies are independent of range. DSIF measurements, which, except for the transponder, are entirely external to the probe, were able to guide Mariner 2 to within 35,000 km of Venus.



Celestial navigation has been employed by terrestrial navigators for centuries to fix their positions on the surface of the Earth. Carefully calculated ephemerides, combined with two or three star observations made with a sextant, are generally adequate to fix a ship's position to within a kilometer or so. In outer space, at least three star or planet observations are needed, as diagrammed in Fig. 7-8. Wheelon has given the following solution to this trigonometric problem (Ref. 7-34):

$$r = \frac{ab \sin (\alpha - \xi - \beta + \eta)}{[a^2 \sin^2 \beta + b^2 \sin^2 \alpha - 2ab \sin \alpha \sin \beta \cos (\alpha - \xi - \beta + \eta)]^{1/2}} \quad (7-3)$$

where all parameters are defined in Fig. 7-8.

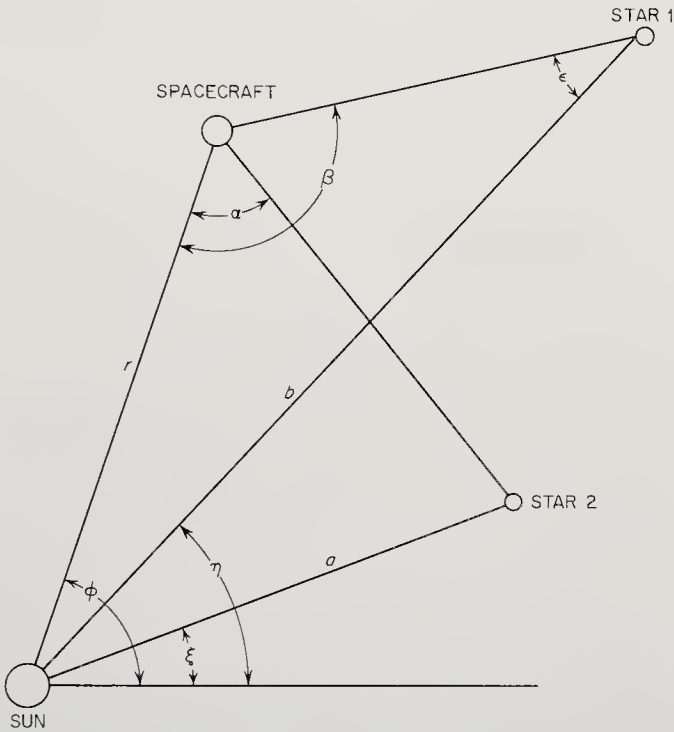


Fig. 7-8. Geometry for celestial navigation. The angles  $\alpha$  and  $\beta$  are measured by sensors on the spacecraft. The parameters  $a$ ,  $b$ ,  $\xi$ , and  $\eta$  are known from ephemerides. (Ref. 7-34)

Celestial navigation is obviously completely internal to the spacecraft. A variety of star-, Sun-, and planet-trackers are available for unmanned spacecraft, but to date no major space probes have utilized celestial navigation.\* This is primarily because the DSIF approach is accurate, simple, and very reliable. In addition, there are no comprehensive ephemerides for space use, though they could be easily constructed.

\* Mariner 4 tracked the star Canopus for attitude-control purposes.

Once the navigational device has accurately measured the deviation of the actual trajectory from the desired one, the magnitude and direction of the midcourse velocity change must be computed. The same procedure was followed with ascent guidance Eq. (7-1). The situation is somewhat more delicate in outer space, because the spacecraft propulsion system must be precisely positioned and the rocket firing carefully timed. Although midcourse maneuvers are small in magnitude (ascent corrections are being corrected), they still have a powerful effect on the accuracy of the terminal portions of the trajectory (Fig. 7-9).

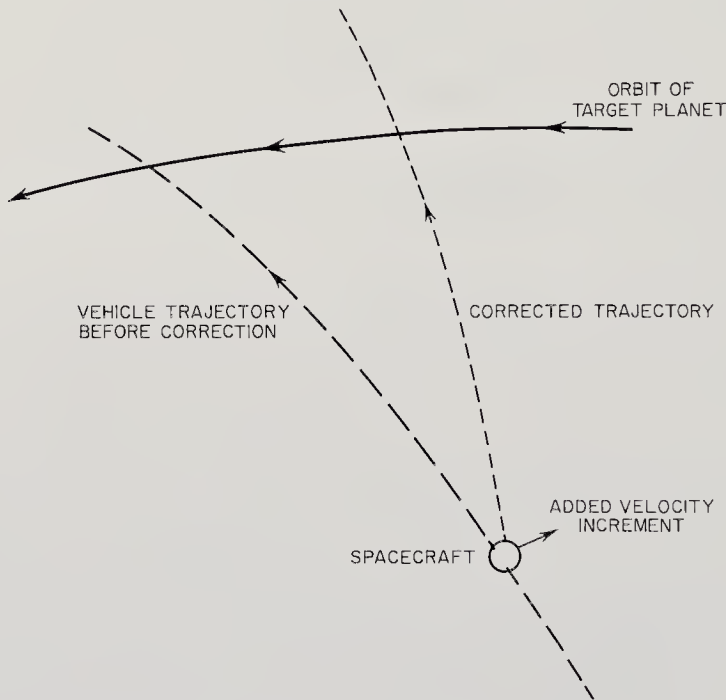


Fig. 7-9. Geometry of the midcourse correction.

If the corrective changes in the actual trajectory are labeled  $dx_1$ ,  $dx_2$ ,  $dx_3$  at a time  $t_2$ , the components of the required velocity increment are given in the equation:

$$\begin{bmatrix} dx_1 \\ dx_2 \\ dx_3 \end{bmatrix}_{t_2} = -H \begin{bmatrix} V_1 \\ V_2 \\ V_3 \end{bmatrix}_{t_1} \quad (7-4)$$

where  $H$  is a three-by-three matrix whose elements are determined from computations made on the standard trajectory at times  $t_1$  and  $t_2$  (Ref. 7-20). Often two midcourse corrections are necessary.

The physical situation can be easily visualized using an aiming plot (Fig. 7-10), which in this case shows the fly-by probe's geometrical target

relative to Venus for the Mariner-2 flight (Ref. 7-1). Mariner 2 was initially injected into a trajectory that would have taken it 373,000 km in front of Venus. This trajectory was well within the accuracy limits of the launch guidance system, but too far from the planet for the scientific instruments. Midcourse maneuver commands were transmitted to Mariner 2 on September 4, 1962, eight days after launch. Two of the commands were directed to the attitude-control subsystem: roll  $-9.33$  degrees and pitch  $-139.83$  degrees to aim the propulsion unit. The third command went to the propulsion unit itself: make a 31.16 m/sec velocity addition to the spacecraft. DSIF communications with the probe confirmed the attitude maneuvers and the firing on the onboard rocket. Mariner 2 eventually passed less than 35,000 km in front of Venus, easily within the aiming plot shown in Fig. 7-10.

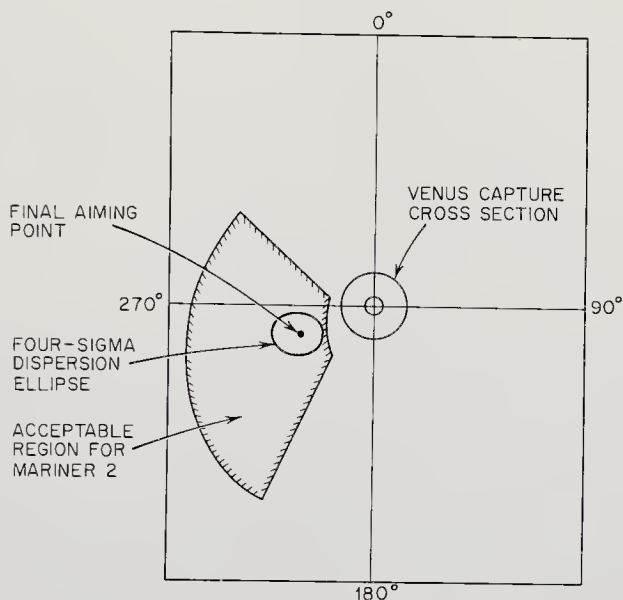


Fig. 7-10. Aiming plot for Mariner-2 shot to Venus in 1962. (Adapted from Ref. 7-1)

In summary, midcourse guidance and maneuvering must remain an essential part of space-probe technology as long as ascent errors are measured in meters per second. In actuality, it is more economical to use simple, vernier midcourse maneuvers than to design superaccurate ascent-guidance systems.

*Terminal Guidance.* During the long months the spacecraft is in transit across interplanetary space, solar radiation pressure and the solar wind are the major sources of trajectory dispersion. As the astronomical target is approached, additional maneuvers may have to be performed to re-

move excessive errors. Maneuvers around the target itself, such as orbital injection, require so much precision that guidance from the Earth is almost out of the question. The transit time of signals from Earth (measured in minutes) rule out external control of probes that may be descending on a planetary surface at 10 km/sec. Except for the relatively undemanding fly-by missions, midcourse guidance is also too coarse for missions involving injection into satellite orbit, hitting a narrow entry corridor, or rendezvous with an asteroid or another spacecraft. Terminal guidance directed from the spacecraft itself is needed.

How does the spacecraft know exactly where it is and what it must do once it has reached the neighborhood of the target? Sightings on the Sun, the Earth, and stars are not precise enough for close-up maneuvers during terminal operations. The target itself must be used as a guide. Optical and infrared sensors provide bearings on the target. An estimate of target range can often be made by measuring the angle subtended by the diameter of the target. Since the true diameter is known from Earth-based astronomical observations, range can be easily calculated by trigonometry. If enough power and weight are available on the spacecraft, radar or laser ranging equipment can be brought to bear, yielding distance, bearing, and range rate. Certainly radar must be used for rendezvous and for delicate landing maneuvers.

In many respects, maneuvers around the target will correspond closely to maneuvers around the Earth. Except for the gas compositions and densities, reentry of the Earth's atmosphere is similar to entry into other planetary atmospheres. Powered descent to a planetary surface has some of the characteristics of the Earth ascent maneuver. In all cases, deviations from the standard or nominal trajectory are sensed by optical, radar, and inertial equipment. Trajectory and attitude corrections can be made by thrust vectoring, and, where an atmosphere is present, by aerodynamic surfaces.

In the case of a precision fly-by, the distance of closest approach has been given by Wheelon (Ref. 7-34) as:

$$\frac{r_0}{l} = \frac{\lambda}{1 + (1 + \lambda^2)^{1/2}} \quad (7-5)$$

where:  $r_0$  = the distance of closest approach (Fig. 7-11) (m)

$l$  = the impact parameter (m)

$\lambda = lV^2/GM$

$V$  = the spacecraft velocity *relative* to the planet (m/sec)

$M$  = the mass of the planet (kg)

$G$  = the universal gravitational constant.

The angular deflection of the spacecraft trajectory after it has passed the planet, assuming no atmospheric braking, is:

$$\psi = 2 \cotan^{-1} (\lambda). \quad (7-6)$$

The distance of closest approach can be made smaller by reducing the relative velocity,  $V$ , or making the impact parameter smaller. Both of these actions are possible with an onboard propulsion subsystem and an attitude-control subsystem. The planetary approach trajectory shown in Fig. 7-11 is hyperbolic because the total spacecraft energy in planet-

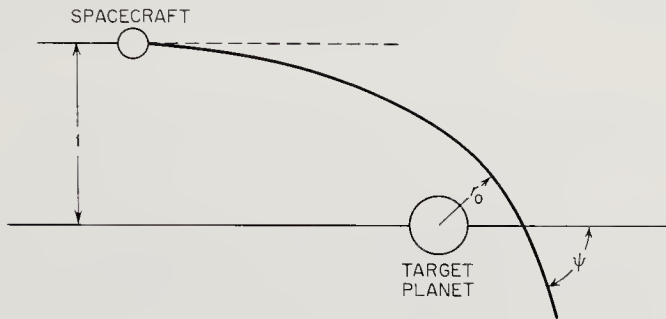


Fig. 7-11. Geometry for determining the distance of closest approach to a planet,  $r_0$ , and the scattering angle  $\psi$ . (Ref. 7-34)

ocentric coordinates is always greater than zero unless a capture maneuver is executed. For planetary capture or satellite orbital injection,  $V$  must be reduced so that:

$$V_c = \left[ \frac{2GM}{r^2} \right]^{1/2}$$

where:  $r$  = the radius of the satellite orbit (m)

$V_c$  = the spacecraft velocity in a circular orbit (m/sec).

Equations (7-5 and 7-6) were derived for planetary approaches without atmospheric drag. When entering an atmosphere at high velocities, the spacecraft must hit a very narrow corridor; otherwise the vehicle will either overshoot and skip out of the atmosphere or it will undershoot and be subjected to excessive deceleration forces. Chapman has derived equations for the width of such corridors (Ref. 7-5). Chapman has also plotted guidance accuracy requirements for entry into different planetary atmospheres. These curves are reproduced in Fig. 7-12. Except for entry into the Jovian atmosphere, the curves show that corridor guidance accuracy requirements are less stringent than they are for ICBMs on the Earth.

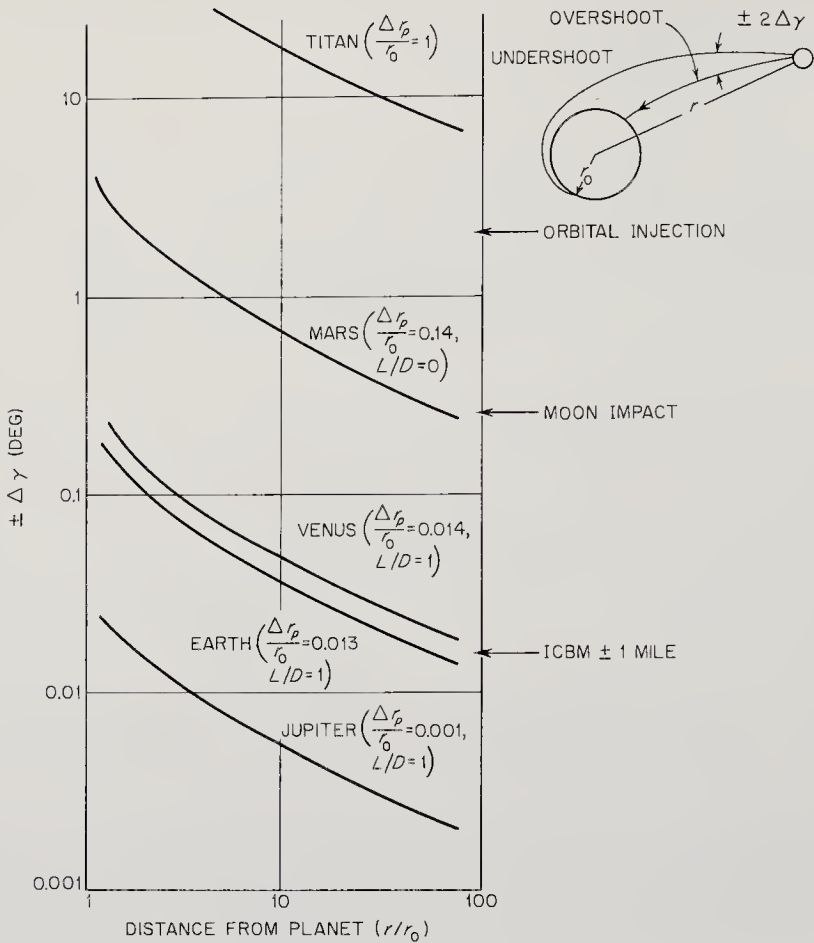


Fig. 7-12. Guidance accuracy requirements on flight angle for single-pass, 10-g maximum, parabolic entries.  $\Delta r_p$  = entry corridor width,  $L/D$  = lift-to-drag ratio. (Ref. 7-5)

All atmospheric entry calculations must be based upon assumptions regarding air density, composition, and distribution. Even with years of telescopic and spectroscopic study of the solar-system planets, the atmospheric models are subject to many uncertainties. Trajectory and guidance computations include this ignorance, making calculated corridor widths for other planets rather questionable. Flyby missions prior to atmospheric entry attempts will undoubtedly sharpen the boundaries of the corridors. One experimental approach involves the launching of a series of experimental entry bodies from a vehicle in a satellite orbit with the purpose of measuring atmospheric properties before committing elaborate and expensive payloads to entry missions. This approach has been termed "precursor guidance." Such preliminary experimentation could also be accomplished from a manned vehicle.

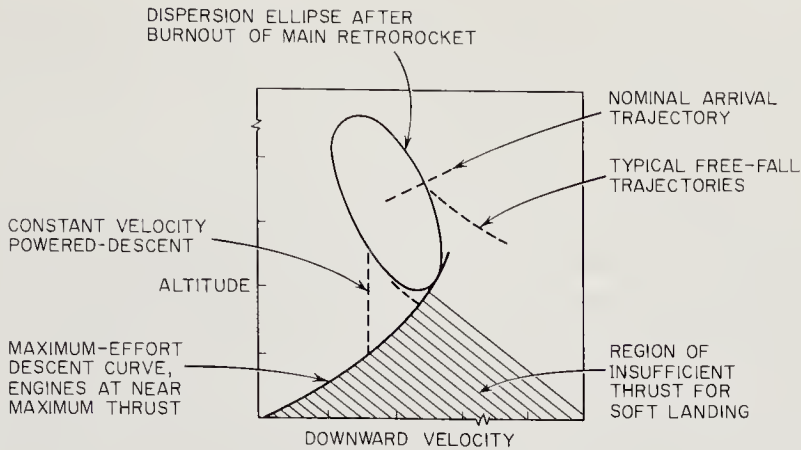


Fig. 7-13. Typical vernier descent trajectory for powered landing on a planet, satellite, or large asteroid. (Adapted from Ref. 7-9)

In the absence of an atmosphere, propulsive braking will be used to set instrumented payloads down gently. The amount of propulsive braking required depends upon the mass of the target and the approach velocity. A general feel for the parameters involved can be acquired from Fig. 7-13. On this altitude-velocity plot, the probe should slide down the slope of the lefthand curve, which is almost perpendicular to the free-fall lines. Ideally, the payload would touch down at zero velocity. Guidance during this delicate maneuver would come from one or more small radars aboard the probe. Figure 7-14 shows a tripod arrangement of radars that would yield altitude above the surface, rate of descent, and possibly spacecraft attitude. Control of the descending

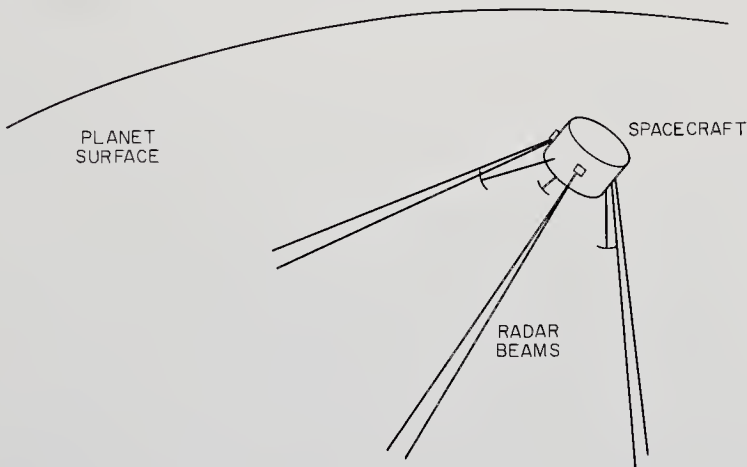


Fig. 7-14. Tripod configuration of radar beams for precision navigation in the vicinity of a planetary surface. Altitude, attitude, and rate of descent can be measured.

vehicle would of necessity reside wholly aboard the spacecraft, not only for the sake of simplicity but also because the long communication lines to the Earth would mean excessive signal delays.

#### 7-4. Other Command and Control Functions

On a spacecraft, just as in a modern home, there are many vital yet unobtrusive control devices. The ubiquitous thermostat that controls the environmental temperature is perhaps the most obvious. The use of spacecraft thermostats to open and close louvers to maintain constant temperature has already been mentioned.

Most of the spacecraft subsystems will incorporate such check-and-balance devices. The power supply, for example, will inevitably boast a voltage regulator. A star tracker will have photosensitive units that will center the tracker on the star of interest. A sophisticated space probe might have dozens of such onboard, self-contained control circuits functioning almost independently of the major channels of command and control.

Many other spacecraft functions are commanded by an internal clock that fixes their sequence and timing. Events like the release of the spacecraft launching shroud, the deployment of the solar-cell panels and communication antennas, and the initial locking of the attitude-control sub-

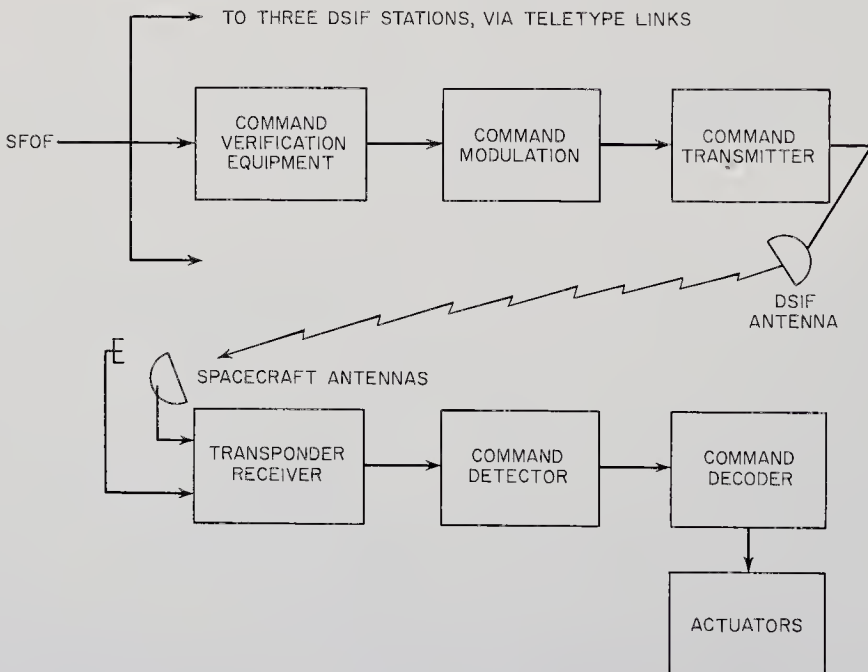


Fig. 7-15. Schematic showing flow of commands from SFOF to actuators on the spacecraft.



system on specific targets are all typical of the commands stored aboard the spacecraft prior to launch. Other commands are not preprogrammed and come directly from the mission director on the Earth through the command communication link. A typical link is shown in Fig. 7-15 and is, of course, part of the regular communication subsystem.

The attitude-control subsystem must properly point the spacecraft scientific sensors, the solar cells, and the communication antennas. During the midcourse maneuver, it must also precisely aim the onboard-propulsion subsystem. In the case of space probes, the spacecraft is usually locked onto specific targets, as mentioned in Sec. 5-6. Since the spacecraft's various degrees of freedom are almost always fixed by reference to sources of electromagnetic energy (visible light, infrared, radio waves), the construction of a closed-loop, source-tracking sensor is an obvious means of guidance. The sensors are linked to gas jets and inertia wheels through conventional control circuitry. The attitude control of a space probe is easier than the stabilization of most Earth satellites, because there is no need for continuous change of attitude as the satellite moves around the Earth.

#### 7-5. Automata

The capabilities of today's machines are well known, but there is intense controversy concerning their ultimate properties, particularly properties related to learning and thinking. Probably the most honest assessment of machines is that their full potential is unknown. Prejudging the situation with generalizations like "Machines will never think, in any sense of the word" or "Thinking machines will eventually control man" is unwise (Refs. 2-24 and 7-24). The facts show that rapid advances are being made in computer technology and in the new discipline of bionics, which is a fusion of biology and electronics. There do not appear to be any provable limitations for machines in the offing.

Today's space probes, except for a few purely internal functions, like temperature control, are, like those of an automobile, all directly manipulated by man. Only the distance between man and machine is different. Now, consider the future—say, the year 2000 A.D.—when technology should have advanced as far again as it did between 1900 and 1950. Already studies of spacecraft data selectors, adaptive planet crawlers, and other partially automated spacecraft are underway. It may eventually be possible to launch probes out beyond Mars with only very general instructions embedded in their computers' memories. Such orders might read:

1. Record all evidences of extraterrestrial life.

2. Bring back ten geological samples from the various moons of Jupiter.
3. Return in five years.

Such instructions are deceptively simple, but no different in character from the "win the game" order given to a chess-playing computer. Probes responding to orders like these would require complex control circuits. There are, however, no fundamental reasons why automated exploring machines cannot be built. In comparison with the "intelligent" automata discussed by MacGowan (Ref. 2-24) probes with functions like those enumerated above would be primitive indeed. The entire solar system can probably be explored with machines not much more advanced than those we already use on Earth today.

In general, the more distant the scientific target, the more adaptive, or intelligent, the machine must be to make up for the loss of Earth communication and command capabilities. When the reliability hurdle has been overcome and spacecraft can operate for several years without human maintenance, then it will be time to talk about reaching out beyond the solar system. On the long trips between the stars, lasting tens of years at least, properties like self-repair and self-maintenance would be valuable. When a target star system is finally approached, a machine with great powers of adaptability will be needed, because the physical conditions at the star, even the number of planets it possesses, will be unknown.

Unless some new method of astronautical transportation is discovered, manned space flight to the major planets and the nearer stars will lag decades behind the probes. Who would wish to spend a lifetime voyaging to a star where only uncertainty waits? Much more likely is the prospect that the first stellar explorations will have the nearest thing to man aboard, a sophisticated, adaptive machine.

There are three approaches to automata:

1. Simple, highly specialized machines with limited memories can be trained by trial and error to run through simple mazes; viz., the mechanical rats that have been so well publicized. These machines are too specialized for most tasks in outer space.

2. General-purpose digital computers that can solve more general problems by trial and error, learning, in a sense, by remembering the correct solutions as they go. Computers can also be given general heuristic rules to follow. Taking an example from Overton (Ref. 7-24), a chess-playing computer should always move a pawn toward the center of the board if it is forking two pieces of equal value. Heuristic rules like this would be useful to a roving machine exploring a planetary surface. An analogous rule might be: When a grade exceeding  $20^\circ$  is encountered,

turn  $45^\circ$  to the right. A machine given enough general rules of this kind would appear superficially to be intelligent. Today's experimental machines that play games and translate languages would have been declared unlikely a few short years ago, and preposterous in 1900.

3. The most general, most adaptive machines are those modeled on the human nervous system. The basic unit, shown in Fig. 7-16, is the

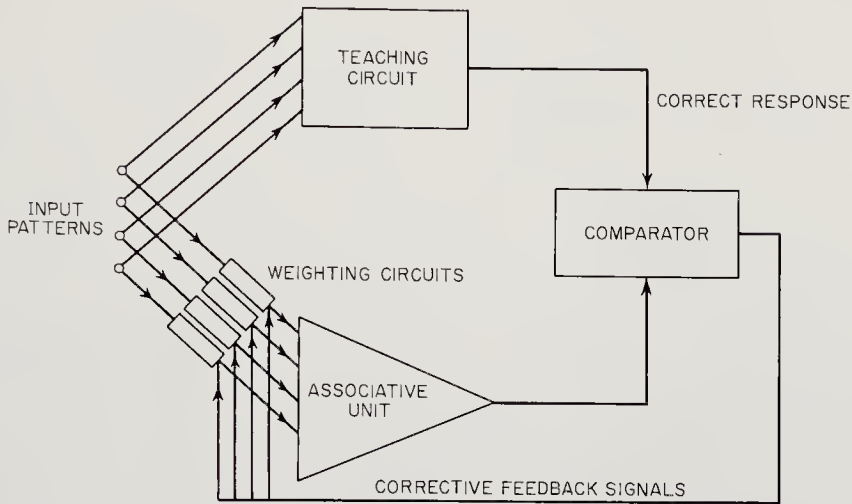


Fig. 7-16. A "learning" experiment in which an incorrect response by the associative circuit results in a modification of the input through adjustments of the weighting circuits.

associative unit, which is crudely analogous to the biological neuron in the animal nervous system. Both are on-off (two-valued) devices. The variation of input signal effectiveness is similar to that of different biological synaptic junctions. The other experimental elements in Fig. 7-16, the teaching circuit and the comparator, can be combined into a learning experiment (Ref. 7-6). Inputs—say from sensors viewing a pattern to be identified or problem to be solved—go to both the associative unit and the teaching circuit. The outputs of the two are compared. If the output of the associative unit is wrong, it is corrected by the teaching circuit, which, of course, knows the right answers. The experiment is repeated until the feedback signals have taught the associative unit to give the right answer. A crude form of learning has transpired.

All three of the approaches just discussed will eventually be used in probe technology. The last is by far the most general, but it is also the least developed. Associative units either based on mechanical or biological neurons can be massed together and function in parallel, rather than in series like the logical elements in a digital computer. In this

way, a machine can be constructed that can be taught to recognize patterns and even situations, depending upon the kind of sensory equipment it has. Circuits can also be installed to permit it to make pretaught, seemingly intelligent action in response to its interpretations of input data. A human observer would undoubtedly be more adaptable, but would also have to be highly trained for the unfamiliar problems to be encountered in space research. The real value of the human would be in handling untaught events. Ultimately, even these situations might be handled by machine. The operational space-probe automaton would be punished for incorrect responses to new situations, perhaps by damage to itself (hopefully self-repairable) or by the loss of data. An astronaut would have to learn by the same unhappy procedure. Automata might not learn as fast as man, but they should be more persistent and rugged.

Although the actions of the machines described above have some of the trappings of intelligence, there are other features, such as deduction and induction, that are difficult to build into machinery. And when can the present heavy, bulky bionic circuitry be made compact enough for spacecraft use? It will be years, perhaps several decades, before spacecraft have many adaptive, cognitive features. Such machine properties are so vital to the exploration of the far reaches of the solar system and, in addition, for penetrating that other hostile frontier, the ocean depths, that there is considerable justification for the development of automata. Little by little, external spacecraft controls will be converted to internal controls, until finally probes can be sent out with only the most general instructions about exploring the universe. One by one they will return with information and samples, paving the way for eventual manned flight beyond Mars and Venus.

# *Chapter 8*

---

## EARTH-BASED FACILITIES AND OPERATIONS

---

---

### 8-1. Prologue

The unmanned interplanetary probes that will be launched during this century will have masses measured in hundreds and even thousands of kilograms. Their launch vehicles will weigh thousands of tons and rival the Washington Monument in height. Even with such gargantuan launch vehicles, if we speak in terms of mass, cost, and complexity, the overwhelming fraction of the total space-probe system never leaves the surface of the Earth. The launch ranges, the Deep Space Instrumentation Facility (DSIF), and the Space Flight Operations Facility (SFOF) must remain behind on Earth to track, communicate with, and process the data sent back across interplanetary space. Modern aircraft, with their large ground crews and support facilities, make a good analogy, but space probes force an even more unequal division of effort. Hundreds of men and billions of dollars' worth of facilities must be assigned to follow the flight of each probe and intercept the data it radiates toward the Earth.

Earth-based facilities become involved long before the booster lifts the space vehicle off the launch pad. When a new space probe is conceived, new ground facilities must be planned or old ones adapted right along with the spacecraft design. There is also reverse economic pressure to use already-developed facilities and launch vehicles that does much to shape the spacecraft design itself. Facility and launch-vehicle compatibility tends to dictate design parameters such as bit rate, spacecraft mass, and launch azimuth. No design starts out with a clean slate. Spacecraft must be built on system foundations that are based in part on Earth-based facilities.

Perhaps it seems a long way from the design of an interplanetary magnetometer experiment to the engineering of a spacecraft umbilical connection at the launch pad, but complete mission success demands that both function properly. Experience has also proven that many seemingly minor engineering tasks are more troublesome and critical to the success of a mission than many a scientific instrument. It is legend that the failure of a ten-cent part can wreck a multimillion-dollar launch vehicle.

Long before the spacecraft is mated with the launch vehicle at the launch site, ground facilities are heavily involved in component testing. Every manufacturer of spacecraft instruments and components is expected to prove his product under simulated flight conditions before it is mounted in the spacecraft. The most thorough *component* testing, however, does not guarantee that the space-probe *system* will function properly. All of the varied mechanical, electrical, and thermal forces that will be impressed on the over-all system during the launch and the flight through space must be duplicated as closely as possible on the ground.

From the point of view of the spacecraft designer, the Earth-based facilities can be divided into three categories:

1. *Test facilities*, where the spacecraft and its components are shaken, heated, put in vacuum chambers, radiated, and bombarded with meteoroid-like particles prior to integration with the launch vehicle.

2. *Checkout and launch facilities*, where the spacecraft interfaces are scrutinized and its instruments calibrated both prior to and after mating with the launch vehicle.

3. *Post-launch facilities*, where the spacecraft is tracked, commanded, and its data received, processed, and presented to human operators and experimenters.

While on the ground, the spacecraft has mechanical, electrical, and many other interfaces with the ground support equipment and the launch vehicle. Once in space, all such ties are severed except the electromagnetic-information interface. The interface diagram, Fig. 8-1, illustrates these spacecraft ties. The most important observation to be drawn from the diagram is that a successful space probe is deeply meshed in a system whose major components are fixed on the Earth. A new probe can be built comparatively easily, but the construction of new launch and tracking facilities is a costly, time-consuming undertaking.

Ground facilities in the three categories just listed have always consumed the major portion of the space dollar. Today, the United States possesses two major launch ranges, several world-wide tracking networks, and dozens of privately and publicly owned test facilities. Most facilities are applicable to many space missions. Even the DSIF and SFOF, which are primarily intended for probe work, are occasionally diverted to other

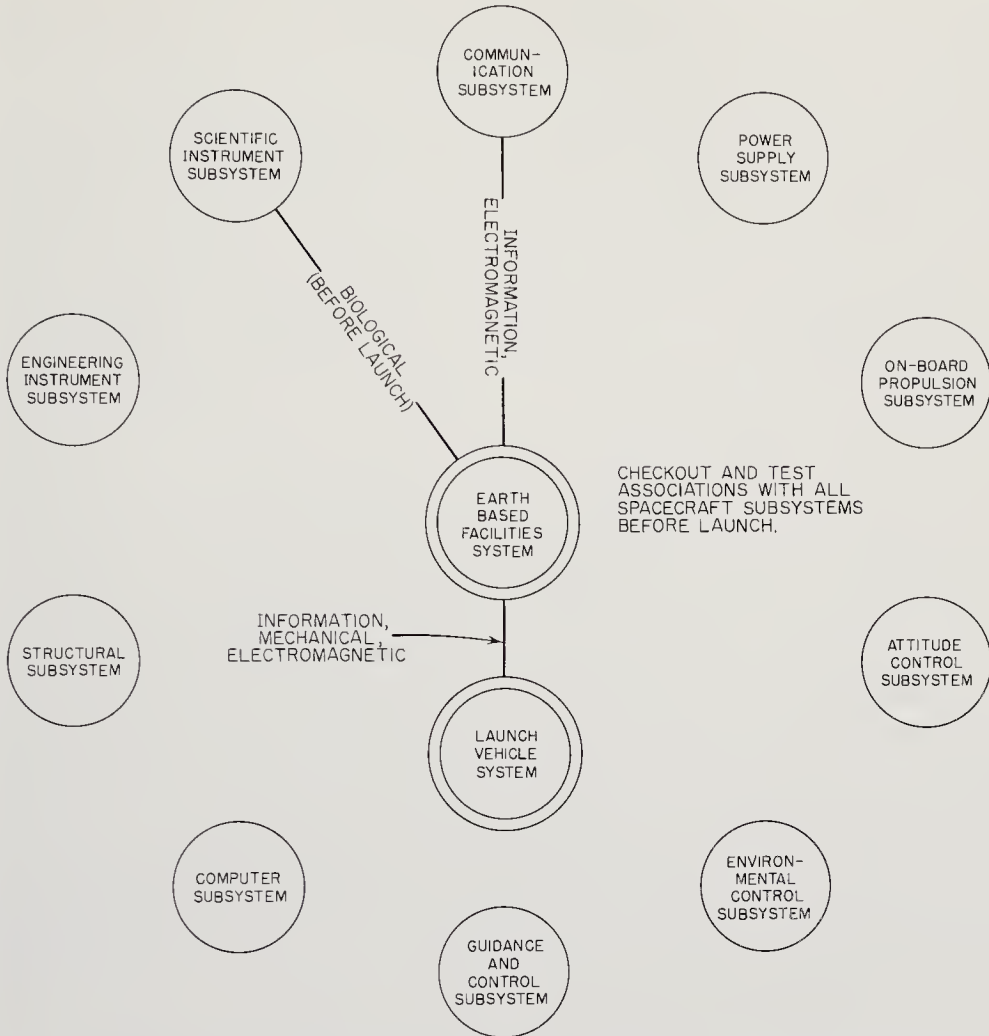


Fig. 8-1. Interface diagram showing the more important relationships between the Earth-based facilities and the rest of the space-probe system.

space activities. Together the Deep Space Net (the DSN includes the DSIF and SFOF) and the Eastern Test Range (ETR) form a billion-dollar complex that can launch probes to the edge of the solar system and record the data they send back.

## 8-2. Spacecraft Testing

Space payloads have dropped back to Earth in flames or have died prematurely once in space because of inadequate testing prior to launch. Of course, undetected poor workmanship and lack of cleanliness have also caused their share of astronomical disasters, but such defects are outside the scope of this chapter. The objective of any preflight test is to determine whether the spacecraft and its component parts will sur-

vive under the forces imposed during launch and out in space. Preflight tests must be distinguished from factory and quality-control checks where parts are examined to see if they meet manufacturing specifications.

The subject of testing is so large that only those aspects pertinent to the spacecraft itself will be dealt with here. Obviously, the launch vehicle, the DSIF-SFOF equipment, and the whole array of ground support equipment must also be tested. Testing should also be separated from checkout. Final checkout takes place on the launch pad just before liftoff. It assumes that the spacecraft and launch vehicle have already proven themselves under simulated mission conditions. The purpose of checkout is to make sure that the space vehicle is ready to go. Checkout queries are electronic in nature; no simulated forces are applied.

The many and diverse forces applied to the spacecraft from launch pad to mission end define the role of preflight testing better than any generalizations about its importance. Such forces arise both within and without the spacecraft. Collectively they make up the spacecraft environment. Not unexpectedly, the internally generated forces (heat, vibration, etc.) can be easily categorized according to the type of interface they bridge. Vibration forces transmitted across the mechanical interface between the launch vehicle and the spacecraft are typical of internal forces. Since the system interfaces are helpful in describing internal forces, perhaps they would also be useful in sorting out the external forces engendered by the vacuum, insolation, and particle fluxes of outer space. Table 8-1 summarizes the total spacecraft environment in terms of interface forces.

TABLE 8-1. DEFINITION OF THE SPACECRAFT ENVIRONMENT

<i>Type of Force</i>	<i>Magnitude</i>	<i>Consequences</i>	<i>Methods of Simulation</i>
Thermal forces:			
Aerodynamic heating	Varies widely	Protective shroud used at launch, ablating nose cone used during reentry.	Wind tunnels, plasma jets
Insolation	1400 w/m <sup>2</sup> at Earth's orbit	Reduces efficiency of solar cells, heat load on spacecraft.	Lamps in space chamber
Planetary thermal radiation	Varies	(Same)	(Same)



TABLE 8-1. Continued

<i>Type of Force</i>	<i>Magnitude</i>	<i>Consequences</i>	<i>Methods of Simulation</i>
Sterilization by heat	125°C for 24 hrs.	May reduce reliability of spacecraft components.	Oven
Internal heat loads	Vary	(Same)	Mission simulation on proof-test model
Mechanical forces:			
Vibration and noise	See Table 8-2 (page 133)	May degrade spacecraft equipment.	Shake tables
Shock	Up to 1000 g for hard landings	(Same)	Drop tests
Inertial	Up to 10 g	(Same)	Centrifuges
Radiative forces:			
Space radiation	See Fig. 3-3 (page 24)	(Same)	Research reactors, accelerators
Nuclear power-plant	Varies	(Same)	(Same)
Magnetic forces:			
Space fields	See Fig. 3-1 (page 21)	May interfere with instrumentation.	Magnets
Internal fields	Varies	(Same)	(Same) And on proof-test model
Other:			
Vacuum	Down to $10^{-8}$ mm Hg	Sublimation of materials	Space chamber
Meteoroid flux	See Fig. 3-5 (page 27)	Physical damage, meteoroid bumpers sometimes used	Light gas guns
Plasma	Up to 1000 protons/cm <sup>2</sup> -sec-steradian	Degrades surfaces	Plasma guns
Time	Years	Reliability effects	Life tests

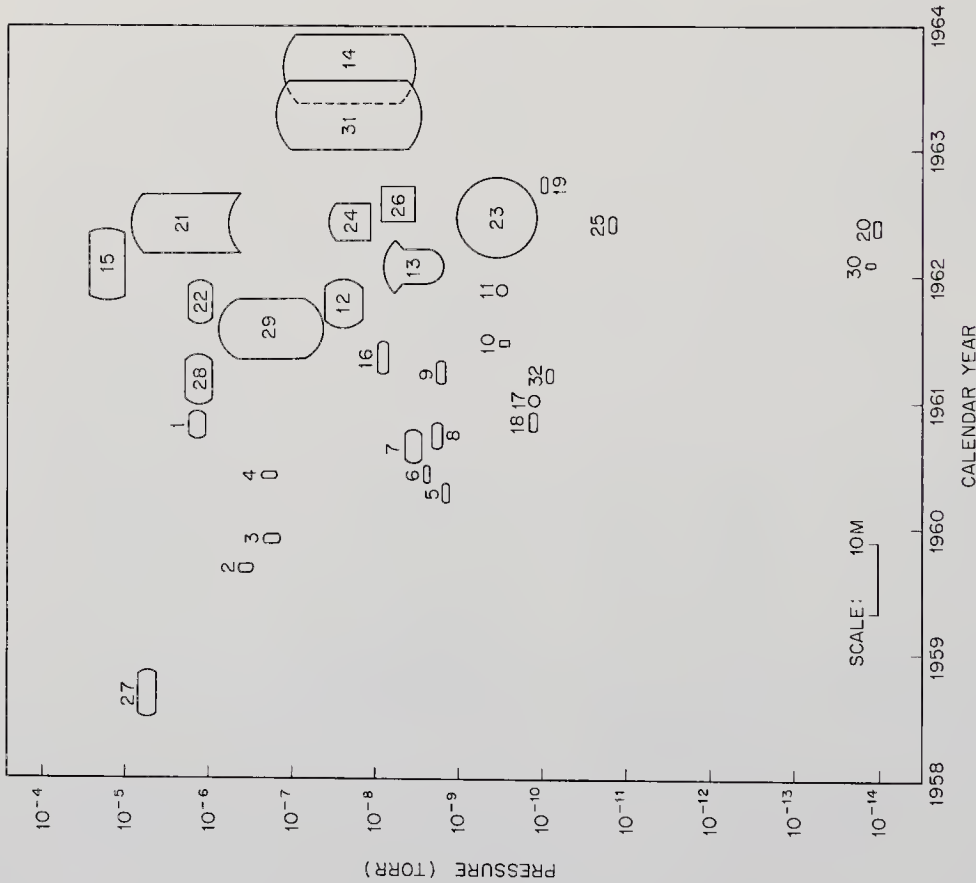


Fig. 8-2. Space-chamber construction history. (Adapted from Ref. 8-11)

1. Thompson Ramo Wooldridge, Cleveland, Ohio
2. USAF, Cambridge Research Center, Cambridge, Mass.
3. Rock Island Arsenal, Rock Island, Ill.
4. Armour Institute of Technology, Chicago, Ill.
5. McDonnell Aircraft Corp., St. Louis, Mo.
6. Fairchild Camera and Instrument, Syosset, L.I., N.Y.
7. Convair, San Diego
8. Grumman, Bethpage, L.I., N.Y.
9. Bendix, Ann Arbor, Mich.
10. Aerojet-General, Azusa, Calif.
11. Electronics Corp. of America, Cambridge, Mass.
12. Bendix, Ann Arbor, Mich.
13. Grumman, Bethpage, L.I., N.Y.
14. USAF, Tullahoma, Tenn.
15. USAF, Tullahoma, Tenn.
16. USAF, Tullahoma, Tenn.
17. National Research Corp., Cambridge, Mass.
18. National Research Corp., Cambridge, Mass.
19. NRC Equipment Corp., Newton, Mass.
20. National Research Corp., Cambridge, Mass.
21. Jet Propulsion Laboratory, Pasadena, Calif.
22. Chance-Vought, Dallas, Texas.
23. General Electric, Valley Forge, Pa.
24. Lockheed, Sunnyvale, Calif.
25. Raytheon, Bedford, Mass.
26. Fairchild Camera and Instrument, Syosset, L.I., N.Y.
27. Litton, Burbank, Calif.
28. Republic, Farmingdale, L.I., N.Y.
29. General Electric, Valley Forge, Pa.
30. NASA-Lewis, Cleveland, Ohio
31. NASA-Goddard, Beltsville, Md.
32. Consolidated Vacuum Corp., Rochester, N.Y.

The final column in Table 8-1 lists representative ways of simulating the different features of the spacecraft environment. The large, evacuated space chamber, with its liquid-nitrogen-cooled walls and artificial sun, is the typical test tool of the space age. Dozens of such space chambers have been built, and more are in the construction stage. The construction histories and vacuum capabilities of these space chambers are summarized in Fig. 8-2 (Ref. 8-11).

Space chambers can simulate the vacuum of space and the Sun's rays, but the magnetic fields, meteoroid fluxes, and nuclear radiations are usually duplicated in separate, specialized facilities. No single facility exists which can simulate all components of the environment. Even when all environmental test facilities are taken collectively, serious gaps in the coverage emerge. The high-velocity end of the meteoroid spectrum cannot yet be duplicated here on Earth. Even the Sun's rays are difficult to duplicate; the rays must be intense ( $1400 \text{ w/m}^2$  at the Earth's orbit) and almost perfectly collimated if heat-transfer experiments are to be accurate. The need for accurate solar simulation was brought out during the Mariner-2 mission to Venus, when the spacecraft experienced much higher temperatures than were expected on the basis of tests using resistance heaters attached to the spacecraft, rather than a radiant heat

TABLE 8-2. TYPICAL SPACECRAFT VIBRATION AND NOISE TESTS\*

*Axial vibration complex wave test:*

Time (sec)	Type of Signal	RMS $G$ Level
0-15	Noise**	1.0
15-30	None	
30-36	Noise**	3.5
36-216	Sinusoid †	1.0
216-516	Noise** plus sinusoid	1.22
	Noise alone	1.0
	Sinusoid alone	0.707

*Pitch and yaw complex vibration test:*

Time (sec)	Type of Signal	RMS $G$ Level
0.15	Noise**	1.0
15-30	None	
30-36	Noise**	4.5
36-186	Sinusoid †	0.5
186-486	Noise** plus sinusoid	1.4
	Noise alone	1.0
	Sinusoid alone	1.0

\* Table adapted from Ref. 8-18.

\*\* White Gaussian noise, band-limited between 15 and 1500 cps.

† Sinusoid-swept from 6 to 40 cps at a rate increasing directly with frequency.

source. Later space-chamber tests with a spare Mariner, using lamps to represent the Sun, confirmed the high temperatures radioed back from the vicinity of Venus (Fig. 8-3). The only true tests come in space itself.

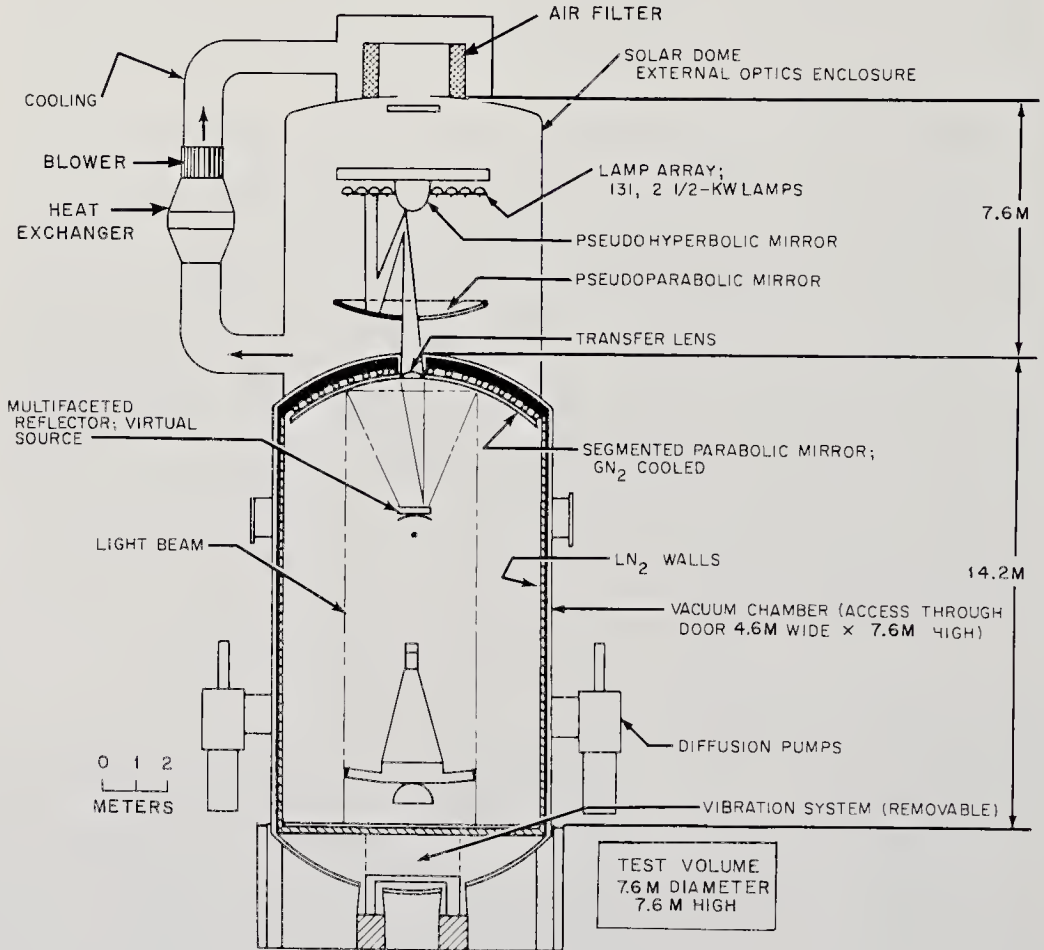


Fig. 8-3. Cross section of the JPL space-probe environmental test chamber. The critical insolation tests are carried out with the lamp-mirror system. (JPL drawing)

In some cases, prototype spacecraft are actually sent into space before launching operational models.

Environmental tests are rigorous and sometimes reveal serious flaws in spacecraft design, but more difficult trials are yet to come. Suppose that a spacecraft has been assembled from components that have survived critical quality-control tests as well as all pertinent environmental tests (Table 8-1). The spacecraft is still a long way from the launch pad. The electrical, mechanical, and thermal bonds that bridge its many interfaces can be completely tested only under dynamic conditions, where the whole system operates as it would in space. A series of tests must

be designed to see whether an assemblage of perfect parts can function together to make a perfect system.

Often a separate proof-test model of the spacecraft is built solely for making system integration tests. At other times, the system integration tests are performed on the actual vehicle to be launched. In many respects, the system integration tests are akin to the system checkout carried out on the launch pad. McGee (Ref. 8-18) has listed the following objectives for a proof-test model:

1. To verify the spacecraft design.
2. To demonstrate compatibility with the launch vehicle.
3. To demonstrate compatibility with the ground-support equipment.
4. To investigate the effects of proposed engineering changes.
5. To carry out special tests such as magnetic interference studies and midcourse engine firings.
6. To finalize test plans and procedures for the flight model.
7. To train personnel.

In addition to the proof-test model, a major space-probe program may require a thermal-control model, a mechanical-test model, a design-evaluation model, and finally a life-test model. (See Fig. 8-4.)

Following McGee's approach, a series of typical spacecraft system tests is described below.

1. *Subsystem tests.* Each subsystem is tested with its associated ground-support equipment to prove that it operates satisfactorily relative to the rest of the space-probe system. Subsystem power levels, cable connections, remote transducers, internal and external RF interference, information interfaces, and other factors are all checked.

2. *Over-all spacecraft test.* This test should verify that the spacecraft will function satisfactorily during flight. All subsystems are carefully monitored to detect any undesirable interactions; viz., RF noise. Usually a number of system tests are needed before all interface problems are identified and corrected.

3. *Weight, moment-of-inertia, and center-of-gravity tests.* Accurate measurements of the static and dynamic properties of the spacecraft are important for attitude-control and guidance-and-control subsystem evaluations.

4. *Radio-frequency-interference test.* Subsystems aboard the spacecraft are operated to determine whether radio interference exists. RF signals from ground-support equipment and the DSIF are also simulated.

5. *Pyrotechnic shock tests.* All pyrotechnics on the spacecraft are fired in proper sequence to determine their shock effects on the operation of the subsystem.

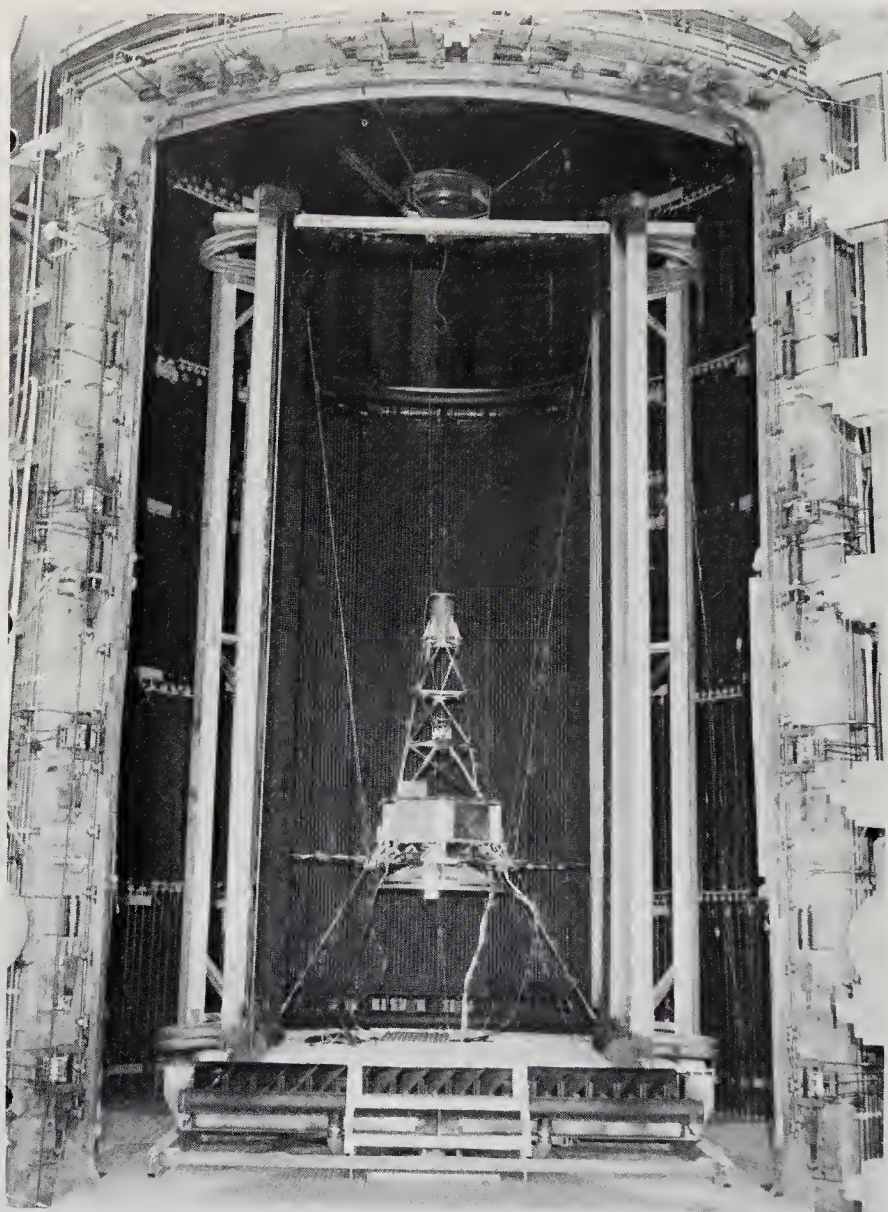


Fig. 8-4. A Mariner-type spacecraft being tested in the JPL space chamber. The temperatures actually observed on the Mariner-2 Venus flight were duplicated later in this chamber. (Courtesy of the Jet Propulsion Laboratory)

6. *Match-mate tests.* Mechanical mating, electrical connections, shroud mounting, and tolerances between the spacecraft and the launch vehicle are checked. The umbilical connections with the ground-support equipment are also tested.

7. *Dummy-run test.* Real-time operations during the preflight count-

down are simulated to establish the dynamic compatibility of the spacecraft and ground-support equipment at the launch pad.

8. *Closed-loop operations test.* These tests check the compatibility of the spacecraft and SFOF. The spacecraft is operated in real time. Telemetered data are radioed directly to the SFOF for a check of data handling, data reduction, information display and analysis.

Most of the tests listed above are performed at the site of spacecraft manufacture. After the arrival of the spacecraft at the launch facility, many of the tests are repeated before the spacecraft is mated to the launch vehicle. Once on the pad, final checkout occurs.

### 8-3. Launch Operations

The spacecraft received at the launch facility has been thoroughly tested under conditions as nearly like those that will be encountered on the mission as possible with terrestrial equipment. The spacecraft, however, is not yet ready for flight. First, it will be taken to a test building well away from any launch pad. There, some of the tests outlined in the preceding section will be repeated to insure that no damage has occurred during transit. The spacecraft then goes to the launch pad for mating with the launch vehicle and final checkout. Assuming a satisfactory checkout and countdown, good weather, and the readiness of downrange equipment and the DSIF-SFOF facilities, launch will take place.

*Checkout and Countdown.* When the spacecraft is finally hoisted and maneuvered into position atop the launch vehicle's uppermost stage, it becomes another component in a complex, far-flung system of ground-support equipment, tracking and communication stations. On the launch pad, the main link between the spacecraft and the rest of the space-probe system is through umbilical connections that consist of connections for electrical power, inert gas, hydraulic pressure, and electrical signals (Fig. 8-5). This link will be severed at launch, leaving the spacecraft to function on its own resources and to communicate through the more tenuous radio link. Before the umbilical is finally broken at liftoff, it carries the long series of electrical checkout interrogations into the spacecraft and returns the responses to the checkout equipment on the launch pad.

Launch-pad checkout and preflight testing are close relatives. The objectives of the final launch-pad checkout are:

1. Final calibration of the onboard instrumentation.
2. The detection and identification of faults that may have occurred since the preflight tests or which may have gone undetected until actual mating with the launch vehicle on the pad.

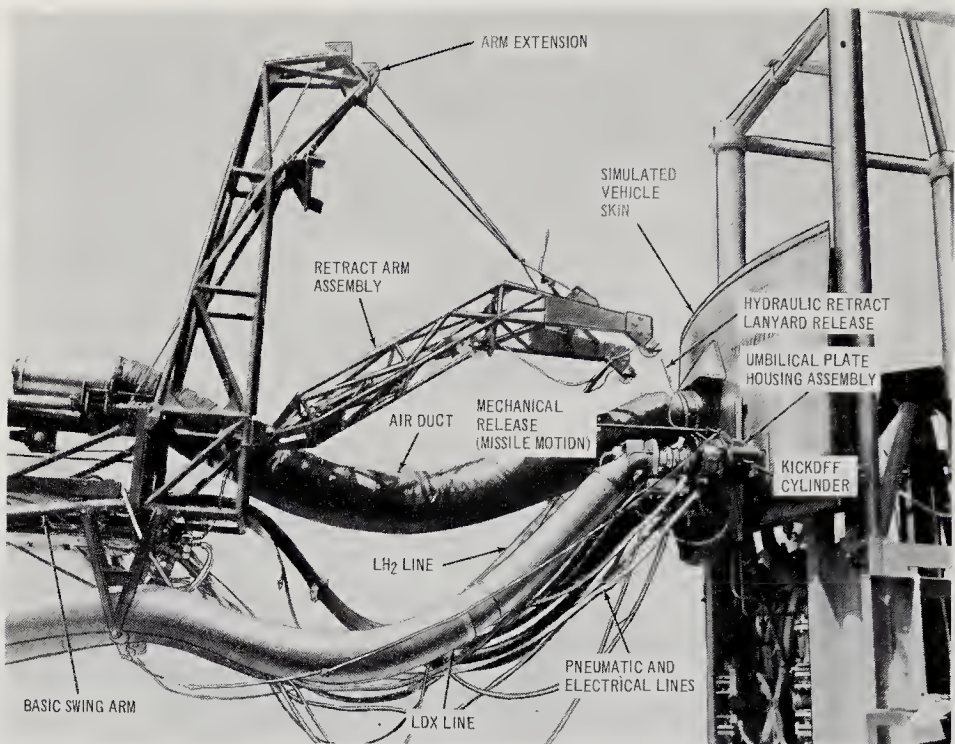


Fig. 8-5. Some of the umbilical connections for the Saturn S-IV stage shown attached to a vehicle simulator. (NASA photograph)

3. Final verification and double-checking of system operational readiness.

Launch-pad checkout has the aspects of a question-and-answer game between the checkout equipment and the spacecraft. A stimulus (question) is sent to the spacecraft through the umbilical connection. A response is received and compared with the correct answer. A wrong answer from the spacecraft will delay launch until the trouble can be spotted and fixed.

Some typical checkout tasks are:

1. Calibration of onboard instrumentation, both scientific and engineering (status-indicating).
2. Electrical continuity tests to pinpoint any damage during final assembly.
3. Spacecraft subsystem interrogation to ascertain flight readiness; viz., measurement of power-supply voltages.
4. Calibration of the communication equipment.
5. Simulated flight test, during which the whole countdown procedure is simulated through launch, ascent, and final spacecraft separation. Responses to simulated commands are also checked.



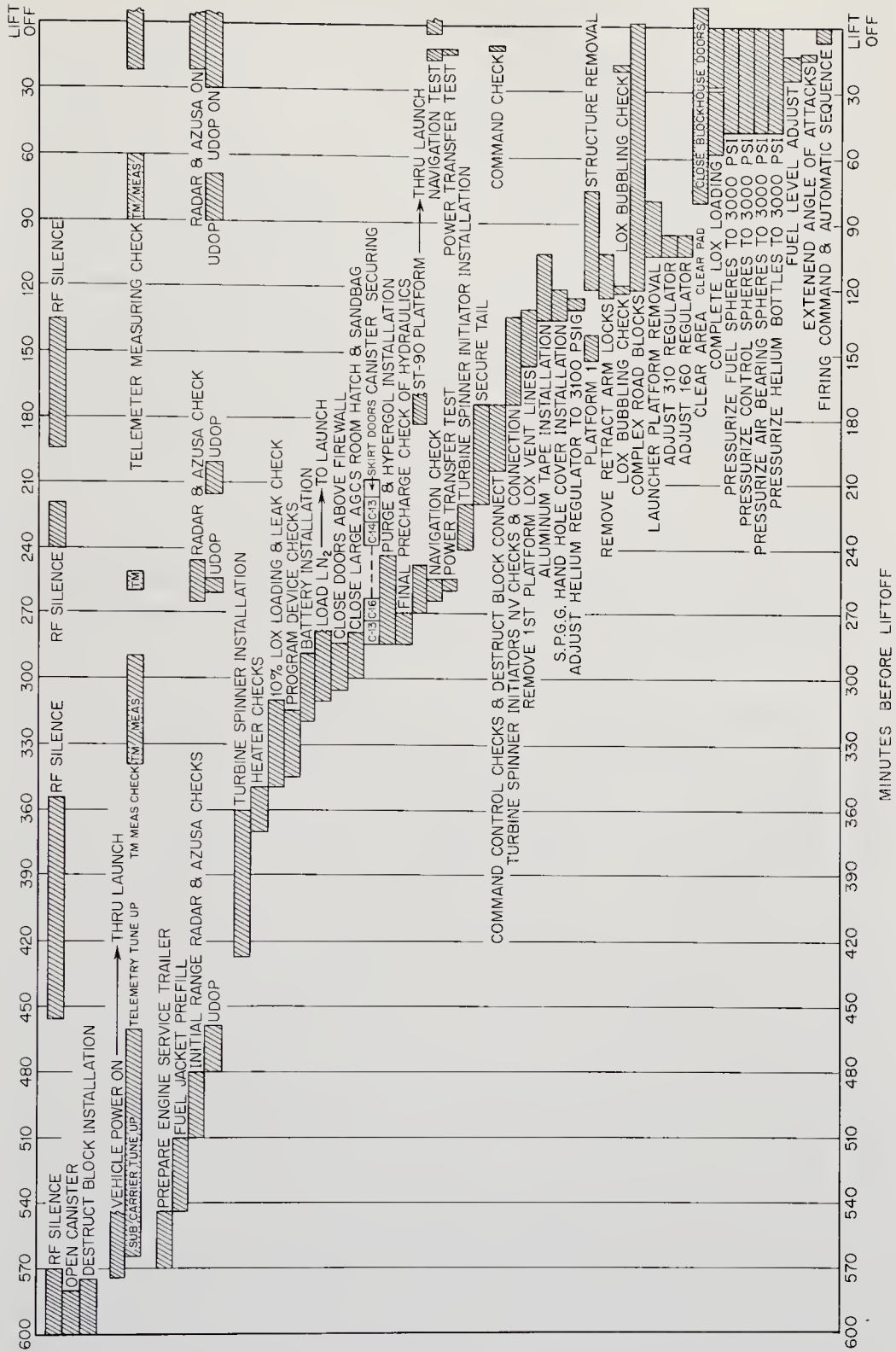


Fig. 8-6. Typical countdown sequence for a large launch vehicle. (NASA drawing)

While the spacecraft is undergoing such questioning, the launch vehicle and all Earth-based facilities receive the same treatment. During the actual countdown, there will be further checkout queries, but then the major operations concern topping the propellant tanks, pressurizing gas bottles, checking for leaks, and starting launch-vehicle rotating equipment. Figure 8-6 summarizes the events that transpire during a typical space vehicle launching.

The subject of Automatic Checkout Equipment (ACE) is controversial. There are conflicting opinions concerning how much automation there should be in the face of several distinct advantages and some serious drawbacks. A discussion of Automatic Checkout Equipment also reveals many of the problems incurred during a vehicle launching. First, some of the advantages:

1. Automatic checkout is faster. (See Table 8-3.)
2. Automatic checkout is more accurate and uniform.
3. Automatic data analysis eliminates the human factor. (This can also be a disadvantage when it comes to spotting malfunctions.)
4. Semi-skilled personnel can sometimes be used.

TABLE 8-3. MAN AND MACHINE CAPABILITIES AND LIMITATIONS\*

<i>Function</i>	<i>Man</i>	<i>Machine</i>
Reaction time	0.15 to 0.45 sec	10 $\mu$ sec
Judgment time	0.5 to 1.5 sec	25 $\mu$ sec
Timing accuracy	0.5 sec	0.01 $\mu$ sec
Reliability in preprogrammed events	2 to 9% error	$10^{-2}$ to $10^{-4}$ % error
Reliability in unprogrammed events	Depends on training, no better than above figure	No capability

\* Adapted from Ref. 8-17.

The major consequence of these facts is that space-vehicle time on the launch pad is shortened considerably with ACE, leading to higher launch rates and a better probability of hitting narrow launch windows. Coupled to these favorable points are the manifestly higher costs of automated equipment and its complexity. Some engineers say, half-jokingly, that checking out Automatic Checkout Equipment is more difficult than checking out the space vehicle. ACE complexity could in fact lower over-all system performance, since total cost and reliability are major space-probe system figures of merit. Cost-effectiveness studies must be carried out for each launch complex to determine the most desirable degree of automation. The final amount of automation used will depend upon the

number of vehicles to be launched, their similarities, and their complexities.

The functional requirements for Automatic Checkout Equipment are much the same as they are for manual checkout. The following list of requirements is taken from Gollomp (Ref. 8-10):

1. It must accept suitable instructions in appropriate form and distribute them in accordance with test system requirements.
2. It must select appropriate stimuli for each test and direct them to proper system excitation terminals.
3. It must select the test points for measuring specific variables and complete the test connections.
4. It must be able to measure many variables of analog and digital character.
5. It must compare the measured parameters against accepted standards.
6. It must communicate the test status and results in graphic, image, or printed form.
7. It must provide controls for the manual override of programmed instructions and for the modification of the test program.
8. It must provide facilities for self-test and monitoring.

*Other Range Support Equipment.* Spacecraft are always small in weight and volume when compared to the launch vehicle. The major activities around the launch site consequently seem to focus on the massive launch vehicle filled with hazardous propellants. Spacecraft assume more importance during checkout and countdown, but for the moment consider how the launch vehicles are handled.

Small stages can be shipped to the launch site aboard large air transports and by road, but the biggest launch vehicles, such as some in the Saturn class, must be barged in from the manufacturing plant in Mississippi. When the stages have been inspected and tested, they are assembled either directly on the launch pad or in a Vertical Assembly Building (VAB). A VAB permits off-pad assembly and checkout of the vehicle, freeing the pad itself for other operations. When the space vehicle is finally ready for the pad, it can be moved intact from the VAB to the launch pad on a massive crawler. The Saturn and Titan-3 launch facilities both employ the Vertical Assembly Building principle. In the case of the Saturns, the booster is attached to the Launcher Umbilical Tower (LUT) while it is being checked out in the VAB. They are moved to the pad with the booster without breaking any of the umbilical connections.\* Such off-pad assembly and checkout allows many more launches from

\*Severing umbilical connections can change instrument calibrations and slow down the launch process.

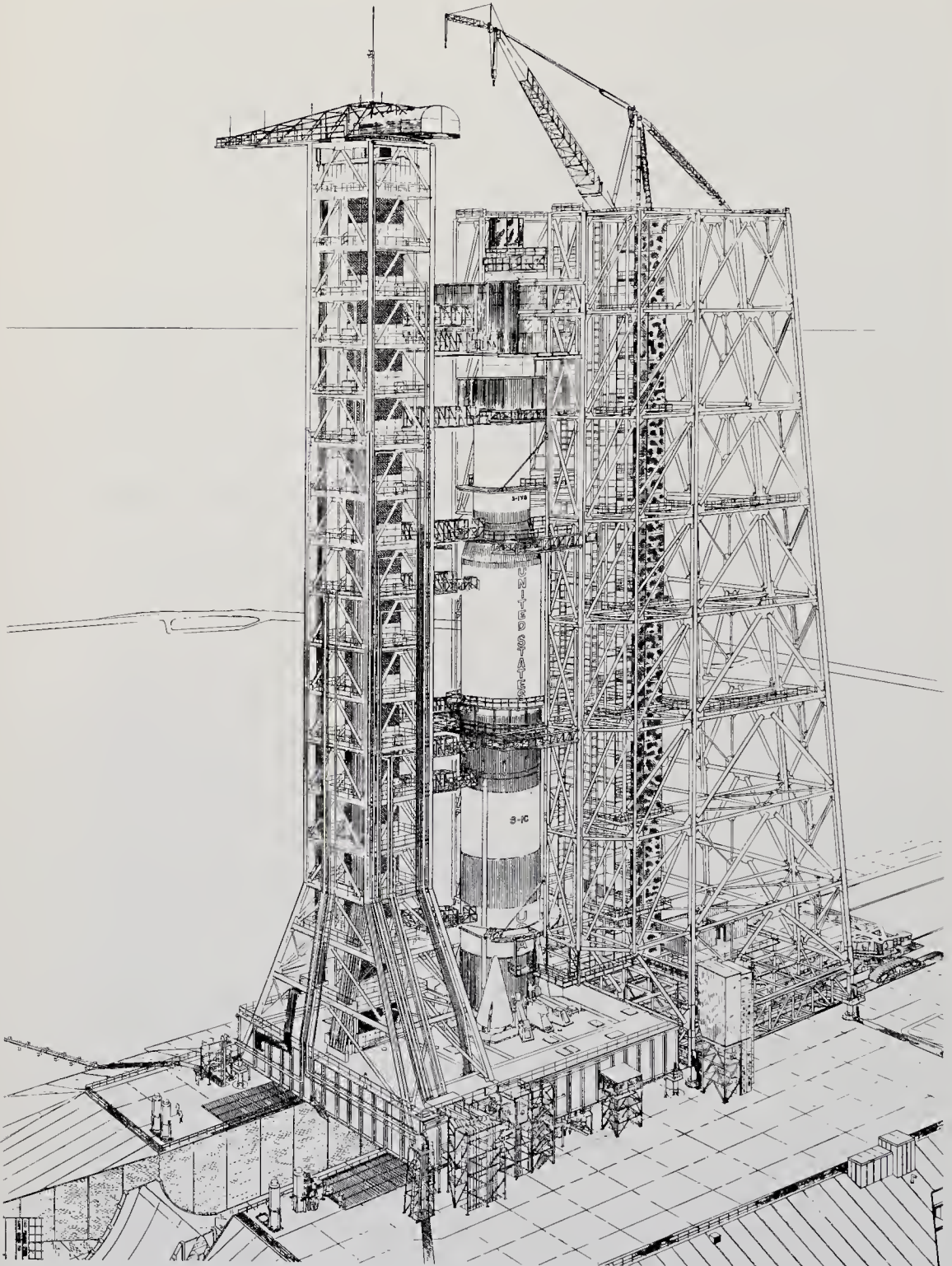


Fig. 8-7. Drawing of the Saturn 5 on its launch pad. The launcher umbilical tower (LUT) is on the left, the service tower on the right. Just before launch, the service tower is moved away from the pad. (NASA drawing)

the same pad. The concept is termed the Mobile System, as opposed to the more common technique, involving assembly, checkout, and launch from a single launch-pad position.

Three major structures make up the launch-pad complex: the launch pad with its pedestal, the launch umbilical tower (LUT), and the service tower (Fig. 8-7).

For the large launch vehicles used in space-probe launchings, the launch-pad structures have no missile guidance function as they do with many small rocket weapons and sounding rockets. The space vehicle sits on an adjustable steel pedestal, beneath which there is a flame deflector, which diverts the hot engine gases away from the launch pad. The vehicle pedestal is supported by a reinforced concrete slab, which also carries the loads of the umbilical and service towers. Drains and holding ponds must be incorporated to handle emergency releases of fuel and oxidizer. A protected pad control room is usually located under the pad to serve as a focal point for checkout and launch preparation. It is of course abandoned for the safer blockhouse during launch. The launch pad shown in Fig. 8-7 was designed for launching the mammoth Saturn 5, a large U.S. launch vehicle under development. The pad hardware, the LUT, and the service tower are analogous to equipment used with smaller boosters. Holddown mechanisms, shown in the illustration, permit the Saturn to build its thrust up to design levels before release. In the case of multiple-engine first stages, the holddown device enables the launch crew to save the vehicle if one or more engines fail to fire.

The LUT, or umbilical tower, has evolved from a simple mast with taped-on cables to the complex structure shown in Fig. 8-7. With Saturn-class vehicles, hundreds of electrical, hydraulic, and gas-supply connections have to be made to the space vehicle through the umbilicals. The design of reliable umbilicals with the complexity shown in Fig. 8-5, page 138, has always been a major task of ground-support equipment engineers. In stark contrast, the umbilicals for military launch vehicles are considerably simpler, sometimes just a single cable, because the payloads are simpler and the vehicles themselves smaller than the Saturns by factors of five to twenty-five. Early space probes have used and will continue to use ICBM boosters and their associated ground-support equipment, but ICBMs are getting smaller (*viz.*, Minuteman) and space probes larger. By 1970, most space probes will use NASA-developed vehicles like the Saturns.

Associated with the umbilical tower is the service structure (Fig. 8-6, page 139). The various platforms permit the launch crew to gain access to the spacecraft and various launch vehicle stages for purposes of checkout and repair. The service structure is mobile, being mounted on a

crawler, and is pulled out of the way before launch. Like the umbilical tower, it is a major design task in itself, one that must be begun years ahead of the first launch.

During an actual space-vehicle launching, all activity is controlled from the blockhouse, or launch control center. The dome-shaped blockhouses (Figs. 8-8 and 8-9) have several floors of electronic gear con-



Fig. 8-8. View of a large blockhouse at Cape Kennedy. (NASA photograph)

nected to the launch pad and vehicle by cable-filled tunnels. Communications are maintained with the downrange stations by microwave links or undersea cables. The vehicle flight can be followed from the blockhouse through the inputs from tracking radars along the length of the range. The possibility of launch-pad explosions and fires requires blockhouses to be heavy structures of reinforced concrete. Blockhouses near the bigger vehicles must be able to withstand overpressures of 100 atmospheres and more.

The dangers during a launch are not confined to fire and explosion. Even the sound pattern during the firing of a large vehicle makes several square miles uninhabitable. With the above dangers in mind, all launches are carefully monitored by a range safety officer, who has the power to destroy the launch vehicle whenever its performance deviates from the design values by more than a specified value.

After a rocket has left the launch pad, and interest has shifted to the tracking stations, the way must be prepared for another space vehicle. Rehabilitating and cleaning the pad may take a month or more for a large vehicle. There may be damage to the service outlets and even the

pad itself. The Mobile System approach is again useful here since one LUT may be moved and rehabilitated away from the pad while another is moved into position.

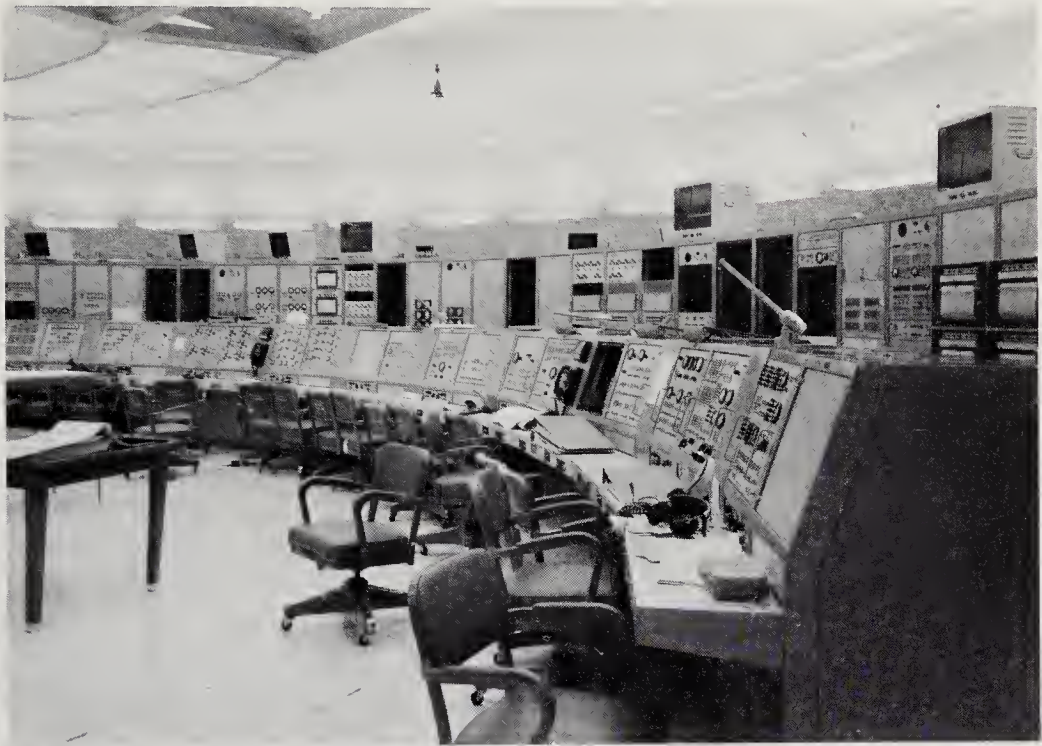


Fig. 8-9. Interior view of Blockhouse 37 at Cape Kennedy, showing some of the consoles and electronic equipment. (NASA photograph)

When timing is critical and a narrow launch window must be hit, the launch vehicle is always backed up by a second vehicle. If the flight is scrubbed on the pad, the first vehicle can be quickly replaced with a new vehicle. If launch-pad damage is severe, another pad would have to be used. Using probability theory and equipment reliability data, it is possible to make an estimate of the chances of hitting a launch window. The probability of a successful launch within the specific window is usually low enough to make it worth-while to prepare a backup vehicle and put it into flight readiness. Of course, hitting launch windows is much more important for manned flights involving orbital rendezvous. If orbital assembly is essential to a space-probe mission, as it might be with extremely large spacecraft, the satellite-rendezvous windows would become important for probes too.

*Launch Ranges.* Soon after liftoff, the space vehicle executes a pitch-over maneuver and heads out over the desolate areas occupied by the downrange tracking stations. Collectively, the downrange stations and

the launch site constitute a tracking range. As their old names imply, the two biggest ranges, the Eastern and Western Test Ranges (formerly the Atlantic Missile Range and the Pacific Missile Range), were built primarily for weapons system testing. They are not tailored specially for space probes in terms of range length, azimuth, or support equipment. However, when the two ranges are supplemented by round-the-world tracking stations, like those in the DSIF (Sec. 8-4), there are essentially no geographical blank spots in tracking and communicating with an ascending space probe. The ETR-DSIF combination has so far proven completely adequate for handling space probes.

Most test ranges are short (hundreds of km) and specialized in terms of certain classes of weapons; viz., the White Sands Missile Range, used for tactical weapons. The two big U.S. ranges, the ETR and WTR, are sufficiently generalized with respect to equipment and have the necessary size to support a large variety of non-military space shots. The WTR, at Pt. Arguello, Calif., is the longer of the two, about 15,000 km, but does not have the instrument coverage of the ETR. The ETR, 8000-km long, is used for most peaceful space activity, including space probes and satellites, manned and unmanned. Most of the ICBM tests have also

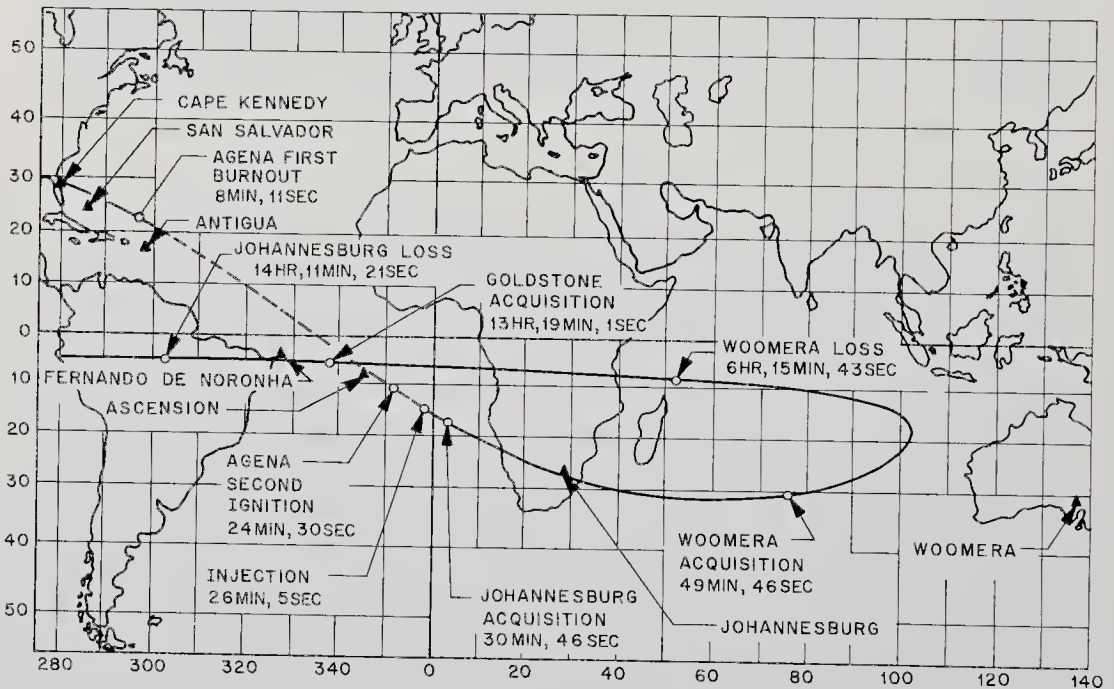


Fig. 8-10. World map showing the ascent of the Mariner-2 Venus probe along the Eastern Test Range and the Deep Space Instrumentation Facility. The apparent retrograde motion of the spacecraft is due to the Earth's rotation. (JPL drawing)



occurred at the ETR. The WTR is the only site in the continental United States where spacecraft ascending to polar orbits do not pass over populous land areas; consequently many military and scientific satellites requiring polar orbits are launched here.

Downrange from the launch pads, island sites and tracking ships analyze vehicle flight, the reentry characteristics, and pinpoint its impact. The same tracking and communication equipment can give valuable information about space-probe trajectories and can monitor spacecraft instruments during the ascent phase. As the spacecraft is passed from one radar to another along the ETR, it eventually reaches the end of the range and must be transferred to the DSIF net. Although the spacecraft is still close to the Earth when it passes over Ascension Island, the last land site in the ETR, it is already in line-of-sight radio contact with the first DSIF site, in South Africa. Expectation would be that the spacecraft would pass over South Africa and soon be acquired by the next DSIF station, at Woomera, Australia, and so on around the Earth. But the rotation of the Earth under the ascending spacecraft can give it an apparent retrograde motion, as shown in Fig. 8-10 for Mariner 2. Eventually the probe is so high above the Earth that it is in line-of-sight contact with almost an entire hemisphere and at least one DSIF station.

The geographical extent of the ETR is also sketched out in Fig. 8-10. The chain of islands and ships stretches from Florida southeast to Ascension Island, in the South Atlantic. The many island sites are supplemented by tracking ships, called ARIS ships (for Advanced Range Instrumentation Ship, Fig. 8-11). The range and accuracy of the radars installed along the ETR are given in Table 8-4.

Considering the billion-dollar-plus investment in the ETR, it is, for all practical purposes, the only U.S. site that will be used for launching

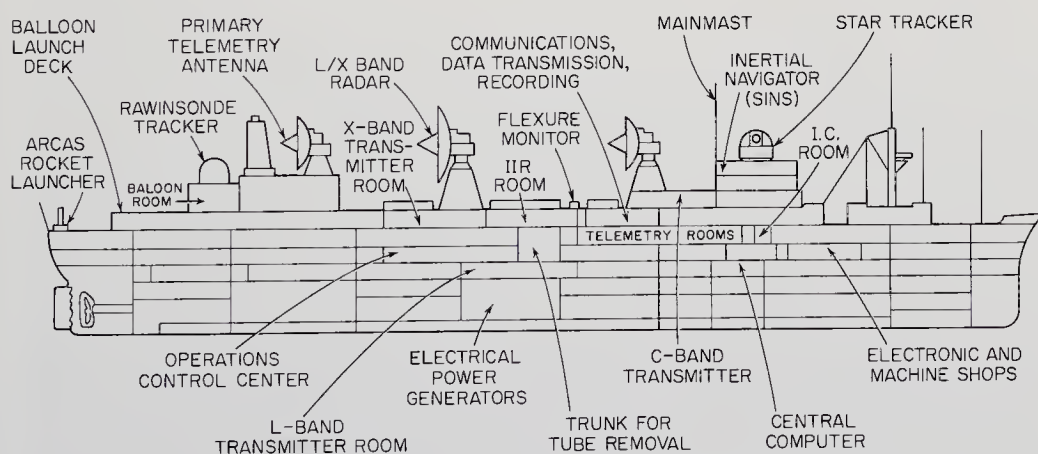


Fig. 8-11. Drawing of a typical range instrumentation ship.

space probes for decades to come. This fact is emphasized by the development of the large and costly Saturn booster pads at the ETR. The Saturns will be the only rockets big enough to launch the large space probes of the future destined for the more distant planets in the solar system. It is very unlikely that this facility investment will be duplicated at the WTR or elsewhere.

The real import of these rather terse descriptions of launch facilities and ranges is not in the statistics of cost and size but rather in the realization of the real magnitude of the total space-probe system and all of the subsystems it encompasses on Earth and in space. The umbilical connections and the radars on an ARIS ship are not irrelevant; they affect spacecraft design as surely as its power supply. The loss of tracking coverage can be as serious as the loss of an onboard scientific experiment through poor design.

TABLE 8-4. TRACKING RADAR CHARACTERISTICS\*

<i>Parameter</i>	<i>Original</i>	<i>Modified</i>	<i>AN/FPQ-6</i>	<i>TRADEX</i>
	<i>AN/FPS-16</i>	<i>AN/FPS-16</i>		
Radar band	C	C	C	UHF+
Frequency (Mc)	5600	5600	5600	425
Peak power (Mw)	1.0	3.0	3.0	4.0
Pulse width ( $\mu$ sec)	1.0	1.7	2.4	50
Repetition rate (pps)	1000	855	640	1500
Average power (kw)	1.0	4.5	4.5	300
Antenna size (m)	4	5	9	25
Beamwidth (mils)	20	14	8	35
Range precision (m)	1.5	2.4	4.6	4.6
Angular precision (mils)	0.2	0.15	0.1	0.3
Doppler precision (m/sec)				0.1

\* Adapted from Ref. 8-2.

#### 8-4. Tracking and Data Acquisition Operations

A newly-launched space probe should be acquired by a DSIF-type tracking and communication station before it is out of range of the well-instrumented launch range. The map in Fig. 8-10 makes it obvious that the first DSIF station needs to be somewhere in South Africa in order to pick up the spacecraft as it gains altitude over Ascension Island. Line-of-sight considerations dictate that there be at least three such tracking stations, located about  $120^\circ$  apart in longitude. The present Deep Space Instrumentation Facility has been built with this geometry. The monetary investment in the DSIF is measured in only a fraction of one per

cent of the ETR investment, yet tens of millions of dollars are involved. Just as it would not be practical to build another ETR for probe launchings, financial considerations make the DSIF a permanent fixture in unmanned exploration of the solar system.

The DSIF consists of three major installations, in California, South Africa, and Australia (Fig. 8-12). It is supplemented by a launch station

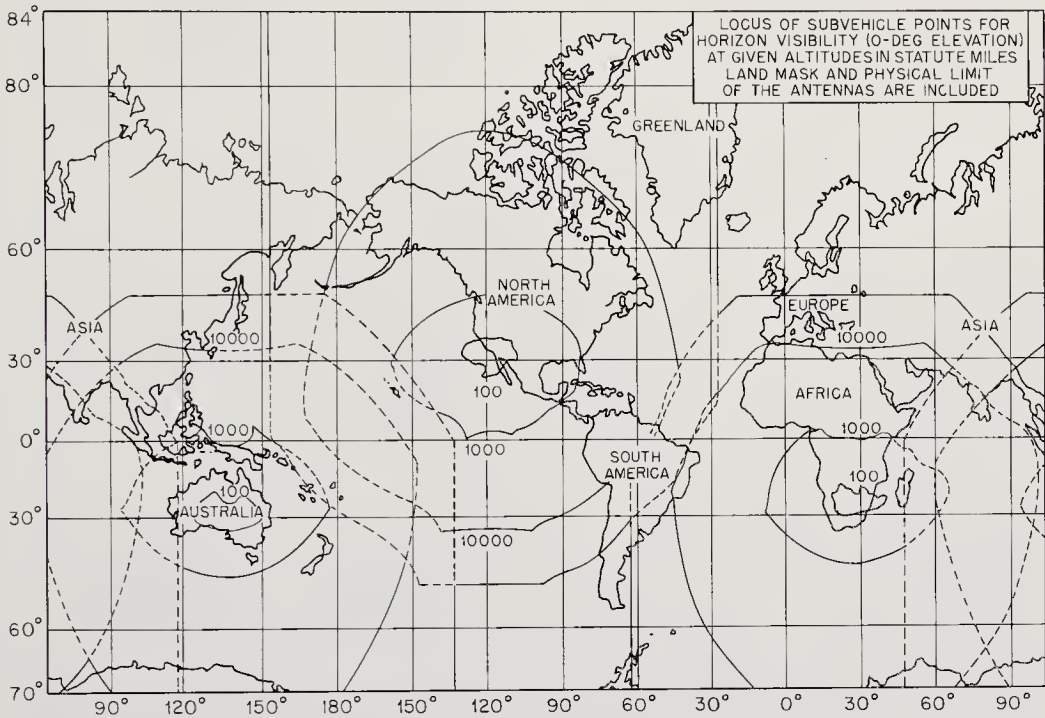


Fig. 8-12. DSIF coverage of ascending spacecraft. Multiply statute miles by 1.61 to obtain kilometers. (NASA drawing)

at Cape Kennedy and a mobile station in South Africa. New stations are being added in Spain and Australia in 1965. The mobile station provides early acquisition of the spacecraft. It has a 3-meter parabolic dish antenna that can command the spacecraft and receive telemetry from injection through to 16,000-km altitude. Eventually it may be possible to eliminate the mobile station. All told, there are six tracking and data receiving antennas in the DSIF complex. These are listed in Tables 8-5 and 8-6.

The DSIF net is connected to the Space Flight Operations Facility (SFOF), in Pasadena, by commercial teletype circuits with a limit of six characters per second. During the flight of a major space probe, the tracking data flowing over these circuits consists mainly of digitally encoded Doppler measurements: two pointing angles, time, and the

TABLE 8-5. LOCATIONS OF THE DSIF STATIONS\*

<i>Location</i>	<i>DSIF Number</i>	<i>Astronomic latitude</i>	<i>Astronomic longitude</i>	<i>Altitude (m)</i>
Cape Kennedy	0	28.48713N	279.42315E	2.57
Mobile (South Africa)	1	varies	varies	varies
Goldstone Pioneer (Calif.)	2	35.38950N	243.15175E	1037.54
Goldstone Echo (Calif.)	3	35.29985N	243.19539E	989.49
Woomera, Australia	4	31.38287S	136.88502E	150.79
Johannesburg, S. Africa	5	25.88735S	27.68478E	1381.92

\* JPL data.

TABLE 8-6. CHARACTERISTICS OF THE DSIF ANTENNAS

<i>Characteristic</i>	<i>DSIF station number</i>		
	<i>0</i>	<i>1</i>	<i>2, 3, 4, 5</i>
Mounting	Az-El	Az-El	HA-Dec
Diameter (m)	1.8	3.0	26
Tracking rate, max. (deg/sec)		20	0.7
Pointing error, max. (deg)		±0.5	±0.1
Range error (m)			±30
Doppler error (m/sec)			±0.2
Angle data		Digitally encoded	Digitally encoded
Drive system	Manual	Electric	Hydraulic

station identification. The sequence is repeated every ten seconds. Range data from time-of-transmission measurements will eventually be added to this format.

The most impressive feature of any DSIF site is the large parabolic antenna (Fig. 6-15, page 99). All except the launch and mobile DSIF sites have the big 26-meter dishes. Located far from concentrations of man-made noise, these large paraboloids can track and receive data from active probes as far out as the edge of the solar system. Formerly, DSIF frequencies were  $890.046 \pm 2$  Mc for transmission to the spacecraft and  $960.05 \pm 2$  Mc for signals from the spacecraft to the Earth. A shift to the following frequencies was made: for transmission from Earth, 2290-2300 Mc; for receiving, 2110-2120 Mc. The large antennas have been designed to operate effectively at these new frequency allocations. The polar-mounted antennas are hydraulically driven and can track rapidly moving spacecraft with high accuracy (Table 8-6). The high tracking precision of the DSIF comes from the careful analysis of the Doppler and pointing-angle data arriving at the SFOF from the three

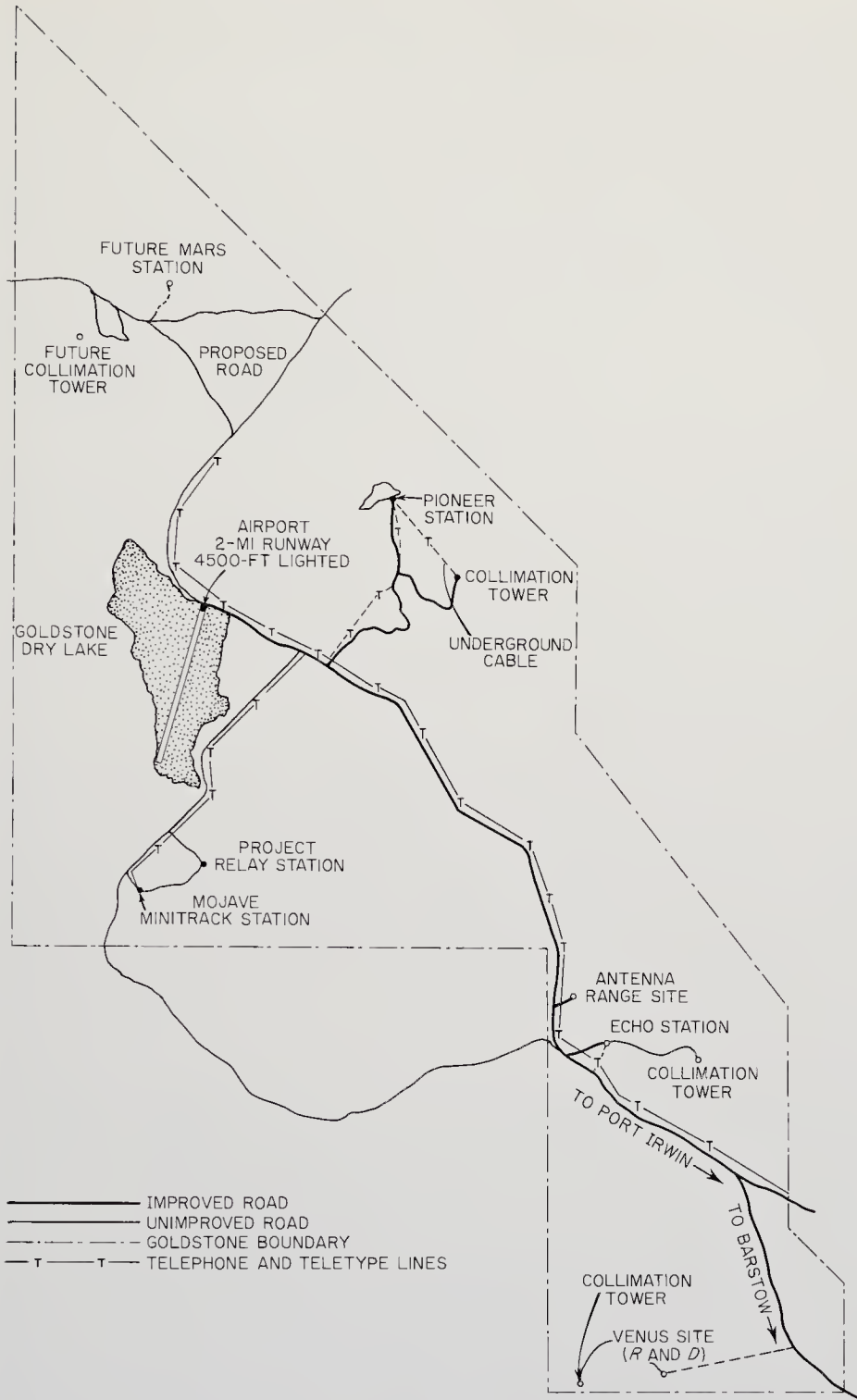


Fig. 8-13. Map of the JPL Goldstone DSIF site, showing the Echo and Pioneer stations 11 km apart. (JPL drawing)

major stations. When the data is analyzed statistically and the most probable trajectory calculated from it, the spacecraft's position in space is pinpointed to within a few kilometers.

DSIF antennas are rugged enough to operate in 30 m/sec winds (hurricanes) and can be stowed to withstand twice this velocity.

The Goldstone site, with its Echo and Pioneer stations (11 km apart) is also instrumented for advanced communications research. The site is located within a natural bowl surrounded by noise-blocking mountains, about 160 km northeast of Los Angeles. The Goldstone site is mapped in Fig. 8-13, showing the over-all size, the positions of the antennas, collimation towers, ranges and other research facilities. All DSIF sites are located in such remote areas and are self-sufficient in terms of power, water, and other services.

The DSIF first proved its value during the Pioneer flights, in 1958 through 1960, although it was still being developed. The facility has also successfully handled the Ranger and Mariner probes. Larger antennas will eventually be added to extend the DSIF range and improve accuracy. Certainly new communications techniques can be expected. The sites and major equipments, however, are expected to retain their present configuration for many years.

Man figures in all Earth-based equipment as radar operator, repairman, data interpreter, and so on, but at many points during every mission his most important faculty, judgment, is called upon to make decisions and issue commands. The Space Flight Operations Facility (SFOF) is at the managerial end of the chain that stretches back from the spacecraft sensors to man himself. The vital teletype and RF communication features of the SFOF have already been covered in Sec. 6-6. Here, some of the physical characteristics of this control center will be briefly described.

The SFOF is located in a three-story building containing about 6000 m<sup>2</sup> of floor space. The building itself is on the Jet Propulsion Laboratory grounds in Pasadena. It became an integral part of NASA space-probe systems on April 1, 1964. The SFOF is especially designed to support the Ranger, Surveyor, Mariner, and Voyager space-probe programs but will also be called upon to take part in other space programs, such as Apollo. The DSIF-SFOF combination has the growth potential to handle several lunar and interplanetary probes at one time. The DSIF antennas would have to be shared between missions, but the SFOF can display mission status and handle technical data for several missions simultaneously. Likewise, decisions and commands can be generated in parallel, though they may have to be transmitted in series by the antenna-limited DSIF. During the 1965-70 time period, there may be as many as six

active lunar probes and perhaps two interplanetary probes operating at a single moment. The possibility of eight far-flung probes, each transmitting diverse data at rates between 10 bits/sec for the distant spacecraft and video for the lunar exploratory vehicles, makes the automatic command and data display features of the SFOF mandatory.

The SFOF is divided into five primary, mission-independent functions:

1. Data processing; addition of time-formatting, etc. (Sec. 6-4).
2. Communications (Sec. 6-6).
3. Display; control boards, status displays, etc.
4. Spacecraft video processing.
5. Support; computers, power, standards, etc.

In addition, the SFOF includes the DSIF Control Room and facilities for monitoring the data and tracking information flowing in from the DSIF. The West Coast switching terminal for the NASA communications system is also housed in the SFOF.

In Chap. 6, the SFOF was likened to a military command center, especially like those of the Air Force concerned with tracking aircraft and missiles. This analogy becomes more apt when the full extent of the space-probe program is considered. The several project managers must have up-to-date status data on their craft and on the Earth-based portion of the system as well. An incorrect decision, perhaps stemming from delayed or poorly formatted status data, could mean the loss of valuable scientific information or even the loss of the probe itself, if it is performing a delicate landing maneuver on a distant planet. The sheer number of probes planned for the future and the avalanches of data they will transmit make automation essential in the DSIF-SFOF portion of the space-probe system.

# Chapter 9

---

## LAUNCH VEHICLES

---

---

### 9-1. Prologue

A space-probe launching, like the suspenseful countdown and fiery liftoff of any space booster, is a most impressive event. The probe's Earth-based facilities work away silently without fanfare and the space probe itself is soon out in space beyond the sight of man, but the liftoff of a large rocket is a great technological spectacle. Many tons of energy-rich chemicals must be burnt within a few minutes to hurl a probe into space and toward the planets. Behind the head-shattering roar and all the pyrotechnics lie years of painstaking design and development. The cornerstone of any space-probe mission will always be the booster, the prime mover that adds enough potential and kinetic energy to the payload to enable it to escape from the Earth's gravitational field.

The prime-mover role of the launch vehicle in interplanetary exploration is self-evident. The physiognomy of the booster is just as clear-cut. There are:

1. The engine, burning a fuel and an oxidizer to generate hot gases that produce a thrust when expanded through a nozzle.
2. Fuel and oxidizer reservoirs, either tanks connected to the engine by pumps, in the case of liquid rockets, or integral solid propellant grains, in the solid rockets.
3. A structure that supports the engine and reservoirs on the pad and during flight.
4. A guidance-and-control system that stabilizes the launch vehicle and keeps it on the calculated trajectory.

A rocket for spacecraft attitude control may be small enough to fit in one's hand. Or a rocket may be more than 100-meters high, such as the Saturn 5, intended for boosting manned lunar vehicles and advanced



probes. This chapter deals with rockets capable of launching space probes to the planets, a distinction that confines the discussion to boosters with thrusts greater than 50,000 kg (110,000 lbs). There is no upper thrust limit in sight.

Just as the United States possesses dovetailing launch ranges and tracking networks, it also boasts a carefully selected "stable" of launch vehicles (Table 9-3). The relatively fixed sizes and shapes of the extant and planned rocket boosters mold the weights and configurations of all space probes, even though the spacecraft itself seems quite negligible, sitting on top of a launch vehicle many stories high.

Other constraints exist, too. A rigorous launch environment is created by a large booster. Shock, vibration, and thermal forces are imposed

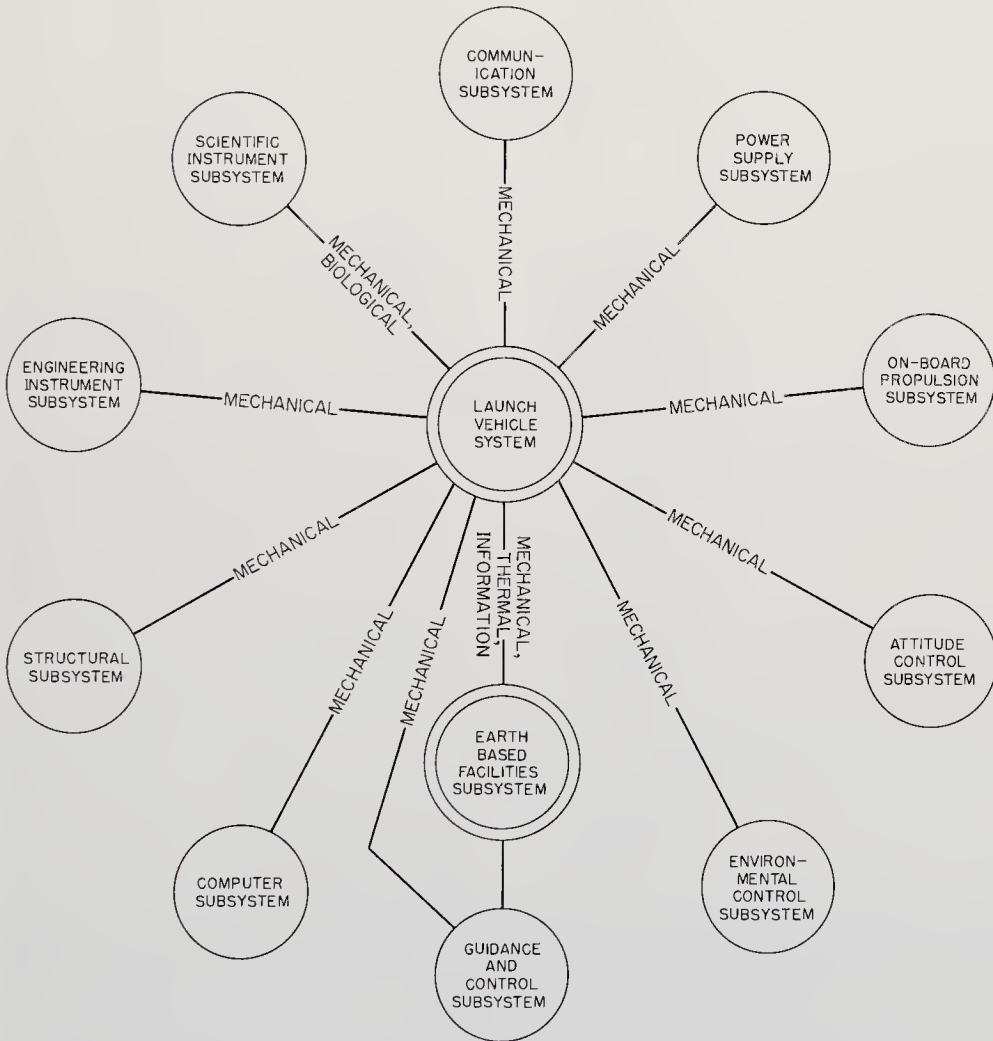


Fig. 9-1. Interface diagram showing the more important relationships between the launch vehicle and the rest of the spaceprobe system.

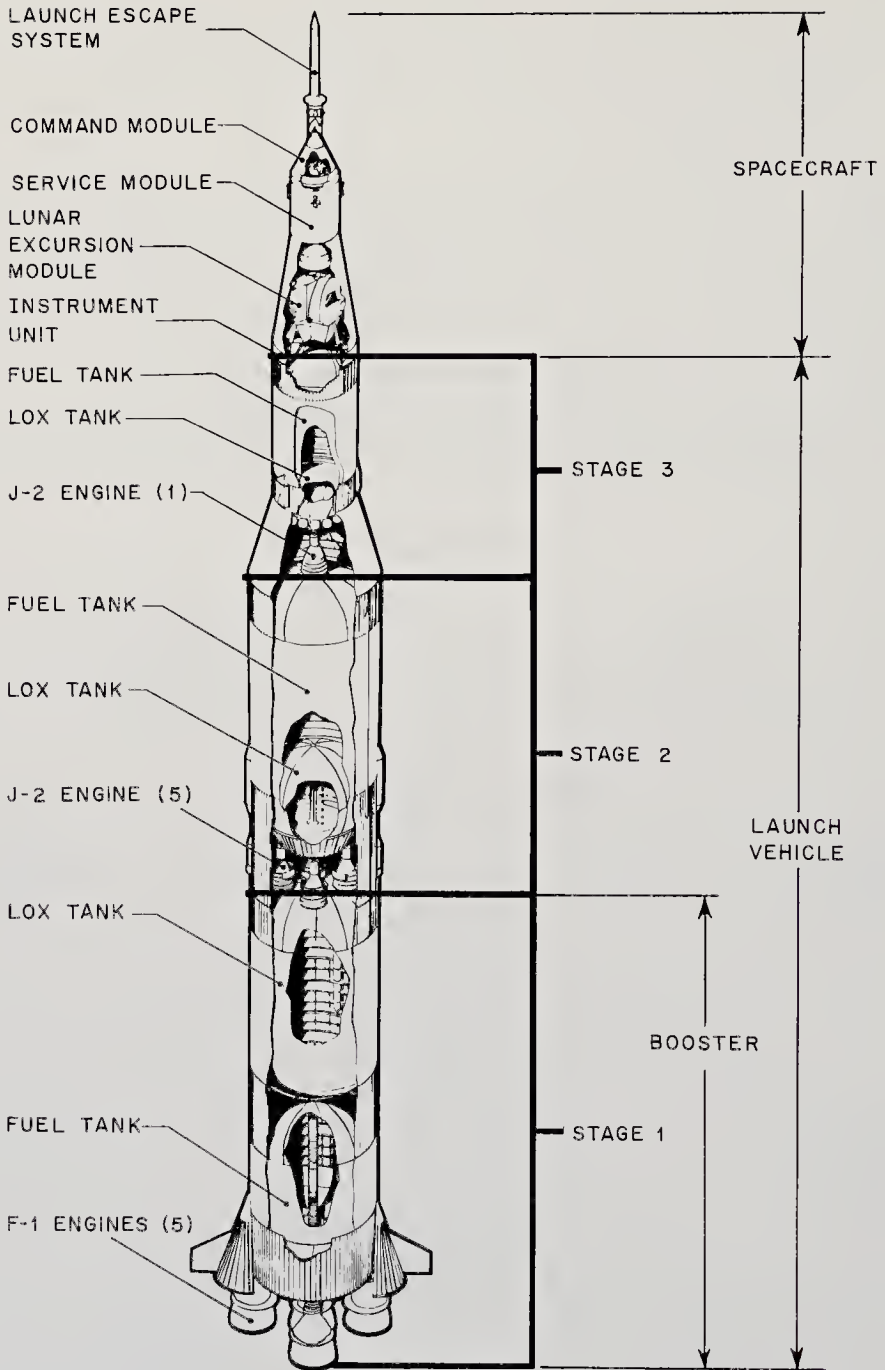


Fig. 9-2. Sketch of the Saturn-5 launch vehicle, showing the general arrangement of stages and engines. The Apollo spacecraft is shown here, but Saturn 5 will also be used to launch large, unmanned space probes in the 1970's.

on the spacecraft across the many interfaces that the launch vehicle shares with the spacecraft. The interface diagram (Fig. 9-1) tabulates the launch vehicle's interfaces with the rest of the space-probe system as they are seen by the system integrator. The mechanical interfaces between the booster and the spacecraft are the most sensitive; ruggedness in spacecraft design is a great virtue. (Fig. 9-2)

Rocket development has historically swung between the solid and liquid types of chemical engines. Congreve's solid war rockets were ascendant during the Eighteenth and Nineteenth centuries, only to be replaced by the V-2 in the 1940's, and finally the liquid ICBM rockets in the 1950's. Now, solid ICBM's (Polaris, Minuteman) are replacing the liquid Thor, Atlas, and Titan missiles. The first large space rockets used liquid engines, but there is a resurgence of solid types, exemplified by the Scout, Titan 3, and some of the post-Saturn-launch-vehicle proposals. At the moment, liquid rockets are the best developed for space-probe work, though design studies show that they will be more complicated and possibly more costly than solid types when the latter are developed. Liquid fuels, on the other hand, are more energetic than solid fuel, yielding more payload for a given gross weight on the launch pad, and also offer the possibility of recovery and reuse. In Sec. 9-3, the trend toward even more powerful liquid fuels, like the hydrogen-fluorine combination, will be discussed. Solids are also being improved; e.g., through the use of metal additives. Beyond the development of better chemicals lies the nuclear heat-transfer rocket. The evolution of launch vehicles is apparently far from finished, either in energy source or in thrust level (Table 9-3). A realistic assessment, however, suggests that liquid chemical rockets are destined to play the major role in space-probe launchings at least until 1975, possibly longer.

## 9-2. Launch-Vehicle Performance

The rocket's role as a prime mover does not exempt it from the dictates of the over-all system figures of merit. The booster must not unduly compromise the system reliability or cost. Fortunately, cost and reliability are easy to relate to launch vehicle performance. A third factor, spacecraft weight, is more elusive.

Booster reliability is simply the ratio of successful launches to the total number of attempts. This factor, plotted in Fig. 9-3, is a good general indicator of booster state of the art. Specific launch vehicles cannot be conveniently plotted on the figure. It suffices to say that any notoriously unreliable booster is soon improved or culled from the stable. ICBM rockets, which were the foundation of the early U.S. space program, are included in Fig. 9-3 only when used for space-vehicle launchings.

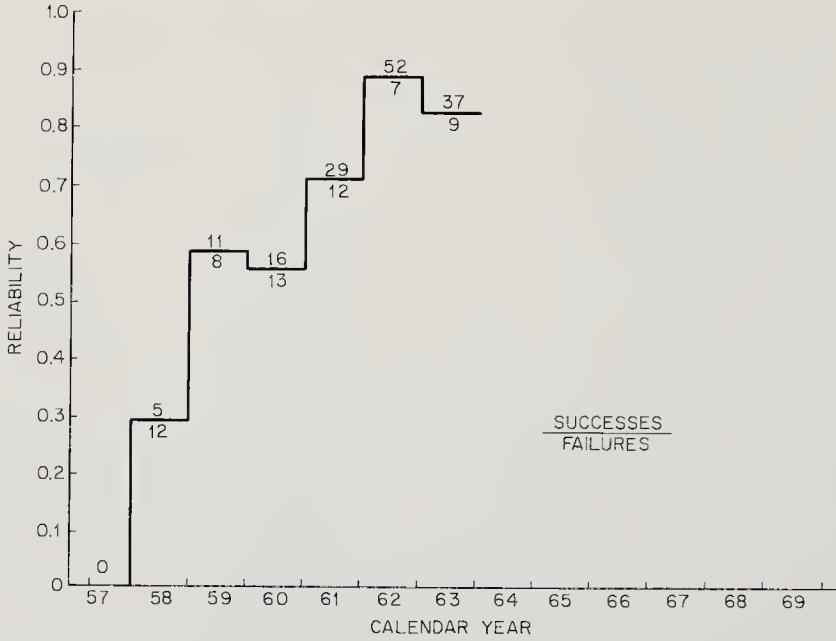


Fig. 9-3. Reliability of launch vehicles in the U.S. space program. Military launches are included only when used for space vehicles. (Data source: STL Spacelog)

The number of ballistic-weapon tests, naturally, is much larger than the number of space shots. Military and peaceful rocketry are mutually beneficial in proving out common techniques and in establishing equipment reliabilities. The reliability improvement shown since 1957 should continue, but at a smaller rate of increase. Launch vehicles do not necessarily get less reliable as size increases. In fact, the Saturn-class

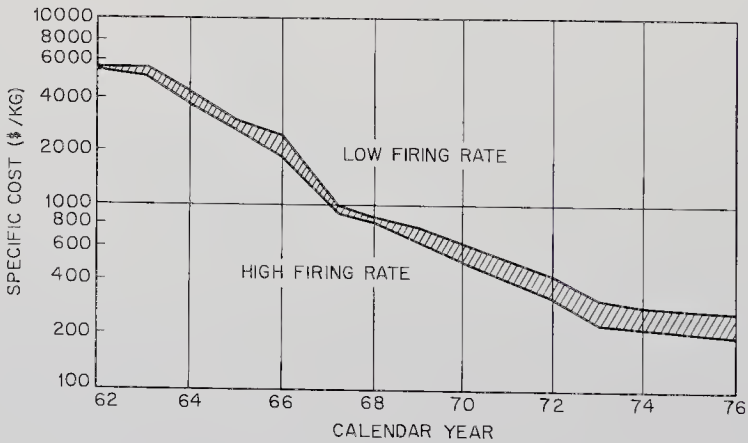


Fig. 9-4. Transportation-cost trends for payloads in 500-km Earth-satellite orbits. (Adapted from Ref. 9-13)

boosters use multiple engines in their first stages, permitting total or partial success to be achieved even with the failure of one engine.\*

Booster costs can be projected from assumptions about material, fabrication method and quantity, and development costs (Ref. 9-13). While not directly applicable to interplanetary payloads, the estimated cost per kilogram in a 500-km orbit (Fig. 9-4) is a useful measure of cost. Space-probe costs per unit mass vary considerably, depending upon the mission. The curves in Fig. 9-4 can be scaled roughly for missions beyond orbit by using a simplified form of Eq. (5-1):

$$\Delta V = g_0 I_{sp} \ln m_0/m_f$$

where:  $\Delta V$  = additional velocity (m/sec)

$g_0$  = acceleration due to gravity (9.8 m/sec<sup>2</sup>)

$I_{sp}$  = engine specific impulse (sec)

$m_0$  = initial mass (kg)

$m_f$  = final mass (kg).

In this case,  $\Delta V$  is the velocity needed beyond a 500-km orbit (Fig. 9-5).

Payload specific cost and its relationship to launch-vehicle cost highlight an often proposed strategem for reducing mission cost—booster recovery and re-use. In such an operation, the expensive first stage of the booster is recovered—say, through the use of parachutes, fixed wings, or paragliders—then refurbished, refueled, and used again. The costs of recovery and refurbishing are usually considerably less than the first cost of the recovered stage, leading to the probable savings shown in Fig. 9-6. Technical papers, however, do not always presage hardware actualities. The cost advantages of recoverable boosters have been recognized for many years, yet no energetic development program exists. The operational use of recoverable boosters is at least as far away as 1970.

Since the beginning of rocketry, there has been extreme pressure exerted on the spacecraft designer to shave the last ounce off his component weight list. At first, the pressure existed because the early launch vehicles could barely struggle into space with a few pounds of payload. During 1959, when converted ICBM boosters were finally able to place hundreds of pounds into low Earth orbits and payload utility became more important than political “firsts,” weight had to be saved to make room for more scientific experiments and better spacecraft instrumentation. There has never been much weight freedom in the closely related field of aircraft design, and the situation will always be worse for spacecraft. Not only does each payload pound sent to the planets cost many thousands of dollars, but each additional payload pound increases the

\* This capability was demonstrated by the successful launch of Saturn SA6 on May 28, 1964.

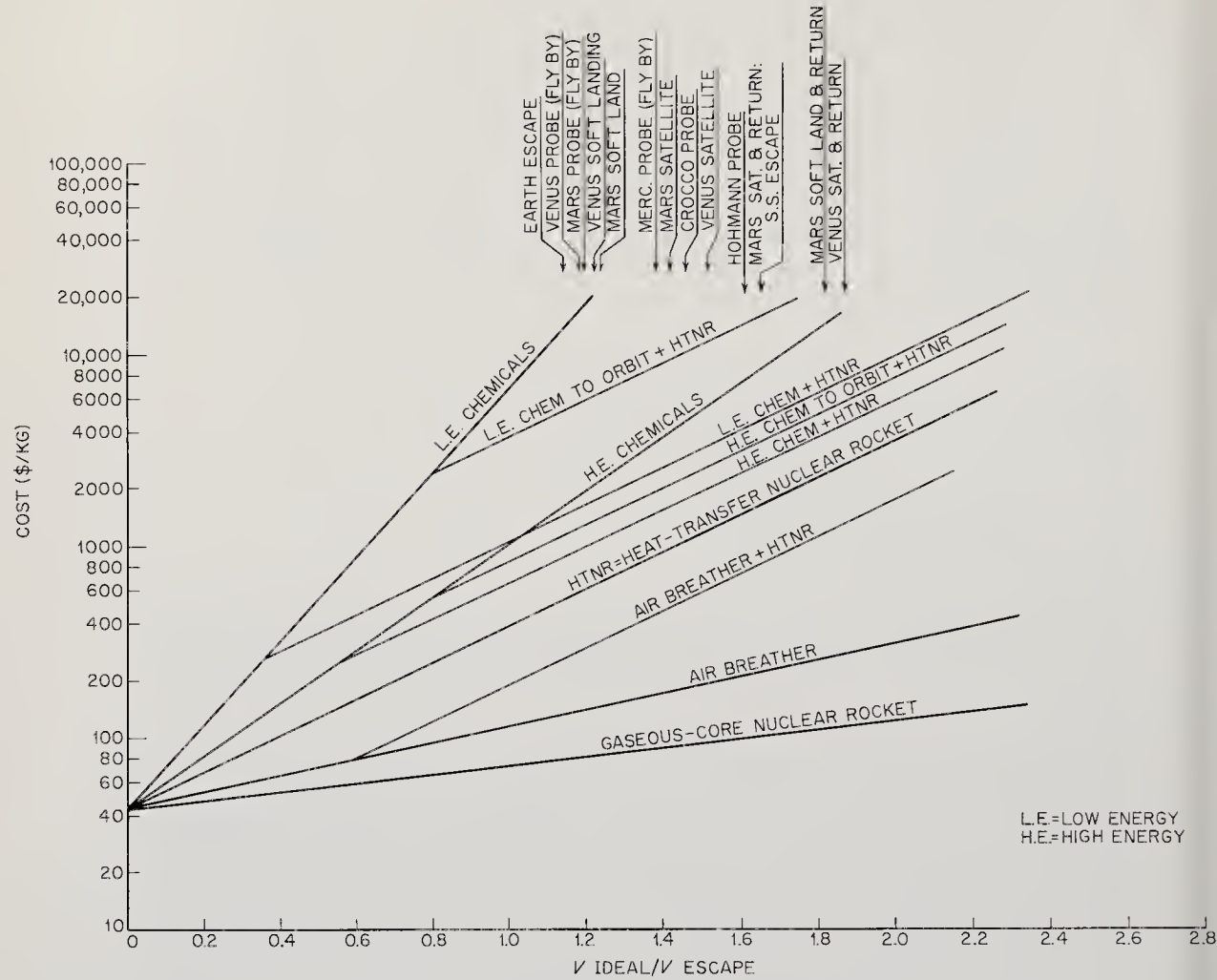


Fig. 9-5. Launch-vehicle costs for several different types of propulsion systems measured in terms of payload accelerated to a given velocity: a. Practical Earth escape; b. Venus-flyby probe; c. Mars-flyby probe; d. Venus soft landing; e. Mars soft landing; f. Mercury-flyby probe; g. Mars satellite; h. Venus satellite; i. Mars satellite and return. Also solar-system escape; j. Mars soft landing and return; k. Venus satellite and return. (NASA drawing)

booster weight by hundreds, perhaps thousands, of pounds. The latter observation, however, is a view from the wrong end of the telescope. When an interplanetary mission is being planned, the fixed mission energy requirements and the capabilities of available boosters fix the spacecraft weight within fairly narrow limits. With this perspective, every pound of launch-vehicle weight saved will be reflected in enhanced payload weight.

Two facets of the booster problem are of interest here. First, if the booster engine specific impulse is fixed by the choice of chemicals, how

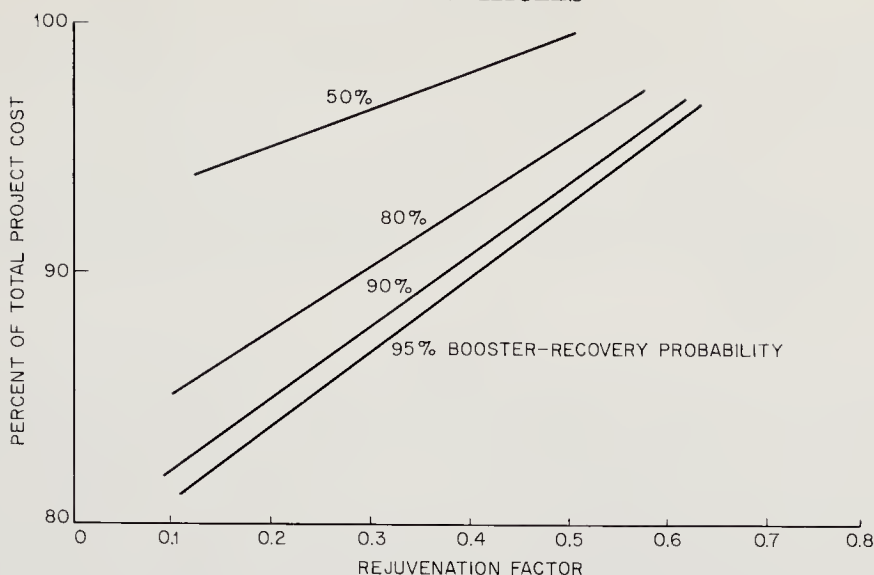


Fig. 9-6. The effect of booster recovery on total project costs. (Ref. 9-12)

can the payload-to-gross-weight ratio be improved beyond the unusable, low, single-stage limits? Second, how can spacecraft weighing many tons be propelled toward the planets without building boosters many times larger than even the immense Saturn 5 and post-Saturn (Nova) rockets? The answers have been well known for many years: Use staging in the first instance and orbital assembly in the second.

All modern space rockets are staged. The payloads of staged vehicles can be calculated by the repeated application of Eq. (5-1). In effect, staging uses lower stages as launching platforms for upper stages. Acquired velocities are just added:

$$\Delta V = \Delta V_1 + \Delta V_2 + \dots + \Delta V_n = g_0 I_{sp} \left[ \ln \frac{m_{10}}{m_{1f}} + \ln \frac{m_{20}}{m_{2f}} + \dots + \ln \frac{m_{n0}}{m_{nf}} \right]$$

where:  $m_{10}$  = the initial mass of stage 1 and its payload  
 $m_{1f}$  = the burnout mass of stage 1 and its payload

and the specific impulses of all stages are equal and constant.  
 Combining the logarithms:

$$\Delta V = g_0 I_{sp} \ln \frac{m_{10} m_{20} \dots m_{n0}}{m_{1f} m_{2f} \dots m_{nf}}$$

This shows no advantage to staging unless  $m_{1f} > m_{20}$  and so on. This state of affairs is easily achieved by discarding the tankage and the no longer pertinent structure of the spent lower stages. This elementary fact about staging is always worth repeating.

To calculate the benefits of staging, a new factor must be introduced

involving the dry weight of the booster stage. A common parameter, but not the only one used in such performance calculations, is the stage structure factor defined by:

$$\delta = \frac{\text{weight of tankage, structure, and propulsion system}}{\text{weight of tankage, structure, propulsion system, and propellant}} \\ = \frac{\text{dry weight}}{\text{wet weight}}$$

The V-2 had a  $\delta = 0.25$ , some modern designs approach  $\delta = 0.10$ , but  $\delta = 0.20$  is a practical value for large boosters. The  $\delta$ 's vary with the type of fuel used. They are higher with liquid hydrogen, which requires thermally insulated tanks, than they are with RP-1 (kerosene), and higher with nuclear engines, because of radiation-shielding requirements.

Orbital assembly represents a special kind of staging, since fuel and oxidizer may be transferred from disposable tanker vehicles to the interplanetary spacecraft. The real import of orbital assembly, however, is in the assembly of small payloads into large vehicles—spacecraft much larger than could be launched from the Earth's surface with available boosters. Orbital assembly is often associated with the manned space missions, because of the large space vehicles needed in this program, but unmanned space probes will eventually tax the capabilities of existing boosters and will have to draw upon orbital assembly, too. Meanwhile, the Saturn-class boosters and post-Saturn (Nova) concepts (Table 9-3, page 172) are large enough to place thousands of kilograms in the neighborhoods of Mars and Venus.

### 9-3. Types of Launch-Vehicle Propulsion Systems

The bulk of a booster's volume is occupied by large fuel and oxidizer tanks. Turbine-driven pumps force the tanks' contents into a comparatively small appendage at the bottom of the booster, called the rocket engine. All rocket engines of the foreseeable future are heat engines; that is, they heat a gas with chemical or nuclear energy and expand it through a nozzle to obtain thrust. The actual mechanical work is accomplished when the expanding gases push on the flared sides of the nozzle.

A rocket engine has another mission besides producing thrust: it must generate a high thrust for each kilogram of fuel-plus-oxidizer consumed each second. The performance parameter describing this property is the specific impulse, defined by:

$$I_{sp} = F/g_0\dot{m} \quad (9-1)$$



where:  $F$  = thrust (newtons)  
 $I_{sp}$  = specific impulse (sec)  
 $g_0$  = acceleration due to gravity (9.8 m/sec<sup>2</sup>)  
 $\dot{m}$  = fuel and oxidizer mass flow rate (kg/sec).

Since the thrust of a rocket engine in empty space is simply  $F = \dot{m}v$ , where  $v$  = the exhaust velocity (m/sec), specific impulse turns out to be directly proportional to the exhaust velocity:

$$I_{sp} = v/g_0.$$

Of course, the value of a high specific impulse is seen when the booster tanks are not drained as rapidly at a given thrust level as they would be at low specific impulses. For a high thrust level at a fixed specific impulse, high mass flow rates are necessary; while a high specific impulse depends upon a high exhaust velocity, regardless of the mass-flow rate.

Specific impulse is proportional to  $\sqrt{T/M}$ . In chemical rockets, both  $T$  and  $M$  are fixed by the fuel-oxidizer combination. Table 9-1 shows the trend from RP-1 and LOX (liquid oxygen) to LH (liquid hydrogen) and LOX. Eventually fluorine may replace oxygen as the oxidizer in chemical engines, but a great deal of development work is required before it is ready for operational use. Usually at least five years are needed between the start of a new engine development and the completion of flight tests. In the case of LH-LOX engines, the problems of storing and handling liquid hydrogen in large quantities had to be solved first. The same will be true for fluorine, which is a relatively difficult element to handle.

The nuclear rocket engines that may be operational in the 1970's offer specific impulses roughly double those of chemical fuels. Interestingly enough, the higher specific impulse comes not from higher temperatures or from the greater energy density of nuclear fuel, but rather from the freedom to use a low-molecular-weight propellant, like hydrogen. Since chemical combustion is unnecessary, propellants can be selected on the basis of molecular weight, cost, and chemical inertness. Only the use of hydrogen and the very high specific impulse it offers make the nuclear rocket worth developing.

To the three basic types of rocket engines listed in Table 9-1—liquid chemical, solid chemical, nuclear—must be added a fourth, the air-breathing engine (Ref. 9-10). The central idea behind using an air-breathing engine on a booster is the reduction of the oxidizer tank size, achieved by extracting the oxidizer directly from the environment. The benefits of scooping up air are reflected in much higher specific impulses, because the  $\dot{m}$  parameter in Eq. (9-1) refers only to the mass flow from the stored

TABLE 9-1. MAJOR ROCKET ENGINES\*

Designation	Thrust		Oxidizer	Sea-level $I_{sp}$ (sec)†	Launch vehicle/ Launch vehicle
	kg (lbs)	Fuel			stage‡
V-2 engine	25,000 (56,000)	Alcohol	LOX	279	V-2
MA-3	82,000 (180,000)	RP-1	LOX	300	Atlas
H-1	85,000 (188,000)	RP-1	LOX	300	Saturn 1 (1st stage)
F-1	680,000 (1,500,000)	RP-1	LOX	300	Saturn 1C
RL-10	6,800 (15,000)	LH	LOX	391	Saturn 4, 5 Centaur
J-2	91,000 (200,000)	LH	LOX	391	Saturn 2, 4B Post Saturn
M-1	545,000 (1,200,000)	LH	LOX	391	Post Saturn
Titan-3 solid	454,000 (1,000,000)	Synthetic rubber polymer	Ammonium perchlorate		Titan 3 (1st stage)
HF engine		LH	LF	410	
Nerva	23,000 (50,000)	U-235	LH propellant (no oxidization)	800	

\* The numbers in this table may change during the development period and with engine model number.

† Specific impulses taken from Table 20.3, *Handbook of Astronautical Engineering*. Actual specific impulses vary with altitude and engine type.

‡ See Table 9-3.

fuel and oxidizer. Turbojet engines, for example, are air-breathers with specific impulses of over 1500 sec, compared with the 300 sec of the RP-1-LOX rocket engine. Of course, air-breathing engines cannot operate outside the atmosphere, but they can materially aid the launch process during the early stages. High-performance jet aircraft have often been proposed (but seldom used) as launch pads for space rockets and ballistic missiles. Like many other apparently attractive booster concepts, air-breathing launch vehicles seem destined to be overwhelmed by the momentum of the established, heavily funded chemical rocket programs. No one can now prove that this concentration of effort is wrong.

*Liquid Chemical Engines.* Liquid chemical fuels supply much higher specific impulses than the lower-energy-density solid fuels, but at a price that includes greater complexity, higher costs, and ground handling problems. The higher specific impulses have been well worth the price ex-

acted until recently, when the sheer size of the space boosters and better solids have forced a reexamination of the tradeoffs.

The liquid engine proper includes a convergent-divergent nozzle, a combustion chamber, fuel and oxidizer pumps, and a forest of associated pipes and valves. A typical liquid chemical engine is shown in Fig. 9-7. In the engine, small portions of fuel and oxidizer are bled off

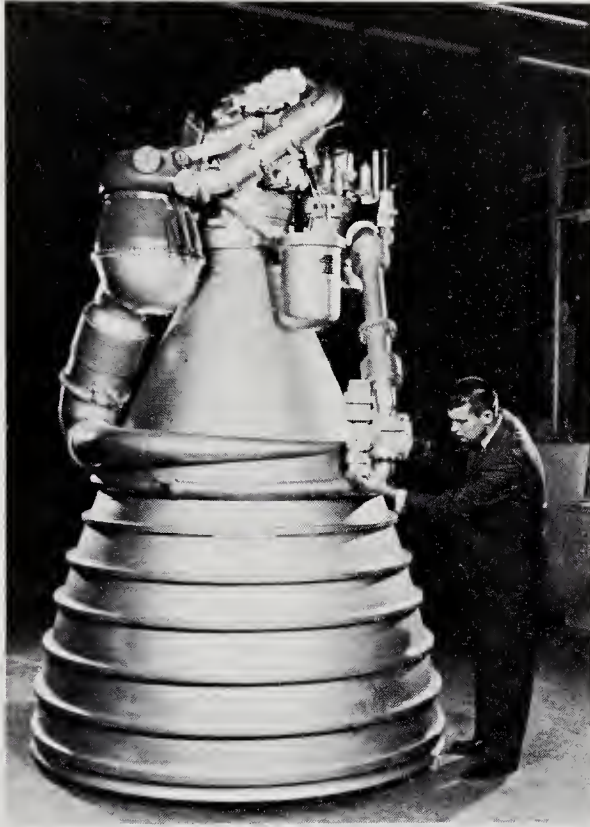


Fig. 9-7. The J-2 liquid chemical rocket engine. Note the size and complicated plumbing. (NASA photo)

from the main streams to power a small gas turbine that drives the pumps. In essence, there are two combustion chambers, the smaller one powering the pumps for the bigger one. After passing through their respective pumps, the main fuel and oxidizer streams are directed through cooling passages lining the engine nozzle. They then enter the combustion chamber through injectors which spray the streams in a pattern that aids burning. The combustion products move through the hot convergent portion of the nozzle, become supersonic in the throat area, and expand isentropically and accelerate in the divergent section of the nozzle. The

reaction force against the nozzle from the gases leaving the engine produces the thrust.

Some aspects of engine design are really more of an art than a science. A new engine must undergo hundreds, and even thousands, of static firing tests before it is committed to a launch vehicle. Combustion instability has been the major affliction of large liquid engines. The F-1 engine, for example, was plagued during development by combustion instabilities that would render the engine useless in actual flight. The instabilities were eliminated largely through experiment and test, rather than through a basic understanding of the engine's combustion processes.

*Solid Chemical Engines.* The venerable history of solid rockets began with toy rockets, centuries ago, in the Orient. The powder-filled tubes used by the Chinese are separated by a huge technological gap from the many-ton grains, 3 meters in diameter, that are strapped on the Titan-3 booster.

A solid chemical rocket has the convergent-divergent nozzle common to most thermal rockets. The hot gases, however, are now generated at the burning wall of a huge solid propellant grain (Fig. 9-8). No pumps

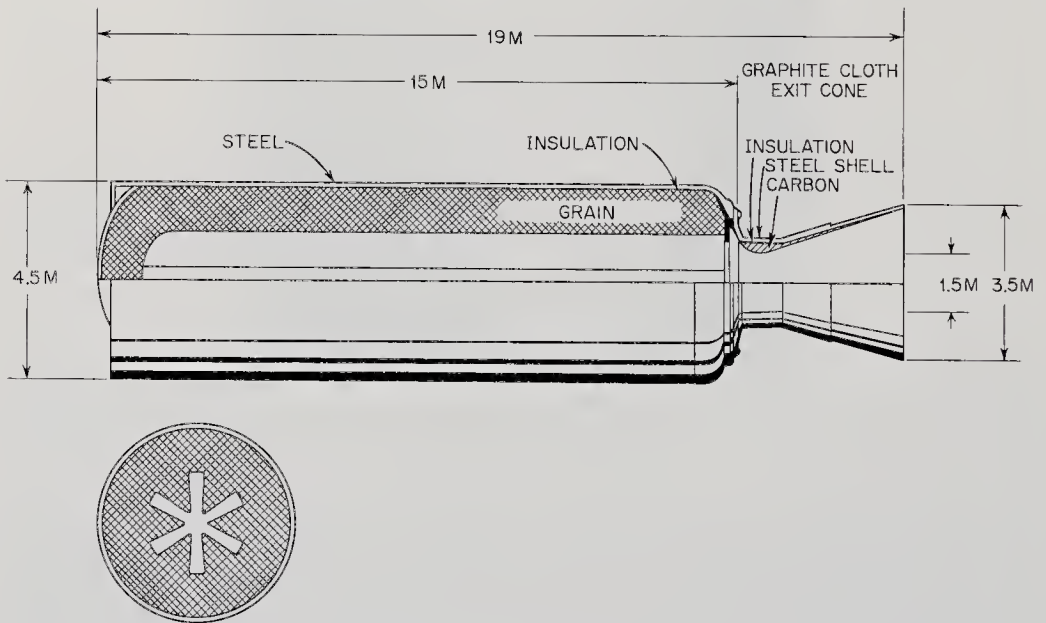


Fig. 9-8. Drawing of a large solid chemical rocket motor. The thrust of such a motor would be approximately 500,000 kg. Dimensions are in meters.

are needed, obviously, but the high pressures generated throughout the large volume of the combustion chamber, which now encloses the whole fuel-oxidizer supply, require that a heavy casing replace the relatively flimsy propellant tanks of the liquid rockets. One of the major accom-

plishments of solid rocket technology has been the development and manufacture of large but lightweight pressure shells. Filament-wound casings, Fig. 9-9, have proven stronger per unit weight than massive metal shells.

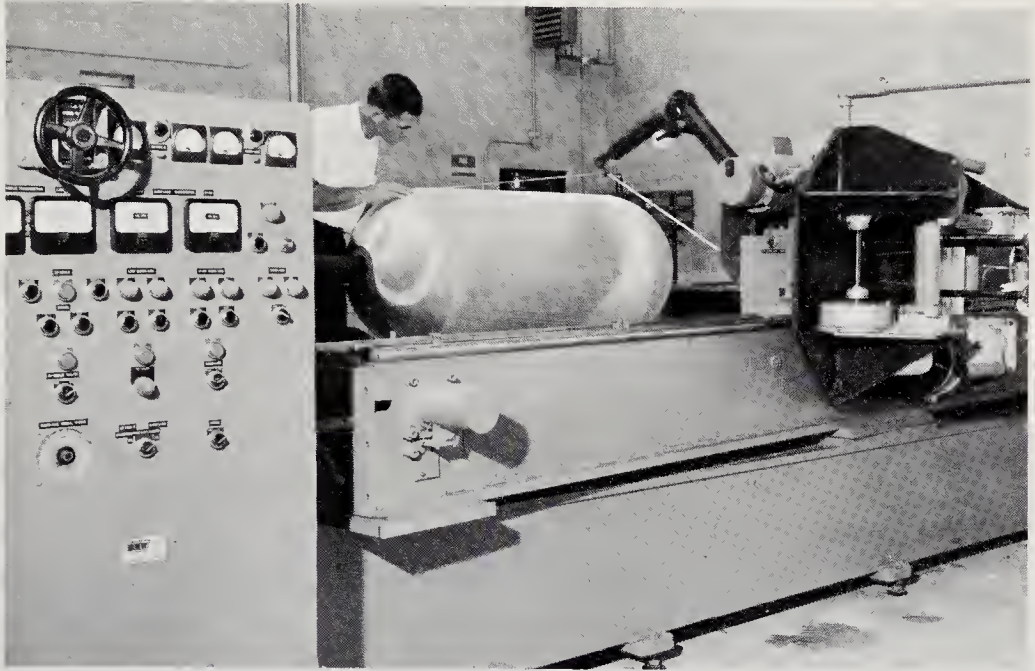


Fig. 9-9. A small solid chemical rocket case being wound with fiberglass on a filament-winding machine. (Courtesy of Thiokol Chemical Corp.)

The erosion of the uncooled nozzle throats of the solid rockets by the hot, reactive, particle-laden combustion products was a serious drawback until ablative materials (viz., graphite), like those used on missile nose cones, were inserted in the most exposed areas.

Originally, solid rockets burned essentially axially inward from the exposed end. Modern solid rockets use propellant grains with a central hole made in the shape of a star, or some reentrant pattern. By shrewd design of the grain's transverse cross section, thrust programs can be created that are constant in time, or time-increasing, or varied in almost any desired way.

Solid rockets took a big step forward when they were adopted for use on the Titan-3 booster. The huge segments, three meters in diameter, are poured and cured away from the launch site, but they are easily transported and assembled on the launch pad or in a Vertical Assembly Building. The convenient building-block approach and the successful firings of large solid-rocket segments with thrusts over a million pounds are partly responsible for the strong resurgence of solid rockets. Solid rockets

are also easily stored and handled. These facts, coupled with their demonstrated high reliability and low cost, place them in strong competition for the first stage of the next generation of booster rockets, the post-Saturn (Nova) series.

*Nuclear Rocket Engines.* The only type of nuclear rocket that might be developed and used operationally before 1975 is the so-called heat-transfer nuclear rocket. The adjectives are derived from the fact that heat from the fissioning uranium in the fuel elements is transferred to the working fluid (hydrogen propellant) by conventional modes of heat transfer (conduction, convection, and radiation) in contrast to kinetic-energy exchange processes used in more advanced nuclear concepts, e.g., the plasma-core approach (Ref. 9-10).

In a nuclear rocket engine, a nuclear reactor replaces the combustion chamber of the liquid chemical rocket (Fig. 9-10). The nuclear reactor

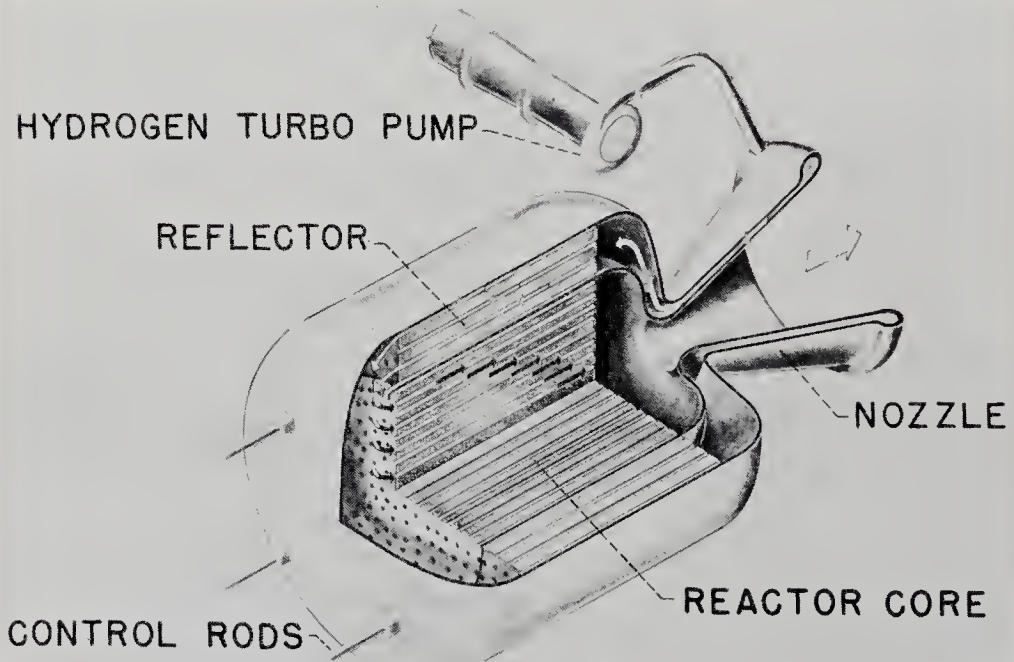


Fig. 9-10. Schematic drawing of a heat-transfer nuclear rocket engine. Hydrogen flow from pump enters nozzle, flows left through the neutron reflector, and then through the nuclear reactor core and out the nozzle. (NASA drawing)

core consists of a geometric lattice of uranium-containing graphite fuel elements. A liquid hydrogen pump impels the propellant through the nozzle cooling channels and then axially along the nuclear fuel elements. The core heats the hydrogen to temperatures in the neighborhood of  $2300^{\circ}\text{K}$ .

On expanding through the nozzle, the low-molecular-weight hydrogen produces thrust at a specific impulse around 800 sec.

The nuclear rocket's specific impulse of 800 sec is about twice that available from chemical rockets and therefore a worthy goal. The high specific impulse is countered, however, by the nuclear rocket's higher structural weights (due to nuclear radiation shielding), high core weight, and the burden of nuclear controls and safeguard devices. When these factors are included in booster performance calculations, the margin of nuclear superiority diminishes considerably.

The United States effort in the nuclear rocket field is concentrated in the Nerva engine (Table 9-1), which is intended to be ready for flight testing about 1970. The major problems encountered with Nerva have been:

1. Core damage, under the influence of high temperatures and the large dynamic loads generated during engine operation.
2. Protection of the public against nuclear hazards arising from a nuclear engine operating in the vicinity of the Earth.
3. Cladding the fuel elements to prevent the diffusion and spread of dangerous fission fragments during normal operations.

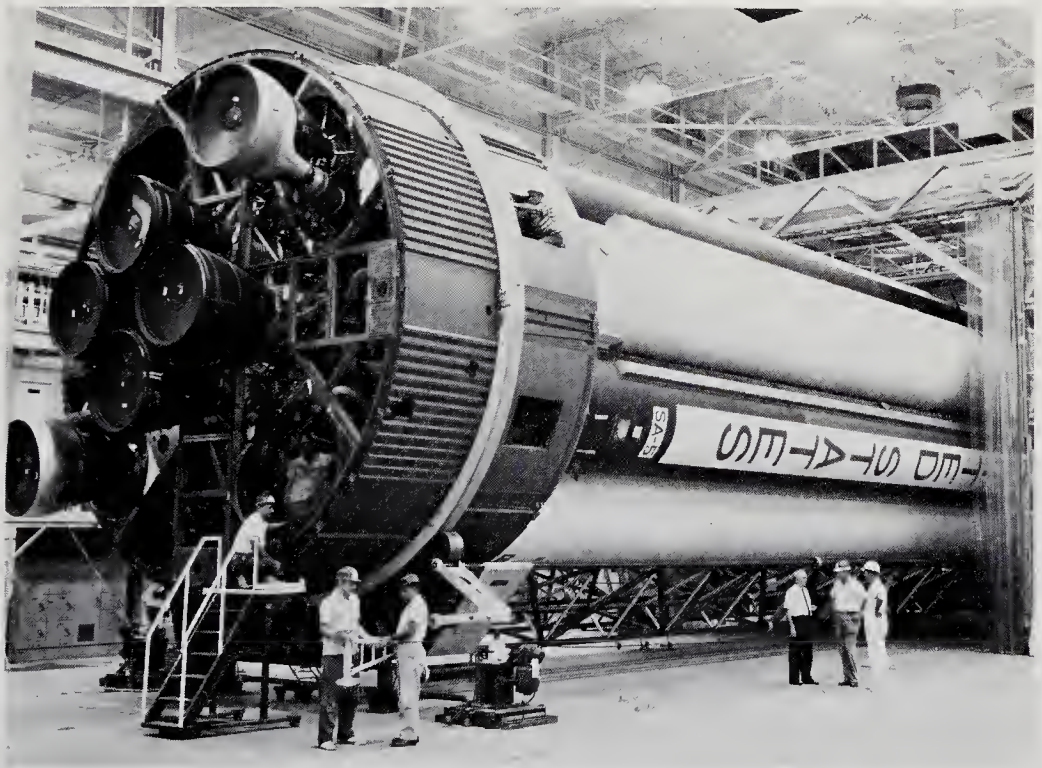


Fig. 9-11. The Saturn-1 stage during construction. Note the intricate structure. (NASA photograph)

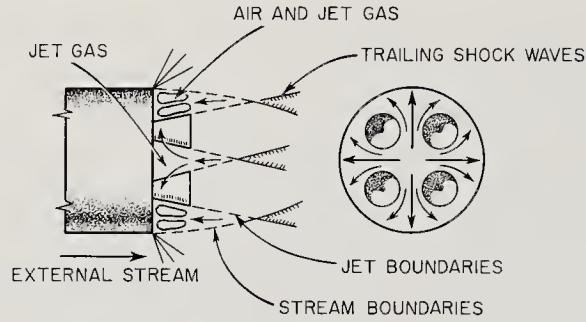


Fig. 9-12. Hot gas streams near the end of a large chemical rocket, showing how they are reflected and circulated. These gases can impose severe thermal loads on the rocket base.

The high costs of nuclear engine development will always make the nuclear rocket fair game during budget-cutting exercises. The additional fact that there are chemical rockets now under development that can do any job the nuclear engine can do, though perhaps not as well, relegates the nuclear-engine program to a lower priority.

#### 9-4. Launch-Vehicle Design Problems

Underneath the sleek, cylindrical skin of the booster as it is usually seen on the launch pad, there are cavernous fuel and oxidizer tanks,

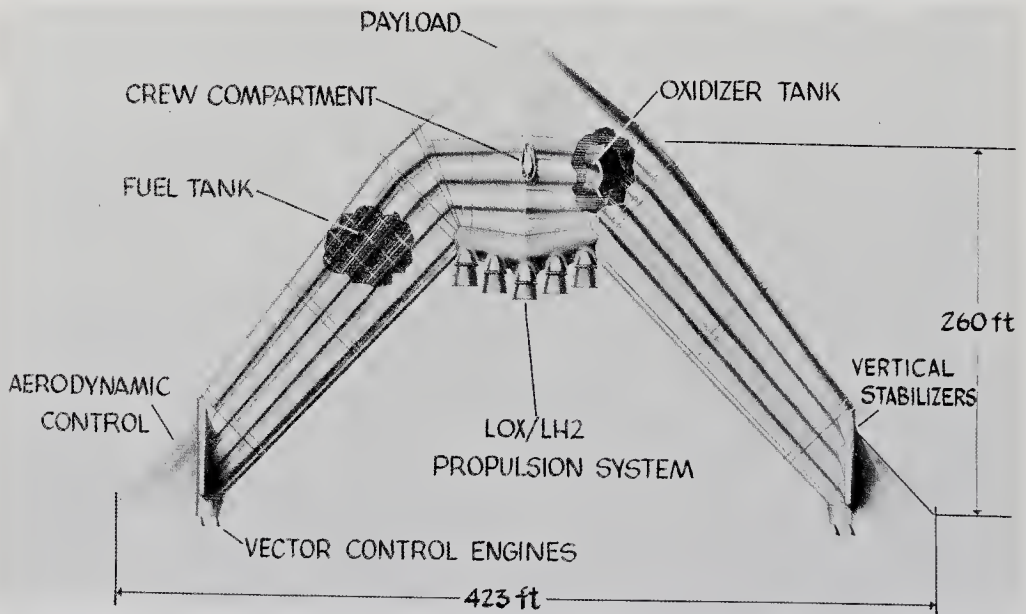


Fig. 9-13. A vertical-takeoff Astroplane concept. This launch vehicle can reenter and land on airfield runways. After refurbishing, it can be reused. (Courtesy of Aerojet-General Corp.)



TABLE 9-2. LAUNCH-VEHICLE DESIGN PROBLEMS

<i>Basic Effect</i>	<i>Description</i>	<i>Implications</i>
Base heating	Hot air reflected from trailing engine shock waves heat booster base. (See Fig. 9-12.)	Thermal insulation and booster skirts needed.
Aerodynamic heating	Aerodynamic heating reaches its maximum around 10-km altitude. Maximum temperature lags slightly.	Internal stresses from differential thermal expansion. Material strengths are reduced.
Ground wind loads	Steady winds cause oscillations of vertical cylinder.	Guidance alignment affected. Structures must be stiffened.
Buffeting	Caused by shock boundary layer interactions, blunt-body separation, and wake buffeting.	Structural damage; viz., first Mercury-Atlas shot. Requires structural stiffening.
Longitudinal bending moments	High altitude winds cause vehicle to fly at an angle of attack near point of maximum dynamic pressure (10-km altitude). Pressure on rocket nose produces a vehicle torque. Maneuvers also generate bending moments.	Autopilot must compensate for pitch forces increasing bending moment. Structure must be stiffened.
Shock and vibration	Ground transportation can cause shocks up to several g. (50 g for railroad humping.) Rocket engine generates vibration. (See Table 8-2, page 133.) Shocks produced by stage-separation pyrotechnics may be 50 to 200 g for 10 msec.	Air transport preferred. Sustained vibration causes structural fatigue. Absorbers and damping devices needed.
Propellant sloshing	Lateral oscillations may cause resonant oscillations in partially filled tanks.	Structural damage may occur. Guidance system may be affected if its resonant frequency is near that of sloshing frequency. Tank baffles needed.

miles of pipes and wiring, a multitude of valves and transducers, and, at the bottom of each stage, an engine and its bell-shaped nozzle (Fig. 9-11). Supporting the heavy loads of propellant and the payload are the tanks themselves and the intertank/interstage structures. Since every pound of structure detracts from launch-vehicle performance, structures are pared to minimum weight and fabricated from high strength-to-weight-ratio materials.

TABLE 9-3. CHARACTERISTICS OF LARGE U.S. LAUNCH VEHICLES\*

<i>Designation</i>	<i>Engine(s)</i>	<i>Thrust kg (lbs)</i>	<i>Height Minus Spacecraft(m)†</i>	<i>Diameter (m)</i>	<i>Payload 500- km Orbit (kg)</i>	<i>Escape Payload (kg)</i>	<i>Opera- tional Date</i>	<i>Assigned Missions</i>
Thor-Able			~24.0		160	39	1958	Pioneer 1, 2, 5
Stage 1	1 MB-1	68,000 (150,000)	19.8	2.4				
Stage 2	1 AJ 10-42	3,500 (7,700)	5.9	0.84				
Stage 3	1 X-248	1,400 (3,100)	1.2	0.56				
Thor-Agena B			23.2		728		1960	Discoverer series, Military satellites
Stage 1	1 MB-3	77,000 (170,000)	17.0	2.4				
Stage 2	1 8018	7,300 (16,000)	8.2	1.5				
Atlas-Agena B†			27.8		2720	340	1961	Ranger series, Mariner series, Military satellites
Stage 1	2 MA-3	167,000 (367,000)	20.6	3.0				
Stage 2	1 8018	7,300 (16,000)	9.4	1.5				
Titan 2			27.4		2720		1963	Gemini
Stage 1	2 XLR-87	195,000 (430,000)		3.0				
Stage 2	1 XLR-91	45,000 (100,000)	9.8	3.0				
Saturn 1			38.2		9100	2300	1964	Apollo
Stage S-I	8 H-1	680,000 (1,500,000)	24.4	6.5				

Stage S-IV	6 RL-10	41,000 (90,000)	13.1					
Stage S-V	2 RL-10	14,000 (30,000)	8.8					
Saturn 1B			45.7	14,500	5900	1964	Apollo	
Stage S-I	8 H-1	680,000 (1,500,000)	24.4	6.4				
Stage S-IVB	1 J-2	91,000 (200,000)	17.7	6.5				
Atlas-Centaur			30.5		1040	1965	Surveyor	
Stage 1-Atlas D	2-MA-3	167,000 (367,000)	20.6	3.0			Probes	
Stage 2-Centaur	2 RL-10	14,000 (30,000)	7.6	3.0				
Titan 3					3600	1965	Space station	
Stage 0	2 solid	910,000 (2,000,000)	31.4		11,400			
Stage 1	2 XLR-87	195,000 (430,000)		3.0				
Stage 2	2 XLR-91	45,000 (100,000)	9.8	3.0				
Transtage		7,300 (10,000)						
Saturn 5			85.3		41,000	1967	Apollo	
Stage S-IC	5 F-1	3,410,000 (7,500,000)	42.1	10.0	100,000			
Stage S-II	5 J-2	454,000 (1,000,000)	25.0	10.0	36,300			
Stage S-IV B	1 J-2	91,000 (200,000)	17.7	6.5	109,000			40,800

TABLE 9-3. CHARACTERISTICS OF LARGE U.S. LAUNCH VEHICLES (cont'd)

Post Saturn (Nova)		~100			
Stage 1	8 F-1	5,460,000 (12,000,000)	15	454,000	123,000
Stage 2	4 M-1	2,180,000 (4,800,000)	15		
Stage 3	1 J-2	91,000 (200,000)	17.7		
Astroplane—10§		76,800,000 (215,000,000)		200,000	1970

\* The numbers in this table may change during the development period and with engine model number.  
 † Some stages nest within others or are connected by transtaging. Stage heights do not necessarily add to give booster total.  
 ‡ The Atlas-D has a 36,400-kg (80,000-lb) sustainer engine.  
 § Aerojet study Ref. 9-17.

The first decisions that must be made when a new launch vehicle is being designed concern such gross problems as:

1. The number of stages to be used.
2. The fuel-oxidizer combination.
3. Over-all vehicle configuration and dimensions.
4. The structural materials to be used.

When such questions have been answered, attention can be turned to the structural problems involving wind loads, aerodynamic heating, noise and vibration, and propellant sloshing. These subjects are so fundamental to booster design that they deserve a few words at this point, even though they are somewhat divorced from the spacecraft proper. For the sake of brevity, these impressed forces and their design consequences are summarized in Table 9-2.

#### **9-5. Characteristics of Major Launch Vehicles**

The United States stable of launch vehicles has grown from a few modified military rockets to the impressive list given in Table 9-3. The most important observation to be drawn from a study of the list is that the U.S. has the capacity to explore the farthest reaches of the solar system with unmanned payloads launched by chemical rockets. Using boosters like post-Saturn (Nova) and orbital assembly, even manned reconnaissance of Mars may be within chemical rocket technology.

# Chapter 10

---

## SPACECRAFT DESIGN

---

---

### 10-1. Prologue

Interplanetary spacecraft tend to be lightweight, butterfly-like structures. Their fragile appearance is deceptive, for these craft are built to withstand the traumas of the launch process and the attrition of years in the interplanetary environment. In addition to mere survival, the probe also is expected to return large quantities of significant scientific data in order to repay its investment. Such qualities do not come easily. A successful space probe is an engineering work of the highest order.

This chapter concentrates on the general engineering of space probes. The discussion will be organized on a subsystem basis. In the chapter following, the details of specific probes that have been built or proposed, viz., Pioneer 5, will be described.

In marveling at the watchlike intricacies of space probes, sight should not be lost of the fact that a probe, even though millions of kilometers away on a ballistic trajectory, is still part of a total system with substantial, active equipment back on Earth. For emphasis, the spacecraft portion of the interface diagram is reproduced in Fig. 10-1, showing the spacecraft broken down into its ten subsystems. Once in space, the vital ties with Earth are kept intact only through electromagnetic information transfer, but among themselves the spacecraft subsystems still manifest a full spectrum of interfaces.

What makes a "good" space probe? The three important figures of merit, as stated earlier, are low weight, low cost, and high reliability—all measured at a constant level of scientific data return, which is hopefully high and significant. Reliability quickly emerges as the dominant factor in spacecraft design, because lacking it the distant parts of the solar system cannot be explored regardless of spacecraft weight and cost.

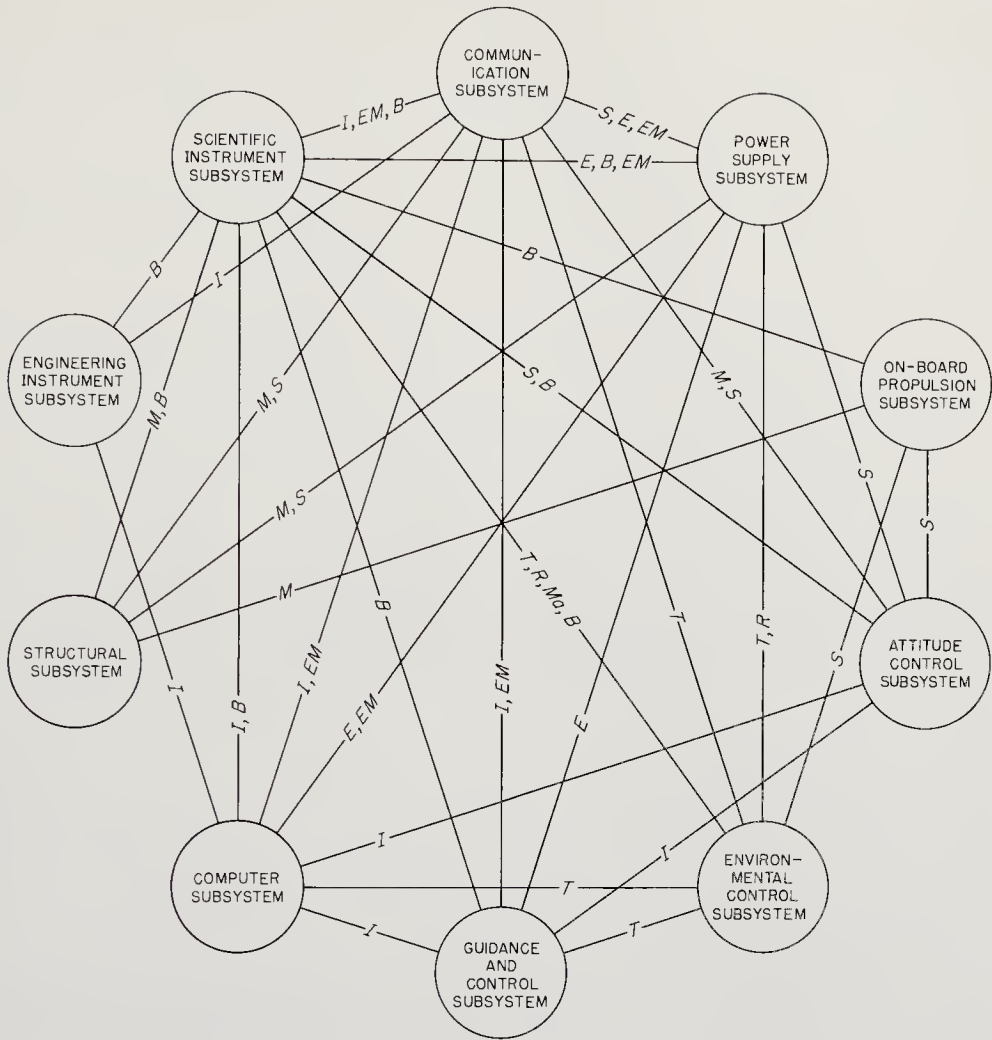


Fig. 10-1. Spacecraft interface diagram. Only the major interfaces are shown. T = thermal, Me = mechanical, S = spatial, E = electrical, R = radiative, Ma = magnetic, I = information, B = biological, EM = electromagnetic.

The magnitude of the reliability problem is highlighted by technical conflicts that have arisen among astronomical engineers. One school believes that more, but simpler, probes should be launched in place of fewer, more complex craft, each carrying dozens of experiments. This simplicity school argues that reliability is on the side of simpler, more frequent probes. Still another group maintains that man should accompany the instruments as far as possible into space; say, on manned flybys where freshly calibrated and activated unmanned capsules could be ejected by astronauts as their craft swings around the target planet. In this philosophy, man is introduced as a maintenance man and repairman, essential to the over-all reliability of the mission. The adverse effect of

heat sterilization on spacecraft reliability forms still another battleground. Finally, there is the conflict between the proponents of electrical propulsion, who claim large payload improvements, and the chemical rocket adherents, who protest that large electrical power plants with the requisite reliabilities are not even on the horizon. The answers to these questions will come only with time. Right now, design decisions must rest on human judgment alone. Present emphasis is on conservatism and simplicity.

The first deep-space probes, the Pioneers, were understandably all aimed in the direction of the Moon, except for Pioneer 5, a true interplanetary probe now in orbit around the Sun. The urgency of the Apollo project has preempted most space-probe activity during the 1960's, in an effort to explore the lunar surface as thoroughly as possible with unmanned devices before committing manned vehicles. The Ranger and Surveyor lunar probes that support Apollo are outside the scope of this book, though there are many areas of overlapping technology, particularly in spacecraft design and scientific instrumentation. In fact, the Ranger spacecraft was generalized to the point where it formed the basic core of the Mariner-2 spacecraft design. The more complex and ambitious post-Mariner probes, in turn, will inherit technology from the simpler Mariners that provide the 1964 state-of-the-art benchmark. Of course, all probes must also pay a debt to the many Earth satellites, which have helped perfect components and improve subsystem reliabilities.

## 10-2. Spacecraft Subsystem Integration

Ten major subsystems make up the spacecraft system defined by the interface matrix (Fig. 10-1). Forty-five subsystem interfaces exist just on the spacecraft alone. Furthermore each interface may be bridged by all nine of the possible interface bonds. These statistics emphasize the complexity of a space probe, but how, amid this superabundance of interconnections, is the spacecraft integrated?

Integration in this instance is the welding together, interface by interface, of the ten diverse spacecraft subsystems into a unit capable of meeting stipulated performance requirements. Performance is measured in terms of weight, cost, and reliability, the three secondary figures of merit introduced in Chap. 4, in lieu of the elusive, single, primary measure of excellence. Tertiary figures of merit, like data bit total and political timing, may also be common currency during the design phase. The really important thing is the designation of a small number of figures of merit that everyone agrees to use in measuring the worth of the system. Only with this decision can system integration proceed.

To be completely objective about system design, the fragmentation



TABLE 10-1. MAJOR TYPES OF SPACECRAFT INTERFACES AND THEIR CONTROL

<i>Interface</i>	<i>Engineering Parameters Involved</i>	<i>Design Implications</i>
Thermal	Temperature, heat flow, material conductivity and surface properties, view factors	Movable louvers, heat transfer convection loops, thermoelectric cooling circuits, optical coatings
Mechanical	Force, torque, vibration, shock	Acoustic insulation, shock absorbers, high strength-to-weight-ratio materials
Spatial	View factors, solid angle	Extendable structures
Electrical	Voltage, current, power, degree of regulation, frequency, impedance.	Parameters must be matched at interfaces.
Radiative	Type of particle, flux, radiation damage	Radiation resistant components, shielding of sensitive components
Magnetic	Flux, frequency	Non-magnetic materials, compensating coils
Information	Data format, bit rate	Parameters must be matched at interfaces.
Electromagnetic	Electromagnetic interference, cross talk, noise	Noisy, interfering components must be eliminated, shielded, or isolated.
Biological	Contamination by microorganisms	Heat and/or radiation sterilization of components. Some components may be "canned."

of the spacecraft into ten subsystems is merely a crutch to help the designers better visualize interactions and design tradeoffs. No matter how carefully the spacecraft is dissected, the resulting model of interlocking subsystems is inferior to a firm grasp of the system-as-a-whole. Accepting the human inability to deal with an unfragmented model, the spacecraft integrator is faced with ten roughly hewn subsystems glued together by a multitude of bonds crossing the forty-five potential interfaces.

Against this backdrop of definitions, and with a list of scientific objectives, the system integrator establishes cost, weight, and reliability budgets for each subsystems. At first, these budgets are assigned on the basis of judgment and experience alone. As the spacecraft takes shape, the initial inequities will be corrected. For example, experience might suggest that a reliability budget of 0.9800 for the communication subsystem is both technically reasonable and acceptable to system goals. The unexpectedly greater complexity of an advanced spacecraft may later force a redistribution of this reliability budget to compensate for the untried features of the new system.

The allocation of the cost, weight, and reliability budgets must be accomplished and monitored in a systematic fashion. The management tools used to control the budgets include Interface Specifications, Approved Parts Lists, and frequent system integration conferences among the subsystem engineers. The interface specifications detail the acceptable ranges of weight and reliability as well as quantitative descriptions of the interface bonds (thermal, electrical, etc.) joining all the subsystems. Sometimes such management tools seem to verge on excessive red tape, but they are essential to a common understanding of the system and provide a bargaining basis for design tradeoffs.

Each experimenter who hopes to place an instrument aboard a spacecraft must adhere to similar weight, reliability, and cost budgets, although they may not be enforced in such a formal fashion. Failures of scientific instruments rarely abort the mission, but they do diminish the final payoff. There can be no compromises in any subsystem without affecting the system as a whole.

The cost and weight parameters are additive and easy to comprehend. So many dollars and kilograms are allotted to each subsystem designer to manipulate in making his subsystem work. Reliability is a more difficult matter. Reliabilities do not add simply and have been the subject of much technical and popular misinterpretation. On top of this, reliability is by far the most critical performance factor in the design of long-lived sterilized probes. In fact, some engineers say that major breakthroughs in component reliability are needed before we can hope to explore beyond Mars and Venus. Further discussion of this all-important parameter is in order.

*Reliability Theory.* Reliability is defined as the probability that a system will perform satisfactorily for a specified period of time under a given set of operating conditions. An interplanetary spacecraft, for example, might have a probability of 0.60 of radioing 10 bits/sec of meaningful scientific data back to Earth from the surface of Mars for 100 hours. The probability and time ingredients of reliability are well understood. More difficult are the specification of the operating conditions and the elucidation of the word "satisfactorily." In the above example, someone must define "meaningful scientific data" before reliability becomes a usable concept. Reliability is a frequently abused parameter. It cannot be employed blindly, because some failures are not due to chance and cannot be properly described by the probabilistic formulas that follow.

The simplest and most easily described kind of reliability occurs when system failures are purely random. In this case:

$$R(t) = \exp(-\rho t) \quad (10-1)$$

where:  $R$  = the system reliability  
 $\rho$  = the chance failure rate (1/hr)  
 $t$  = time (hr).

This simple equation is applicable only to systems which have been adequately debugged (no manufacturing defects), burned in (incipient failures eliminated), and which have not yet reached that point in time where parts begin to wear out. This region of application is illustrated

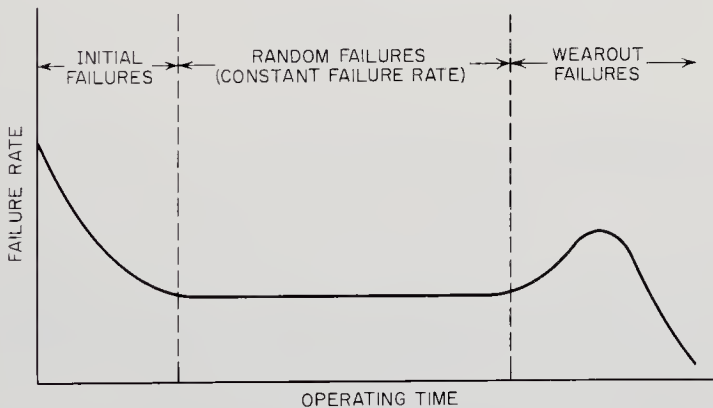


Fig. 10-2. Typical component mortality curve. "Burned-in" spacecraft components operate in the central region. Chapter equations are applicable only in the central region.

in Fig. 10-2, where the mortality curve has flattened out in the middle, yielding a constant failure rate.

The reciprocal of  $\rho$  is the mean time between failures (MTBF), an-

other often-used reliability term. If a system must have a reliability of 0.999999 for one hour, the mean time between failures has to be 1,000,000 hours (over 100 years), according the Eq. (10-1). Such a reliability would be hard to demonstrate experimentally but gives a feeling for the magnitudes involved.

If the system is made up of four devices arranged in series, so that the failure of any one device will fail the whole system, the system reliability,  $R(t)$ , is given by the product rule:

$$R(t) = R_1R_2R_3R_4. \tag{10-2}$$

Referring to Fig. 10-3, the system reliability would be just (0.99) (0.99) (0.95) (0.99) = 0.922. A considerable improvement in system reliability

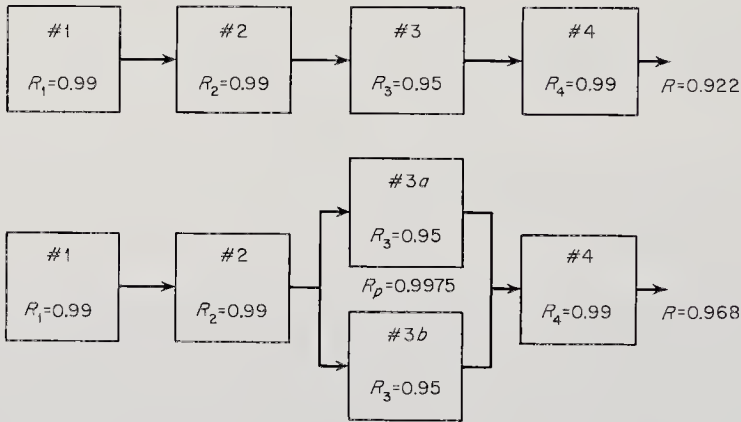


Fig. 10-3. Reliability models of series- and parallel-connected components. Paralleling component #3 significantly improves the over-all reliability. Example from Ref. 10-36.

may be achieved by the paralleling of weak components. The equation for parallel or redundant components is:

$$R_p(t) = 1 - (1 - R_3)^n \tag{10-3}$$

- where:  $R_p$  = the combined reliability of the redundant components
- $R_3$  = the reliability of the individual paralleled components
- $n$  = the number of redundant components.

Using Fig. 10-3 again, the weak third component can be put in parallel with a duplicate of itself so that a failure of one will not fail the whole system. Now the system reliability is:

$$R(t) = (0.99)(0.99) [1 - (0.05)^2] (0.99) = 0.9968,$$

a great improvement (Ref. 10-36).

TABLE 10-2. SURVEYOR STUDY MODEL PARTS LIST\*  
(Approximate Total: 29,000 Parts)

<i>Component</i>	<i>Power Equip- ment</i>	<i>Propulsion Structure Temperature Control</i>	<i>Altitude Control</i>	<i>Sequencer and Computer</i>	<i>Communi- cations and Telemetry</i>	<i>Terminal Guidance Sensors</i>	<i>Tele- vision</i>	<i>Experi- ment Manipula- tion</i>
Electroexplosive devices		6	3					
Pressure regulators		1	1					
Solenoid valves		7	11					
Switches and relays	30	27	25			7		
Electric motors		3	2		2		17	3
Gyros			3					
Accelerometers and transducers			6		2			3
Solar cells	7,000		12					
Battery cells	44							
Crystals				1	9	10		
Memory cores				3,000	500	7	6	
Vacuum tubes			1					
Transistors	32	60	230	840	570	280	127	24
Diodes	77	42	110	2,700	1,800	320	44	48
Resistors	180	160	550	2,200	3,300	690	400	80
Capacitors	190	30	200	870	860	590	90	27
Transformers and inductors	8	6	29	1	46	76	7	

\* Later Surveyor designs may be quite different (Ref. 10-33).

Reliability figures are frequently quoted with confidence levels attached, because it is not a play on words to say that reliability levels themselves are not 100% reliable. To take an example, if a reliability calculation says that a spacecraft has reliability of 0.90 for specified conditions over a given period of time, actual measurements on a series of spacecraft will show a spread of values between 0.00 and 1.00. If the original reliability calculation was based on good component data, most of the experimental reliability points would be clustered in a normal distribution around 0.90. Suppose that half the observed points fall between plus and minus one standard deviation around 0.90, then there is an experimentally observed confidence level of 0.50. Good component reliability data will also give confidence levels. Mathematical techniques are available to handle reliability calculations with attached confidence levels. For the rest of this discussion, only the point values, the peaks of the normal distributions, will be used.

It is worth reemphasizing that the preceding theory assumes a constant failure rate in time (Fig. 10-2). Furthermore, since reliability is a statistical concept, it is necessarily based upon many observations, or, as the phrase goes, "statistically significant data." The point is this: most missiles and spacecraft are classified as *one-shot* systems, which means that there is no recovery, no reuse, and no opportunity for maintenance (Ref. 10-33). The burden on the reliability engineer is magnified by the scarcity of system- and subsystem-reliability data and the extreme scientific, financial, and political pressure for a long active life for the spacecraft. An additional problem is this: planetary landers aimed at Mars, for example, must also be sterilized by heat treatment at 135°C for at least 24 hours, a procedure that demands exceedingly careful selection of components.

The space-probe-reliability quandary is best described by presenting another example. Morrison has published the results of a reliability study completed for one of the Surveyor models (Ref. 10-33). Although Surveyor is a lunar lander, the subsystems are very similar to those that would be used on planetary landers. Tables 10-2, 10-3, and 10-4 present

TABLE 10-3. EXAMPLES OF SURVEYOR STUDY MODEL PART FAILURE RATES\*

Resistors, carbon composition	15	$\times 10^{-9}$ /hour
Resistors, wirewound	150	"
Capacitors, paper	10	"
Transistors, silicon	180	"
Diodes, silicon	40	"
Coils	100	"
Transformers, low voltage	200	"

\* Ref. 10-33.

TABLE 10-4. RELIABILITY ESTIMATES FOR THE SURVEYOR STUDY MODEL, INCLUDING PROSPECTIVE PROBABILITIES OF SUCCESS OF SOME EXPERIMENTS\*

<i>Subsystem</i>	<i>After Landing, Probability of</i>				<i>Total Mission (Flight and 30 days)</i>
	<i>Spacecraft Flight (Boost, Transit, and Landing)</i>	<i>Obtaining One Set TV Pictures (50 hours)</i>	<i>Complete Drilling and Sample Manipulation (9 days)</i>	<i>Other Experiment Manipulation (15 days)</i>	
Propulsion	0.9481				0.9481
Structure	0.9898	0.995	0.995	0.995	0.9849
Power supply	0.994	0.9985	0.9937	0.9894	0.9730
Attitude control	0.9860				0.9860
Sequencer and computer	0.9715				0.9715
Communications and telemetry	0.9932	0.9968	0.9860	0.9766	0.9504
Terminal guidance sensors	0.9841				0.9841
Temperature control and solar panels	0.9988	0.9999	0.9994	0.9970	0.9858
Total spacecraft	0.872	0.9902	0.9743	0.9585	0.802
Television	0.9988	0.9972			0.9748
Drill and sample manipulators	0.9988		0.9898		0.9886
Manipulations of other experiments	0.9988			0.990	0.9814
Spacecraft and experiment total		0.987	0.964	0.949	0.759

\* Later Surveyor designs may differ substantially (Ref. 10-33).

TABLE 10-5. SOME RELIABILITY PREDICTIONS\*

<i>Type of Spacecraft</i>	<i>Rocket Reliability</i>	<i>Lifetime Required</i>	<i>MTBF for Continuous Operations</i>	<i>Reliability of Only Communications</i>	<i>Mission Reliability Including Most Experiments</i>
Interplanetary space probe of 15,000 parts weighing 100 lb; three-stage rocket including IRBM; intermittent 2 percent transmission at 150 watts.	0.75	6 months	100 days	0.7	0.5
Interplanetary orbiting vehicle of 30,000 parts weighing 500 lb; four-stage rocket including ICBM and retro-rocket with terminal guidance; intermittent 2 percent transmission at 150 watts.	0.65	1 year	50 days	0.6	0.4
Interplanetary landing vehicle of 30,000 parts weighing 1,000 lb; five-stage rocket including Saturn and retro-rocket with terminal guidance; intermittent 2 percent transmission at 150 watts.	0.55	1 year	50 days (excluding ground experiments).	0.5	0.3

\* The figures presented here are subject to change as technology improves. The point is that deep-space probes are complex machines. The over-all probability of success is not very high—a fact that makes back-up spacecraft desirable (Ref. 10-33).



these data, beginning with a parts list that is impressive for its totals. Part failure rates and system reliability estimates follow. The subsystem categories used by Morrison do not exactly fit those in the interface matrix—ground-support equipment is omitted—but there is a close parallel. The lesson to be drawn from these tables is that space probes are complex, and, even using the best components obtainable, the system reliability is rather low for a 30-day useful life after landing on the Moon.

The reliability problem of interplanetary spacecraft is brought into focus with Table 10-5, which shows system reliabilities as low as 0.3 for planetary landers. Two solutions to this apparent reliability impasse have been offered:

1. A crash program to improve component reliabilities,
2. The firing of probes in parallel (salvo firing).

The first suggestion aims at the basic problem, but the second can bring acceptable mission reliabilities with today's equipment. Backup spacecraft and salvo firings are admittedly crutches. Ultimately the long-term cost of duplicate firings will have to be compared with that of an all-out component reliability program.

### 10-3. The Communication Subsystem

Three functions may be performed by the spacecraft communications subsystem:

1. Data transmission to the Earth, including both telemetry and video.
2. Command receipt from Earth.
3. Transmission of transponder signals that enable the probe to be tracked from the Earth.

The word "may" is used in the first sentence because the second and third functions can be eliminated in principle by autonomous controls and navigation equipment on the spacecraft. The first major space probes (Mariners and Voyagers) will be dependent on Earth, making all three functions essential. The early spacecraft communication subsystems thus consist of a data encoder/transmitter, a command receiver, and a transponder. Ancillary equipment includes antennas and the cabling to other subsystems for purposes of power, environmental control, and checkout (Fig. 10-4).

The designer of the spacecraft communication equipment cannot have a completely free hand. His apparatus is only part of the much larger communication subsystem stretching from the probe, through the DSIF and SFOF, to man. What is more, all of the internal and external inter-

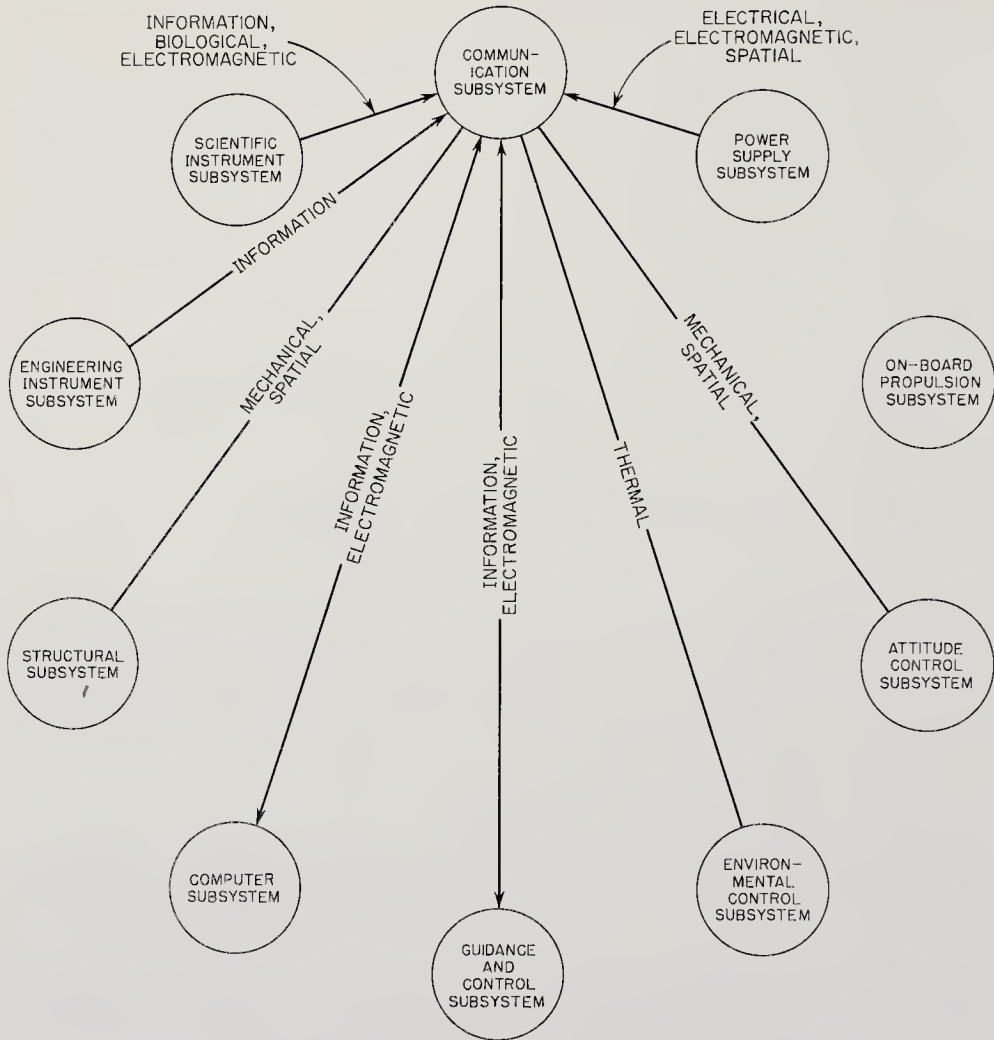


Fig. 10-4. Portion of the spacecraft interface diagram showing the relationships of the communication subsystem to the rest of the subsystems.

faces shown in Fig. 10-4 must be matched, providing still more constraints. On top of this, Nature dictates that a certain range of frequencies be used for interplanetary transmissions. And information theory recommends certain kinds of modulation for space-probe work (see Chap. 6). Such constraints are confirmed on Earth by frequency allocations and large facilities investments that also help to mold the spacecraft parameters.

To narrow the engineering limitations still further, the cost, weight, and reliability budgets enter the picture. Of these three, reliability is the most severe taskmaster, because the electronic parts make up a large fraction of the total number of fallible parts aboard the spacecraft (Table 10-2). Coupled with this fact is the widespread suspicion that electronic com-

ponents are weak links in the spacecraft reliability chain. Boxed in by a multitude of interfaces and overriding figures of merit, space-probe communication subsystems have proven to be surprisingly effective and reliable in practice.

*Matching Communication Subsystem Interfaces.* The communication interface problem is best expressed by Fig. 10-4. Some amplification is warranted, because the communication subsystem interfaces are very similar to those of the other subsystems, discussed later in the chapter. The following paragraphs conform to the kinds of interfaces shown in Fig. 10-1.

In the typical space probe, the communication subsystem will consume a large fraction of the total power generated. Almost all of this energy ultimately appears as heat, which somehow has to be dumped into the space environment or equipment temperatures will rise to excessive values. Conduction and radiation are the simplest and most reliable modes of heat transfer; they are area-limited, however, and may be ineffective in cooling the deep interiors of electronic packages. Convective-cooling loops are useful but should be avoided, because of weight and lack of reliability. Thermoelectric cooling is another technique for removing heat from today's high-part-density electronic equipment. The interface with the environmental control subsystem then is primarily thermal.

A critical mechanical interface connects the booster with the communication subsystem. Across it flow the potentially damaging shocks and vibration spectra of the launch vehicle. The obvious design solution uses insulation and shock mounting. In addition to careful subsystem isolation, each resistor and capacitor should be tied down rather than supported by their leads. Polyurethane foam has been used to ruggedize the electronic packages in spacecraft like Transit.

With small scientific spacecraft, there is always intense competition for every steradian of solid angle. The solar-cell arrays, communication antennas, the environmental control radiators, and the scientific instrumentation all need area access to space to perform their functions properly. The tradeoffs between the competing subsystems involve the spatial interface. Only detailed studies can resolve the arguments in most cases. A spatial interface also links the spacecraft communication and attitude-control subsystems because directional antennas must be pointed accurately to bridge interplanetary distances.

The electrical interface with the power supply involves more than power alone. The power must be of the right sort; i.e., of the proper voltage, frequency, and degree of regulation. Power supply transients could easily insert errors into PCM transmissions.

Nuclear radiation interfaces could be created by radioisotopic and

nuclear-reactor power supplies—say in conjunction with electrical propulsion—or radiation damage could stem from the use of a nuclear rocket during the boost phase. These problems will remain academic until nuclear reactor hardware is developed and tested.\* In any case, radiation shielding, with its weight penalties, could be placed between the radiation source and sensitive components. Since interplanetary spacecraft pass through the Van Allen belts quickly and the radiation levels in deep space are quite low (Fig. 3-3, page 24), environmental shielding is unnecessary.

Magnetic interference with spacecraft scientific instrumentation can be avoided by the use of non-magnetic materials, instrument isolation, and shielding of the offending components. It is difficult to predict magnetic interactions, and most compensation stratagems must wait until systems tests are made during the latter stages of spacecraft development. Compensating circuits are sometimes needed to reduce coupling effects (Sec. 10-7).

Electronic circuits frequently set up interfering electromagnetic fields that disturb not only other portions of the communications subsystem but also nearby equipment, such as the guidance-and-control and scientific-instrument subsystems. This cross talk and noise can be prevented to some extent by good design practice and electromagnetic shielding. Tests with the actual spacecraft, however, usually reveal unpredicted interactions that must be eliminated prior to launch.

The biological interface ties the communication subsystem to the scientific instruments. Residual microorganisms on and within electronics parts, left living despite sterilization on the Earth, may somehow migrate into life-detection experiments and upset the results. Of course, contamination of the target planet might occur too. Mechanical barriers, such as diaphragms, may be interposed to prevent such migration within a spacecraft, but the primary line of defense lies in sterilization by heat (135°C for 24 hrs or more) or nuclear radiation. Both of these accepted treatments may degrade electronic components and reduce reliability. Good design practice obviously decrees the use of heat-tolerant parts and, where possible, components that are more nearly sterile when they come from the factory.

The final interfaces are those where the format and rate of data flow must be matched. Data words flowing between the communication subsystem, the DSIF back on Earth, and the computer subsystem must be of the same length, well synchronized, employ the same conventions, and be transmitted at compatible rates.

\* Only so far as the communication subsystem is concerned. Today's radioisotopic power supplies can seriously interfere with scientific instruments.

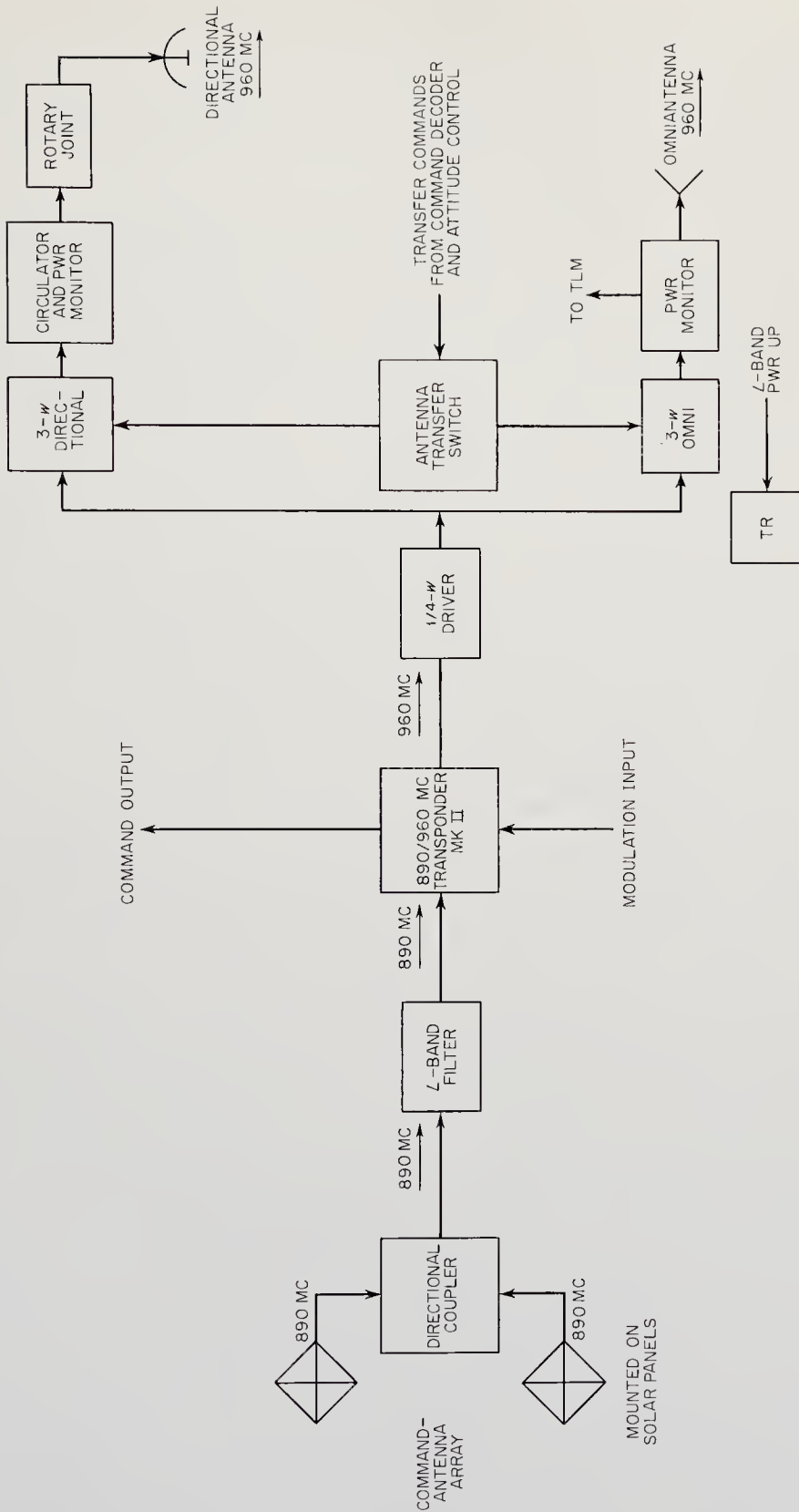


Fig. 10-5. Mariner-2 communication subsystem. The communication functions shown in the diagram are fairly typical of flyby and deep-space probes. (Ref. 10-8)

*Designing the Communication Subsystem.* With all of the preceding admonitions in mind, electronic circuitry must be fashioned into amplifiers, receivers, counters, and the like. The reader's familiarity with basic electronics is assumed here.

Since space probes are all tailored for different particular jobs, generalizations do not come easily. The electronic packages may end up almost anywhere within the confines of the spacecraft. Their positions may even be changed at the last moment, owing to electromagnetic and magnetic interference. It is almost trite to say that the communication equipment has to be rugged, compact, reliable, and consume a minimum of power. Such qualities result mainly from good design practice, exhaustive testing, and careful inspection.

Some specific points can be offered. Equipment should be modular wherever possible so that quick replacement is possible during launch pad checkout. Pursuing the checkout theme, a great deal of thought should be given early in the design to checkout and diagnostic instrumentation and procedures. Finally, reliability can be promoted by using meticulously selected parts in derated situations. Redundancy should be used with discretion. The communication links with the Earth are often duplicated, or alternate links, perhaps using different frequencies and antennas, are provided to back up the primary channels.

Spacecraft communication equipment may be designed in almost infinite variety and yet do its task well. To provide a reference frame, the remainder of this section will use the Mariner-2 communication subsystem as an example (Refs. 6-9 and 10-8). The functional block diagram for the complete subsystem is shown in Fig. 10-5.

In the case of Mariner 2, data had to be transmitted and commands received early in flight, before the midcourse maneuver, regardless of the spacecraft attitude with respect to the Earth. For this reason, a discone omniantenna was mounted on top of the craft. Reception of commands in any attitude was insured by a turnstile antenna on the back side of one solar panel and a dipole antenna on the forward side. Soon after the midcourse maneuver, the spacecraft receded beyond the effective range of the omniantenna. Most communications were then channeled through a large, high-gain, directional antenna. The Mariner-2 high-gain antenna was a 1.22-meter paraboloid with a  $16^\circ$  full-cone-angle beamwidth. Circular polarization was employed. Other antenna combinations would have worked before the midcourse maneuver, but directional antennas are dictated afterward by both distance and the limited power available on the spacecraft.

The transponder used for tracking Mariner 2 received signals from Earth on 890 Mc and responded through a 7-mw transmitter at 960 Mc.

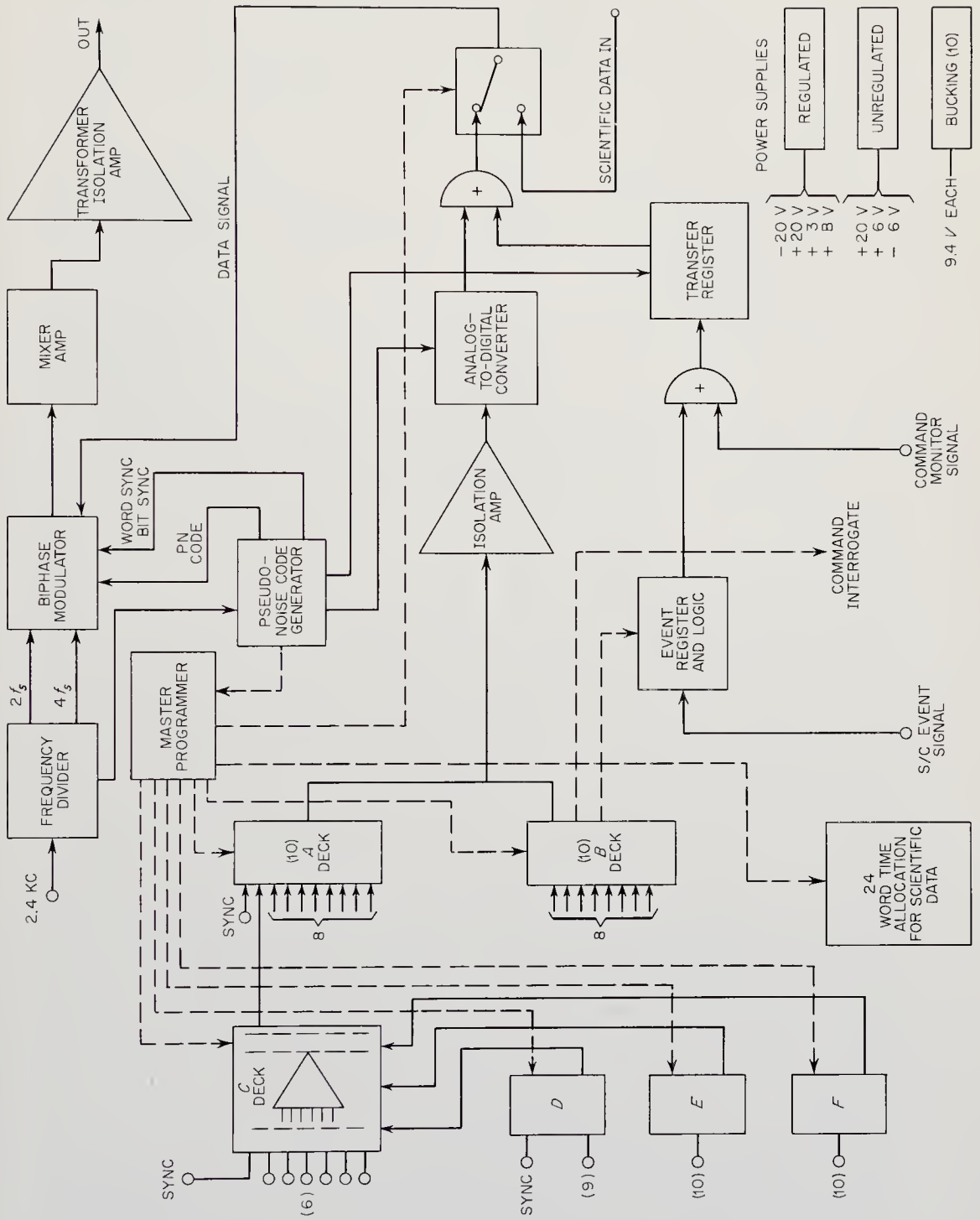


Fig. 10-6. Mariner 2 data encoder. (Ref. 10-8)

The equipment consisted of an extremely narrow-band, double-super-heterodyne, automatic-phase-tracking receiver. Like the bulk of the spacecraft electronic gear, the transponder was entirely transistorized.

Mariner 2's flight command assembly was divided into three functional units (Fig. 10-5), which demodulated the command signals and extracted timing pulses. They were:

1. The command detector.
2. The command decoder, which decoded the commands and timing pulses for other parts of the spacecraft.
3. The transformer-rectifier.

The Mariner-2 data encoder multiplexed engineering and scientific data. It was capable of operating in three modes at two different data rates. To show its intimate connection with the scientific instrumentation, its functional block diagram is presented in Fig. 10-6. During Mode 1, only engineering data were sampled. Engineering and scientific data were time-shared in Mode 2, while only scientific data were transmitted in Mode 3. A bit rate of 107 bits/sec was used near the Earth, but this was reduced to 8.33 bits/sec near Venus, as the distance and limited transmitter power (3 watts) forced the changeover to the lower rate.

The entire Mariner-2 communication subsystem weighed only 12 kg, excluding mounting hardware. Power input was 50 v rms, 2400 cps, square waves at 30 va. Everything was transistorized except for the cavity amplifiers. The most characteristic features were the phase-lock, PCM/PSK modulation concept and the use of a transponder for tracking, both keyed to the DSIF ground equipment. Without question, other design approaches could have worked, but the Mariner-2 communication approach has been validated by its success at Venus. Future probes not only must be matched with the extant DSIF but give good reason for changing from a proven communications approach.

In time, technology undoubtedly will bring surprises that will lead to major performance improvements. Molecular electronics holds out a promise of lower weights, smaller volumes, and reduced power requirements while still performing all the functions of today's electronic equipment.

#### 10-4. The Power Supply Subsystem

The task of the power supply seems so simple—to provide well-regulated electrical power to the spacecraft during all modes of operation—that it is difficult to see why it presents a major problem in spacecraft design. One reason for difficulty is implicit in the load profile for a typical interplanetary exploratory vehicle (Fig. 10-7). Not only do total power



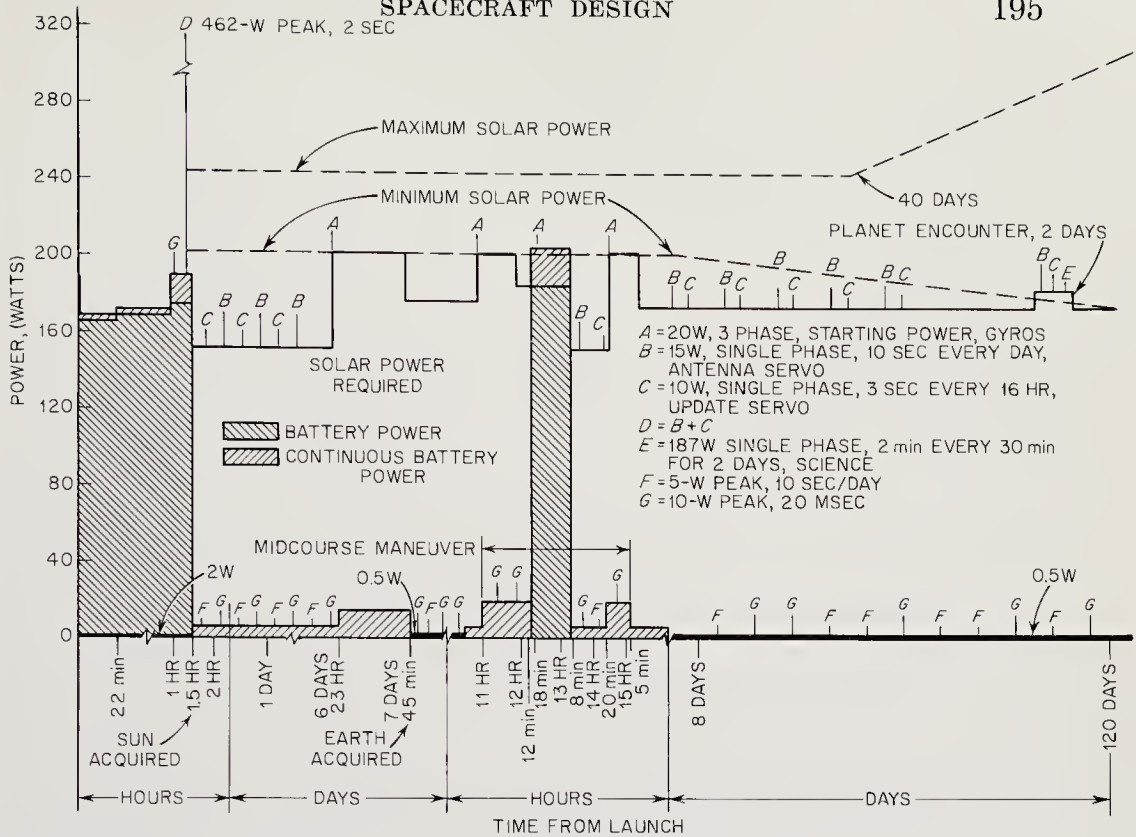


Fig. 10-7. Load profile for Mariner 2. The irregular power demand necessitated an energy accumulator—the battery. (Ref. 10-13)

levels shift radically with time, but the voltages and regulation needed vary, too. The spacecraft power supply is also subject to damage from the environment, particularly from radiation hitting the solar cells. And its complexity (thousands of solar cells) brings about a reliability situation similar to that seen in the communication subsystem.

Perhaps most of the debate in power generation circles today stems from the great variety of competing power sources and power conversion schemes that are being offered for space use. Every purveyor's product, whether it be a fuel cell, nuclear reactor, or thin-film solar cell, is held up as the solution to space power's problems. The best answer to all the contradictory proposals is in the careful study of the mission and a dispassionate selection. The unique characteristics of the interplanetary mission often make the choice easier. Mission durations are months and years, effectively ruling out power supplies based on chemical energy, like batteries, fuel cells, and open-cycle turbomachinery. The interplanetary spacecraft is almost always in full sunlight, a fact which eliminates the Earth-satellite problem of providing power during the shadow periods. On the other hand, the use of solar power is made more difficult by the large changes in the solar constant as the probe moves

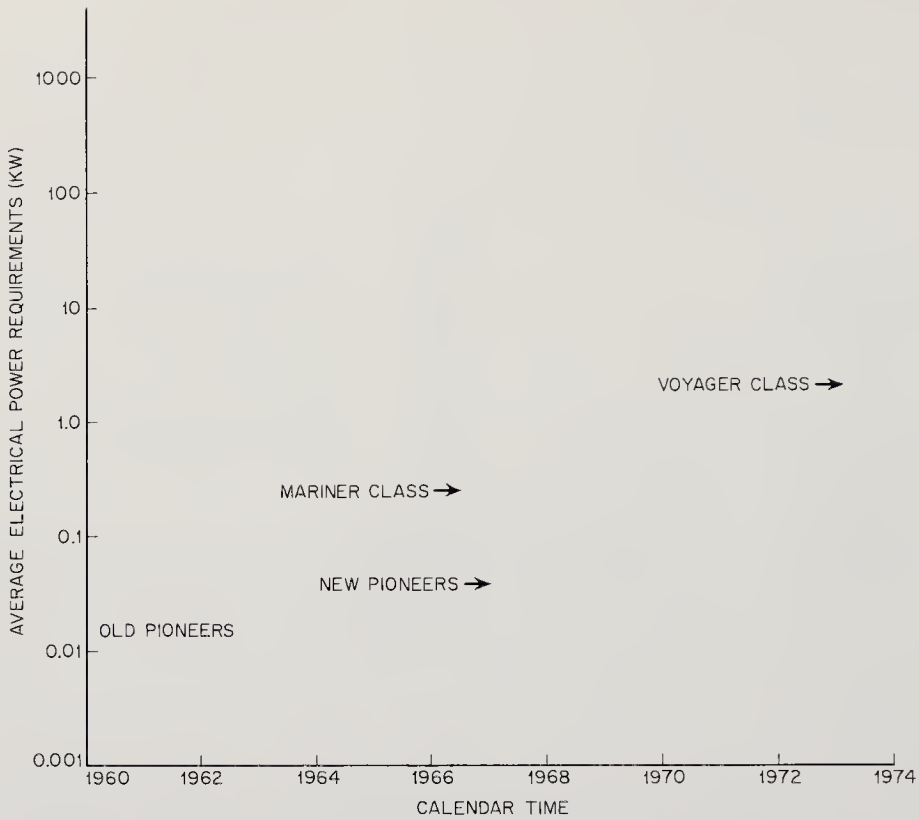


Fig. 10-8. Estimated electrical power requirements for space probes.

toward or away from the Sun. More serious are the opaque and possibly corrosive atmospheres surrounding some of the planets in the solar system. Power requirements, too, are highly variable, starting with tens of watts for simple probes and ending with hundreds of kilowatts for electrically propelled spacecraft (Fig. 10-8).

No single type of electrical power source can meet all load and environmental demands. Only two long-duration power supplies are now operational: solar cells and radioisotopic power generators. Research and development are being carried out on solar-thermionic, solar-thermoelectric, solar-dynamic, and many kinds of nuclear power plants. Just which of these will actually be aboard the space probes of the future cannot be divined at present. Some predictions are shown in Fig. 10-9.

To prepare for interface analysis, examine the block diagram for Mariner 2 (Fig. 10-10). It is far from a simple black box with two terminals. Added to the 2400-cps bus carrying power to the major subsystems are 400-cps lines and a number of connections for ground-support equipment and telemetry monitoring of voltages and currents. These wires constitute the major electrical interfaces.

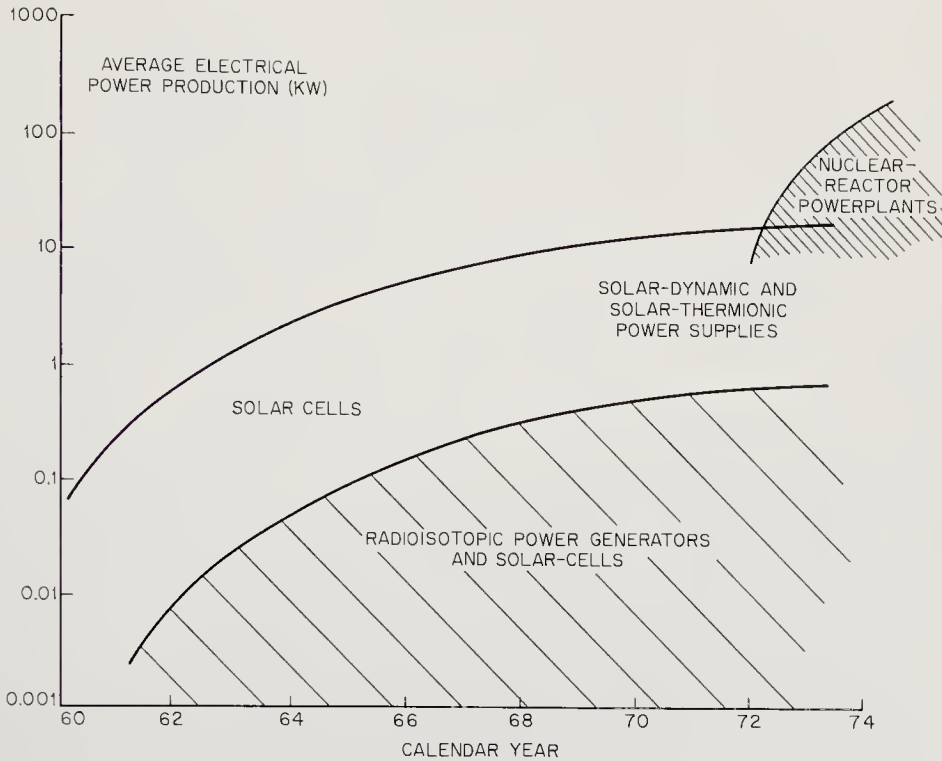


Fig. 10-9. Estimated availability of flight-ready power supplies.

Every power supply has four parts:

1. An energy source.
2. An energy conversion mechanism.
3. A waste heat rejector.
4. A power-conditioning section that regulates and doles out the power according to each subsystem's needs.

Most power research and development concentrates on power sources and energy conversion, although the Mariner-2 block diagram makes it clear that much of the actual hardware is devoted to power conditioning and distribution (Figs. 10-10 and 10-11).

The solar-cell power supply (see Fig. 10-12) is constructed from components rather similar to those in the communication subsystem. Most of the interfaces—mechanical, magnetic, radiative, and spatial—are also similar. Only the thermal interface with the environmental control subsystem differs significantly. Regardless of the type of power supply selected, about 90% of the energy collected or generated turns up as waste

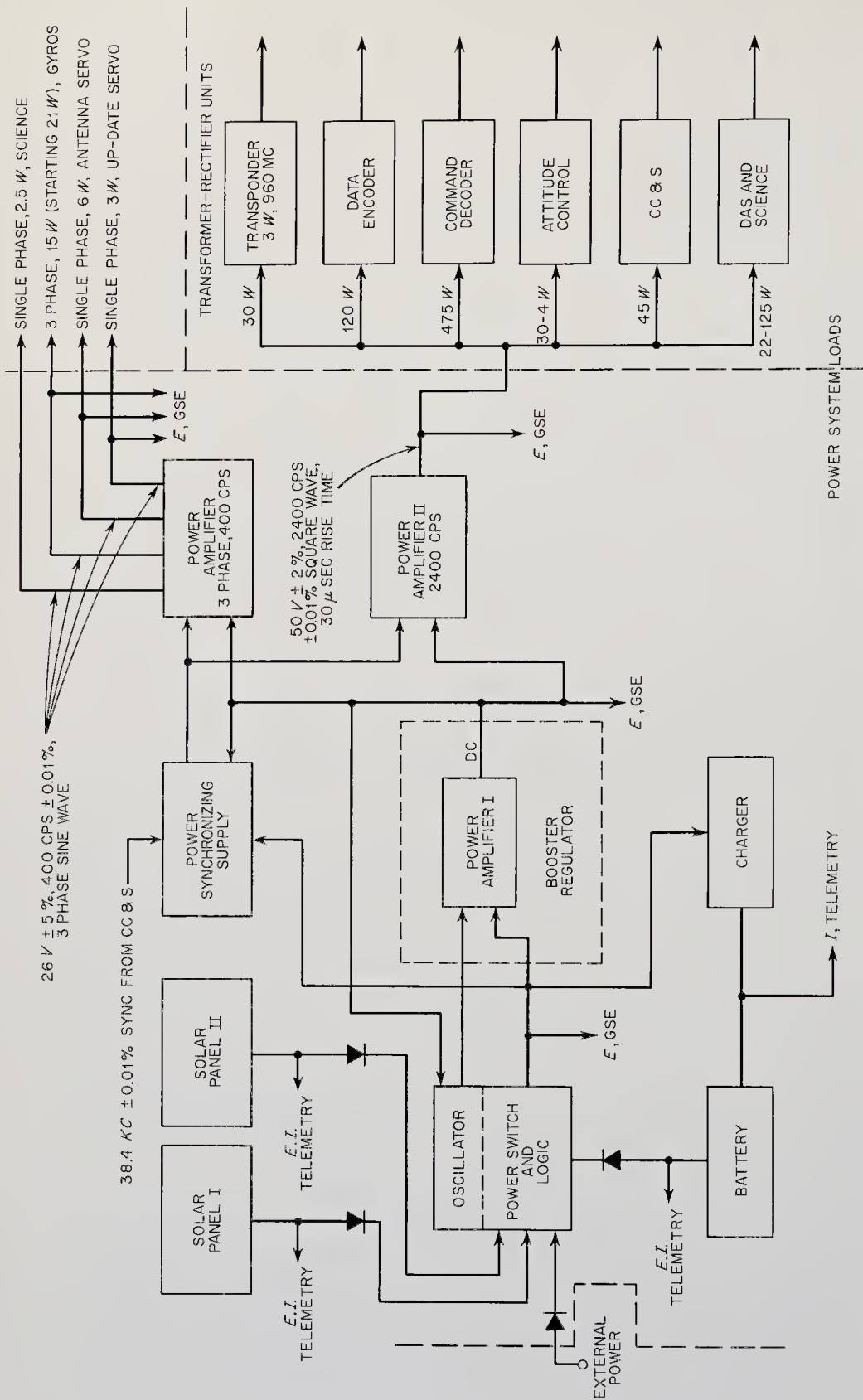


Fig. 10-10. Block diagram of the Mariner 2 power-supply subsystem. Note the extent of the power-conditioning equipment. (Ref. 10-13)

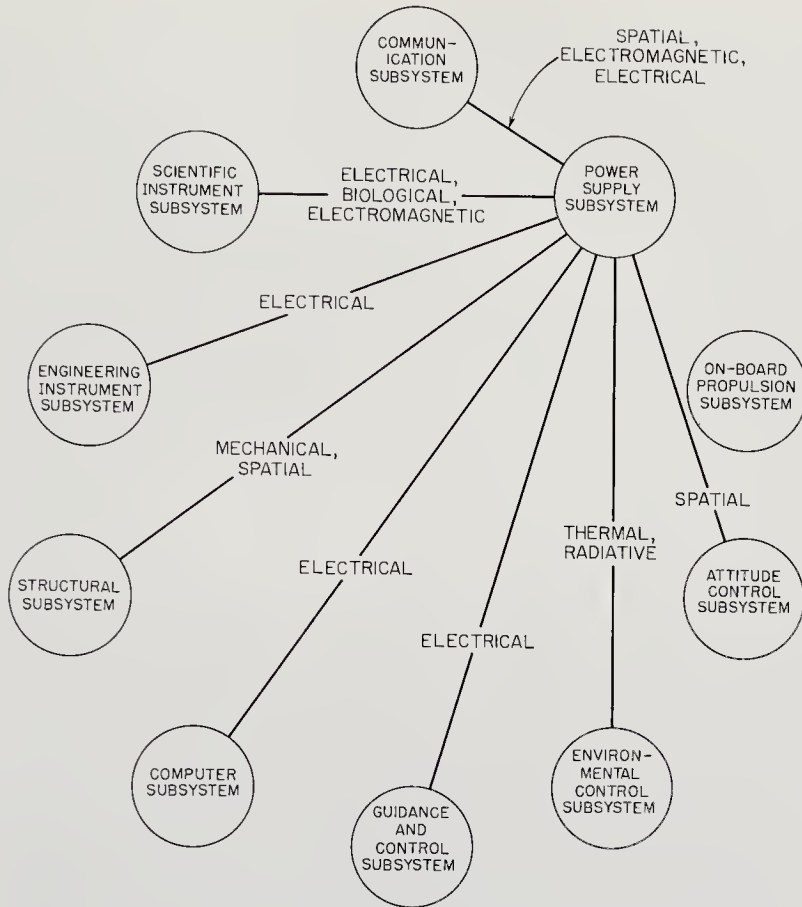


Fig. 10-11. Portion of the spacecraft interface diagram showing the relationship of the power-supply subsystem to the rest of the subsystems.

heat to be disposed of by the power supply. The remaining 10% ultimately appears in the form of heat loads in the other subsystems. Fortunately, solar cells immediately reradiate the heat they absorb from the Sun. The thermal interface becomes a real problem only when there is an onboard source of energy such as a nuclear reactor or isotope. The heavy load of waste heat emanating from these devices must be carefully directed out of the spacecraft and away from heat-sensitive equipment. Since heat rejection must be by thermal radiation, the nuclear power supply is often finned (Fig. 10-13) or uses convection loops and external radiators. Of course, any spacecraft component that optically sees the radiator fins will absorb thermal radiation. Sometimes this heating can be an advantage, as in a planet's shadow or during a lunar night, but usually it is undesirable.

What have been the operational problems encountered with power supplies? Over 90% of the long-lived space vehicles launched so far have

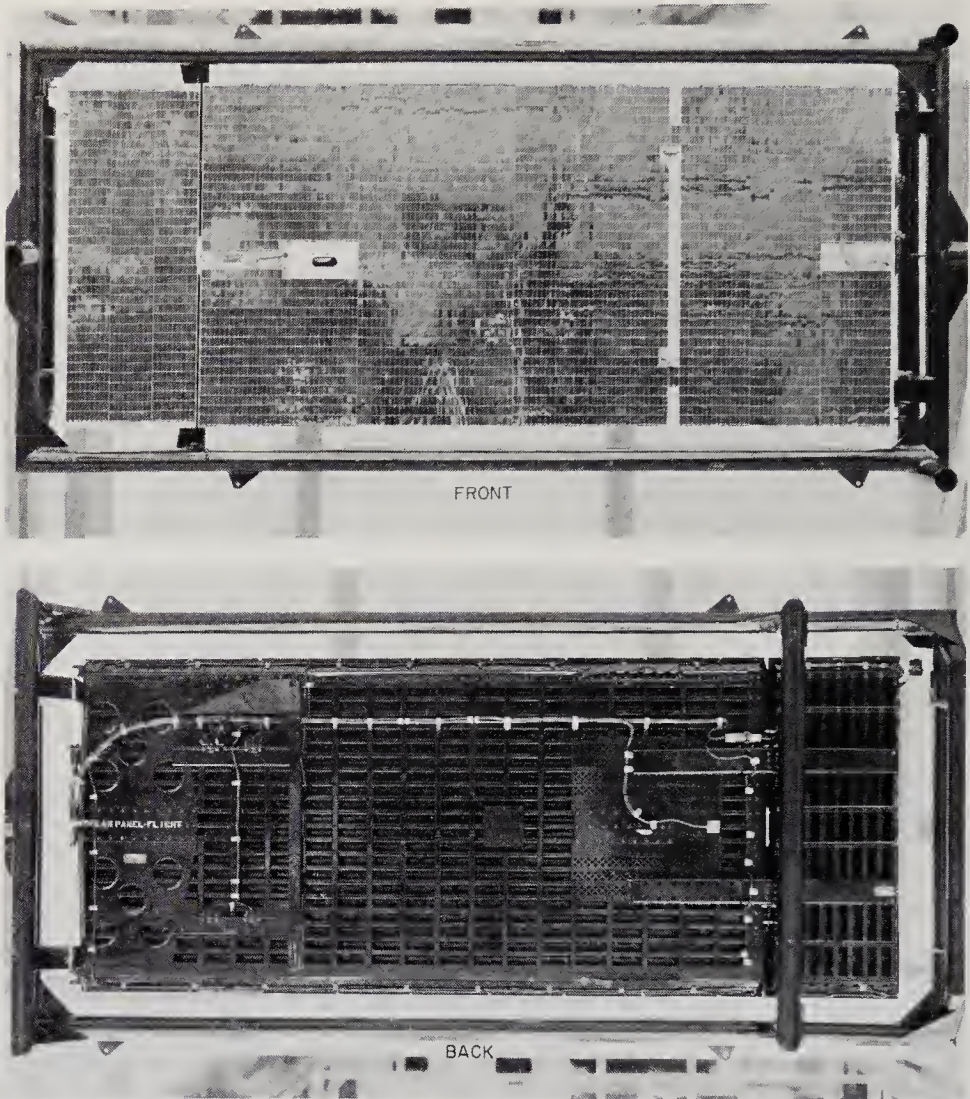


Fig. 10-12. Front and back views of one of the Mariner 2 solar panels. (Courtesy of the Jet Propulsion Laboratory)

employed solar cells. The most publicized problem has been that of radiation damage to the solar cells. Happily, space probes will avoid this since they will not operate within the Earth's Van Allen belts and, hopefully, will avoid those of other planets, if they exist. After the radiation damage problem comes subsystem breakdown due to component failures. Mariner 2, for example, had a short in its solar panels that reduced the amount of power available. Like several other mystifying electronic failures in spacecraft, it first repaired itself and then reappeared. The switching and regulator circuits in the relatively complex power-conditioning equipment have been troublesome for spacecraft with solar cells and also for the

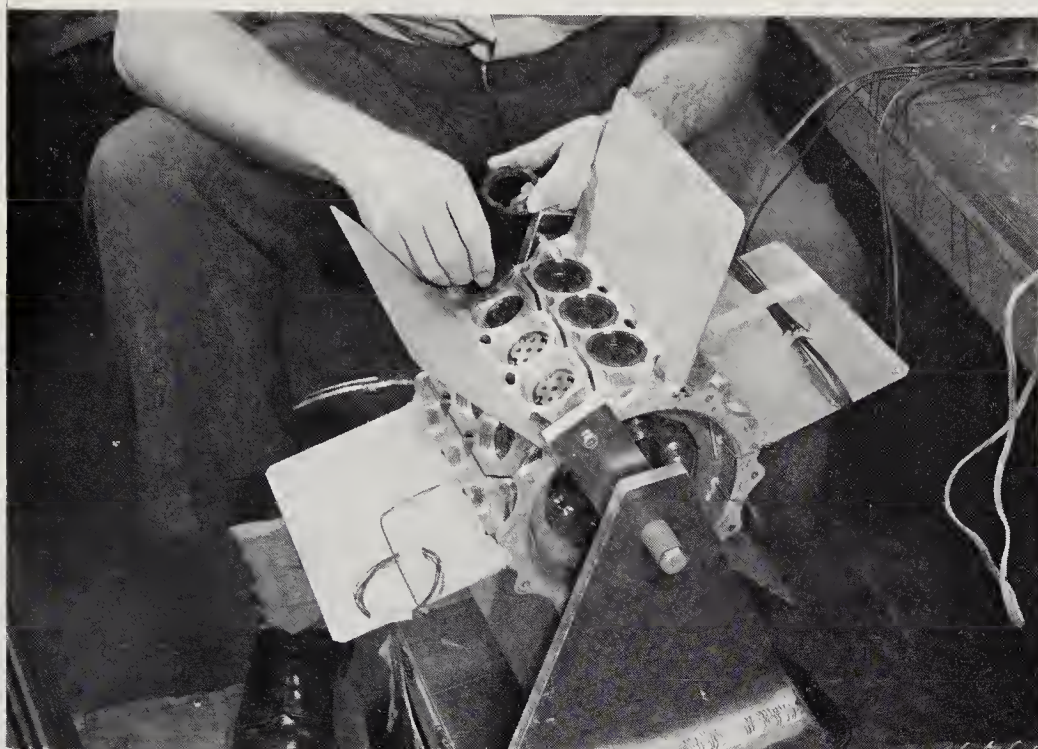


Fig. 10-13. The Snap-9A radioisotopic power generator being assembled. Thermoelectric modules fit in the holes around the central fuel capsule. Note the large radiator fins needed to reject the 500 watts of waste heat. (Courtesy of Martin-Marietta Corp.)

radioisotope-powered Transit satellite. A final operational problem that afflicts solar cells comes from the solar heating of the solar panels: the higher the temperature of the solar cell, the lower its efficiency. Even the higher solar flux on trips toward the Sun does not compensate for this deterioration. Solar probes and missions to Mercury will have their solar-cell power supplies oversized compared to what would be needed close to the Earth to compensate for later degradation.

Solar cells are amply described in the literature (Ref. 10-47). The electromagnetic energy of solar photons is converted into the potential energy of electron-hole pairs in the vicinity of a  $p$ - $n$  junction. These current carriers move across the junction under the influence of the junction's electric field, creating a current flow. Physically, solar cells are thin, semiconductor sheets—usually made from silicon—with several square centimeters of active area. Early cells used a thin layer of  $p$ -silicon diffused on a thick layer of  $n$ -silicon. New radiation-resistant cells reverse the materials.

There are several techniques for assembling the tiny solar cells into the large panels so characteristic of modern spacecraft. In all approaches,

the cells are anchored to a substrate to form modules. Cells are electrically interconnected either by series shingling or by wire connections. Modules are then connected in the series-parallel array that best satisfies the voltage requirements, while still providing part-power protection in the event of circuit failures in some of the strings. Rectifiers must be inserted to prevent current flow between unbalanced series strings and from storage batteries into the cells themselves.

The external surfaces of many satellites are plastered with solar cells. The larger satellites, however, must go to solar paddles to find sufficient area to power their instruments. Deep-space probes also need more power than surface-mounted cells can generate. The familiar wing-like solar-cell panels adorn most space probes. And here is a source of potential failure. Solar panels are stowed inside the booster shroud during the ascent through the atmosphere. After the shroud is blown off, electrical or pressure-powered actuators deploy the solar panels. The electromechanical deployment mechanisms sometimes do not work.

A battery is usually needed in all space power supplies to provide power during peak loads. Solar power plants need the battery for power before solar acquisition and during the midcourse maneuver. If the Sun is accidentally lost, battery power is needed for reacquisition.

The radioisotopic power generator, the only other source of long-duration power sufficiently developed to consider here, receives its thermal energy from decaying radioisotopes, such as Pu-238, Cm-244, and Sr-90. Thermoelectric and thermionic converters change 5-10% of this heat into electricity. The remainder of the heat is radiated to space from the generator surface. Usually a cylindrical geometry like that shown in Fig. 10-13 is used.

One of the major concerns in using nuclear energy is the radiation emanating from the fuel capsule. So long as alpha emitters like Pu-238 and Cm-244 are used and power levels are kept below the kilowatt range, the radiation will be of minor concern to unmanned spacecraft. The intense gamma and bremsstrahlung radiations from the beta-emitting fuels are more serious and necessitate generator shielding (Ref. 10-11).

Another power supply of potential interest focuses sunlight on the cathodes of thermionic converters to generate electricity (Ref. 10-47). Eventually these supplies might produce more power per unit weight than either solar cells or radioisotopic power generators. Fine attitude control (to about one minute) would be needed.

A summary of probable space power supply capabilities is presented in Fig. 10-14, using the conventional parameter of specific mass. Of course, all power-conditioning and mounting equipment is charged to the power supply. Figure 10-9, page 197, shows a well-defined time and



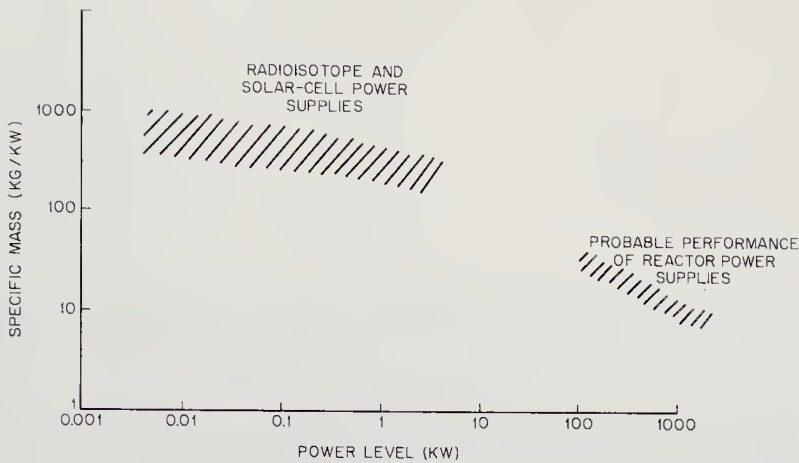


Fig. 10-14. Estimated specific masses of long-duration power supplies available for flight between 1960 and 1975.

technological barrier in space power. This barrier exists because the proven solar cells and radioisotopic units are limited to only a few kilowatts of power for reasons of weight, panel area, and fuel availability. Apparently only nuclear reactor power supplies can overcome this power-level obstruction, but it is unlikely that flight-operational reactor power supplies in the 10-100-kw range will be ready before 1972. This power constraint will undoubtedly hold back both manned and unmanned space exploration.

### 10-5. The Propulsion Subsystem

After the spacecraft has been injected into its trajectory and the last launch-vehicle stage has been discarded, there would seem little left for onboard rocket engines to do. This section owes its existence not to the magnitude of the velocity changes needed but rather to the variety and precision of the propulsion functions that must be performed. Table 10-6 sums the requirements simply. In addition to attitude control, which is discussed in the next section, propulsion is first needed for the small nudges of the correctional maneuvers. Relatively large velocity increments are called for during powered descent to planetary surfaces and the return to Earth of samples from deep space.

The varied propulsive functions and the difficulty of selecting the best propulsion system(s) pose a problem similar to that of choosing the best power supply. As before, the choice of a dependable, operational pro-

TABLE 10-6. ONBOARD PROPULSIVE FUNCTIONS\*

<i>Function</i>	<i>Approximate Velocity Incre- ment (m/sec)</i>	<i>Possible Propulsion System</i>
Midcourse maneuvers	10-500	Solids, liquids, electric
Terminal maneuvers	1-100	Solids, liquids
Orbital injection	10-10000	Solids, liquids
Atmospheric entry	10-10000	Solids, liquids
Powered descent	1000-100,000	Solids, liquids
Rendezvous	1-100	Liquids
Orbital transfer	5000-50,000	Solids, liquids, electric

\* See Table 5-2, page 46, for other propulsive functions and mission types.

pulsion system is limited in terms of possible candidates. The tried and usually true solid- and liquid-chemical rockets are as predominant in onboard propulsion as solar cells are in the power supply. Small, restartable nuclear heat transfer rockets have been studied (Ref. 9-10), but they appear likely to be delayed in development until at least 1980. As with the large nuclear rockets mentioned in Chap. 9, development is slow, and it is hard to see the details beyond the promises of high specific impulse and phenomenal energy density.

Onboard propulsion units will obviously be much smaller than the boosters that started them on their way. More than this, the onboard rocket must survive the long flights through space without fuel deterioration or excessive propellant boiloff. Because they will be used for delicate maneuvers, the onboard rockets have to be precisely controlled not only in thrust level but also in thrust duration and direction. Restartability in space is an additional asset. In fact, the property of restartability tends to separate solid- and liquid-chemical engines, with the

TABLE 10-7. STORABLE FUEL-OXIDIZER COMBINATIONS\*

<i>Fuel</i>	<i>Oxidizer</i>	<i>Vacuum Specific Impulse (sec)</i>
RP-1	IRFNA	314
	N <sub>2</sub> O <sub>4</sub>	323
UDMH	IRFNA	328
	N <sub>2</sub> O <sub>4</sub>	333
N <sub>2</sub> H <sub>4</sub>	IRFNA	328
	N <sub>2</sub> O <sub>4</sub>	339

\* From Tables 20.6 and 20.7, *Handbook of Astronautical Engineering*, H. H. Koelle, ed., McGraw-Hill Book Co., New York, 1961.

solids usually being relegated to one-shot applications, even though much progress has been made in developing restartable solid motors.

Rocket principles and engine configurations are the same for small rockets as they are for large. The discussions of Chap. 9 may thus be applied at this point.

When talking about onboard chemical engines, the list of high-energy fuels (Table 9-1, page 164), must be supplemented with the "storable" fuel-oxidizer combinations, with their markedly lower specific impulses (Table 10-7).

The propulsion subsystem's most sensitive interfaces occur with the

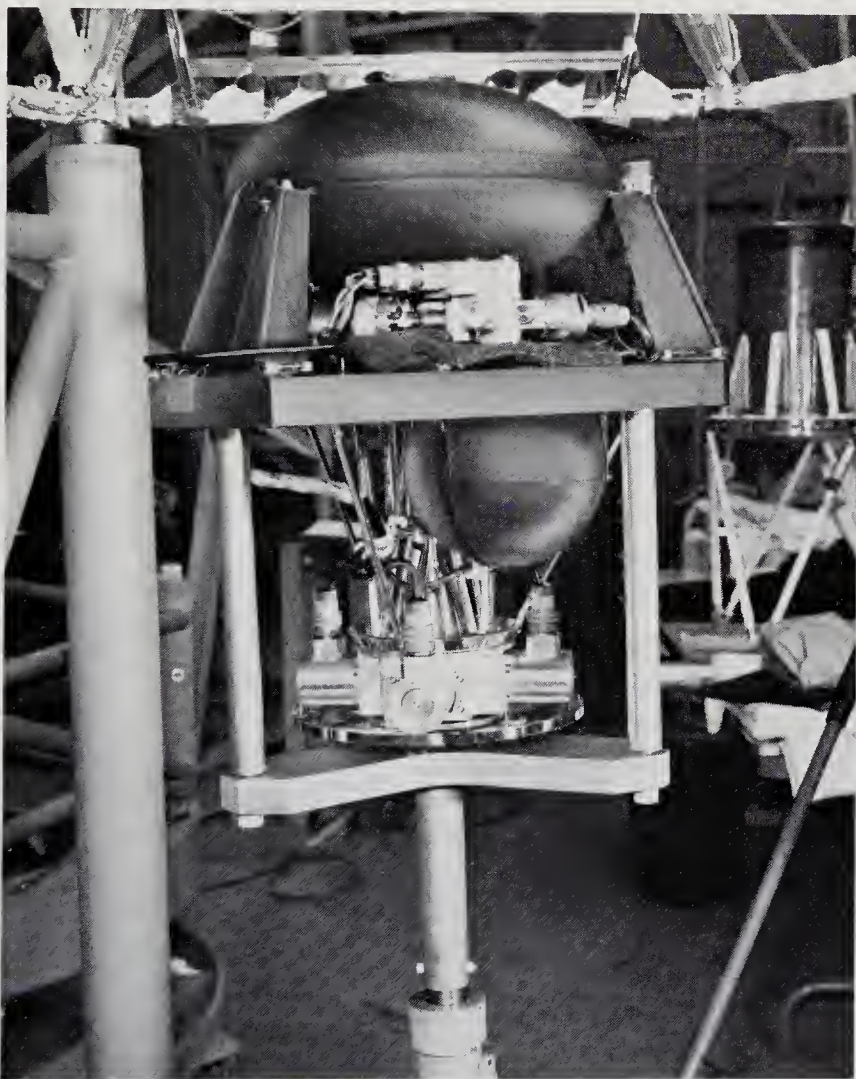


Fig. 10-15. Midcourse propulsion subsystem used on Mariner 2. Bladder is filled with hydrazine under pressure. Rocket nozzles are shown below. (Courtesy of the Jet Propulsion Laboratory)

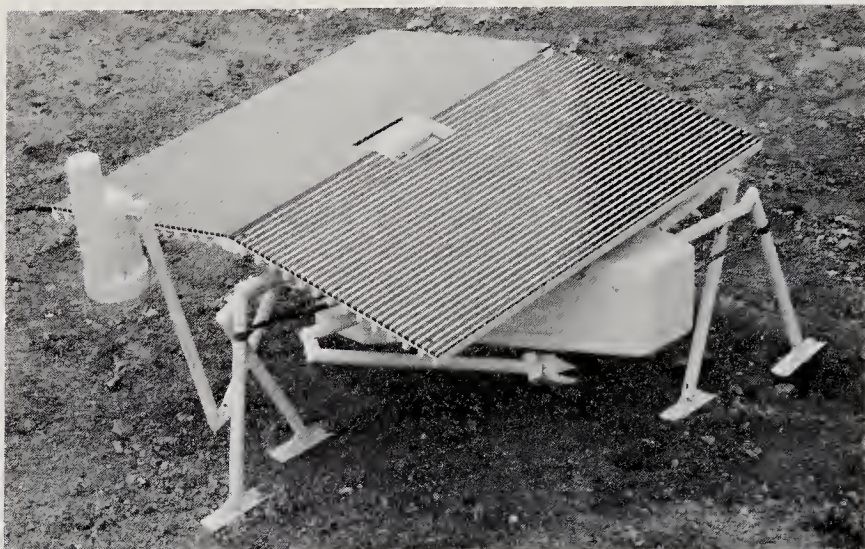


Fig. 10-16. Demonstration model of a walking machine designed for use on planetary and lunar surfaces. (Courtesy of Space General Corp.)

guidance-and-control and attitude-control subsystems. The pertinent function of the guidance-and-control subsystem is to determine the timing, direction, and magnitude of maneuver velocity increments. The attitude-control subsystem should position the spacecraft precisely for the maneuver, or the rocket's action may be worse than useless.

Another interface worth mentioning exists when the engine is fired. In the vacuum of outer space, the exhaust jet will be overexpanded (too fan-like) unless impractically long nozzles are used. The poorly collimated gases may envelope some of the spacecraft surfaces. Back-scattered molecules may even impinge on the solar cells. During powered descent, the hot exhaust gases can interfere with radar altimeters. For these reasons, the engine must be mounted so that its nozzle has a wide field of view. To preclude spinning the spacecraft, the thrust axis should go through the center of mass. The Mariner-2 midcourse propulsion subsystem, shown in Fig. 10-15, illustrates how the problems were met for a flyby probe. A rather unexpected interface occurs between the onboard propulsion subsystem and life-detection instruments. Some rocket propellants are not sterile and, even after combustion, may contaminate instruments with microorganisms in their smoke.

*Surface Propulsion.* When a space probe lands on an unexplored planet, its usefulness will be greatly increased if it is even slightly mobile. But where will the power come from, and what kind of locomotion should be used for unpredictable terrains?

The onboard power-supply subsystem is the manifest source of pro-



Fig. 10-17. Flexibly connected, doughnut-wheeled vehicle for locomotion on planetary and lunar surfaces. (Courtesy of General Motors Corp.)

pulsive energy. If the planet has an atmosphere, it may be opaque to solar rays, chemically active, or a carrier of dust and debris. In view of the environmental hazards, the power supply for early planetary landers seems destined to be fueled with radioisotopes, at least until reactor power plants are available. Whatever energy source is selected, the vehicle motor will probably have only a few hundred watts of electricity to propel the spacecraft.

Potential planetary terrains are so diverse that a great many different kinds of locomotion might be effective (Table 10-8 and Refs. 10-5 and 10-9). Concepts vary from screw-like machines that crawl through dust and sand to insect-like walking machines (see Fig. 10-16). Models of the better concepts have been built and tested in simulated terrains (Fig. 10-17). The only generalization that can be made concerning planetary locomotion is that adaptations of Earth forms of locomotion (wheels and tracks) will probably suffice for most missions and take the least expenditure of research and development.

TABLE 10-8. POSSIBLE TECHNIQUES FOR PLANETARY LOCOMOTION\*

<i>Means of Locomotion</i>	<i>Advantages</i>	<i>Disadvantages</i>	<i>Conclusions</i>
Walkers	<p>Possibility of greatly reduced power requirements compared to a wheel, particularly when operating in soft, loosely packed ground, providing that internal friction of the mechanism can be kept small.</p> <p>Good foldability.</p> <p>Possibility of eliminating exposed rotating joints by using flexible leaf spring joints.</p>	<p>Mechanical complexity.</p> <p>Increased internal friction.</p> <p>Road velocities limited by inertial stresses in leg members, which will be roughly proportional to the square of the speed.</p> <p>Carefully considered design required for feet, which must negotiate and provide useful traction over a variety of random terrains and surfaces.</p> <p>May be subject to excessive vibration.</p>	<p>A practical walking machine for operations is possible providing over-all vehicle size and weight are kept small.</p>
Hoppers	<p>Generally the same advantages and disadvantages summarized above for walking machine with the additional major disadvantage of requiring systems to stabilize the machine's attitude during the ballistic flight phase of the hopping maneuver. Possibility of greatly reduced friction with well designed means of elastic energy absorption upon landing.</p>		<p>Does not seem practical or necessary at this time.</p>
Wheels	<p>Mechanical simplicity.</p> <p>If wheels have large diameters and broad rims, then reasonable coefficients of friction are to be expected.</p> <p>Capable of high speed when negotiating smooth terrain.</p>	<p>Rotating joints require good seals.</p> <p>Large diameters and broad rims suggest possible heavy rim weights.</p>	<p>A planetary vehicle having properly designed wheels, individually powered, can generate sufficient traction for practically any mission except heavy bulldozing.</p>

TABLE 10-8. Continued

<i>Means of Locomotion</i>	<i>Advantages</i>	<i>Disadvantages</i>	<i>Conclusions</i>
Tracks	<p>Good flotation in soft soils.</p> <p>Ability to bridge crevasses and trenches.</p> <p>Capable of the greatest tractive effort of any usual means of locomotion.</p> <p>Capable of negotiating rough terrain.</p>	<p>Mechanically complex.</p> <p>Typical track configurations have many exposed joints.</p> <p>May require frequent maintenance.</p> <p>Have considerable operating friction.</p>	<p>May be the only conventional solution if high traction is a major requirement.</p>
Rocket Sustension	<p>Can overfly rough regions of terrain.</p> <p>Can move short distances at high velocities.</p>	<p>Requires means to stabilize vehicle during flight, which implies a complicated computer.</p> <p>Greatly reduced range for a given quantity of propellant in comparison with a wheeled vehicle.</p>	<p>Not practical from fuel consumption standpoint as a prime means of locomotion during extended cross-country missions.</p>
Rocket-Ballistic Trajectory	<p>Generally the same advantages and disadvantages as enumerated for rocket sustension, but with about three times the range for a given quantity of propellant.</p>		<p>Not satisfactory for deliberate detailed exploration of planetary surfaces.</p>

\* Adapted from Ref. 10-19.

If a planet has an atmosphere, man will inevitably wish to fly probes through it. Therefore, aircraft in alien atmospheres must be considered. Since most planetary atmospheres are nonoxidizing, the conventional jet engine is useless. Rocket planes and helicopters are possible prime movers for unmanned landers, but surface locomotion is much more likely.

*Electrical Propulsion.* The final topic of this section concerns the use of electrical propulsion to increase the spacecraft velocity increment (Ref. 10-43). The considerable research work done in this field indicates that these low-thrust, high-specific-impulse propulsion systems will be most useful during the long flights to the more distant planets. On these

missions their much higher specific impulses (around 10,000 sec) will permit much greater payloads than chemical rockets can promise. There are, however, some disadvantages connected with electrical propulsion. First, the thrust-to-weight ratios are  $10^{-4}$  or less, meaning that travel times between planetary orbits tend to be very long.\* Second, the reliability of the associated large nuclear power plant is therefore an unresolved question. Third, the large nuclear power supplies that can produce hundreds of kilowatts are decades away. Unhappily for the nuclear-electric propulsion systems, the low-specific-impulse chemical rockets have so improved and gained such momentum that it will be difficult to displace them from their dominant role in spacecraft propulsion. Both nuclear rockets and electrical propulsion seem destined to be dominated by chemical rockets during the early exploration of the solar system.

### 10-6. The Attitude-Control Subsystem

The typical space probe is far from isotropic. The communication subsystem, the scientific sensors, and solar power supplies are all direction-sensitive. The spacecraft attitude with respect to the Earth, Sun, and scientific target must be sensed and converted into torques that will align the spacecraft for the business at hand. The physics of attitude control has been covered in Sec. 5-6. The attitude-detecting sensors will be described in Sec. 10-8.

Some of the specific jobs that fall to the attitude-control subsystem at various times after the launch shroud is blown off are:

1. Acquire the Sun for the solar panels in order to relieve spacecraft batteries.
2. Align the spacecraft rocket engine for midcourse and terminal maneuvers and for satellite orbit injection.
3. Acquire the Earth for the high-gain, narrow-beam antennas.
4. Acquire astronomical targets for scientific sensors.
5. During atmospheric entry, present the proper spacecraft angle of attack.
6. During powered descent, assure spacecraft stability and rocket-engine alignment.
7. Compensate for angular disturbances due to unbalanced solar pressure and meteoroid collisions.

With an unjointed spacecraft, some of the above functions are simultaneously incompatible. To illustrate, the Sun may have to be lost during the midcourse maneuver, when the gas jets change the spacecraft attitude,

\* Some low-energy ballistic interplanetary trips may be longer than those of ion rockets, but, in principle, high-thrust, ballistic orbit transfers can always be found that will be faster.



and later be reacquired. Interim power would have to be supplied by batteries during such an occurrence.

The total amount of angular impulse needed during the flight of a space probe varies greatly with vehicle and mission. Simple interplanetary monitoring craft with isotropic sensors, uniformly mounted solar cells, and omniantennas might not require any attitude control at all. Contrast this to a typical, small planetary lander needing  $10^7$  newton-sec ( $2.25 \times 10^6$  lb-sec) of impulse to orient it correctly during all maneuvers. Intermediate missions, like simple planetary flybys, require something like 5000-10,000 newton-sec. Momentum requirements cannot be specified more narrowly than this without going into actual vehicle and mission design.

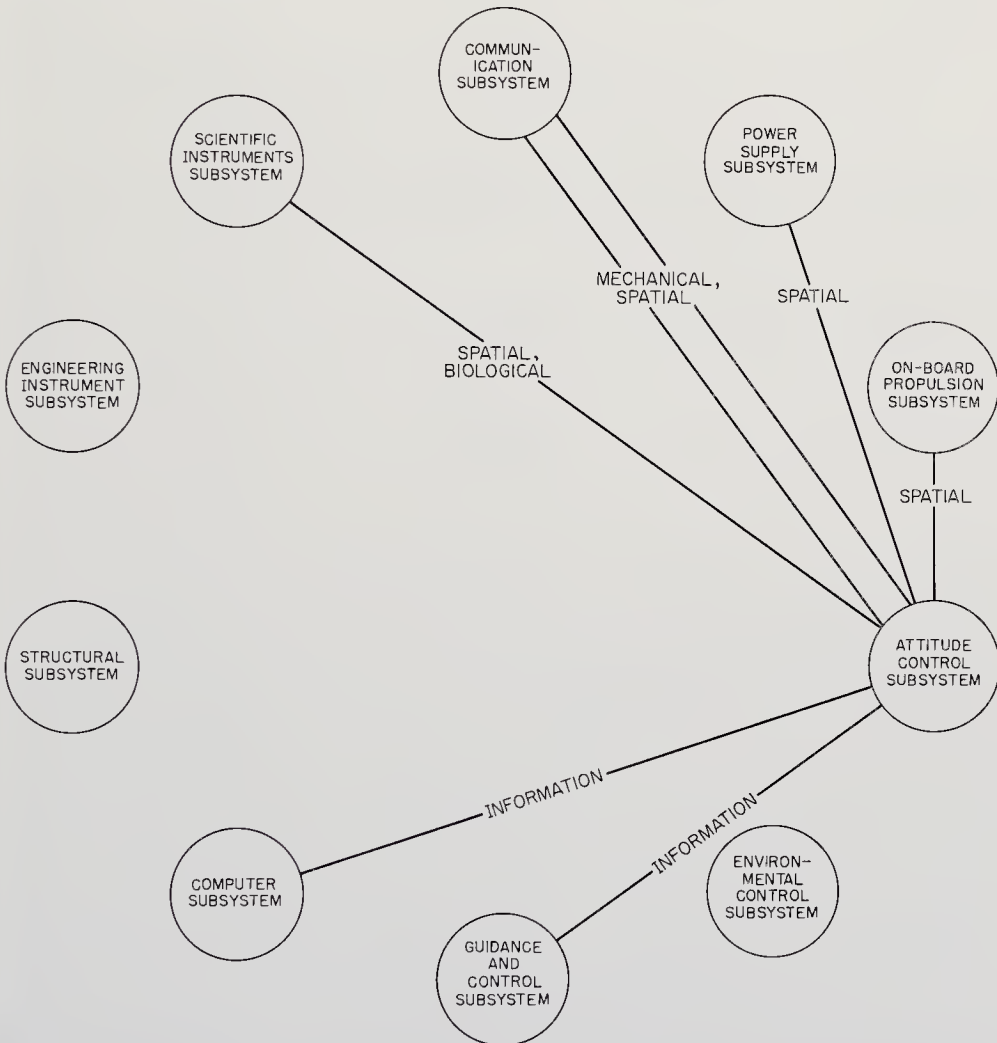


Fig. 10-18. Portion of the spacecraft interface diagram showing the relationship of the attitude-control subsystem to the rest of the subsystems.

The interfaces that the attitude-control subsystem shares with the rest of the spacecraft are summarized in Fig. 10-18. The import of the mechanical interfaces with the communication, propulsion, and power subsystems have already been described. The information interfaces with the guidance-and-control subsystem and the onboard computer may involve attitude instabilities and attitude-control computations that strain the capability of the computer. Luckily, these problems are easier to solve for space probes than they are for Earth satellites, where gravity, drag,

TABLE 10-9. COMPARISON OF ATTITUDE-CONTROL TECHNIQUES

<i>Technique</i>	<i>Specific Impulse (sec)</i>	<i>Torque Range (newton-m or lb-ft)</i>	<i>Remarks</i>
Cold gas jets	80	0.001 to 25	Accurate. High pressure N <sub>2</sub> or Ar stored in vehicle tanks. Good for probes (Fig. 10-20).
Liquid rockets	150-250	0.01 to 80	Can be throttled or used intermittently. Used for resetting saturated inertial devices.
Solid rockets	200-275	0.01 to 80	Best for short burning times. Small gun types ("cap pistols") exist.
Vapor pressure	80	0.001-0.1	Vapor evolved from solid or liquid is expelled through a nozzle.
Inertia wheel		0 to 1	For precision control. Can saturate.
Liquid inertial device		0 to 1	Liquid metal loop driven by electromagnetic pump. Consumes considerable power.
Inertia sphere		0 to 0.03	No cross-coupling, as with wheels. Difficult to build and develop.
Electrical propulsion	10 <sup>3</sup> -10 <sup>5</sup>	10 <sup>-6</sup> to 10 <sup>-4</sup>	Low mass consumption, but power supplies not developed.
Solar pressure		10 <sup>-5</sup> newton/m <sup>2</sup>	Can be used for stabilization. Also a major cause of trajectory dispersion.

and other forces complicate the picture. Experience with the orbiting observatories (OSO and OGO) has been helpful here. Finally, gas jets and rocket exhaust may damage the surfaces of solar cells and scientific sensors if nozzles are not carefully placed. Again the competition for solid angle is manifest.

Approximately 90% of the spacecraft launched to date, including Pioneer 5, have been spin-stabilized because the technique is simple and effective in many applications. Spin stabilization, since it keeps the spacecraft pointed in a fixed direction in inertial space, is unsuited to the highly directional properties desired of advanced space probes. Therefore, some method is needed for parceling out the variously sized bits of angular momentum to accomplish the seven functions just listed.

Two fundamental possibilities exist:

1. Mass expulsion by gas jets, rockets, projectiles, and pyrotechnics.
2. Mass-conservative devices, like gyroscopes and inertia spheres.

The status of these and some other concepts important to the attitude control of interplanetary spacecraft are summarized in Table 10-9. Earth satellites, especially those with sensors continuously pointed at the Earth, have pioneered the use of magnetic bars, gravitational-gradient stabilization, and aerodynamic control. The fields and forces upon which these special attitude-control devices are based are absent or ineffective in

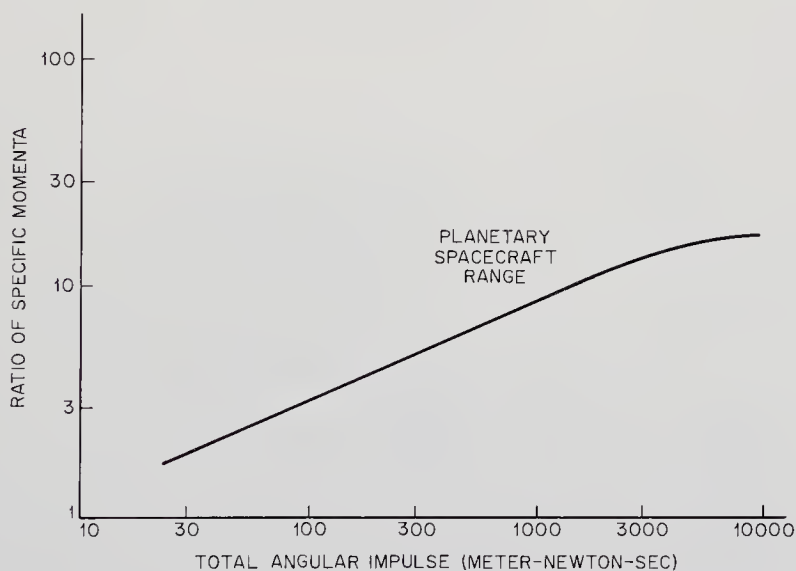


Fig. 10-19. Ratio of specific momenta for cold-gas jets and inertia spheres. (Specific momentum is measured in terms of the momentum per unit mass of the attitude-control subsystem.) (Ref. 7-9)

deep space. As a compensating blessing, they are also too weak to cause significant attitude perturbations.

Space probes have seen the transition from the spin-stabilized Pioneer 5 to the cold-gas-jet-controlled Mariners and Rangers. Gates, Scull, and Watkins have shown that for the Mariner-type flyby missions, cold-gas jets offer more than a ten-to-one margin of superiority over reaction spheres (Fig. 10-19 and Ref. 7-9). A more general comparison of the different mass expulsion possibilities has been published by Romaine (Fig. 10-20 and Ref. 10-38). This comparison is based on total weight,

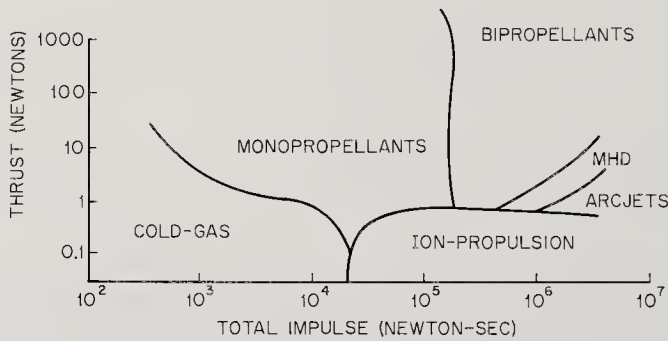
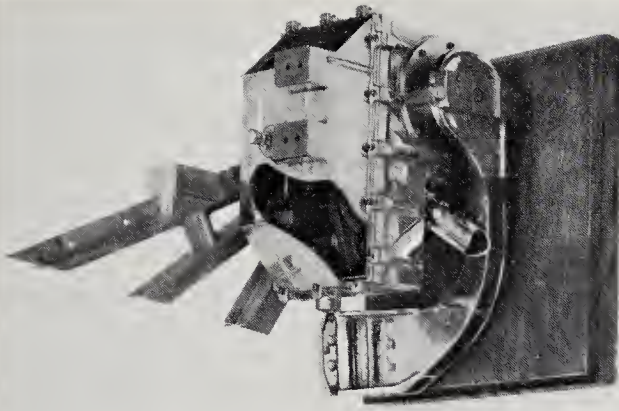


Fig. 10-20. Comparison of attitude-control-system capabilities on a total weight basis showing areas of superiority. Graph assumes that electrical propulsion systems are operational. (Ref. 10-38)

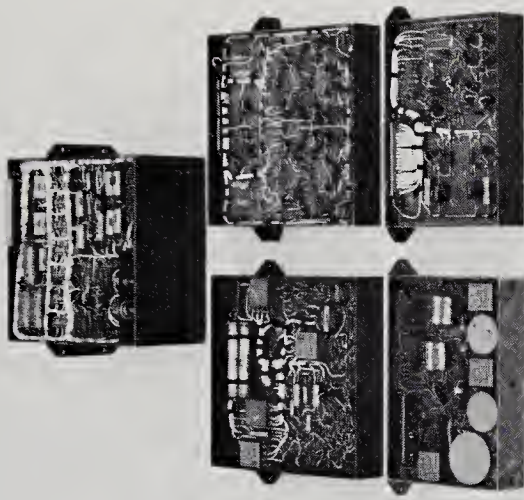
including the thruster and its propellant supply. Unfortunately, the electrical-propulsion attitude-control concepts noted in the figure cannot be used until large, reliable, long-lived power supplies become available. With inertia devices shown to be too heavy in comparison with gas-jets and rocket-engine attitude-control subsystems, the latter two schemes will apparently dominate the scene in deep space for many years to come. Spin stabilization, however, will continue to be useful for probes like Pioneer 6 that require only stabilization in inertial space.

The liquid and solid rockets used in attitude-control subsystems are basically the same as the much larger booster rockets described in Chap. 9. As Table 10-9 indicates, however, the specific impulses of attitude-control rockets suffer considerably in the miniaturization process.

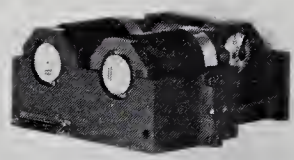
Continuing to use Mariner 2 as a reference space probe, Fig. 10-21 illustrates some of the components of the ten cold-nitrogen gas jets used during the 1962 flight to Venus. The placement of the gas jets about the axes to be controlled during the flight can be seen in the Mariner drawing, Fig. 11-8. Controlling the ten paired gas jets were six solar-aspect sensors, one horizon scanner, and three rate-integrating gyros, all to be discussed in Sec. 10-8.



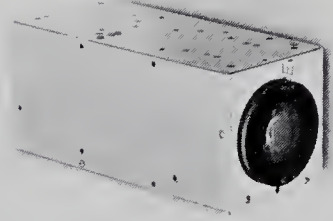
ANTENNA ACTUATOR



ELECTRONICS



GYROS



EARTH SENSOR



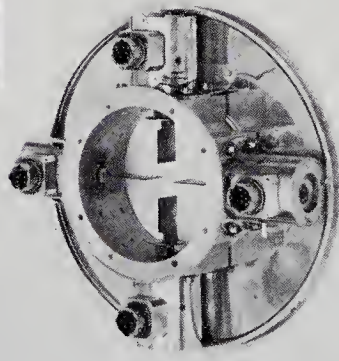
NITROGEN TANK



REGULATOR



VALVE ASSY



JET VANES



SUN SENSORS

Fig. 10-21. Mariner-2 cold-nitrogen-gas-jet attitude-control equipment. (Courtesy of the Jet Propulsion Laboratory)

### 10-7. The Environmental-Control Subsystem

Sophisticated spacecraft use both active and passive means for controlling their environment. Passive devices are preferred, because of their better reliabilities, but some environmental forces—especially thermal forces—that are impressed on the spacecraft are so intense and variable that only active controls yield acceptable solutions.

In this section, three aspects of environmental control will be covered:

1. The maintenance of the spacecraft temperatures within a range where all equipment can operate satisfactorily.
2. The reduction of the nuclear radiation environment to acceptable levels.
3. The reduction of spacecraft-induced magnetic fields to acceptable levels.

These three forces—thermal, radiative, magnetic—may originate on the spacecraft itself or arise in the space environment (Fig. 10-22). Not unexpectedly, the three forces are identical to three of the nine interface forces used in the interface diagrams. A fourth force, mechanical in nature, due to shock and vibration, penetrates the booster interface. It is described in Sec. 10-10. By their very nature, all four forces pervade the entire spacecraft. The environmental-control equipment is therefore intimately intermeshed with all spacecraft subsystems, as illustrated by the ubiquitous thermal-control machinery.

*Thermal Control.* A probe in outer space continually intercepts solar energy, some is reflected, some is converted into heat. A spacecraft also evolves heat internally, because of onboard energy sources and component energy dissipation. For thermal equilibrium, every joule added to the spacecraft must be balanced by a joule radiated from it to empty space. In the absence of equilibrium, spacecraft equipment will eventually become either too hot or too cold for proper operation.

The operating temperature range of most spacecraft equipment is approximately 0-60°C, a little more for some components. Superficially, these broad limits would seem easy to meet with good thermal design. Several factors make the task more challenging. Though the interplanetary spacecraft does not encounter the periodic solar eclipses of the Earth satellites, the Solar Constant does vary considerably from one planetary orbit to another. In the neighborhood of Venus, the solar flux is about twice that near Earth; near Mars, it is only 3/7 that of Earth; at Pluto, only 1/1600 that of Earth. A Mercury-bound spacecraft must be prepared to cool its electronic equipment, while one bound for the outer planets may have to heat it. Furthermore, the heating and cooling actions must

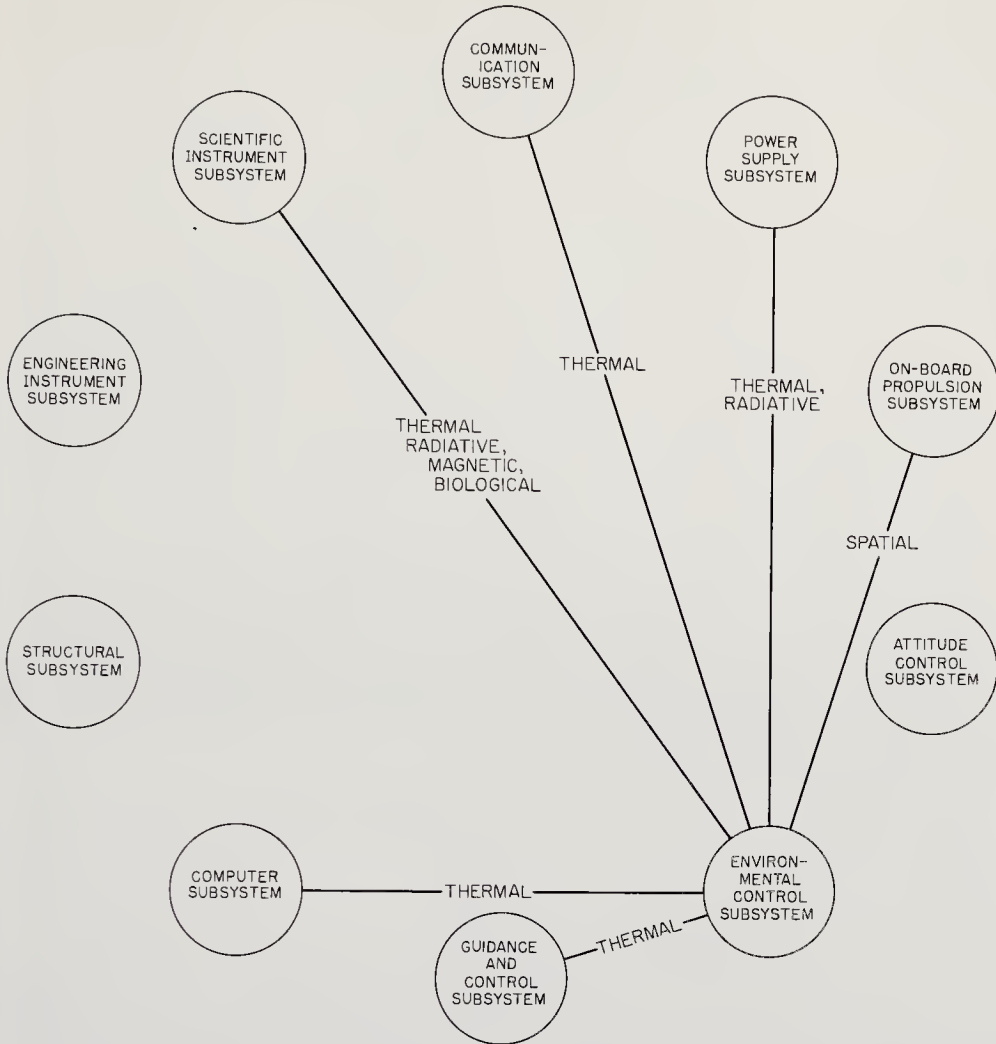


Fig. 10-22. Portion of the spacecraft interface diagram showing the relationship of the environmental-control subsystem to the rest of the subsystems.

vary smoothly with the Solar Constant. The Solar Constant is predictable, but the effects of solar radiation on the properties of spacecraft surfaces is not well known. Ultraviolet radiation and the impact of the interplanetary plasma may degrade or even upgrade surface emissivities and absorptivities. The radiation properties of surfaces are not well known as functions of temperature, although this situation is improving rapidly (Fig. 10-23). A final source of possible errors of calculation is the large increase in thermal resistance across mechanical joints (i.e., riveted pieces) owing to the "cleaning effects" of the space vacuum. Because of these complications, a thermal model of the spacecraft turns out to be an essential part of every probe program. Only in this way can the thermal environment be predicted with confidence.

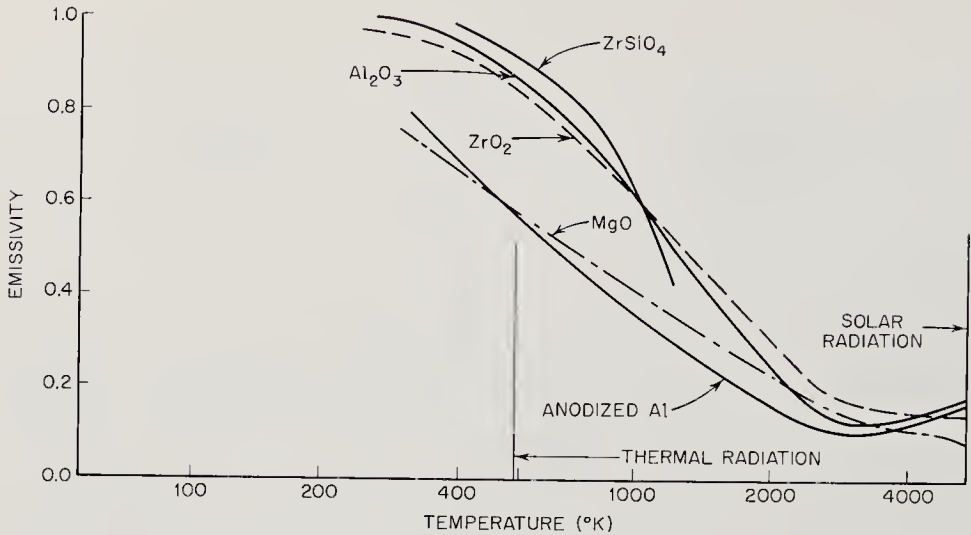


Fig. 10-23. Emissivity vs. temperature for various radiator coatings. (Ref. 10-42)

The importance of a thermal model of the spacecraft is underscored by the spacecraft structure itself, which consists of many shells, wires, struts, and fasteners of different sizes, shapes, and materials. Accurate simulation is needed to support analysis.

Thermal analysis begins with the simple law of heat conduction:

$$Q = kA (T_1 - T_2)$$

where:  $Q$  = the heat flow (watts)  
 $A$  = area (m<sup>2</sup>)  
 $T_1 - T_2$  = the temperature difference (°K)  
 $k$  = thermal conductivity (watts/m<sup>2</sup>-°K)

A simple law, but imagine applying it to a complex structure like Mariner 1 (Fig. 11-8).

The law of radiation heat transfer is scarcely more complicated:

$$Q = \sigma A e F_{12} (T_1^4 - T_2^4)$$

where:  $e$  = the surface emissivity  
 $\sigma$  = the Stefan-Boltzmann constant ( $5.67 \times 10^{-8}$  watt/m<sup>2</sup>-°K<sup>4</sup>)  
 $F_{12}$  = a view factor defined as that fraction of the total energy originating at  $A_1$  which is intercepted by  $A_2$ .

The mathematical difficulty here is that although the laws of heat transfer are quite simple, the actual geometries are extremely involved.

With this handicap in mind, the spacecraft designer can:

1. Construct a simplified analytical model and obtain approximate results under idealistic conditions.



2. Attack the problem on a digital computer, using a more accurate model, in which each differential area and angle is integrated piece by piece on the computer. Almost any spacecraft can be mocked up in this way.
3. Back up all computations with a thermal model.

It is only wise to assume that any analytical attack will be approximate to some degree, say  $\pm 10^{\circ}\text{C}$ , for the most sensitive component. To this uncertainty must be added a safety factor and the dynamic range anticipated during the mission (Ref. 10-31).

Spacecraft thermal calculations deal with only a few kilowatts, but spacecraft have small heat capacities, leading to quick trouble even with small heat unbalances. With such small quantities of energy, heat conduction along wires and struts of small cross section is surprisingly effective in transferring heat. Temperatures are so low that radiative heat transfer between spacecraft components is small but not always negligible.

Passive thermal control uses special surfaces and coatings, applied in patterns calculated to radiate excess heat away and/or absorb solar energy to keep instrument packages warm. Passive surface control usually provides equilibrium solutions only for a fixed environment. As the solar flux waxes or wanes or as subsystem heat loads vary, there must be corresponding changes to preserve the over-all heat balance. In concept, such changes might be carried out passively by surface coatings or thermally conducting members which change with time; say, through sublimation in a vacuum. Use might also be made of the effects of sunlight on the emissivity of a surface. At present, no passive scheme seems to have the dynamic range needed for the thermal control of all space probes.

Active control of the spacecraft thermal environment is more effective. Some possibilities are:

1. Movable surfaces to control radiative heat transfer.
2. Convection heating and cooling.
3. Electrical heating and cooling.

Most spacecraft and many satellites mount thermostatically controlled louvers, slotted disks, and other movable surfaces in strategic positions (see Fig. 10-24). As the controlled component gets hotter, a temperature-sensitive control element, like a bimetallic element or liquid-filler actuator, opens louvers to permit more heat to escape by radiation (Fig. 10-25). If component heating is desired on a trip away from the Sun, the same principle can admit more sunlight or even expose the component to the radiating fins of a radioisotopic power generator.

Convection heating and cooling are not presently used on space probes.

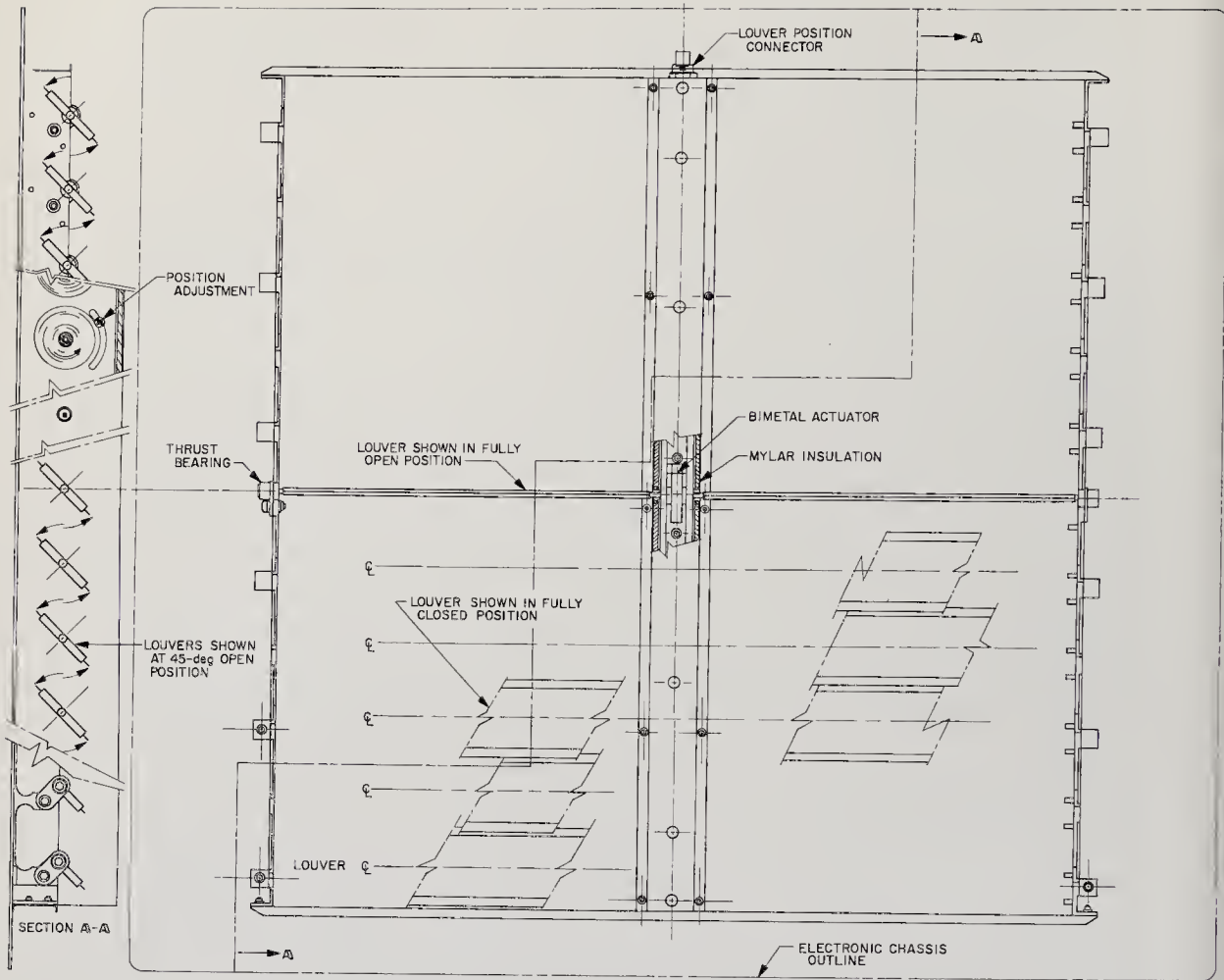


Fig. 10-24. Louver mechanism on Mariner 2 used to control the spacecraft temperature. (JPL drawing)

The larger probes of the future, with deeply buried components, may depend upon streams of liquid metal or organic coolants to carry heat to and from heat-sensitive regions.\* Separate, finned space radiators and an onboard source of electrical energy and heat—perhaps a radioisotopic generator again—are essential features of such schemes. Convection implies moving parts, like pumps and valves. Reliability therefore must sit in judgment when the environmental-control subsystem is considered.

Electricity can be used like convective fluids and beams of radiant energy. Spacecraft often employ small heaters and thermoelectric coolers in special parts of their electronic equipment. Electrical heating and

\* Convective cooling is usually lighter than conduction cooling when space-probe weight exceeds 250 kg.

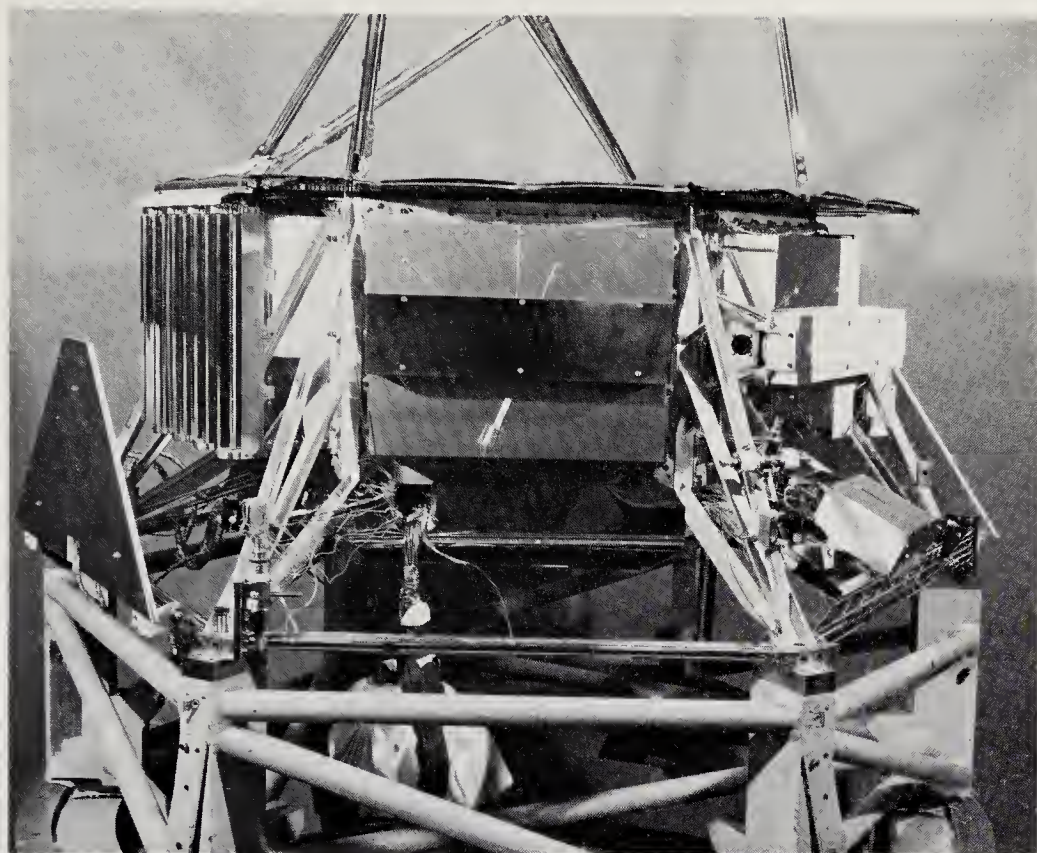


Fig. 10-25. Temperature-controlled louvers on Mariner 2. (Courtesy of the Jet Propulsion Laboratory)

cooling consumes valuable power, but it is also the most flexible means for selectively controlling temperatures throughout the spacecraft.

Most space probes will use some combination of passive and active control.

*Radiation Control.* Damage to spacecraft equipment from space radiation is unimportant for most missions outside the Earth's radiation belts. The fluxes of cosmic and solar flare radiation are not high enough to damage electronic components (Fig. 3-3, page 24). Conceivably some of the other planets, especially Jupiter, might have radiation belts strong enough to cause harm, calling for special shielding. In general, though, the damage threshold is orders of magnitude above expected space-probe exposures.

Nuclear radiation can also interfere with scientific experiments. Neutrons and gamma rays from radioisotopic power sources as well as environmental radiation may interfere with instruments measuring certain restricted portions of the spectrum of particulate radiation. An onboard

nuclear power source creates the most serious radiation problems for space probes. Even radioisotopic power generators with alpha-emitting fuels will produce enough neutrons and gamma rays to make generator shielding mandatory on probes measuring environmental radiation (Ref. 10-11). Beta-emitting fuels, while not now contemplated for probes, produce so many gammas that instrument shielding is difficult and radiation damage to semiconductor components a real possibility. Nuclear reactor power supplies, like Snap-8, produce even more copious radiation.

The sensitivities of spacecraft instruments and components to nuclear radiation vary considerably. A gamma-ray spectrometer may be compromised if bombarded with a few gammas per second. Most transistors can tolerate  $10^{11}$  nvt.\* The radiation levels around nuclear power sources depend upon distance, power level, and the reflection of radiation from surrounding components. Further generalization is difficult.

Components and instruments can be protected from nuclear power supplies by:

1. Distance; viz., mounting either the power supply or the instrument on a long boom.
2. Power-supply shielding (the unit shield concept).
3. Component shielding (patch shielding).
4. A combination of 2 and 3 (split shielding).

In general, dense materials such as lead and tungsten are used to shield against gamma rays; light, hydrogenous substances, like paraffin, make good neutron shields. Radiation levels drop exponentially with the shield thickness. The reader is referred to Blizzard for detailed design procedures (Ref. 10-7). Whatever shield weight is finally calculated, it must be charged against the nuclear power plant.

*Magnetic-Field Control.* The final component of the spacecraft environment that has to be handled on a probe-wide basis originates within the probe itself. Every current flow produces a magnetic field that may disturb magnetometers measuring the weak external fields that amount to only a few gammas. Every piece of magnetic material used potentially distorts the field being measured. Of course, magnetic control is pertinent only where the external field is being monitored, but the magnetic mapping of the solar system holds such great scientific interest that it is hard to imagine a probe without a magnetometer aboard.

Many magnetic-field problems are not recognized until the spacecraft is completely assembled and tested. It would be ridiculous to try to calculate the effect of every current-carrying wire. Instead, design pro-

\* nvt = neutron flux multiplied by time (neutrons/cm<sup>2</sup>).

ceeds on a few basic rules that minimize the resultant spacecraft field:

1. Use nonmagnetic materials where possible.
2. Position major current carriers so that their fields subtract rather than add.
3. Use one of the spacecraft models to detect and eliminate any residual fields.

Remedies at the spacecraft-model stage consist of circuit rearrangement, the use of compensating coils, and the physical isolation of the magnetometer from offending circuits.

### 10-8. The Guidance-and-Control Subsystem

The task of the guidance-and-control subsystem is to detect deviations from proper performance, determine remedial action, and dispatch corrective signals to the actuators. A man in control of an automobile does much the same thing, but steering a spacecraft across millions of kilometers is more difficult by orders of magnitude. In the case of the spacecraft, the major functions to be controlled are:

1. Position and trajectory control in inertial space and on the surfaces of planets.
2. Attitude control.
3. Environmental control.

There are, of course, other controlled quantities, e.g., the power-supply voltages, but, like the spacecraft environment, they are usually controlled by local feedback loops (thermostats) and will not be discussed here. Only the control of position and attitude requires elaborate sensors, computers, and actuators.

The separate mention of computers emphasizes the philosophical isolation of the computer from the guidance-and-control subsystem<sup>31</sup> and the rest of the probe. In many early spacecraft, computers were highly specialized and physically integral with the subsystems they served. Computing, however, is a general type of activity that can easily be centralized on large probes. With this in mind, the computer is treated as a separate subsystem in this book (Sect. 10-9). There is no incontrovertible proof, though, that a centralized computer has any particular advantages over specialized computers.

The information interface between the computer and the guidance-and-control subsystem is most critical. The computer is called upon to make coordinate transformations, calculate midcourse-maneuver propulsion requirements, and so on. The computer does not have to reside in the spacecraft proper and has in many instances remained on Earth.

Other vital information interfaces occur between the guidance-and-control subsystem and the attitude-control and propulsion subsystems. Actuation information must flow accurately and rapidly across these interfaces.

Position- and attitude-finding instruments come in four categories:

1. Inertial devices dependent upon accelerations and gravitational fields.
2. Optical instruments that sense and lock onto light sources.
3. Radar, which is used for determination of distance, direction, and velocity.
4. Earth-based tracking equipment, which can be used to measure spacecraft position and velocity subject to the constraints mentioned in Chap. 9.

*Inertial Sensors.* Inertial devices include gyroscopes, accelerometers, and pendulums. All three of these instruments are customarily used on launch vehicles and satellites. But in deep space, where gravitating bodies are far away and the local vertical has little meaning, pendulums are not employed. Also rejected for probe use is the free gyro, which remains fixed in inertial space but has drift rates so high (0.1-0.5 deg/min) that it is useless on interplanetary flights that are months and years in duration.

The conventional gyroscope has a high-speed, rotating wheel as its inertial member, but many new approaches exist (Table 10-10). Some new designs aim at eliminating the friction-induced bearing torques. Others, like the laser gyros, can measure minute displacement velocities through the change in phase of electromagnetic waves.

Gyroscopes are subdivided into several types. Free gyros, which measure angular displacements about two axes, have already been disposed of for deep-space probe use. The one-degree-of-freedom *rate gyros* have lower drift rates and can be used successfully on long missions. All gyros have signal generators mounted on one or more of their axes. In the free gyro, generator signals drive torque motors, which rotate the gimbals to erect the gyro in the proper position. Rate gyros are mounted with the fixed input axis parallel to the spacecraft axis that is to be monitored. A torque about the input axis will cause the gyro to precess around the output axis. The displacement of the spring-restrained gimbal is proportional to the angular acceleration about the input axis. *Rate-integrating gyros*, which have the lowest drift rates (0.001 deg/hr), generate outputs proportional to the angular displacement around their input axes (Fig. 10-26). A viscous fluid occupies the space between the case and the gimbal, making the rate of gimbal precession a function of the input acceleration and the viscosity of the fluid. Such a gyro integrates the input

TABLE 10-10. PROPERTIES OF UNCONVENTIONAL GYROSCOPES\*

	Estimated Performance (deg/hr)		Input Quantity	Limiting Constraint
	Present	Potential		
Electrostatic gyros	1.0	0.01	Rate, displacement	Mass imbalance, readout
Electromagnetic gyros	2.0	0.001	Rate, displacement	Mass imbalance, readout
Cryogenic electromagnetic gyros	3.0	0.0001	Rate, displacement	Readout, heat transfer
Nuclear-spin gyros	20.0	0.001	Rate, displacement	Relaxation time
Cryogenic nuclear-spin gyros	20.0	0.0001	Rate, displacement	Magnetic noise
Compressible-fluid gyros	0.5	0.2	Acceleration	Pressure detection
Incompressible-fluid gyros	1.0	0.8	Rate, displacement	Thermal conductivity of liquid
Laser gyros		0.001	Rate	Alignment of input axis
Vibrating gyros	8.0	4.0	Rate	Oscillator stability, mass imbalance

\* Ref. 10-30.

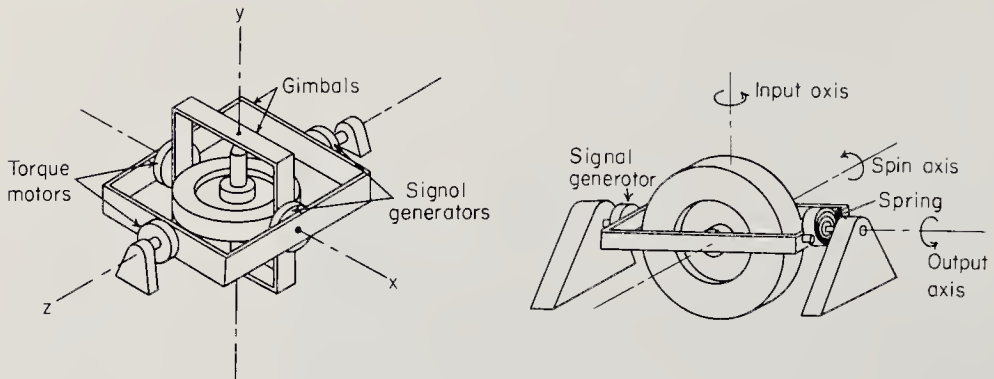


Fig. 10-26. "Free" gyro, left, and "rate" gyro, right.

acceleration over time, the result being the total angular displacement of the gyro (Ref. 10-37). (Fig. 10-27)

In present practice, rate integrating gyros are utilized on space probes during midcourse maneuvers to measure plane changes. To conserve life and power, they are turned off during the coast phases of the mission. Usually there will be at least one gyro for each degree of freedom. Operations near a planet call for the same inertial sensors used on Earth.

*Accelerometers* measure accelerations applied to the spacecraft through the displacement of a spring-loaded mass. Integrating accelerometers like the rate integrating gyros contain a viscous fluid. The total velocity change is then proportional to the total displacement of the mass (Fig. 10-28). Integrating accelerometers have threshold sensitivities of about  $10^{-5}g$ , making them very useful during midcourse, terminal, and rendezvous maneuvers.

*Optical Sensors.* Where inertial sensors falter, optical sensors are available to supplant them. Spacecraft position and attitude can be sensed by sighting on celestial objects. Since the human eye is absent, all optical sensors use photosensitive semiconductors, photocells, iconoscopes, and the like. Accurate pointing always calls for a scanning operation or arrays of fixed, light-sensitive cells, linked with feedback circuits, that center the sensor on the target.

Star trackers home in on point sources of light by focusing their images on photosensitive surfaces with an optical telescope. Typically, a slotted scanning disk rotates in front of the focal plane. Error signals are generated when the target star is not focused on the center of the photosensitive surface. Signal generators attached to the azimuth and elevation axes of the star-tracker mount relay the bearing data to the computer subsystem. The accuracies of star trackers are remarkably good (Table 10-11).



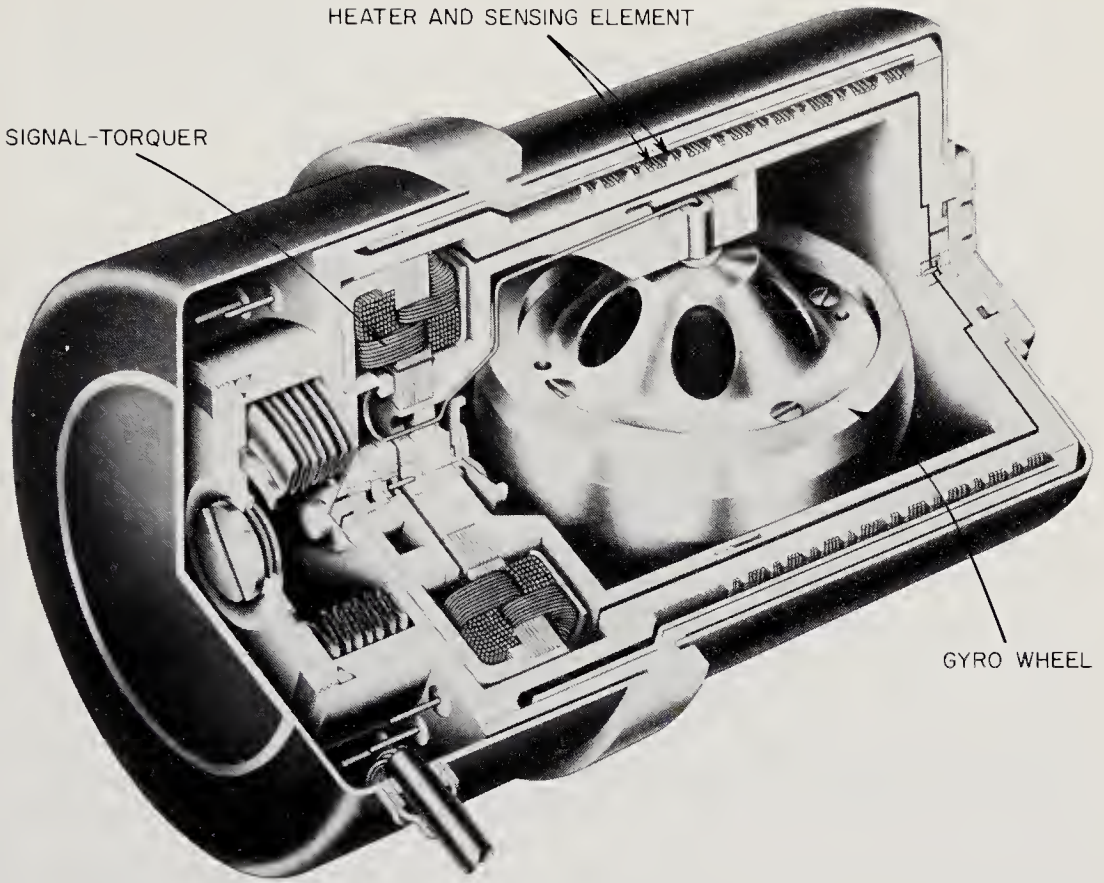


Fig. 10-27. Cutaway view of a miniature integrating gyro. (Courtesy of Minneapolis-Honeywell)

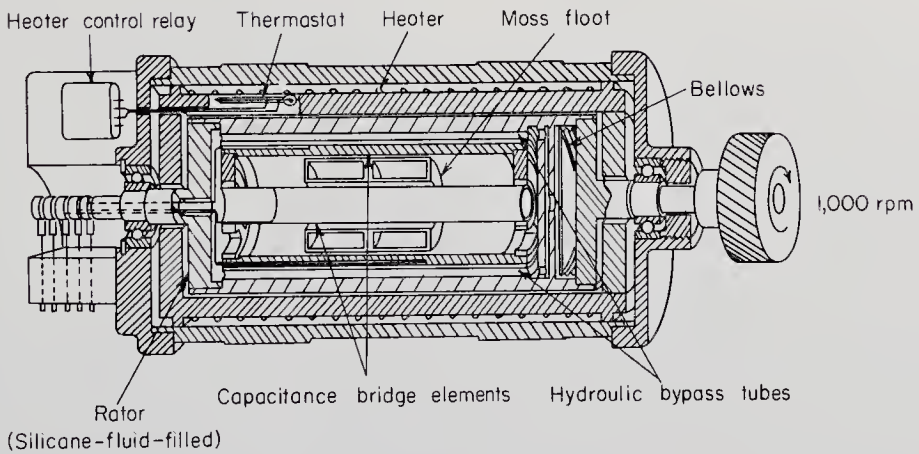


Fig. 10-28. An integrating accelerometer.

TABLE 10-11. SUMMARY OF SENSOR CAPABILITIES\*

Type	Sensing Capability	Accuracy (deg. RMS)	
		Currently Practical	Desired
Sun sensor	Any arbitrary plane in solar system	0.1	0.001
Planet sensor	Any arbitrary plane in solar system	0.2	0.01
Star tracker	Any arbitrary plane in solar system	1	0.001
Horizon scanner	Local vertical	0.2-0.5	0.001
Rate gyro	Rate of deviation from orbital plane	0.2 per hour	0.001 per hour

\* Ref. 10-25.

Extended light sources, like the Sun, the various planets, and their satellites, can also provide valuable navigation information. The feedback loop that centers the optical sensor on an extended source is very similar to that in a star tracker. The image of the object being tracked now fills a large portion of the detector area. A screen splits the image into several parts and directs them to separate photosensitive devices (Fig. 10-29). Error signals, produced when the image is not centered, drive azimuth and elevation motors until the error signals have been reduced to zero (Table 10-11). Solar-aspect sensors are placed on satellites and deep-space probes (Pioneers) to signal the spacecraft orientation relative to the Sun. By placing solar cells at strategic points on the out-

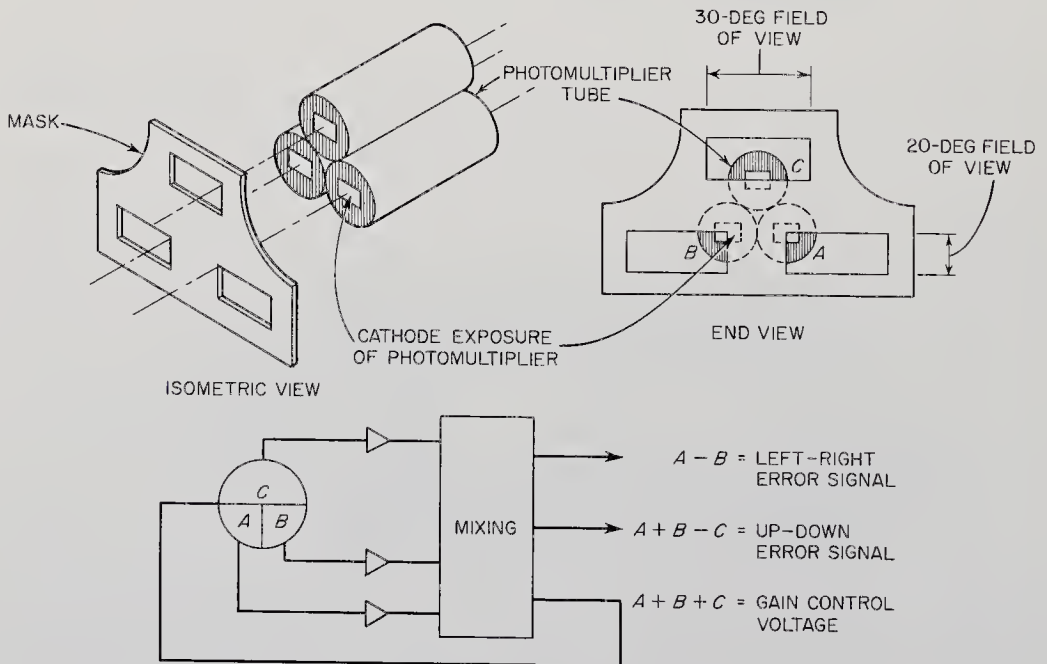


Fig. 10-29. An image splitter for tracking extended bodies. (Ref. 10-40)

side of the spacecraft, i.e., the six faces of a cube, the direction of the Sun can be computed from the simultaneous outputs of the cells.

*Horizon scanners*, like the one shown in Fig. 10-30, are very effective

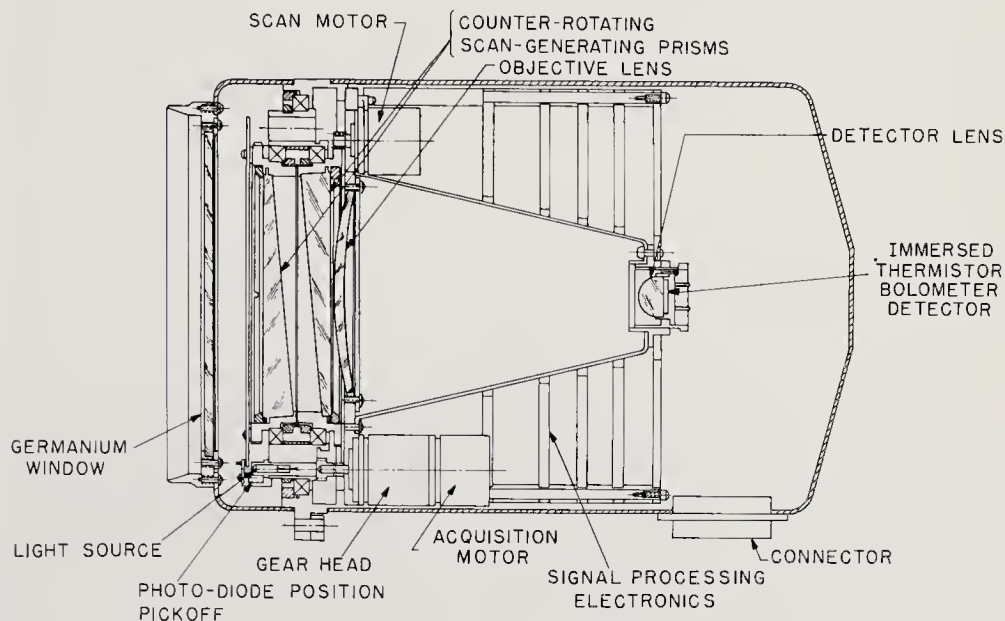


Fig. 10.30. A JPL horizon-scanner design. (Ref. 10-40)

in determining the local vertical near planets warm enough to emit enough infrared radiation. Scanning mirrors or lenses trace the discontinuity in temperature between the warm planetary surface and the cold horizon. If the angle of the scanner axis with the vertical changes, error signals measure the deviation and so inform the guidance-and-control subsystem. In theory, the altitude above the planet can also be computed if its diameter is known.

With modern pattern-recognition equipment, TV cameras can be pointed via a feedback loop until they are centered on specific stars or extended sources. Angle data may then be acquired from the camera drive mechanism. TV cameras are also useful in guiding planetary rovers from the Earth. In principle, a TV camera combined with pattern recognition equipment could automatically locate geological, biological, and other scientific features from a lander vehicle.

The use of radar- and laser-ranging is well understood. These equipments differ from the optical sensors described above in the ability to measure distance and velocity in addition to bearing. As explained in Chap. 7, these active navigation devices must be reserved for close-up planetary and rendezvous maneuvers in order to conserve spacecraft

power. There is no good substitute for active ranging equipment during touchdown and rendezvous operations.

In summary, the guidance-and-control subsystem is the sum total of the navigation sensors and the control and actuation circuits. It must get the spacecraft to the right place at the right time with the proper attitude. Most often this subsystem will be entirely contained within the spacecraft, but many of the early probes will rely on Earth tracking for position information.

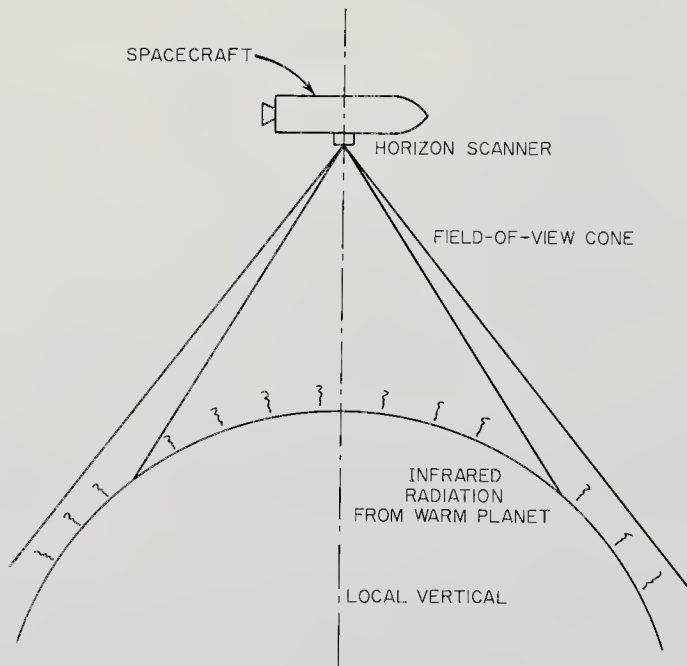


Fig. 10-31. Schematic showing the operational principle of a horizon scanner.

It is much too early to conjure up designs of guidance-and-control circuits for automata. Whatever the spacecraft of the future may be—merely radio-controlled machines or autonomous, cognitive robots—they will be studded with guidance-and-control sensors of all descriptions, for these instruments are the real senses of all spacecraft.

### 10-9. The Computer Subsystem

The computer subsystem serves the spacecraft in four ways:

1. It is a centralized service unit performing computing tasks for all subsystems needing it. Data processing falls in this category.
2. It is a storage unit for data (ephemerides, for example), commands, and the routines used for internal checking, maintenance, and self-repair.

3. It is a timer and sequencer that initiates actions independent of Earth.
4. In the future, it will be the center for onboard cognition and decision making.

Centralized computers will be used on only the larger and more advanced probes. The computer's interfaces are illustrated in Fig. 10-32.

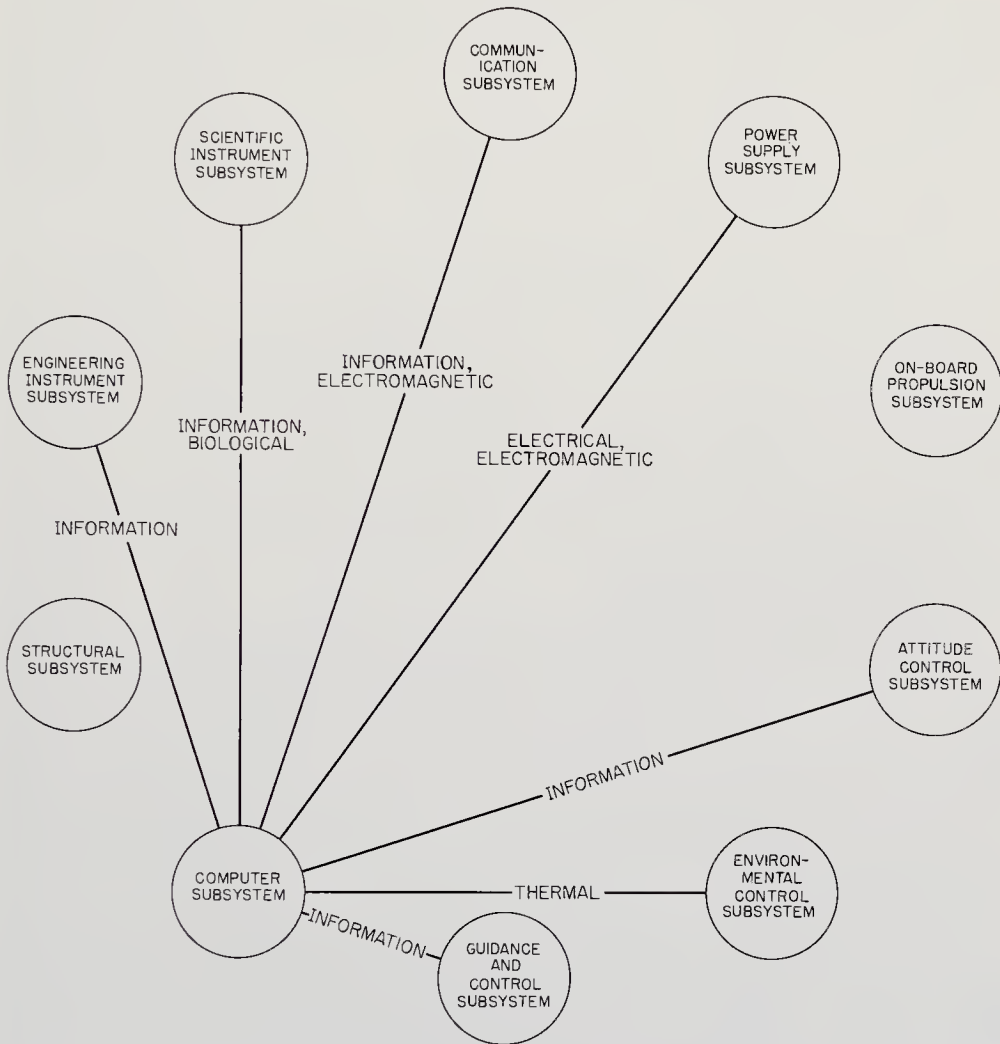


Fig. 10-32. Portion of the spacecraft interface diagram showing the relationship of the onboard-computer subsystem to the rest of the subsystems.

Early spacecraft obviously do not possess all the interfaces shown in the schematic. Some navigation and guidance computations are done on advanced Earth satellites, but most of the computing for space probes is still done on the Earth.

There is an excellent reason for avoiding spacecraft computers. They are complex and unreliable in terms of lengthy interplanetary voyages. Using an example presented by O'Donnell (Ref. 10-35), a typical, real-time computer with 1500 transistors, 10,000 diodes, 500 capacitors, and 2000 resistors would have a mean time between failures of about six days. Such a computer would have only a 50/50 chance of successfully completing a 100-hr mission. The probability of success falls to around  $10^{-17}$  for a 240-day interplanetary mission. No doubt computer improvements will raise this probability several orders of magnitude in the next decade, but not by  $10^{17}$ . Another reliability barrier has been encountered. Again reason dictates that computer equipment be left on the Earth, where it can be repaired when it falters. The burden for computational success is thus placed on the shoulders of the communication subsystem.

Small, highly specialized computers fly on all spacecraft. They are small analog computers with memories in the form of contoured cams and wheel-and-disk mechanisms. Large, general-purpose digital computers will supplant some, but not all, of these simple machines. Can the general-purpose computers be of the analog type? The limited accuracy of the analog computer (about 1 part in 1000) makes this unlikely. Digital computers are not only more precise but much more flexible in terms of the different kinds of jobs they can do. They can probably be made lighter and more compact than the collection of specialized analog computers they will replace.

The general purpose digital computer is buttressed by abundant literature (viz., Ref. 10-21) and will not be discussed further here. It is sufficient to say that the discipline of microelectronics aims at packaging as many as one million components per cubic foot (35,000,000 per cubic meter), and that digital computers can be made small enough for spacecraft. Even the ambitious, complicated automata described earlier seem destined to be brought down to manageable size—eventually. The big problem with computers is reliability, not size.

Mariner 2 used a small digital computer and timer collectively called the Central Computer and Sequencer (CC&S, Fig. 10-33). An electronic clock, using a crystal-controlled oscillator (307.2 kc), provided time pulses which initiated such spacecraft operations as the extension of the solar panels and orientation of the directional radio antenna. Most of the important computations and commands, however, originated on Earth.

#### 10-10. The Structural Subsystem

The structural subsystem is the strong skeleton of the spacecraft. It supports, unites, and protects all of the other subsystems. More than just a framework on which to hang electronics packages, the structure estab-

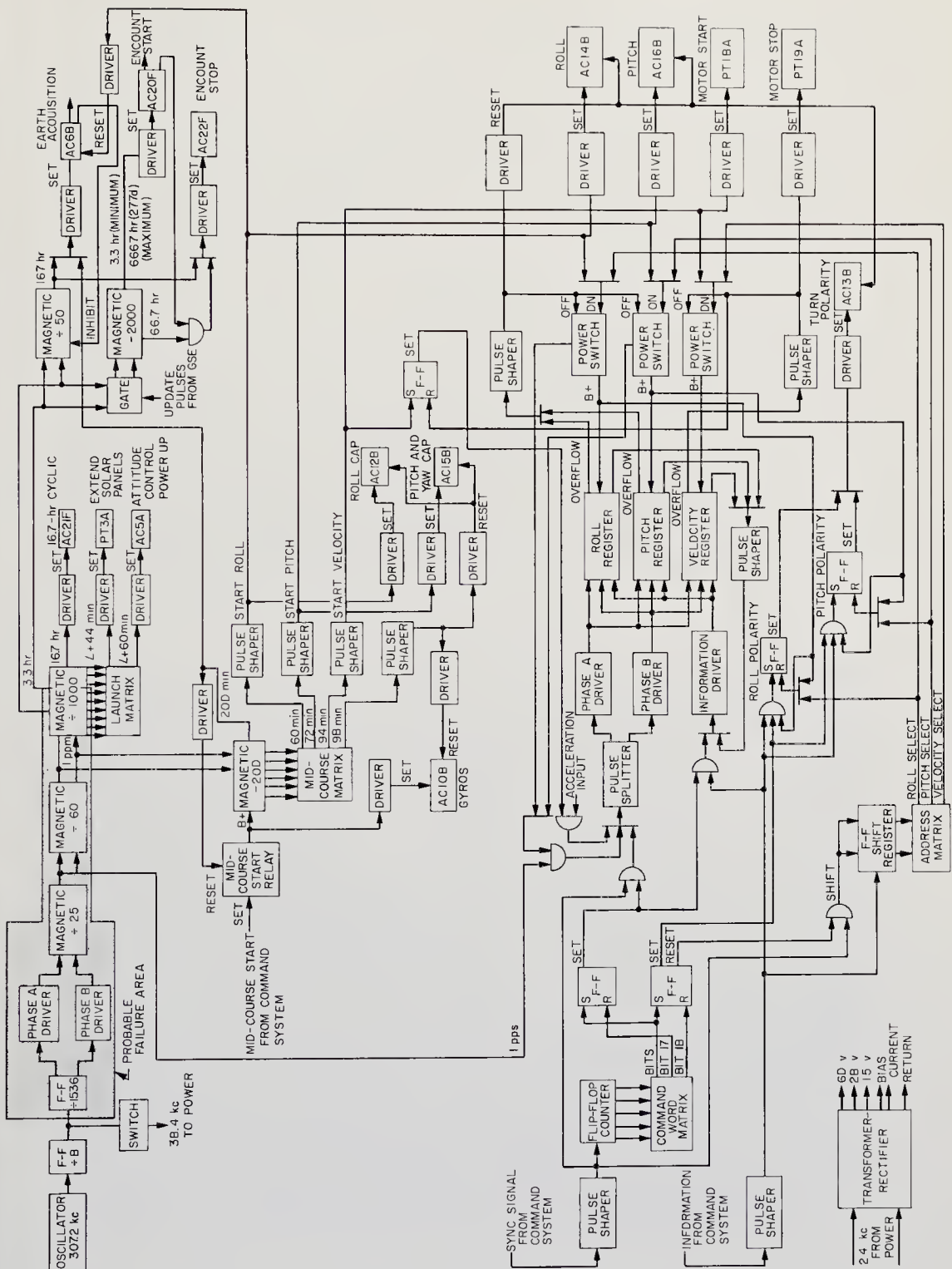


Fig. 10-33. Block diagram of the Mariner-2 Central Computer and Sequencer. (JPL drawing)

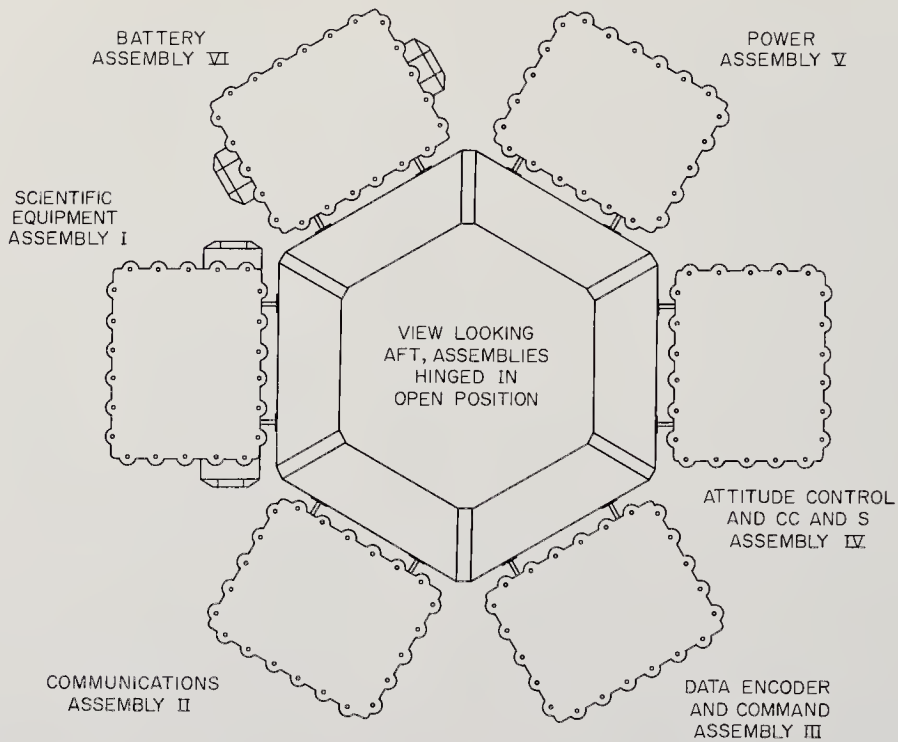


Fig. 10-34. Plan view of the Mariner-2 magnesium chassis in the open position. (JPL drawing)

lishes the geometry of the spacecraft, isolates components on booms, and shields vital equipment from meteoroids and atmospheric-entry forces.

Spacecraft that do not enter planetary atmospheres or impact on surfaces tend to be open structures with unfolding panels and deploying antennas. Obviously all spacecraft must be compact and rugged when they are launched, but once in space, after the protective shroud has been blown off, they can unfold their area-dependent equipment. There can be no increase in the total solid angle seen by the probe, but the total area can be greatly increased by articulated structures. Mariner 1, Fig. 11-8, is typical of an open, jointed spacecraft.

When atmospheric entry and surface landings are planned, rugged, dense structures are preferred until these violent maneuvers have been completed. Once on the ground, a lander will undergo the same sort of metamorphosis as its interplanetary relative. In addition, a lander has to deploy wheels or legs if it is to be mobile.

The powerful urge to gain surface area results directly from the abundance of area-sensitive equipment. Some examples are:

1. The directional spacecraft antennas.
2. The solar panels.



3. Heat rejection surfaces.
4. Scientific sensors like plasma samplers and meteoroid detectors.

Star trackers and other instruments, while not so area-sensitive, need certain fractions of the  $4\pi$  steradians of solid angle that are available. Structural design is further complicated by the need to isolate magnetometers, nuclear power supplies, and other interfering equipment on long booms or structural extensions.

A comparison of probes like Mariner 2 and Ranger 7 with representative Earth satellites like Telstar and Tiros reveals the difference between an open-frame probe and the shell-type satellites. Telstar, for example, consists of an outer shell of solar cells surrounding a cylindrical electronics package supported by nylon cords. The typical probe has a similar, dense electronics package (Fig. 10-34), mounted within a polyhedral framework. A superstructure carrying instruments and antennas is perched on top (Fig. 10-35). The two aims of the superstructure are to increase spacecraft area within the confines of the launch shroud and isolate equipment. The shroud gives probes that customary conical appearance before deployment of the articulated sections. Atmospheric entry shapes also have a similar, but blunter, conical cast.

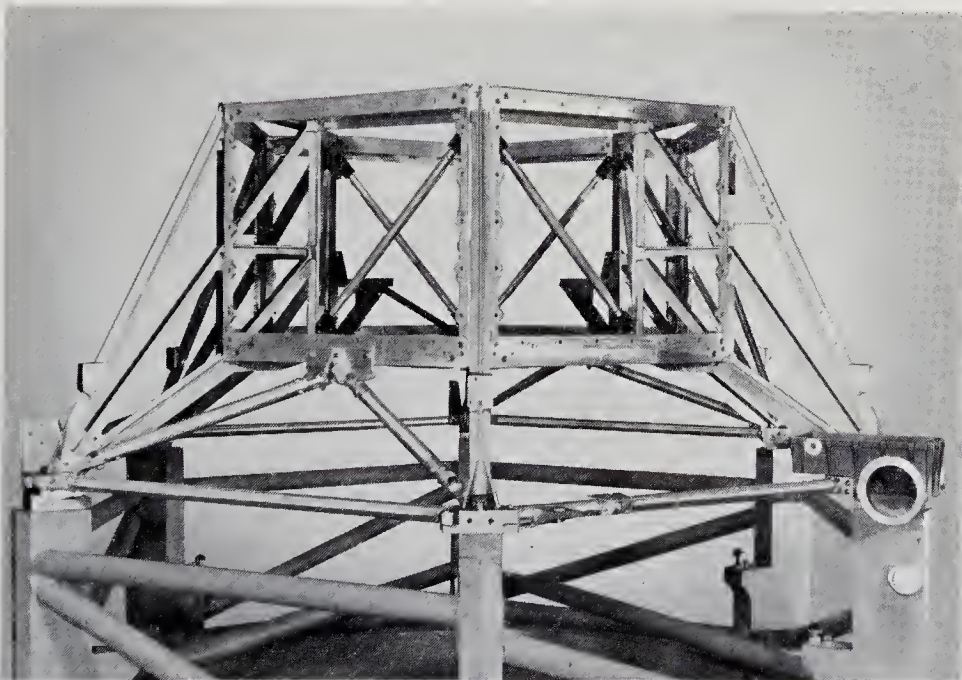


Fig. 10-35. Mariner 2 used a hexagonal frame as its basic structure. The six chassis shown in Fig. 10-34 are hinged to this structure for easy access. (Courtesy of the Jet Propulsion Laboratory)

It is advantageous to modularize spacecraft equipment, so that quick replacement can be made during ground checkout. Figure 10-34 shows the six hinged modules and the hexagonal symmetry of Mariner 2.

Some of the structural interfaces are worth emphasizing. The burden of protecting the spacecraft from the vibrations of the booster falls to the structure. Absorbers must decouple the two systems enough to preclude spacecraft damage. Structural resonances are quite possible. At this point, the reader is referred to several treatises on spacecraft structural design (Refs. 9-1 and 10-24).

A less clearcut interface involves the electrical connections between subsystems. These connections are only wires and waveguides, but instead of just a few wires threading through the structure, there are many thousands. Collectively, they are massed into thick, stiff cables, which not only are hard to install but also transmit vibration and heat.

*Spacecraft Materials.* Spacecraft materials usually operate at low temperatures (0-30°C) in a zero-g environment. Several well-proven, easily joined materials with high strength-to-weight ratios are readily found for such service. Aluminum, magnesium, and beryllium are foremost. Higher temperature service—say, on a hot planetary surface—would call upon steel, titanium, and perhaps molybdenum and columbium, if oxidization can be prevented. In short, there is a wide spectrum of acceptable structural materials available.

Radiation damage to structural materials has already been dismissed as unimportant to most space probes. Surface properties may be affected, however, and the high vacuum may cause sublimation and self-welding of adjoining surfaces (Ref. 10-28).

Metals and their alloys are relatively immune to the threats of sublimation, particle sputtering, and surface degradation in space. Operating temperature is a factor, though, since magnesium begins to sublime rapidly above 175°C. The welding of surfaces in the vacuum may be serious at high temperatures. Davis presents data showing that steel surfaces will weld tightly at 500°C in a vacuum (Ref. 10-14). At lower temperatures and with dissimilar materials, the effect persists, but to a lesser degree. In summary, metals may be used with nearly complete freedom except for the self-welding problem.

Some semiconductors, notably selenium, the phosphides and arsenides, and many polymers, such as nylon and the acrylics, have high sublimation and decomposition rates in vacuum at normal spacecraft operating temperatures. Silicon solar cells, fortunately, are stable. Natural rubber, elastomers like isoprene, the silicone resins, polypropylene, and polyethylene also seem quite stable in a high vacuum. Inorganic coatings for

thermally radiating surfaces have shown both increases and decreases of emissivity upon exposure to space conditions (Ref. 10-14).

General rules concerning the use of materials in space are hard to formulate, except for the liberal guidelines stated for metals. All other materials have to be examined individually.

*Meteoroid Protection.* Meteoroids may damage an unmanned space probe through direct puncture of a pressurized tank, severance electrical connections, surface scouring and attrition, and possibly spalling of wall structures. Probes possess few pressurized compartments, but most of their exterior is covered with active and sensitive surfaces of one sort and another.

The problem of spacecraft protection is made easier by the rapid reduction in meteoroid flux as the probe leaves the vicinity of the Earth. Mariner-2 data suggest that there may be a flux reduction of 10,000 (Fig. 3-5, page 27). Other planets may also have similar halos of cosmic debris.

Our understanding of what happens when a high-velocity meteoroid hits a surface is still incomplete. Following Dubin (Ref. 10-15), designers may use the following penetration equation:

$$p = 2.28 \left( \frac{V}{V_s} \right)^{2/3} \left( \frac{\rho_m}{\rho_t} \right)^{2/3} d$$

where:  $p$  = the depth of penetration (cm)

$d$  = the meteoroid diameter (cm)

$V$  = the meteoroid velocity (cm/sec)

$V_s$  = the velocity of sound in the target material (cm/sec)

$\rho_m$  = the density of the meteoroid (g/cm<sup>3</sup>)

$\rho_t$  = the density of the target material (g/cm<sup>3</sup>).

An average meteoroid velocity of 30 km/sec and a representative density of 2 g/cm<sup>3</sup> are recommended until better data become available.

One or two thin meteoroid bumpers (spaced armor) around the most sensitive equipment may aid survival with a minimum of weight. Impacting meteoroids should be fragmented into many small, relatively innocuous bits by the thin bumpers.

The pitting and erosion of optical surfaces cannot be reduced in this way without affecting light transmission. Calculations for spacecraft far removed from the Earth indicate that surface erosion will probably be less than 1A per year. There appears to be no serious problem, since optical properties should not be hampered until about one tenth of a wavelength has been eroded away.

In general, the meteoroid hazard for deep space vehicles does not seem serious.

*Atmospheric Entry Structures.* A considerable body of data concerning Earth reentry has accumulated during the ballistic missile programs. Much of this information will be applicable to entry into the atmospheres of other planets. The two forces that give the most concern are aerodynamic heating and deceleration. Each planet with an appreciable atmosphere will force the spacecraft to stay within a certain flight corridor to avoid excessive  $g$  forces and overheating (Fig. 10-36). Each planet's

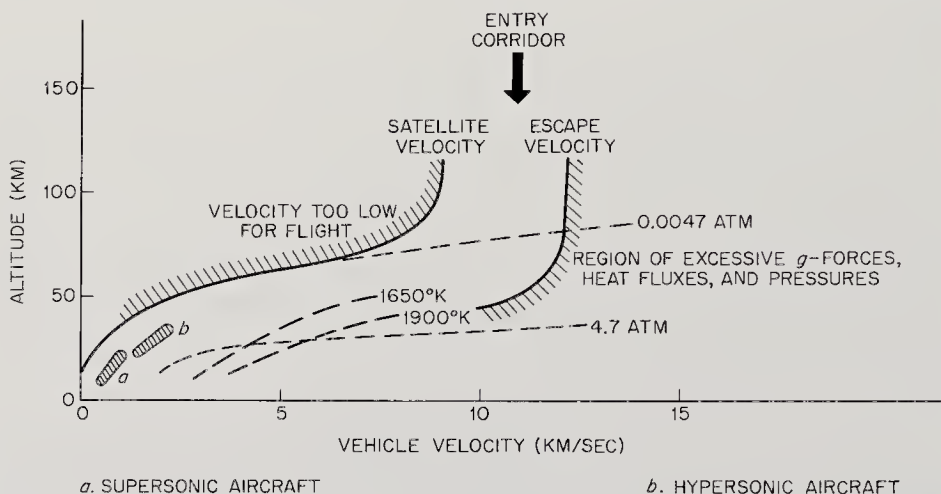


Fig. 10-36. Present limits to flight within the Earth's atmosphere. Similar flight corridors exist for all planets with significant atmospheres.

altitude-velocity chart is obviously different and, except for the Earth's, hypothetical. The mission designer has the option to fly the probe where he wishes within the corridor, placing the burden on the thermal protection structure or on the basic strength of the probe.

High- $g$  loadings are reflected in rugged design, from the nose cone to the scientific instrumentation. The handling of this side of the entry corridor is straightforward: a stronger spacecraft.

On the other side, thermal protection from aerodynamic heating requires special engineering developments. Four possibilities exist:

1. Heat-sink absorption, using materials like copper and beryllium in nose-cone reservoirs that soak up the heat that would otherwise penetrate and damage the spacecraft. This approach is too heavy for probe use.
2. Transpiration cooling, where a heat transfer fluid is forced out of pores on the hottest surfaces. The fluid vaporizes and carries the heat away. This concept is probably too complex for space probes.

3. Radiation cooling, where the burden of heat rejection is placed on a high emissivity nose cone, backed by a layer of thermal insulation. This is a possible solution.
4. Ablation, where the nose cone is protected by a material of low thermal conductivity that melts and transpires in the hot gas stream. Most ICBM nose cones are now made of materials (like phenolic nylon) that char on heating and in the process evolve gases that protect the spacecraft and also carry away the aerodynamic heat.

The heat-transfer analysis of these diverse phenomena is very involved

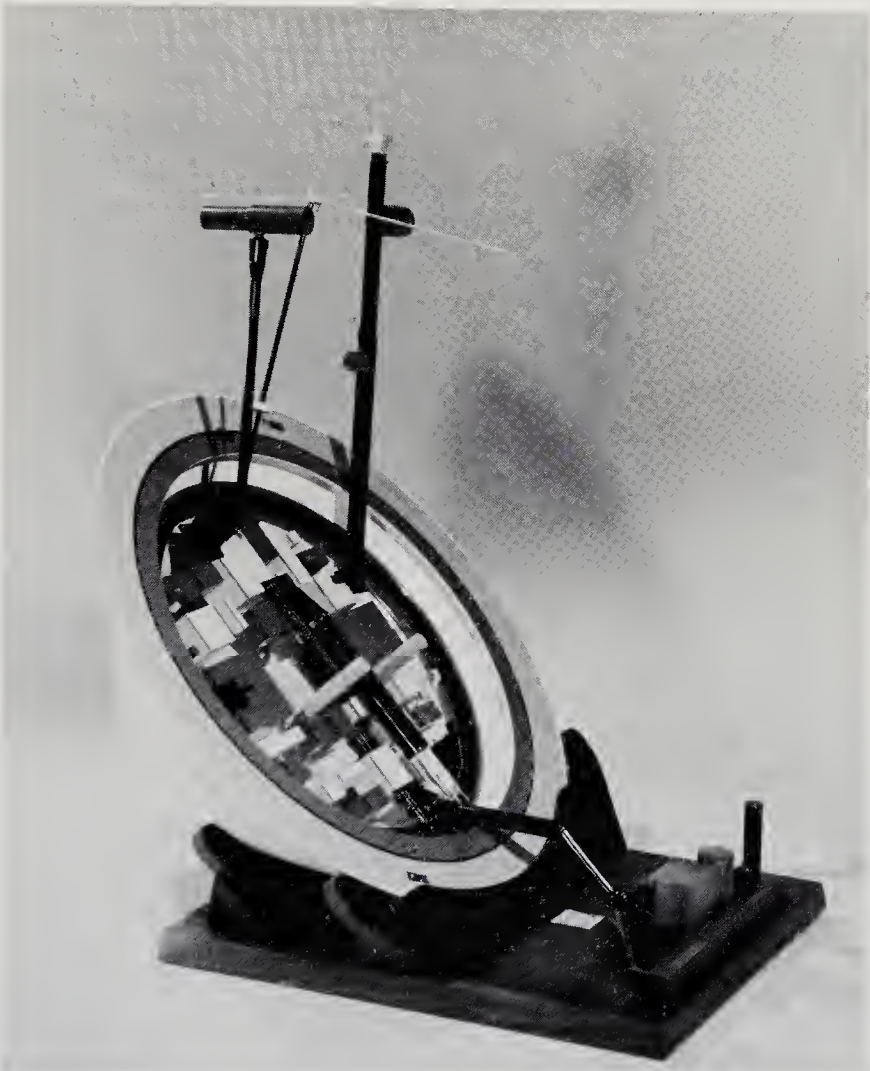


Fig. 10-37. A typical Mars, Voyager-class landing capsule. This design assumes atmospheric braking will be possible on Mars. (Courtesy of General Electric Co.)

and cannot be covered here (see Refs. 10-3 and 10-44). A representative thermal-protection structure for a Mars entry vehicle is shown in Fig. 10-37. The actual shape and materials used would be different for different planets, depending upon the velocity-altitude profile and the composition of the atmosphere.

*Landing Structures.* The final area of specialized structural design appears when the spacecraft must descend to a planetary surface without damaging its cargo of instruments. If there is an atmosphere, the vehicle's descent can be slowed by parachutes, rotors, and the other schemes

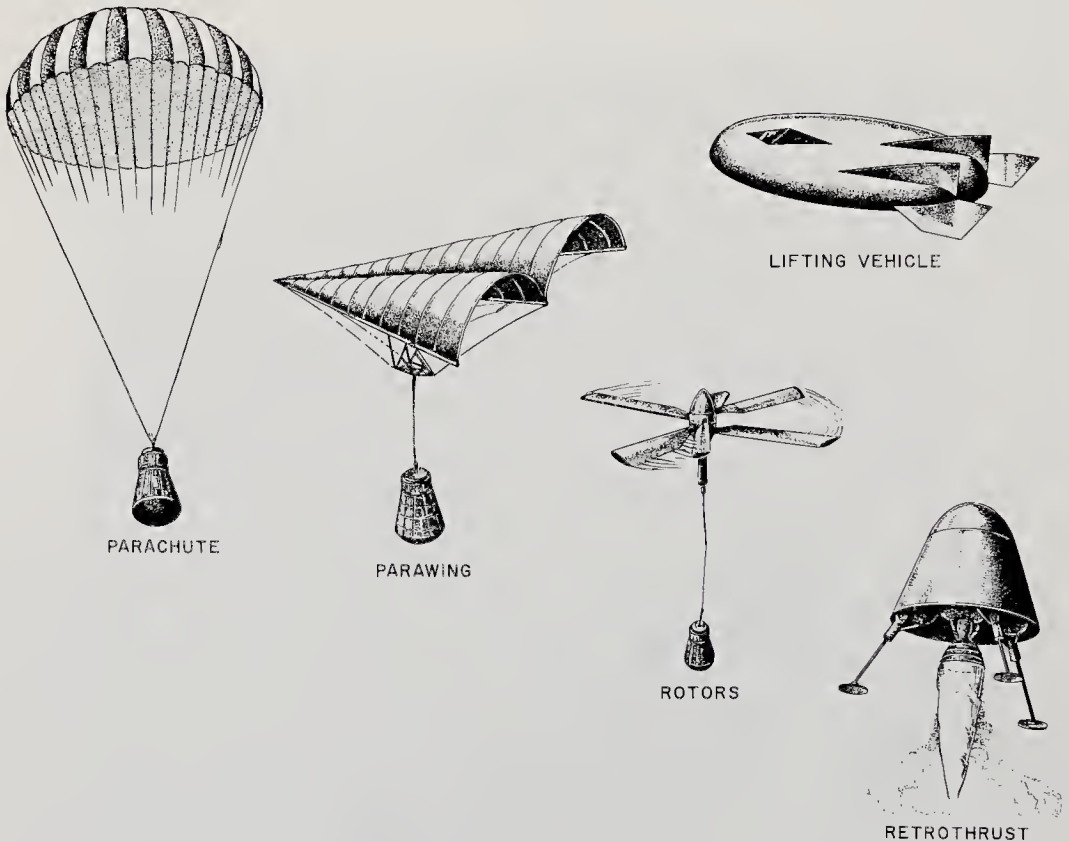


Fig. 10-38. Possible methods of descent after atmospheric deceleration has slowed the spacecraft down. (Ref. 10-17)

shown in Fig. 10-38. Despite such efforts, the impact may result in decelerations of hundreds of g's. Impact cushioning is indicated.

Five energy-absorption methods might be used:

1. Deformation of a structure or material; for example, springs, collapsible honeycombs.
2. Gas compression.

3. Acceleration of external mass, as in water impact.
4. Friction, as produced by a landing spike.
5. Retrorocket thrust.

Esgar (Ref. 10-17) has portrayed these approaches rather vividly as shown in Fig. 10-38. He has also compared their performances under different conditions (Table 10-12).

TABLE 10-12. COMPARISON OF SPACECRAFT LANDING CONCEPTS\*

	<i>Material Deformation</i>	<i>Gas Bags</i>	<i>Collapsi- ble Shell</i>	<i>Retro- rocket</i>	<i>Aerial Snatch</i>	<i>Skid- ding</i>	<i>Bur- rowing Device</i>
Weight System	E†	G	G	G	E	E	F
reliability	E	G	E	G	P-F	F	E
Velocity limitations	F-G	F-G	F-G	E	F	E	F
Stability after impact	F-G	F	F	F-G		G	E
Storage	F-G	E	P-F	F-G	E	E	P-F
Onset rate	P-G	G-E	G-E	E	E	E	P
Terrain limitations	F	F	F	G	E	P	P
Non-Earth landing	G	G	G	E	P	P	P-F
Nonvertical descent	F	F	F	G	G	E	F
Overall rating	G	G	G	G	P-G	P-G	F

\* Ref. 10-17.

† P = Poor, F = fair, G = good, E = excellent.

Each mission must be considered individually. Landings on planets without atmospheres are more restrictive. Spikes assume a yielding surface. Gas bags require inflation, an action which might compromise reliability. There is no panacea. Of all the listed schemes, retrorockets, structure deformation, and gas compression are the most likely.

### 10-11. The Engineering Instrumentation

Part of the telemetry data received at the Earth from the space probe will be diagnostic in character; that is, it monitors the "health" of the spacecraft. The fraction of telemetry time devoted to engineering data is often large, perhaps 50% in early probes, and as little as 5% with well-

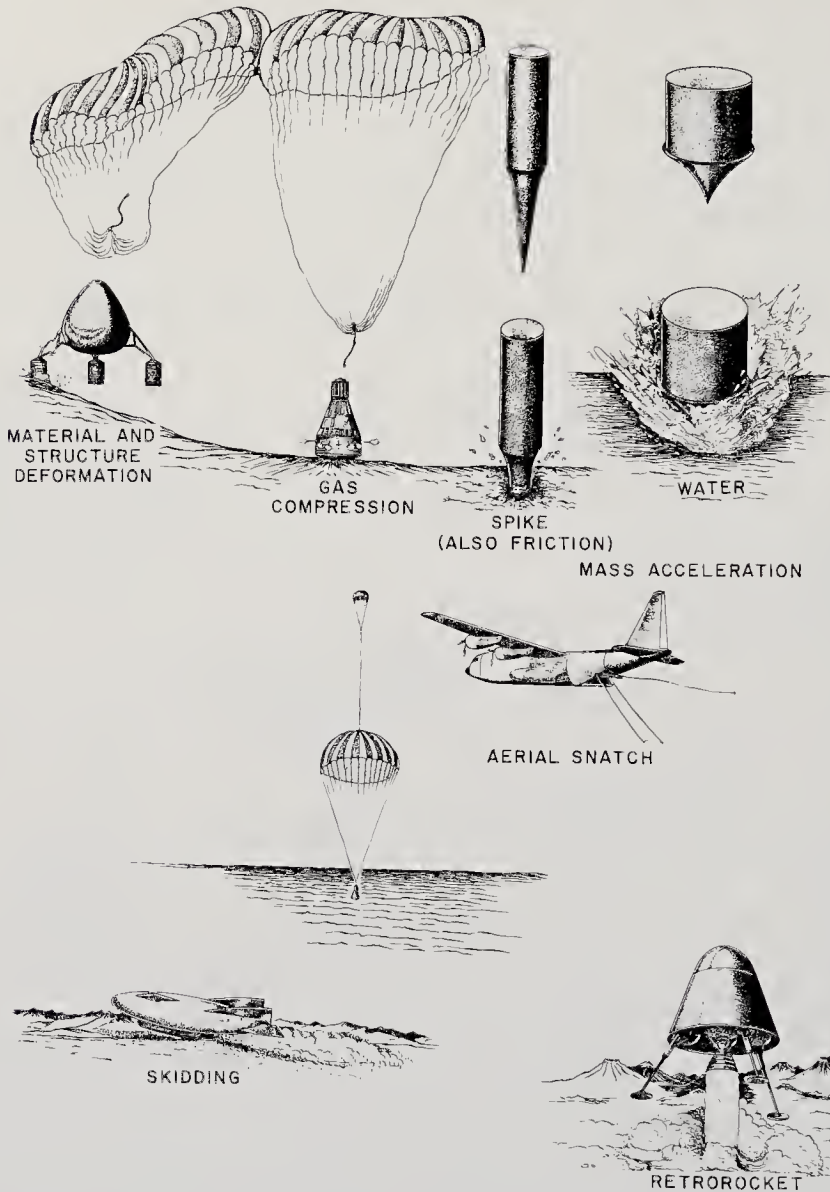


Fig. 10-39. Possible energy-absorption methods for use at surface impact. (Ref. 10-17)

proven spacecraft. The split between scientific and engineering data may be variable upon command from the Earth. During the first part of a voyage, engineering data may be critical in studying the operation of a complex piece of machinery. Later, the scientific target should receive most of the attention.

Just what engineering data should be sent? Generally, temperatures and voltages are easily measured, digitalized, and telemetered. They are diagnostic of many possible spacecraft ills. Electrical current, pressure,



frequency, operational modes, switch positions are all measurable and meaningful. The well-instrumented probe will send back temperatures from critical points on the spacecraft, voltages from the power supply, and status data from important switches.

Consider the following engineering parameters telemetered from IMP (Interplanetary Monitoring Platform):

1. Battery voltage.
2. +50 volt regulated supply voltage.
3. Battery charge current.
4. Spacecraft load current.
5. Skin temperature at top cover above, facet D.
6. Rubidium gas cell temperature.
7. Battery temperature.
8. +12 volt regulated supply voltage.
9. Solar-paddle current.
10. Solar-paddle temperature.
11. Skin temperature at top cover side, facet D.
12. Skin temperature, spring seat.
13. Rubidium lamp temperature.
14. Prime converter temperature.
15. Transmitter temperature.
16. Frame identification.

IMP telemetry consists of sixteen data frames, each with sixteen channels. The third frame, or 1/16th of all telemetry, is assigned to engineering data.

In most spacecraft, engineering instrumentation consists primarily of voltmeters and thermocouples in the most critical parts of the spacecraft.

#### 10-12. The Scientific Instrumentation

The final subsystem, the scientific instrumentation, will be described in detail in Part III of this book. Only the interfaces will be mentioned here (Fig. 10-1, page 177).

Many probe experiments are adversely affected by high temperatures, radiation, vibration; in short, many of the bonds that link the experiments to the rest of the spacecraft. Often experiments must be isolated by distance or by insulating barriers. For these reasons, magnetometers are found on the ends of long booms and gamma-ray spectrometers are surrounded by radiation shielding. The point to emphasize here is that scientific instrumentation cannot be separated from the rest of the spacecraft. It is tied to the other subsystems as surely as the power-supply or communication subsystem.

# *Chapter 11*

---

## CHARACTERISTICS OF SPECIFIC SPACE PROBES

---

---

### 11-1. Prologue

Space probes vary from the simple spin-stabilized Pioneer 5 launched in 1960 to conceptual, multi-ton, planet-walking instrument carriers. The previous chapter dealt with the general design principles applicable to this wide spectrum of probes. Here, attention is directed to specific probes, their characteristics, and how their missions shape their designs.

It is easy to fragment the space-probe spectrum into many small classes and subclasses, but only eight categories of space-probe missions are covered here (Table 5-2, page 46) :

1. Interplanetary missions: the Pioneers, IMP.
2. Planetary-flyby missions: the Mariners.
3. Planetary orbiters.
4. Planetary landers: Voyager.
5. Solar probes.
6. Cometary probes.
7. Asteroidal probes.
8. Interstellar probes.

Each of these eight categories demands probes of unique design.

Probes can be classified further as defunct, active, in development, under study, or conceptual. The following sections and tables embrace probes in all of these classifications, but emphasis is on active spacecraft and those under intense development. Each probe description begins with introductory paragraphs, followed by a comprehensive table summarizing the salient characteristics of the probe. Of course, probes still in the study

or conceptual stage are relatively poorly defined and little can be said about them.

### 11-2. Interplanetary Probes

Interplanetary or deep-space probes are dispatched to explore and map the volume of the ten-billion-kilometer sphere stretching from the Sun to the orbit of Pluto. These probes are aimed at no particular astronomical body but instead are instrumented to record magnetic fields, radiation fluxes, and micrometeoroid densities, or, according to the prevailing jargon, they carry out *fields-and-particles* experiments.

The simplicity of this mission eliminates the usual midcourse and terminal maneuvers. Guidance and control are likewise made easier, since there is no delicate trajectory to shape. Attitude measurement remains important, because many of the properties of space being measured are vector quantities, but usually it is not necessary to orient all axes of the spacecraft precisely.

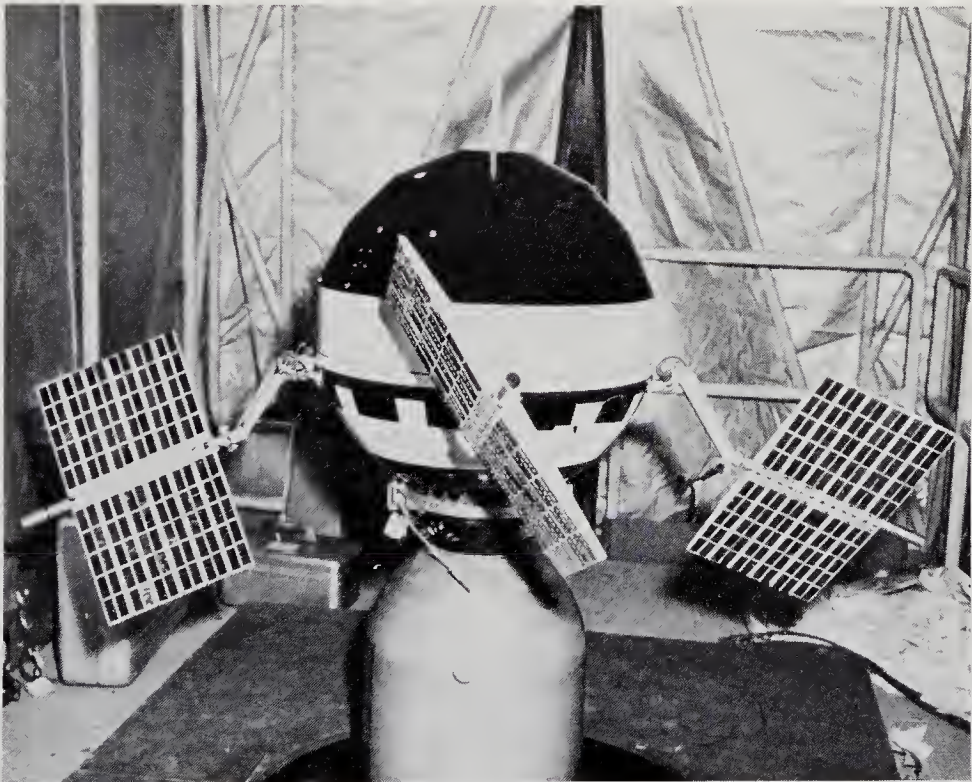


Fig. 11-1. Pioneer 5, one of the first space probes, shown mounted on the third-stage of the Thor-Able launch vehicle. The spheroid was only 63 cm in diameter. (NASA photo)

TABLE 11-1. PIONEER 5

*Mission Objectives:* Originally intended as a Venus-flyby experiment. Changed to deep-space probe when weight goals and launch window couldn't be met. Scientific goals: measure radiation, magnetic fields, and micrometeoroid density.

*Mission Profile:* Simple launch in escape trajectory in general direction of Venus. Actual velocity increment: 11,000 m/sec. Flight-path angle, 78.3°. Azimuth, 93.0°. Burnout time, 322.0 sec.

*Status:* Launched March 11, 1960. Now in 311-day orbit around Sun. Final radio contact was on June 26, 1960, 107 days after launch. Battery could no longer sustain transmitter.

*System Description:*

Launch vehicle: Thor-Able. (See Table 9-3.)

Ground Support: Cape Kennedy. Jodrell Bank radio telescope plus tracking stations at Hawaii, Singapore, and Millstone Hill.

Spacecraft: Spheroid: 66-cm in diameter. Mass 34; kg. (See Fig. 11-1.)

*Spacecraft Subsystem*

Communication

PCM/PM communication system. Transmitter frequency: 378 Mc; receiver: 400-Mc UHF double-conversion superheterodyne command receiver with phase-lock loop. 5-w and 150-w UHF transmitters. Transmitters operated as coherent transponders. Quarter-wave stub antenna. Digital telemetry and command.

Power Supply

4800 silicon solar cells on four paddles oriented so that 23% of area was effective at any attitude. Charging capacity at Earth: 14.8 w. 3-mil glass protective plates on cells. Four paddles released and locked into position following second-stage shut down. 14 Sonotone F (Ni-Cd) cells used as energy accumulators. Power drain: 150 w transmitter on; 523 w, transmitter off; 7 w.

Propulsion

None.

Attitude Control

Spin-stabilized by six solid spin rockets on second stage at 2.4 rps. No active attitude control.

*Comments*

Contrast high power level to Mariner-2's 3-w transmitter. (Ref. 11-5.) No high-gain directional antenna.

Solar cells not locked on Sun.

No maneuvers.

Spacecraft axis fixed in inertial space.

Environmental Control	Temperature range controlled between 0°C and 27°C. Lithium heat sinks at sensitive spots radiated heat to space. Absorptivity and emissivity of spacecraft coating varied with attitude presented to Sun by spin-stabilized probe.	Completely static environmental control.
Guidance and Control	Aspect indicator consisted of a solar cell that triggered a pulse when facing the Sun. Used in interpreting magnetic field and radiation data.	Tracked from Earth. No maneuvers or active altitude control.
Computer	None on spacecraft. All computations done on Earth.	
Structure	Four radial aluminum beams. Central platform constructed of fiberglass honeycomb. Aluminum sheet-metal panels on outside. Instrumentation clustered at platform periphery to increase spin moment of inertia.	
Engineering Instruments	Thermocouples on solar paddles #1 and #2, transmitter heat sink, battery, internal environment, and counter. Battery voltage and receiver phase error monitored.	
Scientific Instruments	Radiation measurements: Geiger-Mueller tube and proportional-counter telescope. Magnetic field measurements: search-coil magnetometer. Micrometeoroid measurements: diaphragm plus microphone and pulse-height analyzer.	First U.S. deep-space measurements.

TABLE 11-2. IMP-1, INTERPLANETARY MONITORING PLATFORM, S-74, EXPLORER 18

*Mission Objectives:* Very high apogee satellite probe designed to monitor solar flare activity for purpose of developing prediction scheme for Apollo astronauts. Also measures solar wind, cosmic rays, interplanetary magnetic fields. Series of probes planned. Descriptions of IMP-1, below, are typical.

*Mission Profile:* Launch into nominal 33° inclined, highly eccentric orbit about Earth. Nominal apogee: 278,000 km. Nominal perigee: 203 km. Nominal period 150-160 hrs. Lifetime about six months.

*Status:* First IMP successfully launched Nov. 26, 1963. Transmissions ceased in May 1964.

*System Description:*

Launch Vehicle: Thor Delta. (See Table 9-3.)

Ground Support: Cape Kennedy. Ground stations at Woomera and Santiago.

Spacecraft: Octagonal cylinder: 71 cm across flats, 30 cm high. Four solar-cell paddles. Magnetometer on boom extending along cylinder axis. Mass about 63 kg. (See Figs. 11-2 through 11-4.)

*Spacecraft Subsystem*

*Description*

*Comments*

Communication Pulsed frequency modulation. Transmitter frequency: 130 Mc. Transmitter power: 4 w. One-month continuous data storage capacity.

Power Supply 11,520 p-n silicon solar cells on four paddles produce 38 w. 12-mil glass covers on cells. Thirteen sealed Ag-Cd cells rated at 5 amp-hrs backup solar cells. Panels 66 x 51 cm.

Propulsion None. No maneuvers.

Attitude Control Spin-stabilized. Yo-yo despin mechanism. Experiments and power supply designed for fixed spin axis.

Environmental Control Passive paints and coatings.

Guidance and Control Solar aspect sensor.

Computer No central computer.

Structure Materials: Aluminum, stainless steel, magnesium. Only iron in cable. Octagonal base with attached booms and solar-cell paddles. Non-ferrous metals dictated by magnetic experiments.

- Engineering Instruments  
Fifteen temperatures, voltages, and currents as listed in Sec. 10-11.
- Scientific Instruments  
Magnetic field measurements: rubidium-vapor and two fluxgate magnetometers. (See Fig. 11-3.)  
Solar wind measurements: charged particle trap, plasma probe, electrostatic analyzer.  
Cosmic ray measurements: solid-state telescope, scintillator detector, Geiger counters.

TABLE 11-3. FOLLOW-ON PIONEER PROBES\*

*Mission Objectives:* Study particles and fields in interplanetary space in conjunction with the International Year of the Quiet Sun and subsequent solar buildup. Series of spacecraft planned.

*Mission Profile:* Direct launch into orbits alternately 0.2 A.U. inside or outside Earth's, i.e., 0.8 and 1.2 A.U. Lifetime about six months.

*Status:* In development. First launch planned for 1965.

*System Description:*

Launch Vehicle: Thor-Delta. (See Table 9-3.)

Ground Support: Cape Kennedy, DSIF, SFOF.

Spacecraft: Cylindrical body with antenna mast parallel to axis. Diameter: 94 cm. Height: 81 cm. Three 165-cm booms erect perpendicular to axis. Mass: 62 kg. (See Figs. 11-5 and 11-6.)

*Spacecraft Subsystem*

*Description*

*Comments*

Communication

Discone omniantenna on top of high-gain antenna mast. Receiver frequency: 2300 Mc. Transmitter frequency: 2300 Mc. PCM/PM phase-lock receiver.

Paraboloid not necessary at planned orbits.

Power Supply

10,368 p-n solar cells in two 48-cm bands around circumference. Battery included for reorientation in case of eclipse. Solar cells produce minimum of 55 w at 1.2 A.U.

Propulsion

No maneuvers.

Attitude Control

Spin stabilized at 60 rpm. Cold-nitrogen-gas jets bring cylinder axis perpendicular to plane of ecliptic. Jets located on one of the three booms.

First Pioneers did not use gas jets.

Environmental Control

Temperature-controlled louvers on bottom of spacecraft cylinder beneath equipment platform. Excess heat is radiated from top and bottom of cylinder, which see empty space. Passive thermal coatings on external components.

Louvers look out perpendicular to plane of the ecliptic.

Guidance and Control

Five Sun sensors actuate attitude-control subsystem. Spacecraft axis parallel to Sun's within  $\pm 1.5^\circ$  and perpendicular to plane of the ecliptic within  $\pm 1^\circ$ .



Computer	Solid-state memory of 14,000 bits for scientific data storage.
Structure	Equipment mounted on an aluminum honeycomb shell. Solar cells attached to a 0.56-cm magnesium shell hanging from shelf. Fiberglass, aluminum-coated antenna mast. Three foldable booms at 120° intervals.
Engineering Instruments	Approximately 40 data points including power-supply voltages and currents, nitrogen gas pressure, spacecraft temperatures at selected points.
Scientific Instruments	Vary from probe to probe.* Micrometeoroid measurements Magnetic field measurements Cosmic ray measurements Plasma probes

\*Descriptive data not firm at time of writing.

All materials should be non-magnetic.

In the broad sense, the interplanetary probe is an extrapolation of the Earth sounding rocket in both purpose and design philosophy. In effect, these probes make weather measurements in deep space. In particular, they record the varying emissions from the Sun and explore the boundaries

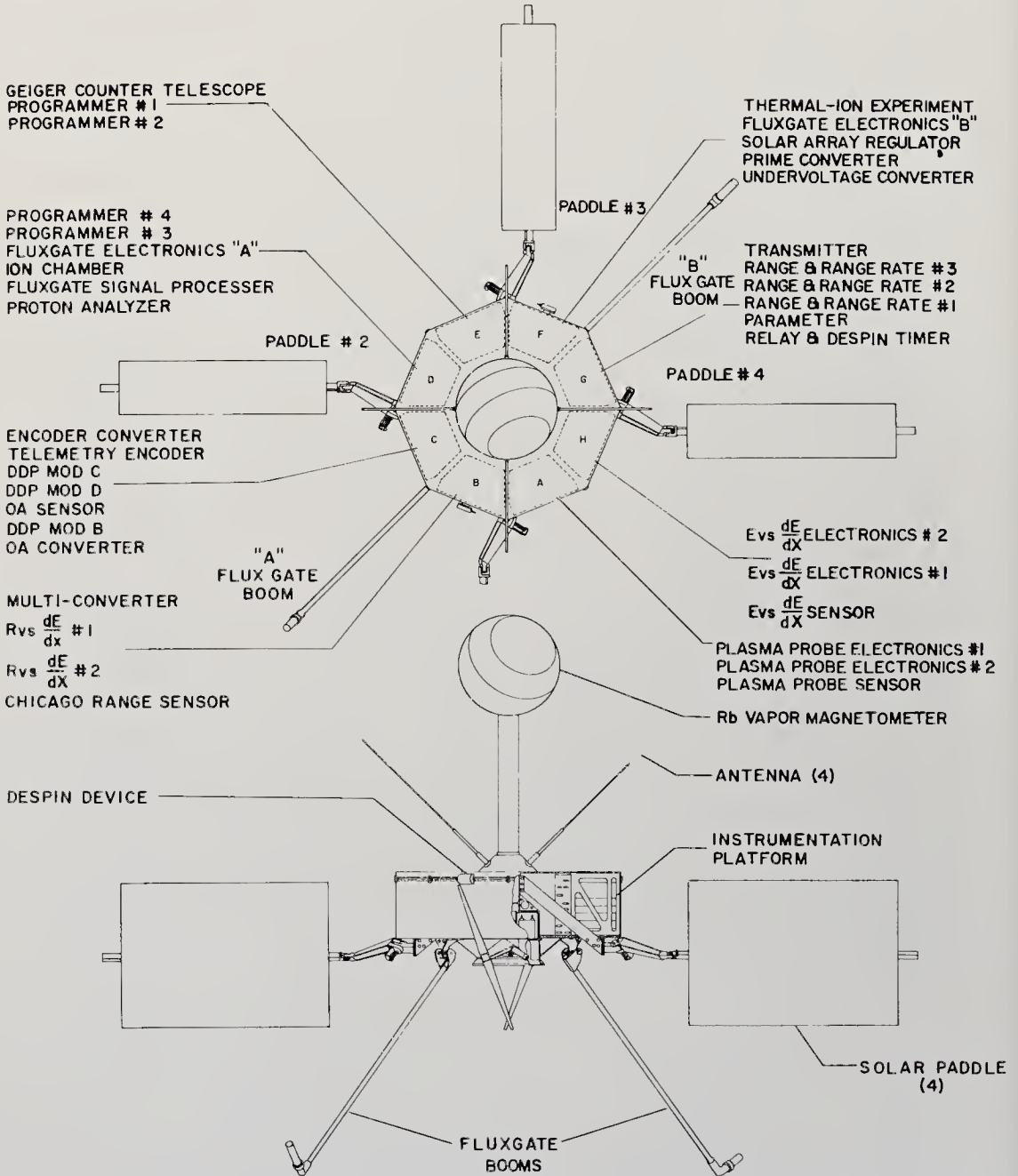


Fig. 11-2. Diagram of the first Interplanetary Monitoring Platform, IMP 1. Distance between the sides of the octahedron is 68 cm. (NASA drawing)

between the terrestrial, solar, and interstellar magnetic fields. They are the simplest of all deep-space research tools.

The first true deep-space probe, Pioneer 5, launched in March, 1960, can be labeled an interplanetary probe even though it was aimed in the general direction of Venus' orbit (Table 11-1). The highly eccentric orbit of IMP (Interplanetary Monitoring Platform) takes it almost 300,000 km into space, making it a valuable addition to the spectrum of space-research vehicles, even though it remains a satellite of Earth (Table 11-2). A new series of Pioneer-class probes, built by Space Technology Laboratories, Inc., will soon begin a systematic, synoptic coverage of the region in space between the orbits of Mars and Venus (Table 11-3). It is not difficult to foresee many small, simple probes similar to the Pioneers being launched on a regular basis as we attempt to understand the transients and the detailed character of the fields and fluxes between the planets.

A special case of the interplanetary probe is the out-of-the-ecliptic

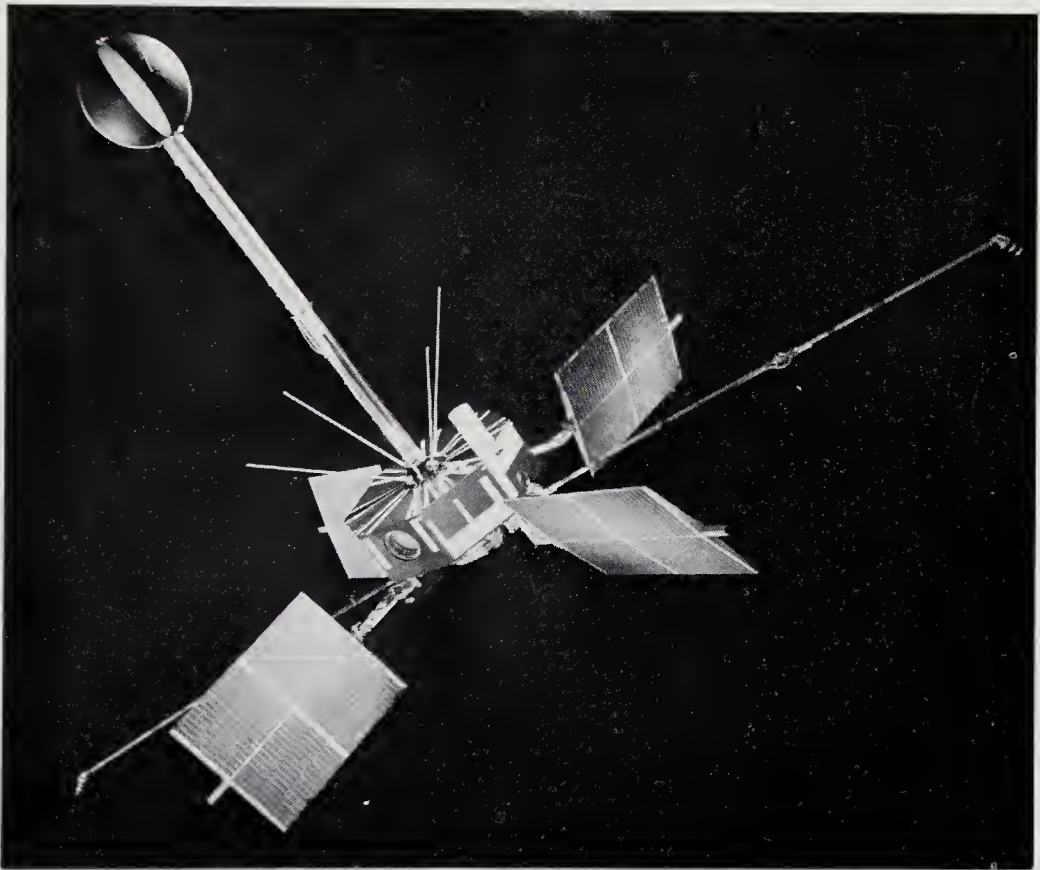


Fig. 11-3. IMP 1, showing solar panels, antennas, and magnetometer sphere in extended positions. (NASA photograph)

probe (Table 11-8). The energy necessary to eject spacecraft into orbital planes at high angles to that of the Earth may be tens of kilometers per second, depending on the inclination desired (Chap. 5). Despite the propulsion challenge, scientific curiosity about the asymmetry of the solar system will force early probing of this vast, neglected region. Most of the dust and debris in the solar system is expected to be concentrated within a narrow angle centered on the plane of the ecliptic. On the other hand, solar flares and cosmic rays, though strongly affected by the Sun's magnetic field, will probably be more nearly isotropic. The probes sent out to investigate the distribution of particles and fields away from the

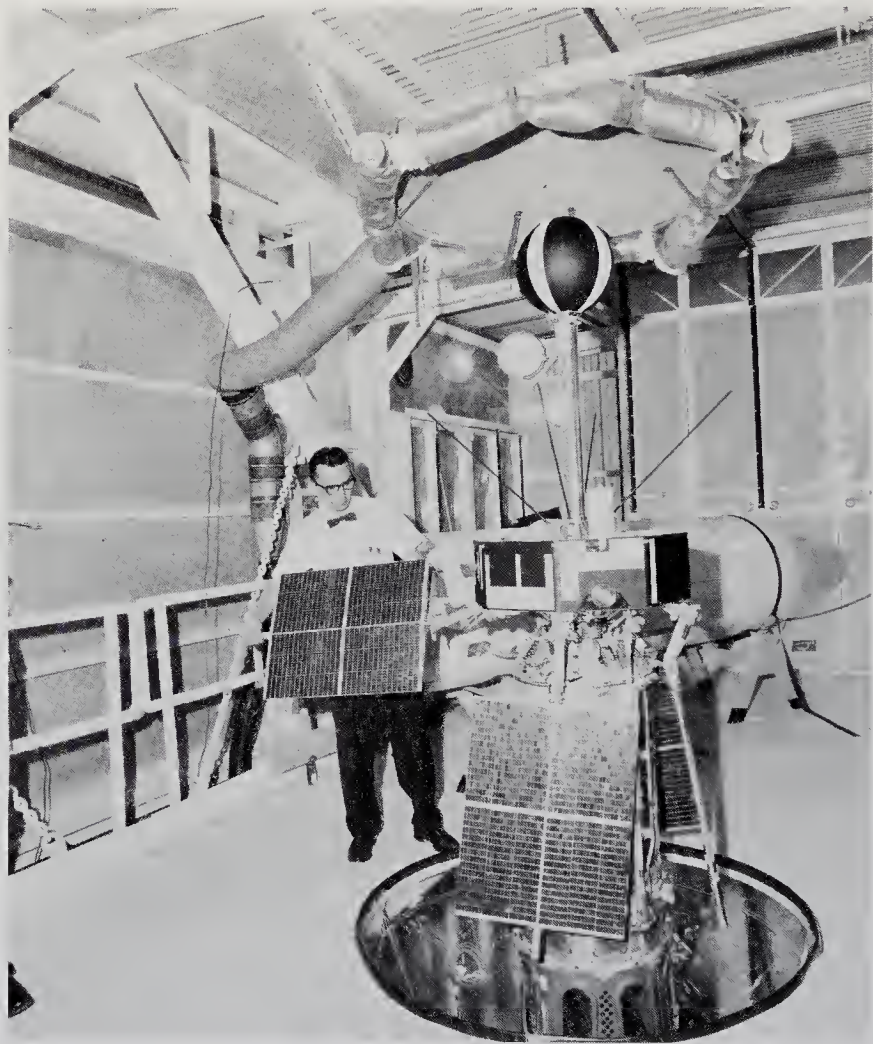


Fig. 11-4. IMP 1, on the launch pad at Cape Kennedy. The Thor Delta launch-vehicle final stage can be seen through the hole in the platform. Space-vehicle shroud is in background. (NASA photograph)

ecliptic will be similar to IMP and the Pioneers in physical construction and instrumentation.

### 11-3. Flyby Probes

By adding a midcourse motor and refining the guidance-and-control subsystem of the interplanetary probe, it can be directed to within a few tens of thousands of kilometers of the surfaces of the inner planets. In passing so close to the planets, flyby probes can resolve questions concerning atmospheric structure and composition. If the surface is visible, photographs or TV pictures can be taken at close range. Before and after

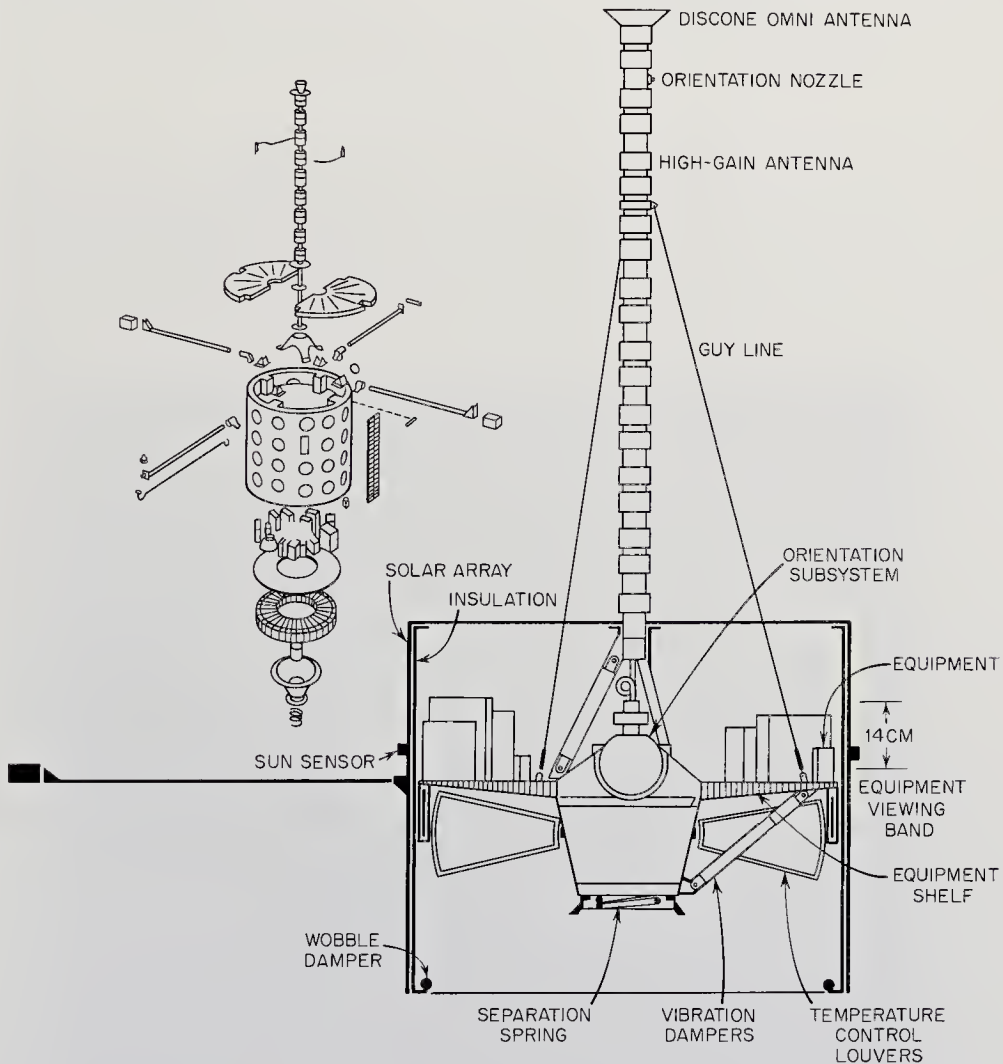


Fig. 11-5. Diagram of the Pioneer-6 spacecraft. Like its predecessor, Pioneer 5, its mission is the exploration of the fields and particles in deep space. (NASA drawing)

planetary encounter, the flyby probe can also function as an interplanetary probe and sample the fields and particles.

The planetary-encounter mode of operation complicates the probe. Instruments scanning the planet's disk must be accurately pointed and swung in the proper arcs to cover the planet's disk and atmosphere. Instrument articulation, added to that of the solar panels and directional antennas, necessitates a sophisticated guidance-and-control subsystem and, in addition, a good attitude-control subsystem.

Aside from the midcourse maneuver and planetary scanning instruments, the flyby probe is much like a scaled-up interplanetary probe. Spacecraft functions like environmental control are performed on a large scale, but the functions themselves are basically the same on Mariner 2 as they are in the new Pioneer series.

The first planetary flyby probe (1961  $\Gamma 1$ ) was launched toward Venus by the Russians, on February 12, 1961. Sputnik 8 was used as a satellite launch vehicle. The spacecraft, pictured in Fig. 11-7, had a mass of 644 kg, much larger than the U.S. Mariner 2 launched a year and a half later. Onboard were instruments to measure the magnetic field, micrometeoroids, charged particles, and cosmic rays. Solar-cell paddles and a large parabolic

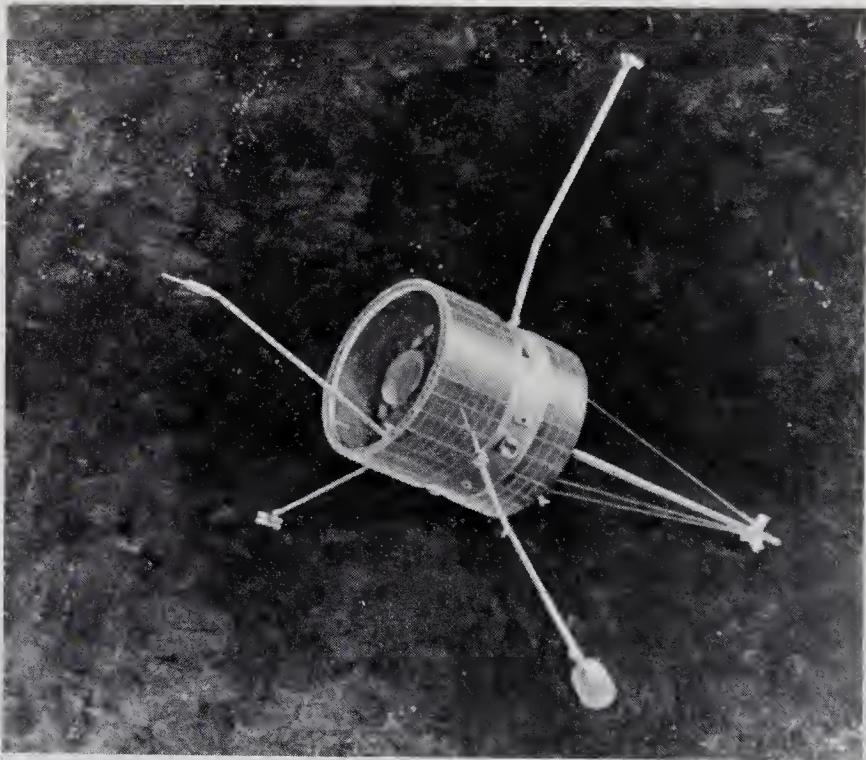


Fig. 11-6. Pioneer 6, showing the instrument booms extended. (NASA photograph)

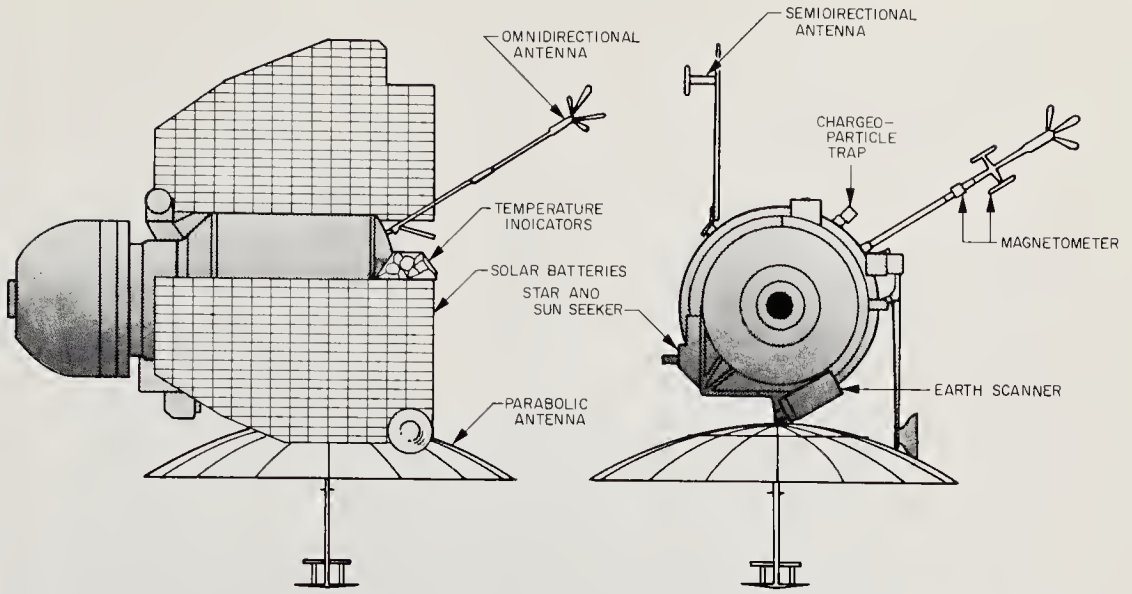


Fig. 11-7. The Russian 1961 Venus probe. This drawing should be compared to that of Mariner 1 (Fig. 11-8) and the many similarities noted.

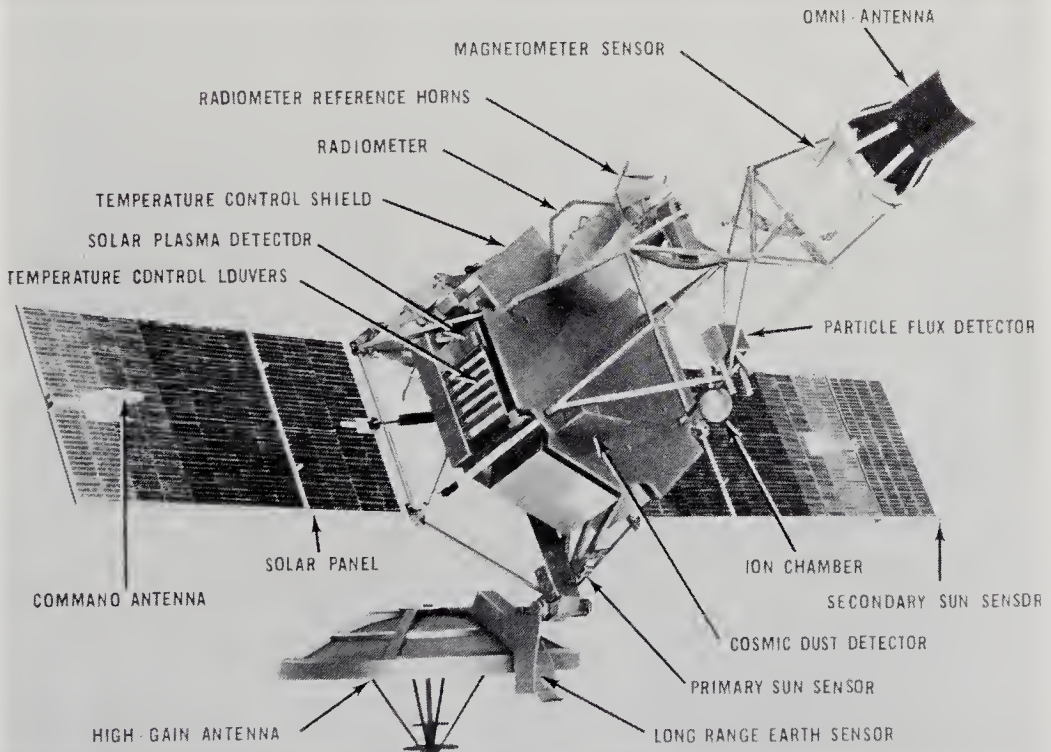


Fig. 11-8. Artist's sketch of the Mariner 1 spacecraft with solar panels and paraboloid antenna extended. Note the superstructure on the hexagonal base. (NASA drawing)

TABLE 11-4. MARINER 2

*Mission Objectives:* To fly by Venus, making infrared and microwave measurements to try to resolve character and temperature of Venus atmosphere. To make fields-and-particles measurements in interplanetary space. To prove out the interplanetary communication system.

*Mission Profile:* Launched Aug. 26, 1962 into parking orbit. Ejected by the Agena stage into a Venus trajectory. Midcourse maneuver on Sept. 4, 1962. Passed within 35,000 km of Venus' sunlit side on Dec. 14, 1962.

*Status:* Launched after the abort of Mariner 1, on July 22, 1962. Communications terminated on Jan. 3, 1963. Now in orbit around the Sun.

*System Description:*

Launch Vehicle: Atlas-Agena B. (See Table 9-3.)

Ground Support: Cape Kennedy, DSIF.

Spacecraft: Hexagonal base with tubular superstructure. Two solar panels and high-gain paraboloid antenna attached to base. Dimensions: 1.52 m at base, 3.02 m high in launch configuration. Mass: 203 kg. (Figures. 11-8 and 11-9.)

*Spacecraft Subsystem*

	<i>Description</i>	<i>Comments</i>
Communication	PCM/PM phase-locked telemetry and commands. Transmitting frequency: 960 Mc. Receiving frequency: 890 Mc. Discone and dipole command antennas. Paraboloid antenna for deep space work. Transmitter power: 3 w.	Established U.S. space communications distance record of 87,000,000 km. See Chap. 6.
Power Supply	9800 silicon solar cells produced minimum of 148 w and maximum of 222 w. Glass covers on solar cells. Ag-Zn backup battery with 1000 w-hr capacity for use during maneuvers and possible loss of Sun-lock.	
Propulsion	Hydrazine-fueled midcourse correction motor providing 23-kg (50 lb) thrust for up to 57 sec. Fuel stored in rubber bladder under pressure.	First U.S. use of midcourse maneuver.
Attitude Control	Ten cold-nitrogen-gas jets. 1-deg pointing accuracy. Earth-lock for antenna, Sun-lock for solar cells, Venus-lock for instrument scanning.	



- Environment Control**  
 Paint patterns, insulating shields, gold plating, and aluminum sheet made up passive control system. Eight polished, aluminum louvers, actuated by bimetallic elements, controlled temperature in CC&S and attitude-control electronics packages.
- Guidance and Control**  
 Three rate-integrating gyros, six Sun sensors, and one Earth sensor. Three modes of operation: launch, midcourse, and encounter, controlled by CC&S below.
- Computer**  
 Central computer and sequencer (CC&S) times spacecraft activities using 307.2-ke crystal oscillator. Some data manipulation done on board.
- Structure**  
 Hexagonal base of magnesium and aluminum. Aluminum tubular truss-type superstructure. Six rectangular chassis mounted inside each hexagon face.
- Engineering Instruments**  
 Approximately 50 data points read repeatedly, including: Earth-sensor temperature; nitrogen pressure; plasma electrometer temperature; propellant tank pressure and temperature; battery voltage, current, and temperature; antenna-hinge angle; Earth brightness.
- Scientific Instruments**  
 Microwave radiometer for surface temperature and water vapor concentration. Infrared radiometer to measure cloud details. Fluxgate magnetometer. Radiation measurements: ion chamber and 3 Geiger-Mueller tubes. Cosmic-dust detector. Solar-plasma detector.

See Chap. 7.

See Chap. 3 for results of scientific measurements. Most Mariner-2 instruments are detailed in Chaps. 13 and 14.

TABLE 11-5. MARINER 4

*Mission Objectives:* To obtain scientific data concerning the Martian atmosphere and surface. To make fields-and-particles measurements between the orbits of Mars and the Earth.

*Mission Profile:* Launched November 28, 1964 into parking orbit. Agena-D stage ejected spacecraft into trajectory towards Mars. Midcourse maneuver occurred Dec. 5. Probe should pass about 8,700 km from sunlit side of Mars on July 14, 1965.

*Status:* Hardware.

*System Description:*

Launch Vehicle: Atlas-Agena D. (See Table 9-3.)

Ground Support: Cape Kennedy, DSIF, SFOF.

Spacecraft: Octagonal base with tubular mast. Four solar panels and high-gain antenna attached to base. Quite similar to Mariner 2. Spacecraft mass approx. 270 kg. (Figs. 11-10 through 11-13.)

#### *Spacecraft Subsystem*

##### Communication

PCM/PM phase-locked telemetry and commands. Transmitting frequency: 2300 Mc. Receiving frequency: 2300 Mc. Omnidirectional antenna for pre-midcourse-maneuver communications. Elliptical parabolic high-gain antenna. Telemetry bit rates,  $33\frac{1}{3}$  near Earth and  $3\frac{1}{3}$  bits/sec near Mars.

##### *Description*

Like Mariner 2, except for shift to higher frequencies.

##### *Comments*

##### Power Supply

Approximately 25,000 solar cells in four oriented panels. Power output about 140 w at Mars orbit. Backup Ag-Zn battery for use during maneuvers and possible loss of Sun-lock.

##### Propulsion

Hydrazine midcourse motor with capability for two starts. Thrust of 23 kg (50 lb). Total velocity increment of 80 m/sec.

Extra start capability over Mariner 2.

##### Attitude Control

Solar pressure vanes for spacecraft stabilization. Cold-nitrogen gas jets for maneuvers and stabilization, solar acquisition, Canopus acquisition, and Mars acquisition.

##### Environment Control

Thermal shielding of components. Paints and metallic coatings used for passive control. Thermostatically controlled louvers make up active control.

- Guidance and Control  
 Canopus star tracker for position and orientation, plus two Sun sensors. Tracking from Earth through transponder signals. See CC&S below.
- Computer  
 Central Computer and Sequencer (CC&S) provides timing, event initiation sequencing, switching and data manipulation.
- Structure  
 Octagonal base with tubular superstructure. Chassis mounted in base. Magnesium and aluminum predominant structural materials.
- Engineering Instruments  
 Similar to Mariner 2.
- Scientific Instruments  
 TV camera for scanning Martian surface  
 Plasma probe  
 Magnetometer measures Martian and interplanetary field  
 Ion chamber  
 Trapped radiation detector  
 Cosmic-dust detector  
 Cosmic-ray telescope  
 S-band radio occultation experiment
- First star tracker on deep-space probes.
- No ferromagnetic materials.
- TV for closeup view of Mars surface. Some Mariner-4 instruments described in Chaps. 13 and 14.

antenna were attached to a pressurized shell containing the electronic instrumentation. In short, the Russian Venus probe differed little from the subsequent U.S. efforts, except for size. Unfortunately, radio contact with the probe was lost on Feb. 27, 1961, when it was about 7,500,000 km from the Earth (Ref. 11-1).

U.S. Venus ventures had to wait for the next firing windows in the late summer of 1962. Mariner 1, launched on July 22, 1962, was destroyed by the range safety officer as it strayed off course. Mariner 2, which was essentially identical to Mariner 1, was successfully launched Aug. 26, 1962. The U.S. press has since reported that the Russians have made several unsuccessful attempts to launch additional planetary probes. One well-publicized Russian probe was the Mars 1, launched on Nov.

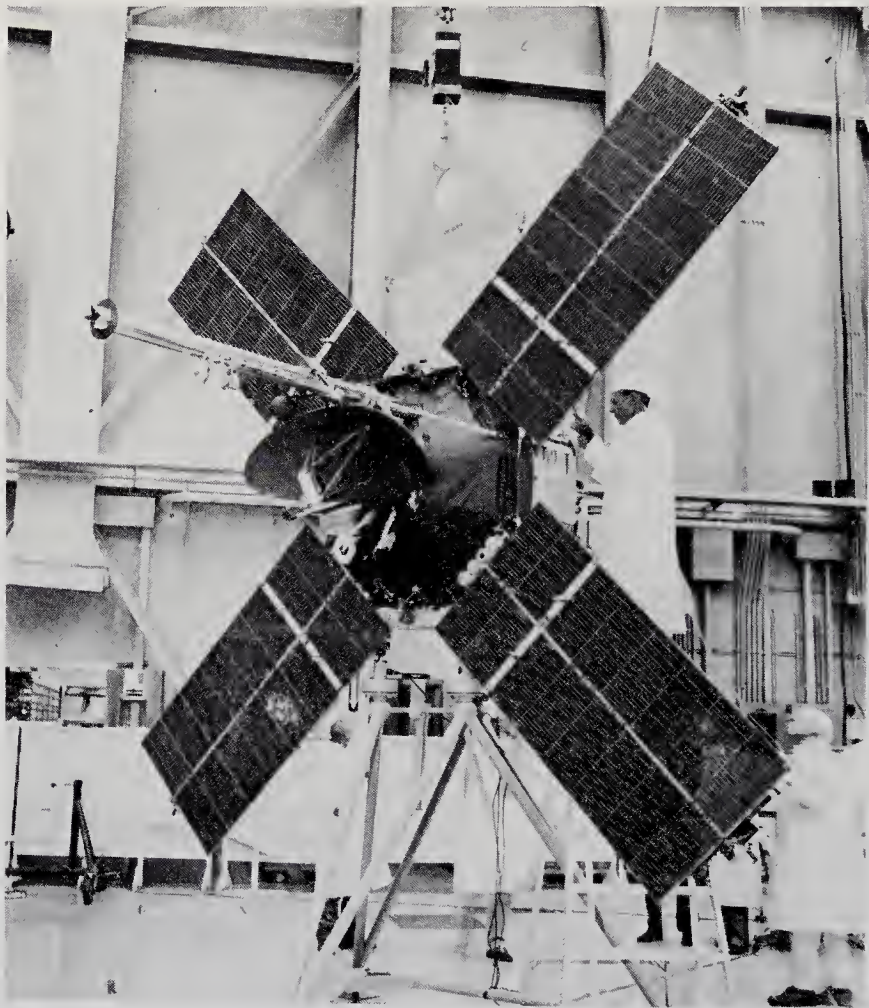


Fig. 11-9. Mariner 1 being mated to the Agena adapter ring prior to mounting on the Atlas-Agena launch vehicle at Cape Kennedy. (NASA photograph)

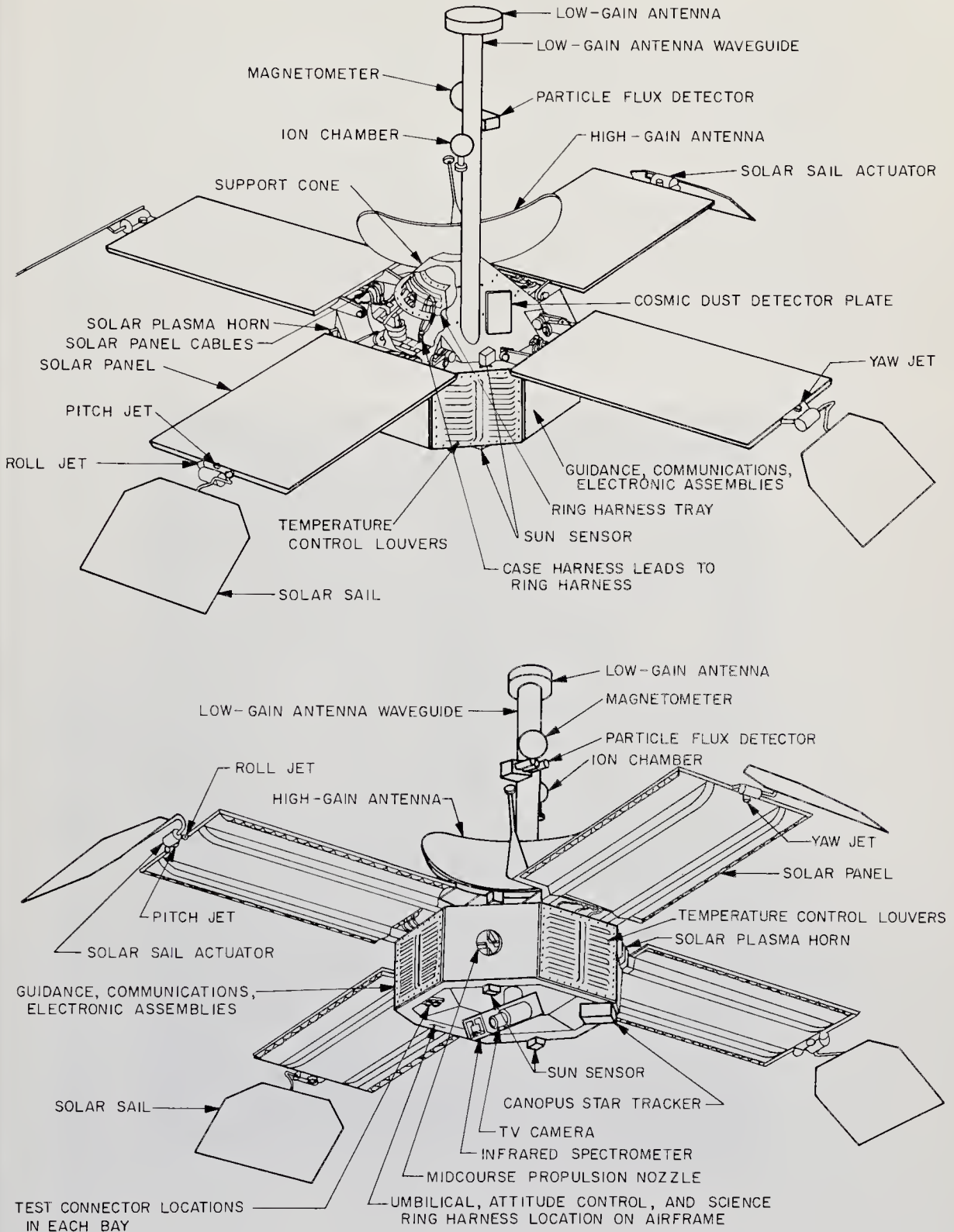


Fig. 11-10. Diagrams of the Mariner-3 spacecraft. (NASA drawing)

1, 1962. Transmissions from this probe failed when it was about 105,000,000 km from Earth. On Nov. 28 1964, the U.S. launched Mariner 4 to Mars. This success was preceded by the launch of Mariner 3 on Nov. 5, 1964, which ended in failure when the launching shroud could not be ejected.

Some of the more advanced Mariner spacecraft may execute a terminal maneuver and inject themselves into an orbit around the target planet (usually Mars). Once in orbit, the planetary surface can be studied more leisurely than from the brief flyby contacts. With the cancellation of the Mariner shot to Mars originally scheduled for 1966, the next Mars opportunity, early in 1969, might logically employ an orbiter. The extra payload needed for an orbiter might be obtained by upgrading the

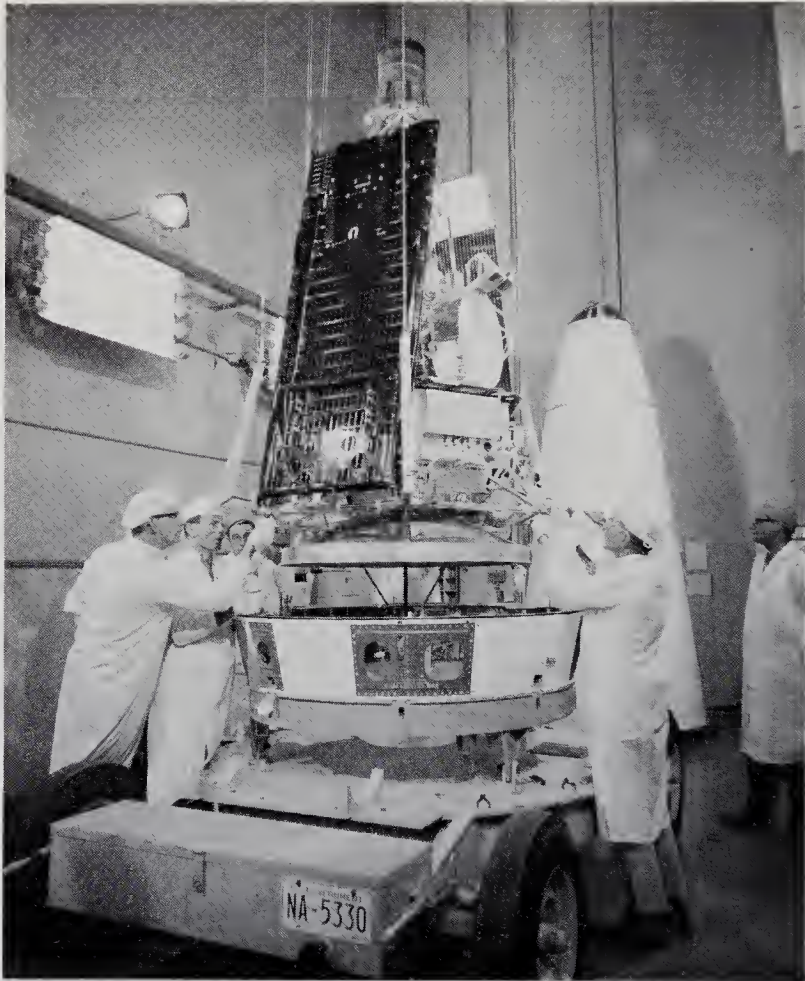


Fig. 11-11. Mariner 3 being prepared for shipment to Cape Kennedy at JPL. (NASA photograph)

Atlas-Centaur launch vehicle through the use of a mixture of fluorine and oxygen (FLOX). These programs are not firm, however.

The flyby probes of the future include not only the U.S. Mars 1969 attempt, but almost certainly some additional Russian tries. Flyby probes to the inner, minor planets will probably bear a strong resemblance to the Mariners (Tables 11-4 and 11-5). Flyby probes to the major planets will claim a legacy from the Mariners but may employ electrical or nuclear propulsion to achieve the higher payload-to-gross-weight ratios that will be needed (Table 11-8). In any event, the flyby probe is a valuable precursor to landings by unmanned exploratory vehicles, and many more of them can be expected.

#### 11-4. Voyager

The NASA Voyager Program comprises a series of studies aimed at defining the next generation of unmanned planetary spacecraft. Many types of spacecraft have been examined, from orbiters to landers. The following data are representative.

A Voyager-class, space-probe system is the most complex of all the probes described in this chapter. The objective of a Voyager spacecraft is the return to Earth of large quantities of meaningful scientific data concerning the atmosphere, surface, and interior of the nearby terrestrial-

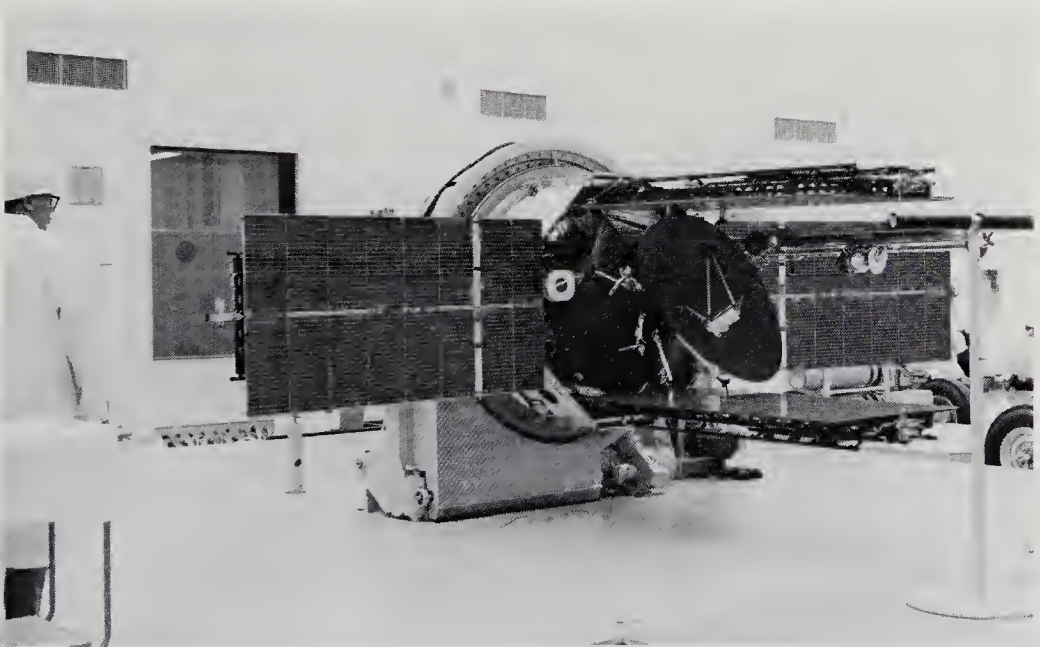


Fig. 11-12. Mariners 3 and 4 at Cape Kennedy before the 1964 launch. (NASA photograph)

TABLE 11-6. REPRESENTATIVE VOYAGER

*Mission Objectives:* To return meteorological, geological, and biological data from the nearby terrestrial-type planets. In the case of Mars, the detection of life has the highest priority.

*Mission Profile:* Launch from Earth followed by midcourse maneuver, cruise, and terminal maneuvers preparatory to orbital injection or landing. Retrorockets for landing capsule ejection.

*Status:* Under study. First launch after 1970.

*System Description:*

*Launch Vehicle:* Not selected. Possibilities include Saturn 1 B and Titan 3. (See Table 9-3.)

*Ground Support:* Cape Kennedy, DSIF, SFOF.

*Spacecraft:* Configuration undetermined. See Fig. 11-14. Spacecraft mass between 1500 and 3000 kg in early versions.

#### *Spacecraft Subsystem*

#### *Description*

#### *Comments*

#### Communication

Probably PCM/PM. Primary and backup links between DSIF, orbiter, and landing capsule may number a dozen. Telemetry and command frequencies in 2000-2500 Mc range. Transmitter power about 50 w.

#### Power Supply

Solar cells in space. Radioisotopic power generator on lander. Batteries for backup. 200-300 w required on orbiter, 50-100 w on lander. Solar cells and batteries too heavy on lander owing to loss of Sun at night or because of clouds.

#### Propulsion

Probably a restartable, bipropellant motor for orbiter and a solid retrorocket for the lander.

#### Attitude Control

Cold-gas jets likely. Similar to Mariners. Small rockets to orient lander package.

#### Environment Control

Thermal shields, paints, coatings, and thermostatically operated louvers. Ablating entry shield for landers. Water-cooling and heating schemes involving radioisotope generator have been suggested.



Guidance and Control	Earth and Sun sensors, possibly a star tracker, and Earth-based tracking for trajectory to Mars. Planet acquisition needed during approach. Orbiter might use horizon sensor for attitude control. Landing radars possible.	
Computer	Small computer likely for data handling. There will probably be a component analogous to the Mariner Central Computer and Sequencer (CC&S).	
Structure	Probably an instrument-platform base with attached superstructure (like Mariner) for orbiter. Lander with blunt entry cone. Parachute descent probable.	Minimum of ferromagnetic materials.
Engineering Instruments Scientific Instruments	Similar to Mariner 2. Particles-and-fields instruments enroute. Orbiters: radiometers, magnetometer, cosmic dust detector, TV for surface studies of Mars. Landers: atmospheric temperature, pressure, density, and composition; TV for surface study, life detectors, microscope for analysis of surface, atmospheric particles, and possible life; drills; chemical analysis of surface.	

type planets. Presumably, Voyager spacecraft are precursors to manned landings.

A Voyager must first intercept the target planet, then hit an entry corridor or inject itself into a satellite orbit, and possibly eject a landing capsule. A capsule, once on the ground, would take a wide spectrum of meteorological, geological, and biological measurements *in situ* or from a roving vehicle. Complexity arises from both the versatility of the

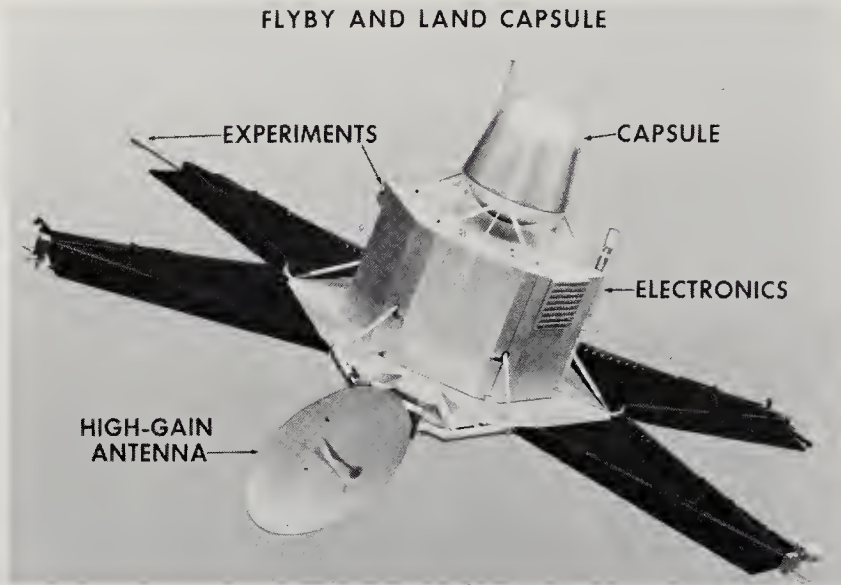


Fig. 11-13. A conceptual drawing of a Mariner-type spacecraft carrying a capsule that would be ejected so that it would enter a planetary atmosphere and land an instrument payload on the planet's surface. (NASA drawing)

scientific instrumentation and the sheer number of spacecraft maneuvers necessary to success. The environment and rotation of the planet may also interfere with power generation for communication and the experiments themselves. A representative Voyager spacecraft is described in Table 11-6. Design problems like atmospheric entry and surface locomotion were covered in the preceding chapter.

During 1963, several industrial organizations carried out Voyager design studies for NASA. With a problem as new and as sweeping as the surface exploration of another planet, many ways to do the job were suggested. The data shown in Table 11-6 are typical but not precise. Voyager must receive a great deal more scrutiny before spacecraft specifications can take final form. Budgets and the parallel Apollo program make it difficult to attach schedule dates to Voyager, but the first mission would not occur until after 1970.

### 11-5. Solar Probes

Superficially, solar probes will seem to be simple extrapolations of interplanetary probes. In fact, they are sometimes called "advanced Pioneers." The major difference is that they operate in that restricted volume within approximately 0.1 A. U. of the Sun. There are three reasons for separating solar probes into a class by themselves:

1. The thermal protection requirements radically affect spacecraft design.

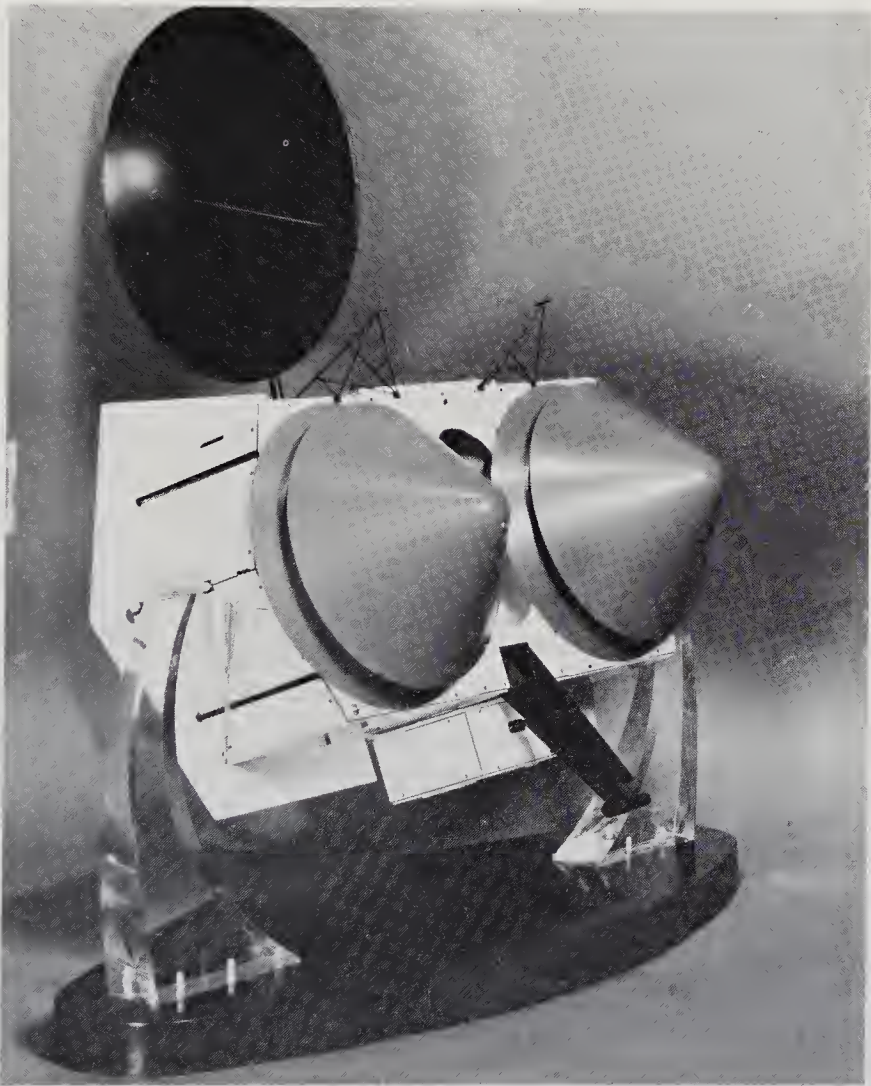


Fig. 11-14. Model of a conceptual Voyager-type spacecraft, showing two conical capsules for projection onto a planetary surface. (Courtesy of General Electric Co.)

2. The power-supply problem becomes more acute as solar cells lose their efficiency in the Sun's heat.
3. Very high velocity increments are needed to get close to the Sun, leading to very small payload-to-gross-weight ratios. (See Chap. 5.)

Other problems arise, too, like the interference of the radio noise of the Sun with communications. The closer the approach to the Sun, the farther the spacecraft design diverges from that of the interplanetary probes.

The scientific payoff resulting from a close approach to the solar disk comes through the close-up view of the Sun's surface, measurements of the fringes of the solar corona, and particles-and-fields experiments near their points of origin.

No solar probes have yet been launched, though Venus probes take instruments to about 0.7 A. U. from the Sun. Numerous studies of solar probes have been carried out by government and industry. Solar probes have been shown to be feasible and within the present state of the art. Their development is primarily a question of mission priority. The Orbiting Solar Observatories (OSO's) are already good outside-the-atmosphere locations for solar instruments. In deciding between solar and planetary probes, priority is usually given to the tiny, dimly seen planets. Nevertheless, the next decade should see one or more solar probes. In fact, the later Pioneer probes might be modified for operation near the Sun.

#### 11-6. Advanced Probe Concepts

In order of scientific priority and our ability to undertake advanced probe missions, the list reads:

1. A flyby of a comet, or preferably a fly-through of the cometary tail.
2. A flyby of one of the larger asteroids, with sample-collecting and analyzing equipment aboard to determine the chemical composition of material in the asteroid belt.
3. An interstellar probe penetrating well beyond the orbit of Pluto.

A little study has been done on each of these probes, but there is not enough agreement or depth to justify extensive presentations. The information in the following paragraphs and Table 11-8 is intended to be representative rather than typical of any of the several rather discordant concepts available from the literature.

*Cometary Probes.* Comets move very rapidly as they approach the perihelia of their highly eccentric orbits around the Sun. In addition, the cometary nuclei are apparently only a few kilometers in diameter. They

TABLE 11-7. REPRESENTATIVE SOLAR PROBE (ADVANCED PIONEER)

<i>Mission Objectives:</i> To make fields-and-particles measurements within 0.1 A. U. of the Sun.		
<i>Mission Profile:</i> Direct launch into orbit around Sun.		
<i>Status:</i> Under study.		
<i>System Description:</i>		
Booster: Possibilities include Atlas-Centaur, Saturn 1, Titan 3.		
Ground Support: Cape Kennedy, DSIF, SFOF.		
Spacecraft: Similar to follow-on Pioneers.		
<i>Spacecraft Subsystem</i>	<i>Description</i>	<i>Comments</i>
Communication	Probably PCM/PM. Directional antenna. Frequencies: 2000 to 3000 Mc. Transmitter power perhaps 5-20 w.	Solar radio noise a problem.
Power Supply	Solar cells, but possibly located on panels inclined at angle with Sun's rays to prevent overheating. Power output: 50-200 w.	
Propulsion	None.	No maneuvers.
Attitude Control	Cold-gas jets for coarse control. Stabilization with one face toward the Sun accomplished through solar pressure and gravity gradients.	At 0.1 A. U., the solar flux and gravitational forces are 100 times those at Earth orbit.
Environment Control	Extensive thermal shielding. Thermostatically controlled louvers on side away from Sun.	High-temperature components should be selected.
Guidance and Control	Sun-horizon and Earth sensors for attitude control and antenna-pointing, respectively.	
Computer	Probably some data storage and handling.	
Structure	Similar to follow-on Pioneers.	
Engineering Instruments	Similar to follow-on Pioneers.	
Scientific Instruments	Magnetometer, plasma probes, cosmic dust detectors. Possibly TV for surface studies. Particle detectors and spectographs.	

are therefore challenging targets with high energy requirements. (See Chap. 5.) Fortunately, the cometary coma is tens of thousands of kilometers in extent and the cometary tails, millions of kilometers long, both present reasonable opportunities for successful fly-throughs.

Small, spin-stabilized probes similar to the advanced Pioneers are big enough to carry TV, plasma probes, a mass spectrometer, and perhaps a few fields-and-particles experiments for use on the trajectory to the cometary intercept (Fig. 11-15). Spacecraft technology for cometary

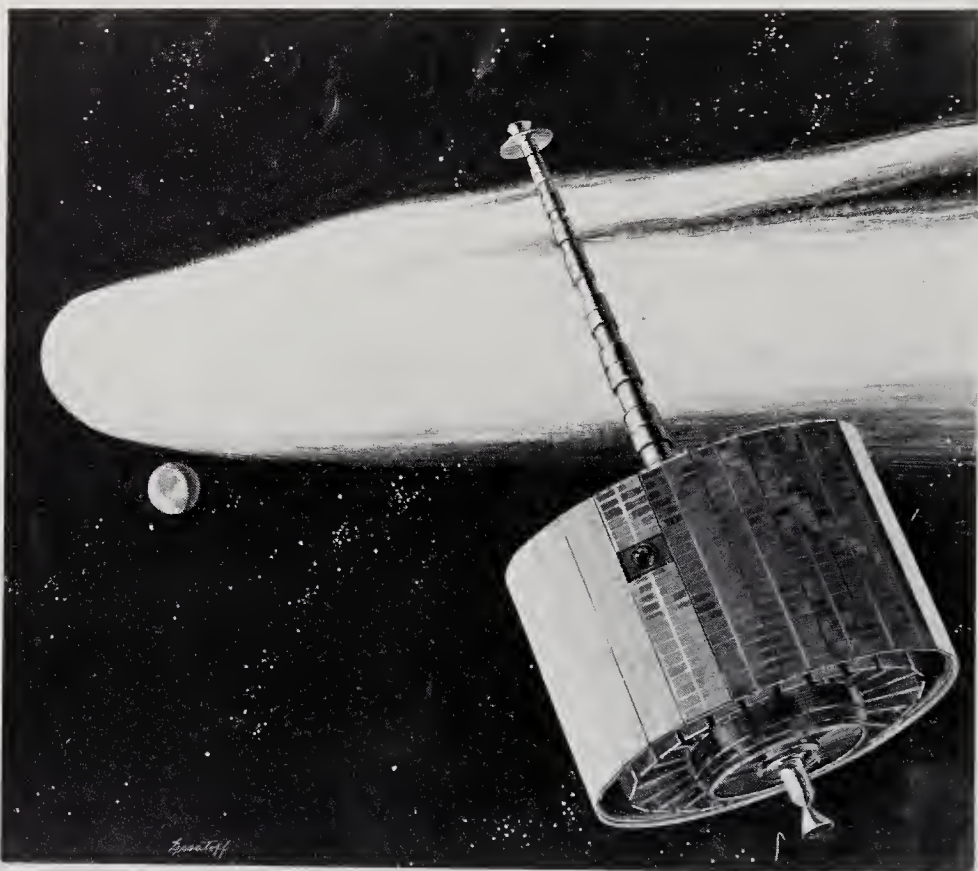


Fig. 11-15. Artist's concept of a cometary probe using Pioneer-type spacecraft technology. (Courtesy of Space Technology Laboratories, Inc.)

probes is based on considerable experience. Furthermore, there will be several dozen acceptable targets between the 1960's and early 1970's (Ref. 11-10). Cometary probes, then, may not be too far off.

The cometary probe would probably make its intercept between the orbits of Mars and Venus, where most spacecraft have been operated. Only two spacecraft subsystems would pose special problems: the propulsion and guidance subsystems. Not only is the target small, but comet

trajectories are not known with anything like the precision of planetary orbits. The burden of intercept—say, a flight through the coma about 40,000 km from the nucleus—rests upon good guidance and well-executed midcourse and terminal maneuvers. Presumably, guidance and correction maneuvers would be controlled from the Earth, with the DSIF providing probe trajectory data and astronomical telescopes the comet's positions.

Data on the size and composition of the comet's tail, coma, and nucleus might help settle the problem of their origin, and if the hypothesis that comets represent the primordial stuff of the solar system is correct, perhaps insight will be gained into the beginnings of the Sun and Earth.

*Asteroidal Probes.* A specimen from that swarm of dust, debris, and planetoids in the asteroid belt would be valuable to astronomers, who have been speculating about the belt's origin for centuries. Relatively little progress has been made in designing spacecraft for such a venture, however. A simple Pioneer-type probe with a magnetometer, plasma probe, and micrometeoroid detector could be lobbed through the belt quite easily. These more or less standard probe instruments would tell us little about the origin of the belt, however. A small asteroid would have to be collected and analyzed on the spacecraft. Or perhaps a close flyby of Ceres or one of the other large planetoids might reveal meaningful physical structures through remote TV. In short, the basic spacecraft itself seems to pose little problem if only a passage through the belt is desired (Table 11-8). The instruments necessary to obtain really significant data should receive the bulk of attention. Of course, if a flyby of a planetoid is deemed desirable, then the guidance and midcourse maneuvers become difficult, just as they did for a comet intercept. Our ignorance about the density and distribution of matter in the asteroid belt may conceal very severe spacecraft design problems, such as structural meteoroid protection or a high probability for the attrition of solar panels. The lack of asteroidal probe studies in the literature implies relative disinterest and low scientific priority. Most investigators believe that the belt originated when a terrestrial-type planet disintegrated. If this is so, a specimen might not yield much new knowledge, or possibly many specimens already exist on Earth in the form of meteorites.

*Interstellar Probes.* The true interstellar probe, with a range of several light years is quite beyond our reach, at least in this century. The energy requirements and reliability roadblock are too formidable. Instead of penetrating into the environs of a neighboring star, it is possible that a shorter journey, just beyond the confines of the solar system would yield important information. For instance, is there a halo of comets far beyond the orbit of Pluto and yet still bound to the Sun by gravitation? What is the make-up of this inferred belt? What is the nature of the

TABLE 11-8. PROBABLE CHARACTERISTICS OF SOME ADVANCED PROBES\*

	<i>Out of Ecliptic</i>	<i>Jupiter Flyby</i>	<i>Mercury Flyby</i>	<i>Cometary</i>	<i>Asteroidal</i>	<i>Interstellar</i>
<i>Objectives</i>	Determine asymmetry of fields and fluxes in solar system.	Determine nature of atmosphere and radiation belts.	Determine character of surface.	Determine composition and size of coma and tail.	Determine density and composition of belts.	Fields and particles measurements. Check on existence of cometary material.
<i>Possible Boosters</i>	Atlas-Centaur, Saturn 1.	Saturn 1, Titan 3, Saturn 1.	Atlas-Centaur, Saturn 1.	Atlas-Centaur.	Atlas-Centaur.	Saturn 5, Post-Saturn (Nova).
<i>Ground Support</i>	Cape Kennedy DSIF, SFOF	Cape Kennedy DSIF, SFOF.	Cape Kennedy, DSIF, SFOF.	Cape Kennedy, DSIF, SFOF.	Cape Kennedy DSIF, SFOF.	Cape Kennedy modified DSIF, SFOF.
<i>Spacecraft</i>	Like Pioneer.	Like Mariner, possibly electrically propelled.	Like Mariner or Pioneer.	Like Mariner or Pioneer.	Like Mariner.	Nuclear-electric.
<i>Communications</i>	Like Pioneer.	Like Mariner or Voyager.	Like Mariner or Pioneer.	Like Mariner or Pioneer.	Like Mariner.	Huge antennas at terminals. Large power requirements.
<i>Power Supply</i>	Solar cells and battery, ~100 w.	Solar cells and battery, >1000 w.	Inclined solar cells and battery, ~200 w.	Solar cells and battery, ~100 w.	Solar cells and battery, ~200 w.	Nuclear reactor, >1000 kw.
<i>Propulsion</i>	None.	Bipropellants for midcourse and terminal maneuvers.	Monopropellant for midcourse maneuver.	Monopropellant for midcourse and terminal maneuver.	Monopropellant for midcourse maneuver.	Electrical propulsion for solar-system escape.



<i>Attitude Control</i>	Spin-stabilized	Cold-gas jets.	Cold-gas jets, solar-pressure stabilization.	Spin-stabilized.	Spin-stabilized.	Electric engines.
<i>Environment Control</i>	Like Pioneer.	Like Mariner.	Like Mariner or Pioneer.	Like Mariner or Pioneer.	Like Mariner.	Convection loops. Louvers.
<i>Guidance and Control</i>	Like Pioneer.	Like Mariner.	Like Mariner or Pioneer.	Like Mariner or Pioneer.	Like Mariner.	Earth sensor to orient antenna. Sun sensor for thrust.
<i>Computer</i>	Like Pioneer.	Like Mariner.	Like Mariner or Pioneer.	Like Mariner or Pioneer.	Like Mariner.	Data conditioning and selection.
<i>Structure</i>	Like Pioneer.	Like Mariner.	Like Mariner or Pioneer.	Like Mariner or Pioneer.	Like Mariner.	(See Fig. 11-16.)
<i>Engineering Instruments</i>	Like Pioneer.	Like Mariner.	Like Mariner or Pioneer.	Like Mariner or Pioneer.	Like Mariner.	Critical temperatures, voltages, currents.
<i>Scientific Instruments</i>	Like Pioneer.	Like Mariner with additional particle detectors to examine radiation belt.	Like Mariner or Pioneer.	Spectroscopes and spectographs to analyze cometary material.	Dust and fragment analyzers. Possibly TV.	Fields and particles instruments. Devices to collect and analyze cometary material.

\* Most of the probes here will be based on two already developed and proven series of spacecraft: the Pioneers and Mariners. Some modifications are inevitable, but it is not feasible to develop new and special spacecraft for each mission from the standpoints of cost and reliability.

interface between the solar system's magnetic field and that of interstellar space?

The last question could be answered by propelling a spacecraft like Pioneer out of the solar system. The magnetometers, plasma probes, and radiation detectors could be designed for this task without much difficulty. The detection and measurement of the cometary material, supposedly aggregations of ices, is a technical problem of the highest order. Most space instrumentation deals with electromagnetic and particle radiation, but this cometary material would be cold, with no self-luminosity. Also, light reflected from the Sun would be small at the distances involved. Thus, instruments based on electromagnetic radiation might be useless. Sampling and analysis instruments would seem to be the best gamble for such a probe.

The probe itself would have to contend with the recession of the sun, with its warmth and power-producing capabilities. Only nuclear power

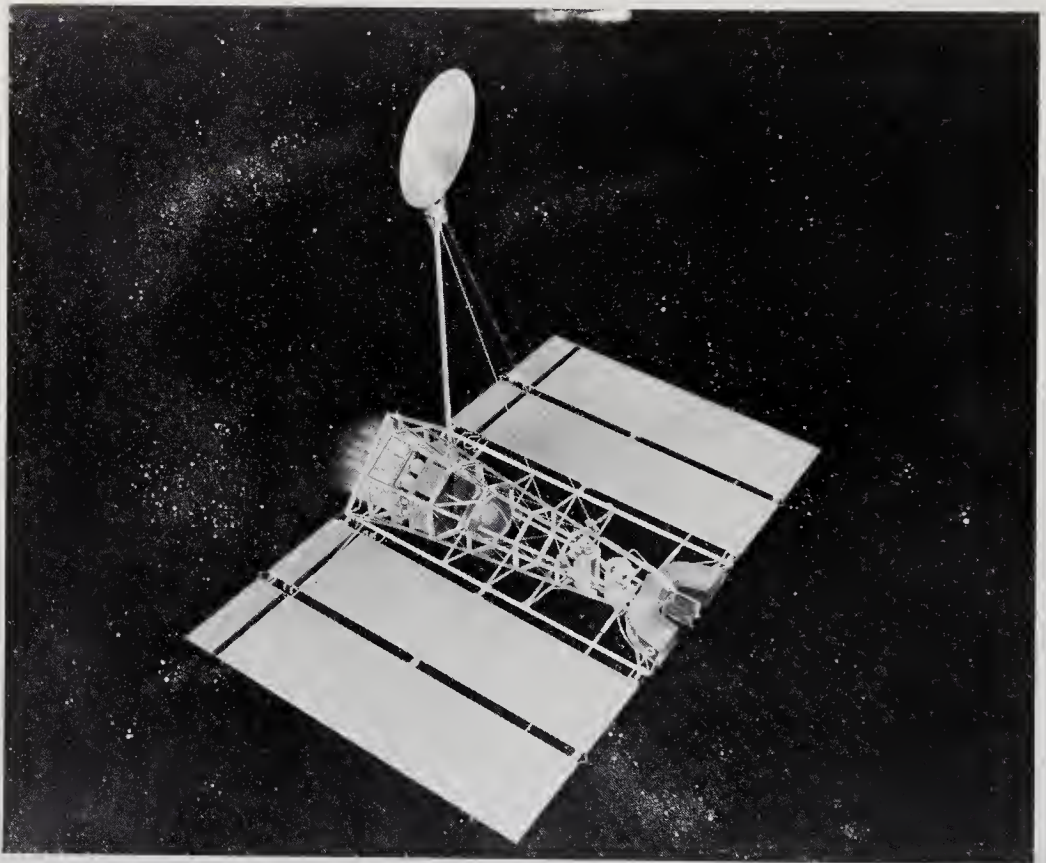


Fig. 11-16. An electrically propelled spacecraft for missions beyond Mars. The "wings" in this conceptual drawing are radiators for the nuclear-electric power supply, not solar-cell panels. Ion beams are shown at left of vehicle structure. (Courtesy of General Electric Co.)

seems reasonable for an interstellar probe. It could provide both electricity and environmental heat. Communicating over a distance of hundreds of A. U. would be impossible without many kilowatts of power and a large directional antenna. The spacecraft image that emerges after such deliberations takes the shape of a large, nuclear-powered craft with large waste-heat radiators and a dominating antenna structure. The scientific instruments themselves would be small in comparison and doubtless isolated from the spacecraft proper by booms.



*Part III*

SCIENTIFIC INSTRUMENTS

---

---



# Chapter 12

---

## SCIENTIFIC EXPERIMENTATION IN SPACE

---

---

### 12-1. Scope and Organization of Part III, Scientific Instruments

The major purpose of a space probe is the transportation of scientific instruments into regions that are otherwise inaccessible to science. The scope and diversity of natural phenomena to be explored outside the Earth's atmosphere encompass all the sciences, including that of life itself. To the list of expected phenomena must be added a generous allowance for the unexpected, those exciting quantum jumps in science that add spice to the launching of space probes.

Space research is a complicated enterprise. Not only are the physical phenomena unpredictable in many ways, but major advances in instrumentation must be made in the areas of reliability, small size, and small power requirements. On top of it all, the experimenter must begin his work about four years before the flight date. Once the probe is launched, he may have to wait another six months to a year before he receives his data. Space-probe research is thus a four-to-five-year gamble; the scientific stakes, however, make the gamble worth taking.

Categorization of the scientific provinces to be investigated in interplanetary space can never be precise, but five roughly hewn groups of experiments can be discerned:

1. Experiments probing the interplanetary medium.
2. Scientific probing of planetary atmospheres.
3. Exploration of planetary surfaces and subsurfaces.
4. The search for extraterrestrial life.
5. A miscellaneous but important group of experiments designed to study the Sun, the comets, the asteroids, and the periphery of the solar system.

To detect and measure the many physical parameters that describe space phenomena in these five classes, approximately 120 different kinds of instruments are now being developed or have already been flown on space probes (Table 12-1). Many instruments designed for balloons, sounding rockets, and Earth satellites are directly adaptable to deep-space probes. In addition, whole new groups of instruments must be invented to investigate the atmospheres, rocky mantles, and cores of the other planets. Just the search for other life forms introduces more than a dozen new instruments. The only types of space instruments not dealt with in the ensuing chapters are those concerned with observational astronomy, which, in the main, can be better done from the Earth's surface or nearby satellites, and some of the advanced instruments on meteorological, navigational, and ionospheric satellites. As pointed out in earlier chapters, the actual data received from space experiments, and their interpretation, are left for the specialized scientific journals.

Space instruments generally resemble terrestrial instruments, if terrestrial counterparts exist, except for weight, size, power consumption, ruggedness, and the enhancement of reliability through redundancy and better construction practices. Many instruments originally designed for terrestrial applications have been gradually modified during the ever-more-demanding succession of high-altitude balloons, sounding rockets, Earth satellites, and finally space probes. Instrument transformation has been gradual during the past twenty years; viz., the development of flight-proven cosmic-ray telescopes. The evolution of radiometers, cosmic-dust detectors, and the like has been more precipitous, but usually the terrestrial roots of the family tree are easily distinguished. In the case of life detection and experiments designed to recognize the products and environments of life, really new instruments come to the fore. There are no terrestrial counterparts to the Multivator or Gulliver.

Space instruments are also characterized by a number of unique requirements:

1. Data transmission rates are restricted to just a few bits per second at planetary distances.
2. Frequent in-flight calibration is needed.
3. There is only a small capacity for internal data storage.
4. No magnetic materials can be used.
5. The high temperatures of heat sterilization (135°C for 24 hours) must be survived.
6. Weight, volume, and electrical power are minimized.
7. Data must ultimately be delivered to the communication subsystem in digital form, in the proper format and word length.



8. The instrument must be rugged enough to withstand the vibration and shocks of launching.

In contrast to the abundant literature referenced in Parts I and II, specialized papers on space instrument design and development are relatively rare. The written word emphasizes the spacecraft and the scientific results obtained, not the instruments themselves. Blanket surveys of space instruments are truly exceptional (Refs. 12-2 and 13-38).

To demonstrate the great variety of probe instruments and also provide a Baedeker for the almost encyclopedic treatment in the following chapters, two general tables are presented here. The first is an inventory of major space-probe instruments and experiments, organized like the rest of the book, with appropriate page references (Table 12-1). The second table (12-2) lists in one place all space-probe instruments flown so far; major characteristics and principal investigators are included. Frequent reference will be made later to this central repository of hardware data.

TABLE 12-1. LIST OF SPACE-PROBE INSTRUMENTS

*Instruments for Studying the Interplanetary Medium (Chap. 13)*

<i>Phenomenon</i>	<i>Instruments and Experiments*</i>	<i>Page</i>
Magnetic field (temporal and spatial variations of flux)	Search-coil magnetometer	298
	Fluxgate magnetometer	301
	Proton-precession magnetometer	305
	Rb-vapor magnetometer	306
	Helium magnetometer	309
Space radiation (corpuscular and gamma radiation)	Geiger-Mueller counter	316
	Proportional counter	317
	Ionization chamber	318
Basic detectors	Channel multiplier	319
	Scintillators	320
	Cerenkov detector	322
	Cadmium-sulfide cell	323
	Solid-state detector	325
	Telescopes (various types)	328
	Magnetic spectrometers	335
Detector combinations	Ionization chamber and Geiger-Mueller counter	337
	Spark chamber	345
Track imagers	Scintillation chamber	347
	Emulsions, cloud and bubble chambers	348
Interplanetary plasma (flux, species, and velocity distributions)	Curved-surface electrostatic analyzers	351
	Faraday-cup probes	356
	Spherical ion traps	361
	Radio-propagation experiments	378

\* It is important to distinguish between the experiments and the instruments used in the experiments. See text.

TABLE 12-1. LIST OF SPACE-PROBE INSTRUMENTS

<i>Instruments for Studying the Interplanetary Medium (Chap. 13)</i>		
<i>Phenomenon</i>	<i>Instruments and Experiments</i>	<i>Page</i>
Micrometeoroids (flux, size, velocity)	Piezoelectric microphone	365
	Piezoelectric ballistic pendulum	369
	Thin-film capacitor detector	370
	Light-flash detector	371
	Pressurized cells	372
	Wire grid detector	373
Structure of the universe	Light-transmission erosion detector	374
	Clock experiments	378
	Red-shift experiments	378
<i>Instruments for Research in Planetary Atmospheres (Chap. 14)</i>		
<i>Phenomenon</i>	<i>Instruments and Experiments</i>	<i>Page</i>
Atmospheric composition and density	Mass spectrometers (various types)	401
	Gas chromatograph	411
	Simple composition sensors (various types)	415
	Ram spectrometers	417
	Alpha and gamma densitometers	417
	Acoustic transmission line	418
Pressure and density	Drag body	423
	Bayard-Alpert gauges	424
	Redhead gauges	424
Meteorological parameters	Alphatron gauges	424
	Pressure gauges	424
	Thermistors	424
Atmospheric electromagnetic transmission, absorption, and emission properties	Resistance thermometers	424
	Anemometers	424
	Radiometers and photometers (various types)	386
Ionosphere characteristics and radio-propagation properties	Spectrometers and spectrophotometers (various types)	395
	Polarimeters	400
	Langmuir probes	420
	Bottomside sounders	420
	Topside sounders	421
	Bistatic radars	421
	Limb diffraction experiment	422
	Sferics detector	422

TABLE 12-1. LIST OF SPACE-PROBE INSTRUMENTS

<i>Instruments for Studying Planetary Surfaces and Subsurfaces (Chap. 15)</i>		
<i>Phenomenon</i>	<i>Instruments and Experiments</i>	<i>Page</i>
Surface composition and density	Infrared spectrometers and photometers	430
	Mass spectrometers	442
	Gas chromatographs	444
	Alpha scattering experiments	447
	X-ray fluorescence spectrometer	449
	Gamma-ray spectrometer	452
	X-ray diffractometers	454
	Neutron activation analysis experiment	456
	Surface densitometer	459
	Differential thermal analysis experiment	461
Petrographic microscopes	462	
Crustal electrical and mechanical properties, seismicity, and topology	Electrical-conductivity meter	467
	Magnetic-inductance meter	467
	Thermal-diffusivity meter	468
	Soil-mechanics experiments (various types)	468
	Seismometers	471
	Television and photography	435
	Bistatic radar	440
	Isotopic dating experiments	462
 <i>Experiment to Detect Life and/or Associated Chemistry (Chap. 16)</i>		
<i>Phenomenon</i>	<i>Instruments and Experiments</i>	<i>Page</i>
Life-associated chemistry	Infrared spectrometers	484
	Mass spectrometers	486
	Chromatographs	487
	Ultraviolet spectrophotometers	487
	Microspectrophotometers	487
	Stain experiments	490
	Optical rotary dispersion	491
Biological activity	Metabolism detectors (Gulliver)	493
	Turbidity and pH detectors (Wolf Trap)	489
	Multivators and minivators	497
Miscellaneous	Microscopes	492
	Television and photography	484
	Radio listening experiments	485

TABLE 12-2. PERFORMANCE CHARACTERISTICS OF SPACE-PROBE INSTRUMENTS

<i>Spacecraft</i>	<i>Instrument</i>	<i>Mass</i> ( <i>kg</i> )	<i>Average Power</i> ( <i>watts</i> )	<i>Range</i>	<i>Principal Investigator (s)</i>	<i>Page</i>
Pioneer 5	Search-coil magnetometer			$> 0.5 \gamma^*$	D. L. Judge	298
	Telescope (Geiger-Mueller)				J. R. Winekler	328
	Telescope (proportional counter)		0.5	$p > 75 \text{ Mev}$	J. A. Simpson	328
	Ionization chamber				R. Arnoldy	318
	Piezoelectric microphone	0.5	0.02	$> 10^{-4} \text{ dyne-sec}$	E. R. Manning, W. M. Alexander	365
Mariner 2	Fluxgate magnetometer	2.1	6.0	$\pm 64 \gamma, \pm 320 \gamma$	P. J. Coleman	301
	Ionization chamber and Geiger-Mueller tubes	1.3	0.4		H. R. Anderson	337
	Piezoelectric microphone	0.6	0.1	$> 7.4 \times 10^{-4} \text{ dyne-sec}$	W. M. Alexander	365
	Curved surface analyzer (plasma)	2.2	1.0	$240 < p < 8400 \text{ ev}$	M. Neugebeuer	361
	Microwave radiometer	9.9	8.9		A. H. Barrett	386
	Infrared radiometer	1.2	2.0		L. D. Kaplan	386
IMP	Fluxgate magnetometers (2)	1.5	1.2		N. F. Ness	301
	Rb-vapor magnetometer	1.4	3.5		N. F. Ness	306
	Ionization chamber and Geiger-Mueller counter	0.9	0.2		K. A. Anderson	337
	Telescope (solid state)	3.3	1.4	$0.6 < p < 200 \text{ Mev}$	J. A. Simpson	328
	Nuclear abundance detector	4.1	1.7	$10\text{-}100 \text{ Mev/nucleon}$	F. B. McDonald	343
	Curved surface analyzer (plasma)	0.9	0.3	$0.2 < p < 20 \text{ kev}$	J. W. Wolfe	351
Pioneer 6	Faraday cup probe	1.7	0.5	thermal <i>e</i> and <i>p</i>	R. Bourdeau	356
	Faraday cup probe	2.2	1.5	$10 < p < 1000 \text{ km/sec}$	H. Bridge	356
	Fluxgate magnetometer	2.6	0.7	$\pm 64 \gamma$	N. F. Ness	301
	Telescope (scintillation)	2.2	1.5	$5 < p < 90 \text{ Mev}, 130 < \alpha < 360$	K. G. McCracken	328
	Telescope (solid state)	1.8	0.7	$1\text{-}200 \text{ Mev/nucleon}$	J. A. Simpson	328

Curved surface analyzer (plasma)	1.4	1.1	$3 < e < 1000 \text{ ev}, 100 < p < 15000 \text{ ev}$	J. W. Wolfe	351
Faraday cup probe	2.0		$0.1 < p < 15 \text{ kev}$	H. Bridge	356
Radio propagation experiments	2.8	1.5		V. R. Eshleman	378
Helium magnetometer	2.5	7.0	$\pm 360 \gamma$	E. J. Smith	309
Mariner 4 Geiger-Mueller counters and solid state detector	1.0	0.36	0.1-50000 counts/sec	J. A. Van Allen	316
Telescope (solid state)	1.2	0.4		J. A. Simpson	328
Ionization chamber and Geiger-Mueller counter	1.2	0.5		H. Neher	337
Faraday cup probe	2.7	2.6	$30 < p < 10000 \text{ ev}$	H. Bridge	356
Piezoelectric microphone	1.0	0.2	$> 10^{-5} \text{ dyne-sec}$	W. M. Alexander	365
Limb diffraction experiment				V. R. Eshleman	422
Vidicon television system	5.3	8.9		R. Leighton	435

\*  $1 \gamma = 10^{-5} \text{ gauss}$ .

12-2. Integration of Experiment and Spacecraft

In this book, the scientific instruments that make up the scientific payload are treated collectively as a subsystem of the spacecraft. The interface diagram linking the instruments with the rest of the space probe system is shown in Fig. 12-1. Scientific sensors and their associated electronics packages connect with the nine other spacecraft subsystems (communication subsystem, the environmental-control subsystem, etc.) through the nine different types of interfaces introduced in Parts I and II:

Mechanical	Electrical	Information
Thermal	Radiative	Electromagnetic
Spatial	Magnetic	Biological

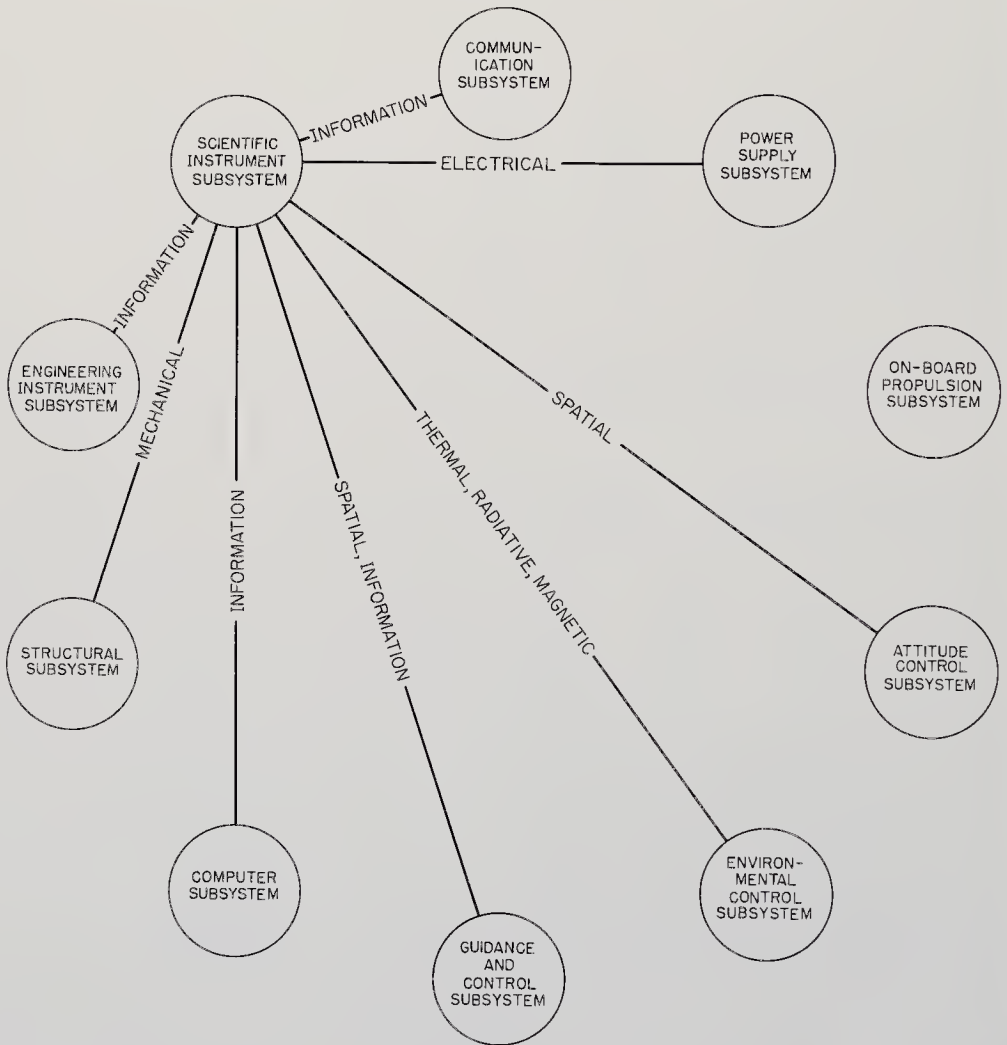


Fig. 12-1. Portion of the spacecraft interface diagram showing the relationship of the scientific instrumentation to the rest of the subsystems.

The definitions of the subsystems and the different interfaces tying them together should be reviewed, in Chap. 4. As before, the discussion will be molded by the formal space-probe-system model constructed from these subsystems and their interlocking interfaces.

Another part of the logical framework involves the three critical figures of merit: reliability, weight, and cost. Experiment design is dominated by these factors and the scientific value of the experiment.

From the experimenter's point of view, the impact of the interface-matching process and the mandates of the figures of merit first come into focus when experiments are being selected for a scientific payload. The next section is assigned to this complex and often controversial subject of experiment choice and priority. In the final competition for payload space—and it is no less than a contest—the desirability of an experiment is measured by its scientific merit, the availability of proven instruments, the figures of merit just mentioned, and the ease of spacecraft integration.

Distinctions must be made between three similar terms: sensor, instrument, and experiment:

1. The *sensor* is a detector of some physical phenomenon. A Geiger-Mueller tube senses the passage of a charge particle. A vidicon images a scene on the Martian surface. All sensors are transducers in that they convert stimuli into signals that can be utilized by the spacecraft. On the spacecraft, the ultimate signal is usually electrical in nature and digital in form.
  2. The *instrument* includes the sensor and all the auxiliary equipment and hardware necessary to obtain the desired data and match the interfaces with the rest of the spacecraft. Included are scanning platforms, structures, lenses, radiation shielding, and all of the electronics needed to feed the digital words into the communication subsystem at the proper rate and in the right format. Typical instruments are spectrometers and seismographs.
  3. The total *experiment*, however, involves many things in addition to the instrument, some not involving hardware directly. In space science, the experimenter cannot be a lone wolf. His every action affects other experimenters. The use of public funds places administrative and moral burdens on him that are over and above those arising from scientific ethics. Some of the points made below are just good design practice. Others have the extra dimensions implied above.
1. *Instrument calibration*. A few instruments are absolute in the sense that the information content of their signals depends only upon the phenomenon being measured, and not the physical design of the experiment;

viz., the absolute, rubidium-vapor magnetometer. Most instruments, though, must be calibrated with acceptable standards before flight and, if possible, during flight, since drift is likely during the long months in space. Associated with calibration is the specification of experimental accuracy. With the limited bandwidths available on deep-space probes, accuracy may be set by the word length assigned rather than by the characteristics of the experiment.

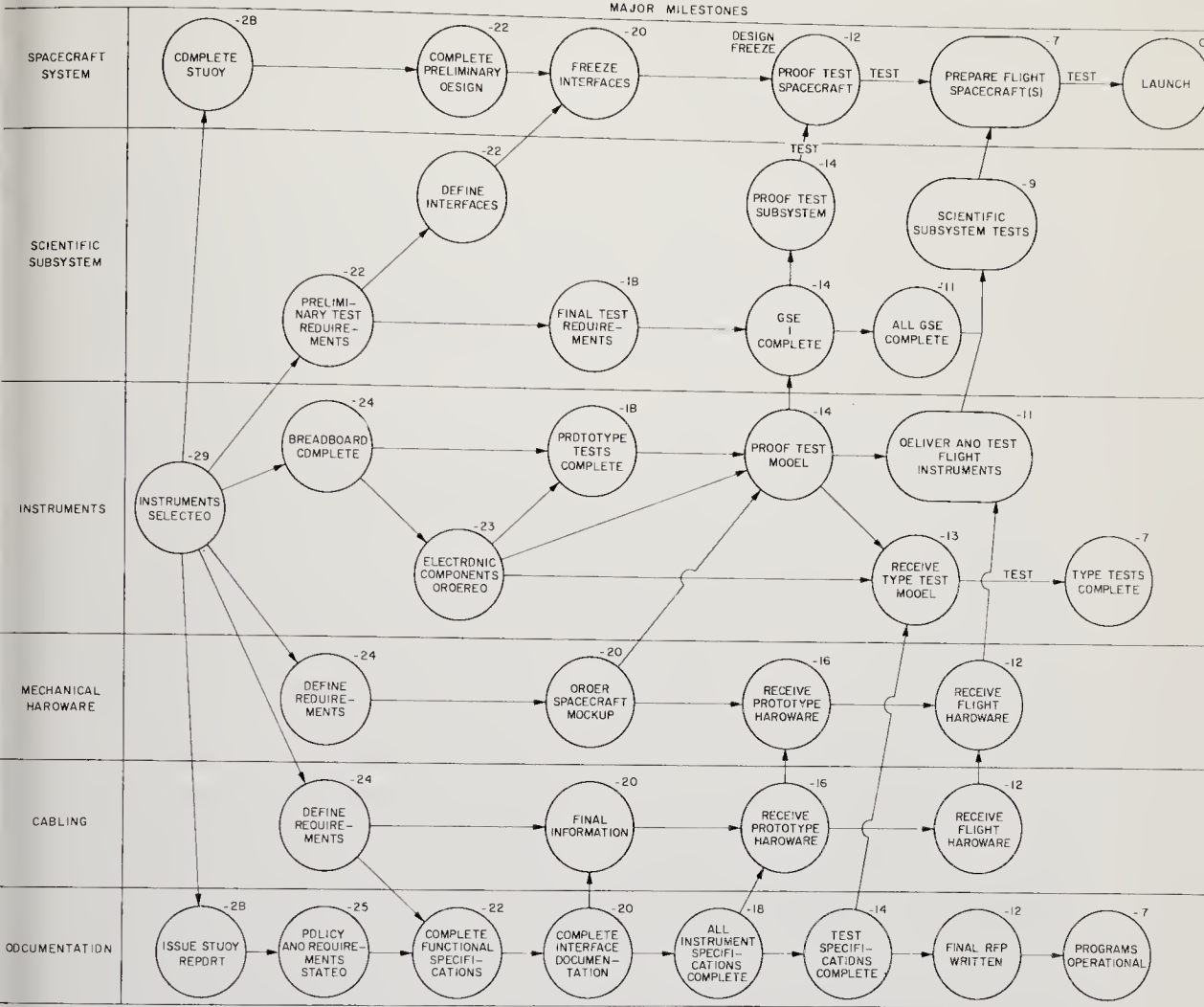
2. *Experiment programing.* Space-probe experiments, in contrast to those of most satellites, are often turned on and off and have their data-sampling rates changed as the probe moves through different scientific provinces. For example, the Mariner-2 radiometers scanned Venus during encounter only. Complete experiment design includes such scheduling and synchronization with the other experiments and spacecraft subsystems. Using the planetary-encounter example again, when a radiometer is turned on, something else must be turned off, because the communication-subsystem capacity is almost always saturated. Similar thinking leads to the establishment of an experiment-sampling rate that depends not so much upon the data-producing capabilities of the experiment as upon the value of its data relative to other measurements (including spacecraft-status information) which must be sent over the same communication channel. Finally, different kinds of instruments often work together in an experiment; viz., the combination of the ionization chamber and the Geiger-Mueller counter. Data from such tandem instruments have to be properly correlated.

3. *Dynamic range.* An experimenter desires a large dynamic range to insure bracketing the phenomenon he is measuring. The accurate range of his instrument provides one limitation, the allotted word length another. A magnetometer with a dynamic range of 0.1-1000 may be restricted to a word length of only eight bits. The over-all experiment's dynamic range is thus 256 instead of  $10^4$ . Non-linear encoding can partially compensate for such restrictions, however.

4. *Data reduction.* Great volumes of machine-printed and magnetically taped data are characteristic of most space experiments. Spacecraft data systems are automated, but, even at the low data rates from distant probes, the pile of data grows inexorably. A properly planned experiment must be prepared for the deluge of information and have facilities ready for the rapid reduction of data and the timely presentation of results to the scientific community.

5. *Experiment flexibility.* Flexibility is the capability of an experiment to recognize and measure a wide range of phenomena. For example, the radiation detectors of the first Explorers were unexpectedly saturated in the Van Allen belts. This fact was deduced from the telemetry, and new





FIGURES NEXT TO EVENTS INDICATE THE NUMBER OF MONTHS BEFORE LAUNCH.

Fig. 12-2. Typical scientific-instrument subsystem design and integration schedule. Numbers shown are months before launch date. (Ref. 12-8)

instruments with modified ranges were quickly flown to encompass the new phenomenon. Space probes, unfortunately, cannot be launched with such dispatch. In addition, the chances of encountering unexpected phenomena would seem greater near the relatively unexplored planets than at 200 km above the Earth's surface. A wide dynamic range can provide a measure of insurance, but the real flexibility must come through the ingenuity of the experimenter and his design.

6. *Management.* An experiment is only one cog in a complex system stretching from the sensors back to the data-readout equipment on Earth. To provide for complete success in the total scientific, political, and financial environment, experiments must be designed in adherence to:

- a. Functional specifications
- b. Design specifications
- c. Interface specifications
- d. Spacecraft schedules (see Fig. 12-2)
- e. Cost allocations

These factors are not so critical in terrestrial experimentation. Management controls on space research have to be considerably tighter because of the source of funds used, the intractability of launch windows, and the fact that every space probe is a group experiment involving thousands of people.

### 12-3. Experiment Selection

Space-probe payloads can accommodate only a small fraction of the experiments proposed for any particular flight. The choice of the few that are finally propelled into space is beset with technical, logical, and emotional problems. If it is hard to agree upon a single, overall figure of merit for a spacecraft system, it is even more perilous to rank scientific experiments in order of desirability. Regardless, decisions must be made and, lacking numerical parameters of excellence, judgment, with all of its arbitrary features, must be applied to the task.

Two philosophies exist regarding payload assignment:

1. Philosophy #1 requires open competition for payload space. This, in theory, is the procedure that is always used. In actual practice, the competition for satellite payload space is more open than it is for the less frequent, payload-limited space probes.

2. Philosophy #2 maintains that there should be "block allocation" of payload space, with space reserved on all or most spacecraft for experimenters or groups with demonstrated records of performance. Or perhaps NASA might assign an entire spacecraft to an institution, reserving for itself only the authority to approve instrument types. Such philosophy would supposedly permit a more orderly, long-term approach to experimental problems. The perpetual proposals and experiment justifications would be virtually eliminated except for newcomers.

The free-enterprise philosophy (#1) permits someone with a good idea for an experiment an equal opportunity in competing with the old hands in space research. Just as in real-world economics, free enterprise in space research is illusory to some extent, because experience and past performance are weighted heavily in the existing selection process. Thus Philosophy #1 tends toward Philosophy #2 in practice. It is difficult, but by no means impossible, for a new experimenter to break into the accepted circle. The heavy weighting given to successful past performance is defensible in part, because mission failures are heavily penalized (techni-

cally and politically) in the infant space-probe program. Who would gamble extremely valuable payload space on an unproven experiment and experimenter? Not many. Only when more payload space becomes available can free enterprise prevail.

With these qualifications in mind, the experiment selection process begins with a list of factors (really figures of merit) to be used in the evaluation. In principle, weights could be assigned to each of the qualities listed below, but no formal scheme exists. Subconsciously, if not consciously, each individual evaluating experiment proposals attaches his own weighting factors. Roughly, then, in order of priority the selection factors are:

1. *Scientific value.* Experiments are rated on the basis of their scientific objectives and appropriateness to the proposed mission. One would expect that each experimenter would favor his own discipline. But there seems to be a general consensus that experiments calculated to search for the existence of extraterrestrial life should be given top priority. After that decision, there is less agreement. Bypassing the lunar program, many would concur that the investigation of the atmospheres of Mars and Venus should be next, closely followed by Martian surface studies. No hard and fast lines are drawn, in any case.

2. *Experiment design.* In general, the factors considered here are technical feasibility, reliability, weight, cost, instrument availability, and interface matching. A vital question is whether the experiment, as designed, will answer the scientific questions that have been posed.

3. *Experimenter qualifications.* What is the proposed experimenter's stature in the scientific community? What has been his experience in terrestrial and space research?

4. *The experimenter's institution.* Here, the organization employing the experimenter is scrutinized. What is its attitude toward research? Does it support its researchers financially and administratively? The record shows that almost all experimenters so far given payload space belong to universities, government research centers, and, on the borderline of industry, the Space Technology Laboratory. To date, industry has been conspicuous by its absence.

The establishment of such a scale of values, though unweighted and admittedly crude, permits the construction of a formal selection process. The steps in the selection sequence are:

1. A decision to fly a particular mission is made and an official NASA program is brought into being.

2. The scientific community is solicited for experiment proposals, some two to four years before the actual flight, by NASA's Office of Space Science and Applications. Announcements are mailed widely and, on oc-

casation, published in the appropriate journals. Spacecraft data, interfaces, and schedules are provided in the solicitation.

3. Proposals are received by NASA. The NASA Space Sciences Steering Committee and its subcommittees review and evaluate each. Both the written proposal and personal presentations made by the experimenter are considered. As many as 50 proposals of widely varying quality may be under study at this time. The experiments are sorted into four categories based on the previously listed judgment factors:

- a. Excellent science. Reasonable schedule.
- b. Good science. Reasonable schedule.
- c. Excellent, but needs considerable development before flight.
- d. Experiment not appropriate to spacecraft mission.

4. Detailed study and evaluation by the subcommittees in conjunction with the experimenters themselves soon produce recommendations that reduce the number of proposals to roughly twice the number that can actually be accommodated on the spacecraft. The authority and responsibility for making decisions rests solely with the Associate Administrator for Space Science and Applications. The time now is roughly three years before flight. Each of the remaining experiments, perhaps ten to twenty of them in the case of deep-space probes, is funded by NASA for further study and development, often up to the breadboard stage.

5. After about a year of development, some of the originally selected experiments will have been dropped for technical reasons. The remainder is now reconsidered by the Space Sciences Steering Committee, its subcommittees, and the experimenters. It is now about two years before flight, and the spacecraft and the surviving experiments are better defined and understood. The final payload of experiments is chosen at this time. Usually, the experiments are ranked in order of priority, so that further elimination can be made if unexpected spacecraft design problems arise and lighten the scientific payload.

The selection process is over. It has been carried out with the aid of the broad spectrum of disciplines represented by members of the Space Sciences Steering Committee and its subcommittees as well as by the experimenters themselves.

The Space Sciences Steering Committee is appointed by the Associate Administrator for Space Science and Applications. It serves as NASA's focal point for space-science activities. The Committee advises the Associate Administrator on experiments and experimenters, supporting research, and long-range space planning. The subcommittees of the Space Science Steering Committee are also appointed by the Associate Administrator for Space Science and Applications. They include scientists

from NASA, other government agencies, universities, and not-for-profit organizations. The subcommittees are discipline oriented:

Astronomy	Particles and fields
Solar physics	Planetology
Planetary atmospheres	Bioscience
Ionospheres and radio physics	

Subcommittee assignments include proposal review and the evaluation and the formulation of recommendations concerning experiments and experimenters, scientific goals in space, supporting research, and general space science planning.

The award of a grant or contract to provide an experiment does not guarantee flight on a specific spacecraft. Sometimes technical problems arise that may eliminate an experiment or defer it until later flights of the same spacecraft. Flight qualification, with its rigorous shock, vibration, thermal, reliability, and other spacecraft integration tests, will further reduce the number of experiments under consideration. Finally, as described earlier with the selection process, some perfectly sound and desirable experiments have to be dropped because of limited payload space. Of course, the knowledge and experience gained even from a dropped experiment is not lost to either the experimenter or space science in general.

In summary, there are necessarily several subjective aspects to experiment selection. A well-defined procedure for submitting experiment proposal exists, and the very best scientific experience is utilized in judging such proposals. Excellence is always recognized, even though lack of experience may penalize an experimenter's proposal to some extent. Space research is not quite an open field. It takes relevant experience or an idea of exceptional promise to fly an experiment on a space probe.

# Chapter 13

## INSTRUMENTS FOR MEASURING THE INTERPLANETARY MEDIUM

### 13-1. Prologue

The average quantity of matter in the vast volume of space between the planets is about 1000 atoms/cm<sup>3</sup>. Flooding through this diffuse medium are fluxes of all descriptions. The magnetic fields of the Sun, the planets, and the galaxy itself are constantly stirring and being stirred in the thin soup of gas, plasma, dust, and particulate radiation.

Four broad classes of phenomena may be distinguished. These are listed in Table 13-1 in their order of development in this chapter. Approximately 40 types of instruments have been developed to map the complex, time-varying fields and fluxes in deep space (see Table 12-1). These

TABLE 13-1. PHYSICAL PHENOMENA IN INTERPLANETARY SPACE\*

<i>Phenomenon</i>	<i>Parameters measured</i>	<i>Measurable effects</i>
Magnetic field	Field strength, direction, fluctuations	Magnetic induction, Zeeman effect, asymmetry of gated ferromagnets
Space radiation	Scalar flux, direction, energy, species	Ionization, fluorescence, creation of lattice defects and electron-hole pairs
Plasma	Scalar flux, direction, energy, species	Conductivity, current flow
Micrometeoroids	Scalar flux, direction, velocity, composition, particle size	Momentum transfer, ionization, physical damage

\* See Chap. 3 for additional discussion.

instruments, based on the diverse measurable effects set down in Table 13-1, must themselves be diverse in character. Generalization is difficult at this point. A short introduction to each instrument class will perform this task later.

The fields, particles, and micrometeoroids were the first features of outer space to be explored in detail, first with balloons, then with sounding rockets, satellites, and space probes. This initial concentration of attention is understandable, since the planets are difficult to reach, while the fluxes and fields of interplanetary space are nearby and produce measurable effects even on the Earth's surface. The consequence is that longer and greater familiarity has bred sophisticated lines of space instrumentation, at least when compared with the apparatus available for planetary research. Most instruments for studying planetary surfaces and detecting life have had to be developed from near zero.

The interplanetary environmental instruments, however, have not been perfected by any means. In each of the four phenomenological territories listed in Table 13-1, major instrument developments are still underway. In magnetic-field studies, new instruments are needed to measure accurately field fluctuations in the turbulence of solar flares. Micrometeoroid velocities cannot now be measured directly. The different nuclear species present in space radiation and plasma must be sorted and better identified. There are frontiers for instrument design everywhere.

### 13-2. Magnetic Field Measurements

Space probes frequently carry magnetometers to measure four important magnetic phenomena in space:

1. The distant geomagnetic field
2. The magnetic fields of the other planets
3. The interplanetary magnetic field
4. The fluctuations of the fields listed above caused by interactions with the solar wind and other magnetohydrodynamic activity.

In comparing the fields measured by space-probe magnetometers with those customarily recorded by Earth-based and satellite instruments, one distinction stands out: Probe magnetometers must measure fields of 1-100  $\gamma$  compared to the nearly 50,000  $\gamma$  (0.5 gauss) at the Earth's surface. The magnetic fields in deep space are extremely weak. Fields below 100  $\gamma$  can be easily overwhelmed by the magnetic field of the spacecraft itself if great care is not exercised. Or the magnetometer calibration may drift a few  $\gamma$ 's and grossly incorrect data will be telemetered. Obviously, the magnetometers used for magnetic studies and geophysical

prospecting on the Earth will require considerable modification for use in space.

What sensitive, dependable, physical phenomena are both easily measurable and simply related to the ambient magnetic field? Magnetic induction and the Zeeman effect immediately come to mind. These and some less obvious phenomena are listed in Table 13-2, along with the five kinds of space magnetometers to be discussed in this section.

The magnetometers in Table 13-2 may be further classified by their ability to distinguish the direction of the ambient field. Only the fluxgate magnetometer is a *vector* instrument. The search coil response is direction-sensitive. The others, the so-called *scalar* magnetometers, depend on physical processes that yield no information about the ambient field's direction. The limitations of scalar magnetometers are sometimes offset by the absolute character of the scalar measurements. That is, the output of scalar magnetometers is often related to the ambient magnetic field only by well-known physical constants so that calibration against a standard field is not needed. The complementary properties of the vector and scalar magnetometers (Table 13-2) may be put to advantage by using the two types together. Explorer 10 and the IMP probes, for example, used an absolute rubidium-vapor instrument alongside two fluxgates, which provided the vector information.

Weight and power consumption are problems for magnetometers as they are for most space instruments. The search coil manages to generate its own signal power—it is in fact a dynamo—but the rubidium-vapor and helium magnetometers demand considerable power for the relatively inefficient process of “optical pumping.” The power and weight characteristics of some flight-qualified magnetometers are listed in Table 12-2, page 286.

From the viewpoint of the magnetometer designer, the most sensitive spacecraft interface is undeniably magnetic in character. “Magnetic cleanliness” has long been a major spacecraft design objective. The intrinsic fields on complex spacecraft like Mariner 2 may be tens of gammas, enough to make the use of absolute magnetometers questionable. To avoid submerging the ambient field in that of the spacecraft, non-magnetic materials must be used in spacecraft construction and current-generated fields should be canceled by opposing currents. Careful design can push the spacecraft fields down below  $1 \gamma$ , as it did on IMP. Extendable booms must still be employed, however, to isolate the magnetometer from the spacecraft. The length of the boom will depend upon the success of the spacecraft magnetic cleanliness program.

*The Search-Coil Magnetometer.* The simplest (and most limited) space magnetometer is the search coil (or spin coil). Used on early probes like



TABLE 13-2. TYPES OF MAGNETOMETERS USED IN DEEP-SPACE RESEARCH

<i>Magnetometer Type</i>	<i>Principle of Operation</i>	<i>Utility and Missions</i>	<i>Remarks</i>
Search coil	Coil spinning with spacecraft cuts lines of force. Generates emf proportional to $dH/dt$ .	Direction-sensitive, not absolute. Pioneer 5.	Obsolete in probe work
Fluxgate	Ambient field gated in a saturable core. Even harmonics in secondary winding proportional to H.	Vector, not absolute. Mariner 2, Pioneer 6, IMP.	
Proton precession	Polarizing field excites protons. When field is removed, protons emit signal with a frequency proportional to field.	Scalar, absolute. Vanguard 3.	Inadequate for deep-space work
Rubidium vapor	Optically pumped Rb atoms are deexcited by electromagnetic field, whose frequency is proportional to magnetic field.	Scalar, absolute. IMP.	Often used with fluxgates
Helium	Same as Rb-vapor.	Scalar, absolute. Mariner 4.	Development lags Rb-vapor instrument

Pioneers 1, 2, and 5, and such satellites as Explorer 6, EGO, and POGO, it is simply a coil of wire that generates an electromotive force as it spins and cuts the lines of the ambient field (Fig. 13-1). The emf generated can be calculated from Faraday's Law. It is proportional to

$$\frac{dH}{dt} \sin \theta$$

where  $H$  = the ambient magnetic field strength  
 $\theta$  = the angle between the coil spin axis and  $H$ .

When the search coil is fixed on a spacecraft and spins with it (Pioneer 5), only the component of the magnetic field perpendicular to the spin axis will be measured. If the probe's spin axis is known, say from a solar-aspect sensor, such measurements are useful. The search coil can also be spun relative to the spacecraft by a motor. The spacecraft-fixed coil, however, measures the true ambient field only and is unaffected by the spacecraft intrinsic field, which, of course, spins with it.

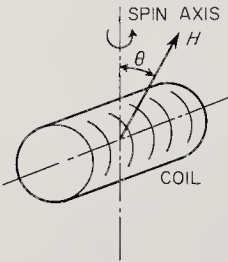


Fig. 13-1. Sketch of a search-coil magnetometer. The coil is usually fixed to the spacecraft and spins with it.

The search coil is unaffected by the spacecraft intrinsic field, which, of course, spins with it.

The output of the search coil is proportional to  $dH/dt$  rather than  $H$ . Integration of the usually sinusoidal signal is electronically easy, resulting only in a  $90^\circ$  change of phase. Magnetic-field transients, however, will be distorted. Another electronic problem arises because the signal is at a very low frequency---just the spin frequency of the spacecraft, a few cycles per second. Since the search coil is not an absolute instrument, it has to be calibrated in a known field before flight.

Despite its simplicity, the search coil has been largely supplanted by the fluxgate and optically pumped magnetometers in recent probes. Pio-

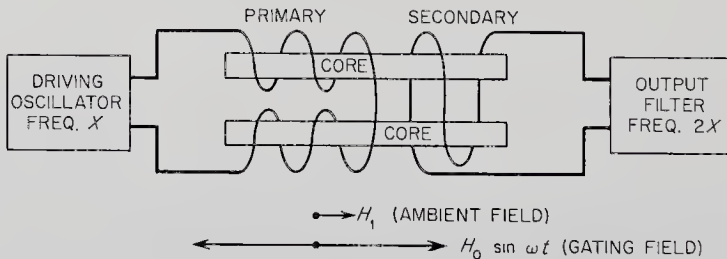


Fig. 13-2. Schematic of the fluxgate magnetometer. Single toroidal cores can also be used.

neer 5 was the only deep-space probe to employ a search coil. This instrument consisted simply of a small coil with 30,000 turns of No. 40 wire. It was fixed to the spacecraft. The weight and power consumption of the coil and associated electronics are shown in Table 12-2.

*The Fluxgate Magnetometer.* The adjective "fluxgate" is derived from a key physical feature of this magnetometer: the "gating" of the ambient field being measured. Consider the two long ferromagnetic cylinders shown in Fig. 13-2. Two external fields are applied to each:  $H_1$ , the field being measured; and  $H_0 \sin \omega t$ , an A.C. gating field impressed by the primary winding around the cylinders. Inside the cylinders, the

total impressed field is  $H = H_0 \sin \omega t + H_1$ . The magnetic induction, found from  $B = \mu \mu_0 H$ , is modified by the saturability of the ferromagnetic core. During the peaks of the gating field, the cylinder cores are saturated at  $\pm B_0$ , and the ambient field is gated. In between the peaks, the induction is  $B = \mu \mu_0 (H \pm H_1)$  (Fig. 13-3). The presence of the ambient field,  $H_1$ , thus introduces an asymmetry into the induction cycle. It is this asymmetry that provides the measure of the ambient field, and the asymmetry appears only in the presence of the gating field.

If the total induction is expanded in a Fourier series,

$$B = a_0 + \Sigma a_n \cos n\omega t + \Sigma b_n \sin n\omega t$$

it can be shown that the source of the asymmetry, the ambient field, is also the source of the even harmonics in the expansion. The logic of the coil arrangement shown in Fig. 13-2 is now apparent. The oppositely wound primaries impress a gating signal at a frequency  $X$  (usually about 10 kc). The output secondary coil is wound around both cores and feeds a filter, which passes only the second harmonic, frequency  $2X$ . The fundamental,  $X$ , and all its odd harmonics are canceled out by the stratagem of winding the primaries in opposite directions.

The magnetometer circuit shown in Fig. 13-2 is of the open-loop type; that is, there is no feedback of the output signal. Its output is an analog signal whose amplitude is proportional to the ambient field. A null-type instrument is more frequently used in which a bucking coil supplies a field in digital steps. This field is adjusted until the ambient field is nulled and all even harmonics disappear. The block diagram of the Mariner-2 instrument is shown in Fig. 13-4.

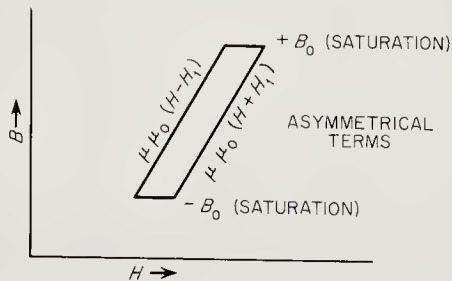


Fig. 13-3. Hysteresis loop for the fluxgate magnetometer.

A fluxgate is sensitive to a tenth of a gamma and can span the range up to thousands of gammas. It is direction-sensitive, and is sometimes teamed with absolute magnetometers because of this property alone.

The fluxgate magnetometer has been used on many spacecraft. Three space probes, Mariner 2, IMP, and Pioneer 6, have carried fluxgates. Some typical fluxgates are described briefly below.

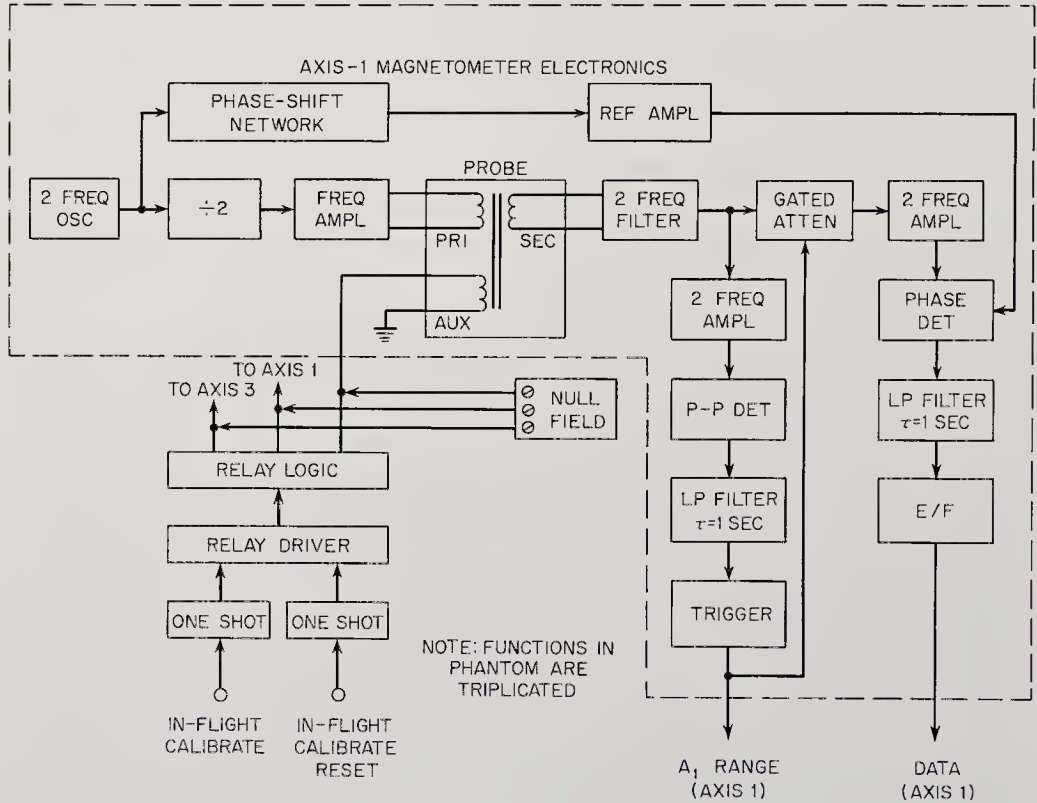


Fig. 13-4. Block diagram for the Mariner-2 fluxgate magnetometer experiment. (Ref. 13-59)

Mariner 2 carried the triaxial fluxgate magnetometer shown in Figs. 13-5 and 13-6. Three orthogonal sensors were positioned to record the three components of the magnetic field. The instrument had two scale ranges:  $\pm 64 \gamma$  and  $\pm 320 \gamma$ . On the low range, the resolution was approximately  $0.6 \gamma$ . Electronic noise in the electronics was equivalent to a fluctuating field of about  $0.25 \gamma$ . Each of the three sensors possessed an added bias coil, carrying enough current to cancel out spacecraft-produced fields measured prior to launch. During operation, the magnetometer sensitivity was checked periodically by the application of a known current to the bias coils (Ref. 13-59). Weight and power consumption for the Mariner-2 magnetometer are given in Table 12-2.

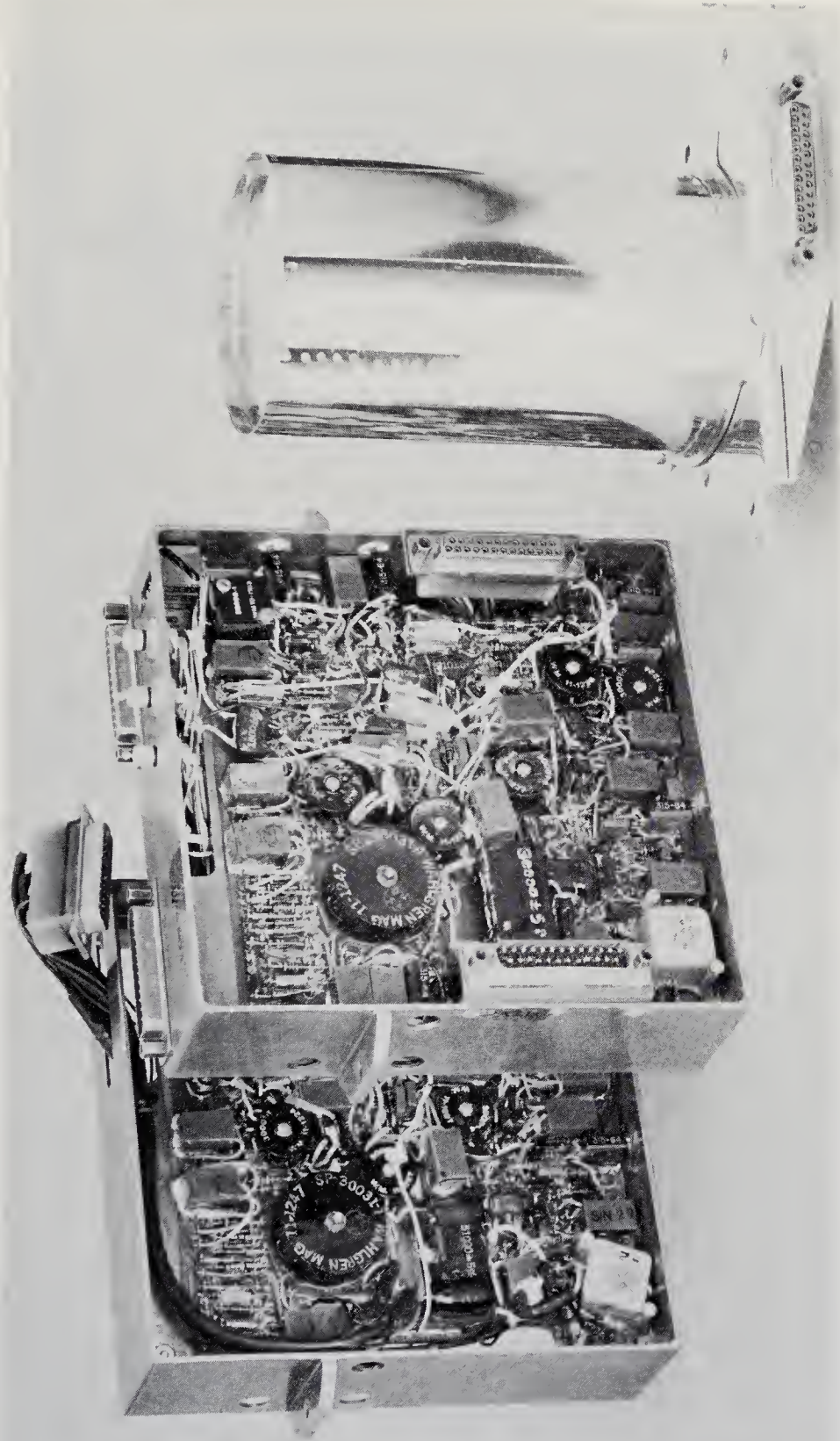


Fig. 13-5. Mariner-2 magnetometer assembly and some of the associated electronic circuits. (Courtesy of the Jet Propulsion Laboratory)

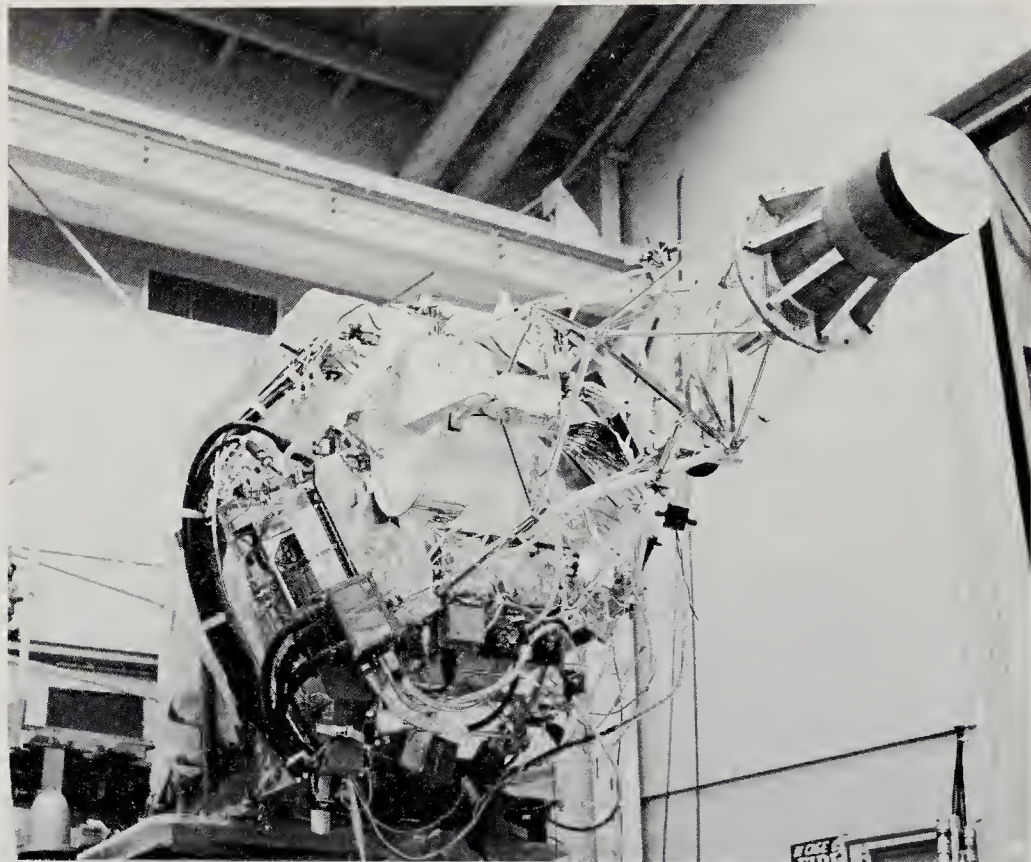


Fig. 13-6. The Mariner-2 magnetometer is shown isolated from spacecraft base at the right-hand end of the superstructure. Mariner 2 is shown on test here, minus its solar panels. (NASA photograph)

Pioneer 6 carried a single-axis fluxgate magnetometer (Fig. 13-7). The 10-ke gating field produced a 20-ke output signal proportional to the ambient magnetic field. A key feature of this instrument is the periodic physical reversal of the sensor, which gives the experimenter data on the magnitude of the errors introduced by any permanent magnetic moment of the core and any electronic drift. Upon command from the Earth, small pyrotechnic squibs are fired, which in turn release escapement mechanisms driven by springs. The lightweight sensor is thus alternately reversed  $180^\circ$ , but only for a finite number of times, eleven in this case. On Pioneer 6, the sensor reversal unit has a mass of only 0.2 kg. Even with this mechanical refinement, the perturbations caused by spacecraft field are not accounted for. In order to reduce the spacecraft field to below  $1 \gamma$ , the magnetometer must be mounted on a boom 1 to 3 meters long. The operating range of the magnetometer is  $\pm 64 \gamma$ , with the minimum recorded field set at  $\pm 0.25 \gamma$  by the digitization of 8 bits per

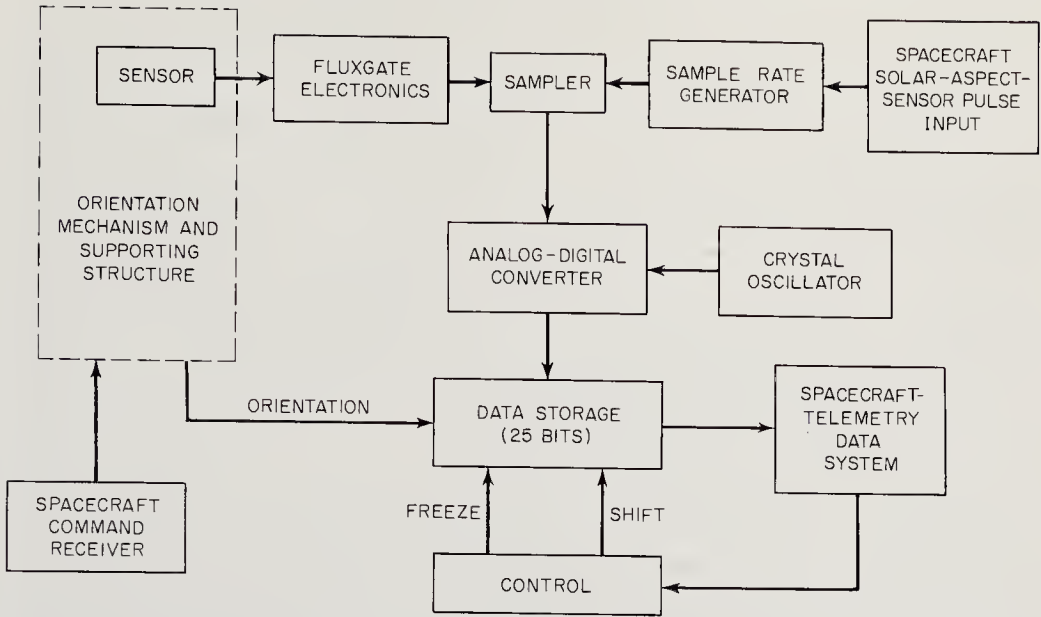
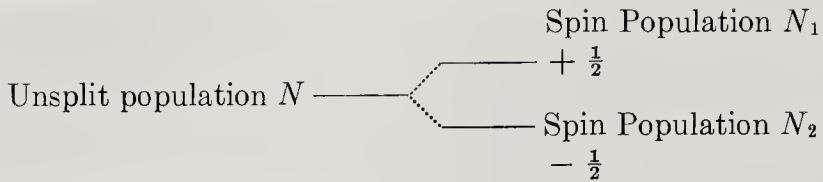


Fig. 13-7. Block diagram of the Pioneer-6 fluxgate magnetometer experiment. (After N. F. Ness)

measurement. The sensor itself is inclined at an angle of  $54^{\circ} 45'$  to the spacecraft spin axis. Spinning in this way, the magnetometer takes measurements every one-third of a revolution. With the addition of solar-aspect data, the single-axis fluxgate can measure all components of the field. With the refinements of sensor reversal, an extendable boom, and an inclined mounting, a simple fluxgate magnetometer can thus measure the total field, and compensate for spacecraft fields, instrument drift, and core magnetic set.

*The Proton Precession Magnetometer.* The proton magnetometer is in common terrestrial use. It is, however, relatively useless for measuring the very weak magnetic fields in deep space. In fact, Vanguard 3 and some early Russian spacecraft have been the only spacecraft to carry proton precession magnetometers. The proton-precession magnetometer was the first of the absolute, scalar magnetometers which depend for their operation upon atomic or nuclear energy states that have been split by the ambient field. It thus has historical as well as instructive value.

Consider a small bottle filled with water or a hydrogen-rich liquid hydrocarbon, such as hexane. If an artificial magnetic field—always much stronger than the ambient field—is applied to the bottle, some of the protons ( $N_1$  of them) in the liquid will be polarized so that their spin axes are aligned with the impressed field. Others ( $N_2$ ) will be aligned in opposition to the field. The creation of two new energy states is analogous to the Zeeman splitting of atomic energy states.



The split populations are related by

$$N_1/N_2 \sim \exp(-\mu H/kT)$$

where  $H$  = the polarizing magnetic field strength

$k$  = Boltzmann's constant ( $1.38 \times 10^{-23}$  joules/°K)

$T$  = the ambient temperature

$\mu$  = the nuclear magnetic moment.

When the impressed field is removed, leaving only the much weaker ambient field, the Zeeman splitting decreases accordingly, and the population ratio changes in response. As protons shift from population  $N_2$  to  $N_1$ , they radiate electromagnetic energy at a frequency proportional in the first order to the ambient magnetic field. The frequency of the radiation is a function only of the magnetic field and physical constants. No calibration is usually needed for this absolute instrument.

The name of this magnetometer comes from the classical mechanistic portrait of protons in a magnetic field, which are pictured as precessing like tops around the ambient magnetic field vector, with a precession frequency proportional to the ambient field. The quantum-mechanical interpretation, given earlier, is preferred and is also more convenient in describing the more complex rubidium-vapor and helium magnetometers.

In actual space operation, a large, power-consuming current must be applied every few seconds to generate the magnetometer's strong polarizing field. After the current is switched off, the electromagnetic energy from the switching proton populations can be picked up as a very weak, exponentially decaying signal. The signal frequency is 4.26 kc/gauss, corresponding to only 0.0426 cycles/gamma. In an ambient field of 10  $\gamma$ , the frequency is still so low that it is difficult to amplify electronically. For this reason, the working range of the proton-precession magnetometer is approximately  $10^4$ - $10^5$   $\gamma$ , not very useful for deep-space research.

*The Rubidium-Vapor Magnetometer.* Like the proton-precession magnetometer, this instrument is an absolute, scalar device whose operation depends upon magnetically split, atomic energy states (Zeeman effect). Instead of using a strong artificial magnetic field to shift populations of excited atoms, the rubidium-vapor magnetometer employs circularly polarized, monochromatic light to "pump" rubidium vapor atoms into long-lived, i.e., "metastable," energy states. These energized rubidium atoms can subsequently be stimulated to leave the metastable state by applying



an artificial electromagnetic field with a frequency equal to the Larmor frequency—which, in the classical view, is the atom's precessional frequency around the ambient magnetic-field vector. As we shall see, the Larmor frequency and the energy gaps between the magnetically split energy levels are both proportional to the ambient magnetic field strength. The scheme is complicated. In essence, a population of excited atoms is artificially created by optical pumping. The population is then destroyed by a signal whose frequency is proportional to the ambient field.

The optical-pumping process so basic to lasers, masers, and rubidium and helium magnetometers has an abstract description. Imagine the experiment pictured in Fig. 13-8. The light from a rubidium lamp is colli-

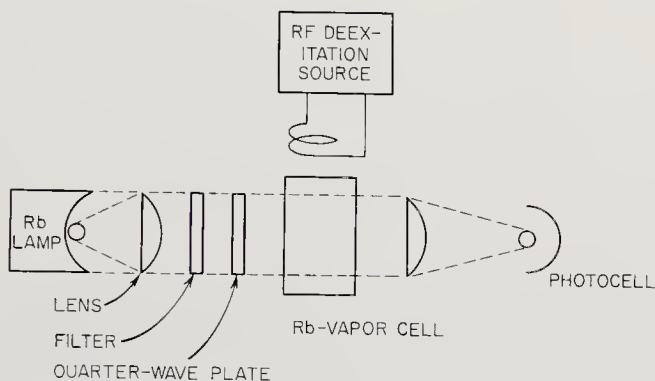


Fig. 13-8. Schematic of a rubidium-vapor magnetometer with no signal feedback.

imated, passed through a filter to remove all wavelengths except the  $D_1$  line at 7947.6Å, and then circularly polarized by a quarter-wave plate. When these monoenergetic photons bombard a rubidium-vapor cell, they have just the right amount of energy to raise some of the atoms from the  $^2S_{1/2}$  state to the  $^2P_{1/2}$  state, as shown in the energy level diagram, Fig. 13-9. If these states are split by an applied magnetic field, quantum-mechanical laws dictate that the magnetic quantum number,  $m$ , can increase only by 1. Energized atoms in the  $^2P_{1/2}$  state, no matter what the value of  $m$ , return to the  $^2S_{1/2}$  state by emitting a photon within about  $10^{-8}$  sec. Clearly, there is no metastable state at the  $^2P_{1/2}$  level. The deenergized atoms, however, return in equal proportions to all eight of the split levels in the  $^2S_{1/2}$  state. The level with  $m = +2$  receives its fair share, but once an atom enters this level it cannot be stimulated to leave again by absorbing one of the incident photons from the rubidium lamp. Why? Because the change in  $m$  must be  $+1$ , and there are no levels in the  $^2P_{1/2}$  state where  $m = +3$ . The  $^2S_{1/2}$ ,  $m = +2$  state is thus a dead end.

Eventually many of the rubidium atoms are pumped into this metastable state. The experimenter can tell when this occurs because the rubidium-vapor cell becomes transparent to the light from the rubidium lamp. There are no longer any atoms that can absorb the light, so the photons pass right through. The secret of pumping, then, is the discovery of a dead-end or near-dead-end state that can be used to shift the normal populations of atoms in a sample.

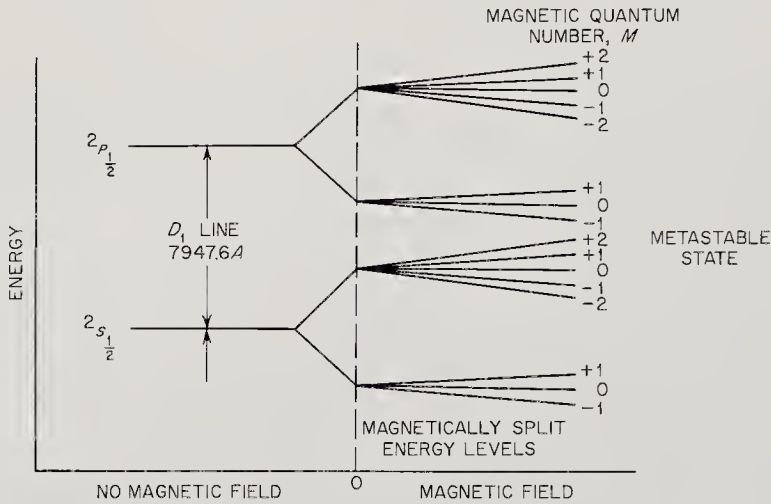


Fig. 13-9. Energy-level diagram for rubidium-87.

Measuring the magnetic field seems rather remotely connected with this complicated procedure. The keys to measuring the ambient field are, first, the observation that the separation of the magnetically split lines is proportional to the ambient field, and second, the application of an electromagnetic wave with just the right frequency perpendicular to the ambient field. The wave with the right frequency is represented in quantum mechanics by a photon whose energy is equal to one of the gaps between the metastable state and the other energy levels. The electromagnetic wave has the effect of ejecting the rubidium atoms from the metastable state. When this occurs, the rubidium vapor cell can again absorb radiation. A photocell on the opposite side of the vapor cell signals the sharp resonance when electromagnetic waves have just the right frequency to depopulate the metastable state. Since the resonant frequency can be measured with precision, the ambient field can be found from the Larmor frequency equation, which specifies about 7 cycles/gamma for a  $\text{Rb}^{87}$  magnetometer.

In practice, rubidium-vapor magnetometers are made to oscillate at the Larmor frequency; that is, the transparency of the vapor cell varies at the Larmor frequency, and this signal is detected and fed back. In

this type of arrangement, the ambient field must be inclined to the axis of the pumping light (Ref. 13-51).

Rubidium-vapor magnetometers using  $\text{Rb}^{85}$  and  $\text{Rb}^{87}$  have been built. Explorer 10, IMP, EGO, and other satellites have used  $\text{Rb}^{87}$  instruments with good success. Usually fluxgates are flown alongside scalar instruments to provide directional data. Offsetting this requirement for directional data is the absolute character of the rubidium-vapor magnetometer. This eliminates the calibration step. Rubidium lamps draw a relatively large amount of electrical power which can be a disadvantage on space probes. The accurate range of the rubidium vapor magnetometer is excellent, roughly  $0.05\text{-}10,000\gamma$ . It is an important research tool in mapping magnetic fields in deep space.

*The Helium Magnetometer.* The great variety of lasers and masers testifies that atoms other than rubidium can be pumped and therefore serve in magnetometers. The metastable,  $^3\text{S}_1$  state of helium has been selected for space magnetometer work. The pumping process, the deexcitation of the metastable state, and the measurement of the ambient magnetic field through the frequency of the deexcitation field are all almost identical to those of the rubidium-vapor magnetometer. Some differences are worth noting, though.

First, the energy-level diagram is quite different (Fig. 13-10). Helium exists in two distinct states, termed *orthohelium* and *parahelium*. The optical pumping described here occurs in orthohelium, which is created by exciting parahelium with a radio-frequency field. Since transitions back to parahelium are statistically unlikely, the orthohelium energy-level diagram of Fig. 13-10 is essentially independent of the parahelium, which may be thought of as a buffer gas. The term "metastable" is ap-

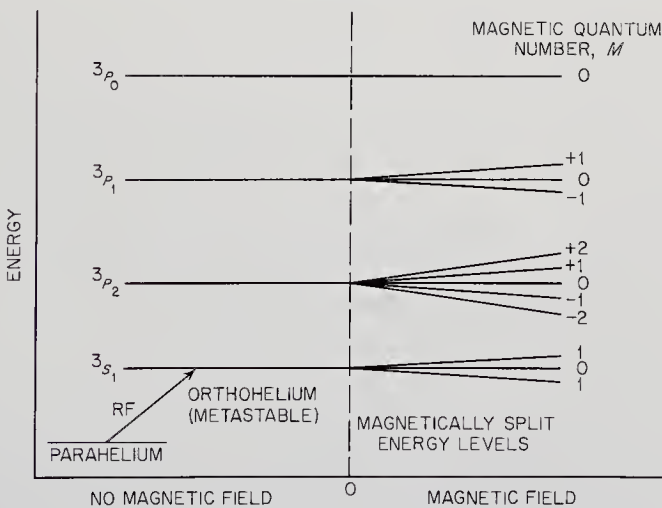


Fig. 13-10. Energy-level diagram for helium.

plied to the entire  ${}^3S_1$  orthohelium population, because all orthohelium energy levels are metastable (long-lived) with respect to parahelium.

Orthohelium is pumped by a helium-discharge lamp where transitions from the  $P_0$ ,  $P_1$ , and  $P_2$  levels to  $S_1$  provide three closely spaced spectral lines. Referring to magnetometer schematic, Fig. 13-11, the interposition

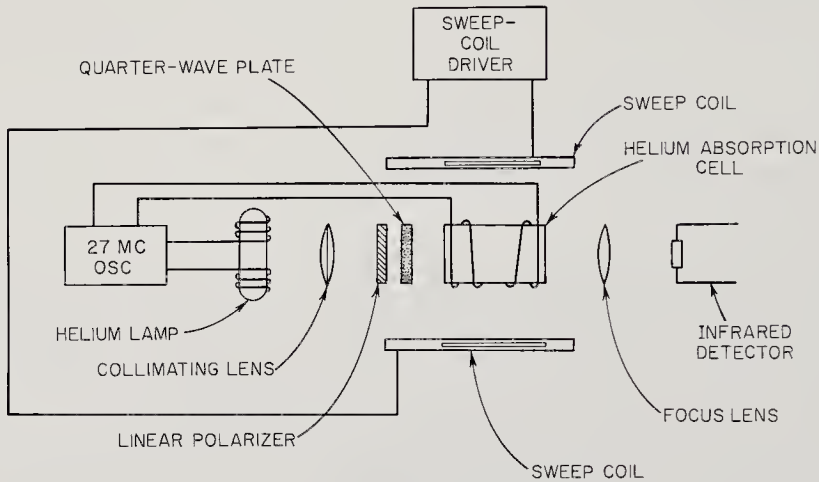


Fig. 13-11. Schematic of the Mariner-3 helium magnetometer. (JPL drawing)

of a quarter-wave plate generates circularly polarized light. The  ${}^3S_1$  atoms, regardless of the value of  $m$ , are excited to the three  $P$  states with the stipulation that  $m = +1$ . The excited  $P$  states quickly decay back to the three  ${}^3S_1$  states with equal probability. The helium pumping is different from rubidium pumping in that the  ${}^3S_1$ ,  $m = +1$  state is not a completely dead-end road. With the stipulation that  $m = +1$ , the  ${}^3S_1$ ,  $m = +1$  atoms can still be excited back to a  $P$  state. The population in the  $S$  state becomes highly skewed, however, because there is only one excitation route open for escaping the  $m = +1$  level; namely,  ${}^3S_1$ ,  $m = +1$  to  ${}^3P_2$ ,  $m = +2$ . There are many more transitions open for the other levels. The result is a population shift strong enough to be detected by a light detector.

Another difference existing between helium and rubidium magnetometers is that the helium pumping light is in the infrared region,  $1.08\mu$ , instead of the visible. An infrared detector, such as lead-sulfide or cadmium-sulfide cell, must replace the photocell.

Helium magnetometers lag behind the rubidium-vapor type in both development and application. The Mariner-3 instrument described below represents the only helium magnetometer flown thus far. Helium magnetometers do have two distinct advantages: a lower power requirement for the helium lamp, and a higher Larmor frequency. The latter is 23

cycles/gamma as opposed to 7 cycles/gamma for rubidium vapor. One infers from this that the accuracy and sensitivity of the helium magnetometer may ultimately be better than they are for its rubidium cousin.

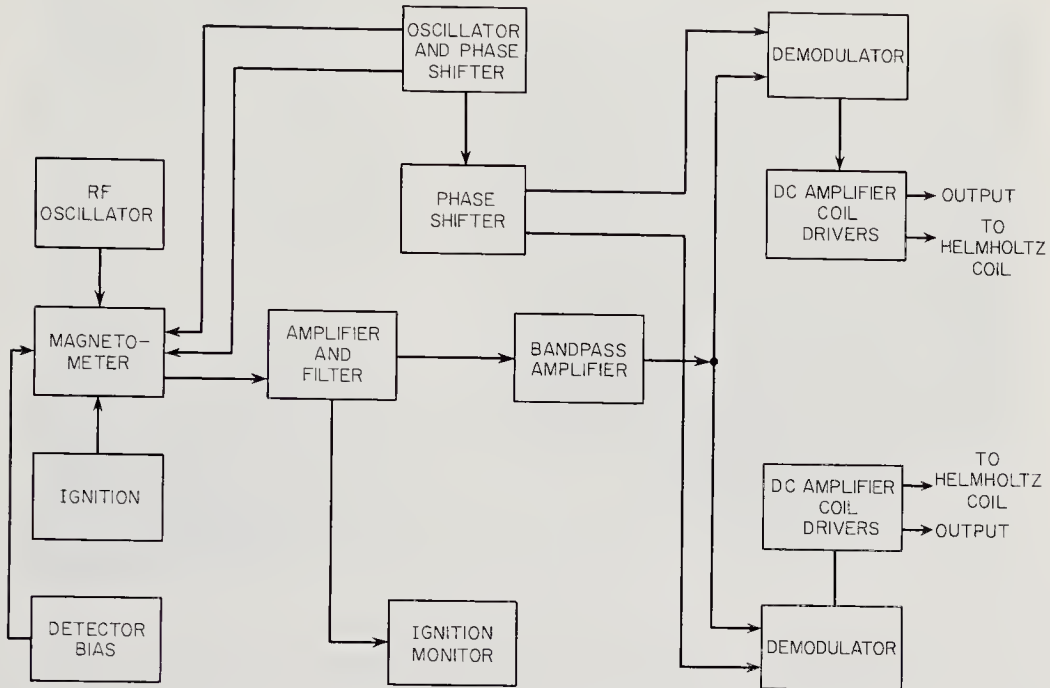


Fig. 13-12. Block diagram of the Mariner-3 helium magnetometer experiment. (JPL drawing)

The Mariner-3 helium magnetometer (Figs. 13-12 and 13-13) is a triaxial instrument. The component of the magnetic field along one axis is measured continuously, while the two other axes are sampled 25 times per second. Its dynamic range is  $\pm 360\gamma$  with a sensitivity of about  $0.5\gamma$  per axis. Although the helium magnetometer is intrinsically an absolute instrument, the Mariner-3 version is not, for rather complicated reasons. In-flight calibration currents from ultrastable voltage sources are thus required. Pumping light in the Mariner-3 magnetometer is obtained from a 27-Mc electrodeless helium discharge lamp. The infrared detector is of the lead sulfide type. Power and weight characteristics are given in Table 12-2. The Mariner-4 instrument was identical.

### 13-3 Space-Radiation Instrumentation

The discovery and mapping of the Van Allen belts represent a classic series of experiments in radiation detection and measurement. Just what new and unexpected fluxes of particles and photons will be uncovered

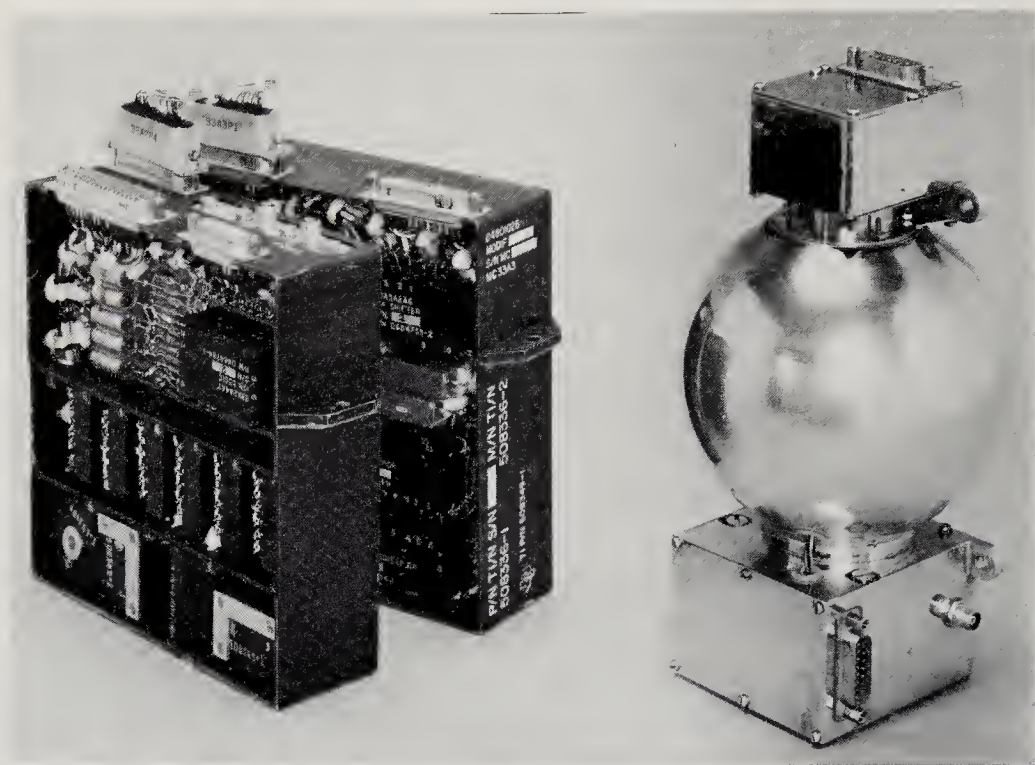


Fig. 13-13. Mariner-3 helium magnetometer and some of the associated electronic circuits. (Courtesy of the Jet Propulsion Laboratory)

in deep space and around the other planets of the solar system remains conjecture. Because of this uncertainty, all space probes carry one or more radiation detectors aboard.

It is convenient to classify particulate and photonic space radiation into four groups, according to apparent source. In Table 13-3, the four

TABLE 13-3. CHARACTERISTICS OF RADIATION ENCOUNTERED IN INTERPLANETARY SPACE\*

<i>Phenomenon</i>	<i>Particles</i>	<i>Energies</i>
Primary cosmic rays	$p, d, \alpha, \beta^{\pm}, \gamma$ , and heavier nuclei up to Fe	$10^4$ to $10^{20}$ ev
Solar energetic particles	$p, d, \alpha, \beta^{\pm}, \gamma$ , X-rays, and heavier nuclei	$10^4$ to $10^9$ ev
Trapped radiation (Van Allen belts)	$p, \beta^-$	$10^4$ to $10^8$ ev
Solar wind (plasma)	$p, \beta^-$ , perhaps a few heavier ions	Up to $2 \times 10^3$ ev

\* See Chap. 3 for further descriptions

categories of radiation are seen to span twenty decades in energy. They encompass dozens of particle species. Despite this rich and tempting variety of phenomena, this section focuses on the instruments themselves rather than the interpretations of their measurements.

When measuring space radiation, there are several physical parameters of concern. First is the *scalar flux*, the number of particles or photons crossing a square centimeter of surface each second, regardless of direction. Next, particle *energy* is of great interest in untangling the origins of the several kinds of radiation. The directional or *vector properties* of the particles may also be indicative of their source. Scalar flux, energy, and direction can all be linked together in the definition of the *differential flux*:

$$F = \int_E \int_{\Omega} \bar{F}(E, \bar{\Omega}) \cdot d\bar{\Omega} dE$$

where  $F$  = the scalar flux or omnidirectional flux  
 $\bar{F}(E, \bar{\Omega})$  = the differential flux  
 $E$  = energy  
 $\Omega$  = solid angle.

Space-radiation studies have continually attempted to increase the resolution of energy and directional measurements. The variation of each flux component with time may also help in deciphering its significance. Last, but not least, is the identification of the particle. In mapping the fluxes of space, therefore, the properties of the ideal radiation instrument should include the capabilities for measuring scalar flux, direction, energy, and species as functions of time.

Radiation is detected primarily by its interactions with matter, especially those interactions that yield electrical and photonic signals. The chief of these reactions is that of bond disruption; an effect including ionization, the creation of lattice defects, and the production of electron-hole pairs. All of the basic detectors described here depend upon some disruptive interaction for signal generation. Since the ultimate signal on a spacecraft must be electrical, if information is to be telemetered back to Earth, all nonelectrical signals (light flashes) must be converted into electrical information, preferably digitally coded electrical signals. Furthermore, the signals should be capable of carrying information beyond the fact that a particle has passed through the detector. In other words, the instrument's dynamic range and the bandwidth of its information channels must be consistent with the aims of the experiment.

To illustrate the taxonomy of radiation detectors, they have been divided into three groups in Table 13-4. Intrinsic in the table is the admission that the simple, basic detectors actually reveal little information

TABLE 13-4. TYPES OF RADIATION INSTRUMENTATION USED IN DEEP-SPACE RESEARCH

<i>Class</i>	<i>Instrument</i>	<i>Principle of Operation</i>	<i>Utility and Missions</i>	<i>Remarks</i>
Basic detector	Geiger-Mueller counter	Particle ionizes gas. Electric field causes avalanche. Counter tube discharges.	Event counter. Used in Little telescopes, etc. Pioneer 5, Mariner 2, IMP, Mariner 4.	Little discrimination of particles. No energy resolution.
Basic detector	Proportional counter	Particle ionizes gas. Electric field causes charge multiplication. No discharge.	Pioneer 5.	Weak analog output signal proportional to the amount of ionization. Rarely used in space.
Basic detector	Ionization chamber	Particle ionizes gas. Ions and electrons collected without multiplication.	Used with other detectors Pioneer 5, Mariner 2, IMP, Mariner 4.	Currents low. Integrating chambers used in space. Measures total ionization.
Basic detector	Channel multiplier	Particle ejects secondary electrons which then multiply by creating more secondaries.	Undetermined at present.	In development stage.
Basic detector	Scintillators	Particle excites crystal lattice. Recombination causes light flash.	Used in telescopes, etc. Pioneer 6, IMP.	Requires photomultiplier tube.
Basic detector	Cerenkov detector	Particle traveling faster than light in medium emits Cerenkov radiation.	Used in telescopes, etc.	Requires photomultiplier tube.
Basic detector	Cadmium-sulfide cell	Particle creates current carriers in cell, reducing its conductivity.	Trapped radiation.	Analog signal. Requires continuous current supply.
Basic detector	Solid-state detector	Particle creates hole-electron pairs, which flow as current under influence of junction emf.	Used in telescopes. IMP, Pioneer 6, Mariner 4.	Generates own signal power. Small active volume often used as a dE/dx detector.



Detector combination	Telescopes	Geometry and electrical circuitry resolve energy and direction.	Energy and direction. Pioneer 5, IMP, Pioneer 6, Mariner 4.	Uses almost any basic detector.
Detector combination	Magnetic spectrometers	Magnetic field disperses particles into array of basic detectors.	Trapped radiation spectrometry.	Magnetic fields often incompatible with magnetometers.
Detector combination	Neutron detectors	(n, $\alpha$ ) reaction creates detectable particles.	Neutrons.	Guard counter needed.
Detector combination	Ionization chamber and Geiger-Mueller counters	GM tube counts events. Chamber integrates their energies.	General radiation measurements. Pioneer 5, Mariner 2, IMP, Mariner 4.	Ubiquitous.
Detector combination	Nuclear-abundance detector	Plot of $\Delta E$ vs $E - \Delta E$ resolves species and energy.	Primarily cosmic-ray work. IMP.	Actually a special kind of telescope.
Detector combination	Double gamma-ray spectrometer	Positron-electron annihilation creates unique detectable gamma rays.	Positrons.	Positron detector.
Track imager	Spark chamber	Ionized track in gas causes sparking between foils.	Track imaging or microphone pickup.	In development for space use.
Track imager	Scintillation chamber	Same as scintillation detector.	Track imaging.	In development stage.
Track imager	Emulsion, cloud and bubble chambers	Ionized trails of particles initiate track forming.	Track imaging.	Generally inferior to above chambers for non-recoverable probes.

when used singly. Auxiliary equipment is needed to help sort out the energies, species, and directions of the radiation. Telescope configurations, different shielding arrangements, and magnetic dispersion are typical of the stratagems used to turn simple event recorders into sophisticated instruments capable of sorting out the welter of particles and photons encountered by space probes.

The ensuing discussion of specific radiation instruments follows the organization of Table 13-4.

### BASIC DETECTORS

*Geiger-Mueller Counters.* The Geiger-Mueller counter is a ubiquitous space-research tool. Not only have Geiger-Mueller tubes flown on almost every satellite and space probe since Explorer 1, but they have been employed in arrays to form cosmic-ray telescopes. Used with magnets, they make spectrometers; combined with other particle detectors, like the ionization chamber, they help to resolve the fluxes, energies, and species of the particles that make up space radiation (Table 13-3).

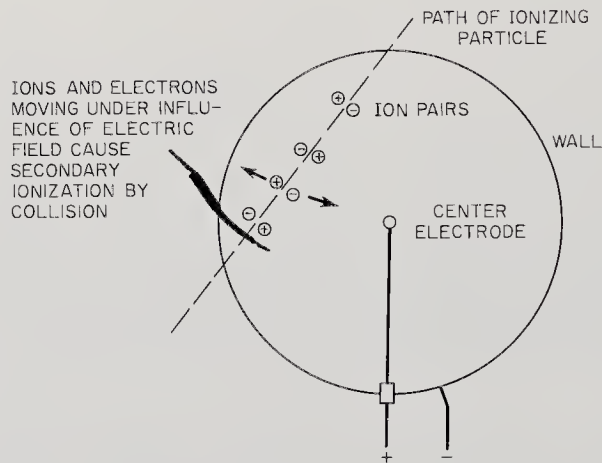


Fig. 13-14. Schematic for detectors which depend upon ionization in a gas. In the Geiger-Mueller tube, the high impressed voltage causes electron avalanches to fill the whole tube. In the proportional counter, the number of ion pairs created by the ionizing particle is multiplied by secondary ionization, but no discharge occurs. There is no secondary ionization at all in the ionization chamber.

A Geiger-Mueller tube usually takes the form of a cylindrical glass or metal tube filled with a gas, like neon or argon (Fig. 13-14). A central wire, positively charged at several hundred to a few thousand volts with respect to the wall, runs along the length of the cylinder. Sometimes a

halogen quenching gas\* is added to reduce resolution times by shortening the length of the tube discharge. The passage of ionizing radiation leaves a trail of electrons and ions, which are accelerated toward the wire and wall respectively. The high voltage gradients soon accelerate the electrons to speeds at which they cause additional ionization. An electrical discharge quickly forms along the length of the tube. The passage of the ionizing particle is thus signaled by a voltage pulse at the tube's output. The simplicity, reliability, and low power requirements of the Geiger-Mueller counter are balanced by several disadvantages:

1. There is no particle species discrimination. Even gammas and X-rays are counted—though with low efficiencies—since they produce secondary electrons in the counter walls which trigger the tube.

2. Even the thinnest tube walls (about  $1 \text{ mg/cm}^2$ ) are too thick to pass any but the most energetic alpha particles and protons.

3. The output pulse gives no information concerning the ionizing particle's energy.

4. The resolving times are long, over  $40 \mu\text{sec}$ . To some degree, these disadvantages can be overcome by telescoping counters and allying them with other detectors. In fact, all space probes have employed Geiger-Mueller tubes either in telescopes or in conjunction with ionization chambers or other basic detectors. (See the later treatment of the Ionization Chamber-Geiger-Mueller Counter combination.) Historically speaking, the earliest Earth satellites carried simple Geiger-Mueller tubes surrounded by various quantities of shielding material. When the complexity of space radiation became apparent—particularly in the vicinity of the Earth—the Geiger-Mueller tube by itself did not have the versatility to sort out the profusion of particle fluxes as functions of energy and species. The instrument vignettes later in this chapter will illustrate how the Geiger-Mueller tube is now used primarily as a detector amid the other apparatus making up the total experiment.

*Proportional Counters.* Like Geiger-Mueller counters, proportional counters have long held an honored place in nuclear instrumentation. Their principle of operation is also similar to that of the Geiger-Mueller tubes (Table 13-4). An ionizing particle penetrates a gas-filled cylindrical tube and creates  $n$  ion pairs (Fig. 13-14). Under the influence of the electrical field impressed between the central wire and the wall, the ions and electrons accelerate in opposite directions. Upon colliding with neutral atoms, the electrons and ions create  $m$  new ion pairs, but because the voltage gradients are smaller than they are in the Geiger-Mueller tube, the charge avalanches are small and localized. No tube discharge

\* Halogens are used for quenching in space because of their longer lifetimes. Alcohol is more common in terrestrial work.

occurs. Instead, the amplitude of the output pulse is proportional to the product  $nm$ , where the quantity  $m$  is called the tube's multiplication factor.

Proportional counters have much shorter resolving times ( $< 1 \mu\text{sec}$ ) than the Geiger-Mueller tubes. Since they do not discharge, they do not need to be quenched. Because the quantity  $n$  is related to the passing particle's species, charge, and energy, the proportional counter provides the experimenter more information than the Geiger-Mueller counter, in which the pulse amplitude is independent of the properties of the triggering particle.

Despite all these advantages, proportional counters are not often used on scientific spacecraft. Their output pulses are so low that very-high-gain amplifiers are required. Even more telling is the need for ultrastable high-voltage power supplies.

Of historical interest is the fact that a triple-coincidence proportional-counter telescope was employed by the University of Chicago group on Pioneer 5 to measure the cosmic-ray flux. They have also been used on Ranger 1, Explorer 6,

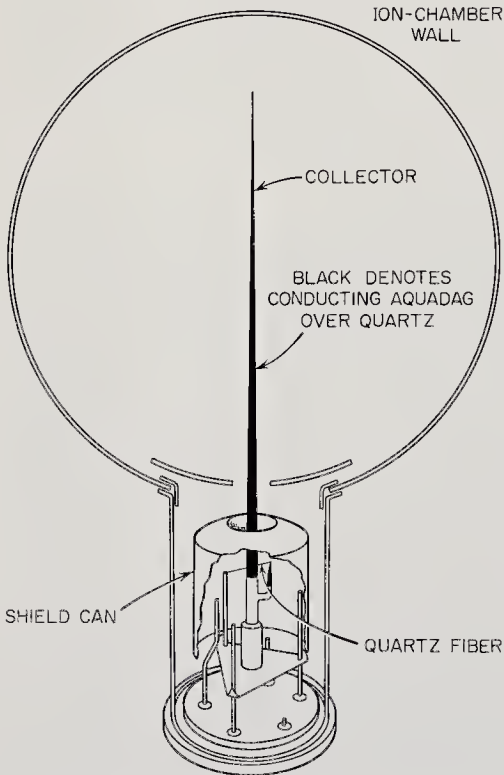


Fig. 13-15. The Neher integrating ionization chamber. This type of chamber was used on Mariner 2 and Pioneer 6. (Ref. 13-59)

and Discoverer 25. In general, however, proportional counters are being displaced by solid-state and scintillation counters, which also provide signals proportional to the energy deposited by the triggering particle.

*Ionization Chambers.* The third member of the family of devices in which particle detection is based upon ionization in a gas is the progenitor of them all, the ionization chamber. In its simplest form, the ionization chamber is a volley-ball-sized sphere—or possibly a cylinder—containing an inert gas under relatively high pressure (usually several atmospheres). The potential difference between the central electrode and the outside wall (Fig. 13-15) is only a few hundred volts, too low for the ion pairs created by the passage of ionizing radiation to cause secondary charge production through collisions (Table 13-4). The ions and electrons

collected by the electrodes thus constitute a current directly related to the total energy deposited in the chamber per unit time. The currents drawn from an ionization chamber (on the order of  $10^{-11}$  amp in space) give the experimenter an integrated energy rate, which, when correlated with particle-count data from Geiger-Mueller tubes, helps to determine individual particle energies and species.

The extremely small current output of the conventional ionization chamber is unhandy in space probes, because it is analog in character and must be amplified many orders of magnitude. The Neher integrating ionization chamber (Fig. 13-15) produces pulses with healthy amplitudes. This type of chamber begins each cycle fully charged by the spacecraft power supply. Ionizing radiation will slowly discharge the chamber, causing the central quartz rod to return to its discharged position in the manner of an electroscope leaf. The moving quartz rod, acting as a switch, ultimately completes an electrical circuit to produce an output pulse and also recharge the chamber. The number of pulses counted per unit time is obviously a measure of the rate at which energy has been deposited in the chamber.

An ionization chamber can be made simple, rugged, and reliable; although their manufacture seems more of an art than a science. Like the Geiger-Mueller counter and the proportional counter, it is easily calibrated by exposure to a known source of radiation. Ionization chambers have been carried on many satellites and several space probes (Pioneer 5, Mariner 2, Mariner 4, and IMP), but only in conjunction with particle counters. Actually, a lone ionization chamber is a rarity on a spacecraft, because it is an integrating instrument that yields little useful data unless coupled to a detector that can differentiate individual particles. Pioneer 1 used an ionization chamber by itself to measure the total amount of ionizing radiation in space, and the Naval Research Laboratory has employed ionization chambers on satellites like Vanguard 3 and Greb 1 to measure the total solar X-ray flux.

*Channel Multipliers.* The channel multiplier is a relatively new type of radiation detector. It is similar to the Geiger-Mueller tube in that it depends upon the avalanching of secondary electrons to produce an output pulse. It is also closely related to the photomultiplier tube, as the following description will show (Ref. 13-23).

Take a long, thin glass tube with a high-resistance coating on its inside surface (Fig. 13-16). Charged particles or energetic photons passing through the tube eject one or more secondary electrons from the inside surface into the central void. The secondary electrons usually possess enough kinetic energy to carry them across the narrow diameter of the tube. There would be no electron-avalanching unless energy were

somehow added to these electrons. In the channel multiplier, a longitudinal electrostatic field of a few thousand volts, applied across the metallized ends of the tube, accelerates the electrons along the axis. The secondary electrons pick up enough kinetic energy to eject more than one tertiary electron upon impact with the tube's inner surface. Multiplication down the channel is rapid, as Fig. 13-16 indicates.

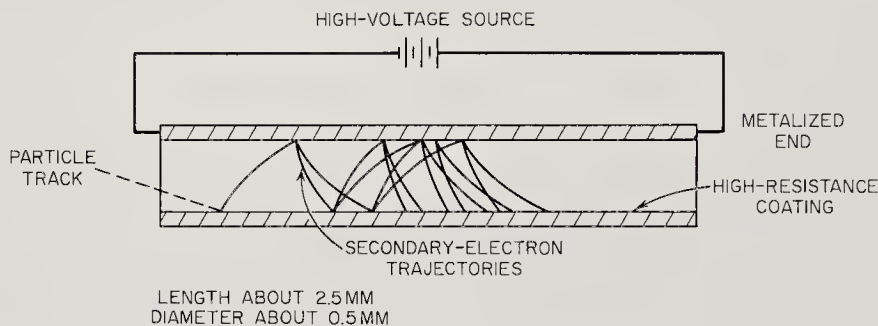


Fig. 13-16. The channel multiplier. Secondary electrons ejected from the wall avalanche down the length of the tube. (Ref. 13-23)

Conceivably, the channel multiplier could be used either for particle detection or in the role of a photomultiplier. It is also being considered for use as an image intensifier. Apparently it will be developed into a rugged, reliable radiation detector.

*Scintillators.* The passage of a high-velocity charged particle or energetic photon through a crystal lattice leaves behind a trail of disrupted bonds and excited atoms. In a number of materials—for example, polystyrene and cesium iodide—some of the energy imparted to the crystal by the ionizing radiation is suddenly re-emitted as a light pulse by the atoms returning to their normal states. In other words, the crystal fluoresces or scintillates when triggered by radiation. Tens of thousands of photons may be generated by the passage of a single energetic particle. The photon flux rises sharply to a peak and then trails off to zero, in times ranging from  $10^{-9}$  to  $10^{-4}$  seconds, depending on the material used.

To make a practical particle detector out of this physical phenomenon, the emitted light must be converted to an electrical signal. The scintillation counter requires the double conversion of energy. The photomultiplier tube or, less frequently, the photodiode, is an essential component of the scintillation counter. Photons impinging on the photomultiplier's cathode cause the photoemission of electrons from its surface. These electrons are accelerated down the tube by a series of dynodes. Electron impacts at these dynodes cause the ejection of several secondary electrons per incident electron from their surfaces. Through this electron

multiplication at the successive dynodes, a large electrical signal can be produced at the output of the photomultiplier tube in response to the input of just a few photons.

A most important property of the scintillation counter is the proportionality of the photomultiplier's output pulse to the amount of energy deposited in the crystal by the triggering radiation. It turns out that the light emitted along the particle's track and the response of the photomultiplier tube are both nearly linear. The addition of a pulse-height analyzer permits particle counts to be sorted according to energy range. A little reflection, however, shows that the light-pulse intensity coming from the scintillator must be a double-valued function when plotted against particle energy (Fig. 13-17). This is because the ionizing ability

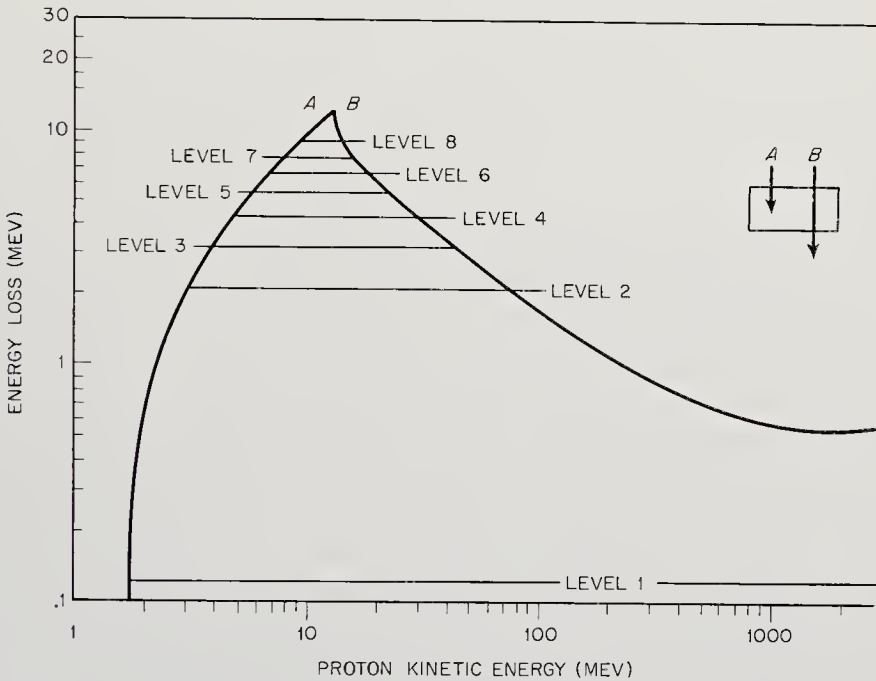


Fig. 13-17. Scintillator-crystal response to energetic protons. Protons to the right of the peak completely penetrate the crystal; those to the left do not. (Ref. 13-41)

of a particle increases as its velocity in the crystal decreases. High-velocity particles (*B* in Fig. 13-17) may whisk right through the crystal and deposit even less energy than a much slower particle. At very high particle energies, pair production again increases the particles' ionizing power (*A* in Fig. 13-17). The shape of the response curve dictates the use of additional scintillators or other companion detectors to remove the energy ambiguity. This is one of the reasons why scintillators are rarely

used alone, but form, instead, the basic sensitive elements in the more sophisticated and versatile telescopes and spectrometers described later.

Scintillator crystals must obviously be transparent to the light they emit. This means that the accompanying photomultiplier tube may see the external environment through the crystal, unless a thin, optically opaque barrier is provided. With this precaution, the scintillation counter is responsive to all energetic charged particles and, to a lesser extent, X-rays and gamma rays.

There are two classes of scintillator materials:

1. Inorganic scintillators, like sodium iodide (NaI) and cesium iodide (CsI), that are doped with an element like thallium (Tl). The heavy thallium converts the energy of gamma rays into detectable electrons and positrons by the pair-production reaction.

2. Organic scintillators, such as anthracene, naphthalene, and polystyrene. These materials are not nearly as sensitive to energetic photons as their inorganic analogs. In addition, their response times ( $10^{-9}$  to  $10^{-8}$  sec) are several orders of magnitude shorter than those of the inorganics.

The scintillators themselves are simple and rugged. To flight-qualify the whole scintillation counter, however, the photo-multipliers with their vibration-and-shock-sensitive dynode structures had to be redesigned and strengthened. Acceptable photomultipliers are now readily available. The dynode accelerators also require the availability of a high-voltage power supply on the spacecraft. The popularity of scintillation counters on spacecraft testifies to their successful adaptation to space.

*Cerenkov Detectors.* When a charged particle moves through a transparent medium at a velocity greater than that of light in the same medium, a cone of light, somewhat analogous to a shock wave in supersonic aerodynamics, is thrown forward. This is the Cerenkov effect, which accounts for the blue glow around the core of swimming-pool nuclear reactors and also serves in radiation detection. The angle of the cone of light is given by:

$$\cos \theta = c/nv$$

where  $\theta$  = the cone's half angle with the particle track (Fig. 13-18).

$c$  = the velocity of light in a vacuum ( $2.99 \times 10^8$  m/sec)

$n$  = the index of refraction of the medium

$v$  = the velocity of the particle (m/sec).

The quantity  $c/n$  represents the velocity of light in the medium and obviously may be less than  $v$ .

The pulse of light from the Cerenkov detector is roughly proportional to the energy of the stimulating particle. The directional characteristics



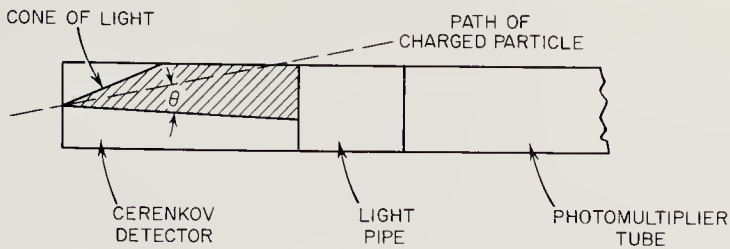


Fig. 13-18. Elements of the Cerenkov counter. Light is thrown ahead of the particle track in a cone.

of the emitted light flash can be of use in defining the geometry of radiation telescopes. Gammas and other energetic photons are not counted by the Cerenkov detector unless a heavy element is introduced into the detector. Lead gamma converters, for example, are used in Cerenkov gamma-ray telescopes to convert incident gammas into positron-electron pairs, which will then trigger the detector. The rapid decay of the Cerenkov light pulse (about  $10^{-9}$  sec) makes it possible, by using two Cerenkov detectors, to measure the velocities of charged particles by time-of-flight techniques.

Cerenkov detectors may be made from almost any transparent material; liquid, solid, or gas. Typical materials used in space research are plexi-glass, lucite, and lead (for gamma conversion) glass. In a practical detector, a cylinder of the chosen material is connected to the photomultiplier tube through a light pipe, or optically bonded directly.

As a basic detector, like the scintillators and Geiger-Mueller tubes, the Cerenkov counter is used most frequently in telescopes and in conjunction with other kinds of detectors. The fact that the response of the Cerenkov detector to radiation is somewhat different from that of the scintillator has made desirable a combination of the two types into an instrument with more energy and species discrimination than either type alone. (See later Cerenkov-Scintillation Counter discussion.)

*Cadmium-Sulfide Cell.* Cadmium sulfide (CdS) is best known as a

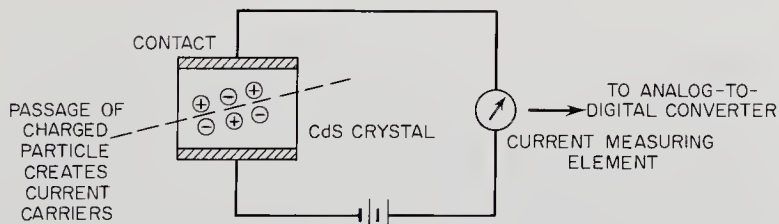


Fig. 13-19. Schematic of a cadmium-sulfide conductive cell. The passage of ionizing radiation creates current carriers in the crystal, lowering its electrical conductivity.

photoconductive detector of infrared light. The passage of ionizing radiation through a crystal of CdS reduces its electrical resistance in the same way photons do, making it also a detector of particulate radiation. The change in the current flowing across a CdS cell is proportional to the energy deposited by the radiation (Fig. 13-19). In other words, the cell conductivity is proportional to the rate of energy deposition. Some scientists term the cadmium-sulfide detector a solid-state ionization chamber, because of the similarity in properties.

In space, the CdS detector must obviously be protected from the influence of the Sun's rays—say by baffles and/or a thin, opaque shield placed around the crystal. Charged particles reaching the crystal with even a few electron volts of energy have a strong effect on its conductivity. This sensitivity to slow particles should not be surprising, since the crystal is affected by infrared photons with far less energy. The common CdS detectors used in space research are sensitive to electrons  $> 100$  ev and to protons  $> 5$  kev. Unless steps are taken to shield or deflect these abundant low-energy particles, the detector will be saturated by them. On several Earth satellites, a "magnetic broom" was installed to sweep away the low-energy fluxes of charged particles which were not germane to the experiments and also provide crude energy measurements through the broom's magnetic spectrometer action. A field of just a few hundred gauss is enough to deflect all electrons under a few hundred kev. Magnetic brooms are usually incompatible with the magnetometer experiments present on most space probes. Since deep-space magnetometers are attempting to measure absolute fields of just a few gammas, seven decades lower than the broom fields, the interference is usually unacceptable.

Cadmium-sulfide detectors have been carried on satellites like Injun, Explorer 12, and the Radiation Satellite (S-46). Their use on probes is restricted to some extent by their small active volumes and their long recovery time from saturation. In deep space, where radiation fluxes are much lower than they are in the Van Allen belts, the CdS cell is sup-

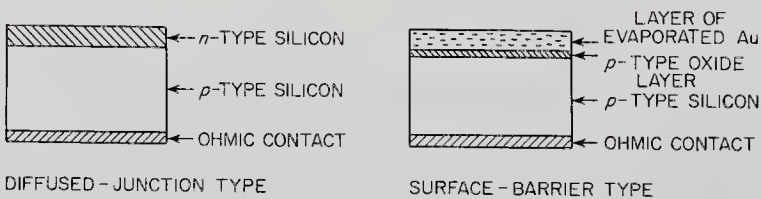


Fig. 13-20. Two major types of solid-state detectors. Electron-hole pairs formed in the vicinity of the junction flow through an external circuit under the influence of the junction-generated field.

planted by the integrating ionization chamber described earlier. The ionization chamber weighs less per unit volume and still can provide the large active volumes needed.

*Solid-State Detectors.* The same physical process that generates power in solar cells can be used to measure space radiation. Particles and photons passing through solids leave trails of electron-hole pairs which may either be drawn off by an impressed voltage (the CdS detector) or forced through an external load by the electromotive force that naturally exists

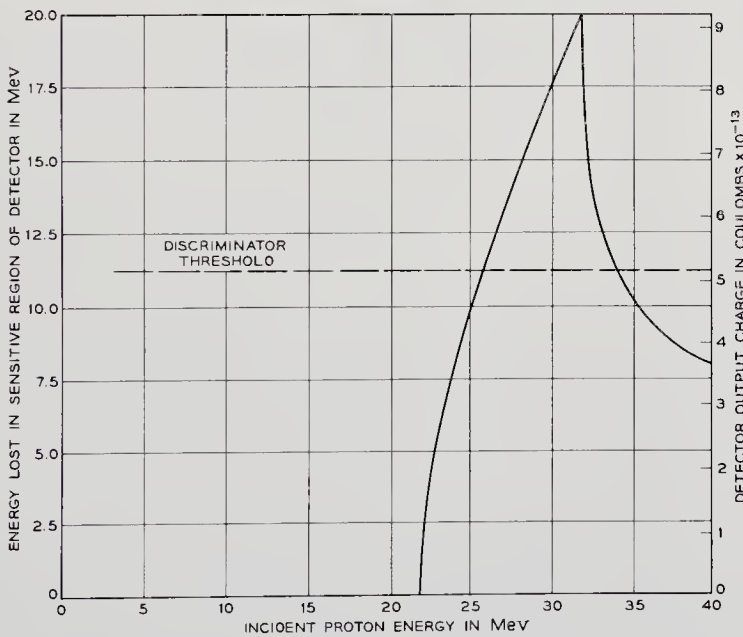
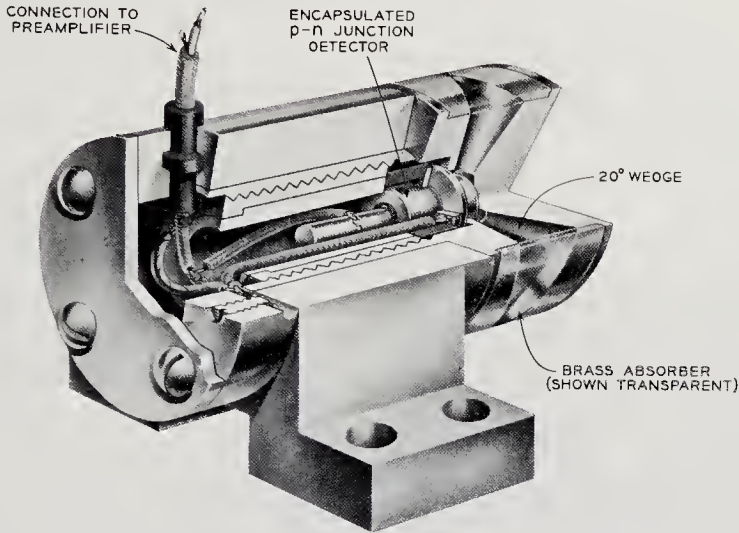


Fig. 13-21. Solid-state detector used on Telstar 1. Its characteristics are shown in the graph. (Ref. 13-13)

across a p-n junction. Since the number of electron-hole pairs created in the neighborhood of a p-n junction is proportional to the energy deposited in this region by the bombarding particles, a solid-state detector has the potential of measuring space radiation. It can provide its own electrical power as well. In effect, the solid-state detectors with p-n junctions act like solid-state ionization chambers in the thin region surrounding this junction, though not throughout the crystal, like the CdS cell. This means that junction-type detectors are  $dE/dx$  devices. Their active volumes are not thick enough to provide integrated energy measure-

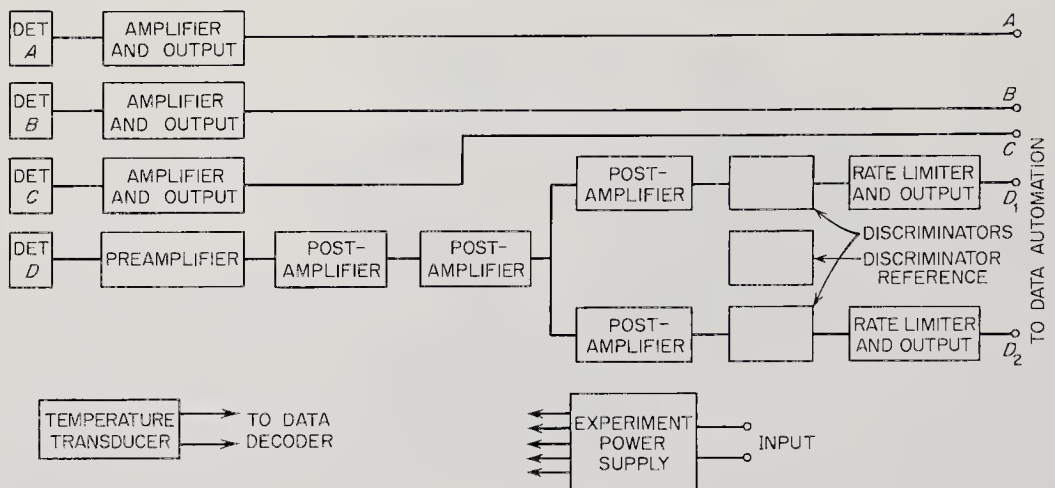


Fig. 13-22. Block diagram for the Mariner-4 trapped-radiation experiment. Detectors A, B, and C are Geiger-Mueller tubes. Detector D is a diffused-junction solid-state detector.

ments. The relatively new "lithium-drifted" semiconductor detectors, however, have much larger active volumes, in the range of  $5 \text{ cm}^3$ . Two types of solid-state detectors (in addition to the CdS detector) have been predominant in space experiments. The "solar-cell," or *diffused-junction* detector and the *surface-barrier* detector (Fig. 13-20). Both operate with the same physical processes occurring near the junction. They are lightweight, rugged, and reliable. Both have short resolution times, around  $10^{-8}$  sec, and both are relatively insensitive to gamma rays and neutrons.

Diffused-junction and solar-cell detectors have flown on such spacecraft as Telstar 1, Injun, and Ranger 1. Generally, when used alone, their energy and directional discrimination is modified by inert shielding and by shielded acceptance cones, as shown in Fig. 13-21 for one of the Telstar-1 detectors. So far, this type of solid-state detector has not been used on any space probes.

In contrast, the surface-barrier solid-state detectors have seen a great deal of service on space probes, mainly as components of cosmic-ray telescopes developed by the University of Chicago group. The IMP, Pioneer-6, and Mariner-4 telescopes, all using gold-silicon surface-barrier detectors, are described later, in the section on telescopes. The versatility and reliability of these simple detectors are attested by their prevalence on recent space probes.

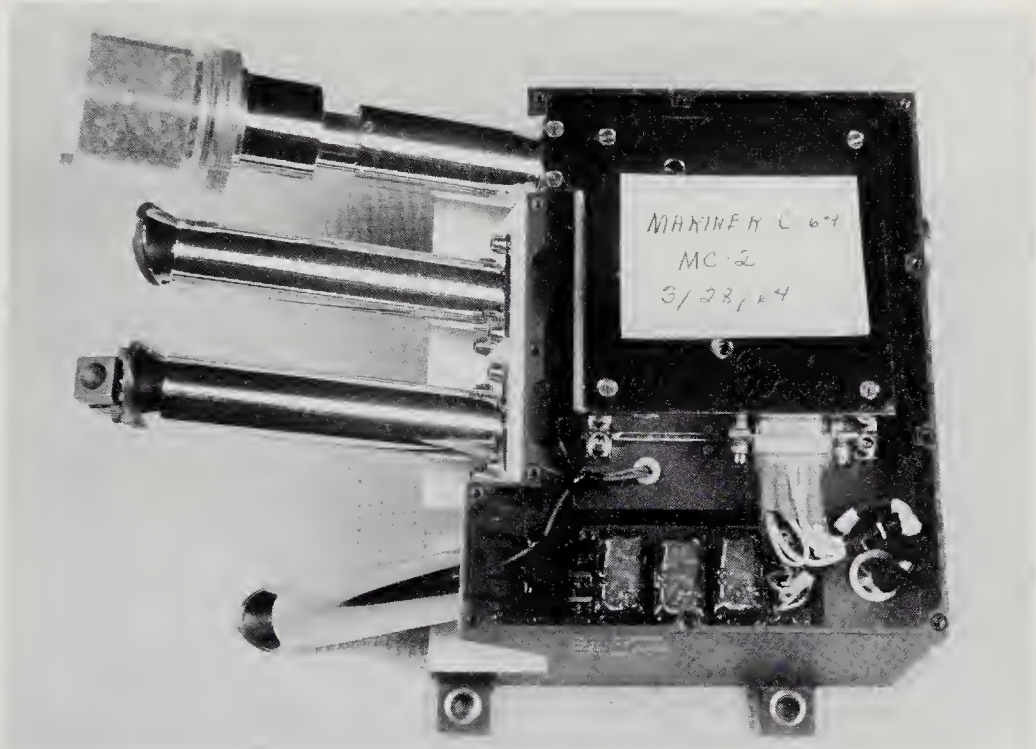


Fig. 13-23. The Mariner-4 trapped-radiation experiment, showing the detectors projecting from the instrument package. (Courtesy of the State University of Iowa)

Besides the cosmic-ray telescope just mentioned, Mariner 4 also carries a trapped radiation detector, designed by the State University of Iowa (Figs. 13-22 and 13-23). Allied with three Anton-213, end-window Geiger-Mueller tubes in this experiment is a silicon surface-barrier diode covered by an opaque, thin nickel foil. The objective of this experiment is to measure the trapped radiation, if any, around Mars. The nickel cover around the solid-state detector stops all but the most energetic electrons and alpha particles. A pulse-height discriminator sorts the output pulses due to protons into two ranges: 0.5-0.8 Mev and 0.9-5.5 Mev. The four detectors were shielded to provide the following experiment characteristics:

<i>Detector</i>	<i>Protons</i>	<i>Electrons</i>	<i>Acceptance-Cone Half Angle</i>
GM tube #1	0.5 Mev	0.04 Mev	135°
GM tube #2	0.5	0.04	70°
GM tube #3	0.9	0.07	70°
Solid-state detector level	10.5-8	none	70°
Solid-state detector level	20.9-5.5	none	70°

See Table 12-2 for other data on this experiment.

#### INSTRUMENTS EMPLOYING COMBINATIONS OF DETECTORS

*Telescopes.* Almost all space probes and many Earth satellites carry some form of radiation telescope. A few of these instruments are X-ray and gamma-ray telescopes for solar studies, but most are cosmic-ray telescopes, designed to resolve the energies and anisotropies of the high-energy particle radiation originating in the Sun and in interstellar space. It is important to propel such cosmic-ray instruments far beyond the geomagnetic cavity to regions where charged particles are not deflected by the Earth's magnetic field. Cosmic-ray telescopes are therefore high-priority space-probe cargo.

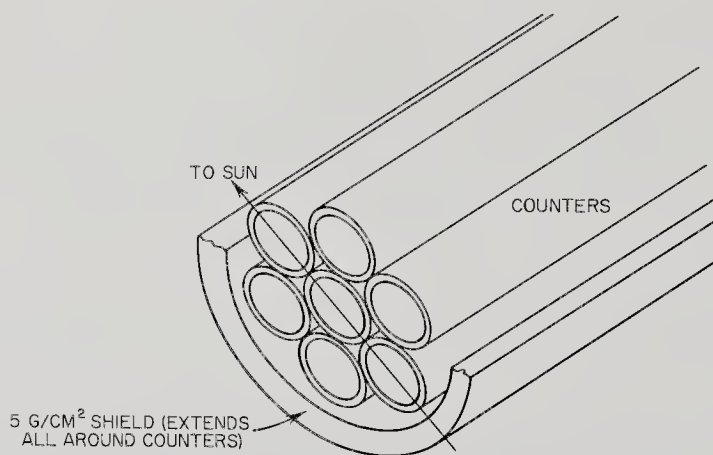


Fig. 13-24. Configuration of the Pioneer-5 triple-coincidence proportional-counter telescope.

Different types of radiation telescopes exist in profusion. The key feature of any telescope is the special geometrical and/or electrical arrangement of two or more detectors. A radiation telescope will resolve particle energies and directions, but it does not magnify anything. The energies of charged particles can be measured either by a detector whose output is proportional to the energy lost in passage by the ionizing

particles or by linear stacks of detectors which signal the depth of penetration of a particle into the stack. Depth of penetration is, of course, related to energy. To measure total particle energy by the pulse-height-analysis method, the particle has to be completely stopped in one of the detectors. Assurance that this occurs must be provided by a guard detector in anticoincidence, which discards particles that completely penetrate the internal detectors (Fig. 13-26). Detector anisotropy can obviously

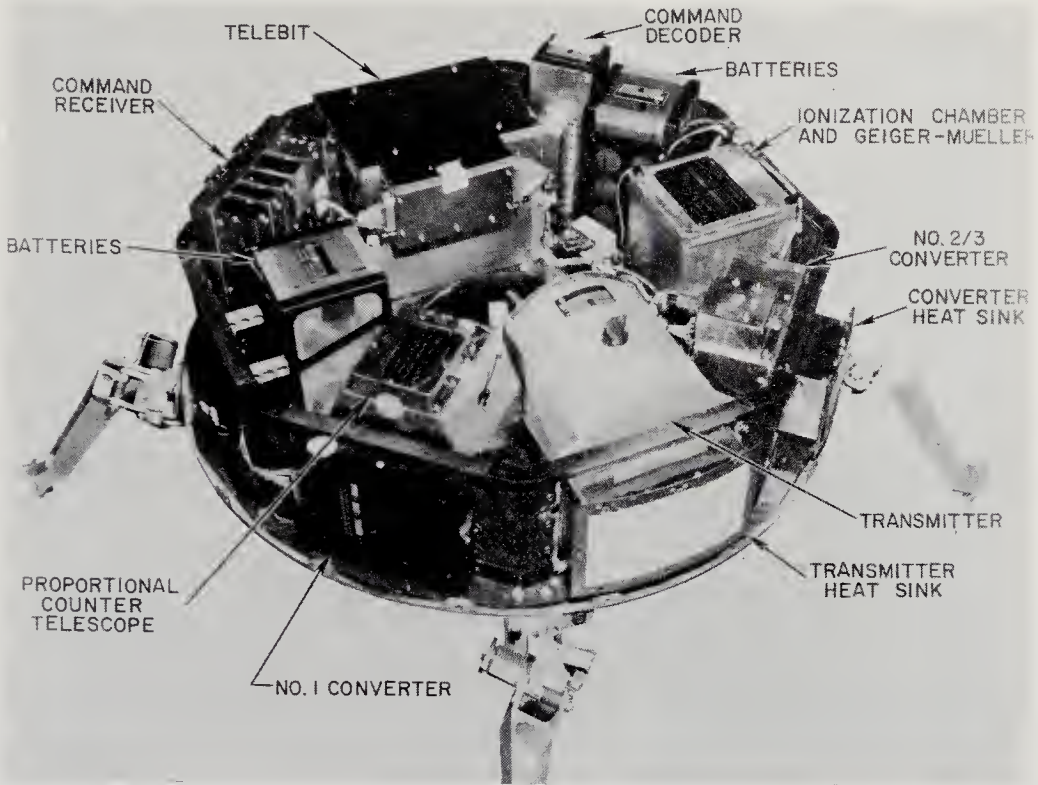


Fig. 13-25. Payload of the Pioneer 5 deep-space probe, showing the telescope assembly, ionization chamber, and Geiger-Mueller counter. Little detail can be seen when the instruments are packaged and mounted. (NASA photograph)

be used to measure direction by scanning space with its open or sensitive area if attitude data are available. It is important to realize that a telescope's anisotropy—in both energy and direction—may be due to either the geometrical stacking of detectors or the electrical selectivity of coincidence and anticoincidence circuitry of an otherwise isotropic group of detectors; e.g., the triple-coincidence proportional-counter telescope described below. Besides the many arrangements of detectors that are possible, the number of telescope varieties is further multiplied by the incorporation in telescopes of at least four of the basic radiation detectors:

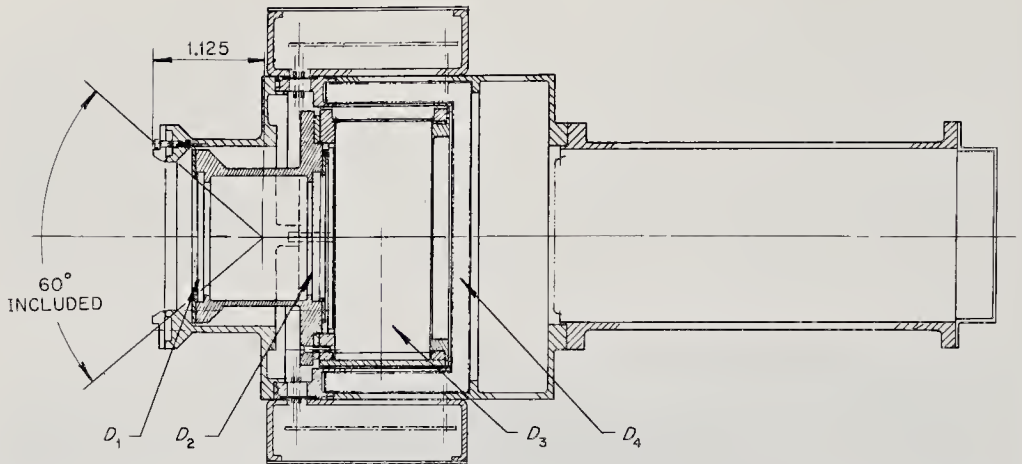


Fig. 13-26. The IMP-1 cosmic-ray telescope. See text for the description of the four detectors:  $D_1$ ,  $D_2$ ,  $D_3$ , and  $D_4$ . (Courtesy of the University of Chicago)

Geiger-Mueller tubes, proportional counters, scintillators, and Cerenkov detectors. Some of these detectors are intermixed in the same instrument.

Rather than delineate all possible telescope types and their widely varying properties, this discussion will concentrate on telescopes that have already flown or are planned for flight on space probes. Several other telescopes illustrating important principles will also be mentioned. Their order will be:

1. The proportional-counter telescope (Pioneer 5).
2. The surface-barrier detector telescopes (IMP, Pioneer 6, Mariner 3).
3. The scintillator telescope.
4. The scintillation-Cerenkov detector telescope.
5. The phoswich.
6. The gamma-ray telescope.

The nuclear-abundance detector and positron detector are also telescopic instruments. They will also be covered.

Pioneer 5 carried the only proportional counters used so far in deep-space probes. Seven Anton 302 proportional counters were arranged in the hexagonal array shown in Fig. 13-24. The whole assembly was shielded with  $5 \text{ g/cm}^2$  of lead shielding. Pulses were registered for both the triple coincidence event (center tube and both outside groups of three) and for the central tube. Triple coincidences required either cosmic-ray protons with energies greater than 75 Mev or electrons over 12 Mev. Isolated counts from the central tube alone indicated the presence of X-rays or bremsstrahlung over 200 kev. Data from the proportional-counter telescope were correlated with the total energy-rate measurements from an integrating ionization chamber of the Neher type. The



two instruments working together permitted better energy and species discrimination. (See the later discussion of the ionization chamber-Geiger-Mueller counter combination.) Similar proportional-counter telescopes have been used on the Explorer-6, Discoverer-25, and Ranger-1 spacecraft.

The Mariner-4 and Pioneer-6 cosmic-ray telescopes were also designed by the University of Chicago group. The objectives of these two experiments are:

1. To measure the heliocentric radial gradient of the proton and alpha-particle flux in different energy ranges.
2. To try to distinguish between low-energy galactic protons and alpha particles and possible persistent, nonrelativistic protons and alpha particles from the Sun that may be distinguishable near the solar minimum.
3. To exploit simultaneous observations from similar instruments on Mariner 4, Pioneer 6, and possibly the POGO satellite in a time-of-flight analyzer built on an interplanetary scale, to study the propagation of solar-initiated shock waves, solar-flare particles, and Forbush decreases.

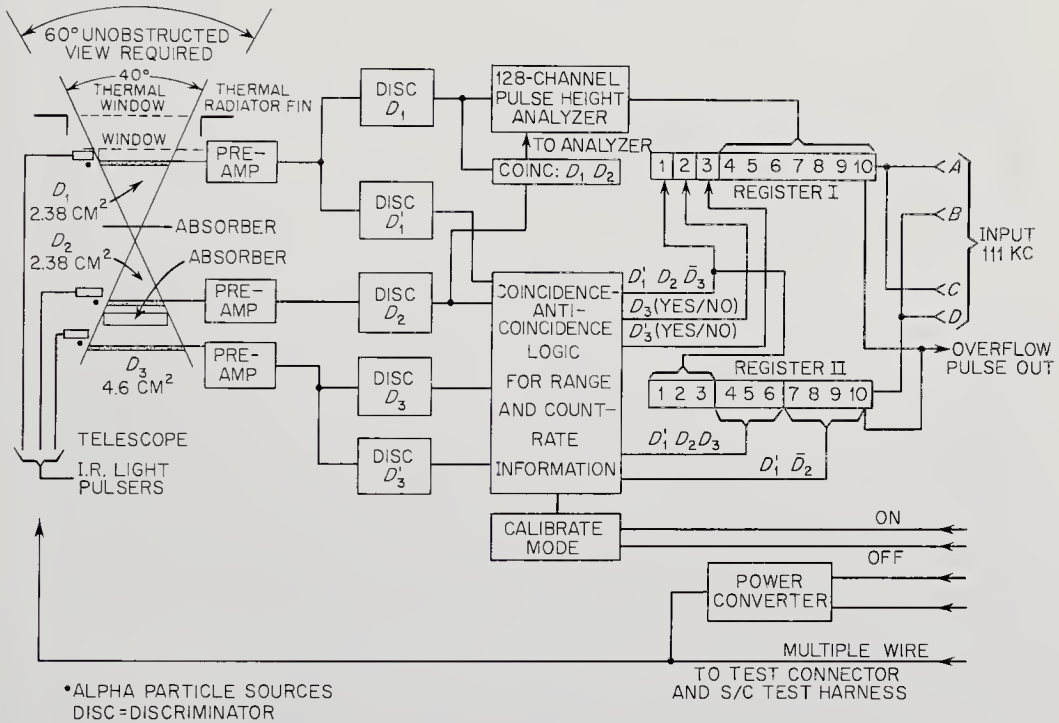


Fig. 13-27. Block diagram of the Mariner-4 cosmic-ray telescope experiment. (University of Chicago drawing)

The University of Chicago cosmic-ray telescope on Mariner 4 consists of three surface-barrier detectors, shown in Fig. 13-27 as  $D_1$ ,  $D_2$ , and  $D_3$ . Each detector produces an electrical pulse with an amplitude proportional

to the energy lost in the barrier region by the impinging charged particle.

This energy loss,  $-dE/dx$ , can be calculated from

$$-\frac{dE}{dx} = \frac{4\pi Z^2 e^4 N z}{m V^2} \left[ \ln \frac{2mV^2}{\bar{I} (1 - \beta^2)} \right]$$

where  $Z$  = the number of electronic charges on the incident particle

$e$  = the electronic charge (coulombs)

$N$  = the number of atoms/cm<sup>3</sup> in the target (1/m<sup>3</sup>)

$z$  = the nuclear charge of the atoms in the target

$V$  = the velocity of the incident particle (m/sec)

$m$  = the mass of the electron (kg)

$\bar{I}$  = the average ionization potential of the electrons in the target

$\beta = V/c$ , where  $c$  = the velocity of light.

The detectors are connected through separate amplifiers to five pulse-height discriminators. The discriminator  $D_3'$  passes pulses representing energy losses of 400 kev or more. The four other discriminators are set with their lower limits at 180 kev. In addition, the discriminator  $D_1$  is connected to a height-to-time converter, which sorts pulses into 128 channels between 180 kev and 5.2 Mev. The coincidence-anticoincidence logic provides output signals when the following events occur:  $D_1' \bar{D}_2$ ,  $D_1' D_2 \bar{D}_3$ , and  $D_1' D_2 D_3$ , where the null bar indicates anticoincidence. When the absorbers placed between the detectors are taken into account, the energy ranges represented by these three events are:

ENERGY RANGE OF PRIMARY PARTICLES (MEV)

<i>Event</i>	<i>Protons</i>	<i>Alphas</i>	<i>Electrons</i>
$D_1' \bar{D}_2$	0.80-15	2-60	0.18-0.35
$D_1' D_2 \bar{D}_3$	15-80	60-320	no sensitivity
$D_1' D_2 D_3$	90-190	320-∞	no sensitivity

The small alpha source shown adjacent to each of the detectors in the illustrations provides coincidence-noncoincidence calibrating pulses at a constant rate. (See Table 12-2 for other performance data.)

A much simpler telescope uses only a pair of scintillator crystals, each viewed by a separate photomultiplier tube. An instrument of this type was built by the Goddard Space Flight Center for the Explorer-12 Earth satellite (Fig. 13-28). Detecting protons in the energy range 100 to 600 Mev by pulse-height analysis and coincidence logic, it is illustrative of early satellite cosmic-ray apparatus.

Scintillation and Cerenkov counters have been combined to make a special type of cosmic-ray telescope (Fig. 13-29 and Ref. 13-45). The

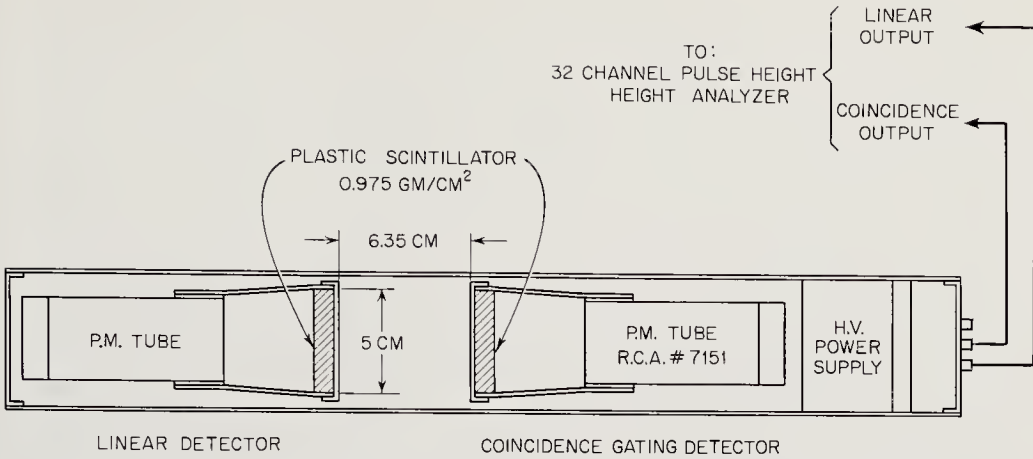


Fig. 13-28. The scintillator telescope used on Explorer 12. (Ref. 13-41)

two detectors are arranged end to end and feed their light pulses into separate photomultiplier tubes. The intensity of each scintillator pulse is proportional to  $Z^2/\beta^2$ , while those from the Cerenkov detector are proportional to  $Z^2/(1 - 1/\beta^2 n^2)$ , where  $Z$  = the particle atomic number,  $\beta$  = the particle velocity/the velocity of light, and  $n$  = the Cerenkov-counter index of refraction. Considering these relationships together, the pulse-height data from the instrument should uniquely determine the charge and velocity of particles between 250 and 1500 Mev/nucleon.

The phoswich is a unique kind of scintillation telescope used to differentiate between photons and charged particles. By using two scintillators with different rates of light-pulse decay, particle coincidences can be distinguished electronically with only one photomultiplier tube. The physical event is sketched in Fig. 13-30 (Ref. 13-55). The neutron phoswich counter designed by Reagan and Smith (Ref. 13-55) is typical of this class of instruments. It uses four lithium-iodide scintillators, surrounded by a plastic guard scintillator, which eliminates charged-particle

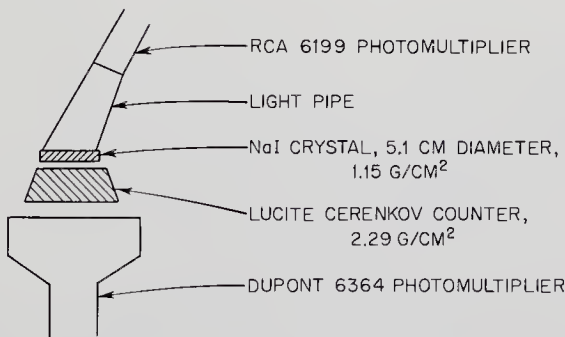


Fig. 13-29. A scintillation-Cerenkov counter. (Ref. 13-45)

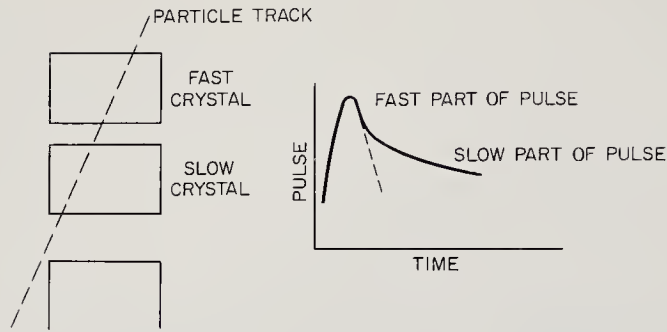


Fig. 13-30. In the phoswich counter, coincidences can be detected by a single photomultiplier through pulse-shape analysis.

counts by anticoincidence logic (Fig. 13-31). The lithium-iodide crystals are made neutron-sensitive by using lithium enriched with the  $\text{Li}^6$  isotope, which has a high cross section for the neutron-alpha reaction. The alphas generated actually trigger the phoswich crystals. (See the later discussion of neutron detectors.)

The final instrument of telescopic configuration to be discussed was flown on the satellite Explorer 11 to measure gamma rays with energies over 100 Mev as a function of direction. The scientific objective here was to test various cosmological hypotheses, which predict different high energy gamma fluxes from interstellar space (Ref. 13-4). Like the neutron phoswich detector, a gamma telescope depends upon a secondary reaction to create charged particles that can be counted by the instrument's detectors. In a gamma-ray telescope, the pair-production reaction is employed. In this sense, the instrument reverses the approach used in the positron detector described in this section of the book. The gamma-ray telescope consists of a sandwich of sodium-iodide and cesium-iodide scintillators viewed by a single photomultiplier tube and, in addition, a

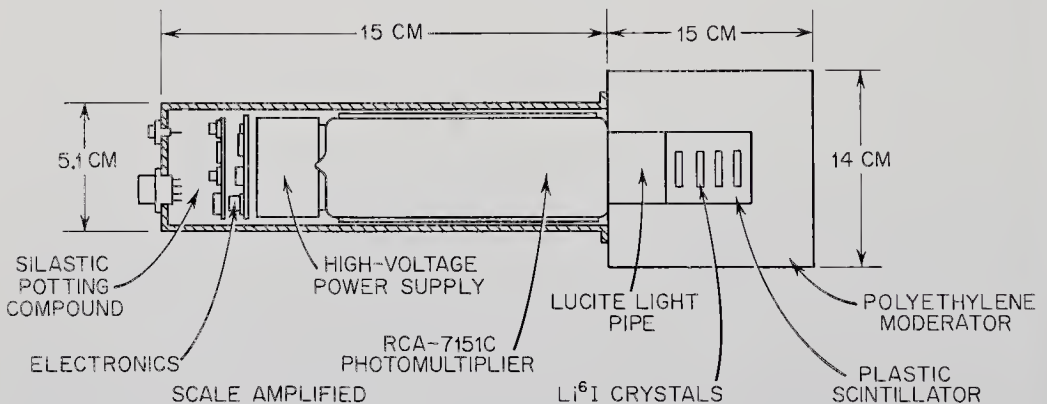


Fig. 13-31. A typical phoswich neutron counter. (Ref. 13-55)

lucite Cerenkov detector seen by two photomultipliers. This detector assembly is surrounded by a shield of scintillating plastic, which is monitored by five photomultiplier tubes. The sandwich provides high-Z material for the pair-production process. The electrons and positrons thus generated enter the Cerenkov detector, which, because of the directional property of Cerenkov light emission, detects only the charged particles moving toward the photomultiplier. Signals from high-energy charged particles in the space environment are eliminated by the outside plastic scintillator used in anticoincidence. Pulses from both the internal scintillator sandwich and Cerenkov counter, in the absence of a signal from the surrounding plastic, indicates that a high-energy gamma ray has passed through the effective aperture of the instrument. Summarizing, the instrument's capabilities are:

1. The detection of gammas in the presence of high-energy charged particles.
2. Gamma-energy sensitivity only above 100 Mev.
3. Crude directional information.

*Magnetic Spectrometers.* In attempting to map the energy spectra of the charged particles in space, the use of telescoped detectors with pulse-height counting has already been described. Separate detectors surrounded by different amounts of shielding material can serve the same purpose, although the spectral measurements here are rather coarse, owing to the

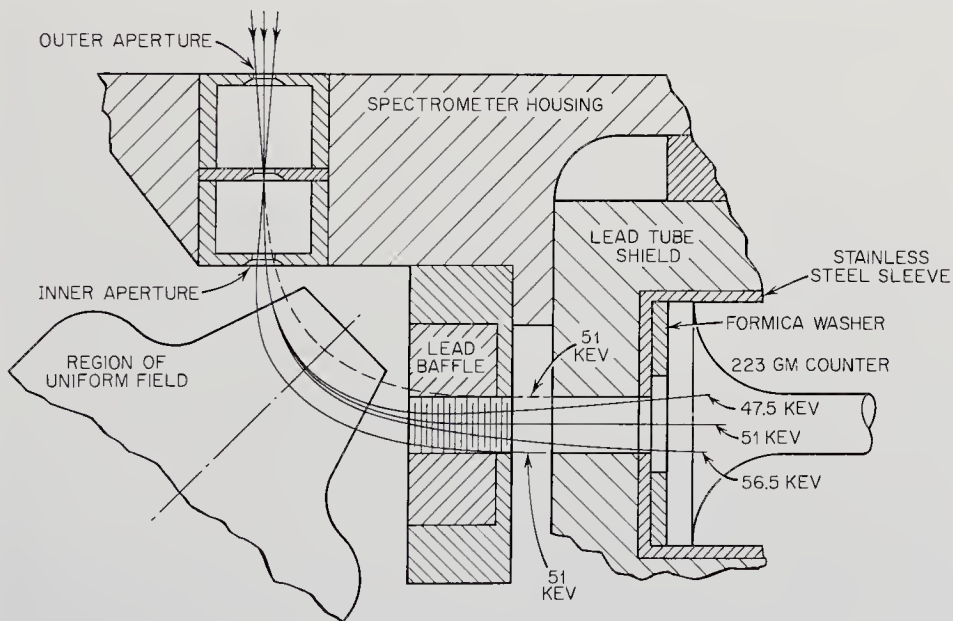


Fig. 13-32. Electron spectrometer used on Explorer S-46. (State University of Iowa drawing)

limited number of shielded detectors that can be carried. The classical way to disperse the energy spectrum of charged particles is through the use of a magnetic field. When a collimated beam of particles with mixed energies enters a magnetic field, particles are deflected by an amount dependent upon their charge-to-mass ratios. An array of detectors, precisely positioned, can intercept and read off the fluxes in different spectral regions. This approach is, of course, limited by the number of detectors that can be carried and the tolerance of other experiments to the strong magnetic fields required for particle dispersion. The latter constraint has prohibited the use of magnetic spectrometers on magnetometer-carrying space probes.

Several magnetic spectrometers have flown on satellites in efforts to better map the energy spectra in the Van Allen belts. One, diagramed in Fig. 13-32, flew on the Radiation Satellite, Explorers S-46. A 1050-gauss field deflected electrons in the narrow range from 47-56 keV into the aperture of a Geiger-Mueller tube. The objective of the experiment was the absolute measurement of flux of this portion of the spectrum. The detector was heavily shielded to preclude triggering by other particles.

Magnetic spectrometers are valuable when particle energies are relatively low and particle deflection easy; i.e., in trapped-radiation fields. Cosmic rays are too energetic for effective magnetic dispersion considering the weight limitations of space probes. The interference of the magnetic field with other instruments also limits the magnetic spectrometer's use in deep space.

*Neutron Detectors.* The neutron's lack of electrical charge and consequent extremely low ionizing power force a modification of the basic charged-particle detectors that were described earlier. In one such modification,  $\text{Li}^6$ , an isotope with a high cross section for alpha particle production, is incorporated in a scintillator material. The secondary alphas produced by the  $\text{Li}^6$  trigger the scintillator. The use of neutron-alpha ( $n, \alpha$ ) reactions is typical in neutron detection. A very common terrestrial counter, for example, is a proportional-counter tube filled with boron trifluoride gas ( $\text{BF}_3$ ). The  $\text{B}^{10}$  isotope, like  $\text{Li}^6$ , has a high cross section for alpha production. Without the  $\text{BF}_3$  gas, proportional counters detect neutrons only with very low efficiencies. Detectors that have been made neutron-sensitive may also be surrounded by a second detector—usually a guard scintillator in anticoincidence—which produces a pulse every time a charged particle penetrates its active volume. By discarding all pulses from the guard detector and all coincident pulses from both detectors, only neutron counts remain. No neutron detectors have yet flown on deep-space probes, although they are under consideration for

solar probes. Neutron detectors are, however, installed on some military satellites for detection of nuclear-weapon explosions.

*Ionization Chamber and Geiger-Mueller Counters.* Following the various kinds of cosmic-ray telescopes, the most frequent type of radiation instrumentation aboard space probes is a combination of an ionization chamber and one or more Geiger-Mueller counters. Geiger-Mueller tubes, variously shielded, can measure the fluxes of ionizing particles in terms of different ranges of penetrating ability. There are several species of penetrating particles in space, however, and the Geiger-Mueller data alone are frequently ambiguous. The addition of an ionization chamber tells the experimenters the total energy being deposited per unit time by the ionizing radiation. With the two kinds of instruments working in unison, unequivocal particle species and energy identifications can often be made. Despite a distinguished history (Pioneer 5, Mariner 2, Mariner 4, and IMP), the ionization chamber-Geiger-Mueller counter alliance is being superseded by more sophisticated experiments, employing scintillators and solid-state detectors; e.g., spectrometers.

The first true space probe, Pioneer 5, used a combination of instruments that logically falls into this category. The ionization chamber was of the Neher, integrating variety. The output of the ionization chamber was correlated with the signals from the triple-coincidence proportional-counter telescope that was described earlier. On Pioneer 5, both instruments had equivalent wall thicknesses (approximately  $1 \text{ g/cm}^2$ ) to enable correlations to be made with confidence. The ionization chamber was a 7.6-cm-diameter sphere filled with argon at 6-atm pressure. The resultant ranges of sensitivity were:

Protons	>10 Mev
Alphas	>40 Mev
Electrons	>0.5 Mev

These characteristics combined with those of the proportional-counter telescope enabled Pioneer 5 to make the first measurements of deep-space radiation levels.

The Mariner-2 ionization chamber-Geiger-Mueller counter combination was perhaps more typical of this experiment class than the Pioneer-5 instruments. The ionization chamber was of the same type used on Pioneer 5, Ranger 1, and Ranger 2. It was a spherical glass shell 0.254-cm thick and 12.5-cm in diameter, filled with argon at 4-atm pressure. Three Geiger-Mueller tubes were employed with different shield thicknesses and the corresponding particle energy ranges shown in Table 12-2 (see Figs. 13-33 and 13-34).

TABLE 13-4. CHARACTERISTICS OF THE IONIZATION CHAMBER AND GEIGER-MUELLER TUBES USED ON MARINER 2\*

<i>Detector</i>	<i>Shielding</i>	<i>Corresponding Energy for Penetration</i>	<i>Geometric Factors</i>	<i>Dynamic Range of Counting Rate†</i>
Integrating ion chamber	0.2 g/cm <sup>2</sup> stainless steel	Protons: $E > 10$ Mev Electrons: $E > 0.5$ Mev	1 liter of argon at 4 atm; $10^{-10}$ coulombs per count	$10^{-3}$ to $10^2$ /sec = $3 \times 10^2$ to $3 \times 10^7$ ion pairs cm <sup>-3</sup> sec <sup>-1</sup> (atm of air) <sup>-1</sup>
GM Tube I RCL 10311	0.030 g/cm <sup>2</sup> glass + 0.160 g/cm <sup>2</sup> stainless steel	Protons: $E > 10$ Mev Electrons: $E > 0.5$ Mev	8.8 cm <sup>2</sup> , omnidirectional	$15$ /sec to $45,000$ /sec
GM Tube II Anton 213	0.0012 g/cm <sup>2</sup> mica window 0.55 g/cm <sup>2</sup> stainless steel and magnesium	Protons: $E > 0.5$ Mev Electrons: $E > 0.040$ Mev	0.1 cm <sup>2</sup> -sterad, unidirectional	0.2/sec to 20,000/sec
GM Tube III RCL 10311	0.030 g/cm <sup>2</sup> glass + 0.113 g/cm <sup>2</sup> beryllium	Protons: $E > 20$ Mev Electrons: $E > 1$ Mev	0.2 cm <sup>2</sup> , omnidirectional	$15$ /sec to $45,000$ /sec

\* Ref. 13-59.

† Minimum rates are those to be expected from galactic cosmic rays; maximum rates are determined by the instruments' responses.



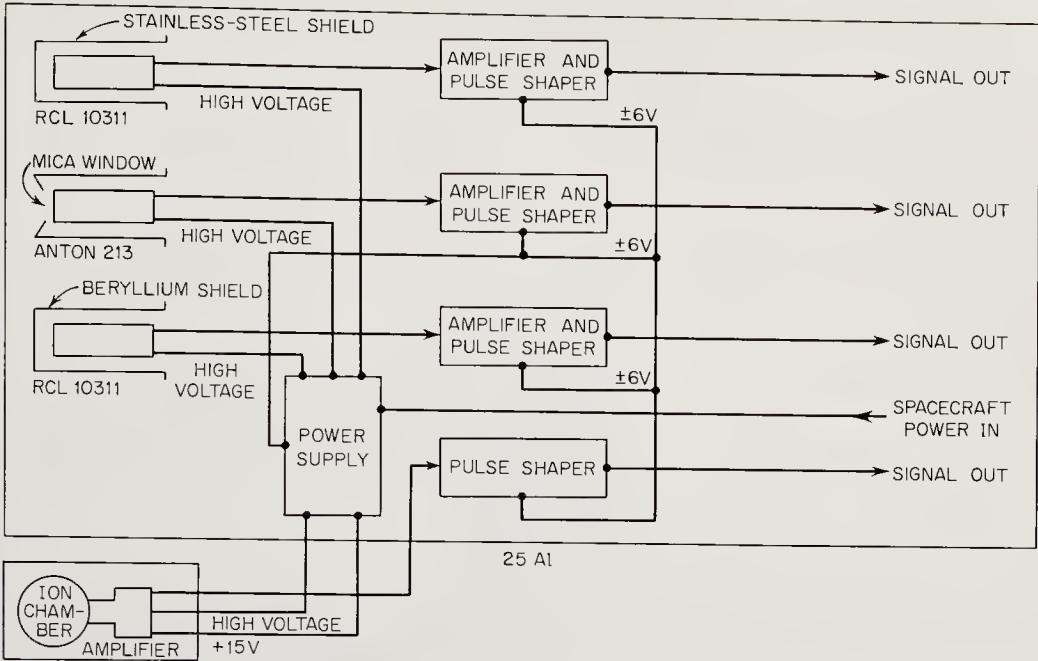


Fig. 13-33. Block diagram for the Mariner-2 ionization chamber and Geiger-Mueller counters. (Ref. 13-59)

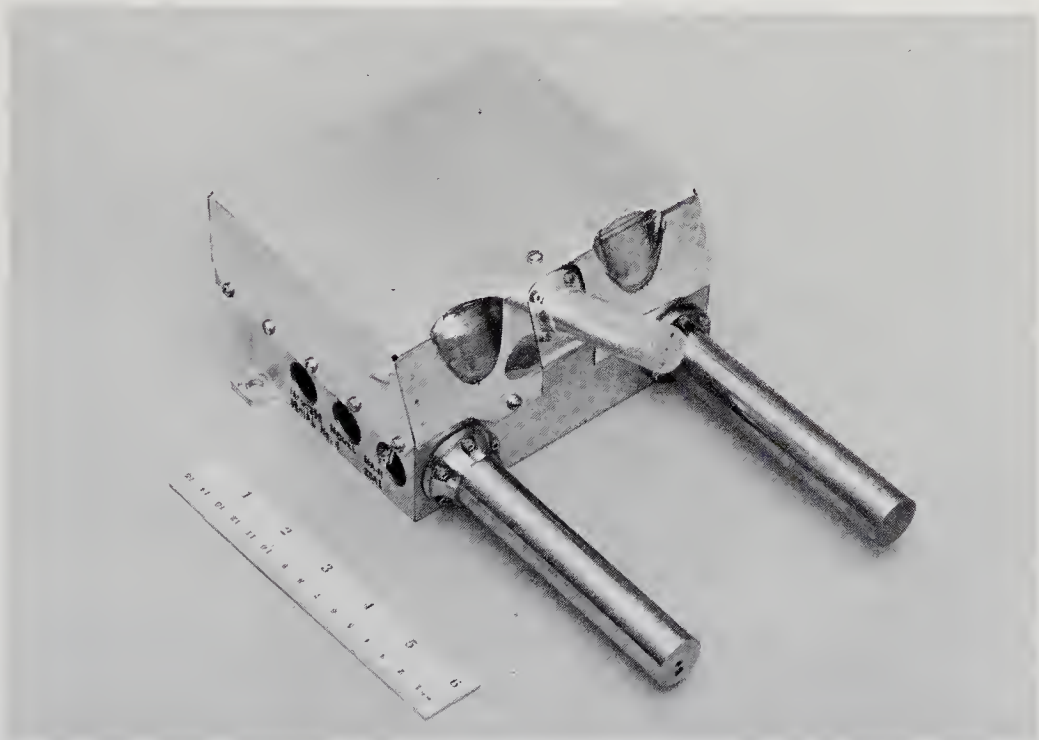


Fig. 13-34. The Mariner-2 Geiger-Mueller-tube package. (Courtesy of the Jet Propulsion Laboratory)

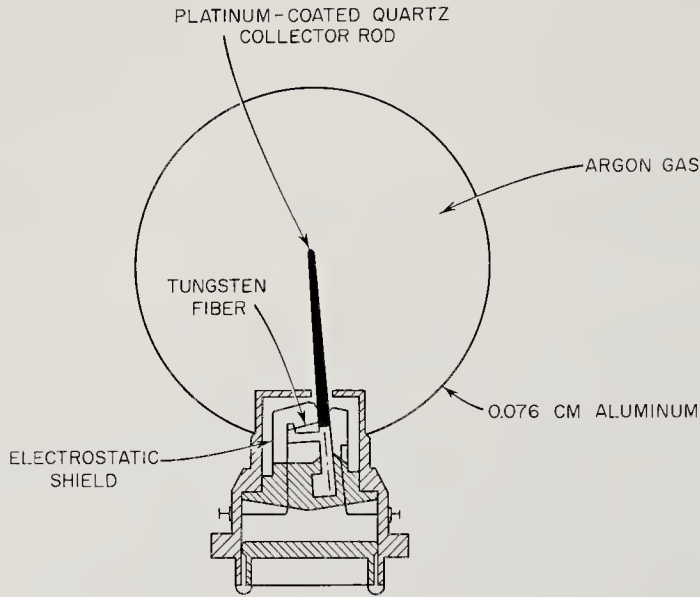


Fig. 13-35. The IMP-1 ionization chamber. It is a Neher, integrating type. (University of California drawing)

The IMP-1 radiation experiment used only two Geiger-Mueller counters, one of which had directional properties; otherwise it bore a great deal of similarity to the Mariner-2 approach. The ionization chamber (Fig. 13-35) is a 7.6-cm aluminum sphere pressurized with argon to seven atmospheres. It was designed and built at the Space Sciences Laboratory at the University of California at Berkeley. Like the Mariner-2 instrument, it is of the Neher, integrating variety. The chamber's output pulse occurs after approximately  $3 \times 10^{-10}$  coulombs of charge have been collected. The chamber's dynamic range is from  $10^{-3}$  pulses/sec (2 mr/hr) to 7 pulses/sec (100 r/hr). The first Geiger-Mueller tube, GM-1 in the drawing of the experiment (Fig. 13-36), is accessible to low-energy electrons in the outside environment through 0.02-cm gold foil. The foil scatters electrons into the tube. The second tube (GM-2) does not possess this window. Both tubes are of the halogen-quenched type with mica end windows. The ionization chamber and Geiger-Mueller tubes are shielded to provide the following detection capabilities. See also Fig. 13-37.

<i>Detector</i>	<i>Shielding</i>	<i>Proton Range</i>	<i>Electron Range</i>
GM-1 (omnidir.)	3.09 g/cm <sup>2</sup>	>52 Mev	>6 Mev
GM-1 (window)	1.7 mg/cm <sup>2</sup>		>45 kev
GM-2	3.09 g/cm <sup>2</sup>	>52 Mev	>6 Mev
Ion Chamber	0.43 g/cm <sup>2</sup>	>17 Mev	>1 Mev

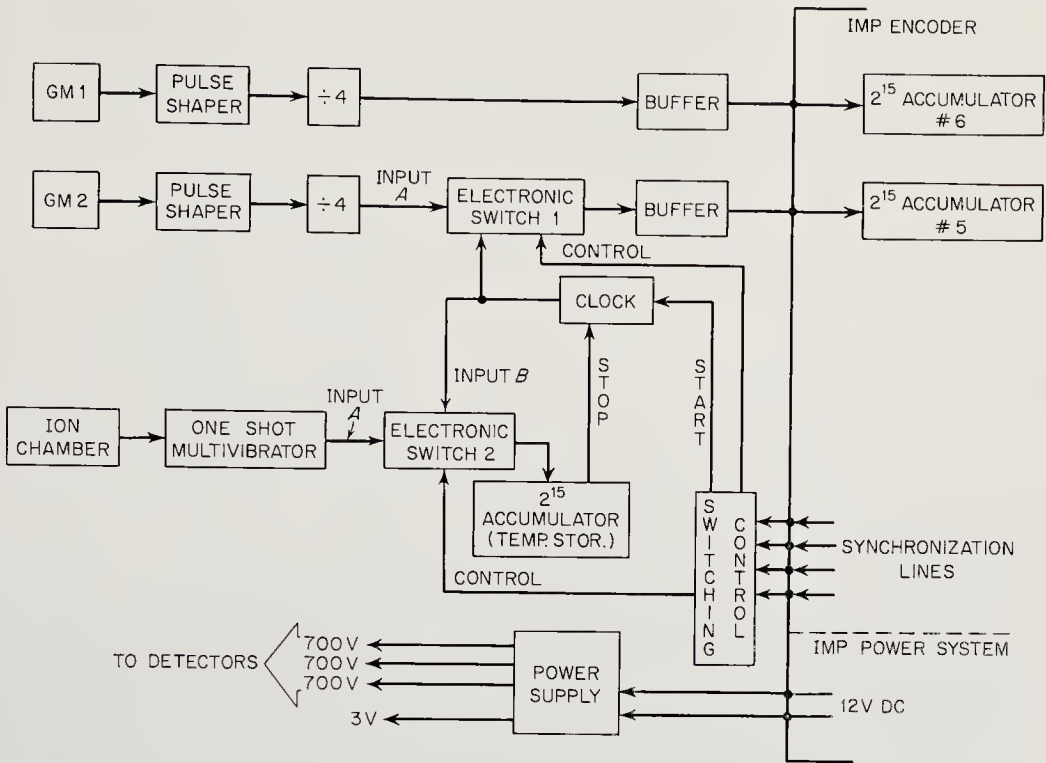


Fig. 13-36. Block diagram for the IMP-1 ionization chamber and Geiger-Mueller counter. (University of California drawing)

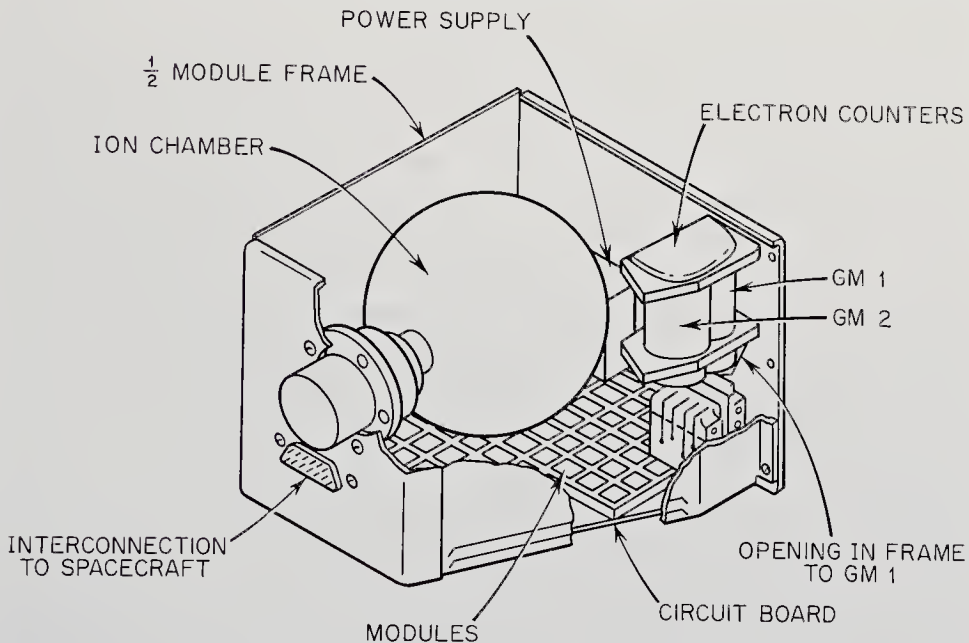


Fig. 13-37. The IMP-1 ionization-chamber and Geiger-Mueller-tube arrangement. Dimensions: 12.4 × 12.4 × 10.0 cm. Mass: 0.87 kg, after potting. (Courtesy of the University of California)

The Mariner-4 experiment is also similar to the Mariner-2 ionization chamber and Geiger-Mueller counter approach. The ionization chamber itself is almost identical to that of Mariner 2 (Fig. 13-15). It is coupled, however, with only one Geiger-Mueller tube. The over-all experiment characteristics are tabulated below.

<i>Detector</i>	<i>Shielding</i>	<i>Proton Range</i>	<i>Electron Range</i>	<i>Dynamic Range</i>
Geiger Tube	0.2 g/cm <sup>2</sup>	>10 Mev	>0.5 Mev	0-50,000 pulses/sec
Ion Chamber	0.199 g/cm <sup>2</sup>	>10 Mev	>0.5 Mev	0-100 pulses/sec

*A Positron Detector.* Several physical processes in interplanetary space can create positrons. Among these are the beta decay of cosmic-ray-excited nuclei and the double decay of pi mesons. The detection and measurement of the positron flux may therefore tell us something about the types and frequencies of high-energy interactions in space. There is also the possibility of measuring directly the low-energy tail of the galactic positron flux that penetrates inward from the boundaries of the solar system.

A positron detector has been developed by the Goddard Space Flight Center for the EGO satellite (Ref. 13-16). This instrument actually detects positron-electron annihilation events rather than positrons. The mutual annihilation of a positron-electron pair yields two 0.51-Mev gammas 180° apart. These gammas are diagnostic for the positron-electron reaction, owing to their unique energies and directional relationship.

The positron detector shown in Fig. 13-38 consists of two cylindrical, thallium-doped, cesium iodide (CsI) crystals, each completely embedded in a plastic scintillator. The two "phoswiches" are optically separated. A third CsI crystal is located in a conical well machined in the joined plastic scintillator blocks. Two photomultiplier tubes separately view the bottom surfaces of the outer scintillators. Another photomultiplier tube sees the crystal in the well through a plastic light pipe.

The incident positron flux is in effect collimated and focused on the well crystal by the encasing plastic scintillators, which are connected in anticoincidence. Positron-electron annihilations occur in the well crystal as the positrons are slowed down. The thickness of the well crystal limits the kinetic energy of reacting positrons to about 2.5 Mev. Small ionizing particles with greater energies will penetrate to the anticoincidence case. Discrimination against particles entering any of the outside plastic is accomplished by circuits sensitive to the light-pulse shape. (See the previous phoswich discussion.)

Positron events may be signaled in three ways. First, two 0.51 Mev

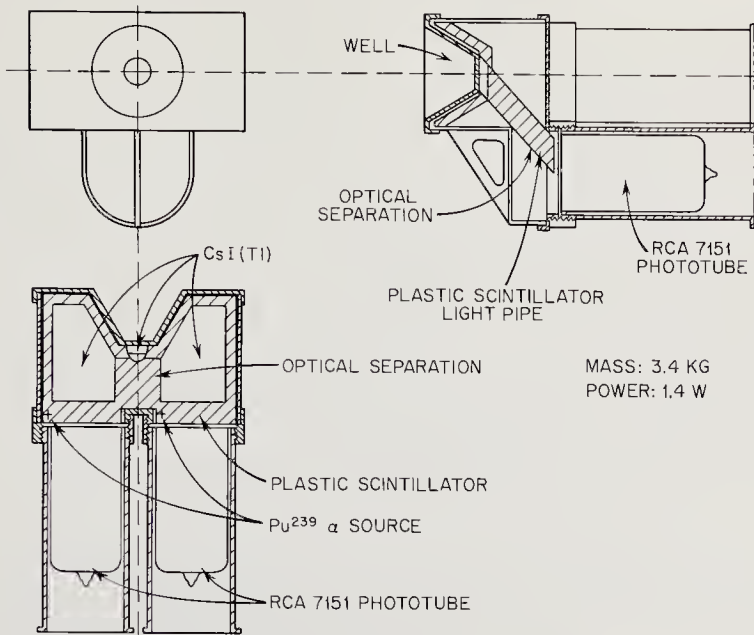


Fig. 13-38. The EGO double gamma-ray spectrometer used to measure the positron flux in outer space. Small plutonium alpha-particle sources are used to calibrate the plastic scintillators. (Ref. 13-16)

gammas,  $180^\circ$  apart, can emerge from the crystal in the well and be recorded by the two side crystal scintillators in coincidence with themselves and the well crystal. Or, less specifically, coincidences between the well crystal and just one of the outer crystal scintillators can also indicate an annihilation reaction. The third method is used to identify non-penetrating positrons. Two coincident gammas may be detected emerging from annihilations in inert portions of the detector. In the EGO positron detector, all three of these detection modes were employed to measure the positron flux and determine background corrections.

*Nuclear-Abundance Detector or E vs.  $dE/dx$  Experiment.* The Goddard Space Flight Center has developed a scintillation telescope of special configuration which can measure cosmic-ray energy spectra in the energy range from 15 to 90 Mev/nucleon for protons through oxygen nuclei. In addition, the instrument can measure the electron spectrum from 2.3 to 20 Mev (Ref. 13-41). A smaller version of the nuclear-abundance detector, capable of analyzing nuclei where  $Z < 3$ , was flown on IMP 1. (See Table 12-2 for performance data.) The full-scale experiment was orbited on the OGO-1 Earth satellite.

The telescope consists of two thallium-doped cesium iodide (CsI) crystal scintillators plus a plastic guard scintillator (Fig. 13-39). The two CsI crystals measure the total energies of the incident charged particles as

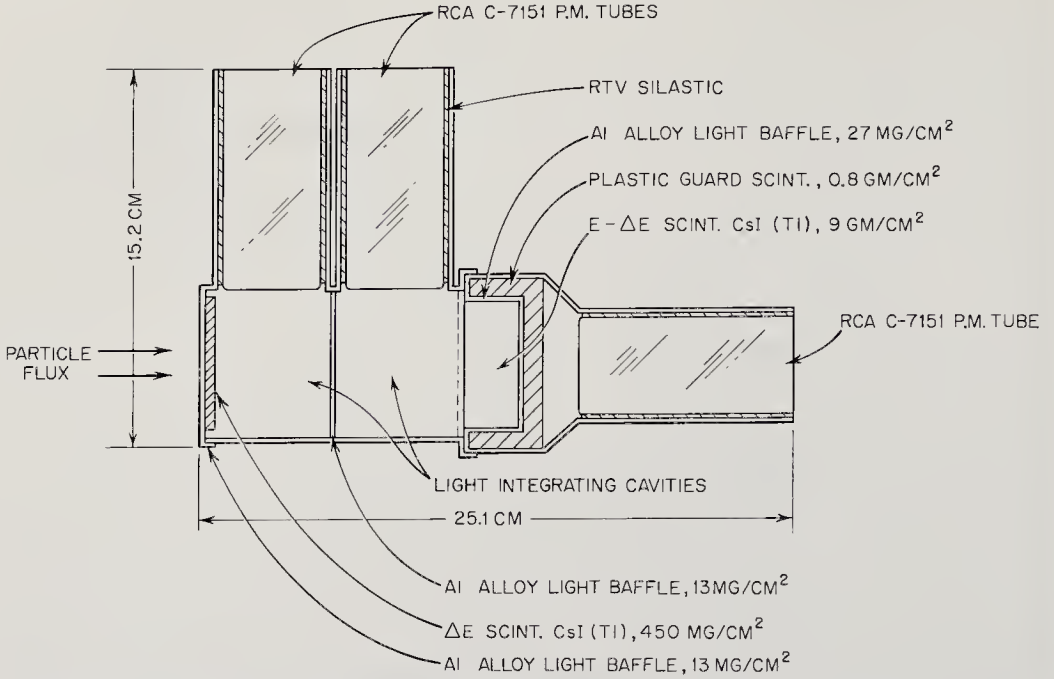


Fig. 13-39. Geometry of a nuclear-abundance detector. It is a  $dE/dx$  vs.  $E$  scintillator telescope. (Ref. 13.41)

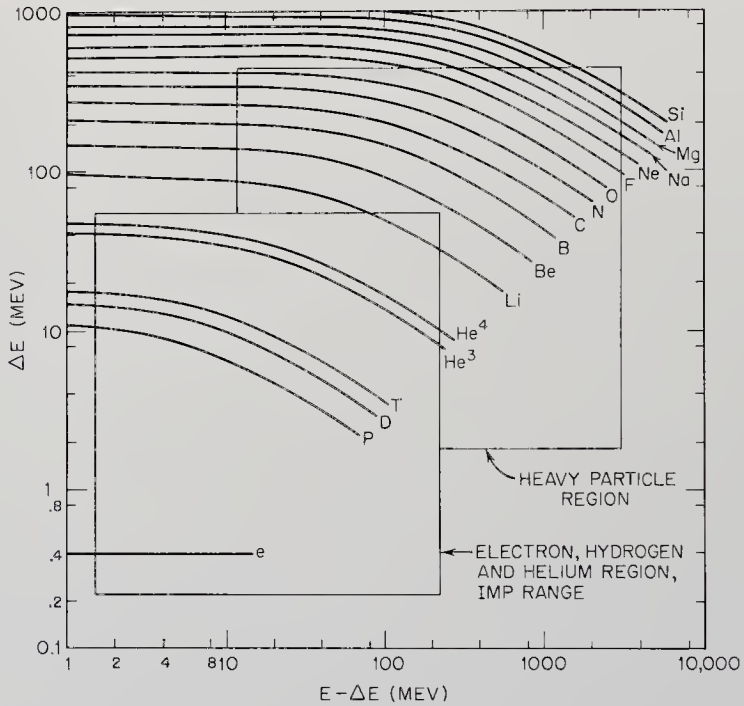


Fig. 13-40. Plot of energy loss in the  $\Delta E$  scintillator as a function of energy loss in the  $E - \Delta E$  scintillator for various particles. The end points of the curves correspond to particles which just penetrate the  $E - \Delta E$  scintillator. (Ref. 13-41)

well as their differential energy losses,  $dE/dx$ . Charged particles entering from the left first pass through a 1-mm crystal that yields a pulse proportional to the energy lost in passage,  $\Delta E$ . The second crystal is 2-cm thick, thick enough to stop particles in the energy range given above. The pulse emitted by the scintillator when the particle is completely stopped is proportional to  $E - \Delta E$ . A Pilot-B plastic guard scintillator is in anticoincidence with the thick crystal to discard events where the particles are not completely stopped. The calibration curves in Fig. 13-40 show how the measurement of both  $E$  and  $E - \Delta E$  can uniquely determine the species of charged particle. The scintillator geometry shown in Fig. 13-39 accepts particles within a cone of half angle of  $25^\circ$ . Output pulses are fed to a pair of 256-channel pulse-height analyzers. (Fig. 13-41)

#### TRACK-IMAGING INSTRUMENTS

*Spark Chambers.* The desire to see the paths traced by charged particles has led to the development of several track-imaging devices. Two of these are actively being adapted for space use.

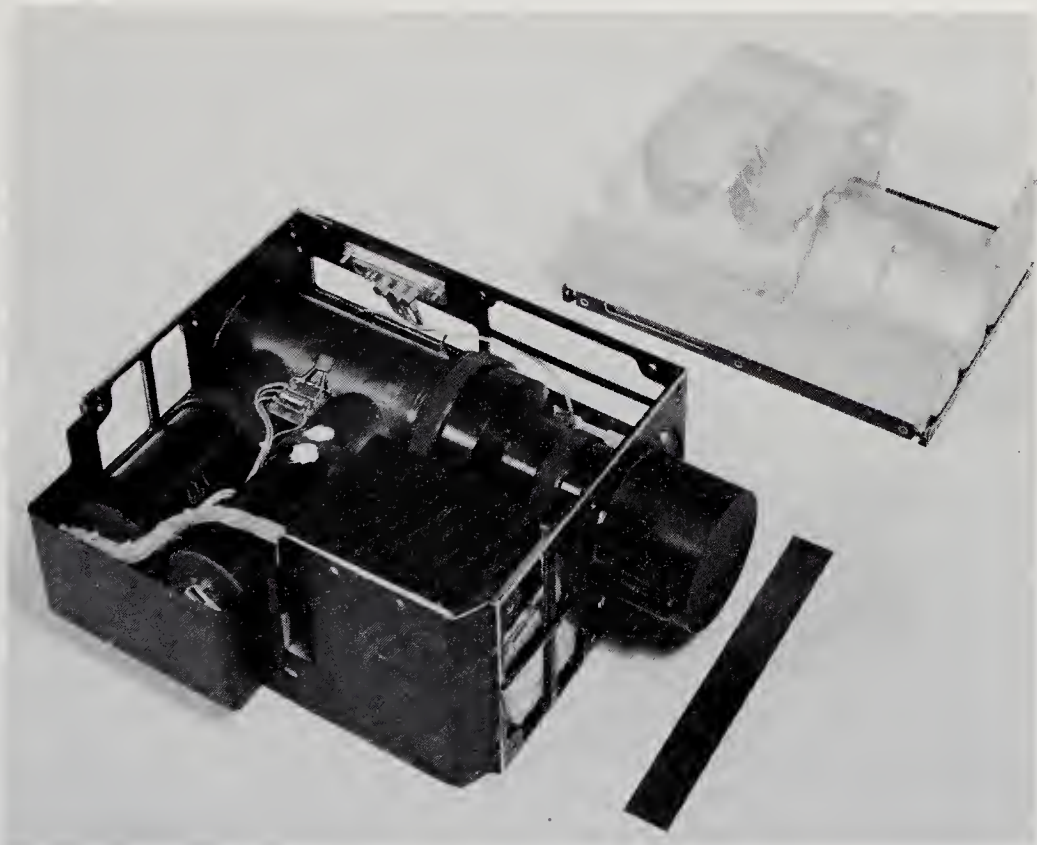


Fig. 13-41. A nuclear-abundance detector with cover removed. Dimensions: approximately 20 cm on a side. (NASA photograph)

One of the more recent track-imaging instruments is the versatile spark chamber, now a common appurtenance to terrestrial high energy physics laboratories. The spark chamber basically consists of a series of parallel, thin metal foils separated by gas-filled gaps of perhaps a millimeter or two. Three-dimensional arrays of wires are also being developed. When voltages on the order of a kilovolt are applied between adjacent plates, or wires, the ionized trails left by charged particles passing through the array of foils reduce the local resistance enough to cause sparks to jump between plates. When the foils are viewed edgewise, each spark forms a segment of the charged particle's track (Fig. 13-42). Of course, in order

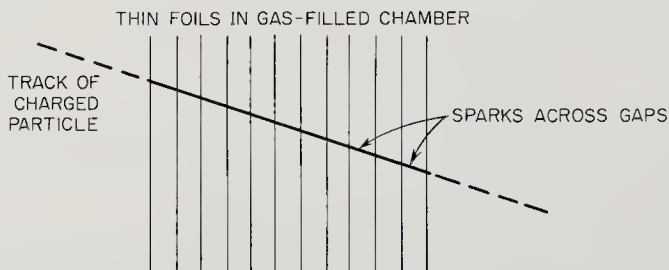


Fig. 13-42. Schematic of a spark chamber.

to view such an event occurring on an unmanned spacecraft, a television circuit must be installed.\* A visual picture of the track gives the experimenter much more information than just a count from a particle detector. Particle species, energy, and direction can be calculated from track measurements. In addition, the secondary particles arising from nuclear reactions can also be followed. Without track imaging, such detail would be impossible. The increase in information content is reflected in the much larger bandwidth needed by the television equipment.

Spark chambers usually contain a discharge-quenching gas, such as argon or xylene. Even though the spark itself may last only  $10^{-9}$  sec, the quenching time is much longer, just as it is in the Geiger-Mueller tube. An experimental disadvantage of the spark chamber is its lack of isotropy and homogeneity; that is, particles see different masses of absorbing material in different directions. As if in compensation, spark chambers are fairly easy to build, even with volumes of several cubic meters. Furthermore, they are reliable, and can be designed to trigger the viewing apparatus only when a particle has passed through.

The spark chambers used in terrestrial laboratories are heavy and cumbersome. Several groups are working at lightening and miniaturizing

\* In a three-dimensional wire chamber being developed at JPL, signals from the wires give the coordinates of the sparks.



these instruments for space use. The high-energy nuclear reactions that experimenters wish to view in space with spark chambers are rather rare, however, and large-volume chambers will be required. This volume problem will probably relegate imaging chambers to near-Earth missions for some time to come.

*Scintillation Chambers.* The crystals used in scintillation counters can be grown to sizes appropriate to small imaging chambers. The inherent sensitivity, reliability, and ruggedness of a solid-state chamber has encouraged the development of scintillation chambers for space research. One advantage of the scintillation chamber over the spark chamber is derived from the higher density of the chamber and the resulting smaller active volume needed for a given experiment. It is also homogeneous throughout its active volume. Like the spark chamber, the scintillation chamber can easily be triggered and can give accurate information on particle species, energy, and direction (Ref. 13-19). On the negative side, scintillation chambers are relatively expensive and will probably require the use of image-intensifier tubes (Fig. 13-43). The scintillation chamber

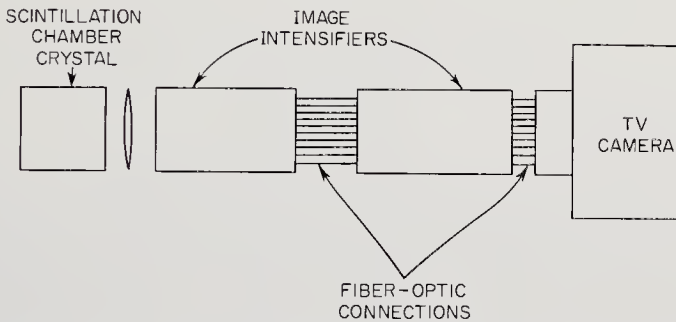


Fig. 13-43. Schematic of a scintillation chamber and associated equipment. Three cameras would be needed for three-dimensional observations.

will also probably be limited to Earth-orbital missions for reasons of weight and bandwidth.

*Other Track-Imaging Instruments.* Three other kinds of imaging devices are frequently employed in terrestrial nuclear physics. All provide good energy, direction and species discrimination. The oldest of these is the photographic emulsion. Thick, three-dimensional stacks of emulsion have been flown frequently on rockets and in recoverable satellites. The prime requirements, however, are recovery, photographic development, and careful examination on the Earth. Recoverable deep-space probes are not even in the planning stage, a fact eliminating emulsions from immediate consideration.

Historically, the cloud chamber was the next track-imaging device.

Both the cloud chamber and the bubble chamber can provide direct views of nuclear tracks. Accompanied by a television camera, these two chambers might be applied to the same purposes as the spark and scintillation chambers. Unfortunately, the cloud and bubble chambers are heavy, possess moving parts, and cannot be rapidly triggered electrically. For these reasons, development efforts have concentrated on the handier spark and scintillation chambers for space research.

#### 13-4. Analysis of the Interplanetary Plasma

A probe launched toward the planets and deep space soon leaves behind the dense cloud of matter surrounding the Earth and becomes submerged in the much more tenuous fluid occupying the space between the planets. The protons, electrons, and the minority of heavier ions making up the interplanetary plasma carry energies up to about 20 kev, many orders of magnitude less than those of the coexisting cosmic-ray fluxes (Table 13-3). The plasma density, though, may be as high as 100 particles/cm<sup>3</sup>. In terms of energy density (ev/cm<sup>3</sup>), then, the low-velocity plasma flux streaming outward from the Sun carries many times more energy than the cosmic rays. The steady-state and transient plasma fluxes, their energy spectra, and their species counts are all diagnostic of important solar system physical processes. Probes necessarily carry plasma probes to map these phenomena.

Just where does the interplanetary plasma begin? For practical purposes, the edge of the Earth's magnetosphere can be taken as a good starting point (Fig. 3-2, page 22). Beyond this surface, solar rather than terrestrial effects dominate. The instruments used beyond the magnetosphere are similar to those used in studying the Earth's ionosphere. A point of significance in comparing instrumentation in the two regions is the mean free path of the particle being measured. In deep space, the mean free paths of protons can be as large as 10<sup>10</sup> cm. Those terrestrial instruments which depend upon thermodynamic effects and the creation of ion sheaths would not be applicable under such conditions. Interplanetary plasma measurements depend more upon analyzing the collisionless trajectories of particles than upon mass action phenomena. Some instruments, like the mass spectrometer, can be used equally well in the upper atmosphere and deep space. Some of these are described in the next chapter along with other atmospheric instruments.

The physical parameters describing interplanetary plasma are the same as those used for radiation studies: scalar flux, direction, energy, and species. Rather than measure the plasma flux by counting individual, penetrating particles, as was done in the case of cosmic rays, charge-collecting surfaces (plates and cups) are connected to photomultiplier or

TABLE 13-5. TYPES OF PLASMA PROBES USED IN SPACE RESEARCH

<i>Instrument</i>	<i>Principle of Operation</i>	<i>Utility and Missions</i>
Curved-surface analyzers	Electrostatic fields separate out particles of equal energy-to-charge ratios. Applied fields nearly normal to trajectories.	Good energy analyzer at upper end of spectrum in deep space. Mariner 2, IMP, Pioneer 6.
Planar probes Faraday-cup probes	Retarding electrostatic fields repel particles in different energy ranges. Applied fields nearly parallel to trajectories.	Good energy analyzer at low end of spectrum and high density. IMP, Pioneer 6.
Spherical ion traps	Same as planar probes	Same as planar probes. Russian probes and satellites.
Plasma-species probes	(See mass spectrometers, Chap. 14)	

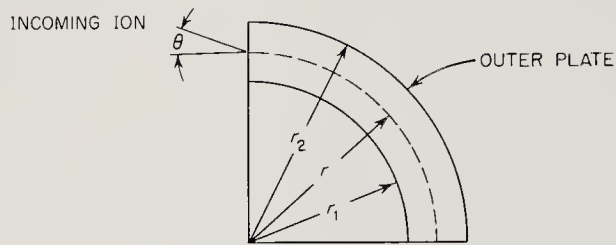


Fig. 13-44. Definitions of symbols used in deriving the energy equation for the curved-surface electrostatic analyzer.

electrometer circuits for current measurements. The plasma flux is too dense and its particles too weak in energy for cosmic-ray counters and counting techniques. To measure plasma flux in the absence of coincidence and anticoincidence counters, experiments fall back on optical geometries, using tube-like collectors which have limited apertures or cones of particle acceptance. Plasma particles outside the desired cone cannot reach the detectors. Particle energies are analyzed by the play of electrostatic forces, which deflect or retard the flow of charged particles. (See curved-surface analyzers and planar plasma probes.) Mass and species discrimination cannot be easily handled with electrostatic fields alone. Plasma-

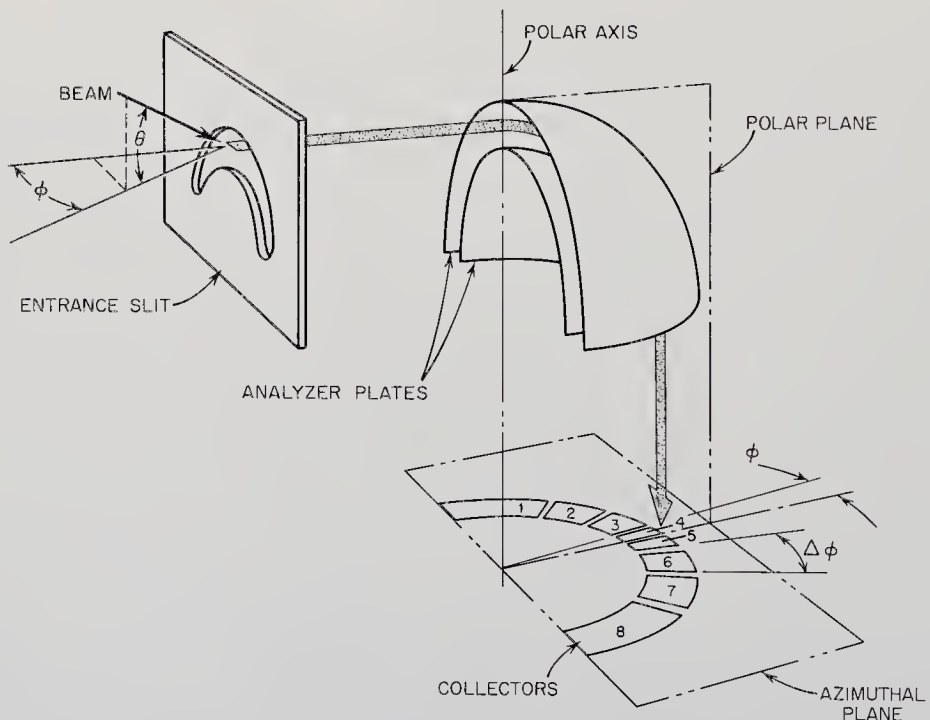


Fig. 13-45. Geometry of the Pioneer-6 spherical electrostatic plasma analyzer. (NASA drawing)

species probes (spectrometers) resort to magnetic and radio-frequency fields.

All instruments affect the phenomena they measure to some extent. Satellites and probes carrying plasma instruments are no exceptions. Several effects have to be compensated for in the instrument-spacecraft design or during the reduction of data:

1. Distorting, fringe electrostatic fields between instrument electrodes and the spacecraft skin.
2. Ram-pressure effects (especially in satellites)
3. Spacecraft magnetic fields may modify the flow of nearby plasma.
4. Photoemission of electrons from spacecraft surfaces.

*Curved-Surface Electrostatic Analyzers.* The energies, directions, and scalar fluxes making up the interplanetary plasma can be partly sorted out by electrostatic analyzers. There is a superficial resemblance between this instrument and the better-known mass spectrometer. While the mass spectrometer separates a monoenergetic beam of charged particles into groups with different mass-to-charge ratios by means of a magnetic field, the electrostatic analyzer splits a flux of charged particles into equal energy-to-charge-ratio groups with an electric field. The functions of the two instruments are actually complementary. The use of both together would provide both mass and energy discrimination, leading to unequivocal analysis of plasma fluxes. This instrument combination has been proposed (Ref. 13-6), but has not been flown yet.

To see how the electrostatic analyzer works, consider the two curved plates shown in Fig. 13-44. The plates may be either spherical or cylindrical. A positively charged particle entering the space between the plates at  $\theta = 0$  will be pulled downward by a negative voltage on the lower plate. If the plates were flat, the particle would quickly impact and be neutralized. Their curvature, however, permits particles with a certain energy-to-charge ratio to travel circular trajectories and reach a detector located at the other ends of the plates. By balancing the centrifugal and electrostatic forces, the radius of the particle's trajectory can be derived:

$$\left. \begin{aligned} \frac{1}{\ln(r_2/r_1)} \cdot \frac{qV}{r} &= \frac{mv^2}{r} = \frac{2E}{r} \\ \frac{E}{q} &= \frac{V}{\ln(r_2/r_1)} \end{aligned} \right\} \text{(for cylinders)}$$

$$\left. \begin{aligned} \frac{r_1 r_2}{r_2 - r_1} \cdot \frac{qV}{r^2} &= \frac{mv^2}{r} = \frac{2E}{r} \\ \frac{E}{q} &= \frac{V r r_1 r_2}{r_2 - r_1} \end{aligned} \right\} \text{(for spheres)}$$

where  $E$  = particle energy (joules)  
 $m$  = particle mass (kg)  
 $v$  = particle velocity (m/sec)  
 $q$  = particle charge (coulombs)  
 $V$  = voltage applied between the plates (volts)  
 $r, r_1, r_2,$  and  $\theta$  are defined in Fig. 13-44.

Particles entering the space between the plates with energy-charge ratios substantially different from that dictated by the dimensions and applied voltage of the analyzer will collide with the walls and not be detected. There is, of course, a small energy range of particles,  $E \pm \Delta E$ , which will just clear the rims of the plates and be detected. The same is true for the elevation angle,  $\theta$ . There is actually a fan of flux that will be accepted and detected. The acceptance angle in the azimuthal plane,

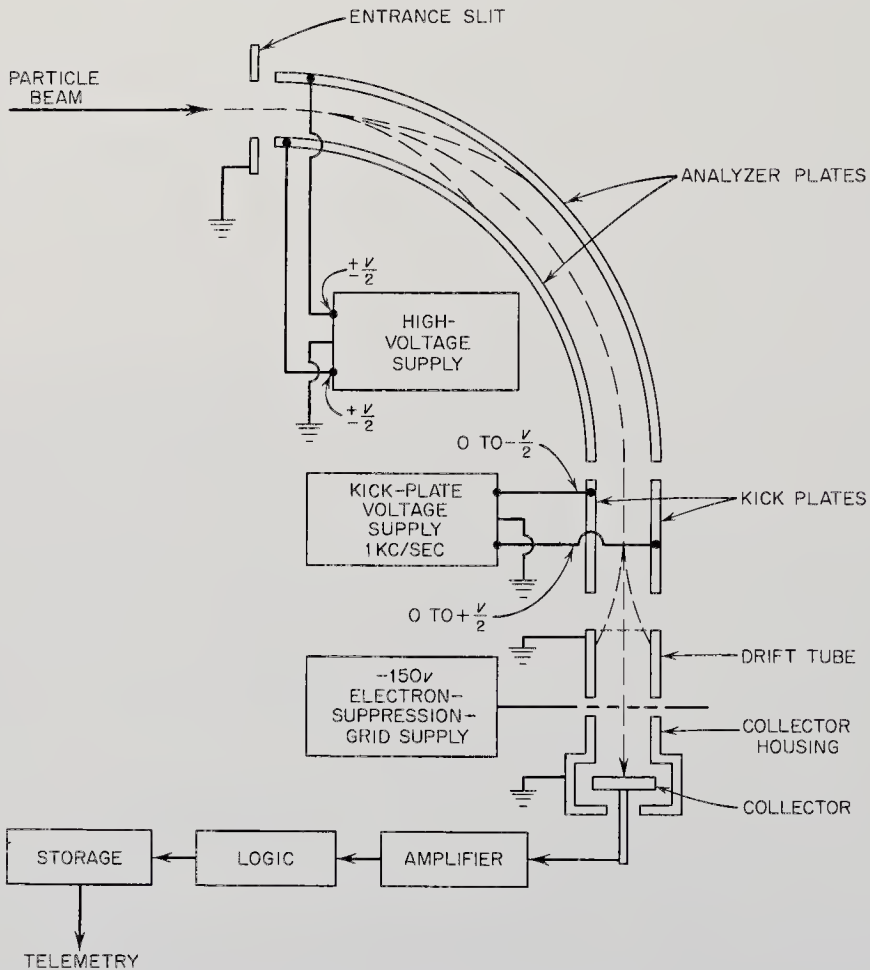


Fig. 13-46. Block diagram of the Pioneer-6 electrostatic analyzer. (NASA drawing)

Fig. 13-45, is small for cylindrical analyzers, but may be nearly  $180^\circ$  for quadrispherical analyzers. In fact, the Pioneer-6 instrument uses an array of eight detectors around the sphere rim to resolve different segments of the azimuthal flux.

At a fixed voltage, the analyzer acts like a narrow energy-to-charge-ratio filter. Voltage stepping allows it to sample different portions of the energy spectrum with time. By synchronizing the detector readings with the voltage steps, energy groups like those shown in Fig. 13-47 and Table 13-6 can be distinguished by electrostatic analyzers. Charges of both signs can be analyzed by reversing the polarity of the plates during the stepping process. Experimenters hope that the incident plasma flux will consist predominantly of protons and electrons, for analysis then is easy. If alpha particles for example are present, they will be indistinguishable from protons with the same  $E/q$ , or, equivalently,  $\sqrt{2}$  times the proton velocity. This ambiguity can be resolved only with further separation by a magnetic field.

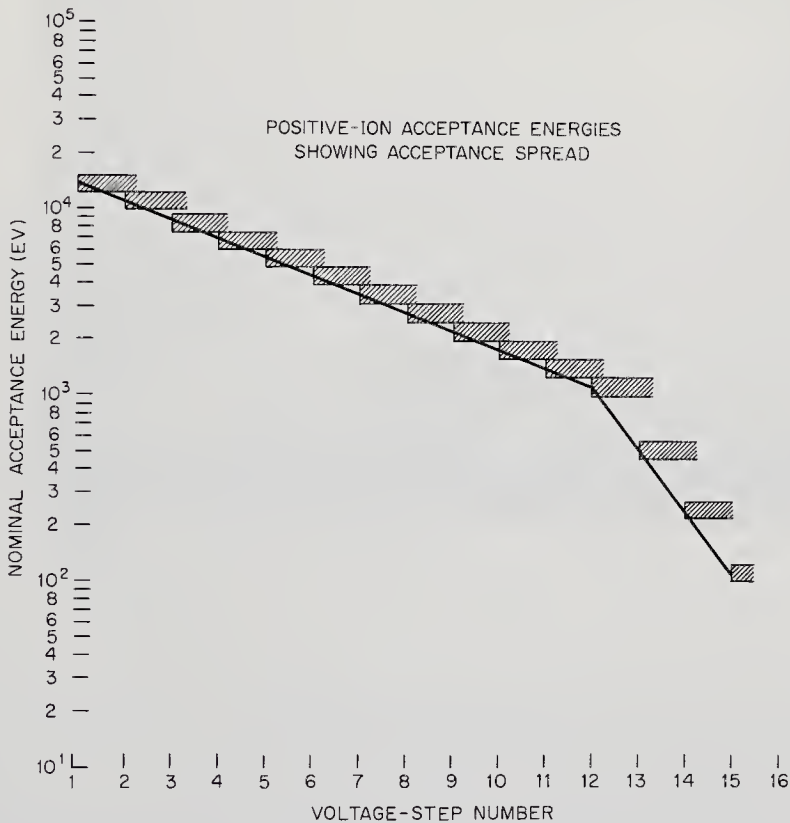


Fig. 13-47. Energy-scanning steps for positive particles (protons) for the Pioneer-6 electrostatic plasma analyzer. A similar scanning diagram exists for electrons when the plate polarity is reversed. Electron-acceptance steps are not as closely spaced. (NASA drawing)

Once a flux of charged particles reaches the detector, a usable signal must be generated. Commonly, a Faraday cup collects the charge and feeds an electrometer tube, which, in turn, is followed by several stages of amplification. Commercially available electrometer tubes can handle the currents of  $10^{-13}$  to  $10^{-7}$  amperes that typify interplanetary plasma measurements. The weak currents, though, are difficult to amplify. Beam modulation has been adopted in the Pioneer-6 instrument to produce a 1-kc, amplitude-modulated signal. The weight of the added modulation circuitry is more than offset by the more easily amplified A. C. signal.

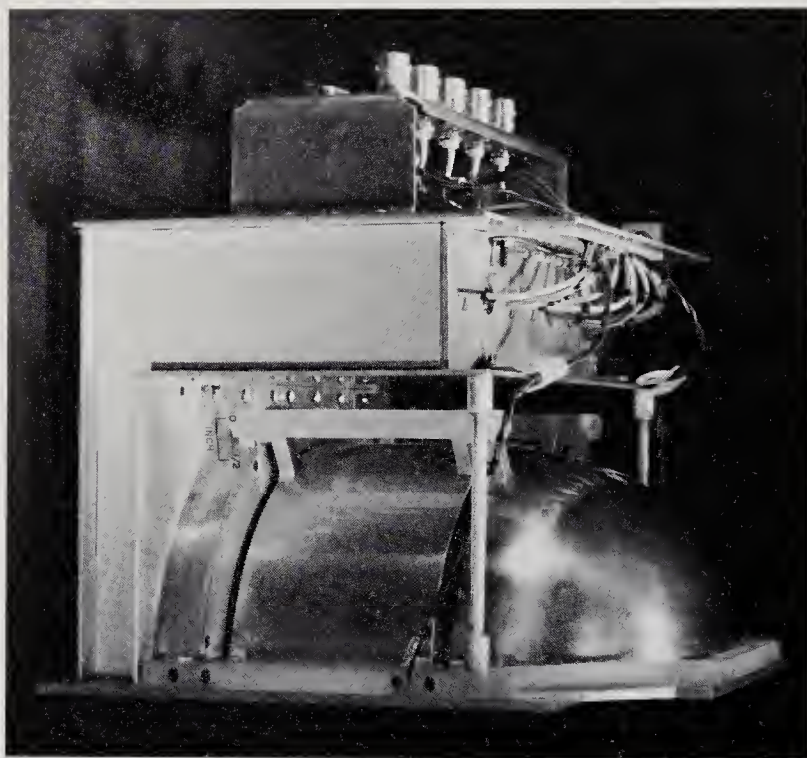


Fig. 13-48. The Pioneer-6, spherical-surface, electrostatic plasma analyzer. (NASA photograph)

Curved-surface electrostatic plasma analyzers will become increasingly sophisticated in terms of energy resolution (more voltage steps) and directional resolution (more detectors). Future analyzers may also include a magnetic stage.

Explorer 12, EGO, IMP, Rangers 1 and 2, and the deep-space probes Mariner 2 and Pioneer 6 have carried curved-surface plasma analyzers. In the case of Pioneer 6, the quadrispherical geometry illustrated in Fig. 13-45 accepts ions through a  $4\text{-cm}^2$  slit open to the environment. The



particles are separated by analyzer plates with a mean radius of 6 cm and a separation of 1 cm. The elevation acceptance angle,  $\theta$ , is about  $20^\circ$ , while particles from  $-80$  to  $+80^\circ$  in azimuth are detected by eight separate collector-electrometer circuits. Protons and electrons are separated by a series of 24 voltage steps (Fig. 13-47). Steps are triggered by the spacecraft solar aspect sensor, sixteen steps are for ions, seven for electrons, and one for a zero step. These voltage steps change so that the energy/unit charge accepted by the analyzer changes after each spacecraft revolution. At the zero-applied-voltage point, step 16, possible contributions from secondary electrons and photoelectrons, stimulated by ultraviolet light scattering into the detector, can be measured. The kick plates modulate the beam of charged particles at 1 kc. Power requirements and weights for existing space-probe plasma instruments are shown in Table 12-2.

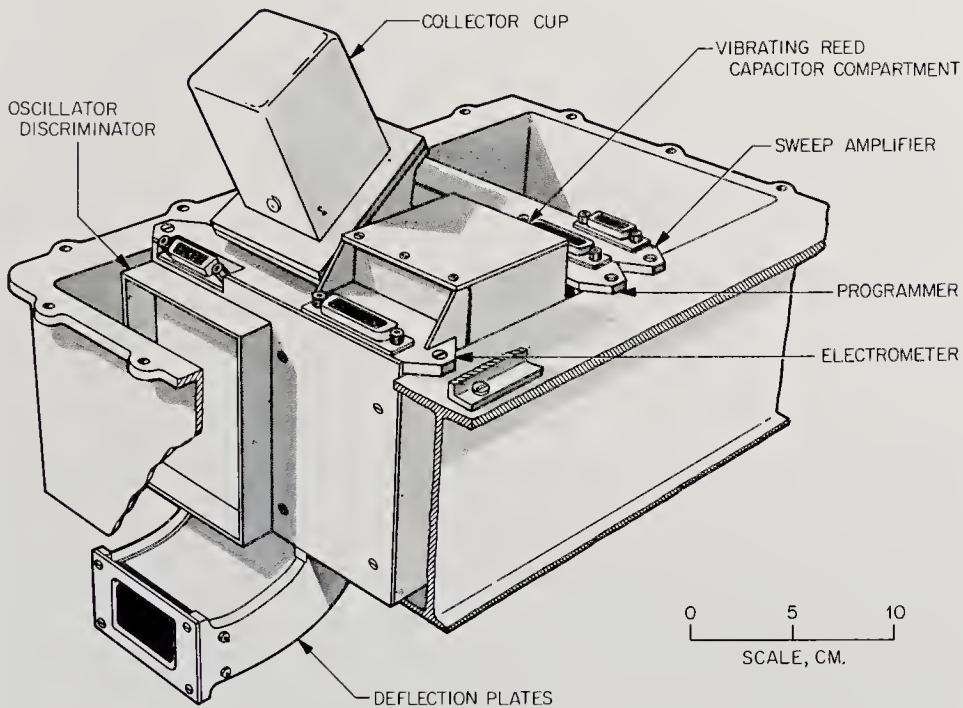


Fig. 13-49. Sketch of the Mariner-2, cylindrical-surface, electrostatic plasma analyzer. (Ref. 13-59)

The Mariner-2 plasma analyzer (Fig. 13-49) employed cylindrical plates, which gave it an acceptance cone of about  $10^\circ$  half angle. Normally, the cone was oriented toward the Sun. No attempt was made to divide the azimuthal plane, as in Pioneer 6. The two curved plates were 11.4 cm and 10.0 cm in radius and covered an angle of  $120^\circ$ . The plates

were made from gold-plated magnesium, coated inside with a layer of gold black to suppress ultraviolet scattering between the plates. There were 12 voltage steps in the 3.7-min voltage cycle, including a step for a zero-current reading and another for calibration by a standard current of  $10^{-10}$  amp. The proton energies and voltage ranges are listed in Table 13-6. Electrons were not measured. Protons (and other positively charged particles) which passed the suppressor grid were collected by a Faraday cup connected to an electrometer circuit. During the flight to Venus, this detector measured a double peak in the plasma energy spectrum that raised suspicions that there is perhaps a significant alpha particle component in the solar plasma.

TABLE 13-6. ENERGY AND VELOCITY OF PROTONS ACCEPTED BY THE MARINER-2 PLASMA ANALYZER IN ITS 10 MEASUREMENT STEPS\*

<i>Step No.</i> †	<i>Proton Energy</i> ( <i>ev</i> )	<i>Proton Velocity</i> ( <i>km/sec</i> )	<i>Plate Voltage</i> ( <i>volts</i> )
1	231	210	60
2	346	257	90
3	516	314	132
4	751	379	196
5	1124	464	290
6	1664	565	425
7	2476	689	630
8	3688	841	950
9	5408	1018	1400
10	8224	1255	2100
11	Zero current reading		-2
12	Calibration		-2

\* Ref. 13-59

† Numbers correspond to the peak of the response function for protons at normal incidence.

*Faraday-Cup Probes (Planar Probes)*. In the studies of the Earth's ionosphere, sounding rockets and satellites have carried a large variety of flush-mounted plasma probes with plane, parallel grids and collectors. With few modifications, these probes have also been employed in interplanetary plasma measurements. The gridded planar probes reject or accept charged particles in various energy ranges by stepping the voltages impressed on their grids. This method of particle energy selection has led to the use of the term "retarding-potential probes" in describing these devices. The applied electrostatic forces tend to be parallel to the ion trajectories rather than perpendicular, as they are in the curved-surface plasma analyzers. The planar probes constitute a large class. There exist many variations in geometry, number of grids, grid-modulation tech-

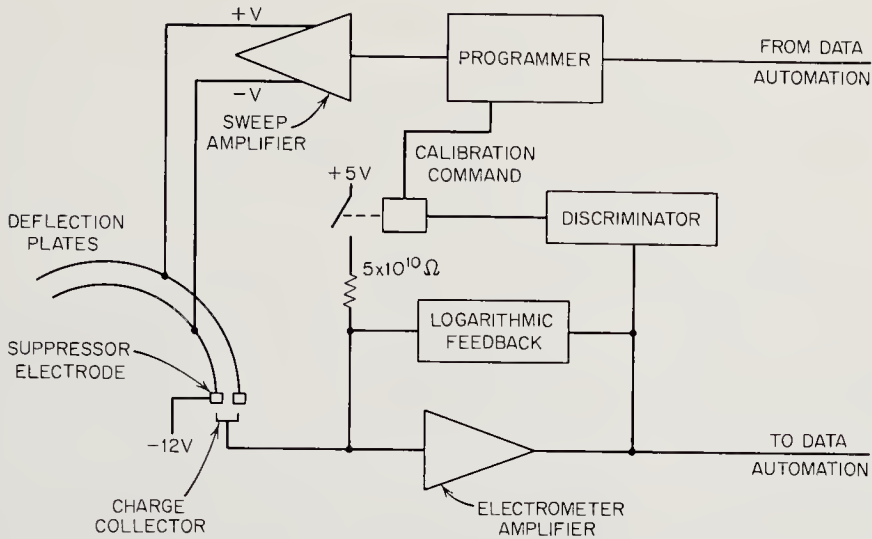


Fig. 13-50. Block diagram of the Mariner-2 plasma experiment. (Ref. 13-59)

niques, and number of collectors. Morphologically, they also bear a resemblance to the RF plasma probe, described in Chap. 14.

Explorer 8 carried a series of planar probes that merits description. The exposition logically begins with a simple, bare collector mounted flush with and electrically insulated from the Explorer-8 satellite skin (Fig. 13-51a). A collector exposed like this measures the total current of incident protons, electrons, other charged particles, and photoelectrons emitted from the collector.

The addition of a single grounded grid and a positively biased collector (Fig. 13-51b) permits the measurement of electron current as a function of satellite attitude. Ambient positive ions are repelled and photoelectrons are pulled back to the collector surface. The recessing of the collector defines a conical acceptance angle. The Explorer-8 experiment sketched in Fig. 13-51b also allows the grid to be swept from  $-1.2$  to  $+8$  volts in order to measure the spacecraft equilibrium potential and the external electron temperature (Ref. 13-9).

The addition of a second grid between the grounded outer grid and the collector enables a probe to measure positive ion and electron currents. Explorer 8 carried two of these three-element probes. One, with the inner grid at  $-15$  volts, collected incoming positive ions while repelling external electrons and suppressing internal photoelectrons. The second probe, with an inner grid bias at  $+25$  volts, measured the incident electron flux and the now unsuppressed photoemission current (Figs. 13-51c and 13-51d). Bourdeau *et al* (Ref. 13-9), at the Goddard Space Flight Center, have approximated the positive-ion current obtained with a three-element planar probe by

$$i = \alpha ANeV \cos \theta$$

- where  $i$  = the positive ion current  
 $\alpha$  = the outer-grid transparency to positive ions  
 $A$  = the probe area  
 $N$  = the ambient positive-ion density  
 $e$  = the charge on the electron  
 $V$  = the satellite velocity  
 $\theta$  = the angle with the probe axis.

This equation is accurate only when  $\theta < 45^\circ$ .

Summarizing the four Explorer-8 probes:

Probe Construction	Figure	Currents Measured
Bare collector	13-51a	electron + positive ion + photoelectron
Two elements	13-51b	electron
Three elements, + bias	13-51c	electron + photoelectron
Three elements, - bias	13-51d	positive ion

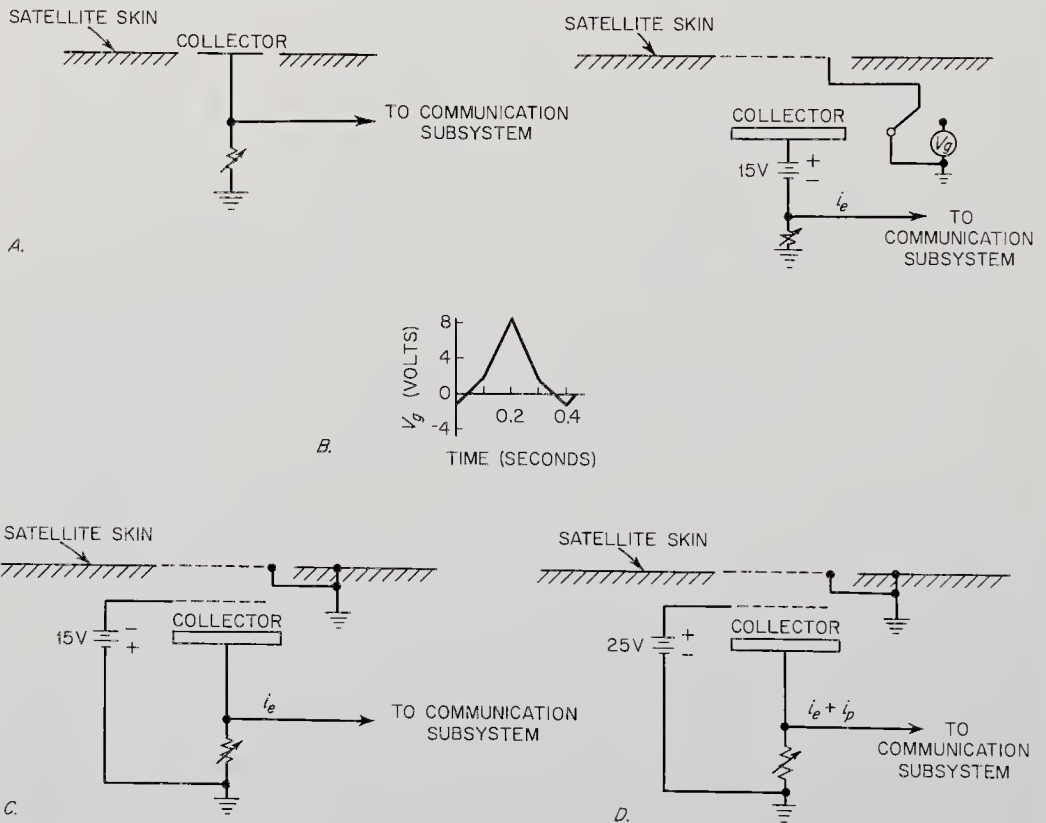


Fig. 13-51. Electrical connections for the four planar plasma probes carried on Explorer 8. a. Total current monitor. b. Electron-temperature probe. c. Ion-current probe. d. Electron-current-probe. (Ref. 13-9)

The grid voltages applied to the Explorer-8 plasma probes were low, just tens of volts. Quite obviously, such probes would not be very effective in interplanetary space, where the proton and electron energies are often measured in kilovolts. Even though the Explorer-8 probes are not directly applicable to deep space probes, only a few modifications are necessary to make them so.

The Goddard Space Flight Center thermal-plasma experiment carried on IMP was, in fact, very similar to the Explorer-8 three-electrode probe (Fig. 13-51a). Provisions were made, however, to apply a series of different grid voltages, so that an energy spectrum could be measured. Power consumption and weight information are given in Table 12-2.

Pioneer 6, Mariner 4, and IMP have all carried cup-like plasma probes designed by the MIT group (Ref. 13-12). Having the walled-in geometry shown in Fig. 13-52, they merit the Faraday-cup appellation. The placement of grids and general operation are similar to those of the unwalled probes.

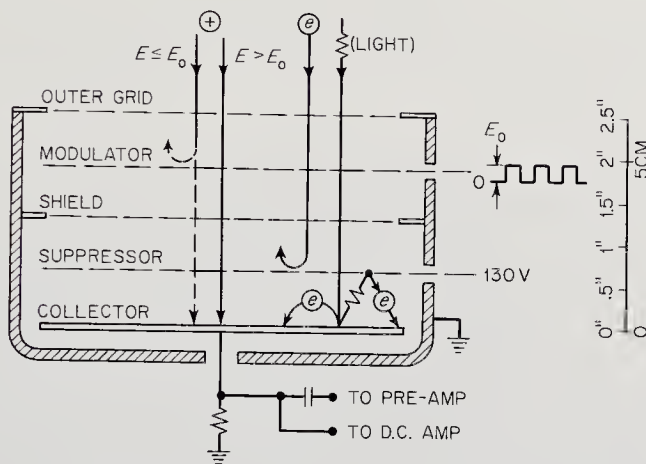


Fig. 13-52. Faraday-cup plasma probe used on Explorer 10. The IMP plasma probe is similar except for a split collector. (Ref. 13-12)

The MIT Faraday-cup plasma probe on IMP was similar to that flown on Explorer 10 except for the use of a split collector. The split detector permits angular information to be recorded, because the cup rim shadows the detectors differently for different angles of flux incidence. The IMP-probe outer grid was about 15 cm in diameter. It was kept at vehicle potential along with the two halves of the collector. Stepped voltages,  $5 < E_0 < 3000$  volts, were applied to a modulating grid, producing modulated signal for protons with energies less than  $E_0$  (ev). Protons with higher energies always reach the collector unmodulated. A shield grid prevents capacitive coupling of the modulating voltage to the

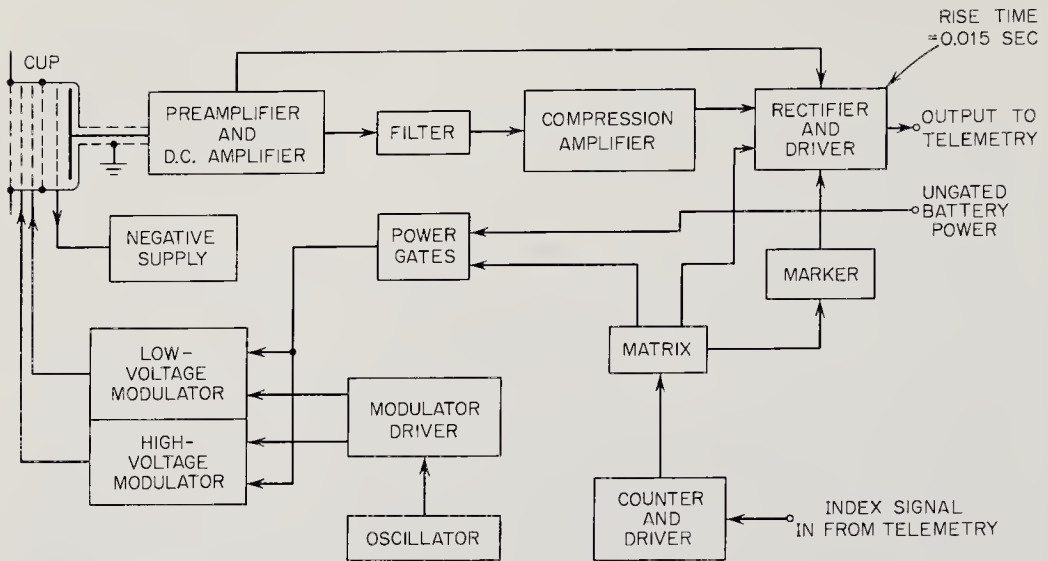


Fig. 13-53. Block diagram for the Explorer-10 Faraday-cup plasma-probe experiment. (Ref. 13-12)

collector. Photoelectrons are suppressed by a grid maintained at  $-130$  volts, located adjacent to the collector. Photoelectrons from the suppressor grid form a steady current that can be easily distinguished from modulated components. The associated circuitry is shown in Fig. 13-53.

The Pioneer-6 probe in turn resembles the IMP instrument, although it is lighter, consumes less power, and uses a smaller bandwidth as a result of the much greater communication distances and tighter performance requirements. The probe axis is perpendicular to the spacecraft spin axis and therefore scans the solar system equatorial plane. Fluxes from  $2 \times 10^5$  to  $2 \times 10^9$  singly charged particles/cm<sup>2</sup>-sec can be measured in the energy range 100 ev to 15 kev. Both ions and electrons can be measured. Sixteen contiguous energy intervals are used. One energy group is monitored for an entire spacecraft rotation for each of the 16 solid-angle windows detectable by the split detector. Sixteen vehicle rotations constitute a complete energy-solid-angle scan of 256 measurements.

Another MIT Faraday-cup probe flew on Mariner 4. The objectives of this experiment included the recording of positive ion fluxes between  $5 \times 10^5$  and  $5 \times 10^9$  particles/cm<sup>2</sup>-sec in the energy range 30 ev to 10 kev. The acceptance cone of the instrument had a half angle of  $15^\circ$  centered  $10^\circ$  off the probe-Sun line. The major geometric difference between the IMP and Mariner-4 probes was the latter's division of its collector into three  $120^\circ$  pie-shaped sectors for the more precise measurements of angular data. The modulating grid was fed a 2-ke, amplitude-modulated square wave. Altogether, there were 144 voltage steps in a complete measurement cycle. Included in the cycle were 128 current measurements

at 32 different voltages for the various combinations of collectors, plus 16 instrument status and calibration measurements.

In summary, the planar probes resemble vacuum tubes in the manner in which they modulate the incoming particles. They are manifestly simpler and lighter in construction than the curved-surface electrostatic analyzers, though their angular resolution is not as good. Planar probes are better energy analyzers at the low-energy end of the spectrum. Both probes suffer from the lack of species discrimination.

*Spherical Ion Traps.* The Russian 1961 Venus probe, the 1959 Luniks, and the 1958 Sputnik 3 all carried three-electrode spherical ion traps (Fig. 13-55). Their principle of operation is essentially identical to that of the three-electrode planar probes just described (Ref. 13-25). On Lunik 2, about which we have some information, the outer spherical grid was biased at three levels during the flight:  $-10$ ,  $-5$ , and  $0$  volts. A second, inner grid was planar and adjacent to the collector on Lunik 2, although in earlier models it was hemispherical and concentric with the outer grid. The current ranges of the Lunik-2 probe were  $10^{-10}$  to  $5 \times 10^{-9}$  amp for ions and  $10^{-10}$  to  $1.5 \times 10^{-10}$  amp for electrons. The threshold flux has been quoted as  $2 \times 10^7$  particles/cm<sup>2</sup>-sec.

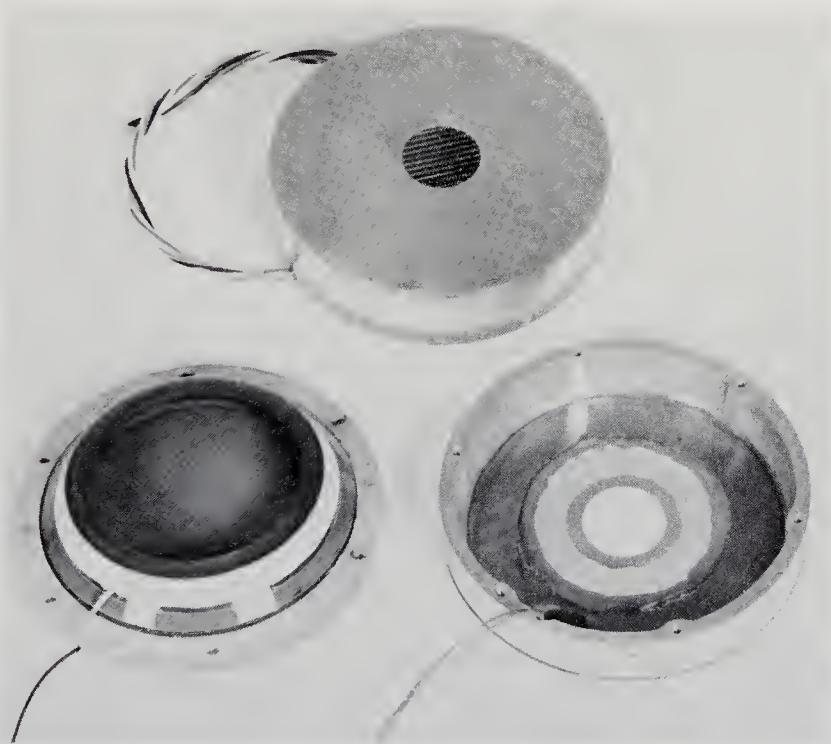


Fig. 13-54. Typical Faraday-cup, retarding-potential plasma probe. (Courtesy of the U.S. Air Force)

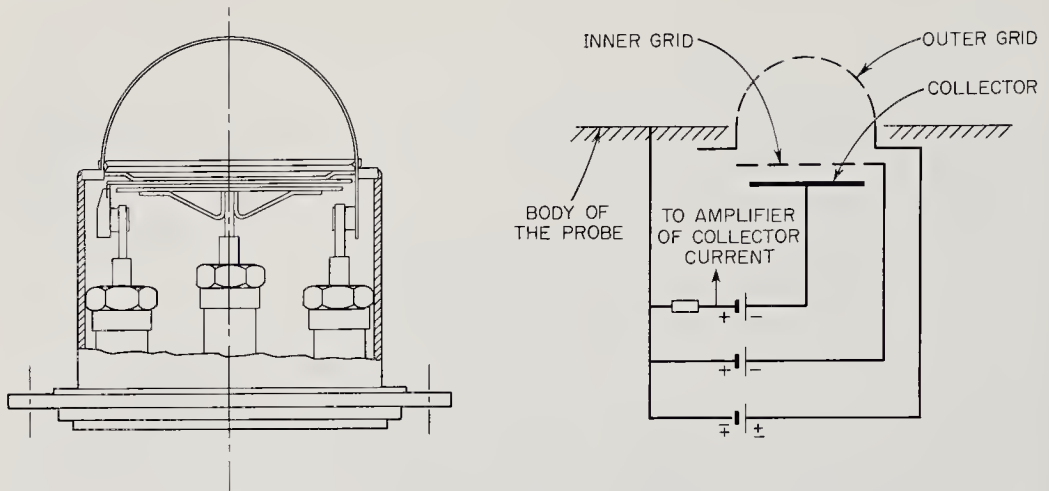


Fig. 13-55. Sketch and electrical diagram for the Lunik-2 three-electrode, spherical ion traps. (Ref. 13-26)

### 13-5. Micrometeoroid Instrumentation

The preceding three sections have dealt with the mutually interacting fields and particles that occupy interplanetary space. The fourth important component of this regime is the micrometeoroid flux; composed of those miniscule bits of matter that the Earth intercepts at speeds between 10 and 70 km/sec. These particles have essentially no interaction with the coexisting space radiation, plasma, and magnetic fields. No one yet knows how many of the micrometeoroids owe their origin to comet tails, the asteroid belt, or ejection by collision from satellite and planetary surfaces. Maps of the meteoroid distribution and chemical analysis will tell science much about the origin and evolution of the solar system. Micrometeoroids, with their capacity for spacecraft damage, present a possible hazard to manned space exploration. From this standpoint alone, it is desirable to understand them better.

The micrometeoroid properties of importance to the scientist differ substantially from those that interest the engineer. The former is concerned with a description of nature, the latter with the effects of nature. The following list of parameters illustrates this division of interest:

<i>Scientific Parameters</i>		<i>Engineering Parameters</i>
Scalar flux	Composition	Scalar flux
Direction	Structure	Direction
Velocity	Charge	Penetrating ability
Size	Radioactivity	Hole size
	Momentum	



What micrometeoroid interactions with sensors might measure the scientific parameters just listed? A meteoroid will impact the spacecraft sensor at such a high velocity that heat evolution, ionization, shock waves, sound, light, and vaporization will result. These physical phenomena form the basis for the surprising variety of micrometeoroid detectors listed in Tables 13-7 and 13-8. Note that none employ magnetic or electrostatic fields to maneuver the meteoroids; their effects are too slight. The abundance of instruments on the lists comes from the diversity of interactions between micrometeoroids and matter. In contrast, the profusion of different radiation instruments stems from combinations of a few basic detectors. Most of the micrometeoroid interactions, instead of revealing fundamental properties like mass and velocity, yield the derived quantities of momentum and energy. This is a serious deficiency when it comes to interpreting data. As with most fluxes, where the number of events recorded depends upon the detector area presented; telescopic arrangements of detectors and baffles can produce the directional information desired.

The first micrometeoroid detectors listened to the sound waves generated from impacts with spacecraft skins, and they measured the damaging effects on pressurized vessels and wire-wound grids. As we shall see, many ingenious schemes have followed, but the mainstay of space research is still the piezoelectric microphone and its close cousin, the piezoelectric ballistic pendulum. The most scientifically significant instrument developments today deal with the direct measurement of velocity through time-of-flight detectors.

Besides being sensitive over a large area, the micrometeoroid detector must, like all space instruments, be rugged, reliable, light-weight, and draw little power. The most serious interface of the sound-sensitive detectors is with spacecraft internal noise (relays, etc.). Detectors using scintillators and photosensitive elements may also be triggered by space radiation and sunlight. Shields and covers are required if discrimination is not feasible. All micrometeoroid sensors compete with other scientific instrumentation for solid angle.

Calibration of micrometeoroid sensors has proven to be a major problem, because terrestrial facilities cannot duplicate the extreme micrometeoroid velocities. Light-gas guns and explosive devices can produce fragments of matter in the lower end of the velocity spectrum. Electrostatic accelerators of charged dust particles are beginning to invade the middle range. As things stand now, we do not know precisely what our micrometeoroid detectors actually measure in space. The historical calibration technique of dropping glass beads on piezoelectric microphones (see page 367) was necessary and reassuring, but possibly misleading.

TABLE 13-7. MAJOR TYPES OF MICROMETEOROID DETECTORS USED IN SPACE RESEARCH\*

<i>Instrument</i>	<i>Principle of Operation</i>	<i>Utility and Missions</i>	<i>Remarks</i>
Piezoelectric microphones	Impact generates elastic waves in plate. Piezoelectric crystal transforms them into electrical signal.	Measures some undetermined function of mass and velocity. Mariner 2, Mariner 4.	Most common micrometeoroid experiment.
Piezoelectric ballistic pendulums	Impact moves ballistic pendulum. Piezoelectric crystals are flexed, generating electric signal.	Measures momentum.	
Capacitor detectors	Passage of particle through metal foil and dielectric causes temporary short and capacitor discharge.	Records event only. Mariner 4.	Used in time-of-flight experiments and as direction indicator.
Light-flash detectors	Impact on crystal causes scintillation which triggers a photomultiplier tube.	Flash proportional to energy. Very sensitive.	Can use with momentum detector to separate mass and velocity.
Wire grids	Impact breaks wire opening an electrical circuit.	Records event. Relation to mass, diameter, and velocity vague. Several satellites.	Engineering experiment. One event per detector.
Pressurized cans	Impact punctures can, releasing gas inside. Pressure-sensitive switch relays signal.	Records event. Relation to mass, diameter, and velocity vague. Several satellites.	Engineering experiment. One event per detector.
Light-transmission erosion experiments	Impact removes bit of opaque layer covering a light-sensitive detector. Sunlight generates signal.	Records event. Relation to mass, diameter, and velocity vague.	Very sensitive.
Time-of-flight experiments	Time of flight over fixed length measured by two "event" recorders.	Measures velocity directly.	Complex.

\* See Table 13-8 for micrometeoroid detectors of lesser importance.

Happily, the calibration problem promises to be solved within the next few years.

*Piezoelectric Microphones.* Many scientific satellites and most space probes have included a micrometeoroid microphone in their inventories of instruments. A thin metal plate with a small piezoelectric crystal bonded to it makes a simple, rugged, and esthetically appealing space instrument (Fig. 13-56). Some questions, however, must be asked about

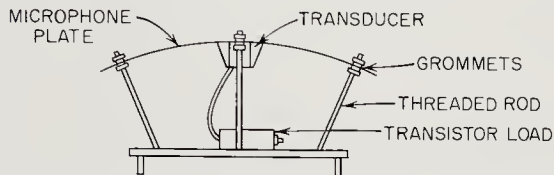


Fig. 13-56. Sketch of the Pioneer-5 microphone-type micrometeoroid detector.

such an instrument. What properties of the meteoroid are actually measured? How is the detection of internal spacecraft mechanical noise avoided? How can the microphone be calibrated?

Consider what happens when a minute bit of matter weighing perhaps  $10^{-12}$  g impacts a metal sheet at 50 km/sec. Some of the micrometeoroid's kinetic energy obviously goes into physically damaging the plate (pitting). This destructive effect has spawned a whole series of other detectors, described later in this section. Another part of the energy is transformed into elastic vibrations, or sound waves, in the plate. The waves propagate outward from the impact point and are distorted by and reflected from plate mountings and edges. The sonic energy of the waves can be coupled to a piezoelectric crystal (made, say, of ammonium phosphate), which will produce an electrical "ringing" signal, an exponentially damped wave train at the characteristic frequency of the plate-crystal assembly. By shaping and bending the plate, perhaps even serrating its edges, wave distortion can be minimized and the entire plate made of relatively uniform impact sensitivity. By decoupling the plate from the spacecraft proper with absorber mountings, internal noise due to solenoids, relays, servo motors, etc., can be attenuated by as much as 80-100 db.

Noise interference can also be reduced considerably by using sensor characteristic frequencies well above the interfering frequencies. It is customary, for example, to tune the stages amplifying the sensor signals to 100 kc.

Early sounding rockets and satellites often attached a piezoelectric crystal transducer directly to the vehicle skin and counted the signals received. This procedure had the advantages of simplicity and large de-

tector areas, but the elastic waves were considerably distorted by the skin structure and internal noise. Understandably, sensor sensitivity varied with impact location. Today, the separate impact plate is the accepted approach.

The voltage peaks produced by the piezoelectric crystals are roughly proportional to the perpendicular component of the impacting particle's momentum at velocities below 10 km/sec when the crystal is compressed along one of its axes. At actual meteoroid velocities, 10 to 70 km/sec relative to the Earth, the relationship is confused. Some results show that the signal amplitude is proportional to the particle's energy rather than momentum. Other data indicate proportionality to (momentum)<sup>1.5</sup>. Until electrostatic accelerators of charged dust (similar to those used in nuclear research) thoroughly explore the high-velocity part of the spec-

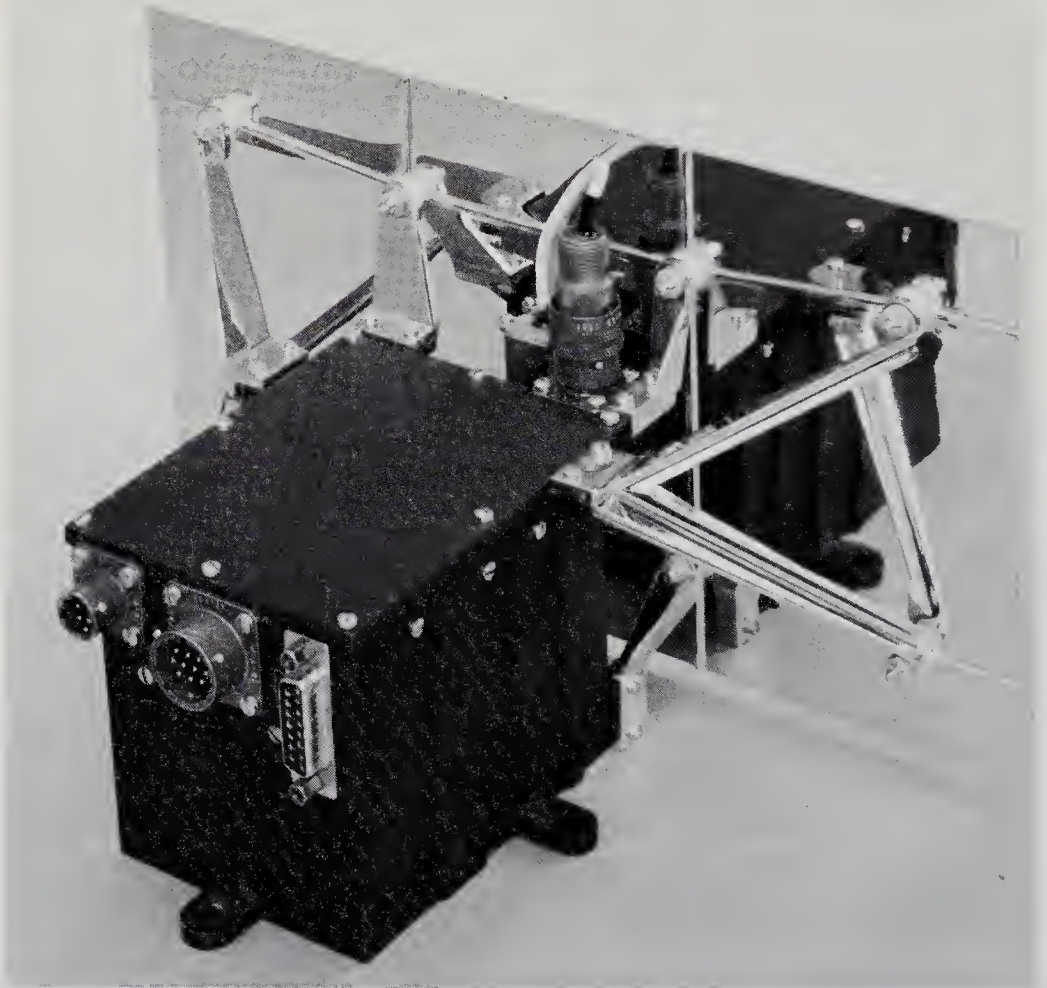


Fig. 13-57. Rear view of the Mariner-2, microphone-type micrometeoroid detector. (Ref. 13-59)

trum, microphone momentum data will be questionable, though impact frequency data are not affected.

Piezoelectric microphones are commonly calibrated by dropping small glass beads a few hundred microns in diameter onto a plate from a height of a few centimeters. Signal amplitudes can then be related to the known momenta of the dropped beads. Spacecraft instruments sometimes employ piezoelectric transducers in reverse for in-flight calibration. That is, an electrical calibrating signal will stimulate a separate piezoelectric crystal to produce a known mechanical impulse to the plate, which is then picked up by the regular crystal sensor.

All of the interplanetary probes have carried piezoelectric instruments, though the first IMP satellite did not. Pioneer 5, Mariner 2, and Mariner 4 used the more or less conventional piezoelectric microphones. V. Rogallo, of NASA's Ames Research Center, has invented a micrometeoroid detector using the piezoelectric crystal in a bending mode, making the instrument effectively a ballistic pendulum rather than a microphone. The following descriptions of the specific instruments will show the trend toward multidetector instruments.

Pioneer 5 employed a curved aluminum plate, 0.038 m<sup>2</sup> in area, mounted to the spacecraft at six points by rubber grommets (Fig. 13-56). Only two pulse-height levels were analyzed. These corresponded to momenta of  $1 \times 10^{-4}$  and  $0.54 \times 10^{-2}$  dyne-sec. Table 12-2 presents weight- and power-requirement data for this and other probe instrumentation.

The Mariner-2 micrometeoroid detector was generally similar to that

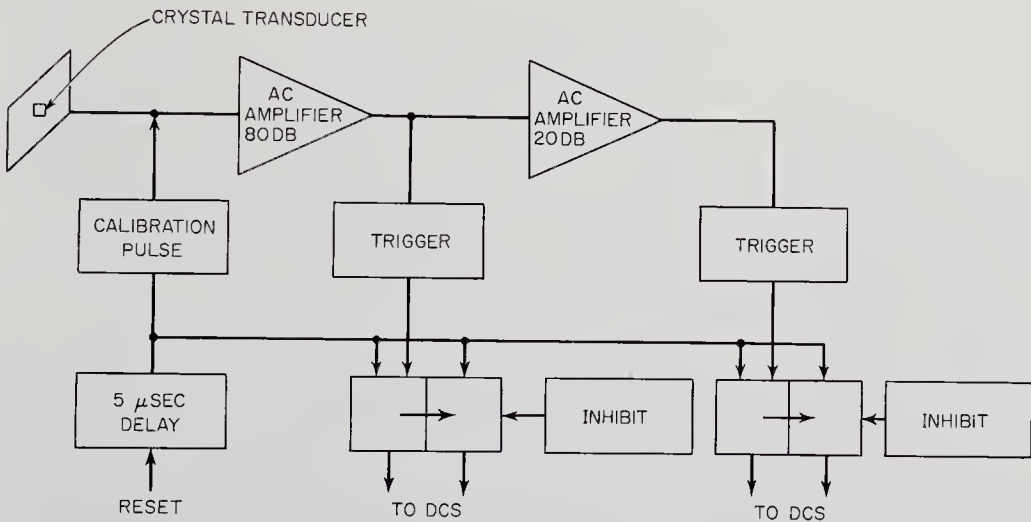


Fig. 13-58. Block diagram of the Mariner-2 micrometeoroid experiment. (Ref. 13-59)

on Pioneer 5. A 0.035-m<sup>2</sup> magnesium plate (14 × 25 cm) was bonded to a crystal whose output fed amplifiers tuned to 100 kc (Figs. 13-57 and 13-58). Again there were two pulse-height channels. The threshold sensitivity for the lower channel varied from 0.9 to 1.1 × 10<sup>-4</sup> dyne-sec over 99% of the exposed area of the plate. The detector was so mounted on the Mariner-2 spacecraft that it pointed forward, in the direction of motion, during the first part of the flight and backward during the last part. It was hoped that a crude idea of the relative magnitudes of the normal and retrograde meteoroid fluxes could be gained by such an arrangement. Unfortunately, the meteoroid flux turned out to be so low that only two impacts were recorded during the entire flight to Venus, and no statistics are available.

The Mariner-4 instrument is a still more sophisticated microphone detector. The basic sensor is an aluminum impact plate 0.076-cm thick, with an area of 0.04 m<sup>2</sup>. The advance over the Mariner-2 instrument was in the use of 5000Å layers of SiO<sub>2</sub> dielectric attached to both faces of the aluminum impact plate. The dielectric then received an evaporated layer of aluminum film to form two capacitors, back to back. (See the later description of capacitor detectors.) Micrometeoroid penetrations of the capacitors cause transient electrical shorting. The electrical signals thus generated indicated not only the side of the plate that was struck but also the total hits down to a threshold of about 10<sup>-6</sup> dyne-sec, an order of magnitude lower than that of the microphone. The output of the lead-

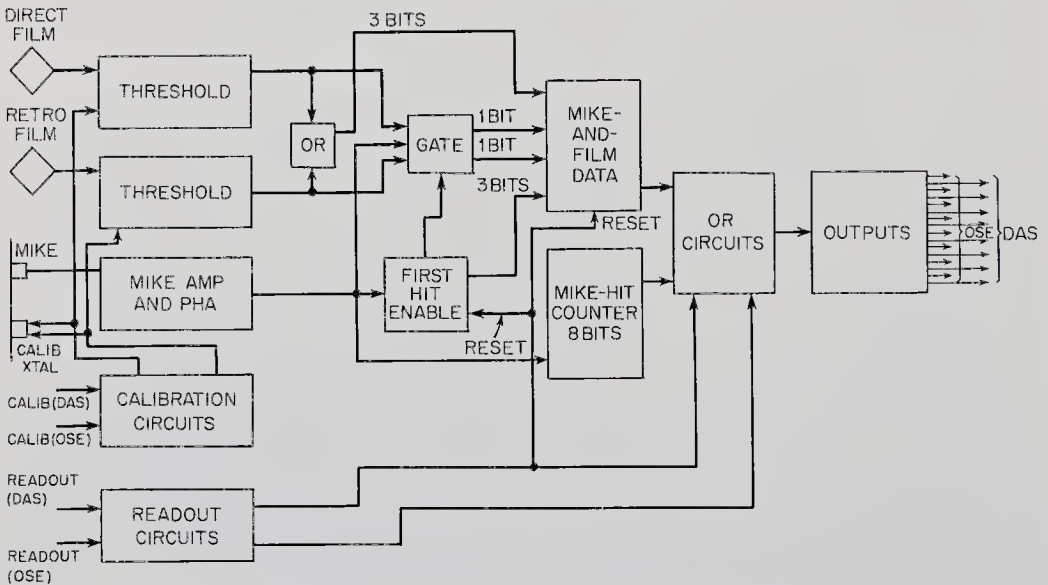


Fig. 13-59. Block diagram of the Mariner-4 microphone-type micrometeoroid experiment. Direction information is derived from the films covering the impact plate. (NASA drawing)

zirconate piezoelectric crystal was fed through amplifiers tuned to 100 kc and then pulse-height-analyzed (Fig. 13-59). Mariner 4 had an in-flight calibration scheme consisting of a separate crystal transducer bonded to the impact plate. When triggered by command, the crystal alternately produced two mechanical signals corresponding to known momentum levels. The microphone sensitivity was about  $10^{-5}$  dyne-sec. The capacitor could detect masses as low as  $10^{-13}$  g with velocities of greater than 1.8 km/sec.

*Piezoelectric Ballistic Pendulums.* The piezoelectric microphone just described uses the crystal detector in its acoustic mode; that is, the vibrations are perpendicular to the bonded axis. The piezoelectric effect is also observed when crystals are suddenly flexed or bent by shear forces. An impact plate, mounted as shown in Fig. 13-60, will transmit shear forces to the crystal when struck by a meteoroid. In effect, we have a ballistic pendulum (Fig. 13-61). Experiments have shown that such a mounting produces electrical signals that are more nearly proportional to the momentum of the impacting particle. Furthermore, the signals are proportional to that component of momentum perpendicular to the plane of the impact plate. The sensitivity threshold of the ballistic pendulum is estimated to be as low as  $10^{-6}$  dyne-sec, so low that spacecraft noise and solar pressure fluctuations due to the spacecraft's spin are limiting conditions. Such characteristics, high sensitivity and momentum proportionality, make the piezoelectric ballistic pendulum a welcome addition to the family of micrometeoroid detectors.

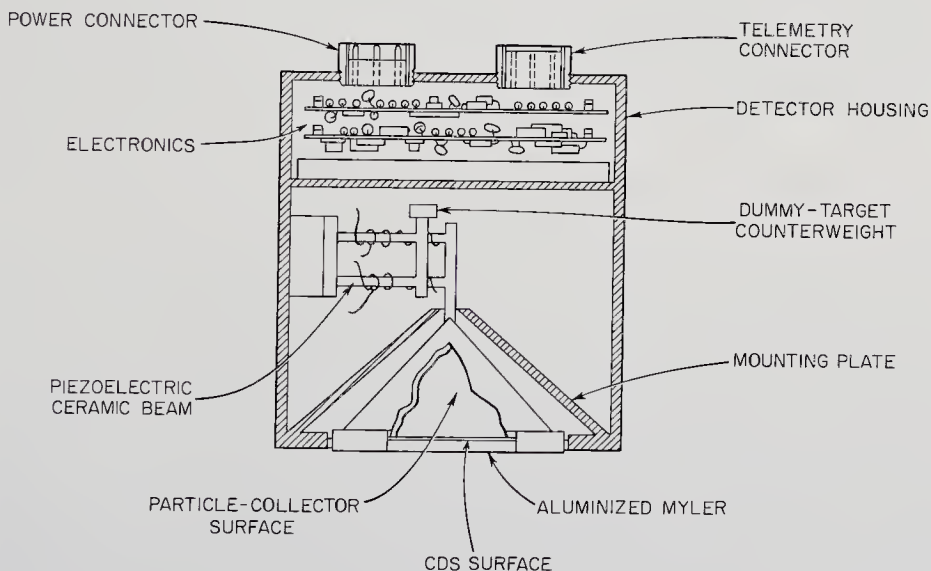


Fig. 13-60. Sketch of the Ames Research Center ballistic-pendulum micrometeoroid detector. (NASA drawing)

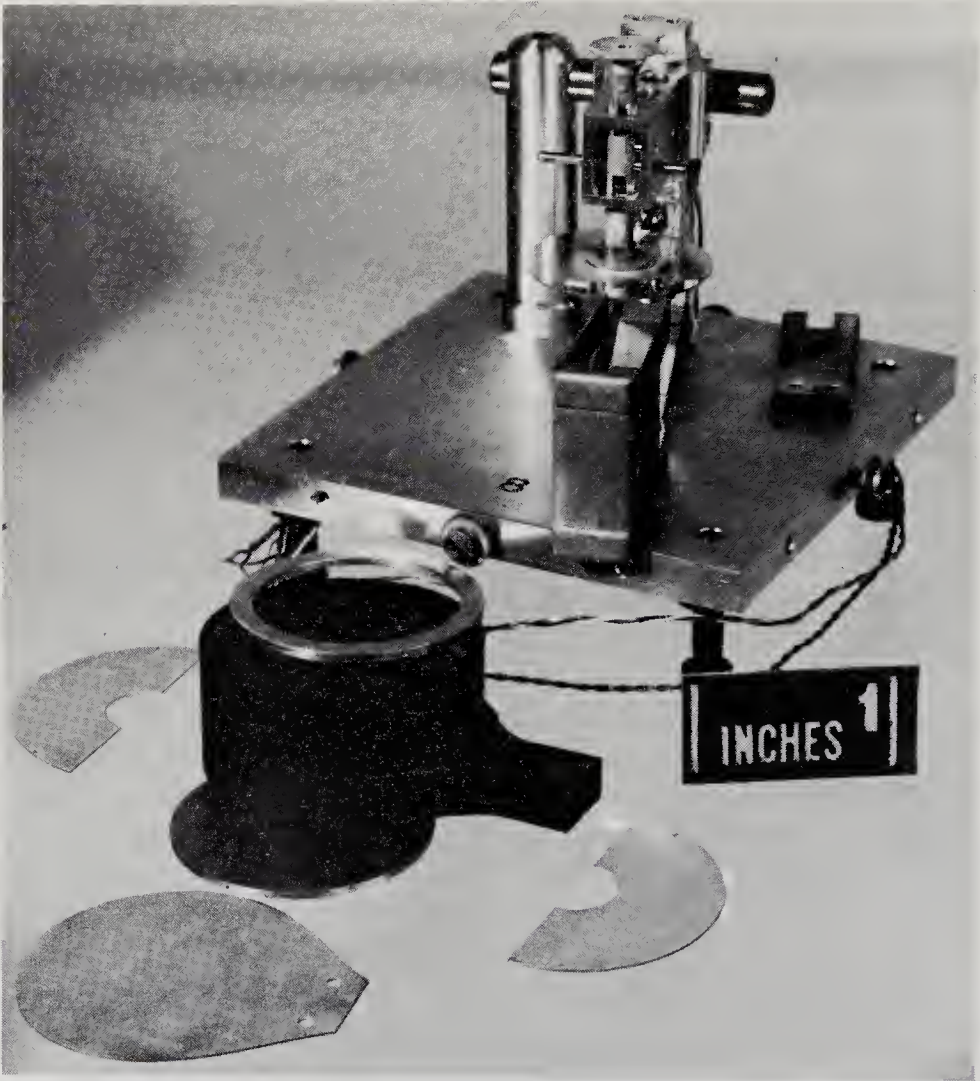


Fig. 13-61. Prototype of the Ames Research Center ballistic-pendulum micro-meteoroid detector. The sounding board is mounted on piezoelectric beams. (NASA photograph)

*Thin-Film Capacitor Detectors.* If a thin layer of dielectric is pierced by a high-velocity micrometeoroid, the trail of ionization and disruption creates a temporary conduction path. By evaporating a thin metallic coat on the side of the dielectric facing the environment, and bonding the other side to a metal plate or perhaps another evaporated metal film, a capacitor detector can be built. This detector will discharge the condenser and generate a signal every time the dielectric is breached. After the event, the ions will recombine and the condenser can be recharged for another event. In practice, capacitor detectors are made by spraying a layer of alumina ( $\text{Al}_2\text{O}_3$ ) on a metal plate and then coating it with



aluminum. Or a detector relatively transparent to micrometeoroids can be made by aluminizing both sides of a thin Mylar plastic film. Two such film-like detectors can then be used to signal the flight of a micrometeoroid over a fixed course in time-of-flight experiments discussed later. The capacitor detector, of course, provides event information only and says nothing about the micrometeoroid properties themselves. It is planned to cover large areas (hundreds of square meters) of spacecraft skin with an aluminized Mylar capacitor detector in future engineering studies.

*Light-Flash Detectors.* When a high velocity micrometeoroid hits a scintillator crystal, a great deal of energy is released in the small volume around the point of impact. The heat, shock waves, and ionization cause the crystal to emit a flash of light, just as it does when penetrated by ionizing radiation (See Sec. 13-3.). The amplitude of the light pulse is proportional to the amount of energy imparted to the crystal. The photons from the event are converted into an electrical signal by a photomultiplier tube adjacent to the scintillator (Fig. 13-62). A pulse-height

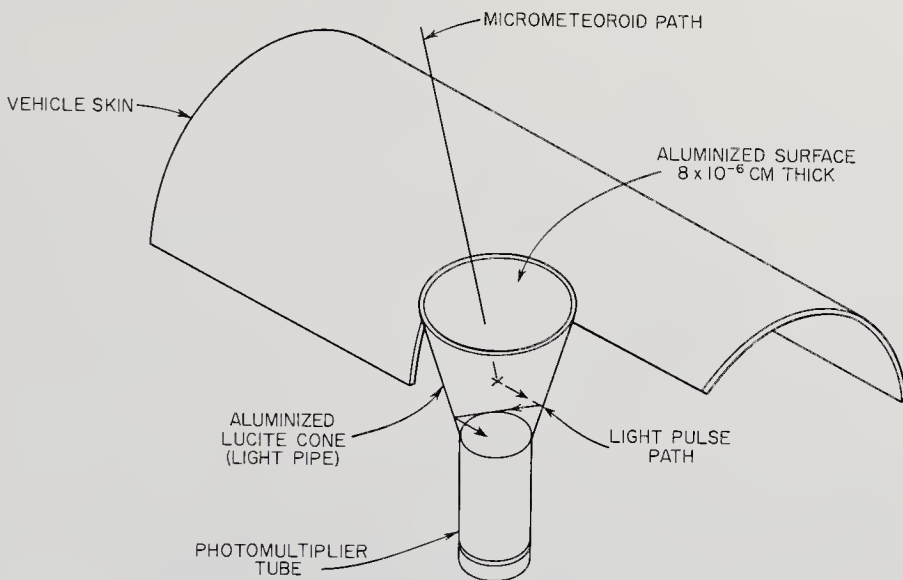


Fig. 13-62. Schematic of a light-flash micrometeoroid detector. (Ref. 13-22)

analyzer following the photomultiplier tube will sort the impacts out according to the amplitudes of the light flashes, which in turn can be related to the particle energy through preflight calibration. The light-flash detector is also sensitive to penetrating radiation, but such signals can be discriminated against by guard counters, like those used in radiation detectors. Some crystals, notably cadmium sulfide, are also photo-

conductive, necessitating an opaque covering. As a family, light-flash detectors are extremely sensitive, probably the most sensitive of all micrometeoroid detectors. Thresholds are as low as  $10^{-14}$  g at 2 km/sec or, equivalently,  $2 \times 10^{-11}$  dyne-sec. The sensor signal is proportional to energy rather than momentum, which brings forward an interesting possibility. A combination instrument using a momentum-sensitive microphone and an energy-sensitive light-flash detector can, though simultaneous measurements, separate the mass and velocity parameters.

Light-flash detectors have been used on Ranger 1 and Explorer 8, but not on any interplanetary probes to date.

*Pressurized Cells.* Here is a very straightforward type of micrometeoroid detector. A particle penetrates a pressurized vessel, usually a cylinder; the gas inside escapes; and a pressure switch sends an electrical signal to the communication subsystem. The cell is useless after one puncture, and information about the meteoroid itself is limited to the knowledge that a certain thickness of metal has been penetrated. Pressurized-cell data are therefore of primary interest to spacecraft designers. Cells with different wall thicknesses can, of course, provide crude size-and-velocity data if reliable terrestrial calibration is available. It has also been proposed that the rate at which gas escapes from a punctured cell measures the hole size and, indirectly, the micrometeoroid size. Here, again, calibration is difficult, because hole size is a complex function of particle energy, mass, size, and possibly shape. Furthermore, the rate of pressure loss would be a parameter difficult to measure and telemeter. Finally, the walls of the pressure cells that are commonly used are very thin ( $25\text{-}100 \mu$ ), and they must be well-protected during the spacecraft launching.

Vanguard 3 carried  $0.162 \text{ m}^2$  of exposed pressure-cell surface in the

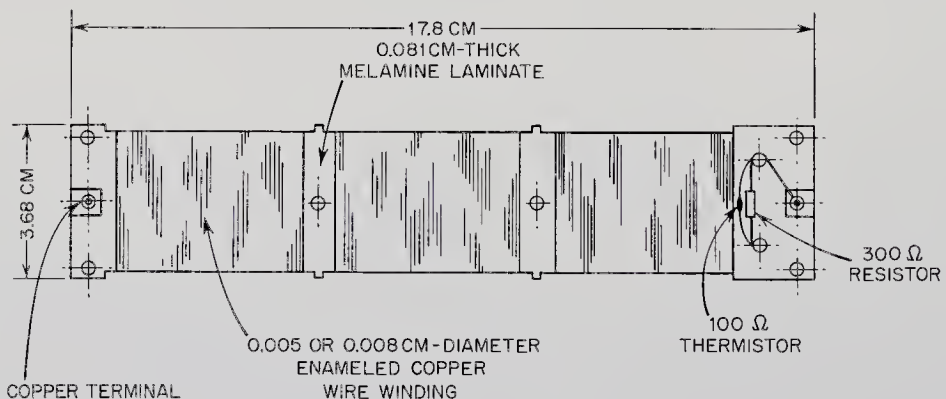


Fig. 13-63. Pressurized cylinders used on Explorer 16 for micrometeoroid puncture detection. (Ref. 13-27)

form of two cylinders with 0.066-cm magnesium walls. The major use of pressure cells to date was on Explorer 16, the Micrometeoroid Satellite. Here, 160 beryllium-copper cylinders were mounted around the final stage rocket. Each cell was filled with helium and included a pressure-sensitive switch (Fig. 13-63). Three different wall thicknesses, 25, 51, and 127  $\mu$  (0.001, 0.002, 0.005 in.), were used. Altogether, the cylinders exposed 0.156 m<sup>2</sup> of area to the environment (Ref. 13-27).

*Wire-Grid Detectors.* The destructive properties of micrometeoroids are put to good use in the wire-grid sensors. The usual form taken is that of enamel-wire-wound cards electrically connected in parallel (Fig. 13-64). A micrometeoroid large enough to sever a wire removes the struck

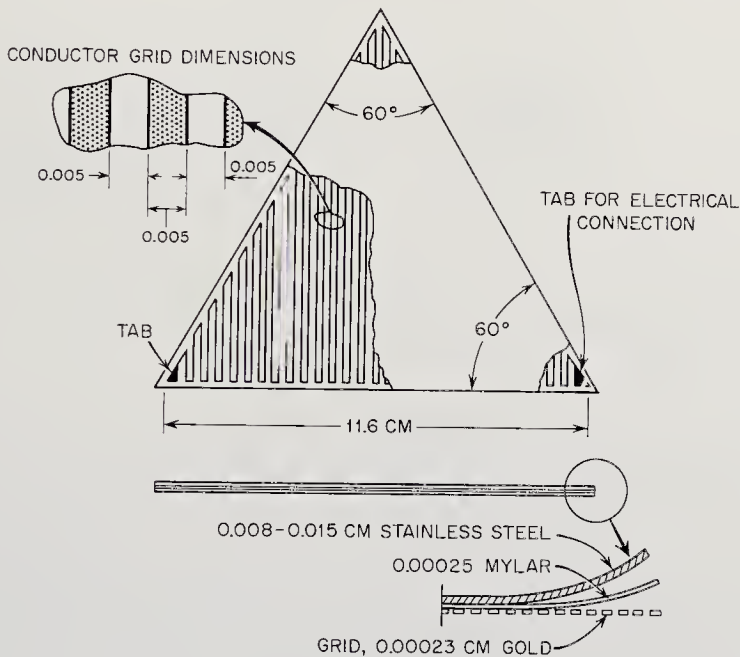


Fig. 13-64. Wire-grid detectors carried on Explorer 16. (Ref. 13-27)

card from the circuit and changes the over-all electrical resistance. This kind of event is convenient to telemeter. But just what does a severed wire mean in terms of micrometeoroid properties? The effect depends upon the particle's size and energy as well as the diameter and composition of the broken wire. Low-velocity calibration experiments have indicated that micrometeoroids may break wires twice their own diameter, but the effects of velocity and wire composition are still vague. At the least, a severed wire signals an event; at the best, there is a crude measure of the micrometeoroid's destructive properties. Although wire-wound cards are light and simple, they are limited to one event apiece,

and even that event yields little information about mass, velocity, and direction. The cards also draw electrical power until a wire is broken.

The first Explorer satellites carried wire grids. The Micrometeoroid Satellite (Explorer 16) used 46 cards like those sketched in Fig. 13-65 and

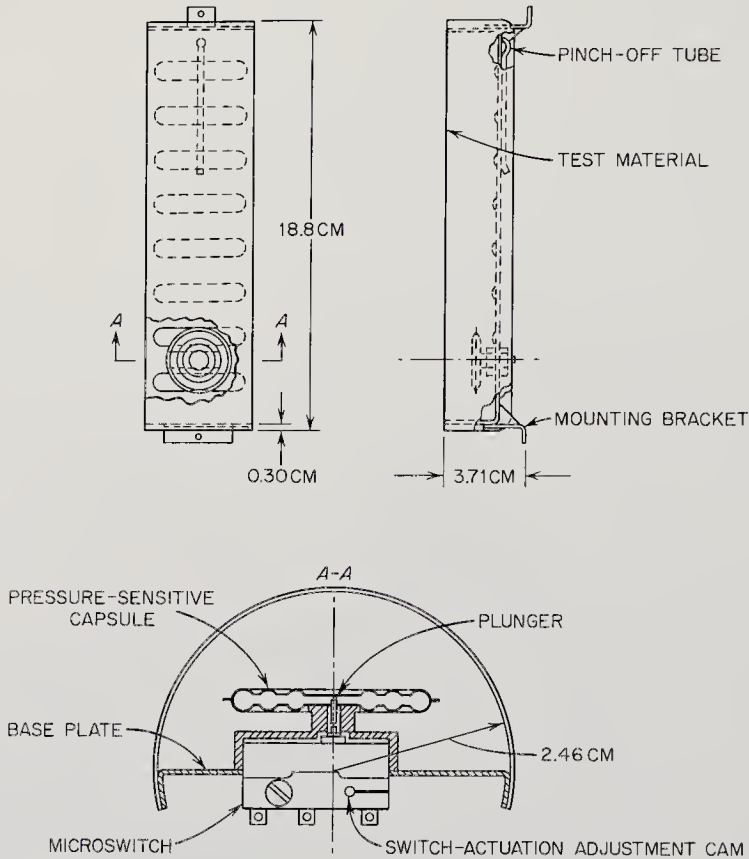


Fig. 13-65. Special wire-grid detector carried on Explorers 13 and 16 (Refs. 13-27 and 13-37)

also carried a more refined detector based on the same principles of operation. Thin grids of conducting gold were deposited on the bottoms of stainless-steel sheets of different thicknesses. A particle penetrating the steel sheet would almost invariably break one of the current channels underneath. Much better engineering penetration data can be recorded in this way (as was the intent) but little is revealed about the intrinsic properties of the bombarding particle.

*Light-Transmission Erosion Detector.* The destructive properties of micrometeoroids are used for measurements in still another way. Holes made by impacts on an opaque film will transmit light in proportion to the collective area of the holes. Hole area can be related empirically

to micrometeoroid diameter on a hypervelocity particle range, but, as usual, the adequacy of velocity simulation is a problem. Either a photomultiplier tube or a photoconductive cell (CdS) can be used as the light detector, the latter being simpler and more rugged but not as sensitive. Holes as small as one and two microns in diameter can be detected. Like most sensors depending upon destructive effects, this type provides only meager information about the meteoroid mass, velocity, and direction.

Light-transmission experiments have flown on Explorers 7, 8, and 16. The Explorer-16 cadmium-cell detector (Fig. 13-66) is perhaps typical

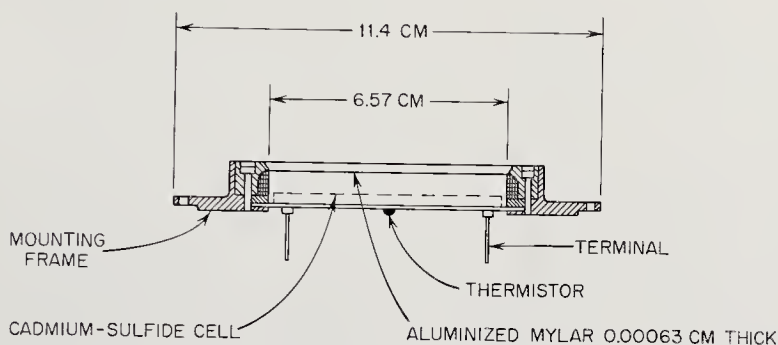


Fig. 13-66. The Explorer-16 light-transmission micrometeoroid detector. Resistance of the CdS cell drops as sunlight passes through holes in the opaque covering. (Ref. 13-27)

of the light-transmission approach. Two such cells, with a total effective area of 48 cm<sup>2</sup>, were deployed on the satellite surface. Explorer 8, in contrast, adopted the photomultiplier-tube approach. Approximately 1000A of aluminum were evaporated onto the face of a commercial photomultiplier tube. Terrestrial calibration indicated that particles as small as 10<sup>-13</sup> g would generate usable signals.

*Miscellaneous Detectors.* Micrometeoroid-detector concepts are legion. Some of the lesser concepts listed in the following table are only ideas; some are in the development stage; some have been tried only to be discarded (Table 13-8).

*Time-of-Flight Measurements.* Since the micrometeoroid velocity is not directly related to the parameters actually measured by most detectors, there has been considerable thinking done about time-of-flight experiments. The average micrometeoroid travels at about 30 km/sec. If there is a distance of 10 cm between two event counters, the associated electrical circuits will have to measure times on the order of two microseconds, an easy feat for today's electronics. The first event detector must be "transparent" and capable of repeated use. Included in this category are the capacitor detector, the plasma detector, the charge-flow detector,

TABLE 13-8. MISCELLANEOUS MICROMETEOROID DETECTORS

<i>Name</i>	<i>Physical Principles</i>	<i>Status</i>
Plasma detector	Trail of plasma left in gas is detected by charged electrodes, in the fashion of ionization chambers.	Idea
Strain-gauge detector	Thin foil transmits impact distortions to strain gauges bonded to rear surface.	In development
Foil-strip erosion detector	Micrometeoroids abrade foil strip, increasing its electrical resistance. Experiments showed punctures instead of erosion.	Discarded (Used on Vanguard 3)
Radioactive-coating erosion detector	Thin surface layer of radioactive material is eroded away, reducing signal to radiation detector.	Idea
Rotating-drum or -vane detector	Slotted drum or vane rotates at high speed. When particle passes through two drum slots, time of flight can be calculated.	Discarded
Crystal erosion detector	Surface of crystal in crystal-controlled oscillator is eroded, changing its characteristic frequency.	In development
Charge-flow detector	Most micrometeoroids are photoelectrically charged. Their passage can be detected by grids and electrodes.	In development
Scattered-light detector	Photons scattered off micrometeoroids are detected by photomultiplier tube.	Idea
Beta back-scattering detector	Back-scattered portion of beta beam is function of thin-target thickness. Erosion rate measured.	Discarded

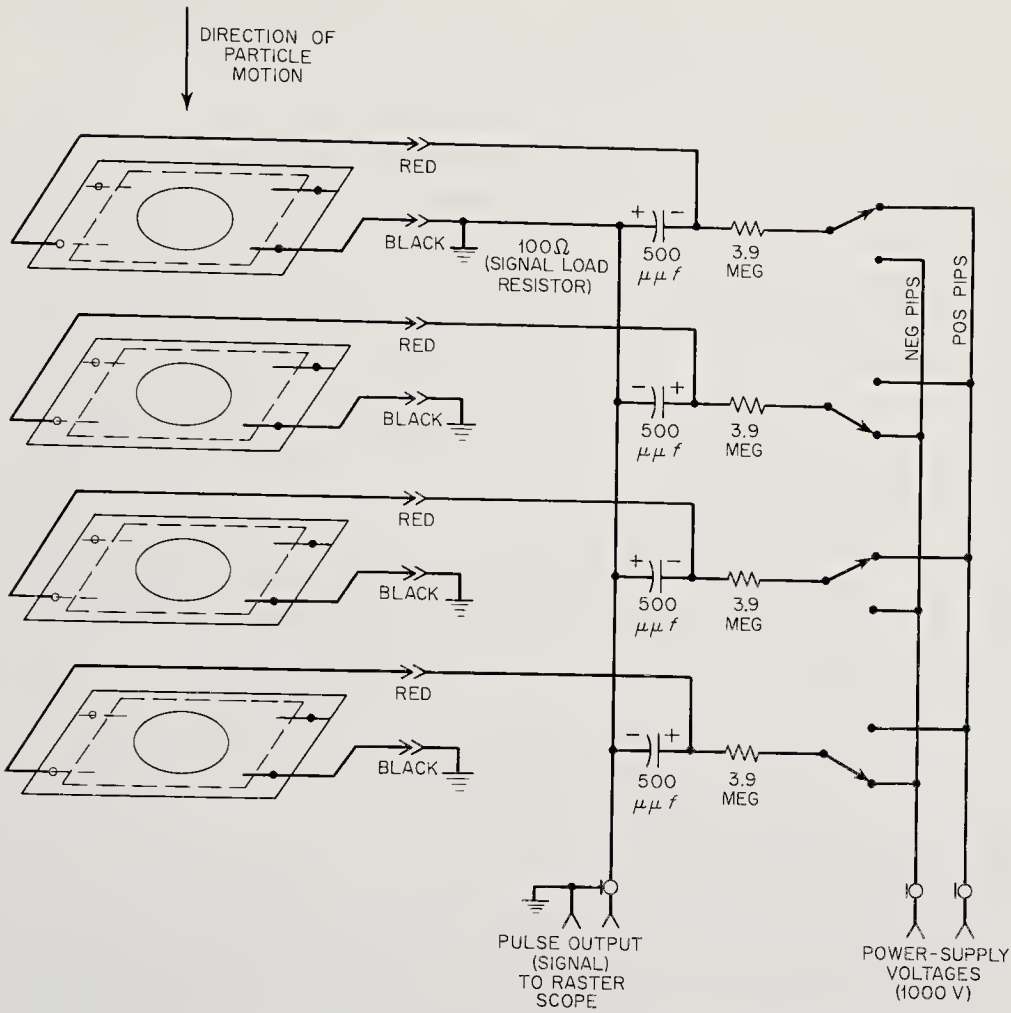


Fig. 13-67. Circuit diagram for a micrometeoroid time-of-flight experiment using capacitor-type detectors as switches. (Ref. 13-22)

and the scattered-light detector. Several combinations of sensors are now being tested in the laboratory. An all-capacitor experiment is illustrated in Fig. 13-67. No spacecraft have carried time-of-flight experiments as yet.

### 13-6. Miscellaneous Experiments in Interplanetary Space

Space probes, by virtue of their great distance from Earth, can help measure more accurate values for the size of the solar system. Space probes are also well out of the gravitational well created by the Earth's field. They are therefore capable of aiding in experiments designed to test the Special and General Theories of Relativity. Finally, the integrated electron density between the Earth and a deep-space probe is

so large that it alters the transmission of radio waves of different frequencies by measurable amounts. In this section, the bases for these three kinds of experiments will be discussed.

*Radio-Propagation Experiments.* Scientists at Stanford University have designed a radio-propagation experiment using the Pioneer-6 deep-space probe. The primary objective is the measurement of the integrated electron density between the Earth and the probe and its variations with time. Secondary goals include a search for postulated anisotropies in radio propagation through the solar wind and diffraction effects occurring when the probe is occulted by the Moon.

The experiment will employ signals transmitted by the Stanford 46-meter, steerable antenna. Two carrier signals will be transmitted, one at 50 Mc and another at 425 Mc. Both signals will be sine-wave modulated at frequencies near 7.7 and 8.7 kc. The space probe will receive the two signals on simple dipole antennas set at an angle to the spacecraft spin axis. The probe equipment will count the number of cycles difference between the 50-Mc carrier and the corresponding subharmonic of the 425-Mc carrier and relay this information back to Earth. A difference of one cycle, for example, implies a change of  $4 \times 10^{14}$  electrons/m<sup>2</sup> over the transmission path. From the measurement of the phase difference between the modulation envelopes of the carriers, the total electron content over the transmission path can be computed. Variations of the integrated electron content may yield more insight into large-scale plasma motion in the solar system, particularly when they are coordinated with local measurements made on one or more spacecraft by plasma probes.

The polarization effects of electrons traveling near the speed of light in outer space can also be measured with the basic Pioneer-6 equipment. If circularly polarized radiowaves are transmitted from Earth, they will be changed into elliptically polarized waves by the high-speed electrons in space. The spinning spacecraft antennas could then measure the amplitudes of the major and minor axes of polarization. (See Table 12-2 for power requirements and weight of the Pioneer-6 propagation experiment.)

*Experiments in Relativity and Gravitation.* Atomic clocks—like the rubidium-vapor frequency standards—could be placed on deep-space probes and flown out of the Earth's gravitational field. If the gravitational potential at the probe's position in space and its velocity are known, the General Theory of Relativity can be checked (Ref. 3-7). The theory predicts a relative frequency shift of

$$\frac{\Delta f}{f} = \sqrt{1 + \frac{2\phi}{c^2}} - \sqrt{1 + \frac{2\phi_0}{c^2}}$$



where  $f$  = the clock frequency  
 $\phi$  = the local gravitational potential at the probe  
 $\phi_0$  = the gravitational potential at the Earth's surface  
 $c$  = the velocity of light.

Without doubt, highly accurate clocks could be made for probe flights, but the same experiments could be carried out more easily on an Earth satellite.

*Measuring the Size of the Solar System.* Radio tracking of Mariner 2 has already provided data for further assessment of the Astronomical Unit (A.U.). Tracking results have generally confirmed radar-ranging data (Ref. 13-3). Both techniques yield values for the A.U. which are so different from the value determined by classical astronomy—they are different by as much as 75,000 km—that a new approach aimed at resolving the disparity is desirable. Kocher and Jamison have described a deep-space triangulation probe to fulfill this need (Ref. 13-33).

The proposed triangulation experiment requires that a probe be launched into an orbit around the Sun. Referring to the Earth-Sun-probe triangle (Fig. 13-68), the distance to the probe,  $d_2$ , as measured in A.U., can be found from:

$$d_2 \text{ (A.U.)} = d_1 \frac{\sin \beta}{\sin (\alpha + \beta)}$$

where the distances and angles are defined in Fig. 13-68. Next, the same distance,  $d_2$ , can be obtained by radio measurements, from  $d_2$  (km) =  $ct/2$ , where  $t$  = the round-trip time for the radio signal. A comparison of the two values for  $d_2$ , measured in A.U. in one case and kilometers in the other, but with the same basic experiment, should yield some insight into the present problem.

The measurement of  $d_2$  in kilometers by radio techniques requires only a transponder aboard the probe. To find  $d_2$  in A.U., two angles,

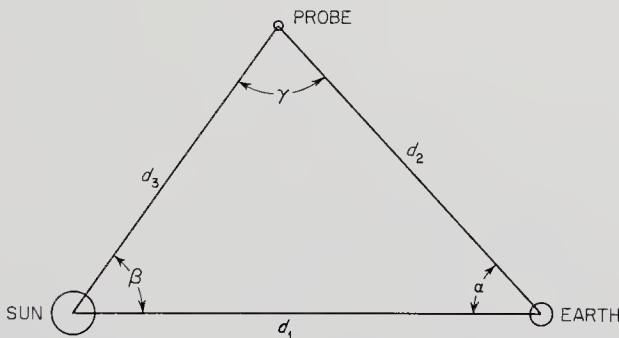


Fig. 13-68. Spatial configuration and definition of symbols for the triangulation-probe experiment. (Ref. 13-33)

$\alpha$  and  $\beta$ , and the distance  $d_1$  must be found in A.U. The ephemeris value of  $d_1$  is given to seven significant figures on a daily basis. The angle  $\alpha$  can be measured by photographing the probe against the stellar background with conventional astronomical instruments. Flat sheets of aluminized plastic two to three meters on a side are suggested to enhance the visibility of the probe. The angle  $\beta$  would be determined by installing a sensor on the probe that would measure the coordinates of the Sun relative to the stellar background. By measuring the direction, relative to the spacecraft, of the Sun and several stars, the longitude of the spacecraft could be found. Given the ephemeris value of the Earth at the same instant,  $\beta$  can be found.

# Chapter 14

---

## INSTRUMENTS FOR MEASURING PLANETARY ATMOSPHERES

---

---

### 14-1. Prologue

Most of the solar-system planets have atmospheres that can be detected from Earth. Even the Moon and Mercury apparently still cling to small residual atmospheres. Although solar system atmospheres have long been studied with Earth-based optical instruments—telescopes, photometers, spectrometers—controversy persists concerning even the closest planets. With the advent of space probes, experiments become possible close to the other planets and, in the more distant future, from within and under their atmospheres. Not only can spacecraft carry instruments to observe details unresolvable on Earth, but remotely controlled experiments can be performed with actual samples of the atmospheres in question. In Table 14-1, the many suggested spacecraft atmospheric instruments have been classified into five groups, according to the physical technique used. The classification is crude, but some sorting out is desirable in the midst of such diversity.

Atmospheric analysis with optical instruments has been well developed during the centuries of observational astronomy. Instruments employing atmospheric sampling have had over two decades of development in conjunction with sounding rockets and satellites. Despite this venerable history, the reader will find that little hardware suitable for probe use is available. The more severe limitations on reliability, weight, and power consumption, cause probe atmospheric instruments to lag behind their counterparts in the interplanetary medium. Furthermore, atmospheric instruments do not receive the developmental benefits of the strong lunar program, like the surface instruments introduced in the next chapter.

TABLE 14-1. INSTRUMENTS USED IN PLANETARY ATMOSPHERIC AND CRUSTAL RESEARCH

<i>Atmospheric Instruments and Experiments</i>	<i>Crustal Instruments</i>	<i>Parameters Measured</i>	<i>Remarks</i>
Radiometer/ Spectrometers	Infrared spectrometer Thermal photography	Atmospheric structure and composition Gas composition by emission and absorption, surface temperature. Surface temperature distribution	Remote analysis of electromagnetic radiation from planet (Secs. 14-2 and 15-2).
Polarimeters	Radar	Atmospheric scattering properties Surface mapping Radar used in ionospheric work	
Mass spectrometer	Television	Surface structure and geology	Solid samples must be vaporized
Gas chromatograph	Mass spectrometer	Abundance v.s. atomic charge-to-mass ratio Composition by sorption-time delay	
Rutherford experiment	Alpha scattering	Abundance v.s. mass number	Rutherford experiment also includes ( $\alpha, p$ ) measurements
Kryptonate experiment		Composition by chemical reactions	Cannot analyze solids
Ram spectrometer Gas densitometer	Spectrometers Densitometer	Composition by emission lines Density by alpha and gamma back-scattering Density, mean molecular weight	Solids must be vaporized
Speed-of-sound experiment	Activation analysis X-ray diffraction Differential thermal analysis Petrographic microscope Isotopic dating	Abundance v.s. isotope Rock structure Composition by thermal properties Rock structure Age	

Langmuir probes	Electron density	} Except for bistatic radar, not applicable to surface studies	} Ionospheric re-search instruments usually using active electromagnetic techniques (Sec. 14-4).
Bottomside sounders	Ionospheric structure		
Topside sounders	Ionospheric structure		
Bistatic radar	Electron-density profile		
Limb-diffraction experiments	Temperature	} Conventional terrestrial instruments modified for probes	} More or less conventional meteorological and geophysical instruments (Secs. 14-5 and 15-4).
Thermometers	Pressure		
Pressure gauges	Wind velocity and direction	} Comparatively specialized probe instruments	} More or less conventional meteorological and geophysical instruments (Secs. 14-5 and 15-4).
Anemometers	Electrical conductivity		
	Magnetic inductance		
	Thermal diffusivity		
	Crustal engineering properties	} Conventional terrestrial instruments modified for probes	} Analysis by vehicle motion (Secs. 14-6 and 15-4).
	Seismic activity, crustal structure, g, crustal tides		
	Density and v.s. altitude	} Conventional terrestrial instruments modified for probes	} Analysis by vehicle motion (Secs. 14-6 and 15-4).
	Planet size and shape		
Drag bodies	Geodetic satellites		

## 14-2. Atmospheric Properties by Analysis of Electromagnetic Radiation

Until the advent of space probes and solar-system-spanning radar, scientists were limited to remote, passive, electromagnetic studies of the planets. The power of conventional astronomy is evident from the immense fund of knowledge that has accumulated over the centuries. (See summarization in Chap. 3.) Probes have made it possible to place instruments much closer to and, on occasion, actually within the atmospheres of interest. Classical astronomy is not at all superseded by close spacecraft reconnaissance. It makes little sense to use expensive probes when equivalent experiments can be performed from the ground or an Earth satellite. Proximity, however, does enlarge the planetary disk to the point where new details and phenomena become measurable (Ref. 14-11). The placement of instruments within, beneath, and behind a planetary atmosphere permits scientists to carry out emission, reflection, and transmission experiments using the Sun or the planetary surface itself as a radiation source. Many of the phenomena expected to be observed from probes (Table 14-2) cannot be seen well from the Earth even with the best telescopes. Some cannot be seen at all. From the analysis of absorption spectra, emission spectra, and polarization, details of atmospheric structure and comparison can be deduced. Active electromagnetic reconnaissance with onboard transmitters, described in Sec. 14-4, will yield even more information. Lasers offer similar opportunities in the shorter wavelengths, but little work has been done here.

There are three basic types of space-probe instruments used in unraveling this mixture:

1. *Radiometers* and *photometers*, which measure electromagnetic fluxes over a few broad spectral areas and/or at several narrow lines in the spectrum. There is no physical dispersion of the spectrum with radiometers. Spectral resolution is accomplished by filters and other methods of tuning (Table 14-3).
2. *Spectrometers* and *spectrophotometers*, which disperse electromagnetic radiation into a spectrum and then scan it with high resolution. The properties of dispersion, spectrum scanning, and high resolution distinguish spectrometers from photometers. Interferometric techniques are sometimes used with spectrometers.
3. *Polarimeters*, which measure the amount of polarization that has been introduced into a beam of radiation in its passage from source to detector.

All probe electromagnetic instruments begin with a lens, mirror, or

TABLE 14-2. TYPES OF OPTICAL INSTRUMENTS FOR ATMOSPHERIC RESEARCH

<i>Instrument Type</i>	<i>Principle of Operation</i>	<i>Phenomena Observed</i>
Radiometer/ photometer	Electromagnetic radiation is focused on a detector which gives a signal proportional to flux. Filters and antennas restrict the spectrum observed to a few specific lines or spectral regions.	Emission: Aurora, permanent airglows, synchrotron radiation, twilight flashes, sferics, fluorescence, resonance radiation
Spectrometer/ spectro- photometer	Electromagnetic radiation is collected, colimated, dispersed, and focused on a detector which scans broad spectrum with high resolution.	Scattering: Aerosol and micrometeoroid scattering, night airglow, halo structures Absorption: Extinction of portions of solar spectrum with atmospheric depth, absorption spectra of planet-emitted thermal radiation, limb studies, atmospheric reflection at angles not observable from earth, "blue-haze" clearing during Mars opposition
Polarimeter	Electromagnetic radiation is passed through an analyzer to determine amount of polarization.	Polarization: Scattering properties of small suspended particles in atmosphere

other flux concentrator that gathers and focuses electromagnetic energy. They all end with a radiation detector that converts the electromagnetic radiation into electrical signals essential for telemetering. In between may lie prisms, analyzers, filters, and other optical devices. Such "optical" instruments may change their character radically with wavelength. Glass, for example, passes only a narrow portion of the spectrum, and the sensitivity of detectors varies greatly from one part of the spectrum to another. Most optical instruments are static, but others are burdened with vibrating reeds and scanning motors. Obviously, there is no typical instrument.

The major interface between the optical instrument and the remainder of the spacecraft is spatial in character. Optical instruments must be able to see their target and gather enough of its light to make good measurements. The field of view needed may vary from a small fraction to several steradians. Electromagnetic observations are often, but not always, directional, which means that the links between the attitude-control and guidance-and-control subsystems are also important.

*Radiometers and Photometers.* When integrated flux measurements are desired over one or more broad portions of the spectrum, or perhaps a few spectral lines, a radiometer or photometer is the appropriate instrument. The term "radiometer" is generally applied at the microwave and infrared ends of the spectrum, while "photometer" is reserved for the shorter wavelengths. Usage is not firm, however. Radiometers and photometers perform the same functions. They both collect radiation, select spectral lines and band-passes, and detect the transmitted fluxes. But they generally employ different components, as shown in Table 14-3.

TABLE 14-3. RADIOMETER AND PHOTOMETER COMPONENTS

<i>Spectral Region</i>	<i>Collectors</i>	<i>Common Selectors</i>	<i>Detectors</i>
Microwave	Dish antenna	Tuned dish and circuits	Antenna diode, thermistor, or bolometer
Infrared	Dish, lens	Filter, grating, interferometer	Thermopiles, CdS, PbSe, and other materials
Visible	Lens, mirror	Filter, grating, prism, interferometer	Photomultiplier, photocell
Ultraviolet	Lens, mirror	Filter, grating, prism	Photomultiplier
X-ray*	None	Shields, radiation telescopes	Ionization chambers, etc.

\* Included for contrast, x-rays are not expected to be important in the analysis of the atmospheres of most solar-system planets.



Radiometers and photometers have long been used on balloons, sounding rockets, and satellites, especially the Tiros series of weather satellites. Microwave and infrared radiometers flew on Mariner 2, and an ultraviolet photometer was designed for Mariner 4. These specific instruments will be used below to illustrate general design principles.

Beginning at the long-wavelength end of the spectrum, the Mariner-2 microwave radiometer was tuned to 13.5 and 19 mm for the purpose of observing limb brightening or darkening during the 1962 Venus encounter. Limb brightening would have inferred an ionospheric origin for the 600°K temperatures that had been observed from the Earth, since more of the ionosphere would have been seen at the planet's edges. In actuality,

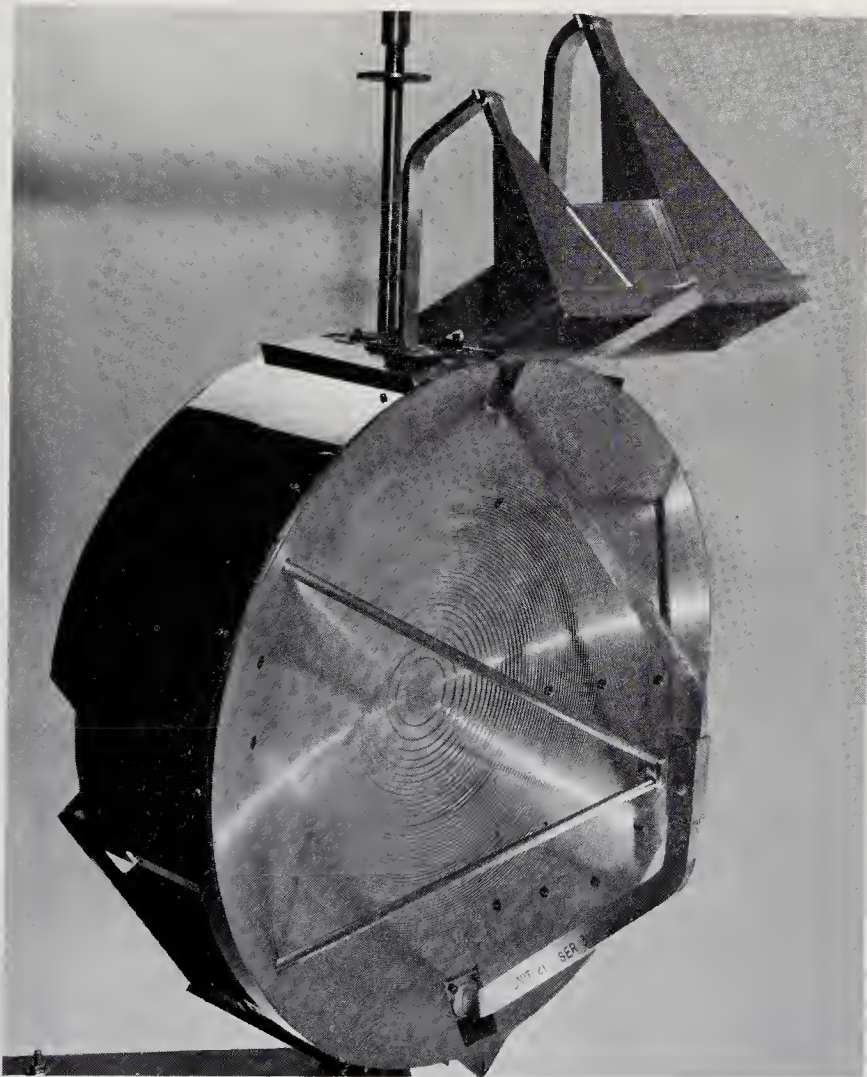


Fig. 14-1. The Mariner-2 microwave radiometer-dish and calibrating-horn antennas. (Courtesy of the Jet Propulsion Laboratory)

limb darkening was detected, indicating that the high temperatures probably originate on the planet's surface. These data support the greenhouse model of the Venusian atmosphere. When the hot planet surface was no longer in the radiometer's field of view, the detector signaled a darkening effect.

A solid, aluminum, parabolic dish 48.5 cm in diameter was used on Mariner 2 (Fig. 14-1). Its field of view was  $2.2^\circ$  and  $2.5^\circ$  in half angle for the 13.5- and 19-mm channels respectively. The ridged surface seen in the photograph diffuses infrared radiation without defocusing the microwaves. Infrared heating of the radiometer is minimized in this way. Ten hours prior to the Venus encounter, the whole dish was driven by a scanning motor in a search mode at  $1^\circ/\text{sec}$ . When the limb of the planet was acquired, the scan rate was reduced to  $0.1^\circ/\text{sec}$ .

The 13.5- and 19-mm signals were fed simultaneously from the antenna through waveguides to the Calibration Directional Coupler shown in Fig. 14-2. Radiometer calibration was achieved by making cold-space

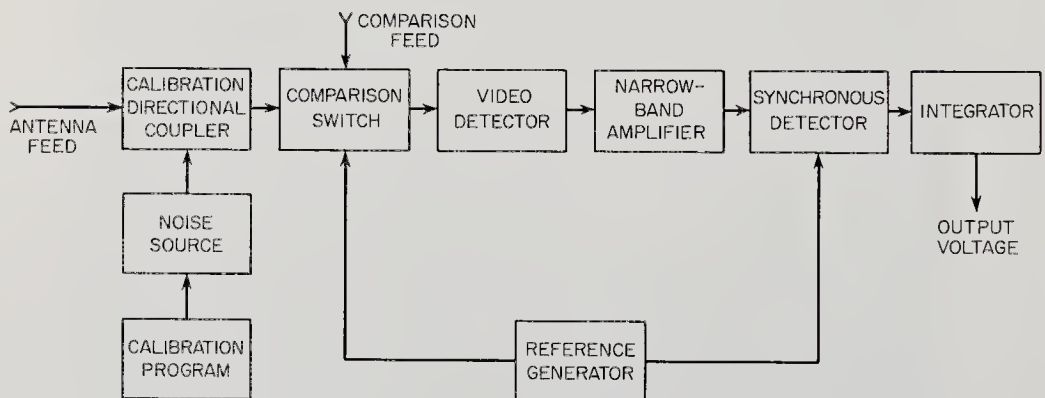


Fig. 14-2. Block diagram for the Mariner-2 microwave radiometer experiment. (Ref. 13-59)

measurements with two horn-type antennas (Fig. 14-1), which were kept pointed away from the Sun and Venus. A noise discharge tube also provided calibrating signal equivalent to approximately  $350^\circ\text{K}$ . Radiometers in which reference signal sources are switched in and out of the main channels are called Dicke radiometers, after R. H. Dicke. The ferrite switches used for this purpose on Mariner 2 had to be shielded electrically and magnetically because of their interference with the rest of the spacecraft. Source and calibration signals were both fed through a crystal video receiver instead of the conventional and more sensitive super-heterodyne receiver. Weight and power consumption restrictions dictated this choice. (See Table 12-2, page 286.)

A modified version of the Mariner-2 radiometer was developed at the Jet Propulsion Laboratory for the canceled 1964 Venus flyby (Ref. 14-1). This instrument was to operate with channels at 8.5 and 33 mm. Crystal video tuned-radio-frequency receivers were to be used on the two channels respectively. Another important difference was the use of a satin, infrared-diffusing antenna surface to replace the Mariner-2 steps, which would have had to be unreasonably small to avoid compromising focusing on the 8.5-mm channel.

In the infrared region of the spectrum, the microwave plumbing and radio-frequency amplifiers are replaced by special lenses, solid state detectors, and mirrors. Again, a Mariner-2 instrument is described as representative of the class.

Instead of a dish antenna, the Mariner-2 infrared radiometer employed a 3.2-cm diameter, germanium objective lens with a focal length of 7.8 cm (Ref. 13-59). The field of view was nominally a square 1.2 degrees on a side. The entire radiometer assembly was rigidly attached to the microwave-dish structure, with both radiometer axes parallel. Both scanned Venus together.

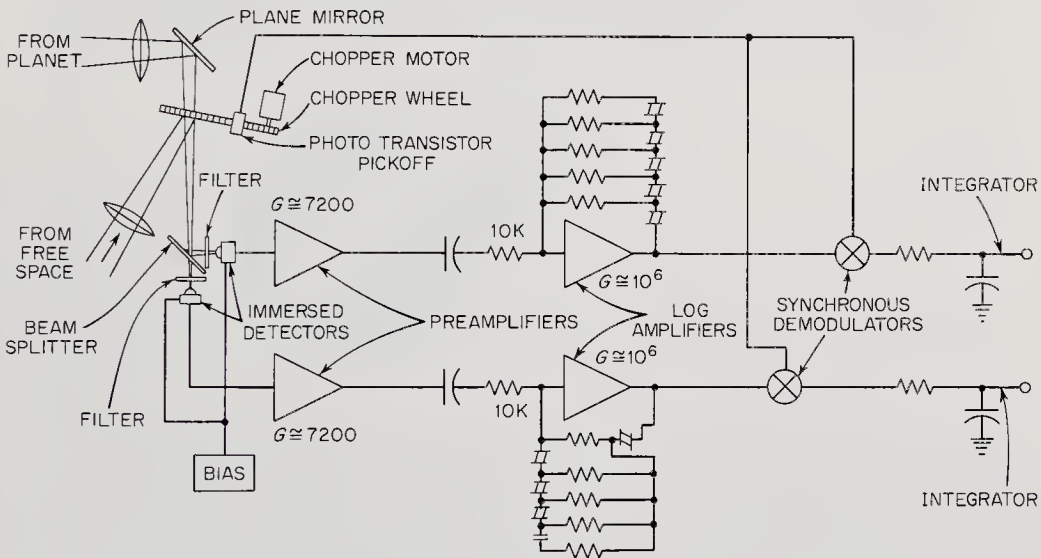


Fig. 14-3. Component arrangement for the Mariner-2 infrared radiometer. (Ref. 13-59)

The infrared radiation beam was chopped twenty times a second by a rotating disk, which alternately exposed the detector to the planet and, for reference purposes, free space (Figs. 14-3 and 14-4). After chopping, the beam was split into two perpendicular components by a dichroic filter or "beam splitter." (Dichroic materials split randomly polarized light

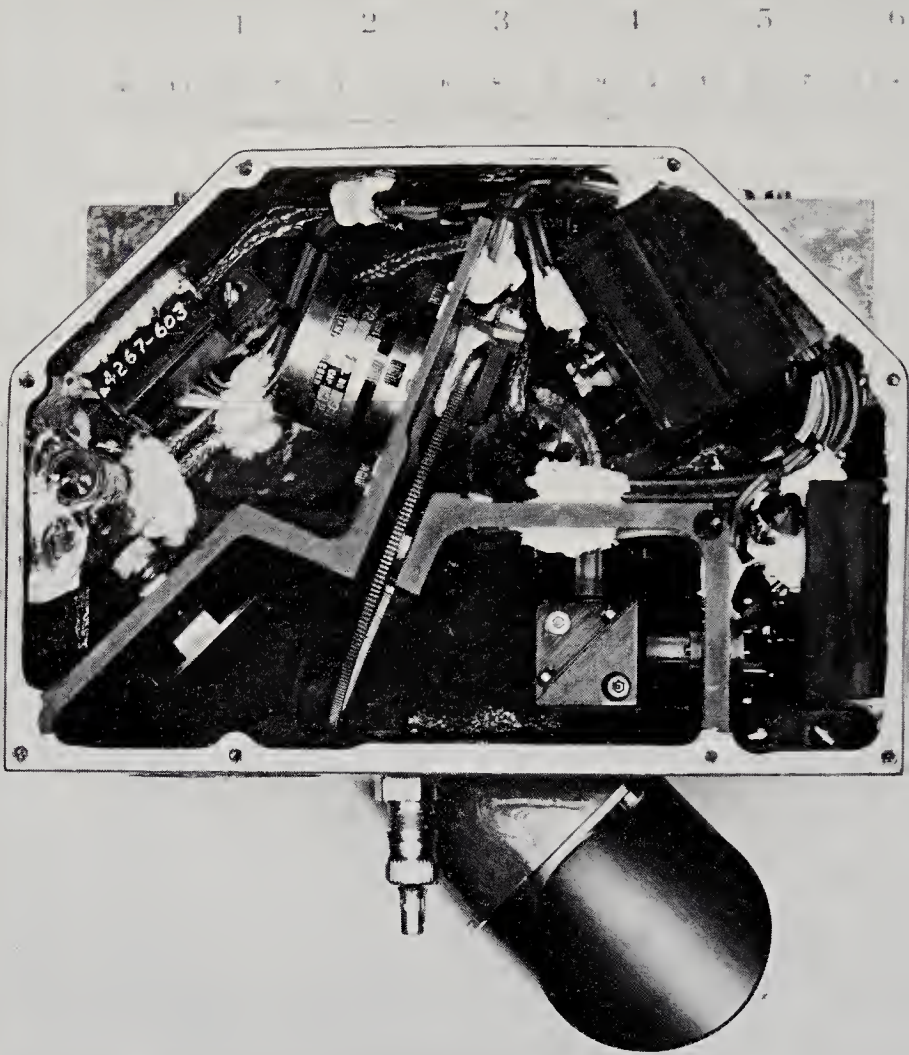


Fig. 14-4. Mariner-2 infrared radiometer with cover plate removed. Toothed chopper wheel is seen end on. (Courtesy of the Jet Propulsion Laboratory)

into two polarized components at right angles.) Interference filters with the characteristics shown in Fig. 14-5 defined the two radiometer channels. The infrared detector consisted of two uncooled, thermistor bolometers immersed in hemispheric germanium lenses. A preamplifier, logarithmic amplifier, and synchronous demodulator followed each detector. (See block diagram, Fig. 14-6. See Table 12-2 for power requirements and mass.)

In addition to terrestrial calibration with a reference blackbody (Ref. 14-8), the radiometer also viewed a reference thermal calibration plate with a telemetered temperature at the end of each scan.

In a sense, the Mariner-2 infrared radiometer was parasitic to the microwave experiment. Even the experimental objectives were largely redundant, a not undesirable feature in space research. It was hoped that the two infrared channels would reveal something about the cloud structure of Venus. One channel was centered on the  $10.3\text{-}\mu$ ,  $\text{CO}_2$  absorption band, and the other on the comparatively absorption-free region around  $8.4\ \mu$ . The theory was that the Venusian surface and lower atmosphere should be visible at  $8.4\ \mu$  but would be obscured by  $\text{CO}_2$  (whose presence was already established) at  $10.3\ \mu$ . No breaks in the cloud cover were observed during planetary encounter.

Other infrared radiometers have been built for satellites. Tiros 2, for instance, carried a five-channel unit. See also Fig. 14-7 for the Mariner-3 three-channel radiometer. Most such radiometers closely resemble the Mariner-2 instrument. A particularly simple, unchopped, low resolution radiometer has been described by Hanel (Ref. 14-17). Such a device would view large areas of a planet and might be used in radiation balance experiments. The Suomi radiometer (after V. E. Suomi) is also of general interest. It consists of four spherical collectors, two coated with materials with different absorptivities and the other two covered by sunshades. Used on a satellite, the Suomi radiometer carries out radiation-balance experiments.

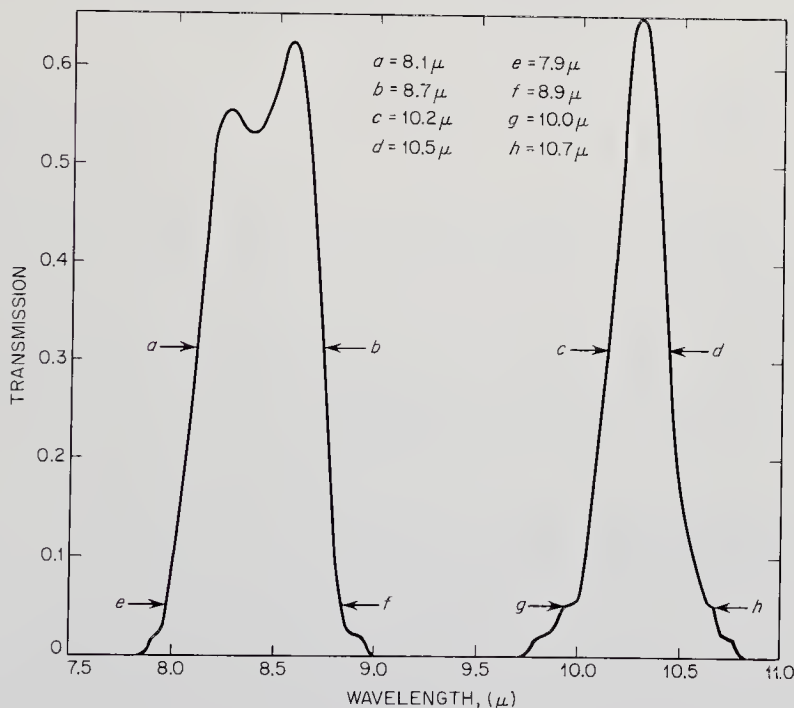


Fig. 14-5. Transmission characteristics of the two filters used in the Mariner-2 infrared radiometer. (Ref. 13-59)

Planetary photometry (and spectrometry, too) in the visible range of the spectrum is usually done more conveniently and economically from the Earth's surface, since the atmosphere offers little hindrance at these wavelengths.

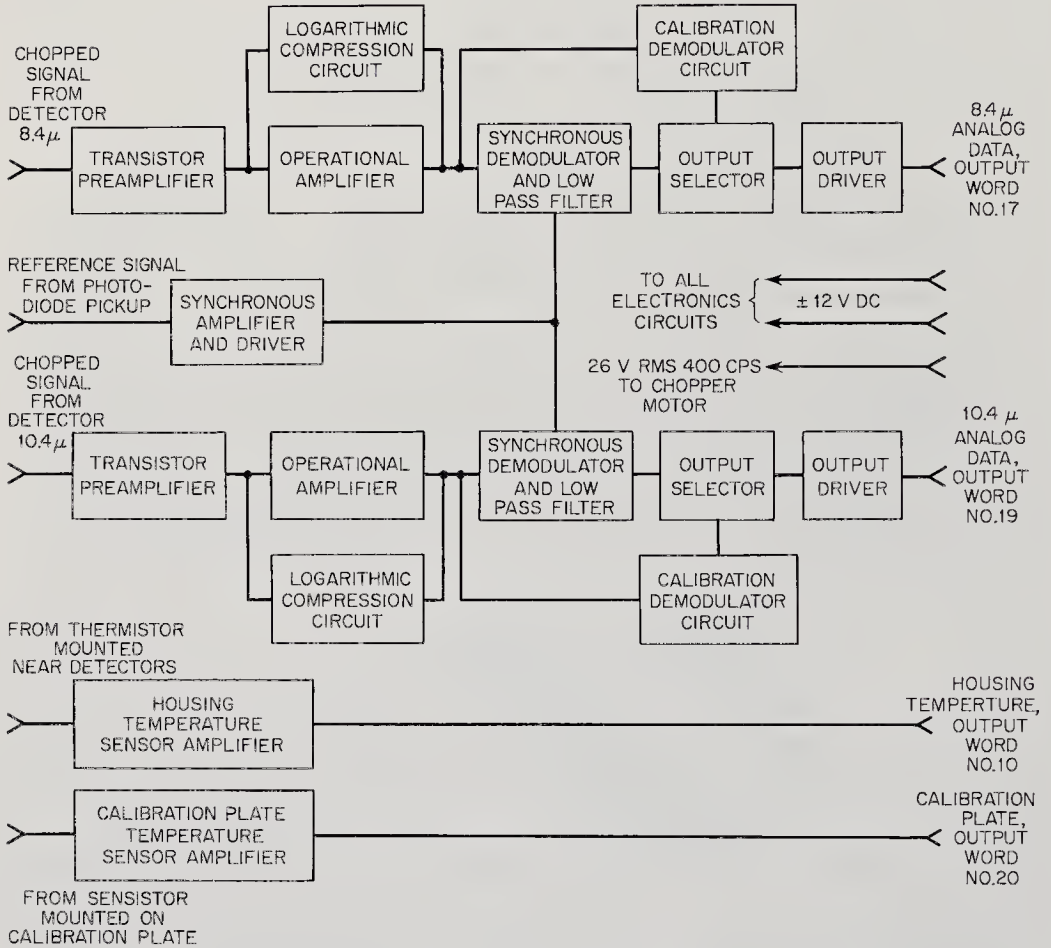


Fig. 14-6. Block diagram for the Mariner-2 infrared radiometer experiment. (Ref. 14-8)

Moving into the ultraviolet region, photometers have been proposed for use on entry vehicles for the measurement of H<sub>2</sub>O, O, O<sub>2</sub>, O<sub>3</sub>, and N<sub>2</sub> densities as functions of altitude by observing the absorption of the solar Lyman  $\alpha$ ,  $\beta$ , and  $\gamma$  lines of hydrogen (1215A, 1026A, and 972A) and the He I and II lines (584A and 304A). (See also the block diagram, Fig. 14-8, of the Mariner-3 photometer.) The proposed instrument would actually consist of five ganged ultraviolet radiometers, each with its own lens, interference filter, and detector. Each of the units would resemble

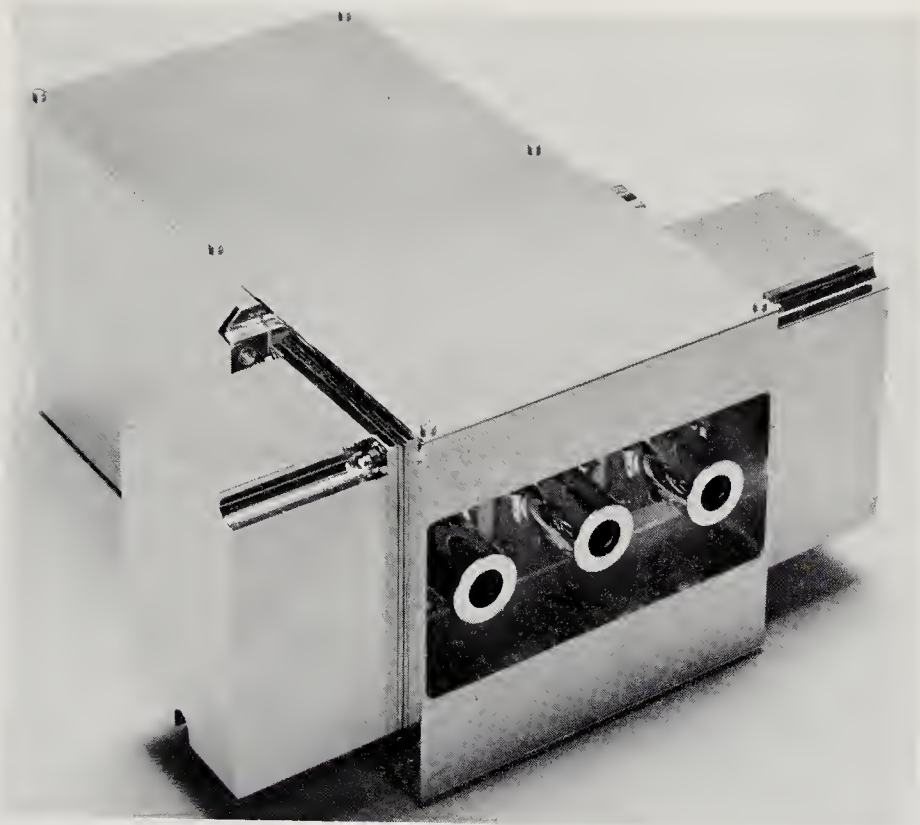


Fig. 14-7. The Mariner-3, three-channel ultraviolet radiometer. (Courtesy of the Jet Propulsion Laboratory)

that shown in Fig. 14-9. Together, they would have a mass of only 0.8 kg and consume about 1.5 watts.

Photometers become even more versatile when a continuously or discretely graded filter wheel rotates in the path of the light beam. A spectrum is obtained in this way without using a dispersive element. Such instruments are called filter spectrometers.

The ultraviolet photometer built for but not flown on the Mariner-3 probe used a signal subtraction technique to isolate the spectral ranges of interest. Three 18-stage photomultiplier tubes (*A*, *B*, and *C*) viewed the planet's image through the following filters:

<i>Tube</i>	<i>Filter</i>	<i>Bandpass</i>	<i>Atmospheric Component Measured</i>
<i>A</i>	lithium fluoride	1050-1800A	
<i>B</i>	calcium fluoride	1250-1800A	
<i>C</i>	barium fluoride	1400-1800A	
<i>A-B</i>		1050-1250A	atomic hydrogen (1215A)
<i>B-C</i>		1250-1400A	atomic oxygen (1300A)

By electrically subtracting the signals from the appropriate photomultiplier tubes, the emission lines and thus the densities of atomic hydrogen and oxygen could be measured.

Tube *A* had a field of view with a  $1.25^\circ$  half angle. *B* and *C* would see the planet through cones with  $0.5^\circ$  half angles. The instrument as a whole was capable of detecting  $1.3 \times 10^{-4}$  erg/cm<sup>2</sup>-sec-steradian at 1216Å. As Fig. 14-7 indicates, the Mariner-3 experimental equipment was particularly simple, with no moving parts. Tube outputs were fed through amplifiers into an analog-to-digital converter (ADC), as shown in the block diagram (Fig. 14-8). The whole photometer would have been mounted on the planetary-scan system.

In-flight calibration of the photometer would have been accomplished by injecting a standardized calibration current into the input amplifier at every sixteenth data frame to check amplifier gain. Eight frames later, the drift offset of the instrument would have been automatically checked.

One constraint applied by the instrument to the attitude-control program was that the photometer axis was not permitted to point within  $10^\circ$

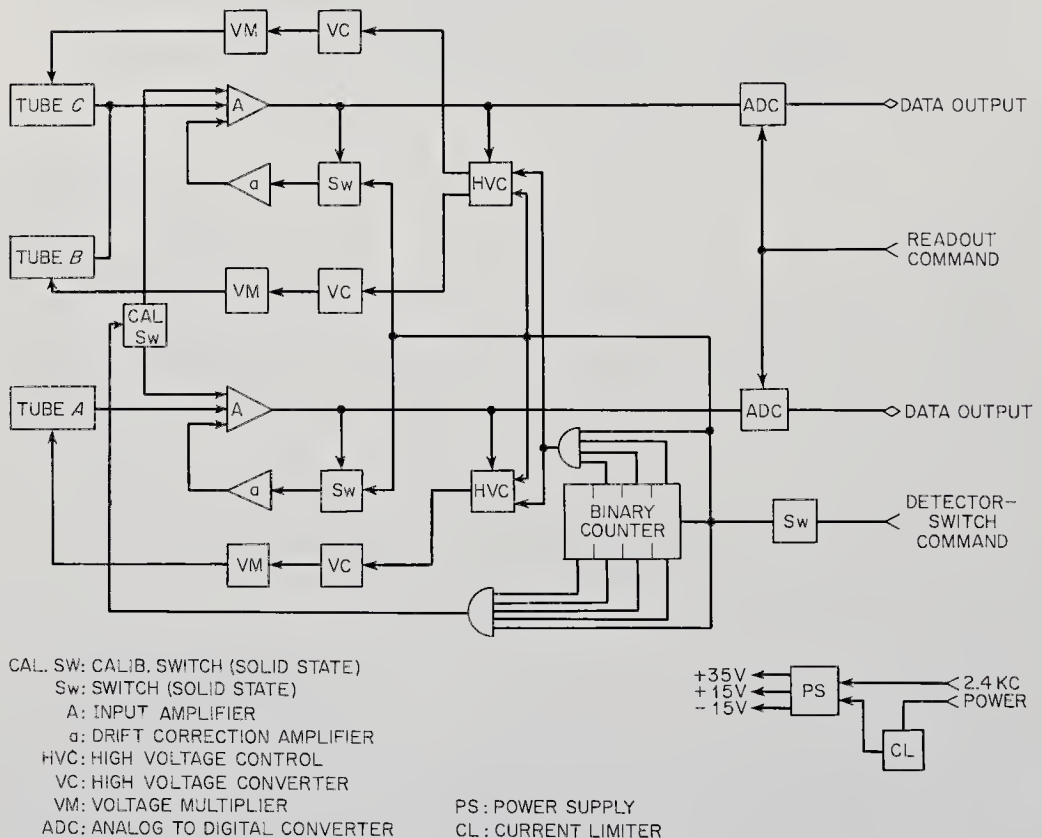


Fig. 14-8. Block diagram of the Mariner-3 ultraviolet photometer. (NASA drawing)



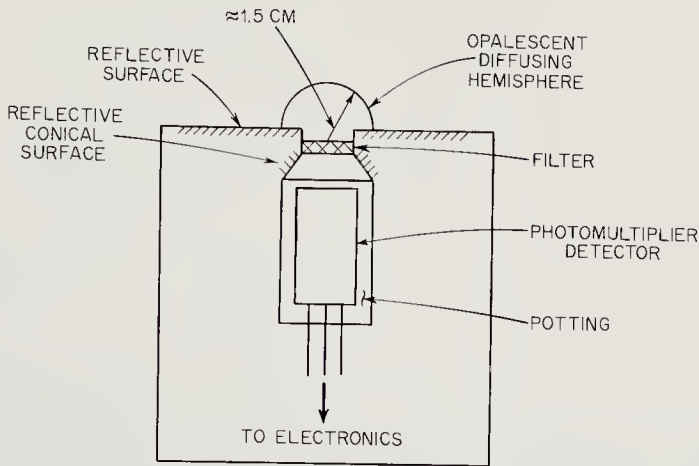


Fig. 14-9. Sketch of a simple ultraviolet radiometer with a field of view of  $2\pi$  steradians. (Ref. 14-15)

of the Sun. Otherwise, the detectors would have been damaged. The final mass of the Mariner-3 photometer was 2.5 kg. It consumed an average of 1.0 watts.

*Spectrometers and Spectrophotometers.* Spectroscopes use prisms and gratings to disperse the electromagnetic spectrum into its emission and absorption lines, which, when analyzed, can reveal a great deal more about a planetary atmosphere than the rather limited photometers just described. With the dispersion of the spectrum, some component of the instrument must be mechanically driven so that a detector can scan the wavelengths of interest. Terrestrial spectrometers perform this feat statically with a long film strip. In space, where electrical signals are the only medium of exchange, either the detector must move or, more conveniently, an optical element must be rotated to sweep the spectrum past a single detector.

The basic functions performed by a spectrometer are light-gathering, focusing and collimation, spectrum dispersion, detection, and spectrum scanning (see Fig. 14-10). The dispersion element replaces the filters used on photometers. There is a great variety of possible arrangements of components. Spacecraft weight and volume restrictions usually dictate "folded" instruments, in which the light is reflected back and forth from components housed in a small volume rather than strung out linearly. Spectrometers are well-established balloon, rocket, and satellite instruments, but they have yet to fly on deep-space probes.

Again it is helpful to divide the instruments into infrared and ultraviolet types.

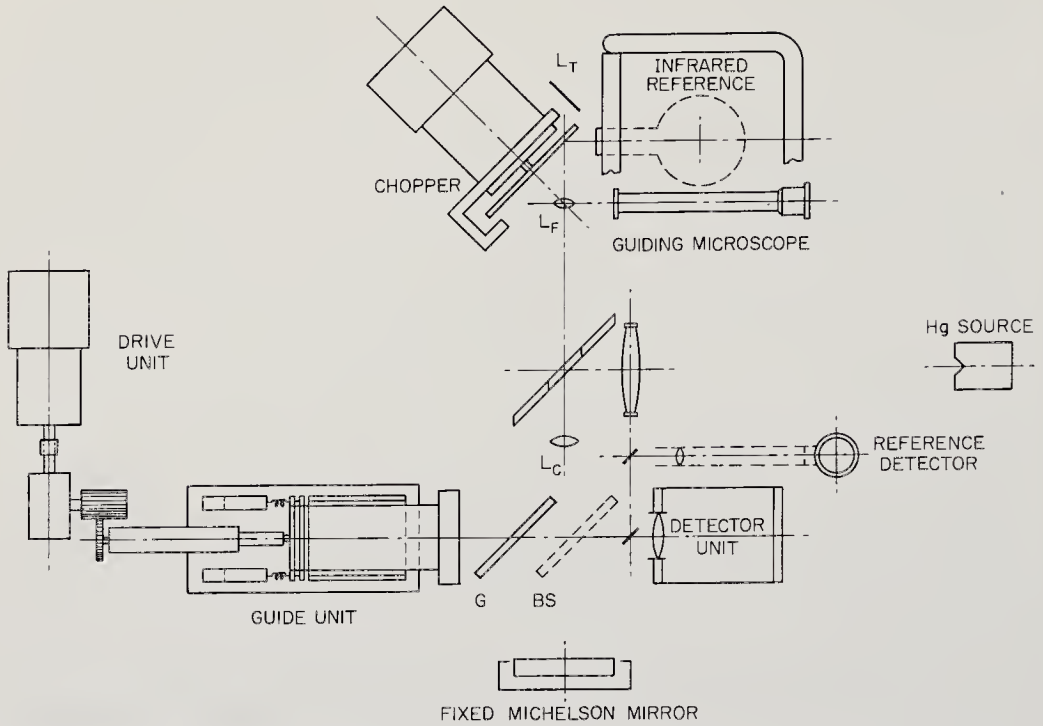


Fig. 14-10. Laboratory setup for an infrared interferometer spectrometer. (Ref. 14-6)

Infrared radiation generally has high penetrating power in atmospheres. Infrared spectrometers can therefore be put to use in thermally mapping a planet's surface. In addition, these instruments can detect the Sinton bands, between 5 and 16  $\mu$ , that are indicative of organic molecules on the surface. Infrared radiation also reveals details of atmospheric structure and composition. For example, carbon dioxide and water have emission bands at 2.7 and 4.3  $\mu$ , respectively. Many other emission and absorption bands exist in the infrared region, so that an infrared spectroscope is a good diagnostic tool in atmospheric research (Ref. 14-11).

An infrared spectrometer proposed by the Jet Propulsion Laboratory for Mariner 2 and the now-canceled Mars 1966 flyby is diagrammed in Fig. 14-11. Light is first collected by a large concave mirror, then reflected off a convex mirror through the entrance slit and on to a monochromator mirror. From here, the light is reflected to the ruled grating where it is dispersed. Ultimately the beam is split into two parts and directed into two cooled detectors. The multiple mirrors and compact, "folded" arrangement of components are typical of the Ebert spectrometer configuration. A tuning-fork-driven chopper at the entrance slit provides the detectors with a modulated light beam for easy amplification.

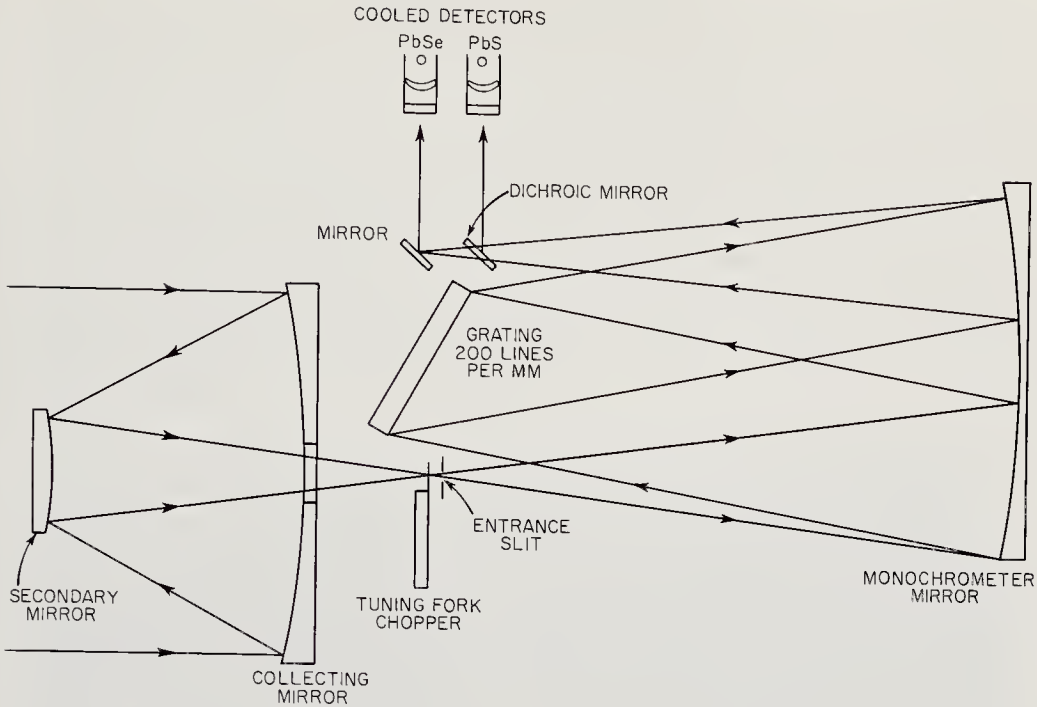


Fig. 14-11. Diagram of an infrared spectrometer suitable for use on a Mars flyby. (JPL drawing)

The light signal eventually reaching the detectors is given by:

$$E_{\lambda} = N_{\lambda} e A_s \frac{A_g}{F^2} \delta\lambda$$

where  $E_{\lambda}$  = the light flux (watts/cm<sup>2</sup>)

$N_{\lambda}$  = the spectral radiance of the source (watts/cm<sup>2</sup>-μ-ster).

$e$  = the instrument optical efficiency. (Including chopper and beam splitting,  $e$  = about 0.2 for an instrument of this type.)

$A_s$  = the slit area illuminated (cm<sup>2</sup>)

$A_g$  = the grating area illuminated (cm<sup>2</sup>)

$F$  = the focal length of the monochromator mirror (cm)

$\delta\lambda$  = the spectral bandpass (μ)

The spectral dispersion is described by the familiar grating equation:

$$d (\sin i + \sin \theta) = m\lambda$$

where  $d$  = the distance between the grating lines (cm)

$i$  = the angle of incidence

$\theta$  = the angle of reflection

$m$  = the order of the spectrum

$\lambda$  = the wavelength (cm).

The grating in Fig. 14-11 is rocked, so that the detectors will scan the desired infrared portion of the spectrum every 60 seconds. Each scan produces about 400 bits of data. In the JPL spectrometer, the 2-6  $\mu$  region is of the greatest interest, leading to the choice of lead sulfide and lead selenide as the materials offering the best compromise between sensitivity and easy cooling. Lead sulfide has the higher sensitivity in the 1-3  $\mu$  range, but this drops rapidly at longer wavelengths. The sensitivity of lead selenide rises to a peak between 3 and 6  $\mu$ . In actual usage, the spectrometer would probably include a reference source of radiation like that in the Mariner-2 infrared radiometer. The instrument just described could probably be built at less than 10 kg and would consume about 5 watts of power.

An interferometer may replace the grating in the infrared spectrometer. Instead of dispersing the spectrum laterally, the interferometer acts somewhat like a variable filter. In essence, this device splits the light beam into two parts and recombines them after they have traveled slightly different distances. If the difference in distance traveled is an integral number of wavelengths, there will be no interference. Otherwise, there will be some cancellation. The linear movement of one of the interferometer mirrors changes the tuning of the instrument and permits the detector to see different parts of the spectrum. Manchester Univer-

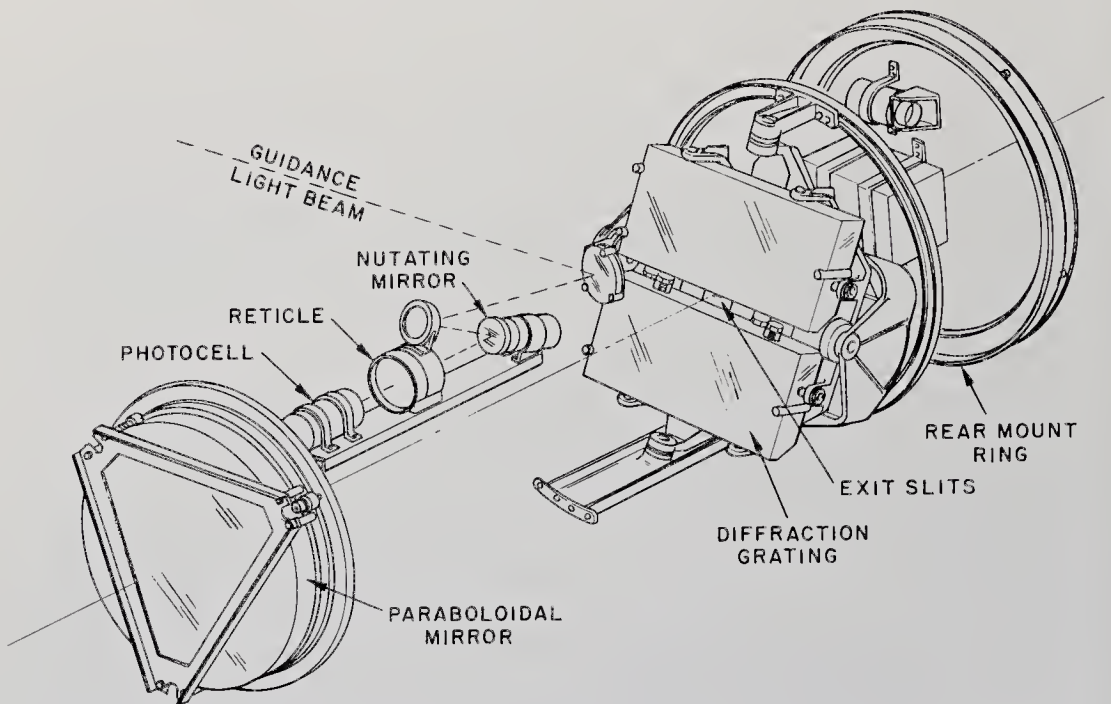


Fig. 14-12. Sketch of a typical rocket-borne ultraviolet spectrometer. (Courtesy of Perkin-Elmer Corp.)

sity, in England, has been experimenting with this type of infrared spectrometer (Ref. 14-6).

The ultraviolet spectrometer was one of the first sounding-rocket instruments. Its purpose, when it first flew in the late 1940's, was the measurement of the solar spectrum in the far ultraviolet, where the Earth's atmosphere is opaque. Figures 14-12 and 14-13 show a recent instrument built for the Aerobee-Hi rocket by Perkin-Elmer Corp. More advanced units of this type will be used on astronomical satellites (OAO's). No ultraviolet spectrometers are being developed for probe flights at present.

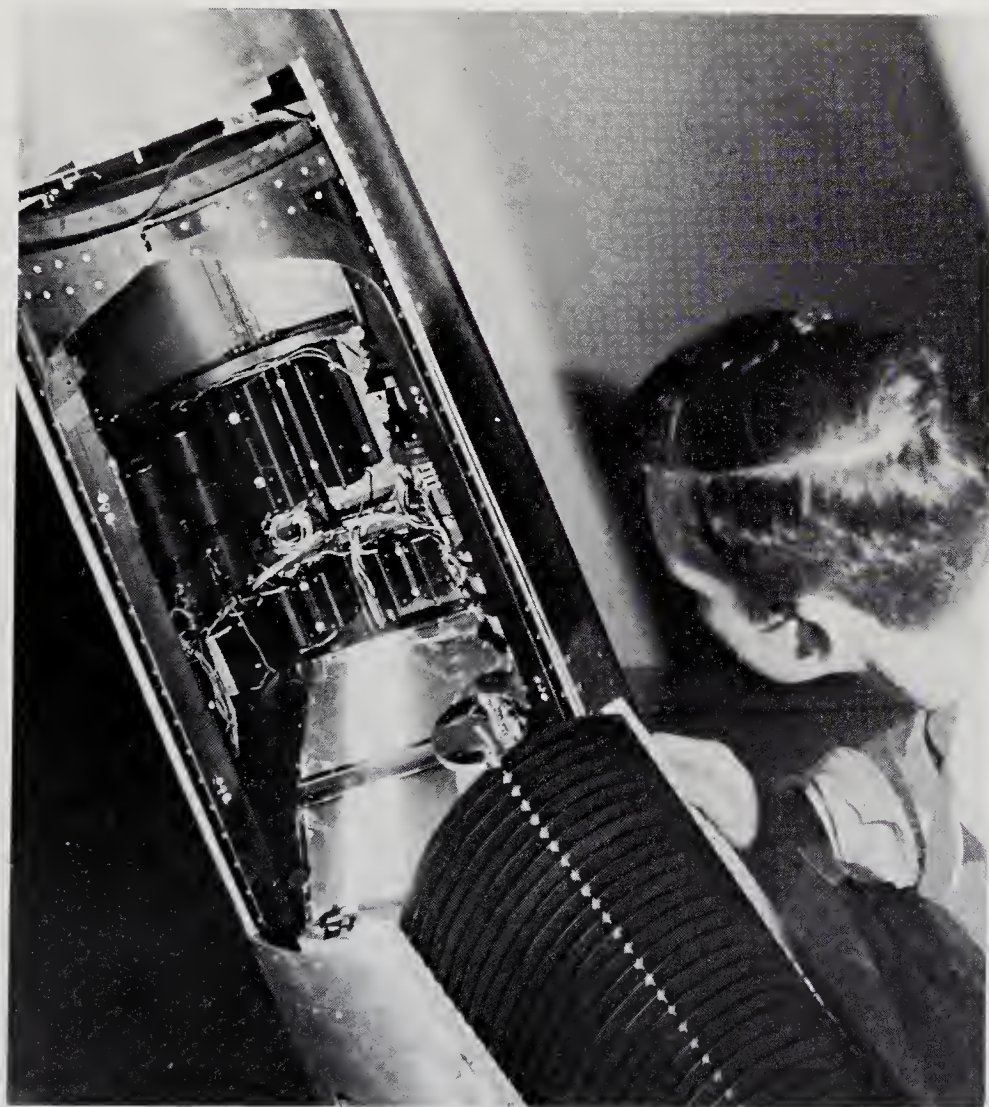


Fig. 14-13. The ultraviolet spectrometer of Fig. 14-12 mounted in an Aerobee-Hi nose. (Courtesy of Perkin-Elmer Corp.)

Ultraviolet light is readily absorbed by O, O<sub>2</sub>, and O<sub>3</sub> in an atmosphere. A spectrometer on an entry vehicle could measure the densities of these and other constituents from their absorption lines and bands in the ultraviolet region. A flyby probe carrying an ultraviolet spectrometer could detect resonance radiation from elements like Ar (1048A), N (1200A), O (1215A), and C (1657A). Chemiluminescence and fluorescence in the upper atmosphere of a planet could also be studied.

The ultraviolet spectrometer of Fig. 14-13 is characteristic of modern rocket instruments of this type. It scans the first-order spectrum from 1750-3200A at 24A/sec and the second-order spectrum from 875-1600A at 12A/sec. The Ebert spectrometer configuration is again used because of its compact nature. In addition to the analyzer section, the spectrometer includes an optical pointing system with a photocell connected to the attitude-control subsystem. The first-order spectrum is detected by a photomultiplier tube, the second-order spectrum by a photocell with a copper oxide cathode. Both detectors are located behind the grating in Fig. 14-13. The instrument's mass is approximately 46 kg; this could probably be reduced significantly for probe use.

*Polarimeters.* It is well known that small particles and gases in the Earth's atmosphere scatter and polarize sunlight. Presumably, the same thing happens in the atmospheres of some of the other planets. A probe carrying a polarimeter could telemeter data from which particle sizes and distribution might be computed.

A polarimeter would consist simply of a lens, a rotating analyzer (a polarizing filter that passes only that light which has its plane of polarization parallel to that of the filter), filters, and a light detector. Basically it is a photometer with an analyzer added. Besides transmitting the detector signal back to Earth, the telemetry includes the analyzer angle, the identity of the filter used, and the direction of the instrument optical axis. There are no space-probe polarimeters under development at present.

### 14-3. Atmospheric Properties by Sample Analysis

The space-probe instruments introduced in this section collect samples of the unknown atmosphere and measure directly parameters like composition and density. The sampling process logically divides these instruments from those described in the preceding section, which employ passive, optical techniques to determine gas properties indirectly from electromagnetic emission, scattering, and transmission evidence. Atmospheric sample collection and analysis is a common terrestrial research technique. Thus, it is not surprising to find terrestrial analogs for many of the instruments in this class. Modifications have to be made before

use in space, of course, but substantial funds of instrument knowhow already exist.

The collection and processing of gas samples almost always necessitates valves, pumps, and other plumbing fixtures. The disadvantage in sampler complexity is counterbalanced by the precision, lack of ambiguity, and the ability to sample directly at various altitudes. Mass spectrometers and gas chromatographs usually produce electrical signals directly, but substitute indicators have to be developed for the common volumetric and colorimetric indicators of conventional chemical analysis.

There are few other generalizations applicable to sampling instruments. Their operation depends upon the atomic mass differences, nuclear cross sections, varying sorptive properties, and specific chemical characteristics like those listed in Table 14-4. Other atmospheric constituents, aerosols and other small particles, can be seen by remote microscopy. This class of instruments is closely associated with life detection and is covered in Chap. 16.

*Mass Spectrometers.* Mass spectrometers separate atoms and molecules possessing differing masses by applying an equal accelerating force to all. As a consequence, the lighter particles acquire more speed in a given time and draw away from their heavier companions. The accelerating force may either be applied perpendicular to the particles' direction of motion, so that the different masses fan out in a spectrum, or it may be parallel causing like particles to clump together, but not alter their direction of flight (Fig. 14-14). In all mass spectrometers there is a *mass scale*, which

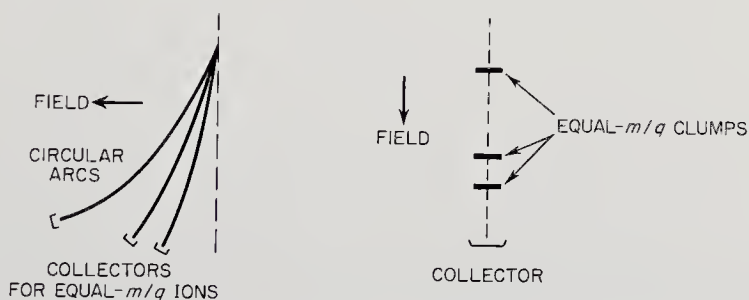


Fig. 14-14. Transverse electrostatic and magnetic forces cause spatial dispersion; longitudinal forces cause segregation by mass number.

is usually made directly proportional to mass. Distance and time of arrival are the mass scales in the simple situations shown in Fig. 14-14.

The application of equal accelerating forces to the different atoms in the sample is easily accomplished by ionizing the particles singly. The presence of electrical charge also provides a means of particle flux measurement. Both electrostatic and magnetic forces,  $\bar{F}_e = q\bar{E}$  and  $\bar{F}_m =$

TABLE 14-4. ATMOSPHERIC RESEARCH INSTRUMENTS USING SAMPLING TECHNIQUES

<i>Instrument Type</i>	<i>Principle of Operation</i>	<i>Parameters Measured</i>
Mass spectrometer	Magnetic and/or electrostatic fields separate ions of varying masses by differential acceleration.	Atmospheric composition Atom abundances by mass
Gas chromatograph	Gas constituents are delayed by varying times in sorptive columns. Time of emergence infers composition.	Atmospheric composition Chemical components and their abundances
Rutherford experiment	Radioactive source creates alphas. Detectors record alpha-scattering and alpha-proton reactions.	Abundances of C <sup>12</sup> , N <sup>14</sup> , O <sup>16</sup> , Ar <sup>40</sup>
Kryptonate experiments	Radioactive Kr <sup>85</sup> is incorporated in various materials. Rate of atmospheric chemical attack on material is measured by loss of Kr <sup>85</sup> .	Abundance of ozone, water vapor, and other selected gases
Ram spectrometer	Ram effect heats gases in front of spacecraft nose cone during entry. Spectroscope analyzes emission.	Atmospheric composition
Gas densitometers	Alpha or gamma sources bombard atmosphere. Back-scattered radiation is a measure of density.	Density
Speed-of-sound experiment	Acoustic generator sends sound waves down tube. Microphones measure wavelength and acoustic impedance.	Gas density, mean molecular weight



$q\bar{v} \times \bar{B}$ , are linear in the charge,  $q$ , and the applied fields,  $E$  and  $B$ . Electrostatic and magnetic analysis both imply precollimated beams of ions, while magnetic separation has the added condition of equal ion velocity.

From these simple considerations, the major components of a mass spectrometer must be:

1. An ionization mechanism, if the population is not already ionized. In this case, we have a neutral gas spectrometer.
2. Collimators, focusing devices, and velocity filters, as needed by the mass-dispersion scheme adopted.
3. A mass-dispersion mechanism, such as the magnetic and electrostatic fields just mentioned. More complicated combinations of static and time-varying fields are presented later.
4. An electric current detector to measure the flow of charged particles meeting the mass-separation criteria.
5. Logic circuitry to make time-of-flight measurements, scan spatially separated detectors, and synchronize the various parts of the instrument.
6. An analog-digital (AD) converter to feed the words in the proper format to the communication subsystem.

All instruments disturb the parameters they measure, and mass spectrometers are no exception. Instrument surfaces, for example, encourage ion recombination. A hot filament emitting ionizing electrons may cause hot-surface chemical reactions. Filaments are usually located away from the main gas stream for this reason. Electrostatic and aerodynamic distortions, like those discussed for the  $E/q$  plasma probes (Sec. 13-4), also apply to the  $m/q$  mass spectrometers.

Five different types of mass spectrometers have been proposed for use in satellites and space probes:

<i>Type</i>	<i>Mass Dispersion Mechanism</i>
Simple mass spectrometer	Magnetic field
Double-focusing mass spectrometer	Electrostatic energy filter plus magnetic field
Quadrupole mass spectrometer	Radio-frequency field superimposed on static field (See discussion)
Time-of-flight mass spectrometer	Time of flight
Radio-frequency mass spectrometer	Resonant grid structure (See discussion)

The first two spectrometers listed require the use of magnetic fields for ion separation. The strong fields set up throughout the spacecraft by such magnetic-dispersion instruments usually preclude their use on spacecraft carrying magnetometers, a fact implying that they will not be used on space probes in the near future.

The mass spectrometers destined for early probing of other planetary atmospheres will be analyzing relatively unknown mixtures of gases. Since present spectrographic measurements of the atmospheres of Mars and Venus are not viewed with high confidence, probe mass spectrometers

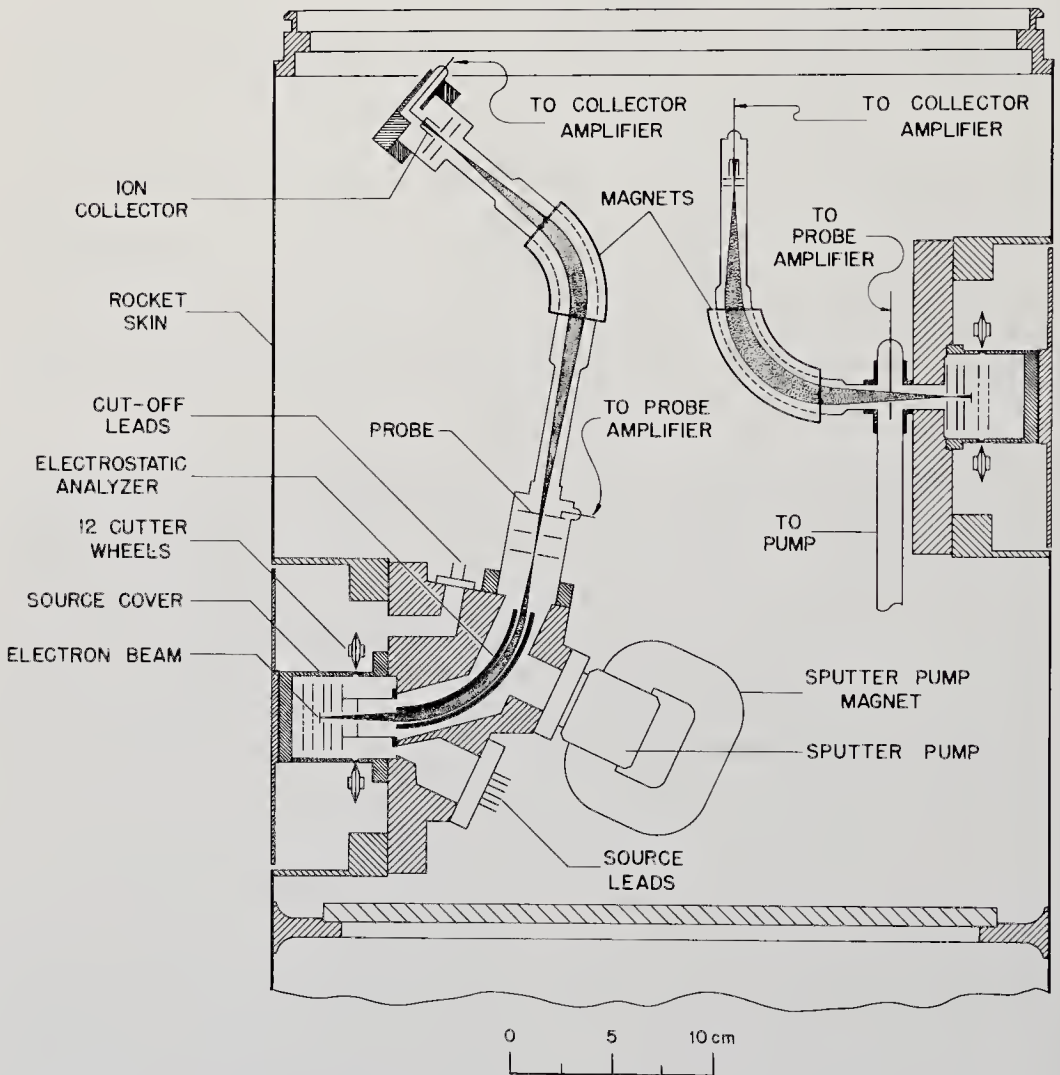


Fig. 14-15. Single- and double-focusing magnetic mass spectrometers carried on an Aerobee sounding rocket. (Courtesy of the University of Minnesota. (Ref. 14-25)

ters must be built to bracket a wide range of masses and also be capable of operating over a broad range of pressures. They will certainly have to be more flexible than mass spectrometers used in the relatively well-known Earth atmosphere.

Two instruments designed by the University of Minnesota group for the Aerobee series of sounding rockets are typical of the single- and double-focusing mass spectrometers that have been used near the Earth (Ref. 14-25). Shown mounted together for redundancy purposes in the Aerobee structure (Fig. 14-15), both employ permanent magnets to disperse ions of different masses laterally into a spectrum. At the same time, the magnetic field focuses ions in equal  $m/q$  groups through the correct exit slits. In both of the spectrometers shown, the neutral gas is ionized by electron bombardment and accelerated by grids through the entrance slits into the analyzer sections. The analyzer sections are evacuated by a single sputter pump to ensure long mean free paths. After the rocket attains an altitude of about 100 km, cutter wheels remove the caps covering the recessed ion sources, exposing them directly to the space environment. Figure 14-15 shows a single ion collector and amplifier for each instrument. Spectrum scanning is accomplished by sweeping the ion accelerator grid voltage from 1000 down to 200 volts every two seconds. This corresponds to a mass sweep from 10 to 50 amu. The major difference between the two units is seen in the electrostatic analyzer used before the magnetic-dispersion stage in the double-focusing spectrometer. As mentioned in Sec. 13-4, a curved-plate electrostatic analyzer provides both energy filtering and spatial focusing. As a result, the double-focusing instrument is more precise; i.e., it has better mass resolution.

A double-focusing mass spectrometer for satellite application has been designed at the NASA Goddard Space Flight Center (Ref. 14-33). One difference between the two double-focusing spectrometers shown in Figs. 14-15 and 14-16 is in the latter's use of an exposed rather than a recessed ion source. More significant, however, is the fixed tuning of the second instrument to masses of 4, 14, 16, 18, 28, and 32, corresponding to major components of the Earth's atmosphere, He, N, O, H<sub>2</sub>O, N<sub>2</sub>, and O<sub>2</sub>. Six separate collectors are connected to a single electrometer tube, which is switched from one collector to another every eight seconds. The detector circuits can measure currents as low as  $10^{-15}$  amp, or, equivalently, partial pressures as low as  $10^{-11}$  mm Hg. Fixed tuning provides more precision than swept tuning, but it is inflexible and presumes prior knowledge of the atmosphere being studied. The mass of the instrument shown in Fig. 14-16 is approximately 5.5 kg, and it consumes an average

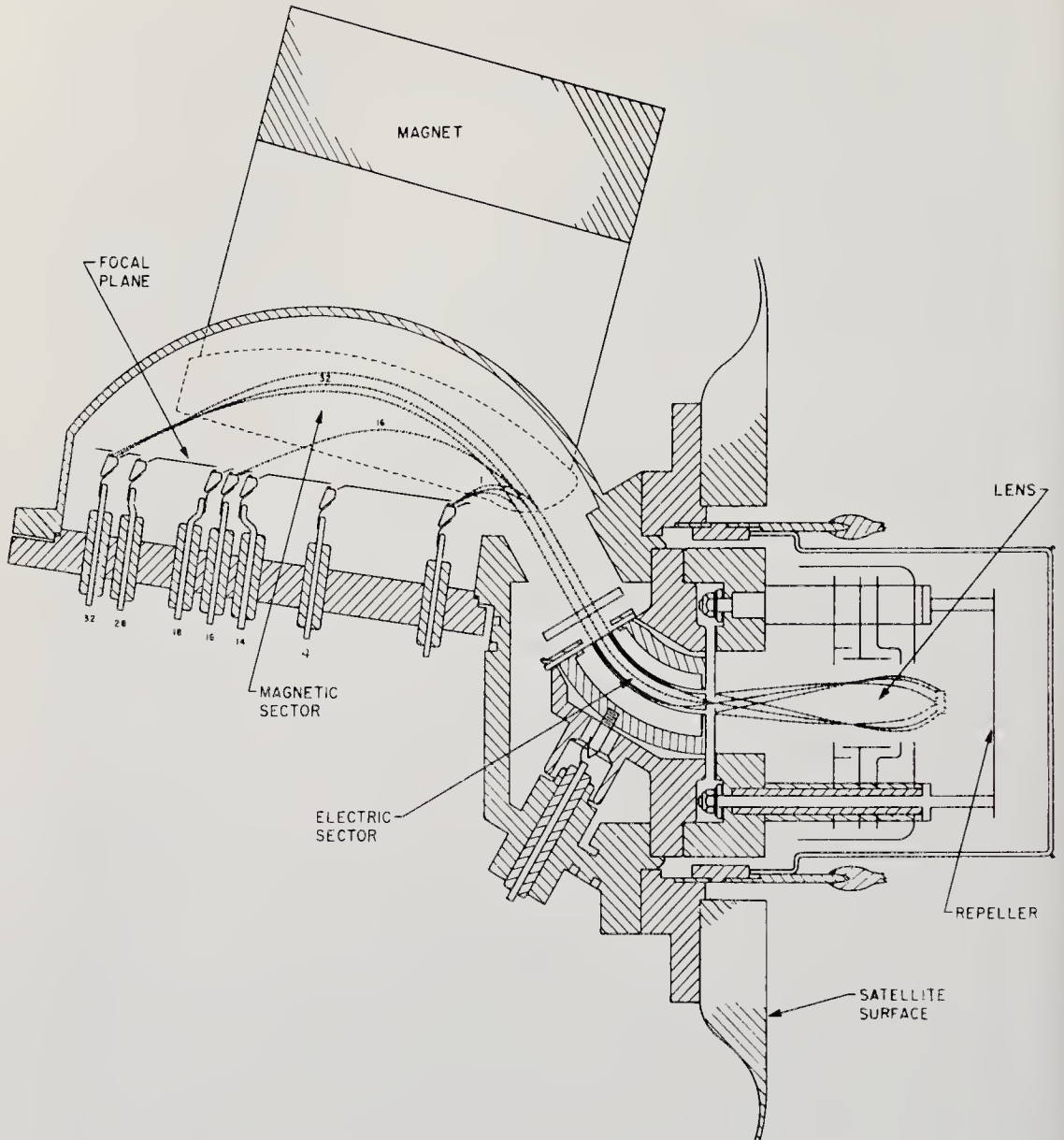


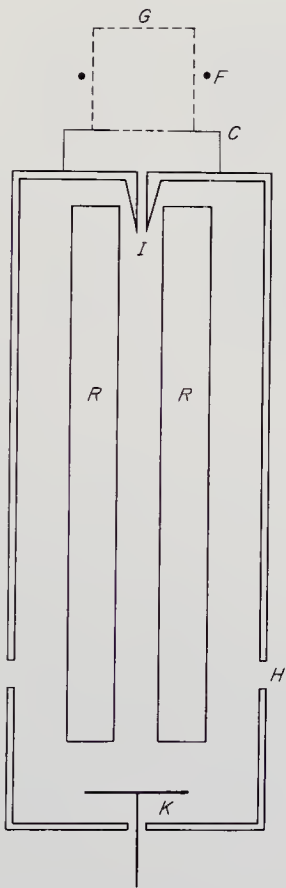
Fig. 14-16. A double-focusing mass spectrometer tuned to six mass components in the Earth's atmosphere. (Ref. 14-33)

of 20 watts. Early space probes would find the magnetic field objectionable and the weight and power requirements high, but double-focusing mass spectrometers are hard to surpass for precision.

Early-flight interest has shifted to the lighter, nonmagnetic instruments, like the quadrupole, time-of-flight, and radio-frequency mass spectrometers. Like the magnetic devices just described, all three are be-

ing developed for space use, but have not been used beyond the sounding-rocket stage yet.

The quadrupole mass spectrometer, or Paul Massenfilter (after W. Paul, Ref. 14-26) has already flown on sounding rockets and promises to be a rugged, lightweight piece of equipment (Ref. 14-31). In essence, it consists of four parallel, cylindrical electrodes arranged on a square pitch (Fig. 14-17). The usual ion source is followed by a grid, which accelerates the mixture of ions into the space running lengthwise between the four cylinder surfaces. The secret of mass separation is the superposition of a radio-frequency field on a steady direct-current field between electrodes. Such a combination of fields forces all except a select group of ions with a specific  $m/q$  ratio into unstable transverse trajectories, so that they eventually collide with the electrodes and are removed from the ion stream. The desired  $m/q$  group travels the full length of the spectrometer to become the detector current. By varying the DC and RF fields, the mass spectrum can be swept.



*F*—FILAMENT, *G*—ACCELERATING GRID,  
*C*—GROUND PLANE, *I*—ION INLET PORT  
 (DIAMETER = 0.081 CM, AREA =  $5.1 \times 10^{-3}$  CM<sup>2</sup>)  
*R*—ANALYZER RODS, *K*—ION COLLECTOR  
*H*—4 BREATHER HOLES (TOTAL AREA = 1.3 CM<sup>2</sup>)

Fig. 14-17. Schematic of a quadrupole mass spectrometer. (Ref. 14-31)

An accurate description of the  $m/q$  filtering action calls upon potential theory. The potential between the four electrodes, assuming electrodes of hyperbolic cross section is:

$$\phi(x, y, z, t) = (A + B \cos \omega t) \frac{x^2 - y^2}{R^2}.$$

The differential equations of motion for an ion in this space are:

$$m\ddot{x} + 2q(A + B \cos \omega t) \cdot \frac{x}{R^2} = 0$$

$$m\ddot{y} - 2q(A + B \cos \omega t) \cdot \frac{y}{R^2} = 0$$

$$m\ddot{z} = 0$$

where  $\phi$  = potential

$x, y, z$  = Cartesian coordinates,  $z$ -axis parallel to the cylinder axes

$t$  = time

$\omega$  =  $2\pi \times$  frequency

$A$  = the applied D.C. voltage

$B$  = the amplitude of the superimposed R.F. voltage

$R$  = one-half the distance between electrode surfaces.

The approximation of hyperbolic electrodes by circular cylinders is acceptable for this instrument. The above equations of motion can be transformed into Mathieu differential equations:

$$\frac{d^2x}{dp^2} + (a + 2b \cos 2p)x = 0$$

$$\frac{d^2y}{dp^2} - (a + 2b \cos 2p)y = 0$$

where:  $p = \omega t/2$

$$a = 8qA/mR^2\omega^2$$

$$b = 4qB/mR^2\omega^2$$

Only for certain small ranges of  $a$  and  $b$  do the equations predict stable transverse ion trajectories. For a fixed  $a/b$  (note  $a/b = 2A/B$ ), only a narrow  $m/q$  group can pass down the instrument's axis without experiencing unstable transverse oscillations and electrode collision.

Scientists at NASA's Ames Research Center have estimated that a quadrupole mass spectrometer suitable for a deep-space probe could be designed at 1.5 kg with an average power drain of 1 watt, assuming pulsed operation. Such a mass spectrometer has been proposed in connection with a curved-plate electrostatic analyzer (Sec. 13-4) to predict plasma species as well as energies. A photograph of a quadrupole mass



Fig. 14-18. A University of Michigan quadrupole mass spectrometer in a sounding-rocket configuration. (Courtesy of the University of Michigan)

spectrometer built and flown in Nike-Cajun sounding rockets is shown in Fig. 14-18 (Ref. 14-30). Although no magnetic field forms in this type of spectrometer to overwhelm the spacecraft magnetometer, the R.F. field must be shielded to preclude disturbing other spacecraft subsystems.

In a time-of-flight mass spectrometer, neutral gas atoms are first ionized and then accelerated in discrete groups by a grid structure such as that shown in Fig. 14-19. Each ion receives the same kinetic-energy increment regardless of mass, so that its time of flight,  $t$ , down a drift tube of length  $S$  is:

$$t = \frac{S}{[2qV/m]^{1/2}}$$

The grid structure also helps to focus the ion beam. In the illustrated

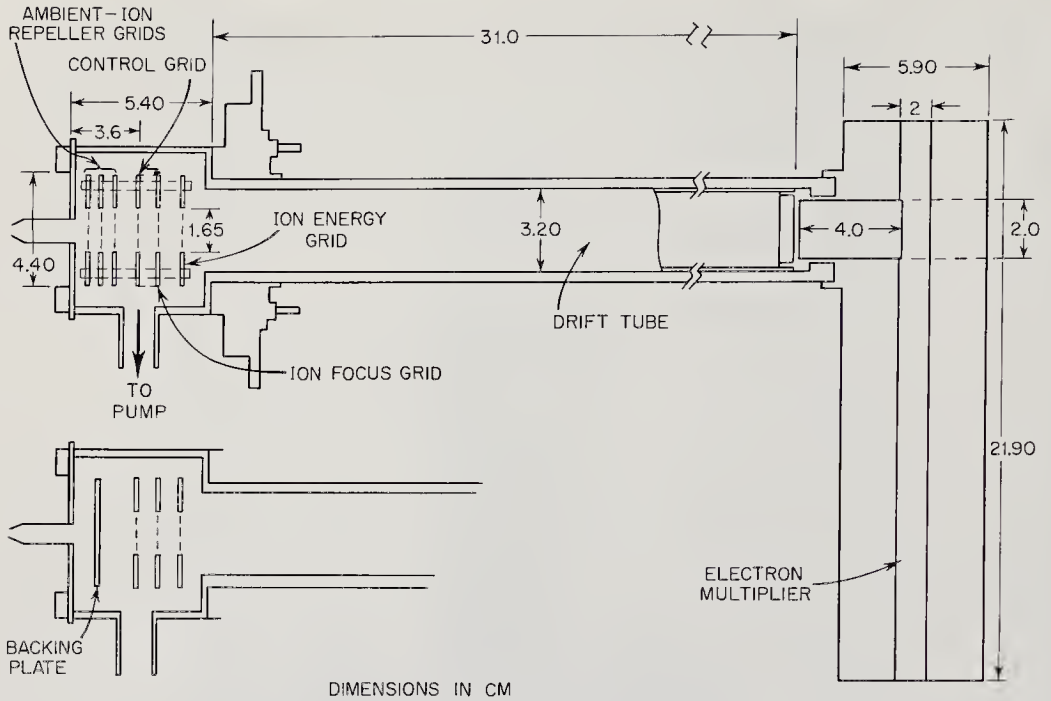


Fig. 14-19. A time-of-flight mass spectrometer designed for spacecraft use. (Ref. 14-23)

Bendix Corporation instrument, the ions impinge on an electron multiplier detector similar to the channel multiplier described in Sec. 13-3. The amplitudes and timing of the signals yield the environmental ion densities and identities.

Superficially, the R.F. mass spectrometer, or Bennett tube, resembles the time-of-flight instrument. Ions of different masses are again separated by grid-produced, axial electrostatic fields (Fig. 14-20). The important difference is the resonant condition set up in the R. F. spectrometer for ion groups with the desired  $m/q$ . Ions are drawn in from the environment or the ion source by a charged grid. A negative, low-frequency sawtooth

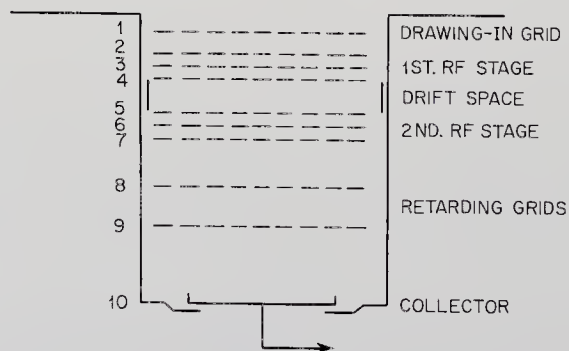


Fig. 14-20. Sketch of an R.F. mass spectrometer.



voltage applied to grid #2 in Fig. 14-20 pulls bunches of these ions into the first R.F. stage. A R.F. field of several megacycles applied to grid #3 imparts kinetic energy to those ions which receive maximum acceleration between grids #2 and #3 and which pass grid #3 at the instant of field reversal. Those ions that pass between grids #3 and #4 at the proper moment are accelerated down the drift tube. Ion sorting depends upon dynamic effects resulting from mass differences. Further filtering occurs farther down the tube. Ions are accepted by the second R.F. stage only if they take an integral number of cycles to clear the drift tube. The retarding grids, #8 and #9, act as another sieve, passing only those ions having a fixed  $m/q$ . R.F. mass spectrometers easily separate ions from 1 to 5 amu and can probably separate the spectrum from 1 to 45 amu. Instruments like the one just described are being developed for the Eccentric Geophysical Observatory (EGO).

*Gas Chromatographs.* A gas chromatograph will chemically separate and identify many of the different molecules present in an unknown planetary atmosphere. The action of this instrument depends upon the different adsorptive properties of special, chemically inert substances packed in columns in granular, fibrous, and other high-surface-area forms. The unknown gas, usually mixed with a carrier gas, is first forced into one end of the column. The different chemical species encounter different resistances to their passage as a result of the selective, adsorptive qualities of the materials packed in the columns. As a function of time, then, the gas component encountering the least resistance will emerge from the other end of the column first. A procession of the dif-

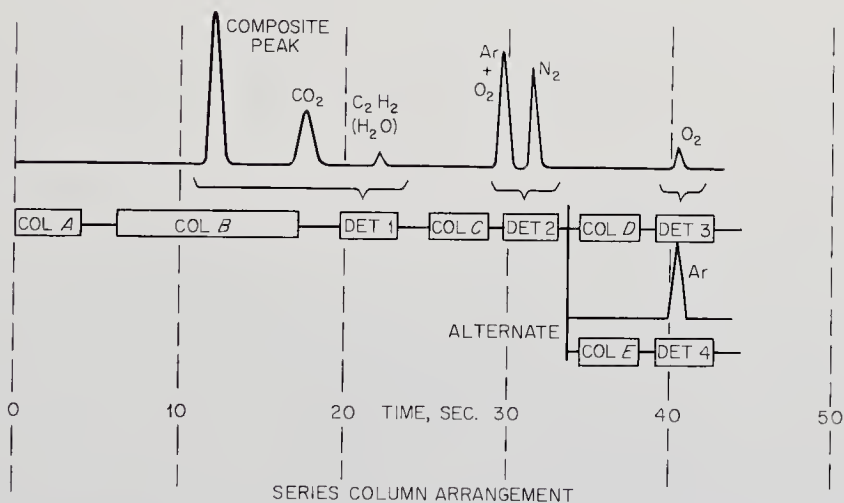


Fig. 14-21. Series-column arrangement for a gas chromatograph for the analysis of the Martian atmosphere. (JPL drawing)

ferent gas constituents will follow, so that a detector sensitive to the thermal conductivity or some similar property of the column efflux will reveal a spectrum in time like the one shown in Fig. 15-12. Note that the order of march depends on adsorptive properties rather than chemical activity or physical parameters like mass. The time of emergence implies the identity of the component. The area under the detector response curve reveals relative concentration. Of course, a spacecraft gas chromatograph would first be calibrated in time and amplitude by a known mixture of gases resembling that expected at the target planet.

The gas chromatograph today is a ubiquitous, highly refined industrial tool. It is accurate, reliable, versatile, in terms of detectable compounds, and possesses a wide dynamic range in terms of concentration. The results at a fixed pressure and temperature can be predicted accurately for many combinations of column materials and gas samples. Furthermore, the basic instrument can also be used to study planetary surface composition by analyzing the pyrolyzed gases from crustal materials. Chemicals associated with life are also susceptible to gas chromatography. In this section, only atmospheric analysis will be discussed, but chromatographs will reappear in Chaps. 15 and 16.

The gas chromatograph of the terrestrial chemical laboratory must obviously be redesigned for space use. It must have the usual qualities of low weight, small size, reliability, ruggedness, and low power consumption. Both the instrument itself and the column materials must be sterilizable. The relatively high temperatures typical of gas chromatograph operation, up to  $400^{\circ}\text{K}$ , must be maintained during operation in the atmosphere under investigation despite its heat transfer properties. If atmosphere analyses are to be made during entry into a planetary atmosphere, chemical determinations must be made within minutes. Fortunately, the gas chromatograph can meet all of these requirements.

In designing a gas chromatograph—say for a Mars probe mission—the chromatograph components would be:

1. A gas-sample collector.
2. A gas pump.
3. Enough columns to separate the expected gas components.
4. A cycling system to permit several rapid analyses in sequence.
5. A sample of known gases for calibration.
6. A detector with an output proportional to the concentration of the gas component emerging from the column.
7. An accurate time scale.
8. An analog-to-digital converter.

A gas chromatograph proposed by the Jet Propulsion Laboratory for

a Mars mission will serve to illustrate typical design problems and their solutions. The Martian atmosphere probably contains  $\text{CO}_2$ , Ar,  $\text{N}_2$ ,  $\text{O}_2$ , and  $\text{H}_2\text{O}$  vapor with a total pressure of just a few millibars. This information helps choose the column packing materials. An impact trajectory permits only a minute or so for the series of sample runs. Under this ground rule, three short runs at different altitudes were proposed for this instrument.

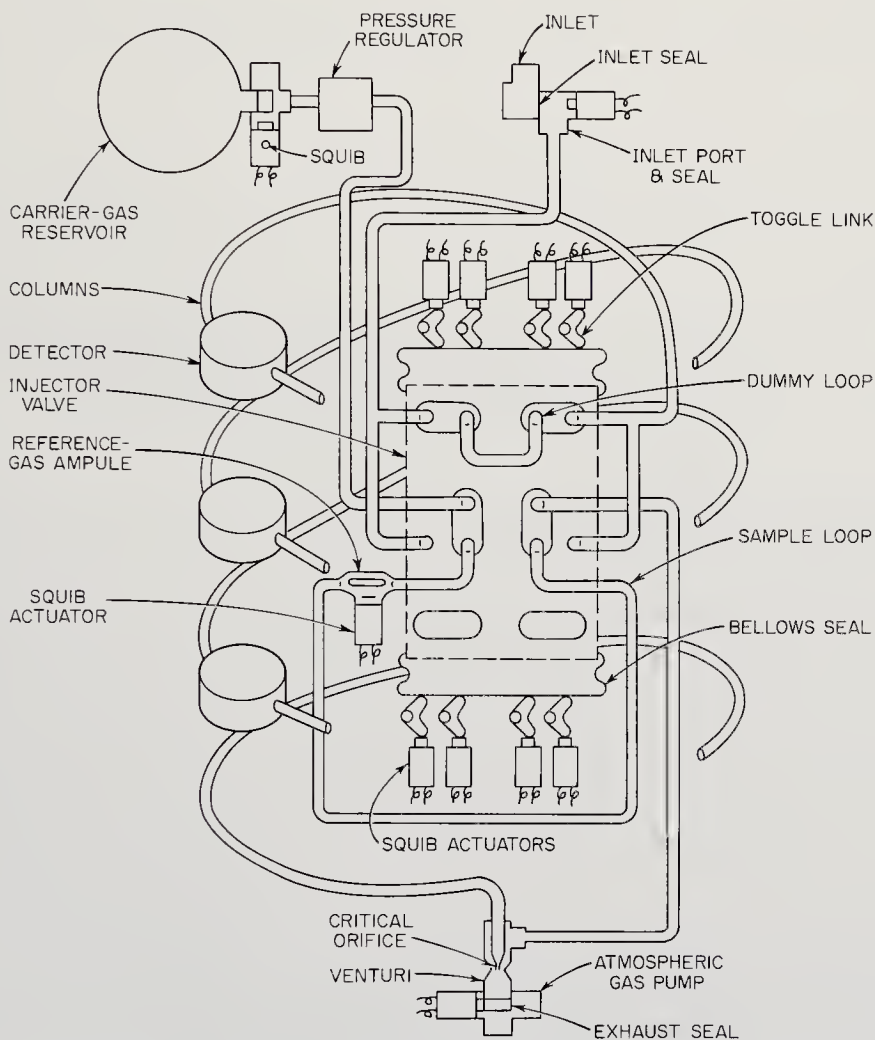


Fig. 14-22. Components of a gas chromatograph for the analysis of the Martian atmosphere. Column detectors are described in the text. (JPL drawing)

The JPL instrument (Fig. 14-22) would be quiescent until about two hours before planetary encounter. A chemical heat source would then bring the instrument up to an operating temperature of  $333^\circ\text{K}$ . A known gas sample would next calibrate the instrument. Upon entering the Mar-

tian atmosphere, a pyrotechnic squib will fire and actuate an injection valve. A bellows arrangement closes the inlet valve after a predetermined amount of gas has been collected. A pressurized, inert carrier gas moving past a Venturi throat establishes a pressure differential that pulls the gas sample through the columns. Figure 14-22 indicates the extensive plumbing necessary for repeated sample collection and column back-flushing.

The four columns and three detectors proposed for the Mars mission are shown in a series arrangement in Fig. 14-21. They are described in more detail below:

<i>Component</i>	<i>Description</i>	<i>Function</i>
Column A	0.95-cm diameter, 3.8-cm long, calcium-carbide filled	Reacts with water vapor to generate acetylene.
Column B	0.16-cm diameter, 244-cm long, 40% Dow Corning 550 silicone oil on 70-80 mesh acid, base washed and silanized diatomaceous earth	Separates sample into composite peak, CO <sub>2</sub> , and acetylene.
Detector 1	Cross-section detector (see later discussion)	Detects composite peak, CO <sub>2</sub> , and acetylene.
Column C	0.16-cm diameter, 23-cm long, 70-80 mesh, acid, base washed and silanized diatomaceous earth. Plus 0.16-cm-diameter, 23-cm-long column with 70-80 mesh activated molecular sieve 5A	First section delays entry of composite peak into molecular sieve 5A column until CO <sub>2</sub> and acetylene are detected. Second section separates N <sub>2</sub> from Ar + O <sub>2</sub> .
Detector 2	Cross-section detector	Detects N <sub>2</sub> and Ar + O <sub>2</sub> .
Column D	0.16-cm diameter, 23-cm long 70-80 mesh, acid, base washed and silanized diatomaceous earth	Delays detection of O <sub>2</sub> until N <sub>2</sub> is detected by detector 2.
Detector 3	Electron-capture detector (see later discussion)	Detects O <sub>2</sub> .

Note that column A is needed to generate acetylene from water vapor, which would otherwise have to be retained in the columns for excessive

lengths of time in order to be detected. The kind of spectrum expected from this gas chromatograph is shown in Fig. 15-12.

The cross-section detectors listed above are small-volume, ionization-cross-section detectors. They are simply small ionization chambers in which the gas being sampled is ionized by a radioactive source (say,  $\text{Sr}^{90}$ ). The current measured is a function of the sum of the ionization cross sections of the molecules present and thus a measure of the sample concentration.

The electron-capture detector is also an ionization chamber using a radioactive source for gas ionization. Its potential, however, is kept just sufficient to collect all of the free electrons produced in the carrier gas. This type of detector responds only to electronegative gases, like oxygen.

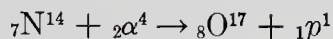
A complete gas chromatograph spectrum entails the transmission of a great deal of information back to Earth. The bandwidth or number of bits may be reduced considerably merely by telemetering the timing and amplitudes of the peaks, though quantitative precision will naturally be lost since the resulting spectral curve is only an approximation.

JPL has estimated that the mass of the gas chromatograph just described should not exceed 2.2 kg and will draw no more than 4 watts during its three cycles of operation.

*Simple-Composition Instruments.* The mass spectrometers and gas chromatograph just presented are spectral instruments; that is, they analyze wide ranges of molecular masses and chemical species. Performance like this almost invariably leads to instrument complexity (Figs. 14-16 and 14-22). The so-called simple-composition instruments form a class of less complex but more restricted instruments for planetary atmospheric measurements. The classifying properties of simplicity and the ability to analyze the composition of a gas can conceivably include a great variety of instruments; however, only a few are under active consideration and only the following two are treated here:

#### The Rutherford experiment Kryptonate analyzers

The Rutherford experiment detects nitrogen-14, the major isotope of nitrogen expected in planetary atmospheres, by observing the protons created by alpha particle bombardment (Ref. 14-22). The Rutherford reaction, first observed by E. Rutherford in 1919, is:



Since other atmospheric isotopes, like  $\text{C}^{12}$ ,  $\text{O}^{16}$ , and  $\text{Ar}^{40}$ , are stable under bombardment by alphas in the 6-Mev range, a Rutherford ( $\alpha, p$ ) experiment would be specific for  $\text{N}^{14}$ . The experiment would consist of an

alpha source, say  $\text{Cm}^{242}$  emitting 6.1-Mev alphas, and a counter sensitive to protons between 2 and 4 Mev (Fig. 14-23). Tests at JPL, where such an instrument is being studied, show characteristic proton energy spectra that, in the case of the Earth's atmosphere, yielded  $80 \pm 2\%$  for the percentage of  $\text{N}_2$ .

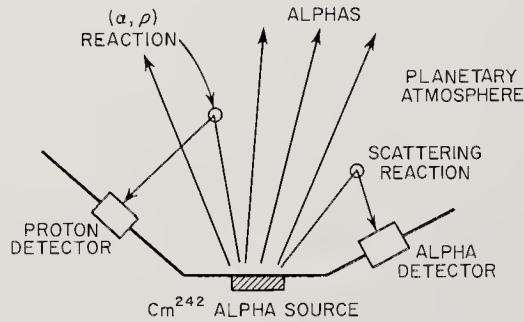


Fig. 14-23. Possible experiment configuration for the Rutherford experiment used to detect the presence of simple gases. (Ref. 15-2)

A detector to count scattered alpha particles can logically be included with the  $\text{N}^{14}$  analyzer. If an alpha source and an alpha detector are arranged as shown in Fig. 14-23, the concentrations of  $\text{C}^{12}$  (presumably in  $\text{CO}_2$ ) and  $\text{Ar}^{40}$  can be measured simultaneously with the  $(\alpha, p)$  determination of  $\text{N}^{14}$ .

Coulomb back-scattering at  $180^\circ$  (also called Rutherford scattering) is described by the following equation:

$$E_s = E_0 \left( \frac{A - 4}{A + 4} \right)^2$$

where  $E_s$  = the energy of the back-scattered alpha

$E_0$  = the initial energy of the alpha

$A$  = the mass number of the target nucleus.

By setting the instrument's electronics to discriminate four alpha energy levels,  $\text{C}^{12}$  and  $\text{Ar}^{40}$  can be analyzed and redundant  $\text{N}^{14}$  and  $\text{O}^{16}$  measurements made. The Rutherford experiment is similar in concept to the one proposed for crustal analysis from the Surveyor lunar soft landing vehicle by A. Turkevich at the University of Chicago (See Sec. 15-3). The Surveyor alpha-scattering experiment will be seen to be much farther along in development.

The kryptonate simple-composition detector works on an entirely different principle, but again it is simple and specific in its analyzing capabilities. Kryptonates are materials in which krypton has been stably

incorporated by electrostatic bombardment or perfusion at high temperatures and pressures (Ref. 14-9). If the krypton trapped in a solid is radioactive  $\text{Kr}^{85}$  (half life = 10.4 years, 0.67-Mev betas), a radiation detector will give a reading proportional to the amount of solid present, assuming a uniform distribution of  $\text{Kr}^{85}$ . If the constituents of the planetary atmosphere under investigation react with the surface of the kryptonated solid and release the bound  $\text{Kr}^{85}$ , the rate of reduction in the radiation level will be a measure of the reaction rate. Reaction rates are highly specific for different combinations of gas and solid. Gases like ozone, sulfur dioxide, hydrogen sulfide, and water vapor have been analyzed terrestrially by such methods. Of course, reaction rates also vary with temperature and pressure, but presumably these data would be known from associated experiments. Kryptonate analyzers are under study by JPL, Parametrics, Inc., and other organizations.

A third simple-composition under active development employs chemiluminescence to indicate the presence of specific atmospheric constituents.

*Ram Spectrometers.* When a spacecraft enters a planetary atmosphere without rocket braking, speeds are so great that an incandescent layer of gases, at temperatures as high as  $7000^\circ\text{K}$ , forms around the nose cone. The radiation emitted from the hot gas can be analyzed by a spacecraft ram spectrometer to reveal the atmospheric composition. Since atmospheric samples are collected and processed, in a sense, this instrument is introduced here rather than placed along with the passive optical instruments in Sec. 14-2.

NASA's Ames Research Center has proposed a ram spectrometer for Martian entry vehicles. Terrestrial experiments using small models launched by light gas guns in test atmospheres containing  $\text{CO}_2$  and  $\text{N}_2$  revealed strong cyanogen (CN) bands. Numerous other bands, indicative of NO,  $\text{C}_2$ ,  $\text{H}_2\text{O}$ , and other compounds, could also be detected with this kind of spectral analysis. The ram spectrometer would be a logical experiment to carry aboard experimental entry vehicles like the drag bodies covered in Sec. 14-6. The spectroscopic experiments described above could also be carried out by a landing vehicle using a small heat source, in the manner of conventional spectroscopy.

*Alpha and Gamma Densitometers.* The fraction of radiation back-scattered from a gas being bombarded with particles and photons from a radioactive source is proportional to the total scattering cross section of the gas. Scattering cross sections vary from element to element, so that a knowledge of atmospheric composition is necessary before data from nuclear back-scatter densitometers can be properly interpreted. Back-scatter data from the alpha-scattering experiment in the Rutherford simple-composition detector would suffice for crude density calcula-

tions. An alpha densitometer would have a component arrangement similar to that shown in Fig. 14-23. Gamma back-scattering might also be used, but gamma rays are much more penetrating than alpha particles, and signals would be weaker. Generally, the embryonic research programs existing in this area favor alpha scattering.

*Acoustic Transmission Line (Speed-of-Sound Experiments).* If the speed of sound can be measured in a gas sample at a known temperature,  $T$  (see Fig. 14-24), the mean molecular weight,  $\bar{M}$ , the density,  $\rho$ ,

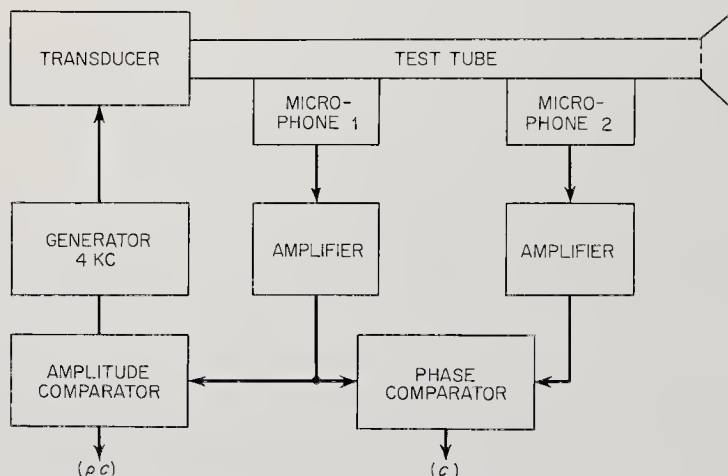


Fig. 14-24. Block diagram for an atmospheric speed-of-sound experiment. (Ref. 14-16)

and the mean specific heat ratio,  $\bar{\gamma} = c_p/c_v$ , can be determined (Ref. 14-15). The pertinent equation is:

$$C^2 = \bar{\gamma}RT/\bar{M}$$

where  $C$  = the velocity of sound in the gas (m/sec)

$R$  = the Universal Gas Constant = 8.31 joules/°K-mole.

In an actual experiment, the unknown atmosphere would be brought into a long, spirally coiled tube (Fig. 14-25). The ratio  $\bar{\gamma}/\bar{M}$  would be determined by measuring  $C$  in the thermostatically controlled transmission line. Next, the acoustical impedance,  $Z = \rho C$ , would be determined in the same apparatus to fix the density,  $\rho$ , at the tube temperature. A knowledge of the ambient temperature—say, from a resistance thermometer—would yield ambient density by inverse scaling. Finally, with density and temperature known, the ideal gas law gives the mean molecular mass, if ambient pressure is known from other instruments:

$$\bar{M} = \rho RT/P.$$



A speed-of-sound experiment for use on the surface of Mars has been proposed by NASA's Goddard Space Flight Center. A spiral tube one meter long with an inner diameter of 0.5 cm admits the atmosphere and raises it to the controlled temperature,  $T$  (Figs. 14-24 and 14-25). At one

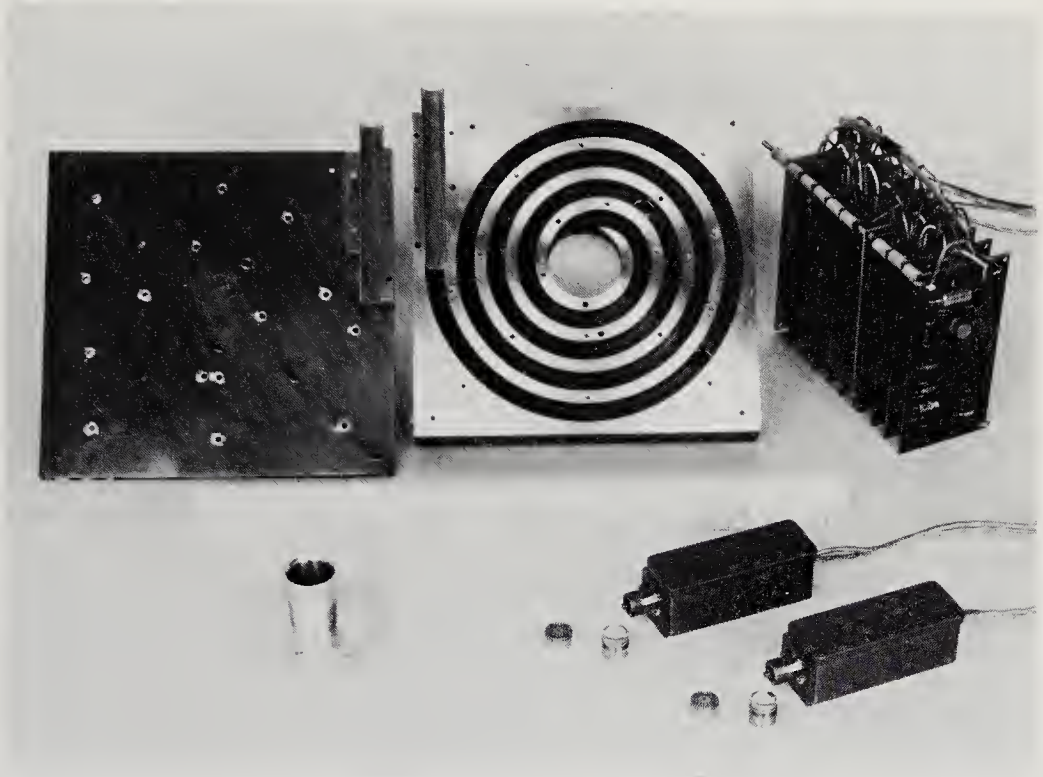


Fig. 14-25. Laboratory speed-of-sound instrument. (NASA photograph)

end of the tube, an acoustic generator produces sound energy at approximately 4000 cycles. Two identical condenser microphones are mounted on the tube wall, separated by approximately nine wavelengths. The tube itself is terminated by a damping material to preclude the formation of standing waves.

The phase shift of the sound waves, as measured by the two microphones and phase comparator, is a function of the wavelength only. Since  $C = \text{frequency} \times \text{wavelength}$ , the speed of sound can be computed. The acoustic impedance can be measured by the same microphones. The mechanical and acoustical impedances of the sound generator can be selected so that the velocity of the diaphragm is practically independent of the acoustic radiation impedance of the tube. The sound pressure in the tube, as recorded by the microphones, is then proportional to the acoustic impedance of the gas. In this way, assuming that data on ambient pres-

sure and temperature are available from other experiments, a speed-of-sound experiment can measure density and mean molecular weight.

#### 14-4. Ionospheric Instruments

The structures and compositions of planetary ionospheres not only reveal the chemical and physical processes occurring under the stimulation of solar radiation but also provide significant information on the neutral compositions of the atmospheres. Historically, the neutral composition and dynamics of the Earth's upper atmosphere were first inferred from ionospheric electromagnetic soundings. The ionospheres of the other planets should be no less revealing.

Ionospheric instruments, with the exception of the Langmuir and certain other probes, rely upon electromagnetic apparatus. While the neutral atmosphere and, to a lesser extent, the ionospheres can be analyzed by observing the effects on electromagnetic radiation generated by the Sun and planets, artificial radio sources on the space probes or back on Earth form the foundation of ionospheric research. Transmitters and receivers must be immersed in, placed beneath, and carried around behind the ionospheres, because no satisfactory natural sources of radiowaves exist in these locations.

The Langmuir probe and some specific ionospheric experiments that have been suggested will now be discussed.

*Langmuir Probe.* This instrument consists of a small cylindrical rod (probe) projecting from and insulated from the spacecraft skin. When a signal with alternating polarity is applied between the probe and the skin, electrons and ions in the ionosphere will flow and be collected. The volt-ampere characteristics of the Langmuir probe in the presence of the plasma reveal both electron density and electron temperature. Typical mass: 1.3 kg. Power consumption: 3 watts. (See Sec. 13.4 for other plasma probes.)

*Bottomside Sounders.* The classical terrestrial ionospheric experiments began with skyward-pointing, ground-based transmitters, or, as they are now rather facetiously called, bottomside sounders. When a beam of radio waves is projected upwards, it encounters a region of high electron density and is refracted. At some critical combination of charge density ( $10^4$  to  $10^6$  electrons/cm<sup>3</sup> in the Earth's ionosphere) and frequency (1 to 10 Mc) the beam is refracted 180° (reflection) and an echo is observed. By sweeping the frequency band, the ionospheric electron density can be plotted. The altitude of reflection can be introduced by pulsing the transmitter and timing the echos. A miniaturized sounder of this type for use on a Mars lander would probably have a mass around 25 kg and draw 25 watts of power when in use. Obviously, bottomside sounders are

heavy and represent substantial power sinks. For this reason, they do not enjoy a high priority on landing-vehicle instrument lists.

*Topside Sounders.* Electromagnetic soundings by flyby probes will almost certainly precede ionospheric experiments from landers. The Mariner class of probes, in fact, could carry such equipment.

A topside sounder would probably consist of a single dipole antenna that would beam radio energy at the target planet during the brief period of encounter. Flattau and Donegan have published the following specifications for such an instrument:

TABLE 14-5. CHARACTERISTICS OF A PLANETARY-PROBE TOPSIDE SOUNDER\*

Planet	Sounding Freq. (Mc)	Radiated Power (watts)	Generated R.F. Power (watts)	Signal Power at	
				Receiver Terminals Max. (dbm)	Max. (dbm)
Mars	1.0	20.0	224.00	-98.7	-73.2
	2.0	16.0	35.0	-98.7	-73.2
	5.0	12.3	15.5	-105.7	-79.9
Venus	4.5	4.5	7.9	-105.7	-81.6
	6.0	4.0	5.6	-107.7	-83.6
	9.0	3.6	4.5	-111.2	-87.1

Maximum sounding range: 40,000 km

Minimum sounding range: 8,000 km

Sounding duration: Three frequencies sequenced, 8-sec sounding time at each frequency

Receiver: Superheterodyne with one stage of tuned R.F. amplification

Mass: 11.6 kg

Power Consumption: Transmitter power supplied by separate battery. One watt from spacecraft power supply continuously.

\* Ref. 14-13.

*Bistatic Radar.* A bistatic radar system (one which places a separate receiver near the target) promises to produce much the same kind of ionospheric data as the topside sounder, without the necessity of carrying a transmitter on the probe itself. In such an experiment, a powerful (~1 Mw), Earth-based radar transmitter sends pulses of electromagnetic energy toward the target planet. A spacecraft near the planet receives two signals: a direct signal from the transmitter and one refracted through the planetary ionosphere and therefore delayed in time. The probe needs only to compute the time delay and telemeter this information back to Earth, where electron-density calculations can be made. A practical study of another planet's ionosphere would entail the use of a

whole range of frequencies. The approximate mass of the probe portion of a bistatic radar system would be 2 to 3 kg, with a power requirement of 2 watts. An added benefit of the bistatic radar is its ability to make planetary-terrain studies with higher frequencies as well as the radio-propagation experiments mentioned in Chapter 13.

*Limb-Diffraction Experiments.* When a circular disk is illuminated by electromagnetic waves from a distant source, a detector placed behind the disk will record the classical Fresnel-diffraction pattern. Surprisingly, Fresnel diffraction results in a bright spot at the center of the circular shadow. In laboratory experiments the bright spot, which is almost as bright as if no disk were there, is surrounded by a series of light and dark rings (Ref. 14-20). Radio waves emanating from a powerful transmitter on the Earth and a planet with a probe-based receiver behind it take the place of the usual laboratory light source, penny, and screen. The probe passing through the planet's shadow will be able to discern the Fresnel pattern as fluctuations in the signal strength of the Earth-based transmitter, though the pattern will probably not be sharp enough to show the central bright spot. Such a diffraction pattern would exist in the absence of a planetary atmosphere. If, however, the planet is surrounded by an atmosphere, the radio waves will also be refracted and distortion of the Fresnel pattern will result. In effect, the Fresnel rings will be stretched, because the radio waves will be bent away from the planet by electrons in its ionosphere. The amount of stretch in the diffraction pattern at various frequencies can be related to ionospheric and atmospheric properties. The limb-diffraction technique is so sensitive that the radio-propagation experiment on the Pioneer-6 deep-space probe is expected to detect the Moon's residual atmosphere as it passes behind the disk. A similar experiment was carried on Mariner 4.

Eshelman and Fjeldbo, at Stanford University, proposed a Martian limb-diffraction experiment for the now-canceled 1966 Mariner flyby. One goal of the experiment would have been the measurement of the stretching of the Fresnel diffraction pattern at the 2300-Mc frequency of the communication subsystem. The spacecraft portion of the experiment would have consisted of a receiver tuned to the Earth-based transmitter. The spacecraft would have digitized and telemetered the fluctuations back to Earth. No mass and power-consumption data are available, but they should be similar to those given for the bistatic radar probe receiver.

*Sferics Detector.* A very simple, broad-band receiver with a whip antenna could monitor sferics caused by electrical discharges (from lightning) in an atmosphere. Such an instrument would record the number and intensities of the discharges. This is a low priority experiment, however. Estimated mass: 1.5 kg. Power consumption: 2 watts.

### 14-5. Meteorological Instruments

Even though the gross features of the other planetary atmospheres are still being debated, speculation concerning meteorological instruments to measure temperature, pressure, and wind velocity and direction are not entirely frivolous. In general, the most rugged and reliable instruments would be counterparts of those that have been developed for remote weather stations on Earth. Probe instruments, as always, should provide electrical and, if possible, digital signals. No meteorological instruments specifically tailored for planetary landings are being developed, but the characteristics shown in Table 14-6 should be representative.

### 14-6. Atmospheric Properties from Drag-Body Experiments

The next logical step beyond the simple planetary flyby probe is the atmospheric entry vehicle launched from a flyby probe. Such a vehicle would descend ballistically through the planet's atmosphere, making measurements until the moment it is destroyed by surface impact. Measured data would be radioed back to the parent probe during descent for retransmission to Earth.

In the short transit time through the atmosphere (just a minute or so in the case of Mars) a surprisingly rich harvest of information may be gathered. The ram spectrometer described in Sec. 14-3 represents one type of instrument that might be carried. Static- and ram-pressure gauges and temperature-indicating instruments similar to those introduced earlier in this chapter are also possibilities. In this section, the dynamic properties of the entry vehicles and the derivation of atmospheric information from their motions will be covered.

The most obvious dynamic effect is that of drag due to atmospheric resistance—thus the term “drag body” (Ref. 14-32). The instantaneous acceleration is a measure of atmospheric density:

$$\frac{C_D \rho V^2 A}{2} = -m \frac{dV}{dt}$$

$$\rho = \frac{2 dV/dt}{V^2 C_D A / m}$$

where  $C_D$  = the drag coefficient  
 $\rho$  = atmospheric density  
 $V$  = entry-vehicle velocity  
 $A$  = area  
 $m$  = entry-vehicle mass  
 $t$  = time.

TABLE 14-6. CHARACTERISTICS OF PLANETARY-LANDER METEOROLOGICAL INSTRUMENTS

<i>Property Measured</i>	<i>Probable Instruments</i>	<i>Instrument Characteristics</i>
Temperature	Resistance thermometer	Platinum or some other material whose resistivity as a function of temperature is well known would be used. Accuracy expected would be 10°C over a range of perhaps 1000°C. Mass: 0.15 kg. Power consumption: 0.1 watt. Analog-to-digital converter needed.
	Thermistor	Thermistors employ ceramic-like semiconductors which have high negative-temperature coefficients. They are more accurate than resistance thermometers, but have more limited ranges of application. Analog-to-digital converter needed. Same mass and power consumption as resistance thermometer.
Pressure	Aneroid gauge	Gas pressure on a diaphragm covering evacuated chamber changes analog signal produced by strain gauge or potentiometer. Mass: 0.15 kg. Power consumption: 1 watt.
	Pirani gauge	Wire filament, whose electrical resistance is a function of temperature, is cooled by atmosphere. Amount of cooling (and therefore filament resistance) depends on pressure. Produces analog signal.
	Redhead gauge	Electrons emitted from a cold cathode ionize gas. Current measured between two electrodes is a measure of pressure. Range: $10^{-5}$ to $10^{-13}$ mm Hg.
	Bayard-Alpert gauge	Electrons which are thermionically emitted from a hot cathode ionize gas. Current measured between two electrodes is a measure of pressure. Range: $10^{-4}$ to $10^{-10}$ mm Hg.
	Alphatron gauge	Alpha particles from radioactive source ionize gas. Current measured between two electrodes is a measure of pressure. Range: 760 to $10^{-9}$ mm Hg.
Wind velocity and direction	Anemometer and vane	Three-dimensional, cruciform-shaped vane is suspended in exposed place. Three orthogonal pressure transducers yield wind velocity and direction. Analog-to-digital converter needed. Mass: 1 kg. Power consumption: 0.5 watt.

The parameters  $C_D$ ,  $A$ , and  $m$  will be known beforehand. The deceleration,  $-dV/dt$ , can be measured by accelerometers within the drag body and telemetered back to the parent probe.  $V$  in the density equation would be obtained by integration:  $V = V_e - \frac{dV}{dt} \cdot dt$ , where  $V_e$  is the calculable entry velocity of the drag body.

As drag body encounters the atmosphere, it will begin to oscillate (pitch and yaw) with a frequency,  $f$ . The measurement of  $f$  by onboard gyroscopes leads to a knowledge of the specific heat ratio,  $\gamma$ , where  $\gamma = c_p/c_v$  (Ref. 14-32). This oscillation frequency would be the same in all noble gases. In fact, it would be the same for all gases with equal specific-heat ratios. The fact that the frequency of oscillation is a sensitive function of  $\gamma$  makes it possible to confirm or refute hypothesized planetary-atmosphere gas mixtures by comparing their calculated specific-heat ratios with those measured by drag bodies.

NASA engineers have proposed both blunt, nearly spherical bodies and slender cylindrical shapes for the experiments described above. The blunt body suffers from communication blackout, due to the formation of a ram-heated plasma sheath during part of its descent. Data in this case would have to be stored and transmitted during the few seconds after the sheath disappears as the probe slows down in the lower atmosphere, and before the transmitter is destroyed at impact. The slender

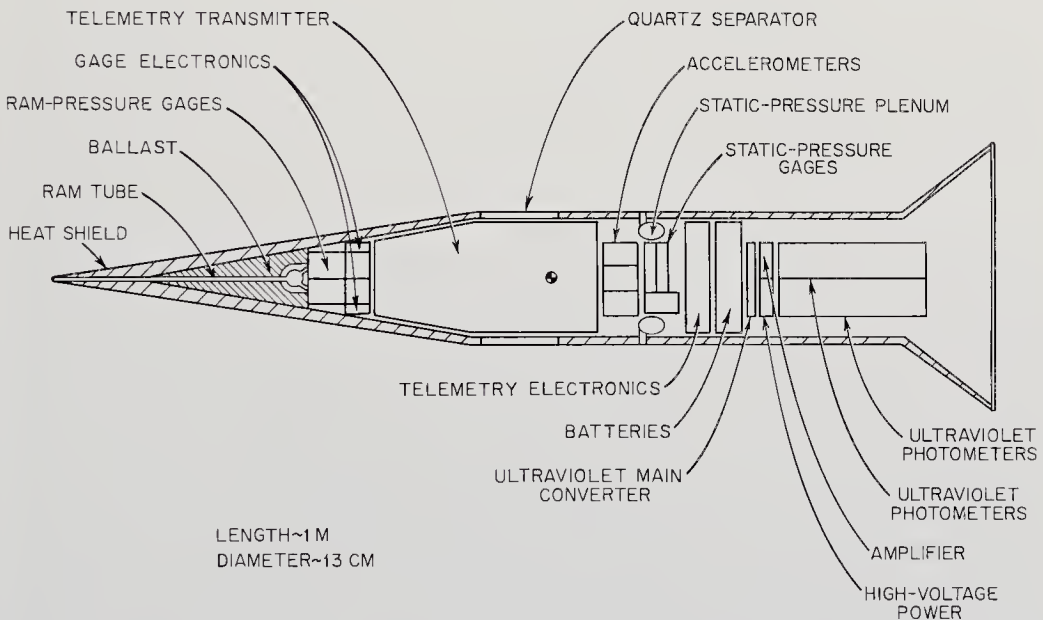


Fig. 14-26. Sketch of a slender, cylindrical drag body for entry experiment in the Martian atmosphere. (NASA drawing)

vehicle does not have the communication problem, but it is more sensitive to perturbing forces. A sketch of the slender cylinder type of drag body proposed by Goddard Space Flight Center for the 1966 Mars flyby is shown in Fig. 14-26 as representative. This drag body would have a mass of around 14 kg, exclusive of the separation mechanism and any momentum equalizer projected in the other direction during launching from the parent probe. Battery-supplied power would amount to roughly 24 watts during the 60-sec penetration of the Martian atmosphere. The total amount of data that would be transmitted would be 60,000 bits for all of the experiments shown in Fig. 14-26.

Analysis of data from all experiments should yield:

1. Ambient pressure as a function of altitude.
2. Ambient atmospheric density as a function of altitude.
3. The ratio of specific heats as a function of altitude.
4. Ambient temperature as a function of altitude.



## *Chapter 15*

---

### INSTRUMENTS FOR ANALYZING A PLANET'S CRUST

---

---

#### 15-1. Prologue

Many of the atmospheric instruments described in the preceding chapter may also be used for crustal analysis after obvious modifications. Some, like the gas chromatograph, merely require that gases be driven from the solid sample collected from the planet's crust. Others, like the alpha-scattering experiment, need only be set down facing the crust instead of the atmosphere. The atmospheric- and crustal-instrument lists were compared in Table 14-1, page 382, to accentuate the similarities. The greatest divergence appears when macroscopic planetary phenomena, like weather and geological structure, are being probed. Instruments that measure microscopic properties—i.e., composition and density—have a great deal in common.

Extraterrestrial geology should not differ too much from terrestrial geology; therefore, the scientific questions to be asked follow familiar lines. The geologist would first like to know the target planet's surface features, texture, composition, and density. The physics-oriented instruments provide atomic and, by inference, molecular abundances in addition to the density. They reveal little, however, about rock structure and the identities of the complex minerals. The petrographic microscope will actually reveal more of a rock's gross features, such as grain size and crystal class, which are commonly used in field identification. For a thorough mineral study, the best instrument is an experienced geologist with a few simple tools. The same comment applies to structural geology. Seismometers, television, and the other instruments in Table 14-1 can only make scoping studies of a planet's surface. Such instruments sup-

TABLE 15-1. ELECTROMAGNETIC RADIATION INSTRUMENTS AND EXPERIMENTS USED IN SPACE-PROBE RESEARCH

<i>Region of Spectrum</i>	<i>Natural Emission</i>	<i>Artificially Induced Emission</i>	<i>Transmission and Reflection</i>
Microwave	Microwave radiometer (Sec. 14-2) (atmospheric structure)		Bistatic radar (Sec. 14-4) (ionospheric structure) Topside and bottomside sounders (Sec. 14-4) (ionospheric structure)
Infrared	Thermal photography (Sec. 15-2) (surface structure) Infrared spectrometers (Secs. 14-2, 15-2, and 16-2) (atmospheric and surface structure, microenvironments, life chemistry)		Radar (Sec. 15-2) (surface relief) Limb-diffraction experiment (Sec. 14-4) (ionospheric structure)
Visible	Infrared radiometer (Sec. 14-2) (atmospheric structure)		Biological microscope (Sec. 16-3) (life) Petrographic microscope (Sec. 15-3) (surface composition) Red-shift experiment (Sec. 13-6) (relativity check) Optical rotary dispersion (Sec. 16-3) (life chemicals) Television (Sec. 15-2) (surface structure, life) Polarimeter (Sec. 14-2) (atmospheric composition)

Ultraviolet	Ultraviolet photometer (Sec. 14-2) (atmospheric composition)	Ram spectrometer (Sec. 14-3) (atmospheric composition)	X-ray diffractometer (Sec. 15-3) (surface composition)
X-ray	Lyman- $\alpha$ detector (solar processes)		Gamma densitometer (Secs. 14-3 and 15-3) (atmospheric and surface densities)
	Thin-window ionization chamber (solar X-rays)	X-ray fluorescence spectrometer (Sec. 15-3) (surface composition)	
Gamma-ray	Gamma spectrometer (Sec. 15-3) (surface composition)	Neutron-activation analysis (Sec. 15-3) (surface composition)	
	Gamma-ray telescope (Sec. 13-3) (galactic $\gamma$ -rays)		
	Ionization chamber (solar $\gamma$ -rays)		

plement the physics data with measurements of seismicity, geological age, engineering properties (hardness), and the surface structure within TV range. Radars can make planet-wide relief studies. Finally, geodetic satellites can grasp the over-all planetary shape, mass distribution, and elasticity. But none can really replace a trained, on-site geologist.

What is the state of development for crustal instruments? Somewhat surprisingly, their general development is farther advanced than it is for their atmospheric counterparts, even though planetary landings will lag flybys by more than ten years. Part of the reason for this disparity is found in the advanced state of geophysical-instrument development for prospecting purposes. More important, though, is the strong current of fallout stemming from the intensive lunar program (Ranger and Surveyor). As the individual instruments are depicted, the extent of these benefits will become more obvious.

### 15-2. Surface Properties by Remote Analysis of Electromagnetic Radiation

One way to study a planetary surface without troublesome sampling is through analysis of the electromagnetic radiation it emits and reflects. Such analysis can be done remotely, even from a flyby spacecraft or orbiter. This convenience over direct sampling is counterbalanced, however, by the lesser amount of information acquired and the greater difficulty in its interpretation. A perusal of Table 15-1 shows that these "remote" surface experiments fall into three categories:

1. Infrared spectroscopy and photometry of the surface, using naturally emitted and reflected light.
2. Television and photography of the surface, using naturally reflected visible light and emitted infrared radiation.
3. Radar, to make topographic and electrical measurements of the surface with artificially created microwaves.

Electromagnetic experiments, as one might expect, closely parallel the atmospheric radiation analyses of Chap. 14. The wavelengths used must, of course, be different in order to penetrate readily the atmospheric absorption windows and the ionosphere.

Since remote surface analysis by flybys may precede lander experiments by ten years, the development of appropriate electromagnetic instruments is being pushed rapidly. Still, in many respects they lag behind the surface-sampling instruments that have borrowed heavily from the Ranger and Surveyor programs.

*Infrared Spectrometers and Photometers.* Spectrometry and photometry in the infrared have important applications in the remote measurement

of surface temperature, surface mineral composition, and the location of coexisting water-vapor concentrations and surface warmth that might indicate surface water and perhaps even life (microenvironments). The use of the infrared instruments in atmospheric study were introduced in Chap. 14, along with the basic operating principles of spectrometers and photometers. This general background will not be repeated here.

A three-channel, planet-mapping, infrared spectrophotometer has been proposed by the University of California group for an early Mars flyby or orbiter. The photometer channels are at:

1.  $2.4\mu$ , just outside the water-vapor absorption band.
2. The  $2.6\mu$  water-vapor absorption band.
3. The  $8-12\mu$  thermal emission band of the Martian surface.

The visible portion of the spectrum is also monitored. The mapping of the Martian surface through these radiation channels offers the following intriguing possibilities:

1. The detection of microenvironments possibly conducive to life, where temperatures and water-vapor pressures are high. The intercomparison of channels 1 and 2 with the visible spectrum could lead to inference of the water-vapor partial pressure. Since surface changes in reflectivity with wavelength might produce the same effects as the presence of water vapor, results would have to be interpreted with great care.
2. The resolution of Martian surface relief (invisible from Earth) by comparing the thermal and visible photometer maps. The different insolation of slopes should force them to stand out as cooler areas, if there is no concurrent change in absorption and emissivity. It is possible that ozone, if present in the upper atmosphere, might hamper absolute temperature measurements with its strong  $9.6\mu$  absorption band.

The Mars-scanner spectrophotometer is mounted on the flyby or orbiter vehicle's planetary-scanning platform, so that several strips a few hundred kilometers wide on the Martian surface will be mapped. Infrared radiation is collected by the 15-cm-diameter Cassegrain mirror shown in Fig. 15-1. Ultimately the light beam is split three times by dichroic mirrors (see Fig. 15-2). Filters are inserted in all channels. The two channels near the water-vapor-absorption band at  $2.6\mu$  will be separated by interference filters before their detection by lead-sulfide photoconductors. A thermistor is proposed for the  $8-12\mu$  thermal radiation channel. The reflected visible light that is collected will be monitored by a photodiode. Mass and power requirements are difficult to estimate for an instrument

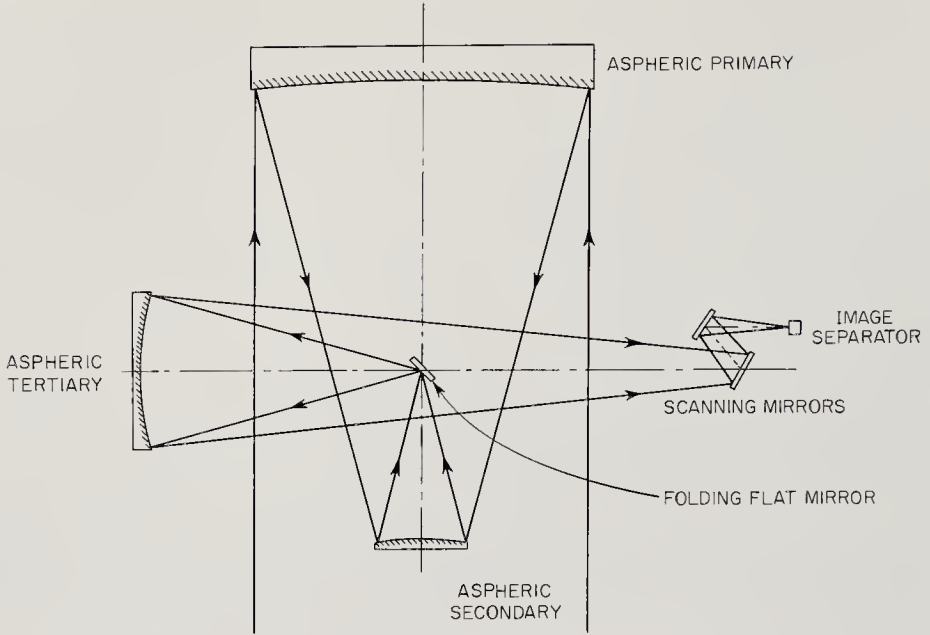


Fig. 15-1. Optical schematic for the Mars scanner, a three-channel radiometer. (TE Company drawing)

in the conceptual stage, but they should fall below 5 kg and 10 watts respectively.

Mapping always generates abundant data. Depending upon the number of digital-signal levels established for each channel, three surface scans,

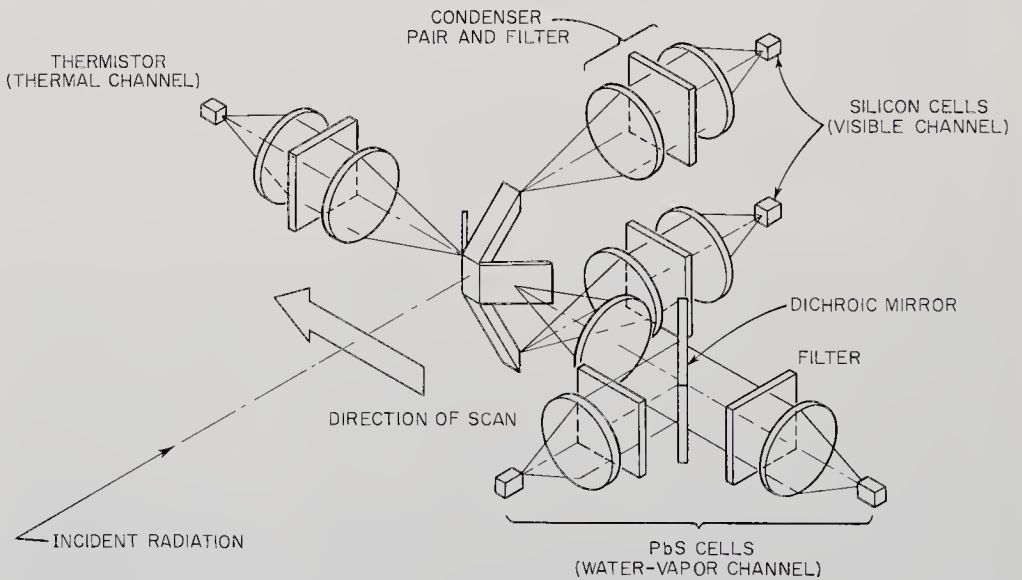


Fig. 15-2. Optical schematic for the image separator portion of the Mars scanner. (TE Company drawing)

corresponding to about 20 min of operation, would accumulate between  $10^6$  and  $10^7$  bits. Storage-space and transmission-time limitations militate for the lower value.

In contrast to the relative simplicity of the three-channel, infrared photometer, Lyon and Burns have suggested a rather sophisticated infrared spectrometer for remote mineral analysis (Refs. 15-6, 15-7, and 15-20). Complexity arises from the need to measure carefully the spectrum of surface emitted radiation with high resolution. Such technical effort would be well worthwhile, since surface composition could be determined on early flybys and orbiters instead of the much later landers using surface-sampling instruments.

The physical basis for remote compositional mapping by emitted infrared radiation is found in the emission process itself. The oscillation of atoms in the solid, a temperature-dependent activity, is the source of electromagnetic radiation. Chemical forces binding the atoms within the solid do not permit the unrestricted motion of such atoms, however. The oscillations are frequency-dependent, giving rise to a varying emissivity curve with occasional abrupt valleys (Fig. 15-3). Such emission

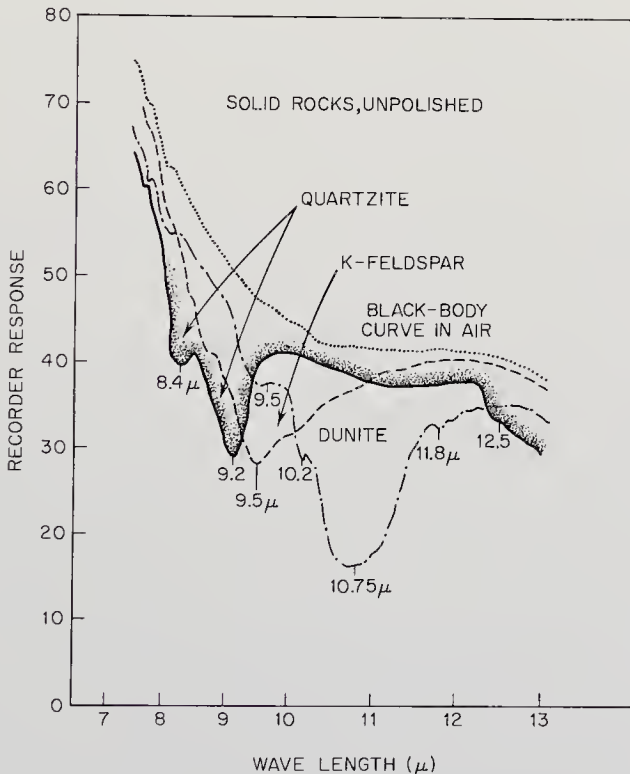


Fig. 15-3. Infrared emission curves for several minerals as functions of wavelength. (Ref. 15-6)

curves are characteristic and may be used for mineral identification, much as the gamma-ray spectrum from neutron-activated samples fingerprints individual isotopes (Sec. 15-3). Libraries of characteristic infrared spectra are available for mineral identification. The characteristic emission curves of planet surfaces are best measured in the infrared portion of the spectrum, where the amount of energy radiated naturally per wavelength interval is high.

The spectra in Fig. 15-3 would vary for the same materials with different degrees of fragmentation. Finely powdered substances (diameters less than  $100\mu$ ) diffuse the emitted light, reflecting it back and forth until the characteristic spectral structure is wiped out and the blackbody curve is approached. In the case of planets with atmospheres, like Mars and Venus, fragmentation from micrometeoroid and plasma bombardment should not be as great as it might be on the airless Moon. Aeolian fragmentation may be important on Mars.

An infrared spectrometer suitable for orbital and flyby analyses was described in Sec. 14-2 and diagramed in Fig. 14-19, page 410. Such an instrument could also be turned to mineral analysis. Important features of instrument adaptation would include:

1. High areal resolution, hopefully finer than  $2 \text{ km}^2$ .
2. Continuous spectral measurement with a resolution of around  $0.1\mu$ .
3. Infrared detectors that do not require large quantities of cryogenic cooling fluid.

As a footnote, we should observe that we must either know that the planet's atmosphere possesses no strong infrared absorption regions (especially the ozone bands) or know the atmosphere well enough to make corrections to the observed spectrum.

Perhaps the greatest challenges proffered the instrument designer are the high areal and wavelength resolutions essential for accurate mineral identification. The higher the resolution in both of these dimensions, the less the amount of light received by the detector. Thus, we have a tradeoff between the light-gathering power of the optics and resolving power. Light-gathering ability depends on mirror area and is strongly linked to instrument weight.

No detailed designs for spacecraft mineral spectrometers exist, but the instrument mass and power consumption should not be far different from those of the infrared spectrometers detailed in Sec. 14-2. Pertinent to the development problem is the fact that several lightweight rocket and satellite infrared spectrometers already exist; viz., the Perkin-Elmer SG-4. One or more of these may be adaptable to remote mineralogy.

Infrared spectrometers and photometers can always give scientists a



fairly accurate idea of surface temperature. For an ideal blackbody, Wien's Displacement Law,  $\lambda_{\max} \cdot T = 2.897 \times 10^6 \text{ m}\mu\text{-}^\circ\text{K}$ , will yield temperature if the peak of the spectrum,  $\lambda_{\max}$ , can be discerned. Naturally, corrections have to be made since no body is perfectly black.

*Television and Photography.* Despite their scientific importance, spectrometers do not have the subjective appeal of a photograph or television image of a scene from a distant planet. Discounting the emotional value of imaging devices, few can deny that they also produce geological, biological, and engineering data of great significance to space flight. Within the scope of the present chapter, no other instrument can as easily resolve surface texture, topology, geological history, and even mineral forms. True, only external structure is revealed, but the use of filters can significantly increase the data returned by providing limited spectral variations. It is not surprising, then, to find television and photographic experiments proposed for most flyby probes and planet landers.

Planetary imaging devices all anticipate the ultimate use of television techniques. Film photography and subsequent recovery have been successful in satellite technology, but cannot be contemplated for many years with deep-space probes. Therefore, data must be returned via electromagnetic waves.

Film, with its high resolution and long image-retention properties, is easily scanned remotely. It deserves a more important place in planetary research than it enjoys. Its long-retention-time feature is especially valuable where images must be stored and transmitted slowly back to Earth over bandwidth-limited communication systems. The familiar, real-time television camera, recording perhaps  $10^7$  bits/sec, can be used on nearby satellites, but not with a 10-bit/sec channel from Mars. The flood of data has to be slowed by image storage on the spacecraft, perhaps with film or magnetic tape film.

Imaging may be carried out in any portion of the spectrum. In fact, the three-channel, infrared Mars scanner mentioned earlier is a crude imager. Films with various spectral sensitivities are obvious possibilities. Vidicons with interchangeable filters also perform a spectrum selection function. Generally, though, fine imaging is done in the visible—perhaps because the results will have more subjective value—with color filters used to increase the scientific value of the pictures. No doubt, stereoscopic imaging will be undertaken soon, because of its value in topographic work.

The principal electro-optical device in space research is the vidicon, a lightweight, rugged instrument with practical image-retention times of up to 30 sec. Referring to Fig. 15-4, the vidicon sensor consists of a

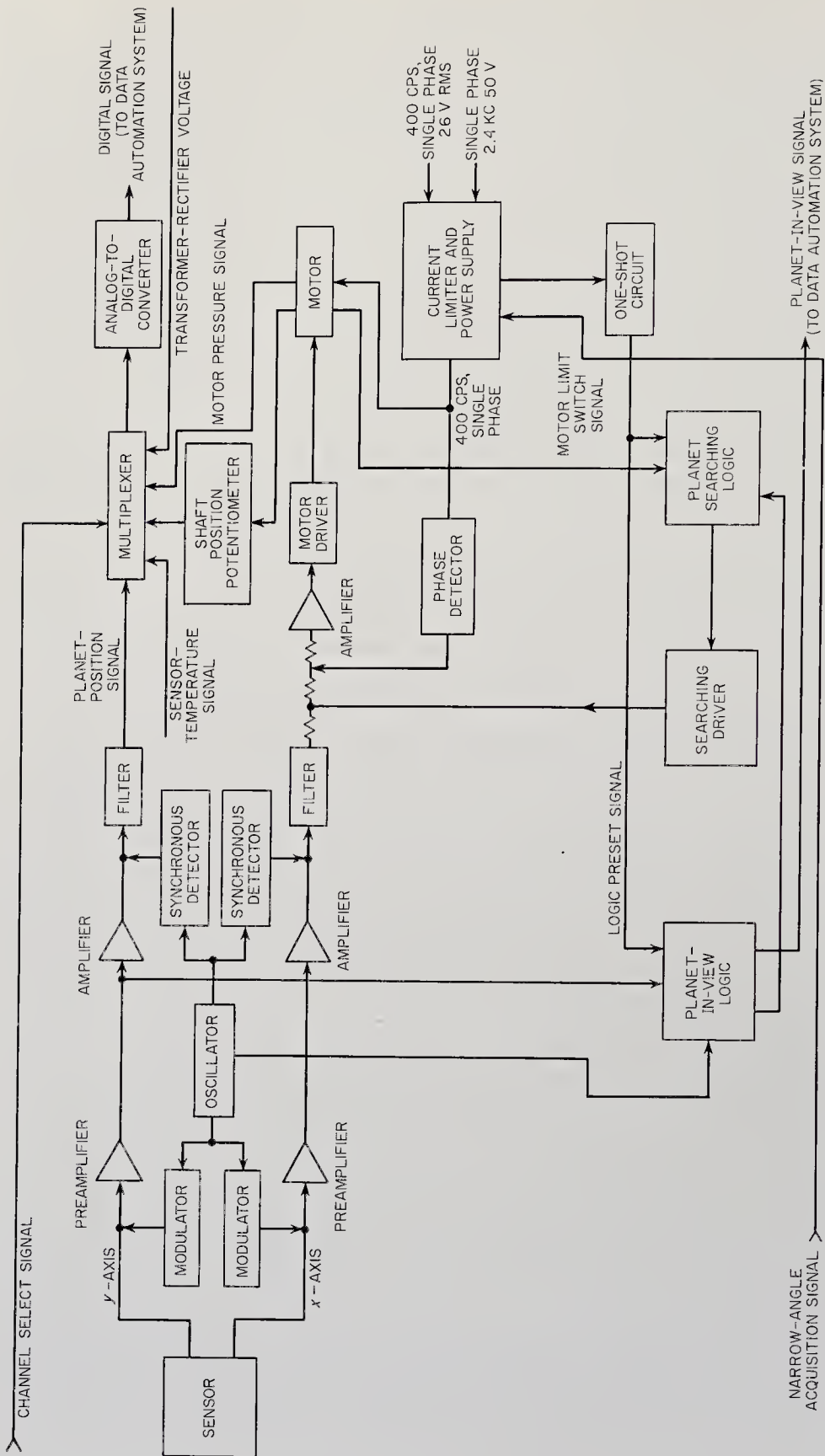


Fig. 15-5. Block diagram of the Mariner-4 television experiment. (JPL drawing)

transparent faceplate coated with a transparent conducting layer. The final piece to the sandwich is a layer of photoconductive material like antimony sulfide oxysulfide, an RCA development. Initially an electron beam deposits a layer of negative charge on the rear surface of the photoconductor, making in effect a charged capacitor, with the photoconductive material as the dielectric. When the instrument shutter is opened and the image focused on the photoconductor, the lighted areas become conducting and the deposited charge flows across to the conducting film. The shutter is then closed and the image is stored as a negative pattern of residual electron density on the rear of the photoconductor. Lateral charge movement and consequent blurring of the image is prevented by the good insulating properties of the dark photoconductor. The vidicon image is read off the photoconductor surface by a slow-scanning electron beam. The beam current will be highest at the light areas, where electrons were drained off by conduction. The resulting analog signal, in the case of planetary space probes, is usually sent to an analog-digital converter. The final step in the vidicon cycle is the erasure of any remnants of the preceding image and the repriming of the photoconductor surface with a new charge layer.

A vidicon includes many auxiliaries. Indeed, the lenses, shutters, electron guns, and control circuitry are far more complex than the basic sensor itself. The full scope of a planetary television camera can be appreciated by a review of the block diagram of the Mariner-4 TV experiment (Fig. 15-5).

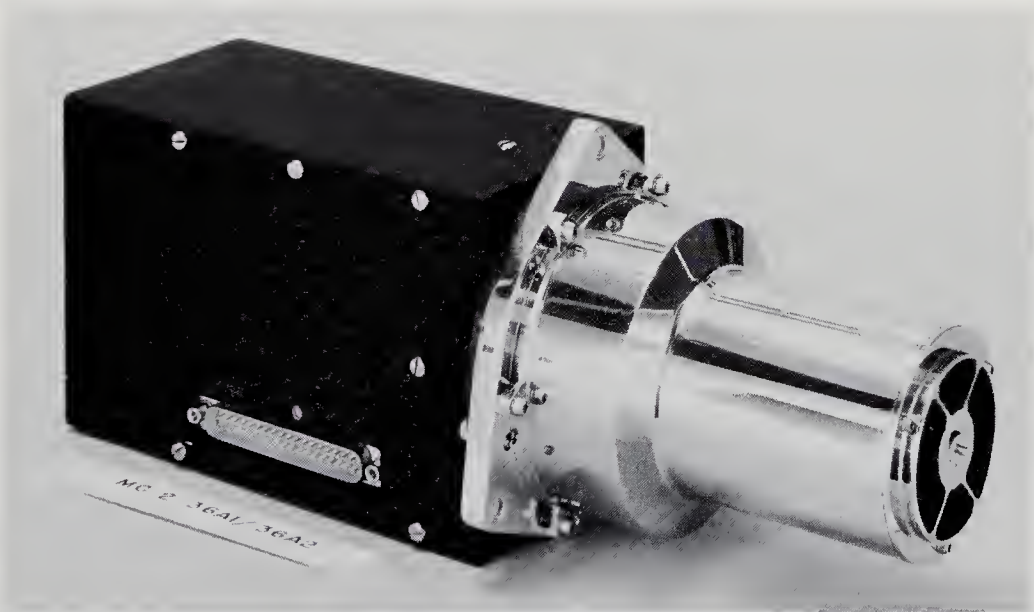


Fig. 15-6. The Mariner-4 television-camera head. (Courtesy of the Jet Propulsion Laboratory)

The major objective of the Mariner-4 flyby experiment was the acquisition of at least twenty pictures of the Martian surface taken through alternate red and green filters. The picture raster consisted of 200 lines, with 200 elements per line, and 64 levels of quantization per element. A complete picture then comprises  $200 \times 200 \times 6 = 240,000$  bits plus line-and-frame encoding. Based on a 19,000-km miss distance, instrument resolution was 2.5 km (more than an order of magnitude better than can be done from Earth), covering an area of  $350 \times 350$  km. An  $f/8$  Cassegrain mirror with a focal length of 30.5 cm and a shutter-filter combination preceded the vidicon sensor. The exposure time was variable from 0.1 to 0.5 sec. The field of view was  $1.05 \times 1.05$  degrees. The vidicon itself used an electrostatic scanning system rather than the heavier magnetic type. A  $0.56 \times 0.56$ -cm square raster was scanned on the selenium-compound photoconductive target. The entire image was read out in 24 sec, digitized, and stored for slow transmission back to Earth. A complete 72-sec picture cycle consisted of two pictures through different filters plus a blank frame. A photograph of the camera head is given in Fig. 15-6. The mass and the average power requirement were about 6.3 kg and 9 watts respectively.

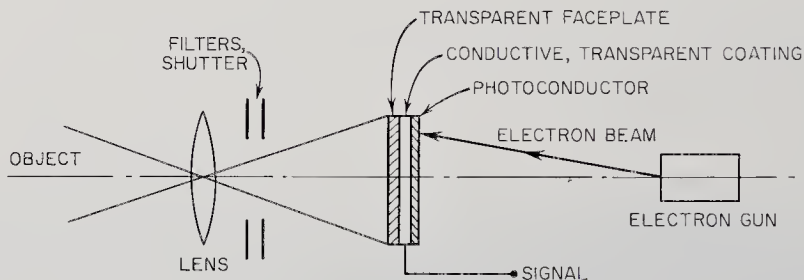


Fig. 15-4. Schematic of a vidicon.

Vidicons were also proposed for inclusion in the payload of the now-cancelled 1966 Mariner flyby of Mars. The objective was similar—obtain twenty photographs of the planet surface—but with much higher resolution than Mariner-4 had. Two modified Mariner-3 cameras were suggested. One would have had a narrow field of view and very high resolution; the other, a new experiment, a wide field of view and low resolution. The objective of the low-resolution experiment is the detection of average height-to-width ratios for large regions of small-scale objects on the surface by observation of their shadow-casting properties, even though the objects themselves are far from resolvable. Example: large areas of vegetation or regular geological structures. The modifica-

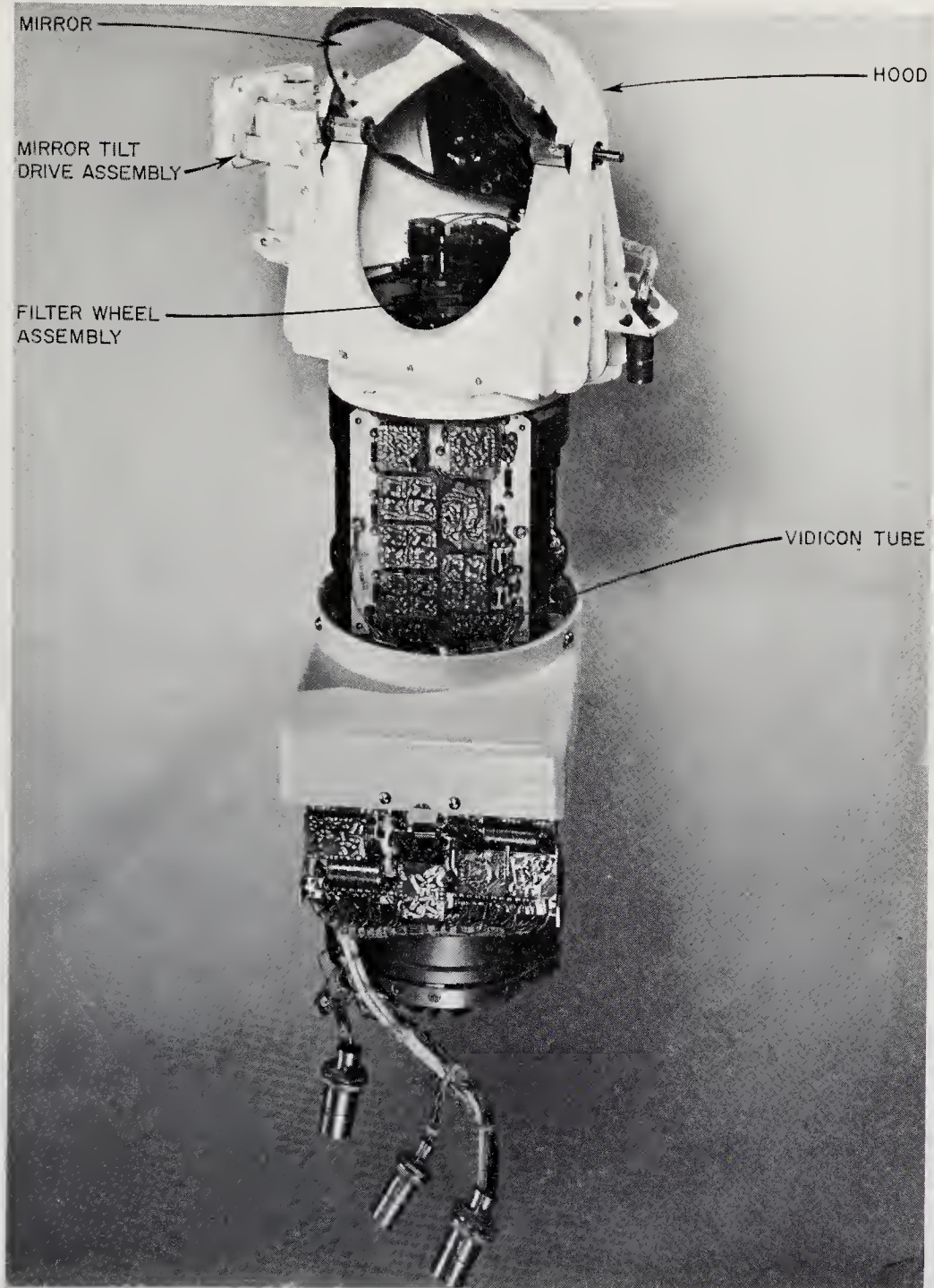


Fig. 15-7. A typical vidicon scanning instrument for observing the landscape in the vicinity of a lander. (Courtesy of the Jet Propulsion Laboratory)

tions to the Mariner-4 camera would have involved the reduction of the raster to 100 lines in one case and the increase to 400 lines for the higher-resolution camera.

Television from a lander for the purpose of geological and biological reconnaissance is a certainty. The Surveyor program has already developed an instrument suitable for lunar applications. A typical camera of this type is shown in Fig. 15-7. Modification for planetary use would not be difficult.

One of the important improvements to be made in planetary-imaging equipment involves data compression and/or selection. Many image data are redundant or trivial; viz., many of the Tiros cloud photographs. Film has another advantage here, because it can be scanned coarsely for pertinence prior to detailed transmission—a form of data selection. To save bandwidth, perhaps a data compressor would transmit only changes in light values. Whatever the solution to the data-abundance problem, most planetary probes will carry television equipment.

*Bistatic Radar.* Bistatic radar equipment, like that described in Sec. 14-4, can in addition to its many other functions measure reflection and roughness parameters for planetary reflection points. An analysis of the

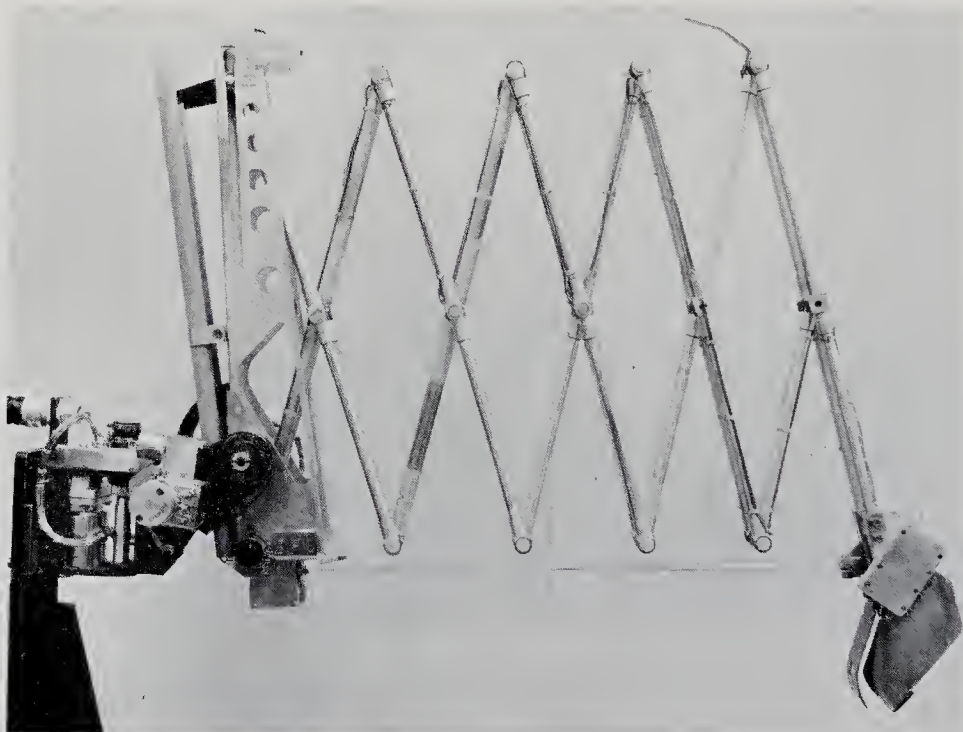


Fig. 15-8. A claw-like sample-collector prototype, designed for lunar missions. (Courtesy of the Hughes Aircraft Co.)

polarization and strength of the reflected signal leads to the evaluation of such parameters. The Brewster angle, at which only the horizontally polarized wave is reflected, can be used to determine the average surface dielectric constant. Furthermore, variations of the dielectric constant from the average are indicative of the magnitude of surface undulations and the slopes of large-scale surface features. By measuring changes of reflectivity and the dielectric constant as functions of frequency, it may be possible to establish how the surface conductivity changes with depth. The lowest frequencies, of course, penetrate the farthest into the crust. Surface-structure measurements such as these can be carried out only with very powerful, Earth-based radar transmitters (Sec. 14-4).

### 15-3. Crustal Properties by Sample Analysis

Surface instruments either require a physical sample of digestible size or they need to be placed within a few centimeters of the crust. This sampling function separates these instruments from the optical devices of the preceding section, which make measurements from afar.

Planetary-instrument designers have often underestimated the difficulty of acquiring and processing samples from unknown surfaces. Sampling mechanisms have to be founded upon (1) best guesses about the character



Fig. 15-9. Pneumatic sample collectors designed for ingesting dust and fine debris from the surface of the Moon or a planet. (Courtesy of the Jet Propulsion Laboratory)

of the target planet's surface, and (2) the admonition that they be flexible enough to cover all likely eventualities. Dust and sand, rock debris, liquids, and perhaps even biological material may be encountered. The best sampling mechanism might be different for each, but initially one will have to be designed for all. The experiments that need only close proximity to the crust—neutron-activation analysis and alpha scattering—are obviously the easiest to set up. On the other hand, the mass spectrometer and gas chromatograph depend upon the pick up and transport of solid material to the instrument for gasification. Claws, sticky tapes, and suction tubes (Figs. 15-8, 15-9, and 16-3, page 488) have been studied, with none meeting universal success in all potential environments. The claw-type mechanism (Fig. 15-8) is adaptable but rather complex. Pneumatic tubes and sticky tapes are simple though applicable only to sand and dust. The weathering of planet surfaces by space radiation, meteorites, and indigenous processes should produce enough fine debris for the illustrated samplers to work.

The great diversity of proposed sampling instruments precludes any fine-mesh classification. In general, all employ physical techniques like nuclear-particle scattering, induced radioactivity, and stimulated light emission (Table 15-2). As pointed out earlier, physical techniques divulge little concerning chemical and crystalline structure. The gas chromatograph, the only really chemical instrument covered in this section, can detect complex molecular species, if they can be made into gases and if the chromatograph is sensitive to them.

*Mass Spectrometers.* The mass spectrometers developed for atmospheric analysis can be taken over bodily for crustal work. First, however, the collected sample must be converted wholly or partially to gas before introduction into the spectrometer. Once the gas is admitted, it is ionized and then separated into ion populations with equal charge-to-mass ratios. The operating principles of the different mass spectrometers were covered in Sec. 14-3.

The conversion of the sample to a gas presents a significant problem. There may be some low-vapor-pressure organics that can be easily driven off by heat, but the mass spectrometer is better adapted to elemental analysis rather than identification of heavy, complex, organic molecules. The gas chromatograph (described next) is better for such heavy-molecule work. Absorbed gases and water of hydration are also possible to unlock by baking in high-temperature ovens. Such pyrolytic techniques will not be adequate to volatilize basic minerals like silica. Electrical discharges are more likely to be successful. Here, the sample forms part of the electrode or is vaporized within the arc. The arc temperatures are high enough to provide the spectrometer with ions of the elements and of



TABLE 15-2. CRUSTAL RESEARCH INSTRUMENTS USING SAMPLING TECHNIQUES

<i>Instrument/Experiment Type</i>	<i>Principle of Operation</i>	<i>Parameters Measured</i>
Mass spectrometers	Magnetic and/or electrostatic fields separate atoms of different masses by differential acceleration (See Sec. 14-3.)	Crustal isotopic composition. Ion abundances by mass number
Gas chromatographs	Gas constituents are delayed by varying amounts in sorptive columns. Time of emergence fixes composition. (See Sec. 14-3.)	Composition of organics in pyrolyzed crustal sample. Abundances by chemical species in gas
Alpha-scattering experiments	Intensity of backscattered alphas from radioactive source depend on atomic number of target. (See Sec. 14-3.)	Abundances of crustal isotopes like C, O, Si
X-ray spectrometers	Artificially induced X-ray emissions diffracted into detectors by crystals. Gammas from natural radioactive elements measured by scintillator.	Crustal composition. Abundances by element and isotope only
Densitometers	Alpha or gamma source bombards atmosphere. Back-scattered radiation is measure of density.	Density
Neutron inelastic scattering experiment	Neutron flux excites elements in crust. Resulting gammas are diagnostic.	Crustal isotopic composition
Neutron-activation analysis	Neutron flux makes crust artificially radioactive. Resulting radiation identifies nuclear species.	Abundances of crustal isotopes
X-ray diffraction	X-rays diffracted by sample form characteristic pattern that identifies mineral.	Crustal composition. Abundances by specific mineral
Differential thermal analysis	Differential heating rate between sample and reference material due to phase transitions identifies mineral.	Crustal composition. Abundances by specific mineral
Petrographic microscopes	Plane and unpolarized light transmitted through powdered sample reveals mineral structure and composition.	Mineral structure and composition
Isotopic-dating experiments	Noble gases evolved by pyrolysis are isotopically separated in mass spectroscopy.	Time of crustal formation Cosmic-ray exposure

simple compounds with strong chemical bonds. Some chemical structure, however, is invariably destroyed in ovens and arcs.

Mass spectrometers capable of handling solid samples on another planet's surface are in a rudimentary state of development. Such an instrument would differ from its atmospheric cousin by the added complexity of sample processing and also the need to span a wider range of elements. Common atmospheric elements of the terrestrial planets do not extend beyond oxygen ( $A = 16$ ), but crustal elements up to iron ( $A = 56$ ) should be detected. Such complexities can be overcome by astute design, but very likely the first crustal analyses will be carried out by the much simpler scattering- and activation-analysis instruments, leaving the mass spectrometer for later, more precise assays.

*Gas Chromatographs.* A gas chromatograph for surface analysis operates under the principles described in Sec. 14-3. The chemical compounds to be identified, however, are no longer simple atmospheric constituents. Instead, there is a host of possible compounds, ranging from water to complicated organics. This fact changes the makeup of the columns. The problem of evolving gases from the solid sample is the same as it was for the mass spectrometer. Gas chromatographs for crustal use must therefore be supplied with a pyrolyzing oven that drives the volatile components out of the retrieved sample and injects them into the carrier gas

TABLE 15-3. CHARACTERISTICS OF THE SURVEYOR GAS CHROMATOGRAPH\*

Components resolved:	Hydrogen	Propionaldehyde
	Oxygen	Formic acid
	Nitrogen	Acetic acid
	Carbon monoxide	Butyric acid
	Carbon dioxide	Benzene
	Methane	Toluene
	Ethane	Acetone
	Propane	Acetonitrile
	Butane	Acetylene
	Methanol	Acrolein
	Ethanol	Hydrogen cyanide
	Propanol	Hydrogen sulfide
	Formaldehyde	Ammonia
	Acetaldehyde	Water
Maximum retention time, min		30
Minimum detectable quantity in oven, mole		$3 \times 10^{-10}$
Minimum dynamic range of detection		$10,000 \times$ minimum detectable quantity
Oven temperature control, °C		10
Oven maximum heating time, min		4

\* Ref. 15-44

that will sweep them into the sorptive columns. One final point, the atmospheric instrument proposed for early probe flights (Sec. 14-3) had to collect and analyze the sample and then telemeter the data all in the minute or so before impact. Hours of analysis time can be assigned to a gas chromatograph on a lander. The upper time limit will be set in this case by the finite supply of carrier gas and energy consumption.

The gas chromatograph described below was developed for the lunar Surveyor program (Refs. 15-32, 15-44, and 15-45). Simplification, weight reduction, and many other modifications would have to be made before it could be taken over directly for the planetary programs.

Despite the present apparent lifelessness of the Moon, the Surveyor gas chromatograph is intended to detect remnants of life or the presence of pre-life chemistry. Consequently, a strong tie exists between this in-

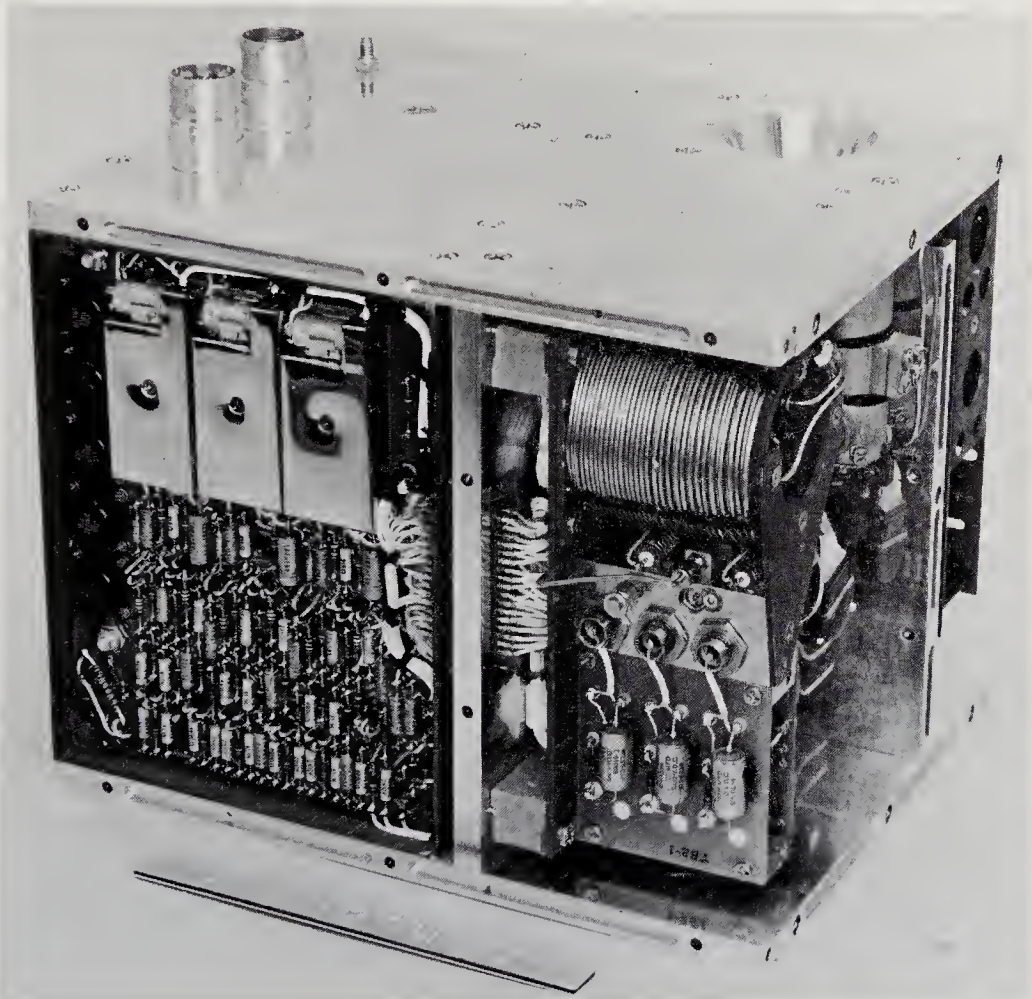


Fig. 15-10. The Surveyor gas chromatograph, prototype P-2. (Courtesy of the Jet Propulsion Laboratory)

strument and the life-detection equipment covered in the next chapter. In addition to the complex organics detectable by the Surveyor chromatograph, water, hydrogen, oxygen, ammonia and some other simple compounds are measurable (Table 15-3).

When a solid sample is dumped into the funnel of the Surveyor gas chromatograph (Fig. 15-10), it falls directly into a pyrolysis oven. After sample receipt, the oven is automatically sealed shut and heated to a ground-commanded temperature of 150, 325, or 500°C. The volatile components from the solid are injected into a helium carrier gas, which transports them into three long columns connected in parallel and wound like wire on a cylinder (Figs. 15-10 and 15-11). The columns have the following characteristics:

- Column 1. a 2.2-m molecular-sieve 5A column that separates the fixed gases.
- Column 2. a 4.6-m column with 15% Carbowax 1540 on T-6 Teflon support that separates water and most of the hydrocarbons.
- Column 3. a 3.7-m column with 15% Apiezon L, 4.5% Carbowax 20M, and 3% phosphoric acid on a Chromosorb support to absorb the organic acids.

In the columns, the various constituents of the gas are delayed for various lengths of time according to their sorptive and chemical-equilibrium

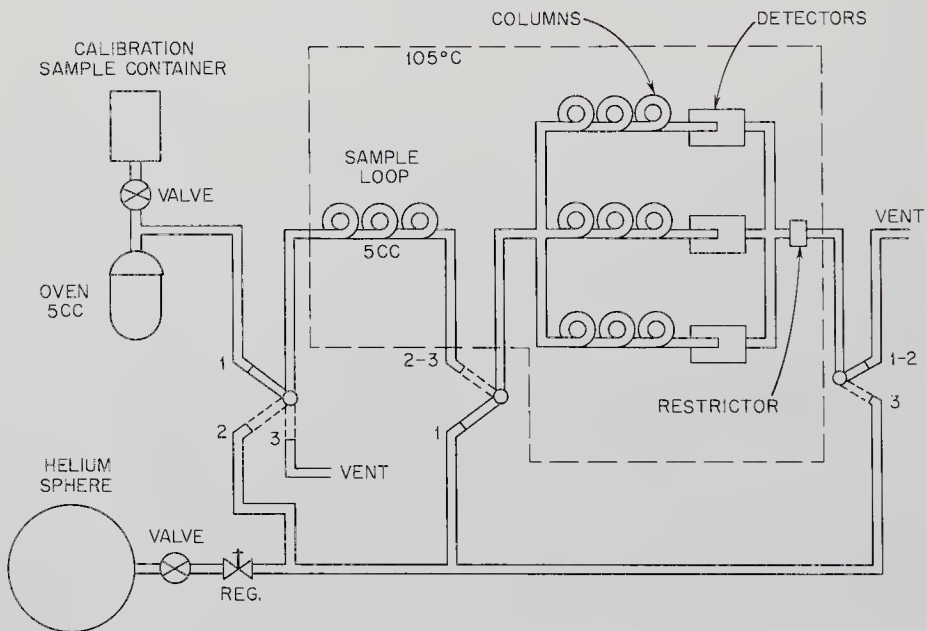


Fig. 15-11. Flow diagram for the Surveyor gas chromatograph. The sample loop insures the injection of a fixed sample of gas. (Ref. 15-44)

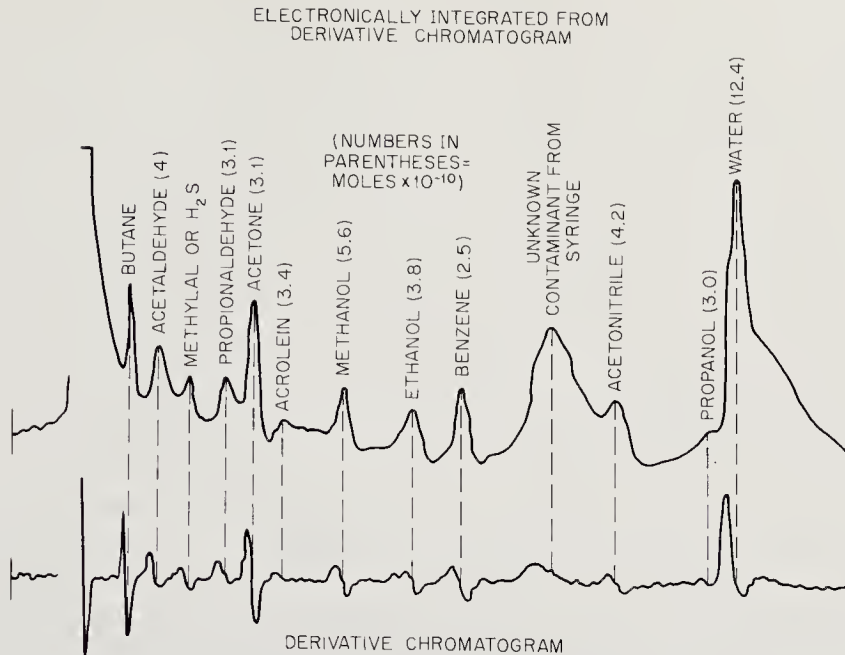


Fig. 15-12. A sample chromatograph for the Surveyor instrument. Time is measured horizontally. (Ref. 15-44)

interactions with the column materials. Each column detector generates a different chromatogram (Fig. 15-12). The time of emergence for a compound is well-defined but not necessarily unique. Pretesting with various substances likely to be found on the target planet should resolve potential ambiguities. The sensitivity of a gas chromatograph to the ambient temperature makes calibration after landing essential. A predetermined calibration sample of gas is carried along for this purpose.

The detectors for all three of the Surveyor chromatograph columns were of the glow-discharge type. First, a voltage-breakdown potential is established in the presence of the pure helium carrier gas. Then, as the time-delayed gases emerge from the columns, they will change the breakdown voltages and produce an analog electrical signal proportional to the concentration of impurities in the helium.

The Model P-2 prototype Surveyor gas chromatograph sketched above was packaged into a nearly perfect cube ( $20 \times 20 \times 25$  cm), with a mass of approximately 6.4 kg. The peak power requirement was 72 watts, but the integrated energy drain during the planned 100 minutes of operation amounted to only 22 watt-hours. As a result of the lunar exploration program, scientists have a well-developed analytical tool for planetary research.

*Alpha-Scattering Experiments.* The Rutherford simple-composition

experiment uses both alpha-scattering and alpha-proton reactions to determine the composition of an unknown atmosphere. An experiment of this type was first proposed by A. Turkevich, University of Chicago, in 1960, for compositional analysis of the lunar surface. The discussion of alpha backscattering presented in Sec. 14-3 is also applicable here. The term  $[(A - 4)/(A + 4)]^2$  in the scattering equation from Sec. 14-3 highlights a limitation of the method when applied to heavy crustal elements. When  $A$ , the atomic mass number, increases, the value of the fraction approaches one, leading to poorer element resolution. Although heavier elements can be detected, the upper limit for good resolution between adjacent mass numbers is at about  $A = 40$ . Atmospheric compositional analysis is little affected by this limit, but many of the heavier elements are important to the geologists. Of course, the most common mineral elements, like O, Si, Al, Mg, and Na are still readily resolved. As with most of the "physical" instruments, elements, and not compounds, are measured. Alpha-scattering experiments seem best for preliminary surface reconnaissance rather than detailed dissection of the chemical makeup of the crust. Measurements, however, are obtained only from a thin upper layer of the crust because of the low penetrating power of the alpha particles.

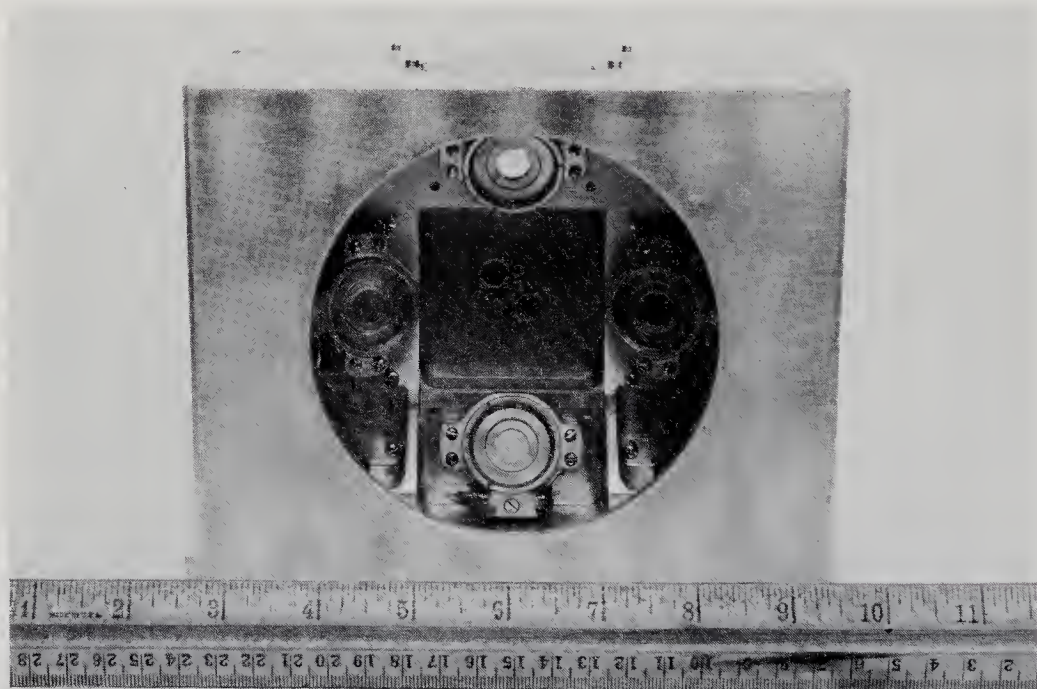


Fig. 15-13. Bottom view of a prototype alpha-scattering instrument. The radioactive alpha-source is surrounded by four alpha detectors. (Courtesy of the Jet Propulsion Laboratory)

A bottom view of a prototype alpha-scattering experiment is shown in Fig. 15-13. The alpha source is placed close to the planet's surface and the back-scattered alphas are detected by the four solid-state detectors shown placed around the source in the photograph. Pulse-height analysis yields the alpha particle and proton energies, and the number of counts per unit time in each channel is proportional to intensity. An alpha-scattering spectrogram like that shown in Fig. 15-14 results. Element identity is

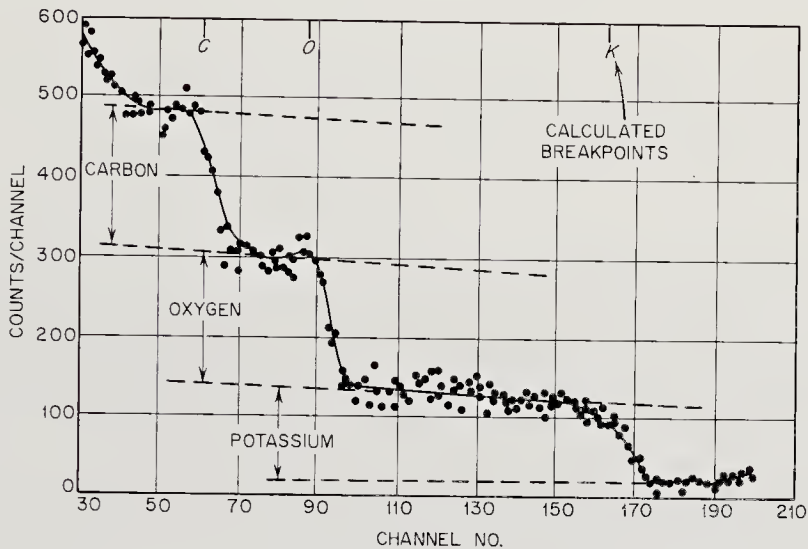


Fig. 15-14. Experimental data from an alpha-scattering instrument taken for  $KCO_3$ . (Ref. 15-12)

indicated by the breakpoints in the curve. Elemental abundances are reflected in the vertical differences between adjacent plateaus.

Experimental results with a breadboard model of the instrument indicate that the minimum detectable amount of an element is roughly 1 atom per cent. Resolution is good enough to distinguish acidic, intermediate, basic, and meteoric rock material. One prototype alpha-scattering instrument had a mass of 3.7 kg and consumed 1.4 watts.

*X-Ray-fluorescence Spectrometers.* Once a sample of a planet's surface is retrieved, it can be artificially induced to emit electromagnetic radiation, revealing its composition. In concept, such spectrometry could be carried out anywhere in the spectrum from the infrared to gamma rays. In practice, though, only X-ray and gamma-ray spectroscopy are popular in space research. The energetic, well-defined photons in these portions of the spectrum are easy to detect and measure; furthermore, the photon energies are highly specific for each isotope. In contrast, visible and ultraviolet spectroscopy mean spectrum scanning and the resolution of many lines and their precise measurement. Also consider-

able power and weight would be required to make samples incandescent. It is more convenient to induce X-ray and gamma-ray emission in the unknown sample.

Imagine a beam of 10-30 kilovolt electrons focused on a powdered sample of a planet's crust, or perhaps in the ultimate case, the crust itself. Some of the inner electrons of the bombarded atoms will be knocked out of the atom by collisions with the electrons in the beam. Atoms with such distorted electronic structures are termed *excited*. One of the electrons in the outer shells quickly moves in to replace the ejected electron. This electronic transition is accompanied by the emission of a characteristic, identifying photon. Because of the high energies involved in transitions deep inside the electronic structure, the emitted photons are in the X-ray region of the spectrum. By measuring the X-ray energies (wavelengths), the emitting atom is identified. In fact, since each element emits only a few characteristic X-rays when stimulated, the complication of spectrum scanning can be bypassed. Separate detectors, each sensitive to one of the characteristic X-rays, can be assigned to each of the elements expected in the sample. This is a lightweight, sensitive approach, but one lacking in flexibility, since the surface composition has been prejudged.

The X-ray-fluorescence spectrometer, illustrated in Fig. 15-15, is tuned to several specific elements. A simple electron gun bombards the target

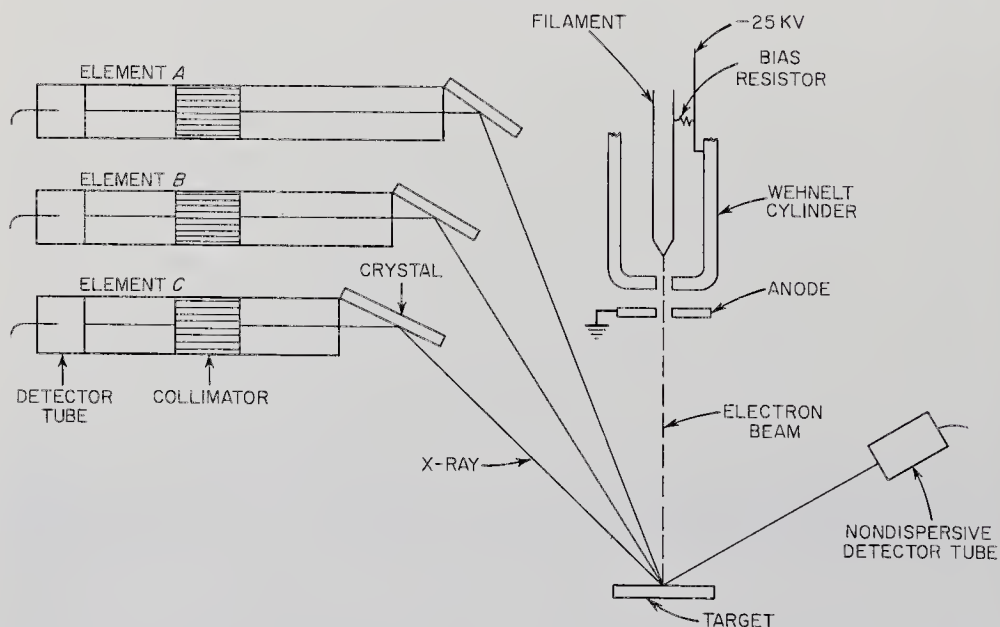


Fig. 15-15. Schematic drawing of the Surveyor X-ray spectrometer. Crystals diffract X-rays into different detectors according to energy. (Ref. 15-26)



(sample) with 12.5- and 25-kv electrons. The characteristic X-rays that are emitted from the target fan out in all directions. These photons must be detected and sorted out according to the few particular energies being monitored. The approach used on the Surveyor program consisted of mounting precisely positioned dispersive crystals and accompanying X-ray detectors around the sample. X-rays of all energies impinge upon all the crystals. They are diffracted according to Bragg's Law:

$$n\lambda = 2d \sin \theta$$

where  $\lambda$  = the wavelength of the X-ray (cm)

$d$  = the interplanar spacings of the different crystals (cm)

$\theta$  = the angle between the incident radiation and the normal to the crystal plane ( $^{\circ}$ )

$n$  = the order of diffraction.

Only the X-rays meeting the Bragg criterion will be diffracted into the associated, well-collimated detector (Fig. 15-15). By the proper choice of  $d$  and  $\theta$ , a highly selective group of X-ray filters can be placed around the sample. In essence, we have a filter spectrometer (or photometer, see Sec. 14-2) which is tuned to the elements anticipated in the crustal sample.

Thirteen separate X-ray channels were incorporated in the first Surveyor prototype X-ray spectrometer (Ref. 15-26). Each channel was sensitive to an element expected in the lunar surface; i.e., Ca, Al, Ni, Si,

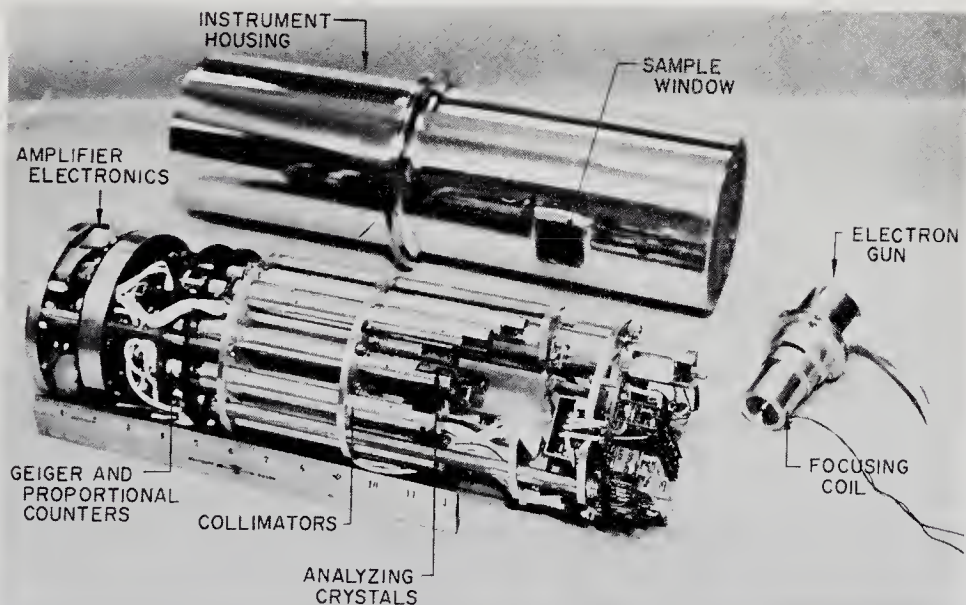


Fig. 15-16. Prototype Surveyor X-ray spectrometer. (Courtesy of the Jet Propulsion Laboratory)

etc. Geiger-Mueller counters (Sec. 13-3), which viewed the different crystals, through flat-bladed collimators, detected the energetic X-rays from the heavier elements (see Fig. 15-16). Proportional counters were assigned to the lighter elements, emitting weaker X-rays. One or two additional proportional counters coupled to a pulse-height analyzer sort out the X-rays according to energy without resorting to dispersive crystals. (Unfortunately, the Surveyor type of X-ray spectrometer is not very sensitive to oxygen and carbon because of this difficulty in detecting very weak X-rays. Rock tests with the breadboard instrument have produced results comparable to those from a commercial X-ray spectrometer.)

One problem encountered during the development of the X-ray spectrometer was the buildup of negative space charge on poorly conducting test samples. The presence of the space charge reduced the intensity of electron emission and caused wide, unpredictable fluctuations in the counting rate. After trying many stratagems aimed at bleeding this charge accumulation from the sample, powdering the sample and mixing it with conducting graphite proved to be the best solution.

With thirteen channels, the Surveyor prototype X-ray spectrometer is a relatively complex instrument. The approximate mass is 12 kg and the power consumption 20 watts. The Surveyor instrument would have to be lightened and simplified considerably prior to deep-space use. A reduction in the number of channels is an obvious possibility, but this would further limit the range of elements detected. A non-dispersive X-ray spectrometer has been proposed as a less sophisticated and simpler instrument which might be better suited to early planetary exploration. The use of a radioisotope source of excitation for nondispersive analysis has also been studied.

*Gamma-ray Spectrometers.* A different spectrometer technique, both simple and appealing, but not as sensitive, measures the photons emitted by naturally occurring radioisotopes in the unknown crust. The most interesting natural radioisotopes are  $K^{40}$ ,  $U^{235}$ ,  $U^{238}$ , and  $Th^{232}$ . The abundance ratios of these four nuclei provide geophysicists with insight into the evolution and differentiation of a planet's crust. When nuclei decay, the energies involved are much larger than those associated with transitions in the surrounding electronic shells. It is not surprising, then, to find that the photons emitted by radioisotopes are energetic, short-wavelength gamma rays. As in the case of X-rays, the gamma-ray energies are characteristic of the atom that emits them, thus providing identification tags for the radioisotopes. The reader will note a strong resemblance between the gamma-ray spectrometer described below and the later neutron-

activation-analysis equipment, in which the measured radioactivity is artificially induced.

Since no artificial excitation is needed with natural radioisotopes, a detector and a pulse-height analyzer complete the instrument (Fig. 15-17). The detector usually proposed is an inorganic scintillator—viz.,

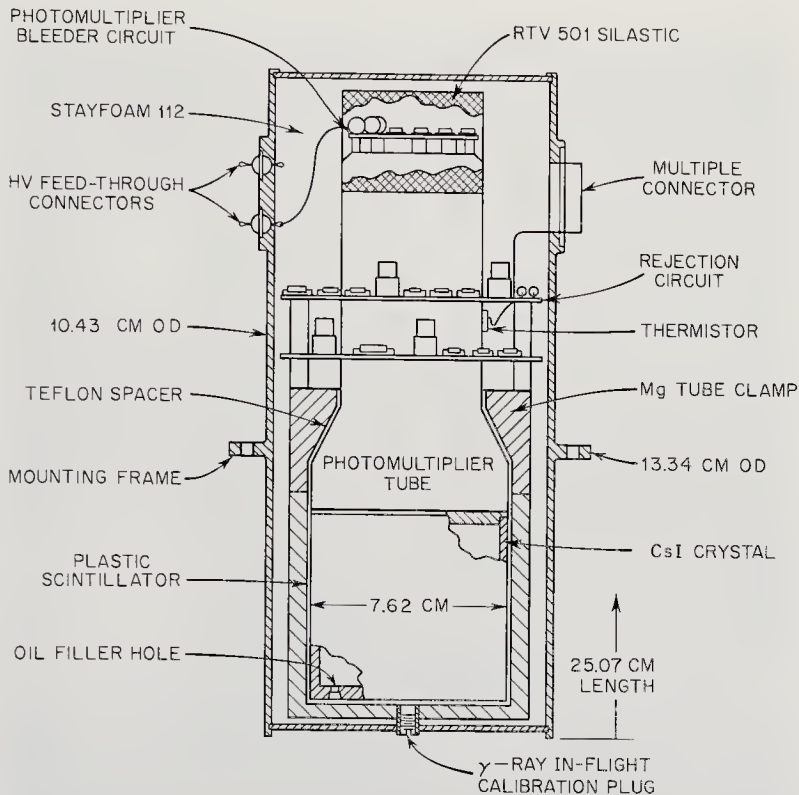


Fig. 15-17. Schematic drawing of the detector portion of the Ranger gamma-ray spectrometer. (Ref. 15-25)

thallium-activated CsI or NaI (Sec. 13-3)—which is large enough to stop the gamma rays being measured. The detector is set down as close as possible to the planet surface. It might be attached on the end of a boom to remove it from any cosmic-ray-induced secondary gammas emanating from the spacecraft. (Note also that a radioisotopic power plant would severely interfere with the measurements.) A photomultiplier tube optically coupled to the scintillator detects the light flashes and delivers a pulse that is proportional to the flash intensity and thus proportional to the energy deposited in the scintillator by intercepted gamma rays and charged particles. A plastic scintillator, which is responsive to charged particles but not gamma rays, surrounds the inorganic

scintillator. The photomultiplier tube sees flashes in both scintillators, but the associated electronic circuits discriminate against the charged particles by rejecting pulses through analysis of their trailing edges in true phoswich fashion (see Sec. 13-3.).

Rangers 3, 4, and 5 carried gamma-ray spectrometers, shown in Figs. 15-17 and 15-18, that made measurements of gamma rays in space during



Fig. 15-18. The Ranger-3 gamma-ray spectrometer disassembled. (Courtesy of the Los Alamos Scientific Laboratory)

the flights to the Moon. The instrument mass was just under 6 kg. The power requirement was approximately 1.5 watts. The detector was designed by the Los Alamos Scientific Laboratory (Ref. 15-43) and integrated into the Ranger spacecraft by the Jet Propulsion Laboratory. A 32-channel pulse-height analyzer followed the detector. In flight, calibration was provided by a small  $\text{Co}^{57}\text{-Hg}^{203}$  source. The spectrometer was mounted on the end of a 2-meter boom.

*X-ray Diffractometers.* The X-ray diffraction pattern formed by a powdered mineral sample can be compared with known patterns and, in the manner of fingerprint identification, be designated as belonging to a specific mineral. The X-ray diffractometer, like the X-ray spectrometer,

employs crystal diffraction, but not for the purpose of energy selection. In X-ray diffractometry, a collimated monoenergetic beam of X-rays illuminates the crystalline sample and is diffracted into a spectrum, according to Bragg's Law. There is no stimulated emission of characteristic X-rays, as there was in the X-ray spectrometer. The geometrical pattern of spots created by diffraction from a single crystal, called a Laué diffraction pattern, can be used to calculate crystal interplane spacings from Bragg's Law. Such spacings vary from mineral to mineral and can form a basis for identification. Few mineral samples, however, come as single, homogeneous crystals. Mineralogists have therefore powdered their specimens (powder size: 100-500A), a process that randomly orients the crystal planes. The new diffraction pattern formed consists of the single-crystal spots smeared into concentric rings with characteristic radii. Extensive libraries of such patterns are available for purposes of mineral identification. X-ray-diffraction experiments from a planetary lander involve measuring the diffraction pattern of a powdered sample and telemetering the data back to Earth for comparison with known patterns.

Even though the smallest laboratory diffractometer weighs more than half a ton, modern miniaturization has produced a prototype Surveyor X-ray diffractometer that has a mass of approximately 10 kg. The instrument schematic, Fig. 15-19, shows a small, 25-kv X-ray tube with a cop-

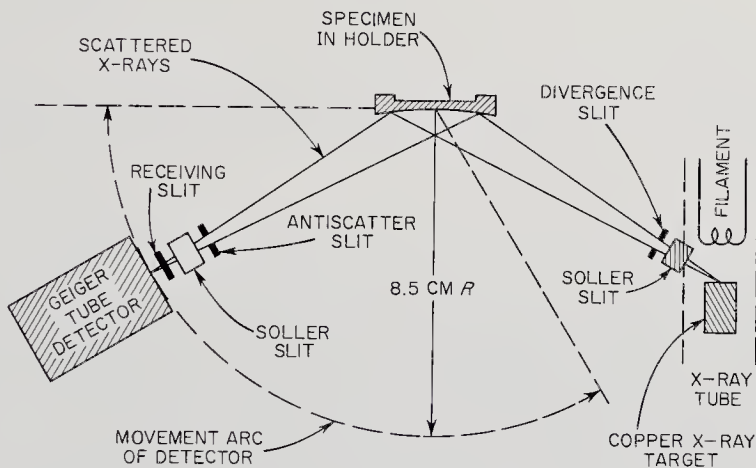


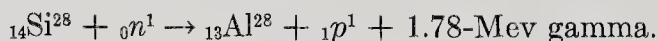
Fig. 15-19. Schematic drawing of the Surveyor X-ray diffractometer. Crustal sample diffracts X-ray beam into a spectrum.

per target. The resulting X-rays are collimated by leaf-like soller slits and impinge on the powdered sample. The diffraction pattern is viewed by a Geiger-Mueller counter, which is driven from  $20^\circ$  to  $90^\circ$  around the 8.5-cm arc by a small motor. The Geiger-Mueller counter signals replace

the images formed on the more customary photographic film. The number of Geiger-Mueller tube discharges per unit time are proportional to the intensity of the pattern at each angular position. Tests with the Surveyor prototype, manufactured by Philips Space Development, Inc., have shown that the miniaturized equipment is nearly comparable in performance with the much larger (but cheaper) laboratory models. Flight models of the diffractometer are each expected to consume about 15 watts of power and have a mass under 5 kg.

*Neutron-Activation Analysis.* Neutron bombardment can stimulate an atom's nucleus to emit characteristic gamma radiation, just as electrons induced the emission of identifying X-rays from electron shells. Being uncharged, neutrons can penetrate the atom's electrostatic fields and initiate three pertinent types of nuclear reactions:

1. *Inelastic scattering*, where the bombarding neutron is inelastically scattered out by the target nucleus, leaving some of its energy behind. The excited nucleus ( $A^*$ ) decays quickly ( $\sim 10^{-12}$  sec), emitting its excess energy in the form of gamma rays possessing energies characteristic of the nucleus ( $A$ ).
2. *Radiative capture*, where the neutron is absorbed by the target nucleus ( $A$ ) to form a new isotope of the same element, ( $A + 1$ ). Excess energy appears again as characteristic gamma radiation. Capture gamma rays from a number of elements, such as hydrogen, silicon, and iron, can be important in mineral analysis using neutron activation.
3. *Activation*, where the bombarding neutron causes a transformation of nucleus ( $A$ ) into a new element ( $B$ ) that is radioactive. A typical reaction of this type is:



Besides gamma rays, protons, beta particles, neutrons, and other particles may be emitted by the newly created radioisotope. The particle identities, energies, and half lives are all diagnostic; that is, they all help identify the new nucleus ( $B$ ).

For the activation process, unlike the cases of inelastic scattering and radiative capture, a simple inference must be made to determine nucleus ( $A$ ) from the properties of the nuclei  $A + 1$  and  $B$ . This contrasts with gamma-ray spectroscopy of natural radioisotopes, where the measured radiations are specific for indigenous elements. Inference, however, is no real problem and artificial activation by neutrons, protons, and gamma rays opens up most of the Periodic Table to analysis (Fig. 15-20).

The picture of the neutron-activation analysis instrument that emerges

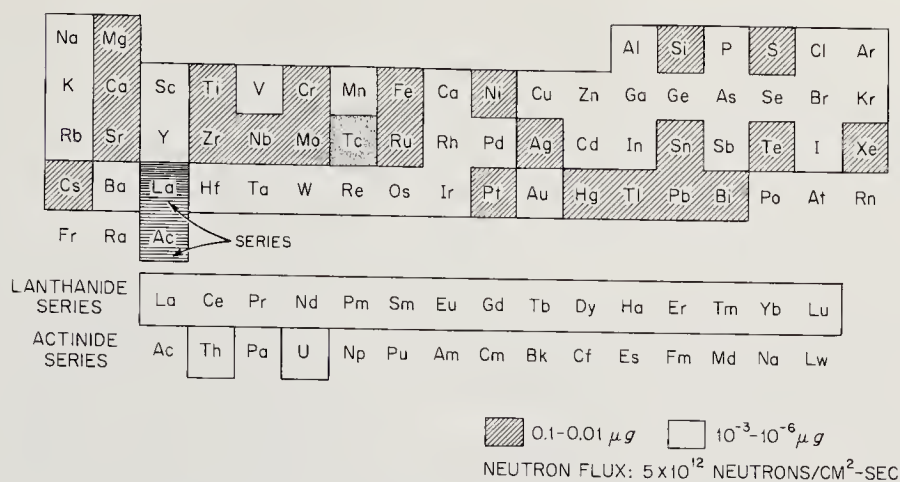


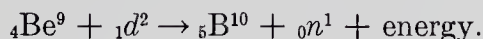
Fig. 15-20. Sensitivity of the neutron-activation-analysis technique. Elements in white blocks are easily detected. Those not shown at all are not susceptible.

from the basic physical facts consists of a neutron source for bombarding the target sample and a detector to measure the resulting radiation fluxes and their energies as functions of time. In space instrumentation, neutrons are useful activating particles, because of the high fluxes that can be generated and their high penetrating power. In comparison with the charged particles emitted by radioactive nuclei, gamma rays possess a distinct set of energies for each radioisotope and are not readily absorbed in the sample itself.

Not all elements are detected with equal ease. In particular, some of the light elements are inaccessible to neutron activation analysis. Some, for example, have neutron-activation cross sections that are unusably low. Most elements, however, can be activated easily by neutrons. Some typical reactions are:

Target Element	Activated Nucleus	Activating Reaction	Activated Nucleus Gamma Rays (Mev)	Half Life
Al <sup>27</sup>	Mg <sup>27</sup>	(n, p)	0.83, 1.01, 0.18	9.45 min
Fe <sup>56</sup>	Mn <sup>56</sup>	(n, p)	0.84, 1.81, 2.12	2.58 hr
Mg <sup>24</sup>	Na <sup>24</sup>	(n, p)	2.75, 1.37	15. hr
Si <sup>28</sup>	Al <sup>28</sup>	(n, p)	1.78	2.27 min

Under the Surveyor program, considerable feasibility work has been completed on a neutron-activation mineral-analysis instrument (Refs. 15-21, 15-27, and 15-36). A miniature electrostatic accelerator irradiates a beryllium target with a beam of deuterons. Neutrons are produced by the reaction.



Typically  $10^7$  to  $10^{10}$  14-Mev neutrons can be produced every second by such a source. An accelerator-type neutron source is used, in preference to the common terrestrial Ra-Be and Pu-Be radioactive neutron sources, because it can be turned on and off and the desire to keep planetary surfaces free from large quantities of introduced radioisotopes. On the other hand, the use of a radioactive neutron source would save weight and reduce power consumption. A scintillation detector and photomultiplier tube unite to deliver pulses proportional to the gamma-ray energies to a pulse-height analyzer. Here, the pulses are sorted according to energy to produce a spectrum like that illustrated in Fig. 15-21. The spectrum, one

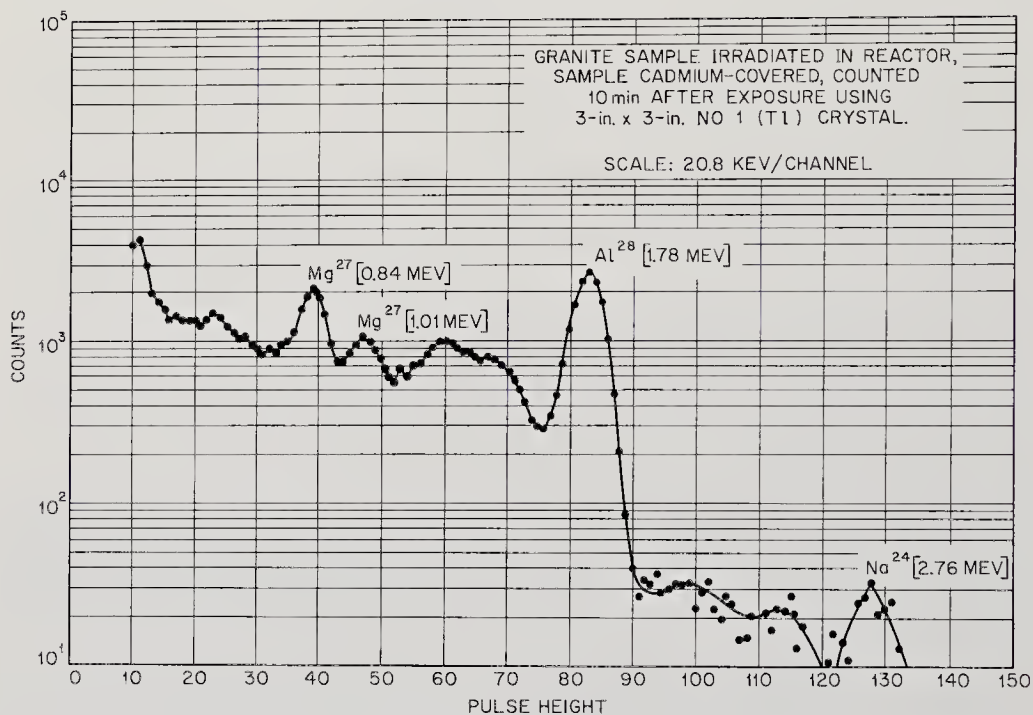


Fig. 15-21. Sample spectrum from a neutron-activation-analysis experiment. (Ref. 15-22)

should note, represents the sum of counts from all radioisotopes by channel. In other words, the spectra are additive, and if the spectrum of a known radioisotope is subtracted (stripped) from the totals, the remaining elements may be made to stand out more clearly. Even without "spectrum stripping," the distinctive peaks readily lead to element identification.

There is a striking similarity between the detector part of the neutron-activation-analysis instrument and the gamma-ray spectrometer. One could, in fact, use the neutron-activation-analysis equipment for gamma-



ray spectroscopy of the naturally occurring radioisotopes before the neutron source is turned on.

An instrument designed primarily for neutron inelastic scattering experiments has been brought close to the prototype state with a mass and power consumption of 10 kg and 20 watts respectively (see Fig. 15-22);

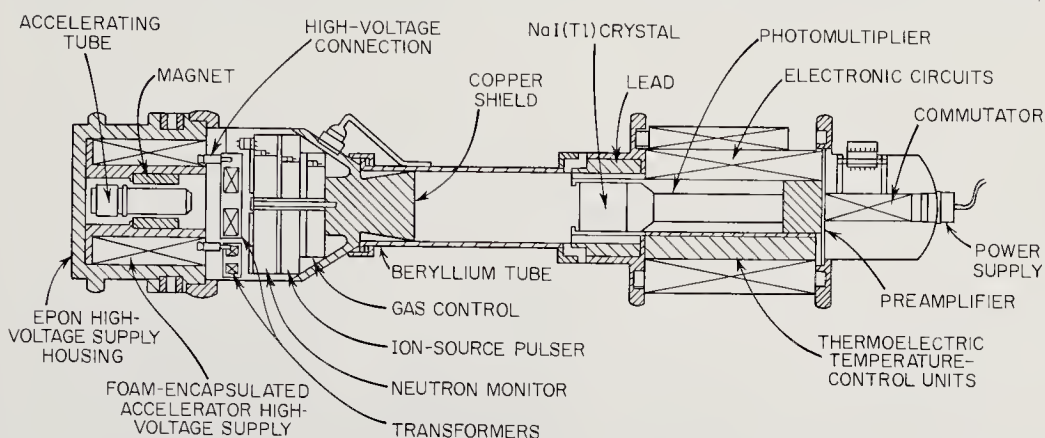


Fig. 15-22. Drawing of a prototype inelastic-scattering instrument. Neutron source is on left, detector on the right. Since neutrons are emitted isotropically from the beryllium target, instrument could be placed horizontally on the planet surface and secondary-gamma rays would enter detector acceptance cone. (Ref. 15-37)

present estimates for a system using neutron activation and the radiative capture reaction run 50 per cent higher in mass and power consumption.

Some redundancy in terms of element identification can be seen if all the physical experiments covered in this section are compared. Each experiment has its areas of strength and weakness. The great power of neutron-activation analysis is its ability to function with little or no sample preparation, the penetrating power of the neutrons, and its sensitivity to a large fraction of the elements in the Periodic Table, especially the heavier elements which cannot be touched by alpha-scattering instruments and X-ray spectroscopy. The common weakness of physical experiments (analysis by element rather than compound) applies to neutron activation analysis too. In addition, instruments like that pictured in Fig. 15-22 reproduce electromagnetic, magnetic, and radiation fields, which may interfere with other experiments and spacecraft equipment.

*Surface Densitometers.* Knowledge of the density of surface rocks is important in unraveling a planet's evolution. Some notion of the density may be obtained from the intensity of the radiation induced by neutron activation, but a more precise, even if partly redundant, density measurement is desirable. The same gamma back-scattering technique used in

determining atmospheric density may be employed to advantage here.

A radioactive gamma source (say, a few millicuries of  $\text{Ir}^{192}$ ) can be placed close to the planet's surface. Shields would separate the source from the detector, a few centimeters away (Ref. 15-11). Gamma rays scattered into the detector generate a two-valued function when plotted against density (Fig. 15-23). Low-density materials do not scatter gamma

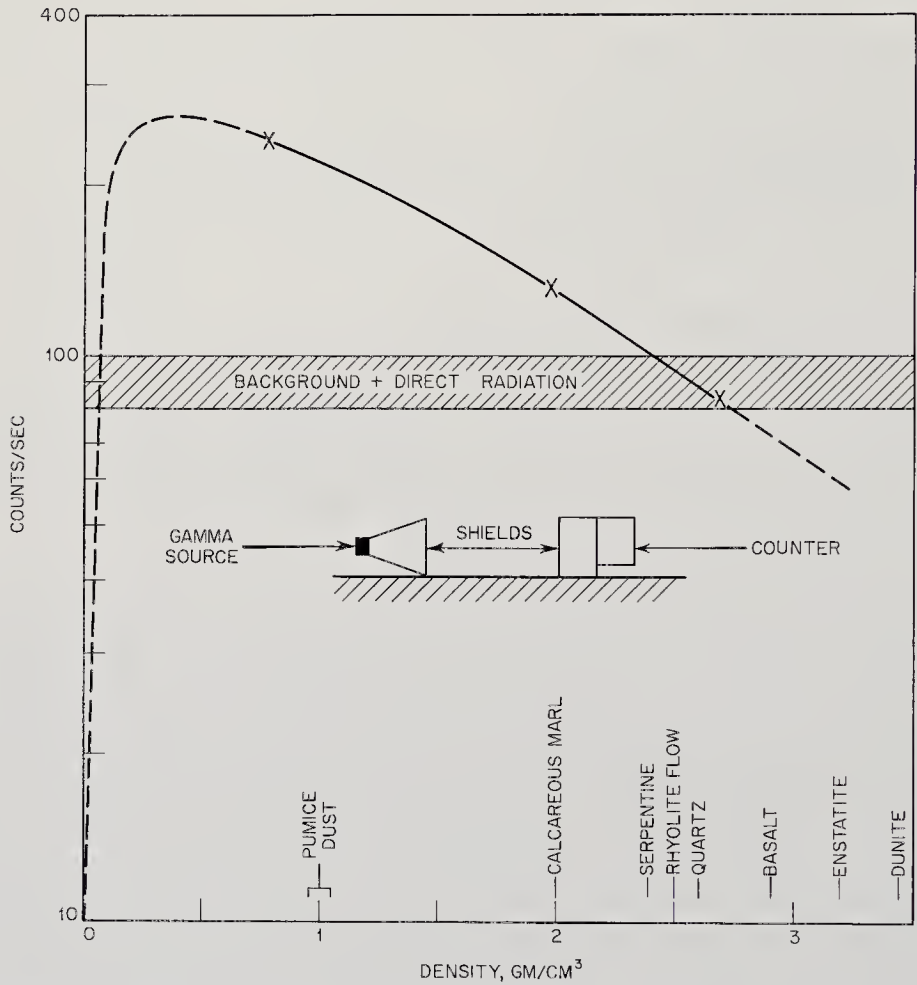


Fig. 15-23. Experimental arrangement and typical curve for a gamma-ray backscatter densitometer. Ref. 15-11)

rays very well, causing the initial dip. High density, good scatterers will also strongly absorb gamma rays, leading to final depression of the curve. Such a densitometer, though extremely simple, can measure density to  $0.1 \text{ g/cm}^3$ , below  $2 \text{ g/cm}^3$ , and to 5%, from 2 to  $4 \text{ g/cm}^3$ , for smooth-surfaced samples. Empirical corrections can be applied when rough surfaces are analyzed.

A gamma-back-scatter densitometer for planetary use could be built at around 1 kg, with a power consumption of about 2 watts.

*Differential Thermal Analysis.* Still in the research stage, differential thermal analysis is an appealing technique using phase-transition detection as an indicator of mineral identity. A schematic for a differential thermal analysis experiment is illustrated in Fig. 15-24. One of the two

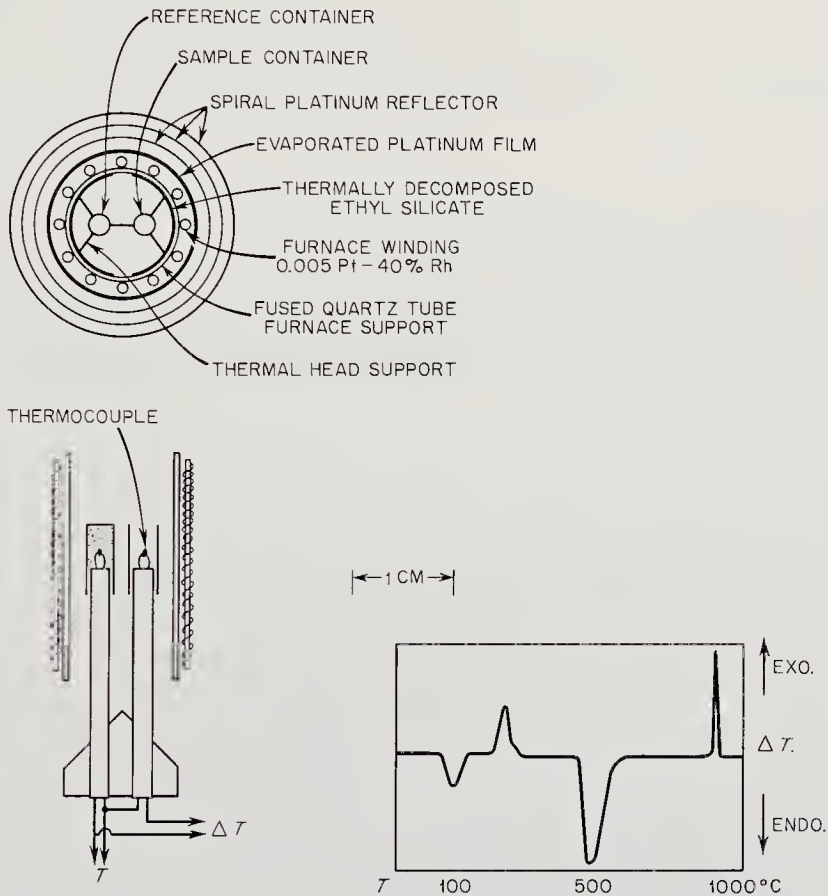


Fig. 15-24. Experimental curve and arrangement for a differential-thermal-analysis (DTA) instrument. (JPL drawing)

cups shown is filled with the unknown powdered sample, the other with a reference material (commonly alumina,  $Al_2O_3$ ). When heat is slowly applied to both cups, their temperatures will rise equally (ignoring their insignificantly different thermal capacities). The temperature difference measured between them thus remains fixed. When the unknown sample undergoes a structural phase change, however, heat will be either absorbed or evolved, as shown in the plot of temperature versus temperature difference (Fig. 15-24). Most minerals of interest in planetary research

have characteristic  $\Delta T$  vs.  $T$  curves, making differential thermal analysis a possible diagnostic tool for space-probe use.

*Petrographic Microscopes.* One of the most technically difficult of all sampling instruments is the petrographic microscope. The challenge lies not only in sample collection and preparation, but in forming a suitable image, relaying it to Earth, and then interpreting the received picture.

Earthbound geologists have long employed petrographic microscopes to view light transmitted through thin sections of rock sample. Extensive experience in the interpretation of such images has been accumulated. The information to be derived includes crystal structure, glass content, mineral identity, and, in the case of powdered samples, particle size and shape.

There are three major parts to a remotely operated petrographic microscope:

1. The sample collector and preparer.
2. The microscope itself.
3. A vidicon or some other imaging device for converting the image into electrical signals.

The first and last, more generalized, components are described elsewhere (Secs. 15-3 and 15-2). Two points concerning them should be made here, however. First, any imaging device collects a lot of information. The value of that information should be weighed against the difficulties of transmitting it. Second, sample collection is extremely difficult. Thin, polished rock sections are apparently out of the question. Samples for the microscope will have to consist of indigenous or artificially prepared powder. Unfortunately, there is considerably less experience available in the interpretation of images obtained from powdered samples.

The Jet Propulsion Laboratory and Armour Research Foundation have been developing petrographic microscopes for the space program. Preparation of a powdered sample for viewing involves immersing the powder in a thermoplastic tape, which is then carried to the microscope. In the microscope, the sample is viewed by plane and unpolarized light. Many adjustments must be made remotely: focus, sample orientation, light source, intensity, and filter identity. Though still in the research stage, a space-adapted petrographic microscope with its associated vidicon has been estimated to have a mass of about 15 kg, and it would consume perhaps 30 watts of power, both exclusive of the sample collector. Because of its size and complexity in terms of the value of the data returned, the petrographic microscope has low priority at present.

*Isotopic Dating.* Cosmology, geology, archaeology, and other sciences have come to depend upon isotopic dating as a useful tool, though one

that demands careful interpretation of results. Remote isotopic dating of the materials encountered on a planetary surface is certainly no more difficult technically than many of the experiments already mentioned. A successful series of dating experiments could provide insight into:

1. The times at which geological differentiation processes and mineral crystallizations occurred on the planet; viz., when the crust was formed.
2. The length of time surface material has been exposed to cosmic radiation.
3. The final stages of nucleosynthetic processes which helped form the planets.

P. Eberhardt and J. Geiss, at the University of Bern, have studied lunar isotopic dating under a NASA contract. They have concluded that isotopic analysis of the noble gases represents the simplest approach to remote dating. The experimental steps would be: extraction of gases from the sample, gas purification, and, finally, the separation of the noble gas

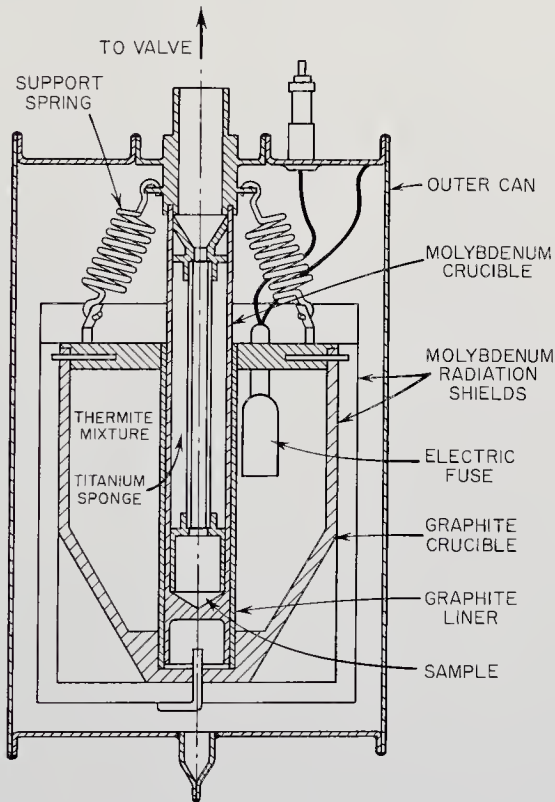


Fig. 15-25. Prototype thermite device for evolving and purifying noble gases from crustal samples prior to isotopic separation for age measurements. (NASA drawing)

isotopes. Pyrolysis of the crustal sample at temperatures over 1500°C, using a thermite reaction, is suggested (Fig. 15-25). The evolved gases, except for helium, argon, and other inert gases, would be absorbed in a titanium sponge. Isotopic separation of the purified gases could be done most easily by one of the mass spectrometers discussed earlier in this chapter. The ratios of the isotopic abundances would be calculated on Earth.

The  $\text{Ar}^{40}$  and  $\text{He}^4$  concentrations should not be higher than 6 and  $2 \times 10^{-5}$  cc/g, if the planetary surface is similar to the chondrite class of meteorites. The extraction and analysis of such small quantities of gas seem within the capabilities of instrument technology. Isotopic dating of a planetary surface will probably be delayed, however, until crustal composition and the major geological features have been resolved.

#### 15-4. Geophysical Instruments

During the centuries that man has studied the Earth's surface, geophysical instruments have evolved that are destined to be vital in exploring the other planets. No cleancut division exists between the physical instruments of Sec. 15-3 and the geophysical devices introduced here. Generally speaking, the former measure microscopic parameters like crustal isotopic composition and density using techniques recently borrowed from physics. The latter instruments are more concerned with the delineation of macroscopic geological and engineering features of the planetary crust. They have been evolved by the mineral and petroleum industries after a long marriage with physics.

Categorically speaking, all geophysical and geochemical instruments are adaptable to planetary exploration. The total number of possible devices is seemingly endless. For practical purposes, the discussion here must be confined to the most important and best developed types. In terms of development, all geophysical instruments owe a large debt to the Surveyor program, where seismometers, drills, and other familiar tools have been modified for space use.

Many geophysical instruments require only proximity to the surface. The seismograph and other soil-mechanics experiments usually demand leveling, calibration, and sometimes special preparation of the surface. In fact, the single unifying characteristic of the geophysical class of instruments might be said to be their physical coupling to the subsurface, as opposed to the remote-radiation and sample-dissection instruments of Secs. 15-2 and 15-3. Table 15-4 shows that the coupling schemes are many: magnetic, electrical, kinetic, gravitational. Except for gravity, most of the coupling forces are induced by *active* transducers that are integral parts of the instruments.

TABLE 15-4. GEOPHYSICAL RESEARCH INSTRUMENTS

<i>Instrument Type</i>	<i>Principle of Operation</i>	<i>Parameters Measured</i>
Electrical-conductivity meter	$Q$ of resonant tank circuit placed near crust depends on crust resistivity.	Crustal electrical conductivity
Magnetic-inductance meter	Increase in mutual inductance of two coils placed close to crust depends on crust's susceptibility.	Crustal magnetic susceptibility
Thermal-diffusivity meter	Heat source added or withdrawn from crust causes crust's temperature to vary. Curve analysis yields diffusivity.	Crustal thermal inertia, conductivity, and diffusivity
Soil-mechanics instruments	Forces required to penetrate, depress, scrape surface are measured.	Crustal texture, structure, degree of consolidation, hardness, bearing and traction strengths
Seismometers	Relative motion between elastically suspended mass and frame coupled to surface measured.	Seismicity, crustal structure, crustal density
Gravimeters	Frequency of pendulum observed.	Acceleration due to gravity
Magnetometers	See Chap. 13.	Magnetic field and its fluctuations
Subsurface sondes and drills	Not instruments per se.	
Geodetic satellite	Orbit determination by precision tracking stations.	Size, mass, and shape of planet

Forecasts of payload-launching capabilities insist that geophysical instruments wait until after the remote analyses from flybys and some of the simpler sampling instruments have carried out preliminary reconnaissance of the planetary surfaces. In this light, the Martian surface probably will not see a geophysical instrument until 1975. There are several reasons why:

1. Geophysical instruments are generally heavier and more complex than others. Furthermore, they must be landed and carefully positioned.
2. Scientific interest is first in the microscopic physical parameters; i.e., composition; and then in the macroscopic crustal and subsurface properties.
3. The proper design of geophysical instruments depends to some extent upon the data obtained from flybys and early sampling experiments.

The scientific importance of geophysical devices should not be obscured by timetables. No other class of instruments can better unravel the

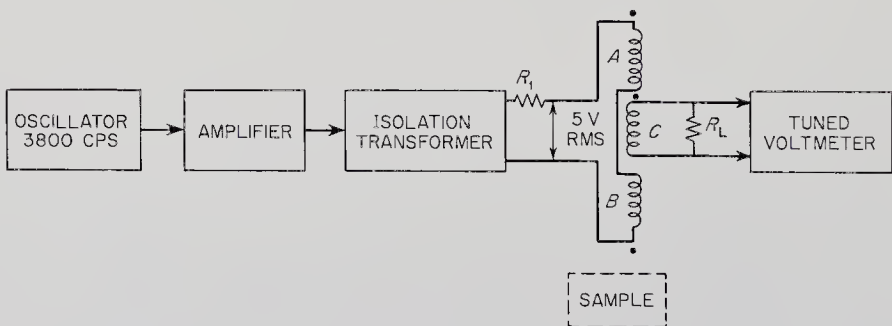
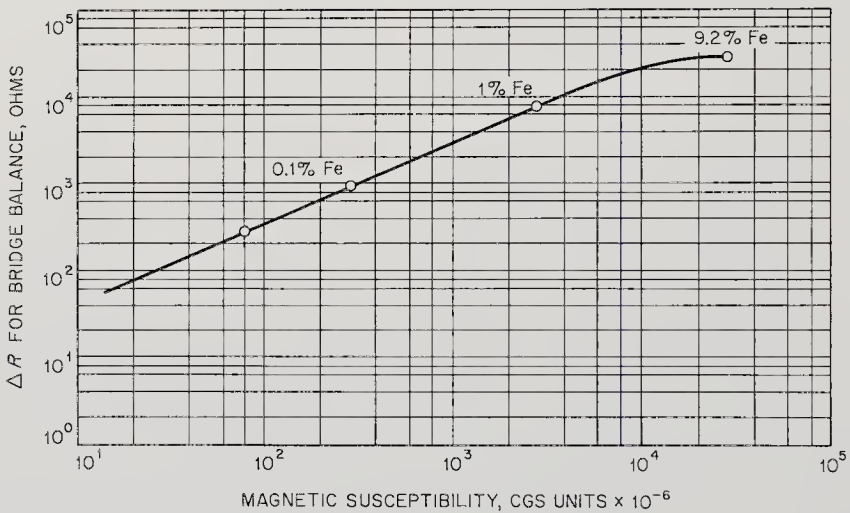


Fig. 15-26. Typical experimental data and block diagram for a magnetic-susceptibility experiment.



structure and evolutionary history of one of the terrestrial planets by remote control.

*Electrical-Conductivity Meter.* The electrical conductivity of a planet's crust can be measured by placing a high-frequency resonant tank circuit near the crust and measuring the  $Q$  of the circuit. The oscillating electromagnetic field of the circuit is pulsed to induce crustal currents, which damp out at a rate dependent on the soil's electrical resistivity. The crust's electrical conductivity is one of several properties which, when taken together, are indicative of composition. Magnetic susceptibility and thermal diffusivity, discussed next, are in this class.

No extensive instrument development work has been done on electrical-conductivity meters. Studies have estimated that a relatively lightweight, compact instrument should result: mass, about 0.5 kg; power consumption, about 1 watt.

*Magnetic-Inductance Meter.* Like electrical conductivity, magnetic susceptibility can be used in the identification of crustal composition. Some typical values measured with a prototype Surveyor instrument are illustrated in Fig. 15-26 (Refs. 15-5 and 15-9).

Crust susceptibility can be measured by placing two coils close to the surface and observing the changes in mutual inductance occasioned by the presence of the crust. The prototype instrument mentioned above used a single receiver coil, whose magnetic field was initially bucked out by two transmitter coils. If the receiver coil is connected into a bridge circuit, small distortions due to the presence of the crust can be easily measured by the imbalance in the bridge.

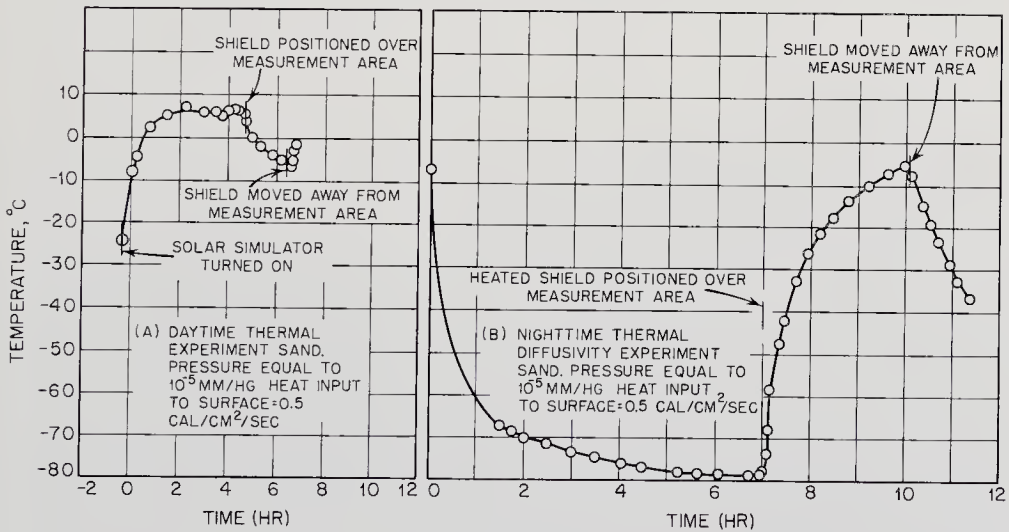


Fig. 15-27. Typical experimental data for a thermal-diffusivity experiment, in which heat sources are added and removed. (JPL drawing)

Both surface and subsurface susceptibility meters have been examined under the Surveyor program. These instruments are simple, rugged, and lightweight. Mass and power requirements are about the same as they are for the electrical-conductivity meter.

*Thermal-Diffusivity Meter.* When a section of planetary crust is suddenly exposed to a heat source (or perhaps deprived of solar heat), its temperature will change in the manner shown in Fig. 15-27. By proper interpretation of such curves, the thermal inertia, thermal conductivity, and thermal diffusivity of the crust can be inferred. These crustal properties, added to magnetic susceptibility and electrical conductivity, can help pinpoint crustal composition and degree of consolidation.

The use of an artificial heat source rather than insolation is preferable for planetary work—sunlight is weak at Mars, and Venus is cloud-covered. An electrically heated source drawing about 25 watts of power would be placed in thermal contact with the crust, and the temperature of the crust measured as a function of time by a small thermistor. The entire experiment would have a mass of less than 0.5 kg. Some development of thermal-diffusivity instrumentation has already been accomplished under the Surveyor program (Ref. 15-9).

*Soil-Mechanics Experiments.* The landing of vehicles, especially manned ones, on the Moon or planets requires prior knowledge of the so-called engineering properties of the crust if the lander is to be designed correctly. Through the use of various transducers that penetrate and interact with the crust, unmanned spacecraft can early determine surface parameters like load-bearing capability, degree of surface-material consolidation, and traction properties for mobile vehicles. Four types of instruments and experiments have been studied under the Surveyor program:

1. Penetrometers.
2. Load-bearing and traction experiments.
3. Instrumented surface samplers.
4. Touchdown-dynamics experiments.

These experiments are redundant when taken together, and no single spacecraft would carry all of them. The first Surveyor soft lunar landers will carry only experiments 3 and 4. The adjective "engineering" perhaps implies that soil-mechanics experiments have no scientific value. To the contrary, the character of the planetary crust, as measured by soil-mechanics experiments, has an important bearing on the interpretation of the planet's evolution.

Penetrometers are simply weights with conical or hemispheric ends (Fig. 15-28) that are permitted to drop onto and penetrate the crust. By

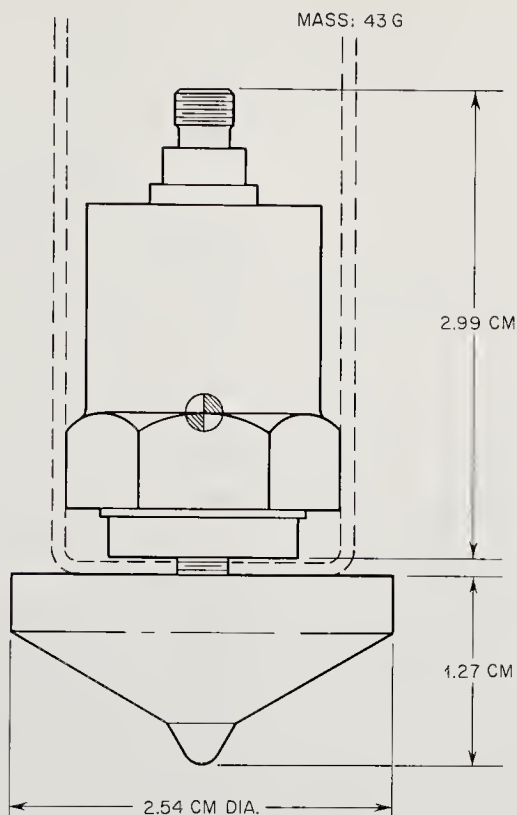


Fig. 15-28. A typical penetrometer. (Ref. 15-9)

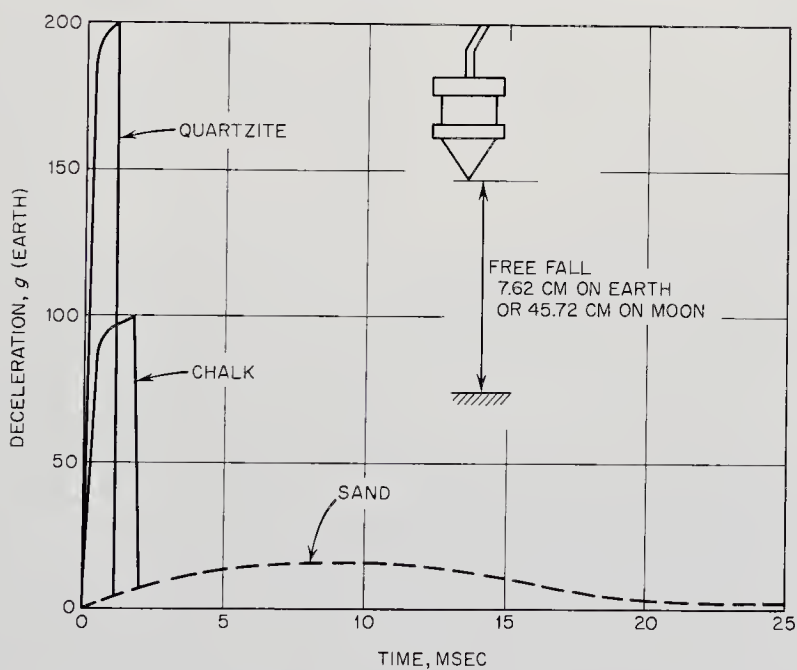


Fig. 15-29. Penetrometer curves for different materials. (Ref. 15-9)

placing a small piezoelectric-crystal accelerometer within the weight, the deceleration-time history can be measured and telemetered back to Earth. Figure 15-29 shows how such information is indicative of the type of

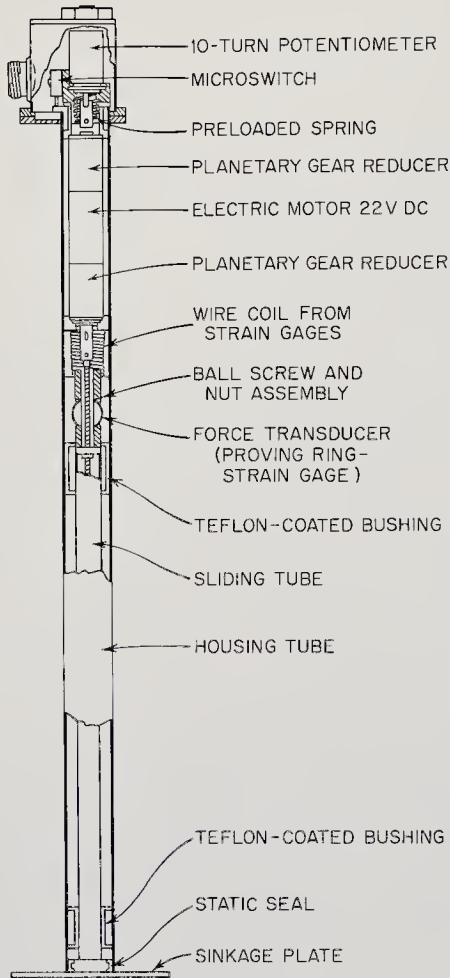


Fig. 15-30. Load-bearing experiment. Traction experiment is similar, but has an annular ring at base and an applied torque in addition to axial load. (JPL drawing)

rock and the degree of consolidation. Penetrometers, including an arm and release mechanism, have masses of less than a kilogram and consume only a few tenths of a watt of power when in operation.

A load-bearing experiment measures the distance of sinkage of a flat plate as a function of the applied load. Traction capability or crustal shear strength can be measured in a plane parallel to the surface by monitoring the torque necessary to achieve a given angular displacement of a spudded annular ring bearing down on the surface with a constant axial load. Prototypes of both experiments have been constructed. Both take the form of long vertical cylinders with a flat plate or ring in contact with the crust (Fig. 15-30). Combined, the two cylinders and their associated electronics have a mass of about 6.5 kg. Only a couple watt-hours of energy would be needed for the full experiment.

The Surveyor soil-mechanics experiment includes an instrumented sample collector (see Fig. 15-8) which by probing and scraping the lunar surface should collect quan-

titative information on the mechanical properties of the surface. Surface load-bearing strength and the presence or lack of any layered structures can probably be detected by the instrumented sampler.

The Surveyor sample collector, essentially a scraper, will be instrumented to record the following data:

1. Azimuth, elevation, and extension of the sampler.

2. Radial horizontal and vertical applied forces.
3. Accelerometers will measure sampler deceleration at crustal contacts in penetrometer fashion.

Of course, operations of the sampler will also be observed by television to supplement the above data.

Since Surveyor's landing gear is strut-like, one can instrument the legs themselves as if they were penetrometers and obtain dynamic data at the moment of touchdown. NASA's Langley Research Center will carry out an experiment like this on Surveyor. The touchdown-dynamics experiment objectives are:

1. Determine linear and angular acceleration, angular velocity, and displacement of the spacecraft during touchdown.
2. Determine the bearing strength and shear resistance of the lunar surface.
3. Determine the depth of the spacecraft penetration into the lunar surface.
4. Determine the surface contour in the landing area.

The first objective can be accomplished by installing three linear accelerometers, three angular-rate gyroscopes, and linear-displacement indicators on the leg-shock-absorber combinations. Data measured with these instruments must be combined with that from the following transducers to fulfill the objectives listed above.

Strain-gauge bridges attached to the six leg struts and to each of the three shock absorber struts will measure axial loads. Finally, auxiliary data are available from other sources. These include the spacecraft dimensions, particularly the areas of the surfaces contacting the surface, and doppler velocity and altimeter data from the guidance-and-control subsystem.

Quite obviously, the Surveyor touchdown-dynamics experiments are more or less immersed in the spacecraft itself; that is, there is no single, separable instrument one can point to. Instead, the experiments involve attaching very simple transducers to several functional parts of the spacecraft. The acquired data must then be analyzed collectively along with spacecraft dimensions and touchdown information if the results are to be significant.

*Seismometers.* On Earth, seismometers are best known for their earthquake-detecting abilities. They are more versatile than that. We may expect a seismometer placed on the Martian surface to record data leading to the following insights:

1. The frequency, intensity, and direction of quakes.

2. The crustal structure. Is it layered or monolithic?
3. The existence or lack of a fluid core.
4. Crustal composition and/or density from velocity data.
5. The frequency of nearby meteorite impacts and thermal activity if the background signal level is low.

Because we wish to know the same things about the Moon, a substantial amount of seismometer development has already been accomplished under the Ranger and Surveyor programs. Much of this work can be transferred bodily to the planetary programs.

The principles of seismometer operation are well known. Mechanical vibrations in the crust are transferred to the seismometer body. A large mass is suspended from the frame by a spring or some other elastic device. When the frame moves, the mass remains nearly fixed, permitting displacement between the frame and mass to be recorded by a distance-to-electrical-signal transducer. This is reminiscent of the linear accelerometer. Of course, there must be a separate mass suspension for each of the three axes if a complete record of crustal movement is desired. A single-axis vertical seismograph is a simpler, lighter, but still useful instrument, especially for preliminary scoping measurements. In addition to the number of axes recorded, each seismometer, like any structure, boasts a natural frequency at which it is extremely sensitive to induced vibrations. Within limits, the sensitivity curve can be made to peak almost anywhere. Many seismometers are tuned to the strongest frequency components in earthquakes. In the exploration of a planet, a broad range of frequencies should be investigated. For example, each solid planet will possess a resonant frequency of its own, with a period possibly as long as several hours. Or perhaps the seismometer will be designed to measure crustal tides, the distortions caused by rotation in the gravitational field of another large body. Untuned seismometers, with broad frequency responses, seem desirable for initial reconnaissance.

The mechanical interface with the remainder of the lander is critical for seismometers. Almost every payload will include noisy experiments, with closing relays, moving arms, vibrating reeds, and so on. These experiments must either be turned off during quakes or the seismometer must be adequately decoupled from the spacecraft. Also, while in flight and during the touchdown itself, the seismometer mass must be caged to prevent damaging the transducers. Finally, seismograms, like optical spectra, contain a great deal of information, more than can be telemetered in real time. Data storage facilities must therefore be incorporated into the instrument.

Of the several space seismographs that have been or are being devel-

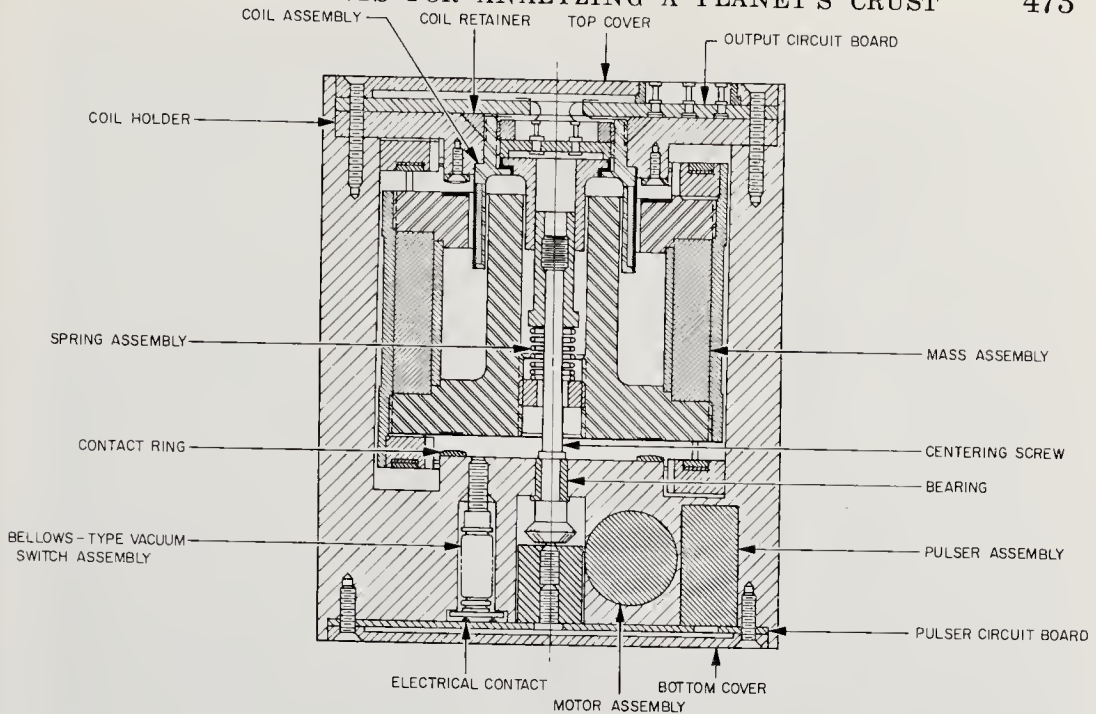


Fig. 15-31. The Ranger single-axis seismometer. (Ref. 15-1)

oped, two have special interest here. The first is the single-axis, hard-lunar-landing Ranger seismometer pictured in Fig. 15-31. The basic instrument consisted of a coil, a spring-suspended magnet, and an internal calibration device (Ref. 15-1). The coil was rigidly attached to the instrument case. Movement of the spring-suspended magnet induced a current in the coil proportional to the rate at which lines of flux are cut. The natural period of the Ranger seismometer was nominally 0.4 sec, but the mounting of several additional permanent magnets inside the case extended the natural period to about one second. With this period, the sensitivity was 0.80 microvolt/ $m\mu$  of peak-to-peak crustal deflection. By sending a known current through a coil, the suspended mass could be deflected a known amount for calibration purposes. In order to survive the 3000-g lunar landing, the seismometer mass was caged in fluid (*n*-heptane), which was to be drained when the lander was in position on the lunar surface. Total mass of the instrument, with caging fluid, was 3.3 kg. The Surveyor soft lunar landing seismometer, the second instrument of interest, is also a single-axis system (Fig. 15-32). It is slightly more sensitive and uses a mechanical rather than fluid caging device. The instrument mass with caging and electronics is about 3.5 kg.

Eventually, scientists can expect active rather than passive seismic experiments. Possibly the other planets will not be as cooperative as the Earth in the production of frequent quakes to help plumb their interiors.

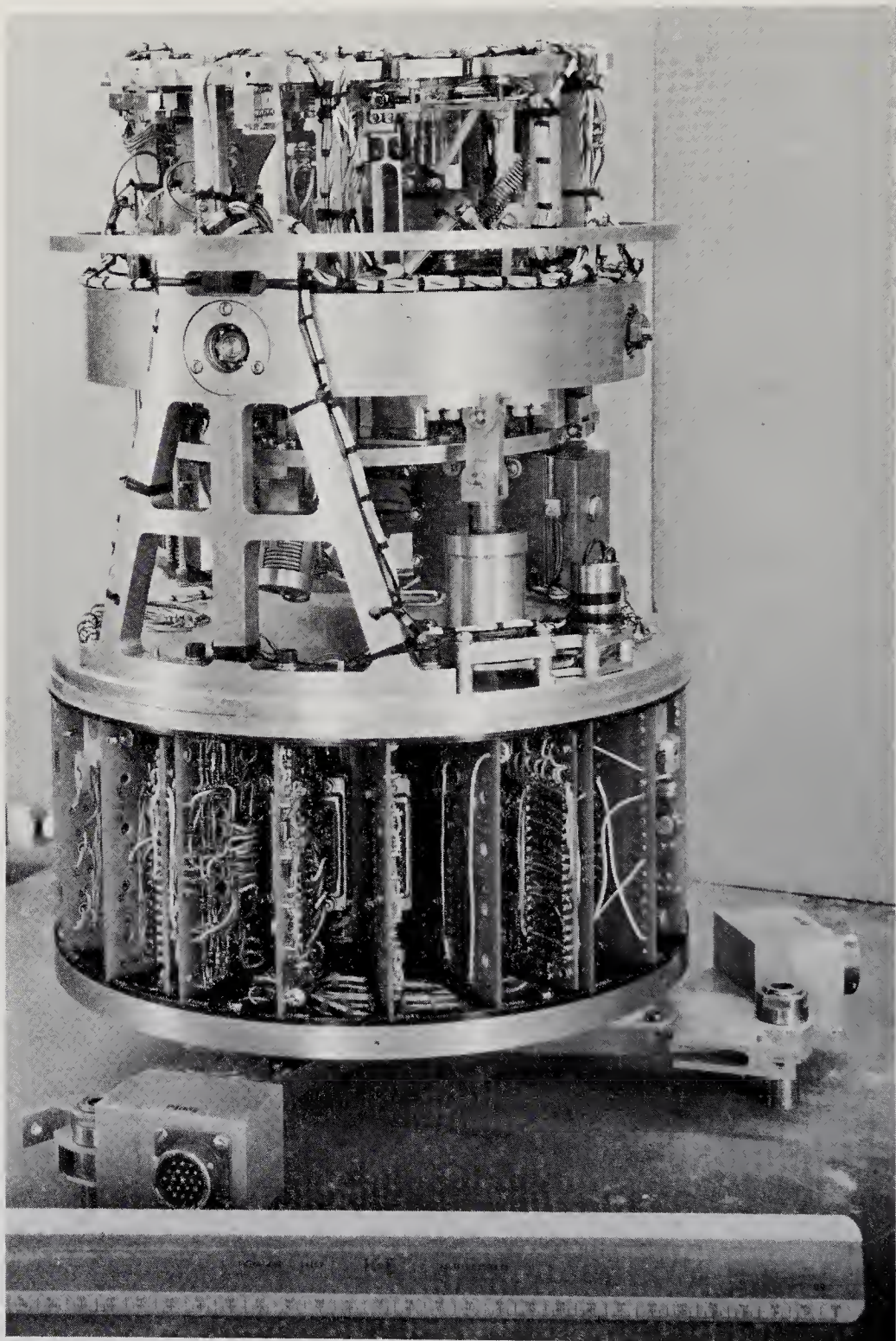


Fig. 15-32. A Surveyor seismometer. (Courtesy of Columbia University)



Active seismic experiments would involve the detonation of an explosive charge and listening to the reflected and/or refracted seismic waves with an array of geophones, after the fashion of petroleum prospecting. Strata could be measured in this way and, by observing the dispersion of propagation velocity with depth, some idea about the depth-density relationship for the planet could be gained. A complete active seismic experiment with four dispersible geophones has been estimated to have a mass of 40 kg and a power requirement of 5 watts.

One final seismic experiment, which could be carried out with the equipment just described or with a much simpler setup, is the measurement of the velocity of sound in the crust. One or two strategically placed detectors (geophones) could record the sound waves sent through the crust by a succession of small squib detonations (Ref. 15-16). Knowledge of the distances and travel times would lead directly to the velocity of sound. Knowledge of the velocity of sound, in turn, would give geophysicists a good idea about the density of the surface rocks.

*Other Geophysical Experiments.* The impressive number and variety of geophysical instruments have already been mentioned. Typical of those that have not been mentioned are the gravimeter and magnetometer. From a fixed lander, these two instruments would measure the planet's surface acceleration due to gravity and the time variation of the magnetic field. Ultimately, vehicles could carry the instruments over the face of the planet to help unravel subsurface geology in the same way that aircraft are used to search for mineral deposits on Earth.

Initially, a drill was to have been included on the early Surveyor spacecraft in order to place a sonde beneath the Moon's surface to measure, from a better vantage point, parameters such as thermal diffusivity, the speed of sound, magnetic susceptibility, and the crust's engineering properties. The complexity, power consumption, and weight of the equipment have deferred its use until later lunar shots. Weight and reliability are even more critical on deep-space missions, so that drills and sondes, despite their admitted advantages in crustal research, will have to remain until later when larger landers will be available.

A relatively new geophysical instrument is the geodetic satellite. By careful observation over long periods of time, an artificial satellite can help fix the size, mass, and shape of a planet. An artificial satellite becomes a geodetic satellite when accouterments such as flashing lights are added to aid ground-based tracking. A man-made satellite circling another planet in the solar system would not be visually observable from Earth. Automatic, remote tracking from the planet itself appears too difficult. Manned, planet-based, tracking stations present the best hope,

but they are a good many years away. In this same desirable-but-difficult category we would have to place the planet-based sounding rocket, designed to make upper atmosphere measurements at a more leisurely pace than that possible during the trauma of entry from outer space.

# Chapter 16

---

## INSTRUMENTS FOR DETECTING LIFE

---

---

### 16-1. Prologue

Is there life on Mars? This is perhaps the most persistent and ubiquitous question in all of astronautics. Despite the question's emotional appeal, the scope of biology far transcends the restricted yes-or-no answer we hope to receive from unmanned probes within the next decade. Biology, like any other science, tries to construct the most general, most accurate, and most elegant description of the universe possible. The simple discovery of life on another planet without detailed study of that life, though it would greatly enlarge our biological universe, represents no new triumph of understanding but simply more grist for the mill that ultimately produces our broad scientific generalizations. Indeed, some biologists already base their theories on the existence of life outside the Earth. The fact of life on Mars by itself would give biology no real insight into this life's origin, its variety, or evolution (Refs. 16-3, 16-9, 16-25). *Detailed studies* of extraterrestrial life, in contrast, would be immensely stimulating to biology, a science overwhelmed with observations but possessing few broad generalizations. The discovery of life forms existing beyond the limited sphere of the Earth, perhaps with different genetic and metabolic schemes, might provide that additional breadth necessary for the formulation of powerful new theories.

The newly named discipline of exobiology encompasses both life detection and the study of this life. This book covers only that part of exobiology concerned with the instrumentation of unmanned space probes. The very newness of the field makes this more a chapter of ideas and research than hardware description. While the interplanetary, atmospheric, and surface instruments have had the advantage of many years of development on sounding rockets, balloons, and satellites, biologists have

usually had no opportunities or scientific justifications for placing life-detection equipment aboard these vehicles. Abundant life for scientific research has always been present on Earth in every pinch of sand and drop of water. The design of remote life-detection instrumentation is a new scientific venture. The much more important *study of life* with remote equipment has hardly been considered at all. Consequently, the great bulk of discussion will concentrate on the simple detection or non-detection of life; the yes or no.

There is a question of what constitutes life detection. Amino acids, for example, are linked together to form proteins in all terrestrial organisms. Would the detection of amino acids indicate the presence of life on another planet? Not necessarily, because they may have been synthesized from simpler chemicals with the help of non-life processes; say, electrical discharges. If an experiment could be designed that appeared to detect proteins, a biologist would then have more confidence that life truly existed on the planet. There would still be questions, however, about incomplete sterilization of Earth-built equipment, equipment defects, and chemical poisoning of the experiment. Short of seeing life forms through a television circuit, there can be no real certainty that life has or has not been detected. Every life-detection experiment so far proposed can be faulted by the skeptics—and there are more skeptics where life detection is concerned than in the rest of space research.

Human nature being what it is, a series of life-detection experiments all yielding positive results will sway more and more scientists at each step, perhaps after the fashion of the “confidence” curve, Fig. 16-1. A small minority of scientists are already convinced that extraterrestrial life exists, even before the first probe experiments; therefore the curve cannot start at zero. A single positive or negative result will be instrumental in swinging the opinions of many. Two successive positive or negative experiments will convince more, and so on, as shown in Fig. 16-1. But both curves are asymptotic. The whole universe would have to be explored to be sure of a no. And there will always be the doubters that make certain proof impossible, and rightfully so, since none of the life-detection devices is completely foolproof. Between the positive and negative branches of the curve lie the frustrating situations where mixed yeses and noes are received on the telemetry channels. The cause may lie in faulty equipment or possibly because the wrong questions are being asked. (The right questions on Earth might be the wrong questions on Mars.)

Just what are the right questions? None of the experiments listed in Table 16-1 really gives the yes or no answer desired. Experimental answers are quite different and far more limited. Take the optical rotary-dispersion experiment as an example. It asks if there are substances on

the target planet that rotate the plane of polarized light. The experiment can tell both the amount and direction of the rotation, but such data are separated from the desired yes or no by human interpretation and opinion, which always keep the curves in Fig. 16-1 asymptotic.

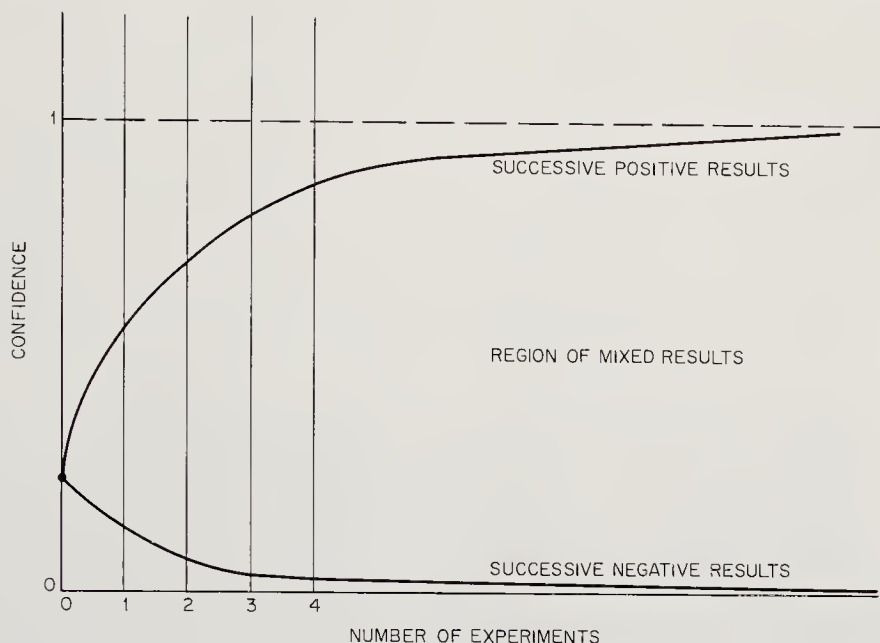


Fig. 16-1. "Confidence" in the existence of extraterrestrial life as a function of the number of experiments performed.

Scanning the major life-detection experiments listed in Table 16-1, one may separate the experimental queries into three groups:

1. Those that ask whether there are chemical compounds on the target planet that are usually associated with terrestrial life (amino acids).
2. Those that ask whether, given Earth-type nutrients, there are chemical reactions like those associated with terrestrial life (metabolism).
3. Those that ask whether life forms, remnants of life, or artifacts can be seen (animals, fossils, "canals").

"Life detection" experiments, then, except perhaps for those in category 3, do not really detect life directly. Even the imaging experiments in category 3 may be fooled by lifelike forms; viz., the controversy over the organized elements in meteoroids. Thus qualified, this chapter's title will be retained.

In the discussion so far, it has been assumed that a well-defined taxonomic wall separates life from non-life. The wall is none too strong. Life seems best defined by its most distinctive attributes:

TABLE 16-1. INSTRUMENTS USED IN "LIFE DETECTION" \*

<i>Instrument/Experiment</i>	<i>Principle of Operation</i>	<i>Parameters Measured</i>
Infrared spectrometers	Emitted or reflected radiation is dispersed by grating or prism into spectrum. IR detector produces electrical signal proportional to light intensity.	Absorption and emission spectra due to organic molecules.
Television	Vidicon camera stores electrostatic image on photoconductor-backed plate. Image is scanned by electron beam.	Images of life forms, fossils, and artifacts.
Radio listening	Radio receiver detects "intelligent" or non-random signals.	Possible existence of intelligence, but not necessarily life as defined in Sec. 16-1.
Mass spectrometers	Electromagnetic force fields separate ions according to mass. Ion detectors measure abundances of macromolecular fragments. See Sec. 15-3.	Abundance vs. molecular weight of ionized fragments.
Chromatographs	Sorptive columns or paper strips separate chemical components. See Sec. 15-3.	Abundance vs. chemical compound.
Ultraviolet spectrophotometer	Absorption due to peptide bonds is measured by conventional filter spectrometer. See Sec. 14-3.	Amount of absorption vs. time.
Turbidity and pH	Photocell measures solution turbidity vs. time. Glass electrodes measure pH vs. time.	Turbidity and pH vs. time.
Stain experiments (J-band detectors)	Aggregation of certain dyes cause proteins to absorb strongly in the visible. Effect is measured by conventional filter spectrometer. See Sec. 14-2.	Amount of absorption vs. time.
Bioluminescence	Absorption of light causes several biologically significant molecules to fluoresce.	Amount of fluorescence vs. time.
Redox-potential experiments	Electrodes in culture cell measure potential difference if reduction-oxidization reactions are occurring.	Potential difference vs. time.

## Optical rotary dispersion

Activated molecules in solution rotate plane of polarized light. Polaroid analyzer measures direction and amount of polarization.

Direction and amount of polarization leads to knowledge of abundance vs. chemical compound.

## Microscopes

Lenses magnify object. Vidicon camera transmits images of particles placed in focal plane.

Images of life forms, fossils, and artifacts.

## Metabolism detectors

Radioactively tagged culture is fed to sample. Metabolism evolves gases, which are detected by a counter.

Evolution of gases vs. time.

## Isotope interchange experiment

Water-based life should possess catalysts that stimulate oxygen exchange between water and oxygen anions important in metabolism. Exchange of isotopically tagged oxygen detected with mass spectrometer.

Presence of oxygen-exchange catalysis.

\* See text for qualification of this term.

1. Metabolism.
2. Reproduction.
3. Evolution or mutation.

Like all definitions, that of life is arbitrary. For the purposes of this book, life must have all three of the attributes just listed. Our primitive life-detection experiments cannot confirm singly or collectively the existence of all three attributes.

What exactly should life-detection equipment look for on a planet and where should it look? There seem to be six definable "states" of life (Ref. 16-25):

1. Protolife, where chemical evolution has proceeded to a point where necessary precursor molecules (e.g., amino acids, fatty acids, etc.) are present in detectable amounts, under environmental conditions suitable for the synthesis of still more complex molecules; i.e., reducing atmosphere, energy sources, etc.
2. Primitive life, where protolife has become replicating, metabolizing, and mutating.
3. Diverse forms of animal and vegetable life, including perhaps "intelligent" life.
4. Artifacts of a once-living biosphere and perhaps culture.
5. No evidence of life at all.
6. Something beyond our present comprehension; that is, life as we do *not* know it.

It is possible, of course, that the life forms and chemistries, if discovered, may be radically different from our own.

It is popular to talk about the probabilities of discovering life. This is not the place to indulge in such exercises, since the decision to look for life has already been made. The probability of finding life during a single experiment, however, can probably be improved by placing the instruments in likely spots. In choosing planets and specific locations on planets for experiments, mission planners can only assume that Earth-like environments are the most likely to harbor life. The Mars scanner described in Sec. 15-2 is, in fact, designed to detect microenvironments on Mars, where temperature and water-vapor concentrations are higher than normal. Such favored spots would be logical targets for the first planetary landing vehicles.

Once landed, most life-detection instruments must obtain a sample of the planet's life to work on. Except for some of the imaging experiments, microorganisms have been selected for collection and experimentation. No matter how much or what kind of life is present, if life is present at all,



there should be microorganisms available. They are expected to be hardy and yet simple to work with. It will still be difficult, however, to collect and study microorganisms by remote control. The scrapers, aspirators, and sticky strings introduced in Sec. 15-3 are all pertinent here. All samplers must assume that dust, aerosols, and other fine materials will contain microorganisms, just as they do on Earth. Some instruments, like the microscope, also require rather elaborate sample processing before the experiment can begin.

Possibly the biggest obstacle to life-detection-instrument design is the sterilization requirement. All terrestrial organisms obviously must be eliminated, at least from metabolic chambers, where life processes are to be detected. Sterilization processes may not need to be applied so rigorously to other parts of the instruments, but there must be adequate barriers to preclude the migration of Earth organisms from the rest of the spacecraft and the instrument proper into life-sensitive parts of the equipment.\* Note that the over-all spacecraft sterilization requirements specify only a certain upper limit to the probability of planet contamination ( $10^{-4}$  for Mars) and do not require complete sterilization of all components. In any case, the sterilizing processes—heat and gas soaking—are severe enough to damage many conventional components. Finally, the contamination of Mars itself by Earth microorganisms must be prevented during the early biological explorations. The contamination of Mars might ruin forever our chances of obtaining a clearcut answer to our questions about life beyond the Earth.

In the rest of the chapter, the life-detection instruments have been divided into three groups, after the fashion of Chapters 14 and 15. First, there are the experiments which attempt to detect life or the chemistry associated with life from a distance, through analysis of emitted or reflected electromagnetic radiation. The imaging devices and probe spectrometers fall in this category. Next come the sample processors and, lastly, the "biological" experiments, which are analogous to the macroscopic meteorological and geophysical experiments of the preceding chapters.

## 16-2. Life Detection by Remote Analysis of Electromagnetic Radiation

The first planetary probes will be flyby and orbiter spacecraft. Therefore, the first attempts to detect life on the other planets will be simply extensions of techniques already tried from the Earth's surface—the ad-

\* It has been found, for example, that solid rocket fuels, such as those used for braking the fall of impacting space probes, may be contaminated. Bits of unburnt fuel may contaminate large areas with Earth life.

vantage of the spacecraft being, of course, proximity. Distance during a planetary flyby is reduced by a factor of  $10^4$  or more. Electromagnetic instruments, if they are light and rugged enough to be placed on probes, can therefore be used to advantage in the search for life. The numbers and kinds of electromagnetic experiments possible from a distance, as indicated below, are rather limited. In essence, a distant instrument can either look for the spectra of chemicals associated with life or attempt to image life forms directly.

*Infrared Spectrometers.* The spectrum of infrared radiation emitted and reflected from a planet's surface may indicate the presence of complex organic materials as well as rock compositions and temperatures. Sinton has made infrared measurements of the Martian disk from Earth and has found absorption bands located at 3.45, 3.58, and  $3.69\mu$  (Ref. 16-18). Though Sinton's spectra are subject to non-life interpretations, some, but not all, scientists agree that they closely correspond to those of Earth-based organic molecules. Unfortunately, Sinton's experiment was hampered by the low spatial resolution of his optical equipment, approximately half a planetary diameter. Observations did, however, indicate stronger absorption bands in the dark areas (maria) of Mars. These same areas become even darker with the advent of the Martian spring. It is easy to leap to a positive conclusion concerning life on Mars from such measurements.

A flyby probe carrying an infrared spectrometer could repeat Sinton's measurements with much better areal resolution. This experiment, however, is not being considered seriously for probes at present because great improvements in resolution can still be obtained with Earth-based telescopes.

*Television.* One of the most convincing demonstrations of life on another planet would be the transmission of images showing undeniably living forms, fossils, or the engineering works of intelligent beings. From an orbit about Mars, for example, photography plus subsequent high resolution scanning of the film might reveal the true nature of the controversial "canals." The resolution of surface objects on the Martian surface might be reduced from the present hundreds of kilometers, attainable with Earth-based telescopes, down to tens of meters, with an orbiter telescope-film-vidicon combination (see Sec. 15-3).

Television equipment on a lander might be able to distinguish individual life forms or their aggregations. The Surveyor television unit would be adaptable to this role. Life on Mars, if it exists, is expected to be plant-like. Magnification of the scene surveyed by the lander will be desired for detailed studies of such organisms and potential fossil deposits. The Surveyor instrument, with adaptations for continuous focus-

ing and lens changes, would be a very heavy instrument for a planetary lander. Yet, it could give us pictures, probably the most direct and certainly the most subjectively satisfying proofs of life. The same reasoning applies to the microscopes covered in Sec. 16-3.

*Radio-Listening Experiments.* Scientists do not really expect to find other intelligent life within the solar system. All efforts, such as Project Ozma, to communicate by radio with other technically inclined life forms beyond the Earth have been confined to interstellar searchings (Ref. 16-4). Surely, the logic goes, if intelligent life forms with advanced technologies existed on the other planets of the solar system, we should be able to detect their radio signals by now. Perhaps that's true, if the signals were strong enough and of the right frequencies to penetrate the ionospheres of both planets. Consequently, radio listening from a planetary probe must be assigned a very low priority in the hierarchy of life-detection experiments because of the extremely low probability that any useful information could be acquired by such an experiment.

### 16-3. Life Detection by Sample Analysis

More convincing than the electromagnetic observations from flybys and orbiters will be the signals sent by instruments that have obtained and made measurements upon actual samples of the target planet's crust or, more positively, its biosphere. The instruments described in this section all depend upon the detection of some physical or chemical property of the sample which characterizes life. No uniquely biological properties are measured by these instruments. Metabolism, reproduction, and mutation, the three defining attributes of life, are not perceived directly or indirectly. The parameters measured are thus at least once removed from life's defining properties. One notes further that inescapable necessity of assuming that extraterrestrial life is like Earth life.

The sampling instruments previously listed in Table 16-1 can be classified into five groups according to their operating principle:

<i>Group</i>	<i>Objective</i>	<i>Instruments/Experiments</i>
1	Identify chemicals associated with life.	Mass spectrometers Chromatographs Ultraviolet spectrophotometer
2	Identify chemical processes associated with life.	Turbidity and pH experiments Stain experiments Bioluminescence Redox-potential experiments Isotope interchange experiment

<i>Group</i>	<i>Objective</i>	<i>Instruments/Experiments</i>
3	Identify physical phenomena associated with life.	Optical rotary dispersion
4	Identify images of lifeforms.	Microscopes
5	Identify biological processes.	Metabolism detectors

Group 5 is discussed in the next section, along with the Multivator/Minivator, multiple-experiment device, which straddles both Secs. 16-3 and 16-4.

Mass spectrometers and chromatographs are well down the development path as atmospheric and crustal-analysis instruments. The microscope, spectrophotometer, and the optical rotary-dispersion experiment represent space-probe adaptations of common terrestrial instruments. The remainder, however, are relative newcomers to space instrumentation. None, however, is unique to the space program. All have firm foundations in terrestrial laboratory experience.

*Mass Spectrometers.* Since a mass spectrometer accepts only gaseous inputs, any life forms present in the collected sample cannot avoid being broken down into much simpler compounds by the preparation process—usually pyrolysis and subsequent ionization. Mass spectrometry, moreover, is a better analytical tool when studying the lighter, simpler compounds, which are distinguishable by appreciable charge-to-mass-ratio differences (see Sec. 14-3). The role of the mass spectrometer in life detection is in the identification of biologically important chemical compounds, like the amino acids and peptides, through a mass analysis of their pyrolysis and ionization products. There are two opposing tradeoffs in this kind of mass spectrometry. The smaller the fragments being analyzed (molecular weights are usually well under 250), the more accurate the spectrometer. Unhappily, the likelihood of identifying the parent macromolecules from their fragments drops rapidly as the molecular weights of the constituents decrease. Experiments at MIT using conventional laboratory mass spectrometers reveal that many of the amino acids show a pyrolysis- and ionization-product peak at a molecular weight of 74, indicating a common fragment. Other peaks found in test spectra will probably enable scientists to identify specific amino acids from their pieces without ambiguity.

Once the technical feasibility of macromolecule identification by mass spectroscopy has been established in the laboratory, instruments light enough for probe use will have to be developed. The principles and guidelines presented for atmospheric mass spectrometers will apply here. No

space-vehicle mass spectrometers tailored to the life-detection task have yet been built.

*Chromatographs.* Much of what has been said about mass spectrometers also applies to gas chromatographs. That is, analysis of the pyrolysis products will probably permit identification of biologically significant parent macromolecules. The list of compounds detectable by the Surveyor gas chromatograph (see Sec. 15-3) emphasizes its ability to detect heavier, more complex molecules than the mass spectrograph. Chromatographs may therefore assay a crustal sample for macromolecules with less ambiguity.

Although the Surveyor gas chromatograph has been specifically constructed for lunar use, the engineering knowledge gained will be useful for life detection on the planets. In fact, one of the scientific objectives on the lunar surface is the detection of organic materials that have either been transported to the Moon (panspermia or space probes) or still remain as relics of an ancient biosphere. Similar objectives hold for planetary biological experiments, but, of course, the probability seems higher that living samples may be collected on the planets (Sec. 16-1). Except for reducing the weight of the Surveyor instrument, its configuration and general operating principles can be taken over directly for use by a planetary lander (see Sec. 15-3). Oyama has indicated that a gas chromatograph for use on Mars, incorporating hot-wire pyrolysis and only two columns, can probably be built for about 2.5 kg, with a power consumption of about 4 watts (Ref. 16-14). Another possibility, now being explored at Florida State University, is the use of paper chromatography to detect macromolecules directly without the necessity of destructive pyrolysis.

*Ultraviolet Spectrophotometers.* Besides identifying macromolecules by the masses and sorptive properties of their pyrolysis products, one can study their absorption spectra for clues. The different wavelengths of light absorbed by a liquid containing macromolecules indicate chemical-bond resonances. More specifically, proteins are observed to absorb strongly in the region of 1950A, in the ultraviolet. Photons with this particular wavelength are absorbed by the peptide bond that links amino acids together to form the polypeptides, a chemical class which includes the proteins. The more peptide bonds in a macromolecule, the stronger the absorption at the 1950A band, and the larger the polypeptide macromolecules.

A one-channel photometer, Fig. 16-2, at 1950A, seems rather simple after the multichannel photometers described for atmospheric work (Sec. 14-2). The problem is complicated, though, by the fact that other chemicals, not so closely associated with life, also absorb strongly in the

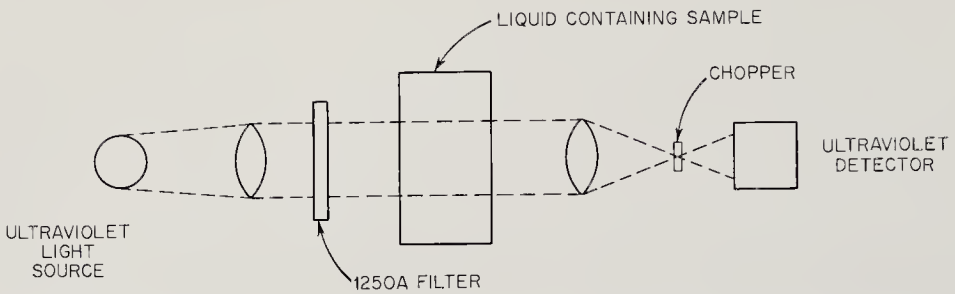


Fig. 16-2. Operating principle for a one-channel ultraviolet spectrophotometer that might be used in detecting peptide bonds and, by inference, proteins.

neighborhood of 1950Å. Any instrument built based on peptide-bond absorption will have to distinguish between the different possibilities. One scheme that has been advanced involves the hydrolysis of the sample after an initial set of measurements. Hydrolysis will then break any peptide bonds present and greatly reduce the absorption at 1950Å when a second set of measurements is made. Other chemicals absorbing at these wavelengths would probably not be affected by hydrolysis. No

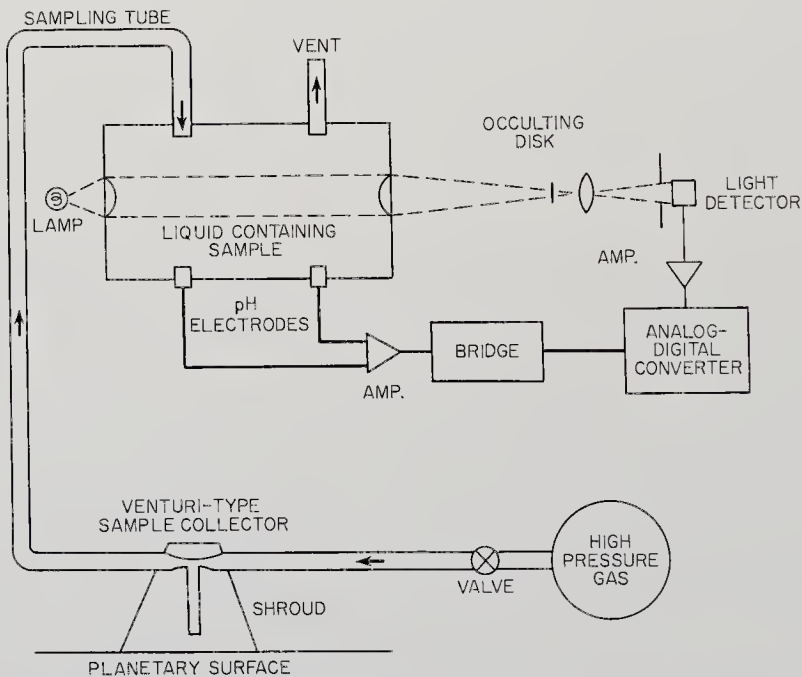


Fig. 16-3. Schematic drawing of the Wolf Trap. Dust is sucked up from planetary surface and blown into culture chamber. Changes in light transmission measure turbidity as a function of time. Electrodes measure pH. Occulting disk provides A.C. signal for amplifier. (Adapted from U. of Rochester drawing)

marked change in the spectrum would be observed in the absence of polypeptides.

An ultraviolet spectrophotometer for probe use is being studied by Melpar, Inc. (Ref. 16-1).

*Turbidity and pH Experiments.* When organisms grow in a fluid culture medium, the fluid usually becomes more turbid (cloudy), a photo-metrically measurable phenomenon. The acidity of the fluid medium almost always increases, too. The latter change is easily measurable with standard electrochemical techniques. Together the two phenomena form the basis for the Wolf trap, a life-detection instrument named after its proponent and designer, Wolf Vishniac, now at the University of Rochester (Refs. 16-23 and 16-24).

In actuality, of course, the Wolf Trap, like most instruments described in this chapter, does not really detect life, but rather signals changes in turbidity and pH. A fine, but sterile sample of Martian dust, for example, might keep the fluid medium turbid for days. If the dust happened to be acid, too, misinterpretations might easily occur. This objection can

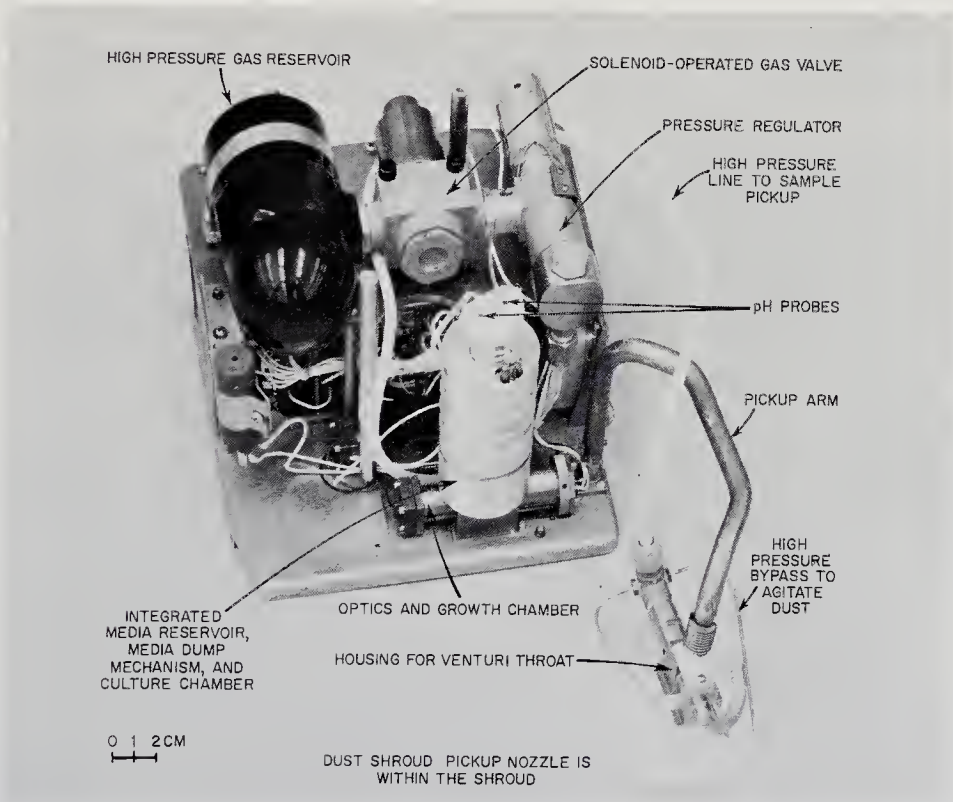


Fig. 16-4. A recent breadboard model of the Wolf Trap. The culture chamber itself is dwarfed by the sample collector and other auxiliaries, a common situation in space research. (Courtesy of the U. of Rochester)

be met by observing the time history of the fluid turbidity and pH. If the surface sample is truly sterile, turbidity should decrease eventually. If life forms exist which can multiply in the culture medium, an increase in turbidity should be noted, perhaps after an initial decrease, as the dust settles out. An experimental check and balance can be introduced through the addition of a culture chamber that receives no sample. Comparison of measurements from the two chambers can be used to check sensor and electronics operation.

The complete Wolf Trap consists of the sample collector and perhaps 10 to 20 culture chambers. This multiexperiment approach is similar to that used in the Multivators and Minivators covered in the next section. The turbidity and pH sensors and culture chambers can be made very simple and compact, as shown in Figs. 16-3, 16-4, and 16-5. A lamp-photo cell combination monitors the turbidity as a function of time, while two electrodes measure the pH. The Venturi-type sample collector shown in the same diagram is an interesting variation of the aspirator mentioned in Sec. 14-1. Though the instrument is still in the research stage, the culture chambers and their detectors have been made very small and lightweight.

*Stain Experiments.* Proteins and other macromolecules associated with terrestrial life characteristically absorb many kinds of dyes. This behav-

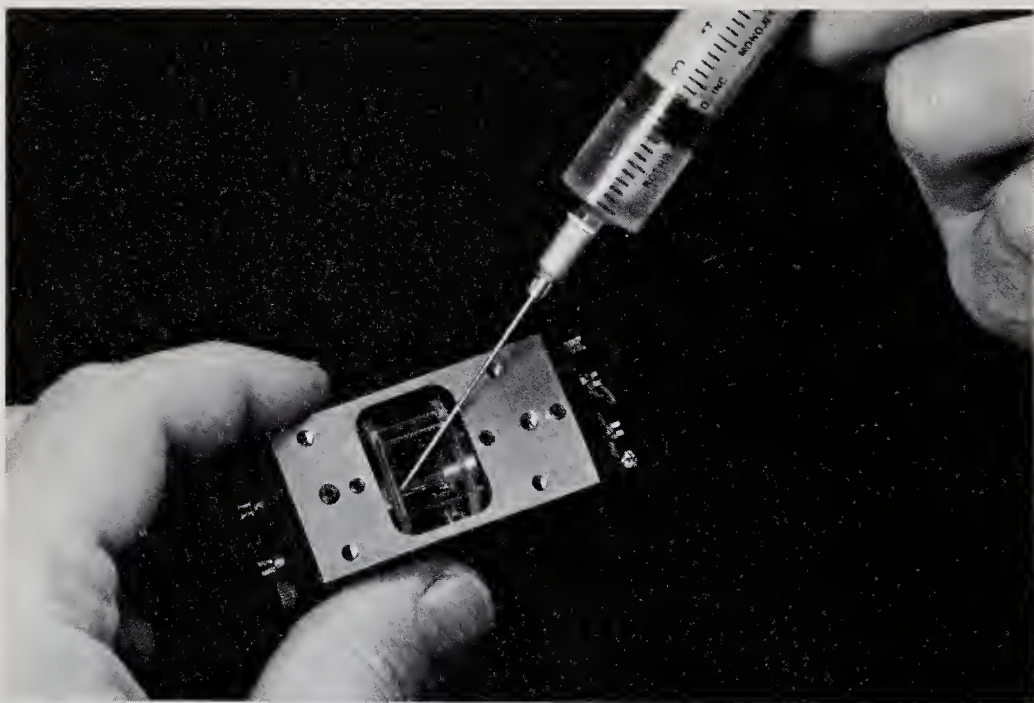


Fig. 16-5. Wolf Trap culture chamber. Note small size. (Courtesy of the U. of Rochester)



ior is the basis for the cell-staining techniques employed in the biological laboratory. Although some (supposedly) non-life substances, viz., the organized elements found in meteorites, also take up these dyes, staining is so closely associated with life that it forms the foundation for another kind of life-detection instrument, the so-called J-band detector.

When proteins, polynucleic acids, polysaccharides, and other macromolecules absorb dyes like dibenzo-thiocarbocyanine, the new bonds that are formed create strong absorption bands between 4500A and 6500A, in the visible portion of the spectrum. Molecular absorption bands in the visible are not very common, and the formation of J bands seems to offer a clearcut indication of the presence of macromolecules—at least terrestrial macromolecules.

The translation of the J-band concept into hardware is particularly simple. A light source in the visible, a sample chamber, an interference filter, a chopper, and photocell are all that are needed. The experimental schematic is, in fact, similar to that of the ultraviolet spectrophotometer, Fig. 16-2, except for the wavelengths employed.

*Optical-Rotary-Dispersion Experiments.* One of the strangest properties of terrestrial life is its apparently exclusive production of optically active substances; that is, substances which rotate the plane of polarized light. Sugars and other life-associated compounds which are optically active can be made in both dextro- and levo- forms. If a mixture of dextro- and levo-nutrients is carefully prepared so that the optical activities cancel one another out, extraterrestrial microorganisms eating the nutrients would be expected to disturb this balance. That extraterrestrial life would possess asymmetries in its chemical processes is expected philosophically but is not known for certain. All life-detection equipment extrapolates terrestrial biology to the other planets, and the same assumption applies to this class of instruments.

More specifically, the proteins and nucleic acids, which are closely associated with terrestrial life and possess little optical activity by themselves, can be made strongly optically active in the neighborhood of their ultraviolet absorption bands by the addition of sugar and other optically active molecules to the macromolecules.

Again the resulting instrument bears a strong resemblance to the ultraviolet spectrophotometer. The major difference is the insertion of polarizers and analyzers into the optical system. By measuring the amount and direction of optical rotation experienced by the polarized light as it passes through a solution containing the optically activated sample, scientists can deduce whether macromolecules are present in the sample. Space instruments using optical rotary dispersion are being studied at Melpar, Inc.

*Microscopes.* More convincing than any telemetry signal from abstract physical and chemical experiments would be a picture of an undeniably living organism. The vidicon cameras described earlier could provide such pictures if life forms happen to be large enough singly or in aggregate to be identified from the lander with telescopic attachments. The greatest number of terrestrial life forms, however, are microscopic. Primitive life, in particular, is likely to be too small to be seen with the naked eye or with vidicon telescopes. A space adaptation of the laboratory microscope therefore seems to have merit as a life-detection tool.

Just what will a microscope tell us? It cannot detect easily the three major features of life: metabolism, reproduction, and mutation. However, by focusing a microscope on dust and aerosols brought in by a sample collector, one could hope to determine particle form, size, symmetry, color, optical properties, and reaction to various biological staining techniques. Interpretation will admittedly be difficult. Again, the controversy over organized elements found in meteorites serves as a good example of the kind of disagreement that can develop over the analysis of visual images, even with staining.

One of the problems encountered with the petrographic microscope, Sec. 15-3, was the preparation of the sample. The same problem crops up here. An extraterrestrial microtome would be well beyond the state of the art. Furthermore, we don't know anything about the specimens. If life is as prevalent on the target planet as it is on Earth, every cubic centimeter of atmosphere and every bit of dust blown up from the surface will contain microorganisms. The first and simplest collection scheme is just the exposure of a sticky plate to aerosols and dust that may be naturally settling to the surface—the lander itself may stir up clouds of such material. The plates, after varying exposures, are moved into the focal plane of the microscope, and the images of the collected aerosols and dust particles transmitted back to Earth via a vidicon camera. A more forceful approach involves blowing the atmosphere into the microscope proper, Fig. 16-6, and onto a sticky, aerosol impaction plate. Dust stirred up from the surface could also be carried into the plate by this means. Studies show that pneumatic sample collection is probably simpler and more reliable than any scraping or pulverizing scheme (Ref. 16-6). Since the aerosols and dust particles seem very likely to be carriers of life, most life samplers have taken this road.

The Jet Propulsion Laboratory and Stanford University have been studying a simple, fixed-focus microscope for space use. One version of the abbreviated, phase-contrast microscope that has evolved from the program is drawn in cross section in Fig. 16-6. The vidicon and sampler are not shown. In fact, both might be shared with other instruments.



Fig. 16-6. An aerosol impact microscope. Dust and aerosol samples are blown into the microscope through the tube connection. Sticky plate at focal plane is illuminated by lamp at far left. TV camera at right would view the magnified image. (Courtesy of the Jet Propulsion Laboratory)

Preliminary specifications for the JPL-Stanford instrument include a  $100\mu$  field with a resolution of  $0.5 \mu$ . Eight brightness levels have been selected for each spot in the 400-line picture raster. As in the case of the other imaging devices described in Sec. 15-3, very large quantities of information must be transmitted for each picture, about 500,000 bits in this case. Exclusive of the vidicon and sampler, the abbreviated microscope can probably be built at about 2 kg, a small mass penalty for the scientific value that might be returned.

Advanced microscope programs involve some obvious sophistications: automatic focusing and magnification control; sample staining; the use of ultraviolet light to observe the spectral absorption of macromolecules in the 2600 to 2800A region (ultraviolet microspectrophotometry), and the use of photographic film to improve the resolution.

#### 16-4. Biological Experiments

The metabolism experiments are so distinct that, although they also involve sample collection and experimentation with samples, they are treated in a separate section. Metabolism—the energy-exchange process whereby organisms take food from their environments, process it, extract energy, and eliminate the residue—is one of the three defining attributes of life (Sec. 16-1). A successful, positive metabolism experiment would be much more convincing than data from an instrument measuring secondary, one-step-removed parameters. The two instruments introduced here, Gulliver and the Multivator, strike at the heart of the life-detection problem. Each has several years of study and research behind it, and, in comparison with most other instruments covered in this chapter, each is well into the prototype stage.

*Metabolism Detectors, "Gulliver."* If metabolism is a universal char-

acteristic of life, instruments that can detect this property will be valuable additions to the space scientist's arsenal. The attributes of metabolism that might be detected are the consumption of food, the evolution of wastes, and the production of heat. Growth is sometimes associated with metabolism, but by no means is it an essential feature. The metabolism detector discussed below is sensitive to the evolution of radioactive carbon dioxide or other gaseous wastes from metabolizing organisms that consume a radioactively tagged culture medium. There are obvious objections to such an approach:

1. The sample organisms may not metabolize the culture sent along on the space probe.
2. They may not evolve gases.
3. There may be enough radioactivity on the planetary surface to mask any life effects, though anticoincidence counting and energy discrimination could reduce the effects of this interference.

In all life detection, the search is first for Earth-like organisms; therefore, items 1 and 2 are temporarily set aside. If the probe lands on an inner planet, item 3 is unlikely to be significant.

Many types of metabolism experiments can be visualized, but the  $C^{14}$  tracer experiment being developed by Hazelton Laboratories, Inc., is typical and by far the most advanced in terms of hardware (Refs. 16-7, 16-10, and 16-11). The instrument is named Gulliver after Swift's character who discovered many unusual forms of life in distant lands.

Three steps make up the Gulliver cycle. In essence, they are: collect

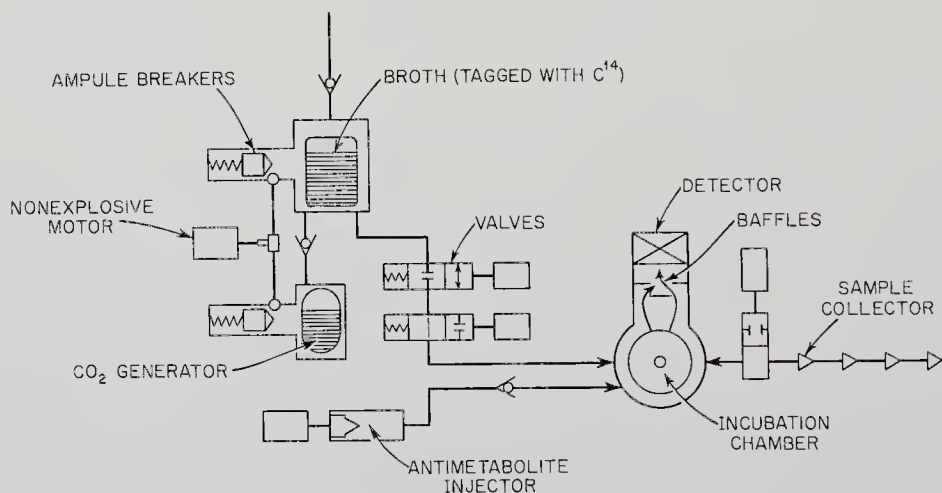


Fig. 16-7. Schematic for the Gulliver metabolism detector. Later versions incorporate a separate control chamber inoculated with an antimetabolite. (Ref. 16-10)

a sample, feed it radioactively tagged food, and detect any tagged gaseous waste products. Gulliver, whose design is tailored to a Mars mission, accomplishes these steps in the following ways:

1. Two 8-m lines are fired from the instrument (prototype shown in Fig. 16-8) attached to "bullets." The lines are coated with silicone grease, or some other substance that will remain sticky at Martian surface temperatures. Dust and other material adhere to the lines as they are retrieved by a motor. The sample-laden strings are deposited in a reaction chamber, which is then sealed off from the outside environment (see Fig. 16-7).
2. An ampule containing a culture medium tagged with  $C^{14}$  or other radioisotopes\* and which is designed to support the metabolism of a wide spectrum of terrestrial organisms (Table 16-2) is broken by

TABLE 16-2. A BASIC TEST MEDIUM USED FOR GULLIVER

<i>Component</i>	<i>Amount</i>
$K_2HPO_4$	1.0 g
$KNO_3$	0.5 g
$MgSO_4 \cdot 7H_2O$	0.2 g
NaCl	0.1 g

a dimple motor and forced into the reaction chamber by pressurized  $CO_2$  gas. If Earth-like metabolism takes place,  $C^{14}O_2$  and other gases will evolve. As the gases contact a thin getter layer covering the window of a Geiger-Mueller counter, they become fixed and available for counting.

3. The beta particles emitted by  $C^{14}$  (half life = 5600 yr), for example, are detected by the Geiger-Mueller counter (described in Sec. 13-3).

Note that the Geiger-Mueller tube is shielded by a baffle from the betas emitted by the culture. The data are then telemetered to earth for analysis.

A number of  $C^{14}$ - and  $S^{35}$ -labeled compounds have been investigated, including sodium formate, glucose, sodium acetate, cysteine, sodium thio-sulfate, yeast, and *Escherichia-coli* extracts. Obviously, the culture employed should sustain a great variety of organisms. The culture medium developed by Hazelton Laboratories, Inc. (described in Table 16-2), has been shown to support a great variety of terrestrial microorganisms. Both levo and dextro forms of the key culture molecules will be included in case Martian microorganisms prefer the mirror images.

\*  $S^{35}$  and  $H^3$  are also being considered.

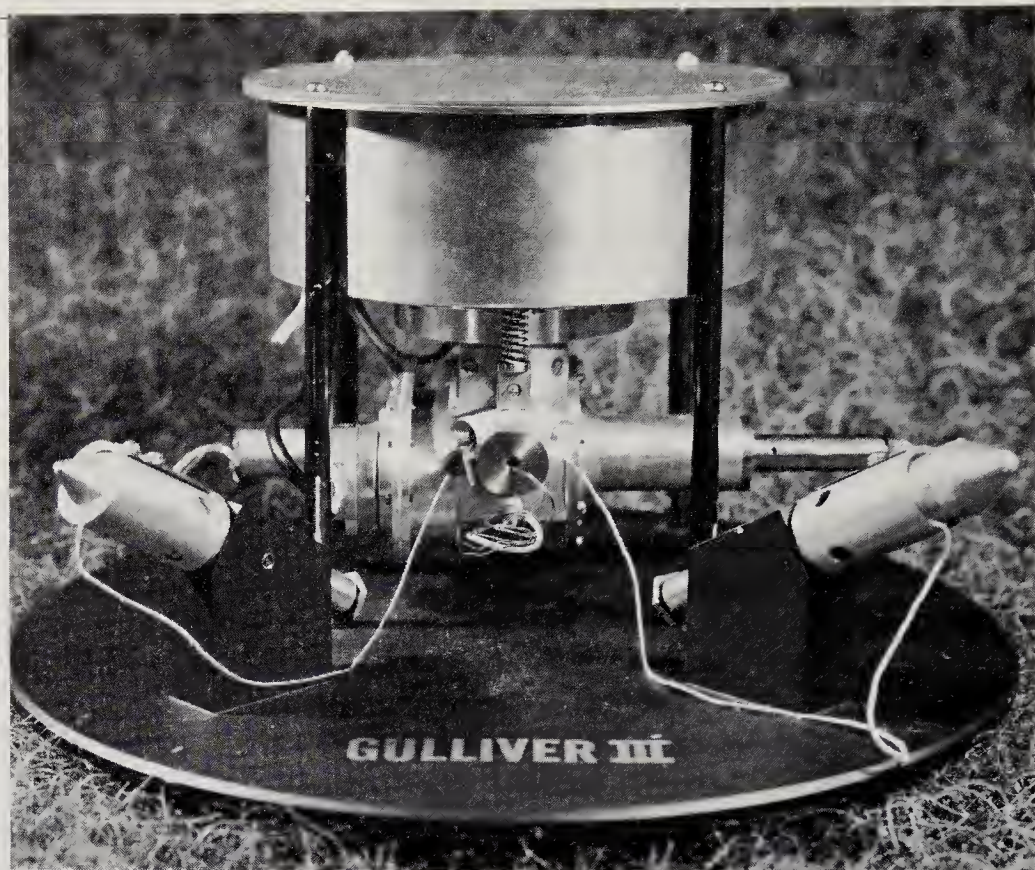


Fig. 16-8. Gulliver, Model Mark III. This model shoots out two 8-meter sticky strings, which are then retrieved by a motor. The strings and adhering dust are deposited in a reaction chamber. (Courtesy of Hazelton Laboratories)

The complete Gulliver instrument (see Fig. 16-8 and also Fig. 16-9) has a mass of less than a kilogram, including a duplicate reaction chamber inoculated with an antimetabolite that serves as a control. Less than a watt is required for the incubation and measurement period, while about two watts are needed for the three-minute sample collection period.

Tests with Gulliver prototypes have proven very successful in many locations around the United States, including deserts, mountain tops, and deciduous forests. The curve illustrated in Fig. 16-10 (taken in a Washington, D.C., park) is representative. The double, possibly triple, hump may be interpreted as showing the existence of two or three different organisms with different generation times. Metabolism in the absence of reproduction and growth in a sample would be indicated by a curve that gradually acquires a constant slope. An advanced version of Gulliver will incorporate light and dark cycles to determine the presence



Fig. 16-9. Gulliver field-test unit. Units like this have successfully detected terrestrial life in a variety of locations. (Courtesy of Hazelton Laboratories)

of photosynthesizing organisms. Gulliver has generally proven itself to be a versatile, lightweight, rugged life detector.

*Multivators and Minivators.* One problem with all life detectors described so far is limited versatility. In a sense, each instrument asks one or two questions. The answer to any single question does not take science very far up or down the confidence curve (Fig. 16-1). To be sure, several different experiments can and probably will be used on each planetary lander. In some cases, as with the Wolf Trap, the basic detectors are so tiny that different culture media can be used in duplicate instruments. This stratagem will also probably be put into effect. The Multivator/Minivator, in contrast, performs many different experiments all within the same instrument, creating in effect a miniaturized, automatic biological laboratory that performs experiments using wet-chemical processes. A well-functioning Multivator thus could take the observer up or down the confidence curve rather quickly.

The original Multivator was proposed by J. Lederberg, of Stanford University. In the original design, over thirty separate experimental re-

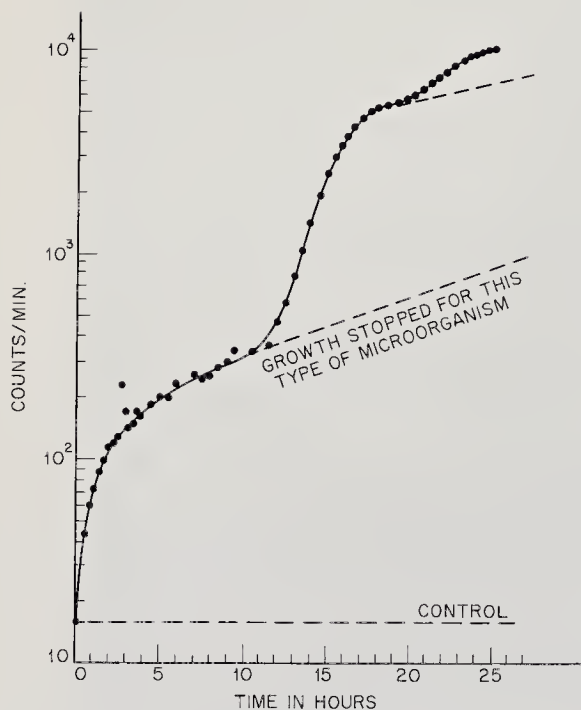


Fig. 16-10. Typical experimental curve obtained with Gulliver. Humps are caused by presence of several types of microorganisms with different growth curves.

action chambers were contemplated, giving rise to the "multi" prefix. Later, engineers at the Jet Propulsion Laboratory, concerned about complexity and weight, began studying a Multivator with less than ten reaction chambers. The prefix "mini" naturally came into use. At the present time, although designs are not firm, both Multivator and Minivator have about fifteen chambers. There are few differences between the two instruments.

The sketch of Fig. 16-11 illustrates the basic chamber idea for both Multivator and Minivator. A fine, filtered sample from the planet's crust is blown into the chamber by a sample collector. A substrate (possibly a culture medium) is already located in the chamber in dry form. Once the sample is introduced and the chamber sealed off, a solvent or some other chemical is released and the reaction begins. A

detector appropriate to the reaction is nearby, and it sends data to the data-processing and communication subsystems. Figure 16-11 shows the set-up for the phosphatase reaction described in more detail below, but many other reactions have been suggested (Ref. 16-3). A partial list follows:

1. The turbidity experiment (Sec. 16-3).
2. The pH experiment (Sec. 16-3).
3. The optical-rotary-dispersion experiment (Sec. 16-3).
4. The radioisotope-tagged metabolism experiment (Sec. 16-4).
5. Wet-chemical analysis of the sample for organic compounds.
6. Bioluminescence experiments (Table 16-1).
7. Redox-potential experiments (Table 16-1).
8. Measurement of total carbon by electrical conductivity.

The phosphatase experiment has received the most effort by the Stan-



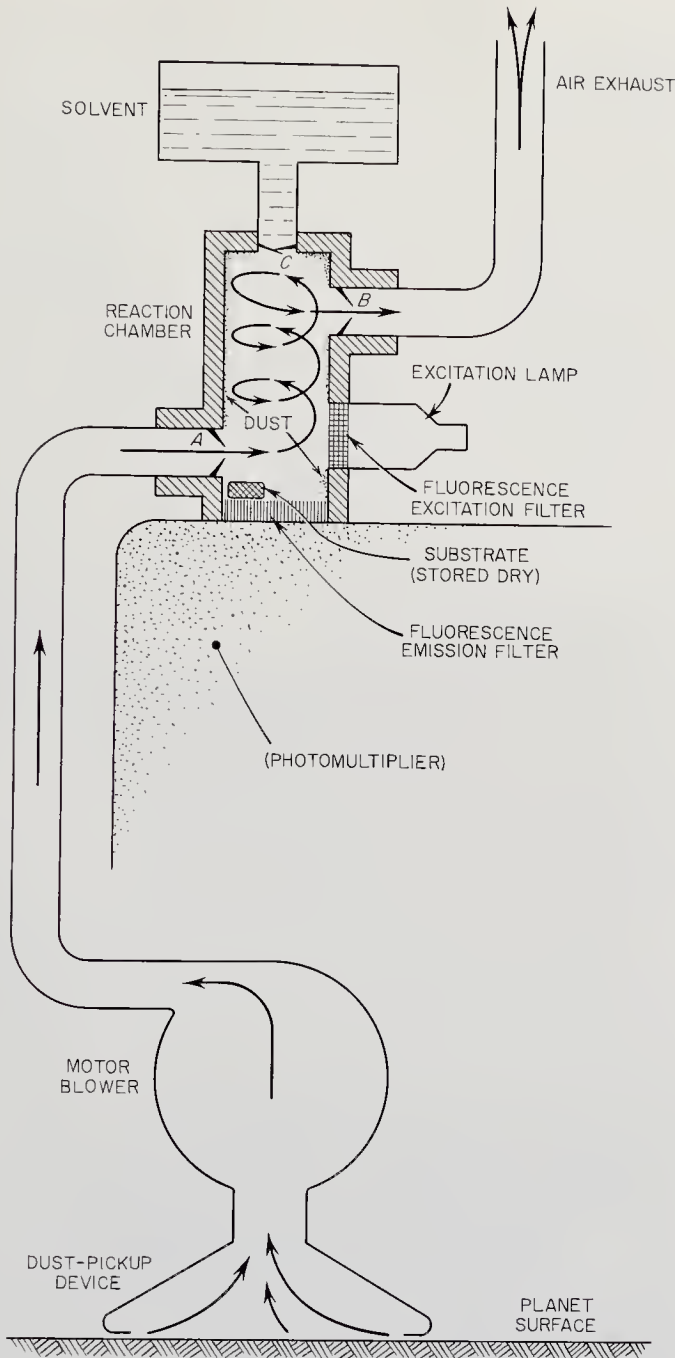
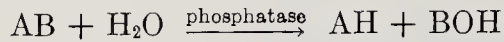


Fig. 16-11. Schematic of an experiment using phosphatase enzymes being considered for one or more of the Multivator chambers. (Ref. 16-12)

ford Multivator group. The logic underlying the experiment goes like this: The phosphatase enzymes are very common in terrestrial organisms and are also assumed to be prevalent in extraterrestrial life. Phosphatases catalyze the hydrolysis of phosphate esters with high specificity.

The product of several hydrolysis reactions can be detected with high sensitivity, using fluorescence techniques. A typical reaction would be:



where AB = a non-fluorescent phosphate ester  
AH = the fluorescent product.

The phosphatase enzymes, assumed present in the life-form sample, are essential to the hydrolysis reaction. Unfortunately, the action of phosphatase can be simulated by several other conditions, i.e., high pH and high temperature (Ref. 16-3).

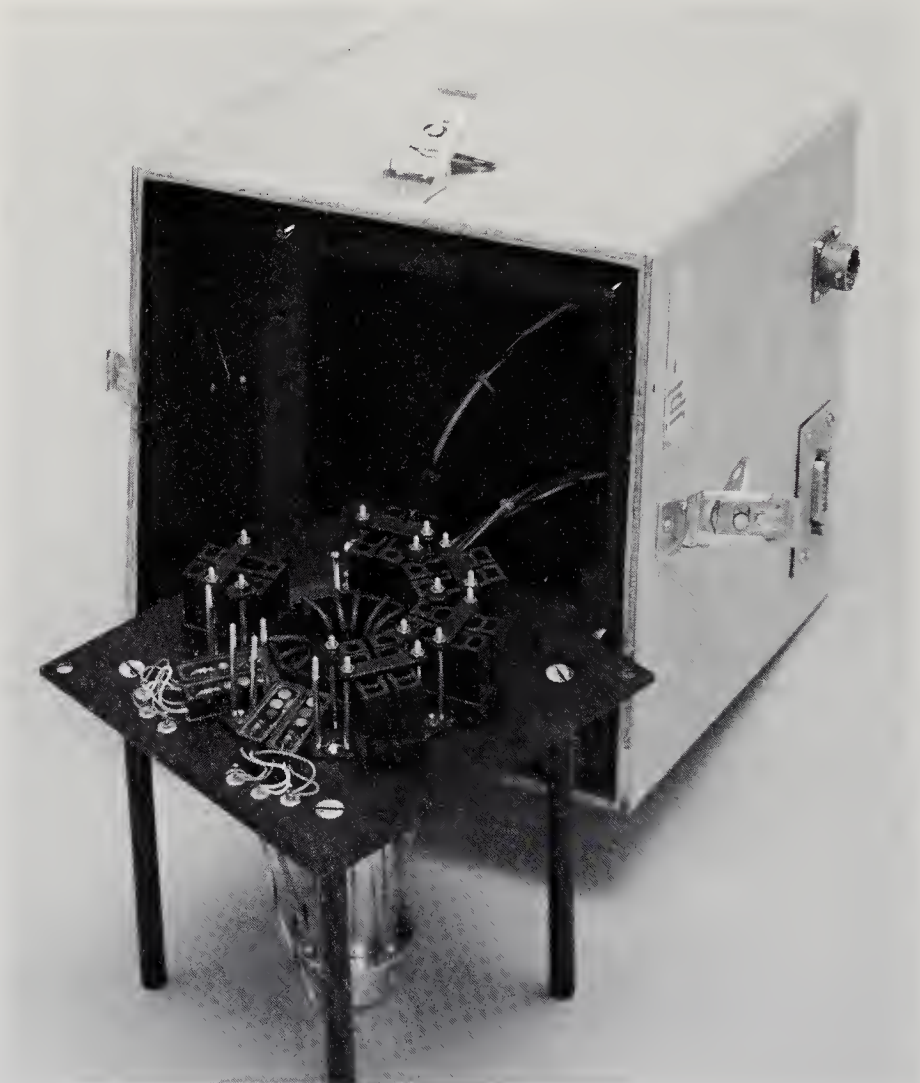


Fig. 16-12. An early breadboard model of the JPL Minivator. In the original Minivator concept, the chambers would have been tested sequentially by a moving arm. (Courtesy of the Jet Propulsion Laboratory)



Fig. 16-13. One of the Multivator prototypes. This model shows fifteen reaction chambers and a photomultiplier tube, which is used with those chambers employing light signals. Dust and aerosol samples are blown into the radial chambers. (Courtesy of Stanford University)

An early Minivator is shown in Fig. 16-12; a prototype Multivator is illustrated in Fig. 16-13. In spite of the multiple reaction chambers, the latter remains a compact instrument that can probably be built in flight configuration for about a kilogram. The Multivator and Minivator possess separate detectors for each reaction chamber and employ simultaneous sample inoculation for all active chambers. Multivator and Minivator chambers are removable and interchangeable. Both employ blank control chambers. In addition, some of the more critical experiments would be performed in duplicate to improve the over-all probability of getting answers. While the Multivator and Minivator are considerably more complex than any of the single experiments previously described, they both provide more answers about extraterrestrial life per kilogram of mass and watt of power invested.

A logical extrapolation of the multiexperiment philosophy is the Automated Biological Laboratory (ABL) being developed for post-1970 missions to Mars. The ABL would incorporate Gullivers, Multivators, Wolf Traps, and other life-detection experiments. Its mass would be between one and two metric tons and would require the Saturn-5 launch vehicle.

In closing this chapter, the primitive character of the foregoing experiments should be emphasized. Generally, they are aimed at a life-or-no-life answer. If several convincing yeses are ultimately received via the telemetry circuits, the real instrumentation task will begin: that of determining the precise character of extraterrestrial life, its impact upon biological theory, and its importance to human philosophy.

# Chapter 17

---

## INSTRUMENTS USED ON SOLAR, COMETARY, AND ASTEROIDAL PROBES

---

---

### 17-1. Prologue

Although planetary exploration and the plumbing of the interplanetary medium have the highest scientific priorities, the fascination of the Sun, the comets, and the asteroids shapes the research efforts of many scientists. The Sun is the nearest star and the energy source for the entire solar system. The comets are probably the unaltered primordial stuff from which the solar system was formed, while the asteroids, some hundreds of kilometers across, have hardly been explored at all by Earth-based instruments.

Launching space probes to these other occupants of our star system represents a more difficult feat than flying past Mars or Venus. The energy requirements are large, and timing, except for the solar probes, is critical (see Chap. 5). Furthermore, many pertinent astronomical observations can be made from the Orbiting Astronomical Observatory (OAO) class of satellites. Why fly special probes to these bodies at all?

On the pro side of the argument, several important factors can be listed:

1. Proximity permits more accurate measurements and often opens up wider ranges of phenomena. Magnetic fields, solar-plasma mapping, and cometary spectroscopy are typical of the phenomena where a closer look would be a big help.
2. An escape from the Earth's magnetic field, its halo of dust, and the radiation belts would be welcome in many experiments.
3. Orbiting observatories encounter problems with fine pointing because of the target's distance. The eclipsing of the Sun and target

object cause power losses, temperature cycling of the spacecraft equipment, and the need for frequent reacquisition of the target.

Counterbalancing these advantages are some probe problems:

1. The greater mission propulsion and guidance requirements radically reduce payload size.
2. Diminution of solar power and spacecraft cooling occurs as the Sun recedes, overheating, as the probes fall in toward the Sun.
3. Communication over interplanetary distances is far more difficult than it is from an Earth satellite.
4. Perhaps most telling is the long travel time to the target (many months and even years in some cases). A reliability engineer would calculate a much lower probability for successful data return after a six months' flight than he would for immediate satellite transmission.

In the face of these advantages and disadvantages, the road to take is fairly obvious. Assign a somewhat lower priority to solar, cometary, and asteroidal probes than that accorded the planetary probes and deep-space monitors. Meanwhile, emphasize more strongly Earth-based and satellite-based observations, which, particularly in the case of comets, represent fertile fields for additional research.

Looking next at the instruments which might form the scientific payloads of these more advanced probes, it will become apparent in the following sections and tables that these instruments are predominantly old friends, used in planetary research and the study of the interplanetary medium. This fact should not be surprising, because the asteroids are essentially small planets, and the Sun is the maker of the interplanetary weather. Only in the case of the comets, where novel ices and free radicals exist, will new kinds of instruments have to be devised.

## 17-2. Solar-Probe Research

Solar probes will undoubtedly precede cometary and asteroidal spacecraft. Indeed, *Mariner 2* was a solar probe in the sense that it carried instruments farther in toward the Sun than ever before, on its way past Venus. The advanced Pioneer probes, scheduled for about 1968, were formerly termed solar probes, even though they will only penetrate to within 0.8 A.U. of the Sun. (Now, the designation solar probe is reserved for probes passing within 0.2 A.U. of the Sun.)

Solar-probe instruments will first of all encompass all five classes of interplanetary experiments described in Chap. 13: magnetic, radiation, plasma, micrometeoroid, and cosmological. Besides mapping the fine

TABLE 17-1. POSSIBLE SOLAR-PROBE EXPERIMENTS\*

<i>Experimental Objectives</i>	<i>Possible Instruments</i>	<i>Reference Chapters</i>
Measure line profiles of the integrated monochromatic light from discrete active regions.	Filter photometers	14, 15
Measure the intensity vs. wavelength of light from discrete active regions.	Scanning spectrometers	14, 15
Obtain high-resolution profile data for lines at 1216A, 304A and 584A.	Spectrometers, filter photometers	14, 15
General mapping of magnetic field, radiation, plasma, and micrometeoroids in vicinity of Sun.	See Chapter 13	13

\* Only those experiments are included where proximity offers special advantages over Earth satellites.

TABLE 17-2. POSSIBLE COMETARY-PROBE EXPERIMENTS\*

<i>Experimental Objectives</i>	<i>Possible Instruments</i>	<i>Reference Chapters</i>
Obtain image of the nucleus to determine its size and structure.	Vidicon telescopes	15
Map magnetic field around nucleus and in tail.	Magnetometers	13
Measure surface temperature of nucleus.	Infrared spectrometers	14
Qualitative and quantitative analysis of whole comet from emission and induced fluorescence.	Spectrometers	14, 15
Measure the sizes of small, solid particles in coma and tail by their light-scattering properties; also during fly-through by direct detection.	Polarimeters, micrometeoroid detectors	13, 14
Sample tail during fly through and analyze gas and particles.	Mass spectrometers	14
Measure ionization levels and plasma densities in tail.	Radio transmission experiments, plasma probes	13, 14

\* Only those experiments are included where proximity offers special advantages.



structures and temporal variations of the fields and particle fluxes in the neighborhood of the Sun, it is desirable to obtain closer scrutiny of the Sun's surface with telescopes and spectrometers. A list of possible solar-probe experiments and their pertinent (and familiar) instruments is presented in Table 17-1.

### 17-3. Cometary-Probe Research

Comets remain objects of comparative mystery. Proposals have suggested flying by them, flying through their tails, flying alongside them in matched trajectories, and instrument landings on their nuclei. Artificial comets, launched near the Earth for better observation, have also been proposed (Ref. 17-10). Since only a ton or so of comet ices ( $\text{H}_2\text{O}$ ,  $\text{NH}_3$ ,  $\text{CO}_2$ , etc.) would be needed, this idea is not as radical as one might think. Fly-throughs of cometary tails will probably come first on the schedule, though even they are perhaps a decade away, because of high velocity requirements, low mission priority, and the normal spacecraft development time. Sampling instruments, similar to but much larger than those employed in planetary atmosphere research, would have to be developed to acquire usable amounts of the very diffuse matter making up the cometary tails. The list of desirable experiments, Table 17-2, includes some other new challenges to the instrument designer. There is also considerable equipment that has been described before. Generally, the new instruments are just in the thinking stage and cannot be described in detail.

### 17-4. Asteroidal-Probe Research

Everyone presumes that the asteroids are fragments of a former planet. The largest asteroids will have negligible atmospheres, and there is even less chance of a biosphere. Except as possible repositories of solar system history—in terms of dust deposits, radioisotopes created by cosmic-ray bombardment, and space flotsam and jetsam (panspermia?)—the asteroids seem deader than our own Moon. It would be of interest, however, to land instruments on some of the larger bodies to check out our suppositions. It would also be desirable to examine planet fragments for clues about planetary origin and evolution. The instrument payloads and experimental objectives would be similar to those of a planetary lander, except for the de-emphasis of life-detection and atmospheric instruments.

## BIBLIOGRAPHY

---

---

### 1. General References

- 1-1. Berkner, L. V. and Odishaw, H., eds.: *Science in Space*, McGraw-Hill Book Co., New York, 1961.
- 1-2. Bourke, D. G.: *Deep Space Exploration and the Probability of Success*, Jet Propulsion Laboratory, *TM 33-88*, 1962.
- 1-3. de Vaucouleurs, G.: *Reconnaissance of the Nearer Planets*, Air Force Office of Scientific Research, *AD 276 833*, 1961.
- 1-4. Eimer, M.: *The Scientific Exploration of Deep Space*, in *Proceedings of the NASA-University Conference on the Science and Technology of Space Exploration*, 1, 155, Government Printing Office, Washington, 1962.
- 1-5. Fry, B. M. and Mohrhardt, F. E., eds.: *Space Science and Technology*, John Wiley & Sons, New York, 1964.
- 1-6. Hibbs, A. R.: *Exploring the Solar System with Probes*, in *Space Science*, D. P. Le Galley, ed., John Wiley & Sons, New York, 1963.
- 1-7. Hibbs, A. R.: *The Exploration of the Moon, the Planets, and Interplanetary Space*, in *Space Age Astronomy*, A. J. Deutsch and W. B. Klemperer, eds., Academic Press, New York, 1962.
- 1-8. Hyatt, A.: *Planning for the Future Goals of NASA*, in *Proceedings of the NASA-University Conference on the Science and Technology of Space Exploration* 1, 15, Government Printing Office, Washington, 1962.
- 1-9. Kallmann Bijl, H., ed.: *Space Research*, Interscience Publishers, New York, 1960.
- 1-10. Koelle, H. H., ed.: *Handbook of Astronautical Engineering*, McGraw-Hill Book Co., New York, 1961.
- 1-11. Le Galley, D. P., ed.: *Space Science*, John Wiley & Sons, New York, 1963.
- 1-12. Le Galley, D. P. and Rosen, A., eds.: *Space Physics*, John Wiley & Sons, New York, 1964.
- 1-13. Muller, P., ed.: *Space Research IV*, Interscience Publishers, New York, 1964.
- 1-14. Newell, H. E.: *What We Have Learned and Hope to Learn from Space Exploration*, in *Proceedings of the NASA-University Conference on the Science and Technology of Space Exploration*, 1, 59, Government Printing Office, Washington, 1962.
- 1-15. Ordway, F. I., Gardner, J. P., and Sharpe, M. R.: *Basic Astronautics*, Prentice-Hall, Inc., Englewood Cliffs, 1962.

- 1-16. Ordway, F. I. *et al*: *Applied Astronautics, An Introduction to Space Flight*, Prentice-Hall, Inc., Englewood Cliffs, 1963.
- 1-17. Priester, W.: *Space Research III*, Interscience Publishers, New York, 1963.
- 1-18. Riley, F. E. and Sailor, J. D.: *Space Systems Engineering*, McGraw-Hill Book Co., New York, 1962.
- 1-19. Seifert, H. S., ed.: *Space Technology*, John Wiley & Sons, New York, 1959.
- 1-20. Starkey, D. G.: The Space Vehicle—Manned Versus Unmanned, *Aerospace Eng.*, **21**, 88, Sept. 1962.
- 1-21. U.S. Government: *The Next Ten Years in Space, 1959-1969*, Government Printing Office, Washington, 1959.
- 1-22. U.S. Government: *A Review of Space Research*, National Academy of Science, *NAS/NRC 1079*, 1962.
- 1-23. U.S. Government, Hearings before the Committee on Science and Astronautics: *1965 NASA Authorization*, Parts I through V, Government Printing Office, Washington, 1964. (See also previous years' hearings.)
- 1-24. van de Hulst, H. C., de Jager, C., and Moore, A. F.: *Space Research II*, Interscience Publishers, New York, 1961.
- 1-25. Wolff, E. A.: *Spacecraft Technology*, Spartan Books, Washington, 1962.

## 2. History of Interplanetary Inquiry and Exploration

- 2-1. Adams, C. C.: *Space Flight*, McGraw-Hill Book Co., New York, 1958.
- 2-2. Burgess, E. and Cross, C. A.: The Martian Probe, *J. Brit. Interplanetary Soc.*, **12**, 72, 1953.
- 2-3. Burgess, E.: High Altitude Research, *J. Brit. Interplanetary Soc.*, **15**, 261, 1956.
- 2-4. Clarke, A. C.: Stationary Orbits, *J. Brit. Astron. Assoc.*, **57**, 232, 1947.
- 2-5. Clarke, A. C.: Electronics and Space-Flight, *J. Brit. Interplanetary Soc.*, **7**, 49, March 1948.
- 2-6. Cleator, P. E.: *Rockets through Space: The Dawn of Inter-Planetary Travel*, Simon and Schuster, New York, 1936.
- 2-7. Clynes, M. E. and Kline, N. S.: Cyborgs and Space, *Astronautics*, **5**, 26, Sept. 1960.
- 2-8. Cross, C. A.: The Use of Probe Rockets, *J. Brit. Interplanetary Soc.*, **16**, 148, 1957.
- 2-9. Debus, K. H.: The Evolution of Launch Concepts and Space Flight Operations, in *Astronautical Engineering and Science*, E. Stuhlinger *et al.*, eds., McGraw-Hill Book Co., New York, 1963.
- 2-10. Ehricke, K. A.: *Space Flight, 1. Environment and Celestial Mechanics*, D. Van Nostrand Co., Princeton, 1960.
- 2-11. Esnault-Pelterie, R.: *L'Astronautique*, A. Lahure, Paris, 1930.
- 2-12. Farrior, J. S.: Inertial Guidance, Its Evolution and Future Potential, in *Astronautical Engineering and Science*, E. Stuhlinger *et al.*, eds., McGraw-Hill Book Co., New York, 1963.
- 2-13. Franklin Institute: *Ten Steps into Space*, Monograph 6, Philadelphia, 1958.
- 2-14. Gatland, K. W., Kunesch, A. M., and Dixon, A. E.: Minimum Satellite Vehicles, *J. Brit. Interplanetary Soc.*, **10**, 287, Nov. 1951.
- 2-15. Goddard, R. H.: A Method of Reaching Extreme Altitudes, in *Smithsonian Miscellaneous Collections, LXXI, no. 2*, Smithsonian Institution, Washington, 1919.

- 2-16. Haley, A. G.: *Rocketry and Space Exploration*, D. Van Nostrand Co., Princeton, 1958.
- 2-17. Herrick, S.: Space Rocket Trajectories, *J. Brit. Interplanetary Soc.*, **9**, 235, Sept. 1950.
- 2-18. Hohmann, W.: *The Attainability of Celestial Bodies*, R. Oldenburg, Munich, 1926.
- 2-19. Koelle, D. E.: Milestones of Astronautical History, in *Handbook of Astronautical Engineering*, H. H. Koelle, ed., McGraw-Hill Book Co., New York, 1961.
- 2-20. Kooy, J. M. J. and Uytendogaart, J. W. H.: *Ballistics of the Future*, McGraw-Hill Book Co., New York, 1946.
- 2-21. Lasswitz, K.: *Of Two Planets*, Leipzig, 1897.
- 2-22. Lawden, D. F.: Fundamentals of Space Navigation, *J. Brit. Interplanetary Soc.*, **13**, 87, March 1954.
- 2-23. Ley, W.: *Rockets, Missiles, and Space Travel*, The Viking Press, New York, 1958.
- 2-24. MacGowan, R. A.: On the Possibilities of the Existence of Extraterrestrial Intelligence, in *Advances in Space Science and Technology*, **4**, F. I. Ordway, ed., Academic Press, New York, 1962.
- 2-25. Maxwell, W. R.: Some Aspects of the Origins and Early Development of Astronautics, *J. Brit. Interplanetary Soc.*, **18**, 415, 1962.
- 2-26. Oberth, H.: *Rocket to Outer Space*, R. Oldenbourg-Verlag, Munich, 1923. Revised and reissued in 1929.
- 2-27. Ordway, F. I.: A Chronology of Space Carrier Vehicle Launchings, 1957 through 1962, in *Astronautical Engineering and Science*, E. Stuhlinger et al., eds., McGraw-Hill Book Co., New York, 1963.
- 2-28. Preston-Thomas, H.: Generalized Interplanetary Orbits, *J. Brit. Interplanetary Soc.*, **11**, 76, March 1952.
- 2-29. Roberson, R. E.: Attitude Control of a Satellite Vehicle—An Outline of the Problem, in *Proceedings of the VIIIth International Astronautical Congress*, F. Hecht, ed., Springer-Verlag, Vienna, 1958.
- 2-30. Schuler, M.: The Disturbance of Pendulum and Gyroscopic Apparatus by the Acceleration of the Vehicle, *Phys. Zeits.*, **24**, 344, 1923.
- 2-31. Shannon, C. E. and McCarthy, J., eds.: *Automata Studies*, Princeton University Press, Princeton, 1956.
- 2-32. Singer, S. F.: Interplanetary Ballistic Missiles—A New Astrophysical Research Tool, in *Proceedings of the VIIIth. International Astronautical Congress*, F. Hecht, ed., Springer-Verlag, Vienna, 1958.
- 2-33. Spitzer, L.: Interplanetary Travel between Satellite Orbits., *J. Brit. Interplanetary Soc.*, **10**, 249, Nov. 1951.
- 2-34. Tsien, H. S.: Take-off from Satellite Orbit, *J. Amer. Rocket Soc.*, **23**, 233, July 1953.
- 2-35. Von Pirquet, G.: Space Travel, *Die Rakete*, **2**, 117, Aug. 1928.
- 2-36. Wiener, N.: *Cybernetics*, John Wiley & Sons, New York, 1948.
- 2-37. Ziolkovsky, K. E.: *Exploration of Planetary Space with Reactive Equipment*, Nauchnoye Obozrenie, 1903.

### 3. The Status of Interplanetary Exploration

- 3-1. Berman, A. I.: Observatories in Space, *Scientific American*, **209**, 29, August 1963.

- 3-2. Blanco, V. M. and McCuskey, S. W.: *Basic Physics of the Solar System*, Addison-Wesley Publishing Co., Reading, Mass. 1961.
- 3-3. Briggs, M. H.: Venus: A Summary of Present Knowledge, *J. Brit. Interplanetary Soc.*, **19**, 45, 1963.
- 3-4. Cahill, L. J.: The Geomagnetic Field, in *Space Physics*, D. P. Le Galley and A. Rosen, eds., John Wiley & Sons, New York, 1964.
- 3-5. Dauvillier, A.: *Cosmic Dust*, Philosophical Library, New York, 1964.
- 3-6. Davis, L.: Theoretical and Experimental Aspects of Cosmic Rays, in *Space Science*, D. P. Le Galley, ed., John Wiley & Sons, New York, 1963.
- 3-7. Dicke, R. H.: The Nature of Gravitation, in *Science in Space*, L. V. Berkner and H. Odishaw, eds., McGraw-Hill Book Co., New York, 1961.
- 3-8. Dubin, M.: Meteoroid Effects on Space Exploration, *NASA TN D-1839*, 1963.
- 3-9. Eshleman, V. R.: Radio Exploration of the Solar System, in *Space Science*, D. P. Le Galley, ed., John Wiley & Sons, New York, 1963.
- 3-10. Friedman, H.: Solar Radiation, *Astronautics*, **7**, 14, Aug. 1962.
- 3-11. Friedman, H.: X-Ray Astronomy, *Scientific American*, **210**, 36, June 1964.
- 3-12. Gold, T.: Cosmic Rays and the Interplanetary Medium, *Astronautics*, **7**, 43, Aug. 1962.
- 3-13. Goldberg, L. and Dyer, E. R.: The Sun., in *Science in Space*, L. V. Berkner and H. Odishaw, eds., McGraw-Hill Book Co., New York, 1961.
- 3-14. Goldberg, L.: The Physics of the Sun—Its Nature, Structure, and Emission Properties, in *Space Science*, D. P. Le Galley, ed., John Wiley & Sons, New York, 1963.
- 3-15. Hamermesh, B.: Micrometeoroids, in *Space Physics*, D. P. Le Galley and A. Rosen, eds., John Wiley & Sons, New York, 1964.
- 3-16. Hess, S. L.: Mars as an Astronautical Objective, in *Advances in Space Science and Technology*, **3**, F. I. Ordway, ed., Academic Press, New York, 1961.
- 3-17. Hines, C. O.: The Magnetopause: A New Frontier in Space, *Science*, **141**, 130, July 12, 1963.
- 3-18. Jastrow, J.: *The Exploration of Space*, The Macmillan Co., New York, 1960.
- 3-19. Johnson, F. S.: Physics of the Atmosphere and Space, *Astronautics*, **7**, 72, Nov. 1962.
- 3-20. Kellogg, W. W.: Mars, *International Science and Technology*, no. 26, 40, Feb. 1964.
- 3-21. Kellogg, W. W. and Sagan, C.: The Atmospheres of Mars and Venus, National Academy of Sciences, *NRC-944*, Washington, 1961.
- 3-22. Kern, J. W. and Vestine, E. H.: Magnetic Fields of the Earth and Planets, *Space Science Rev.*, **2**, 136, 1963.
- 3-23. Kupperian, J. E. and Zeimer, R. R.: Satellite Astronomy, *International Science and Technology*, **48**, 1962.
- 3-24. Lederberg, J.: Exobiology: Experimental Approaches to Life beyond the Earth, *Science*, **132**, 393, 1960.
- 3-25. Ludwig, G. H.: Particles and Fields Research in Space, in *Proceedings of the NASA-University Conference on the Science and Technology of Space Exploration*, **1**, 129, Government Printing Office, Washington, 1962.
- 3-26. Manring, E.: Interplanetary Matter, in *Advances in Space Science and Technology*, **3**, F. I. Ordway, ed., Academic Press, New York, 1961.

- 3-27. Mayer, C. H.: The Temperatures of the Planets, *Scientific American*, **204**, 58, May 1961.
- 3-28. McDonald, F. B., ed.: Solar Proton Manual, *NASA TR R-169*, 1963.
- 3-29. McGuire, J. B., Spangler, E. R., and Wong, L.: The Size of the Solar System: *Scientific American*, **204**, 64, April 1961.
- 3-30. Middlehurst, B. M. and Kuiper, G. P.: *The Moons, Meteorites, and Comets*, University of Chicago Press, Chicago, 1963.
- 3-31. Moore, P.: *The Planets*, W. W. Norton & Co., New York, 1962.
- 3-32. Moore, P. and Greenwood, S. W.: Venus as an Astronautical Objective, in *Advances in Space Science and Technology*, **3**, F. I. Ordway, ed., Academic Press, New York, 1961.
- 3-33. Newburn, R. L.: The Exploration of Mercury, the Asteroids, the Major Planets and Their Satellite Systems, and Pluto, in *Advances in Space Science and Technology*, **3**, F. I. Ordway, ed., Academic Press, New York, 1961.
- 3-34. Newburn, R. L.: Planetary Astrophysics and the Exploration of the Solar System, in *Proceedings of the NASA-University Conference on the Science and Technology of Space Exploration*, **1**, 197, Government Printing Office, Washington, 1962.
- 3-35. Opik, E. J.: Atmosphere and Surface Properties of Mars and Venus, in *Progress in the Astronautical Sciences*, **1**, S. F. Singer, ed., Interscience Publishers, New York, 1962.
- 3-36. Parker, E. N.: The Interplanetary Gas and Magnetic Fields, in *Science in Space*, L. V. Berkner and H. Odishaw, eds., McGraw-Hill Book Co., New York, 1961.
- 3-37. Parker, E. N.: *Interplanetary Dynamical Processes*, Interscience Publishers, New York, 1963.
- 3-38. Parker, E. N.: The Solar Wind, *Scientific American*, **210**, 66, 1964.
- 3-39. Rasool, S. I. and Jastrow, R.: The Atmospheres of Mars, Venus, and Jupiter, *NASA TN D-2303*, 1964.
- 3-40. Rosen, A. and Vogl, J. L.: Cosmic Rays in Space, in *Space Physics*, D. P. Le Galley and A. Rosen, eds., John Wiley & Sons, New York, 1964.
- 3-41. Sagan, C.: Venus, *International Science and Technology*, no. 13, 86, March 1963.
- 3-42. Sagan, C.: The Physical Environment of Venus: Models and Prospects, in *Space Age Astronomy*, A. J. Deutsch and W. B. Klemperer, eds., Academic Press, New York, 1962.
- 3-43. Simpson, J. A.: Physics of Fields and Energetic Particles in Space, in *Science in Space*, L. V. Berkner and H. Odishaw, eds., McGraw-Hill Book Co., New York, 1961.
- 3-44. Smith, E. J.: Interplanetary Magnetic Fields, in *Space Physics*, D. P. Le Galley and A. Rosen, eds., John Wiley & Sons, New York, 1964.
- 3-45. Snyder, C. *et al.*: Interplanetary Space Physics, in *Proceedings of the NASA-University Conference on the Science and Technology of Space Exploration*, **1**, 163, Government Printing Office, Washington, 1962.
- 3-46. Sonett, C. P.: Magnetic Fields in Space, *Astronautics*, **7**, 34, Aug. 1962.
- 3-47. Sonett, C. P.: Rocket Experiments in Cosmic Magnetism and Their Significance, in *Space Science*, D. P. Le Galley, ed., John Wiley & Sons, New York, 1963.
- 3-48. Tilson, S.: Planet Mars, *Space/Aeronautics*, **42**, 46, July 1964.

- 3-49. Urey, H. C.: The Planets, in *Science in Space*, L. V. Berkner and H. Odishaw, eds., McGraw-Hill Book Co., New York, 1961.
- 3-50. Valley, S. L., ed.: *Space and Planetary Environments*, AFCRL-62-270, 1962.
- 3-51. Victor, W. K.: Radar Astronomy, in *Proceedings of the NASA-University Conference on the Science and Technology of Space Exploration*, 1, Government Printing Office, Washington, 1962.
- 3-52. Winckler, J. R.: The Production and Propagation of Energetic Particles from the Sun, in *Space Science*, D. P. Le Galley, ed., John Wiley & Sons, New York, 1963.
- 3-53. Young, R. S.: Exobiology, in *Proceedings of the NASA-University Conference on the Science and Technology of Space Exploration*, 1, 423, Government Printing Office, Washington, 1962.

#### 4. Integrating the Space Vehicle, Earth-Based Facilities, and Instrumentation

- 4-1. Barton, M. V.: Integrated Design Analysis, in *Space Technology*, H. S. Seifert, ed., John Wiley & Sons, New York, 1959.
- 4-2. Bazovsky, I.: *Reliability Theory and Practice*, Prentice-Hall, Inc., Englewood Cliffs, 1961.
- 4-3. Brooks, J. E.: Propulsion Interface, in *Ballistic Missile and Space Vehicle Systems*, H. S. Seifert and K. Brown, eds., John Wiley & Sons, New York, 1961.
- 4-4. Fletcher, J. C.: The Integration of Design; Overall System Considerations, in *Guided Missile Engineering*, A. E. Puckett, and S. Ramo, eds., McGraw-Hill Book Co., New York, 1959.
- 4-5. Powell, H. R.: Reliability, in *Ground Support Systems for Missiles and Space Vehicles*, K. Brown and P. Weiser, eds., McGraw-Hill Book Co., New York, 1961.
- 4-6. Robertson, A. E. and Fatianow, P. R.: Optimizing Space Programs, in *Technology of Lunar Exploration*, C. I. Cummings and H. R. Lawrence, eds., Academic Press, New York, 1963.
- 4-7. Whitaker, A. B. and Schuhlein, C.: Integrating Spacecraft Electronics, *Space/Aeronautics*, 42, 53, Aug. 1964.

#### 5. Interplanetary Transportation and Space Mechanics

- 5-1. Baker, R. M. L.: *Introduction of Astrodynamics*, Academic Press, New York, 1960.
- 5-2. Bellman, R.: *Dynamic Programming*, Princeton University Press, Princeton, 1957.
- 5-3. Berman, A. I.: *The Physical Principles of Astronautics*, John Wiley & Sons, New York, 1961.
- 5-4. Bollman, W. E.: The Engineering Design of Interplanetary Ballistic Trajectories, *AIAA Paper 63-414*, 1963.
- 5-5. Breakwell, J. V. and Gillespie, R. W.: Missions Normal to the Ecliptic, *Astronautics*, 7, 59, Sept. 1962.
- 5-6. Breakwell, J. V., Gillespie, R. W., and Ross, S.: Researches in Interplanetary Transfer, *ARS J.*, 31, 201, Feb. 1961.
- 5-7. Burley, R. R.: Out-of-Ecliptic Trajectories, *ARS J.*, 32, 1104, July 1962.

- 5-8. Chapman, D. R.: An Approximate Analytic Method for Studying Entry into Planetary Atmospheres, *NASA TR R-11*, 1959.
- 5-9. Clarke, V. C.: Summary of the Characteristics of Ballistic Interplanetary Trajectories, 1962-1977, Jet Propulsion Laboratory, *TR-32-209*, 1962.
- 5-10. Clarke, V. C. *et al.*: Design Parameters for Ballistic Interplanetary Trajectories, Jet Propulsion Laboratory, *TR-32-77*, 1963.
- 5-11. Cohen, A. D. and Beers, L. S.: What Kind of Upper-Stage Propulsion for Mars Missions?, *Astro. and Aerosp. Eng.*, **1**, 98, Aug. 1963.
- 5-12. Cole, D. M.: Astronautical Applications of the Asteroids, Amer. Astro. Soc. paper, 1963.
- 5-13. Dugan, D. W.: A Preliminary Study of a Solar Probe Mission, *NASA TN D-783*, 1961.
- 5-14. Edelbaum, T. N.: Some Extensions of the Hohmann Transfer Maneuver, *ARS J.*, **29**, 864, Nov. 1959.
- 5-15. Ehricke, K. A.: *Space Flight, 2, Dynamics*, D. Van Nostrand Co., Princeton, 1962.
- 5-16. Foelsche, T.: Relativistic Treatment of an Optimum Rocket Propulsion System under Consideration of Nuclear Data, *AD 214006, AFMDC-TN-59-8*, 1959.
- 5-17. Gillespie, R. W., Ragsac, R. V., and Ross, S. E.: Prospects for Early Manned Interplanetary Flights, *Astro. and Aerosp. Eng.*, **1**, 16, Aug. 1963.
- 5-18. Gobetz, F. W.: Optimum Transfers between Hyperbolic Asymptotes, *AIAA J.*, **1**, 2034, Sept. 1963.
- 5-19. Hunter, M. W.: Future Unmanned Exploration of the Solar System, *Astronautics and Aeronautics*, **2**, 16, May 1964.
- 5-20. Huth, J.: Relativistic Theory of Rocket Flight with Advanced Propulsion Systems, *ARS J.*, **30**, 250, March 1960.
- 5-21. Irving, J. H. and Blum, E. K.: Comparative Performance of Ballistic and Low-thrust Vehicles for Flight to Mars, in *Vistas in Astronautics*, **2**, M. Alperin and H. F. Gregory, eds., Pergamon Press, New York, 1959.
- 5-22. Lawden, D. F.: Interplanetary Rocket Trajectories, in *Advances in Space Science*, **1**, F. I. Ordway, ed., Academic Press, New York, 1959.
- 5-23. Laxdal, A. L. and Holdridge, D. B.: The JPL Trajectory System, *IAS Paper 63-85*, 1963.
- 5-24. Leitmann, G.: The Optimization of Rocket Trajectories—A Survey, in *Progress in the Astronautical Sciences*, **1**, S. F. Singer, ed., Interscience Publishers, New York, 1962.
- 5-25. Levin, E.: Low Acceleration Transfer Orbits, in *Handbook of Astronautical Engineering*, H. H. Koelle, ed., McGraw-Hill Book Co., New York, 1961.
- 5-26. Lorell, J.: Two-Dimensional Analysis of Interplanetary Flight Schedules, Jet Propulsion Laboratory, *TM 30-13*, 1959.
- 5-27. Melbourne, W. G.: Space Flight Optimization, in *Proceedings of the NASA-University Conference on the Science and Technology of Space Exploration*, **1**, 261, Government Printing Office, Washington, 1962.
- 5-28. Moeckel, W.: Trajectories with Constant Tangential Thrust in Central Gravitational Fields, *NASA TR R-53*, 1960.
- 5-29. Moeckel, W.: Interplanetary Trajectories with Excess Energy, in *Proceedings of the IXth International Astronautical Congress*, **1**, F. Hecht, ed., Springer-Verlag, Vienna, 1959.



- 5-30. Park, R. A.: Intercepting a Comet, *Astronautics and Aeronautics*, **2**, 54, Aug. 1964.
- 5-31. Park, R. A., Page, R. M., and Stableford, C. V.: Trajectory Considerations for a Cometary Mission, *AIAA Paper 63-413*, 1963.
- 5-32. Pauson, W. M.: Time Relationships for Interplanetary Trajectories, *ARS J.*, **31**, 128, Sept. 1961.
- 5-33. Pontryagin, L. S. *et al.*: *The Mathematical Theory of Optimum Processes*, John Wiley & Sons, New York, 1962.
- 5-34. Roberson, R. E.: Attitude Control of Satellites and Space Vehicles, in *Advances in Space Science*, **2**, F. I. Ordway, ed., Academic Press, New York, 1960.
- 5-35. Ross, S. *et al.*: *Planetary Flight Handbook*, NASA SP-35, 1963. (Three vols.)
- 5-36. Ruppe, H. O.: Minimum Energy Requirements for Space Travel, in *Proceedings of the Xth International Congress*, **1**, F. Hecht, ed., Springer-Verlag, Vienna, 1960.
- 5-37. Spencer, D. F. and Jaffe, L. D.: Feasibility of Interstellar Travel, *Astronautica Acta*, **9**, 49, 1963.
- 5-38. Thomson, W. T.: *Introduction to Space Dynamics*, John Wiley & Sons, New York, 1961.
- 5-39. Tsu, T. C.: Requirements of Interstellar Flight, *Astronautica Acta*, **6**, 247, 1960.
- 5-40. Ulam, S.: On the Possibility of Extracting Energy from Gravitational Systems by Navigating Space Vehicles, Los Alamos Scientific Laboratory, LAMS-2219, 1958.
- 5-41. von Hoerner, S.: The General Limits of Space Travel, *Science*, **137**, 18, July 6, 1962.
- 5-42. Vertregt, M.: *Principles of Astronautics*, Elsevier Publishing Co., New York, 1960.

## 6. Space Communications and Data Handling

- 6-1. Bayley, D. S.: The Interplanetary and Interstellar Communication Potential of the LASER, *Proceedings, National Aerospace Electronics Conference*, Dayton, 1962.
- 6-2. Creveling, C. J., Ferris, A. G., and Stout, C. M.: Automatic Data Processing, *IRE Trans.*, **SET-8**, 124, June 1962.
- 6-3. Higa, W. H.: Low-noise Receivers, in *Space Communications*, A. V. Balakrishnan, ed., McGraw-Hill Book Co., New York, 1963.
- 6-4. Hughes Aircraft Co.: Deep Space Optical Communications Study, NASA CR-73, 1964.
- 6-5. Institution of Electrical Engineers: *Proceedings, International Telemetry Conference, London, England*. Sept. 23-27, 1963, London.
- 6-6. Kirsten, C. C.: Data Acquisition at Planetary Ranges, in *Proceedings of the NASA-University Conference on the Science and Technology of Space Exploration*, **1**, 319, Government Printing Office, Washington, 1962.
- 6-7. Krassner, G. N. and Michaels, J. V., eds.: *An Introduction to Space Communication Systems*, McGraw-Hill Book Co., New York, 1964.
- 6-8. Lehan, F. W.: Space Communication Implementation Problems, in *Space Technology*, H. S. Seifert, ed., John Wiley & Sons, New York, 1959.

- 6-9. Martin, B. D.: The Mariner Planetary Communication System Design, in *Space Research*, 2, H. C. van de Hulst, C. de Jager, and A. F. Moore, eds., Interscience Publishers, New York, 1961.
- 6-10. Martin, B. D.: The Pioneer IV Lunar Probe: A Minimum-Power FM/PM System Design, Jet Propulsion Laboratory, *TR 32-215*, Pasadena, 1962.
- 6-11. Mathison, R. P.: Constraints in Space Telecommunications Systems, Jet Propulsion Laboratory, *TR 32-260*, Pasadena, 1962.
- 6-12. Pierce, J. R. and Cutler, C. C.: Interplanetary Communications, in *Advances in Space Science*, 1, F. I. Ordway, ed., Academic Press, New York, 1959.
- 6-13. Potter, P. D., Stevens, R., and Wells, W. H.: Radio and Optial Space Communications, Jet Propulsion Laboratory, *TM 33-85*, 1962.
- 6-14. Potter, P. D.: Antennas, in *Space Communications*, A. V. Balakrishnan, ed., McGraw-Hill Book Co., New York, 1963.
- 6-15. Rechtin, E., Rule, B., and Stevens, R.: Large Ground Antennas, Jet Propulsion Laboratory, *TR 32-213*, 1962.
- 6-16. Rechtin, E.: Deep Space Communications, *Astronautics*, 6, 26, May 1961.
- 6-17. Rechtin, E.: Basic Constraints of Space Communication Systems, in *Space Communications*, A. V. Balakrishnan, ed., McGraw-Hill Book Co., New York, 1963.
- 6-18. Rechtin, E.: Feasibility of Space Communications, in *Space Technology*, H. S. Seifert, ed., John Wiley & Sons, New York, 1959.
- 6-19. Sanders, R.: Sampled Data Modulation Systems, in *Space Communications*, A. V. Balakrishnan, ed., McGraw-Hill Book Co., New York, 1963.
- 6-20. Stephenson, R. D.: External Noise, in *Space Communications*, A. V. Balakrishnan, ed., McGraw-Hill Book Co., New York, 1963.
- 6-21. Stephenson, R. G.: Spaae Communications, in *Space Logistics Engineering*, K. Brown and L. D. Ely, eds., John Wiley & Sons, New York, 1962.
- 6-22. Stiltz, H. L., ed.: *Aerospace Telemetry*, Prentice-Hall, Inc., Englewood Cliffs, 1961.
- 6-23. Stoller, M. J.: Satellite Telemetry and Data Recovery Systems, in *Space Research II*, H. C. van de Hulst, C. de Jager and A. F. Moore, eds., Interscience Publishers, New York, 1961.
- 6-24. Thatcher, J. W.: Deep Space Communications, *Space/Aeronautics*, 42, 54, July 1964.
- 6-25. Viterbi, A. J.: Phase-lock-loop Systems, in *Space Communications*, A. V. Balakrishnan, ed., McGraw-Hill Book Co., New York, 1963.

## 7. Navigation, Guidance, and Control of Interplanetary Spacecraft

- 7-1. Barnes, F. L. *et al.*: Mariner 2 Flight to Venus, *Astronautics*, 7, 66, Dec. 1962.
- 7-2. Battin, R.: *Astronautical Guidance*, McGraw-Hill Book Co., New York, 1964.
- 7-3. Boek, C. D. and Mundo, C. J.: Guidance Techniques for Interplanetary Travel, *ARS J.*, 29, 931, Dec. 1959.
- 7-4. Breckenridge, W. G.: Ascent Guidance Aceuracy Studies, Jet Propulsion Laboratory, *SPS 37-23*, 4, 32, 1963.
- 7-5. Chapman, D. R.: An Analysis of the Corridor and Guidance Requirements for Supercircular Entry into Planetary Atmospheres, *NASA TR R-55*, 1960.

- 7-6. Daly, J., Joseph, R. D., and Kelly, P. M.: Self-organizing Logic Systems, *Astronautica Acta*, **8**, 376, 1962.
- 7-7. Fogel, L. J.: *Biotechnology: Concepts and Applications*, Chap. 10, Prentice-Hall, Inc., Englewood Cliffs, 1963.
- 7-8. Friedlander, A. L. and Harry, D. P.: A Study of Statistical Data-Adjustment and Logic Techniques as Applied to the Interplanetary Midcourse Guidance Problem, *NASA TR R-113*, 1961.
- 7-9. Gates, C. R., Scull, J. R., and Watkins, K. S.: Space Guidance, *Astronautics*, **6**, 24, Nov. 1961.
- 7-10. Gordon, H. J.: A Study of Injection Guidance Accuracy as Applied to Lunar and Interplanetary Missions, in *Guidance and Control*, R. E. Roberson and J. S. Farrior, eds., Academic Press, New York, 1962.
- 7-11. Haviland, R. P. and House, C. M.: Celestial Navigation in Space, in *Advances in the Astronautical Sciences*, **13**, E. Burgess, ed., Western Periodicals Co., North Hollywood, 1963.
- 7-12. Horsfall, R. B.: Celestial Guidance, *ARS J.*, **29**, 981, Dec. 1959.
- 7-13. Kochi, K. C. and Dibble, H. L.: Stellar Techniques for Midcourse Navigation-Guidance, *AIAA Paper 63-357*, 1963.
- 7-14. Lawden, D. F.: Fundamentals of Space Navigation, *J. Brit. Interplanetary Soc.*, **13**, 87, 1954.
- 7-15. Mathison, R. P.: Tracking Techniques for Interplanetary Spacecraft, Jet Propulsion Laboratory, *TR 32-284*, Pasadena, 1962.
- 7-16. Minsky, M.: Steps Toward Artificial Intelligence, *Proc. IRE*, **49**, 8, 1961.
- 7-17. Mishkin, E. and Braun, L.: *Adaptive Control Systems*, McGraw-Hill Book Co., New York, 1960.
- 7-18. Mullen, E. B. and Woods, C. R.: State of the Art in Radio Tracking, in *Proceedings. XIth. International Astronautical Congress*, C. W. P. Reutersward, ed., Springer-Verlag, Vienna, 1961.
- 7-19. Newell, D. H.: Orbital Transfer Guidance Analysis, Jet Propulsion Laboratory, *SPS 37-23*, **4**, 23, 1963.
- 7-20. Noton, A. R. M., Cutting, E., and Barnes, F. L.: Analysis of Radio Command Midcourse Guidance, Jet Propulsion Laboratory, *TR 32-28*, 1960.
- 7-21. Noton, A. R. M.: The Statistical Analysis of Space Guidance Systems, Jet Propulsion Laboratory, *TM 33-15*, 1960.
- 7-22. O'Donnell, C. F., ed.: *Inertial Navigation Analysis and Design*, McGraw-Hill Book Co., New York, 1963.
- 7-23. Oliver, E. F.: Interplanetary Navigation, *Navigation*, **10**, 373, Winter 1963-1964.
- 7-24. Overton, R. K.: The Truth about Learning Machines, *Ind. Res.*, **36**, Oct. 1963.
- 7-25. Pfeiffer, C. G.: Guidance Analysis, in *Lunar Missions and Exploration*, C. T. Leondes and H. C. Vance, John Wiley & Sons, New York, 1964.
- 7-26. Pfeiffer, C. G.: Guidance of Unmanned Lunar and Interplanetary Spacecraft, *AIAA Paper 63-399*, 1963.
- 7-27. Renzetti, N. A. *et al.*: Radio Tracking Techniques and Performance of the United States Deep Space Instrumentation Facility, in *Space Research II*, H. C. van de Hulst, C. de Jager, and A. F. Moore, eds., Interscience Publishers, New York, 1961.
- 7-28. Roberson, R. E. and Farrior, J. S., eds.: *Guidance and Control*, Academic Press, New York, 1962.

- 7-29. Schmieder, D. H. and Winch, J. B.: Adaptive Guidance, in *Proceedings of the NASA-University Conference on the Science and Technology of Space Exploration*, **1**, 339, Government Printing Office, Washington, 1962.
- 7-30. Springett, J. C.: Command Techniques for the Remote Control of Interplanetary Spacecraft, Jet Propulsion Laboratory, *TR 32-314*, 1962.
- 7-31. Stearns, E. V. B.: *Navigation and Guidance in Space*, Prentice-Hall, Inc., Englewood Cliffs, 1963.
- 7-32. Truxal, J. G.: *Automatic Feedback Control Synthesis*, McGraw-Hill Book Co., New York, 1955.
- 7-33. Vertregt, M.: Orientation in Space, *J. Brit. Interplanetary Soc.*, **15**, 324, 1956.
- 7-34. Wheelon, A. D.: Midcourse and Terminal Guidance, in *Space Technology*, H. S. Seifert, ed., John Wiley & Sons, New York, 1959.
- 7-35. Wingrove, R. C.: Study of Atmosphere Re-entry Guidance and Control Methods, *AIAA J.*, **1**, 2019, Sept. 1963.

## 8. Earth-Based Facilities

- 8-1. Barnett, R. M. and Thiele, C.: JPL Advanced Solar Simulator, Design Type A, Jet Propulsion Laboratory, *TM 33-141*, 1963.
- 8-2. Barton, D. K.: Recent Developments in Radar Instrumentation, *Astro. and Aerosp. Eng.*, **1**, 54, July, 1963.
- 8-3. Brown, K. and Weiser, P., eds.: *Ground Support Systems for Missiles and Space Vehicles*, McGraw-Hill Book Co., New York, 1961.
- 8-4. Buchanan, D. D.: Saturn V Launch Environment and GSE Design, *Astronautics and Aeronautics*, **2**, 30, March 1964.
- 8-5. Burrill, E. A.: Simulating Space Radiation, *Space/Aeronautics*, **41**, 78, May 1964.
- 8-6. Debus, K. H.: Launching the Moon Rocket, *Astro and Aerosp. Eng.*, **1**, 20, March 1963.
- 8-7. Debus, K. and Gruene, H. F., eds.: Launching Sites and Space Ports, in *Handbook of Astronautical Engineering*, H. H. Koelle, ed., McGraw-Hill Book Co., New York, 1961.
- 8-8. Duberg, J. A.: Space Vehicle Environment and Some NASA Facilities for Their Simulation, paper presented at the 31st. Symposium on Shock, Vibration, and Associated Environments, Phoenix, 1962. *NASA Abstract N63-17734*.
- 8-9. Godfrey, R. V. and Carroll, C. L.: Range Instrumentation for Space Vehicle Operations, *ARS Preprint 2061-61*, 1961.
- 8-10. Gollomp, B., Lawton, J., and Van Rennes, A. B.: Evolution of Automatic Checkout Equipment, *J. Brit. Interplanetary Soc.*, **19**, 223, Oct. 1963.
- 8-11. Hnlicka, M. P. and Geiger, K. A.: Simulating Interplanetary Space, *Astro. and Aerosp. Eng.*, **1**, 31, July 1963.
- 8-12. Hueter, H. and Stamy, J. L., eds.: Special Launch-Operations Support Equipment, in *Handbook of Astronautical Engineering*, H. H. Koelle, ed., McGraw-Hill Book Co., New York, 1961.
- 8-13. Jet Propulsion Laboratory: *Space Programs Summary*, Nos. 37-20 and 37-21, **6**, Jet Propulsion Laboratory, 1963.
- 8-14. Johnson, D. R.: Future Land and Water Launch Facilities, *Astro. and Aerosp. Eng.*, **1**, 45, March 1963.

- 8-15. Lewis, D. E. and Shubert, G. H.: Efficiency in Space-Rocket Launching Operations: Recent Advances and Future Opportunities, Rand Corp., *RM-9313-PR, AD 429 979*, 1963.
- 8-16. Mann, J. F. and Cohen, J.: Advanced Range Instrumentation Ship Data Handling, *ARS Preprint 63097*, 1963.
- 8-17. Mast, L. T.: Automatic Test and Checkout in Missile and Space Systems, *Astro and Aerosp. Eng.*, **1**, 41, March 1963.
- 8-18. McGee, J. F.: System Checkout and Flight Testing of Unmanned Lunar and Planetary Spacecraft, *AIAA Preprint 63104*, 1963.
- 8-19. Munday, R. T. G.: System Design of Space Simulation Chambers, *J. Brit. Interplanetary Soc.*, **19**, 272, Feb. 1964.
- 8-20. Peterson, M. C.: System Checkout and Launch Control Equipment, in *Ground Support Systems for Missiles and Space Vehicles*, K. Brown and P. Weiser, eds., McGraw-Hill Book Co., New York, 1961.
- 8-21. Renzetti, N. A. *et al.*: Radio Tracking Techniques and Performance of the United States Deep Space Instrumentation Facility, in *Space Research II*, H. C. van de Hulst, C. de Jager, and A. F. Moore, eds., Interscience Publishers, New York, 1961.
- 8-22. Riise, H. N.: Modifications to the Solar Simulation System of the JPL 25-ft Space Simulator, *Jet Propulsion Laboratory, SPS 37-19*, **4**, 94, 1963.

## 9. Launch Vehicles

- 9-1. Abraham, L. H.: *Structural Design of Missiles and Spacecraft*, McGraw-Hill Book Co., New York, 1962.
- 9-2. Alberi, A. and Rosenkranz, C.: Structures of Carrier and Space Vehicles, in *Advances in Space Science and Technology*, **3**, F. I. Ordway, ed., Academic Press, New York, 1961.
- 9-3. American Institute of Aeronautics and Astronautics: The Saturn Program, *Astronautics*, **7**, Feb. 1962 (whole issue).
- 9-4. American Institute of Aeronautics and Astronautics: Reusable Launch Systems, *Astronautics and Aeronautics*, **2**, Jan. 1964 (whole issue).
- 9-5. Anonymous: Launch Vehicles, *NASA SP-10*, Washington, 1962.
- 9-6. Boswinkle, R. W.: Aerodynamic Problems of Launch Vehicles, in *Proceedings of the NASA-University Conference on the Science and Technology of Space Exploration*, **2**, 193, Government Printing Office, Washington, 1962.
- 9-7. Burlage, H.: Liquid Engines for Advanced Launch Vehicles, *Astronautics and Aeronautics*, **2**, 42, July 1964.
- 9-8. Canright, R. B. and Rafel, N.: Nonrecoverable Boosters, *Astronautics*, **8**, 26, Jan. 1963.
- 9-9. Cohen, W.: Solid Fuel Boosters, *International Science and Technology*, **66**, Sept. 1963.
- 9-10. Corliss, W. R.: *Propulsion Systems for Space Flight*, McGraw-Hill Book Co., New York, 1960.
- 9-11. Hyatt, A.: NASA Launch Vehicle Development Program, in *Space Age Astronomy*, A. J. Deutsch and W. B. Klemperer, eds., Academic Press, New York, 1962.
- 9-12. Koelle, H. H., ed.: Long Range Planning for Space Transportation Systems, *NASA TN D-597*, 1961.
- 9-13. Koelle, H. H. ed.: Missiles and Space Systems—1962, *Astronautics*, **7**, 29, Nov. 1962.

- 9-14. Kovit, B.: The Saturns, *Space/Aeronautics*, **42**, 40, Aug. 1964.
- 9-15. Lange, O. H. and Stein, R. J.: *Space Carrier Vehicles*, Academic Press, New York, 1963.
- 9-16. Lange, O. H.: Development of the Saturn Space Carrier Vehicle, in *Astronautical Engineering and Science*, E. Stuhlinger *et al*, eds., McGraw-Hill Book Co., New York, 1963.
- 9-17. Moise, J. C., Henry, C. S., and Swanson, R. S.: Astroplane: A Reusable Orbital Booster Utilizing Lifting Tankage, *AIAA Preprint 63-283*, 1963.
- 9-18. Nylander, H. E. and Hopper, F. W.: The Development of Multiple Staging in Military and Space Carrier Vehicles, in *Advances in Space Science and Technology*, **4**, F. I. Ordway, ed., Academic Press, New York, 1962.
- 9-19. Ordway, F. I.: United States Carrier Vehicle and Spacecraft Developments, *Astronautica Acta*, **7**, 103, 1961.
- 9-20. Rosen, M. W.: Big Rockets, *International Science and Technology*, **66**, Dec. 1962.
- 9-21. Stafford, W. H., Harlin, S. H., and Catalfamo, C. R.: Performance Analysis of High-Energy Chemical Stages for Interplanetary Missions, *NASA TN D-1829*, 1964.
- 9-22. Stambler, I.: Titan III, *Space/Aeronautics*, **40**, 72, Aug. 1963.
- 9-23. Stambler, I.: Centaur, *Space/Aeronautics*, **40**, 70, Oct. 1963.
- 9-24. von Braun, W.: Launch Vehicles and Launch Operations, *NASA SP-8*, 1962.

## 10. Spacecraft Design

- 10-1. Acord, J. D. and Nicklas, J. C.: Theoretical and Practical Aspects of Solar Pressure Attitude Control for Interplanetary Spacecraft, *AIAA Preprint 63-327*, 1963.
- 10-2. Alexander, A. L.: Thermal Control in Space Vehicles, *Science*, **143**, 654, Feb. 14, 1964.
- 10-3. Allen, H. J.: Gas Dynamics Problems of Space Vehicles, in *Proceedings of the NASA-University Conference on the Science and Technology of Space Exploration*, **2**, 251, Government Printing Office, Washington, 1962.
- 10-4. Becker, J. V.: Re-entry from Space, *Scientific American*, **204**, 49, Jan. 1961.
- 10-5. Bekker, M. G.: Land Locomotion on the Surface of a Planet, *ARS J.*, **32**, 1651, Nov. 1962.
- 10-6. Black, R. J.: Quadrupedal Landing Gear Systems for Spacecraft, *J. Spacecraft and Rockets*, **1**, 196, March-April, 1964.
- 10-7. Blizard, E. P.: *Reactor Handbook*, **3B**, *Shielding*, Interscience Publishers, New York, 1963.
- 10-8. Bryden, J. N.: Mariner (Venus '62) Flight Telecommunication System, Jet Propulsion Laboratory, *TR-32-377*, Pasadena, 1963.
- 10-9. Cartaino, T. F.: Vehicles for Exploration on Mars, *ARS Preprint 1090-60*, 1960.
- 10-10. Corliss, W. R.: Survey of Space Power Requirements, in *Power Systems for Space Flight*, M. A. Zipkin and R. N. Edwards, eds., Academic Press, New York, 1963.
- 10-11. Corliss, W. R. and Harvey, D. G.: *Radioisotopic Power Generation*, Prentice-Hall, Inc., Englewood Cliffs, 1964.
- 10-12. Coppa, A. P.: Collapsible Shell Structures for Lunar Landing, *ARS Preprint 2156-61*, 1961.

- 10-13. Costogue, E. N.: Mariner Venus Power-Supply System, Jet Propulsion Laboratory, *TR 32-424*, Pasadena, 1963.
- 10-14. Davis, D. D.: Space Environment and Its Effects on Materials, in *Proceedings of the NASA-University Conference on the Science and Technology of Space Exploration*, 2, 439, Government Printing Office, Washington, 1962.
- 10-15. Dubin, M.: Meteoroid Effects on Space Exploration, *NASA TN D-1839*, 1963.
- 10-16. Dzilvelis, A. A.: Satellite Attitude Control Systems, *Astro. and Aerosp. Eng.*, 1, 78, March 1963.
- 10-17. Esgar, J. B.: Survey of Energy-Absorption Devices for Soft Landing of Space Vehicles, *NASA TN D-1308*, 1962.
- 10-18. Forney, R. G.: Mariner II Attitude Control System, *IAF Paper*, 1963.
- 10-19. Froehlich, J. E. and Hazard, A. B.: Lunar Exploration Vehicles and Equipment, in *Manned Lunar Flight*, G. W. Morgenthaler and H. Jacobs, eds., Western Periodicals Co., North Hollywood, 1963.
- 10-20. Gin, W. and Piasecki, L. R.: Solid Rockets for Lunar and Planetary Spacecraft, Jet Propulsion Laboratory, *TR 34-158*, Pasadena, 1960.
- 10-21. Grabbe, E. M., Ramo, S., and Wooldridge, D. E., eds.: *Handbook of Automation, Computation, and Control*, John Wiley & Sons, New York, 1958.
- 10-22. Graves, C. D. and Park, R. A.: Spacecraft Design for Scientific Missions, in *Space Physics*, D. P. Le Galley and A. Rosen, eds., John Wiley & Sons, New York, 1964.
- 10-23. Haeussermann, W.: Recent Advances in Attitude Control of Space Vehicles, *ARS J.*, 32, 188, Feb. 1962.
- 10-24. Hellebrand, E. A.: Structural Analysis, in *Handbook of Astronautical Engineering*, H. H. Koelle, ed., McGraw-Hill Book Co., New York, 1961.
- 10-25. Holahan, J.: Attitude Control for Unmanned Spacecraft, *Space/Aeronautics*, 39, 78, Feb. 1963.
- 10-26. Jaffe, L. D.: Sterilizing Unmanned Spacecraft, *Astronautics and Aerospace Eng.*, 1, 22, Aug. 1963.
- 10-27. Jaffe, L. D.: Sterilization of Unmanned Planetary and Lunar Space Vehicles—An Engineering Examination, Jet Propulsion Laboratory, *TR 32-325 Rev.*, 1963.
- 10-28. Jaffe, L. D. and Rittenhouse, J. B.: Behavior of Materials in Space Environments, *ARS J.*, 32, 320, Mar. 1962.
- 10-29. Keller, J. W. *et al.*: Problems in Radiation Shielding of Space Vehicles, in *Astronautical Engineering and Science*, E. Stuhlinger *et al.*, eds., McGraw-Hill Book Co., New York, 1963.
- 10-30. LaVan, J. T.: Unconventional Inertial Sensors, *Space/Aeronautics*, 40, 73, Dec. 1963.
- 10-31. Lewis, D. W. *et al.*: Final Report on Mariner-2 Temperature Control, Jet Propulsion Laboratory, *TM 33-140*, 1963.
- 10-32. McDonald, J. C. *et al.*: *Materials for Missiles and Spacecraft*, McGraw-Hill Book Co., New York, 1963.
- 10-33. Morrison, S. C.: Maximizing Reliability for One-Shot Space Missions, *Aerospace Eng.*, 21, 54, March 1962.
- 10-34. Nelson, E. C.: Digital Computers, in *Guided Missile Engineering*, A. E. Puckett and S. Ramo, eds., McGraw-Hill Book Co., New York, 1959.
- 10-35. O'Donnell, C. F.: On Board Computers, in *Handbook of Astronautical Engineering*, H. H. Koelle, ed., McGraw-Hill Book Co., New York, 1961.

- 10-36. Powell, H. R.: Reliability, in *Ground Support Systems for Missiles and Space Vehicles*, K. Brown and P. Weiser, eds., McGraw-Hill Book Co., New York, 1961.
- 10-37. Riley, F. E. and Sailor, J. D.: *Space Systems Engineering*, McGraw-Hill Book Co., New York, 1962.
- 10-38. Romaine, O.: Secondary Rockets, *Space/Aeronautics*, **39**, 83, May 1963.
- 10-39. Sanders, N. D. *et al.*: Power for Spacecraft, in *Proceedings of the NASA-University Conference on the Science and Technology of Space Exploration*, **2**, 125, Government Printing Office, Washington, 1962.
- 10-40. Scull, J. R.: The Application of Optical Sensors for Lunar and Planetary Space Vehicles, Jet Propulsion Laboratory, *TR 32-274*, 1962.
- 10-41. Slater, J. M.: Guidance and Control Components, in *Handbook of Astronautical Engineering*, H. H. Koelle, ed., McGraw-Hill Book Co., New York, 1961.
- 10-42. Stevenson, J. A. and Grafton, J. C.: Radiation Heat Transfer Analysis for Space Vehicles, U.S. Air Force, *ASD TR 61-119*, 1961.
- 10-43. Stuhlinger, E., ed.: *Electric Propulsion Development*, Academic Press, New York, 1963.
- 10-44. Tucker, M.: Spacecraft Entry and Landing in Planetary Atmospheres, in *Advances in Space Science and Technology*, **4**, F. I. Ordway, ed., Academic Press, New York, 1962.
- 10-45. Van Lear, G. A. and Lassen, H. A.: Instrumental Gyroscopy, in *Guided Missile Engineering*, A. E. Puckett and S. Ramo., eds., McGraw-Hill Book Co., New York, 1959.
- 10-46. Whipple, F. L.: On Meteoroids and Penetration, *J. Geophys. Res.*, **68**, 4929, Sept. 1, 1963.
- 10-47. Zipkin, M. A. and Edwards, R. N., eds.: *Power Systems for Space Flight*, Academic Press, New York, 1963.
- 10-48. Zoutendyk, J. A., Vondra, R. J., and Smith, A. H.: Mariner 2 Solar Panel Design and Flight Performance, Jet Propulsion Laboratory, *TR 32-455*, 1963.

## 11. Characteristics of Specific Space Probes

- 11-1. Anonymous: Mission to Venus, *Spaceflight*, **3**, 114, July 1961.
- 11-2. Beale, R. J.: Systems Engineering of a Nuclear-Electric Spacecraft, Jet Propulsion Laboratory, *TR 32-158*, 1961.
- 11-3. Beale, R. J., Speiser, E. W., and Womeck, J. R.: The Electric Space Cruiser for High Energy Missions, *AIAA Preprint 63007-63*, 1963.
- 11-4. Dugan, D. W.: A Preliminary Study of a Solar Probe Mission, *NASA TN D-783*, 1961.
- 11-5. Glaser, P.: Pioneer V Communication System, in *Space Communications*, A. V. Balakrishnan, ed., McGraw-Hill Book Co., New York, 1963.
- 11-6. Hall, C. F., Nothwang, G. J., Hornyby, H.: A Feasibility Study of Solar Probes, *Aerospace Eng.*, **21**, 22, May 1962.
- 11-7. Hibben, R. D.: IMP Will Warn of Dangerous Solar Flares, *Aviation Week*, **79**, 28, Nov. 4, 1963.
- 11-8. Mueller, G. E.: Pioneer V and Explorer VI, Systems Engineered Space Probes, in *Proceedings of the XIth. International Astronautical Congress*, C. W. P. Reutersward, ed., Springer-Verlag, Vienna, 1961.



- 11-9. Paulson, J. J.: Triune: Three-in-One Nuclear Electric Saturn Probe, *Space/Aeronautics*, **38**, A-14, July 1962.
- 11-10. Space Technology Laboratories: Comet Intercept Study, *Report 8668-6002-RU-000*, 1963.
- 11-11. Stafford, W. H. and Croft, R. M.: Artificial Earth Satellites and Successful Solar Probes, *NASA TN D-601*, 1961.
- 11-12. Stambler, I.: Interplanetary Probes, *Space/Aeronautics*, **42**, 36, July 1964.
- 11-13. Stambler, I.: The New Pioneer Satellites, *Space/Aeronautics*, **40**, 58, Nov. 1963.
- 11-14. Stambler, I.: Mariner 2, *Space/Aeronautics*, **38**, 65, Nov. 1962.
- 11-15. Stone, I.: Mariner Design Modified for Mars Flyby, *Aviation Week*, **78**, 50, May 6, 1963.
- 11-16. Wheelock, H. J., comp.: *Mariner, Mission to Venus*, McGraw-Hill Book Co., New York, 1963. (Paperback.)

## 12. Scientific Experimentation in Space

- 12-1. Brown, W. E.: Measurement Problems of Space Vehicle Experiments, *IRE Trans.*, **I-11**, 86, Dec. 1962.
- 12-2. Electro-Optical Systems, Inc.: Space Measurements Survey, *DASA 1277, AD 415161*, 1962.
- 12-3. Graves, C. D. and Park, R. A.: Spacecraft Design for Scientific Missions, in *Space Physics*, D. P. Le Galley and A. Rosen, eds., John Wiley & Sons, New York, 1964.
- 12-4. Heacock, R. L.: Problems in Instrument Design, *Nucleonics*, **20**, 55, Oct. 1962.
- 12-5. Heacock, R. L.: Scientific Instruments in Space Exploration, *Science*, **142**, 188, Oct. 11, 1963.
- 12-6. Ludwig, G. H.: Spacecraft Information Systems, *NASA TN D-1348*, 1962.
- 12-7. Nicks, O. W.: Some Aspects of Preparing Scientific Payloads for Lunar and Planetary Payloads, speech before the American Geophysical Union, 1961.
- 12-8. Schutz, F. L.: Incorporation of Scientific Instruments into Deep Space Probes, Jet Propulsion Laboratory paper, 1964.

## 13. Instruments for Measuring the Interplanetary Medium

- 13-1. Alexander, W. M. *et al.*: Review of Direct Measurements of Interplanetary Dust from Satellites and Probes, in *Space Research III*, W. Priester, ed., Interscience Publishers, New York, 1963.
- 13-2. Anderson, H. R.: Ionizing Radiation Measured between Earth and Venus by Mariner II, *COSPAR Paper*, 1964.
- 13-3. Anderson, J. D. and Null, G. W.: The Evaluation of Certain Physical Constants from the Radio Tracking of Mariner II, *AIAA Paper 63-424*, 1963.
- 13-4. Anonymous: High Energy Gamma-Ray Telescope, *Nucleonics*, **20**, 69, Oct. 1962.
- 13-5. Arnold, J. T.: Spin Precession Magnetometers for Applications in Space, Instrument Society of America, *Proceedings, 1962 National Aerospace Instrument Symposium*, 1962.

- 13-6. Bader, M., Fryer, T. B., and Witteborn, F. C.: Two Instruments for Measuring Distributions of Low-Energy Charged Particles in Space, *NASA TN D-1035*, 1961.
- 13-7. Bernstein, W.: The Solar Plasma—Its Detection, Measurement, and Significance, in *Space Physics*, D. P. Le Galley and A. Rosen, eds., John Wiley & Sons, New York, 1964.
- 13-8. Biermann *et al.*: Study of the Interplanetary Media by Means of the Artificial Ionized Clouds, *AD 282654*, 1962.
- 13-9. Bourdeau, R. E., Donley, J. L., and Whipple, E. C.: Instrumentation of the Ionosphere Direct Measurements Satellite (Explorer VIII), *NASA TN D-414*, 1962.
- 13-10. Bourdeau, R. E. and Donley, J. L.: Explorer VIII Satellite Measurements in the Upper Ionosphere, *NASA TN D-2150*, 1964.
- 13-11. Bridge, H. S. *et al.*: Plasma Probe Instrumentation on Explorer X, in *Space Research III*, W. Priester, ed., Interscience Publishers, New York, 1963.
- 13-12. Bridge, H. S. *et al.*: An Instrument for the Investigation of Interplanetary Plasma, *J. Geophys. Res.*, **65**, 3053, Oct. 1960.
- 13-13. Brown, W. L. *et al.*: The Spacecraft Radiation Experiments, in *Telstar I*, **1**, *NASA SP-32*, 899, 1963.
- 13-14. Bryant, D. A., Ludwig, G. H., and McDonald, F. B.: A Scintillation Counter Telescope for Charge and Mass Identification of Primary Cosmic Rays, *IRE Trans.*, **NS-9**, 376, June 1962.
- 13-15. Cahill, L. J.: Magnetic Field Measurements in Space, *Space Science Rev.*, **1**, 399, 1963.
- 13-16. Cline, T. L., Serlemitsos, P., and Hones, E. W.: A Double Gamma-Ray Spectrometer to Search for Positrons in Space, *NASA TN D-1464*, 1962.
- 13-17. Davison, E. H. and Winslow, P. C.: Micrometeoroid Satellite (Explorer XVI) Stainless-Steel Penetration Rate Experiment, *NASA TN D-2445*, 1964.
- 13-18. Dolginov, S. Sh., Zhuzgov, L. N., and Seliutin, V. A.: Magnetometric Equipment of the Third Soviet Satellite, translated in *ARS J.*, **31**, 1329, Sept. 1961.
- 13-19. Doolittle, R. F., and Graves, C. D.: The Application of Scintillation Chambers to Space Research, paper presented at the Second Symposium on Photo-Electric Image Devices, London, 1961.
- 13-20. Fillius, R. W. and McIlwain, C. E.: Solid-State Detectors for Inner Zone Protons, in *Space Research III*, W. Priester, ed., Interscience Publishers, New York, 1963.
- 13-21. Friedland, S. S. *et al.*: Application of Nuclear Semiconductor Detectors for Space Spectrometry, *IRE Trans.*, **NS-9**, 391, June 1962.
- 13-22. Goettelman, R. C.: The Meteoroid and Cosmic Ray Environments of Space Vehicles and Techniques for Measuring Parameters Affecting Them, *WADD TR 60-846*, *AD 262013*, 1960.
- 13-23. Goodrich, G. W. and Wiley, W. C.: Experiments with the Bendix Continuous-Channel Multiplier, Image Intensifier Symposium, *NASA SP-2*, 211, 1961.
- 13-24. Goulding, F. S.: Semiconductor Detectors—Their Properties and Applications, *Nucleonics*, **22**, 54, May 1964.
- 13-25. Gringauz, K. I.: Some Results of Experiments in Interplanetary Space

- by Means of Charged Particle Traps on Soviet Space Probes, in *Space Research II*, H. C. van de Hulst, C. de Jager, and A. F. Moore, eds., Interscience Publishers, New York, 1961.
- 13-26. Gringauz, K. I.: Investigation of Interplanetary Plasma and Planetary Ionospheres by Means of Charged Particle Traps on Space Rockets, *Proceedings of the XIIIth. International Astronautical Congress*, R. M. L. Baker, and M. W. Makemson, eds., Academic Press, New York, 1963.
- 13-27. Hastings, E. C., comp.: The Explorer XVI Micrometeoroid Satellite—Description and Preliminary Results for the Period December 16, 1962 through January 13, 1963, *NASA TM X-810*, 1963.
- 13-28. Haymes, R. C.: Fast Neutrons in the Earth's Atmosphere, *J. Geophys. Res.*, **69**, 841, March 1, 1964.
- 13-29. Holms, A. G.: The Design of Micrometeoroid Penetration Experiments as Single-Sampling Life-Test Sampling Plans, *NASA TN D-1989*, 1964.
- 13-30. Hubbard, E. L.: Nuclear Particle Spectrometers for Satellites and Space Probes, *IRE Trans.*, **NS-9**, 357, June 1962.
- 13-31. Josias, C. and Lawrence, J.: An Instrument for the Measurement of the Interplanetary Solar Plasma, Jet Propulsion Laboratory, *TR 32-492*, 1964.
- 13-32. Judge, D. L., McLeod, M. G., and Sims, A. R.: The Pioneer I, Explorer VI and Pioneer V High-Sensitivity Transistorized Search Coil Magnetometer, *IRE Trans.*, **SET-6**, 114, Sept. 1960.
- 13-33. Kocher, G. E. and Jamison, D. T.: A Deep-Space Triangulation Probe to Determine the Astronomical Unit, Rand Corp., *RM-4014-NASA*, 1964.
- 13-34. Lampert, J. E.: Instrumentation for the Measurements of Energetic Particles in Space, *Instrument Society of America Proceedings, 1962 National Aerospace Instrument Symposium*, 1962.
- 13-35. Lawrence, J. L. and Norris, D. D.: Mariner C Magnetometer, Jet Propulsion Laboratory, *SPS 37-26*, **4**, 1964.
- 13-36. Leavitt, C. P.: High Energy Gamma Ray Satellite Experiment, *IRE Trans.*, **NS-9**, 400, June 1962.
- 13-37. Lewis Research Center Staff: Micrometeoroid Satellite (Explorer XIII) Stainless-Steel Penetration Rate Experiment, *NASA TN D-1986*, 1963.
- 13-38. Lindner, J. W.: Experimental Techniques Employed in Space Physics, in *Space Physics*, D. P. Le Galley and A. Rosen, eds., John Wiley & Sons, New York, 1964.
- 13-39. Ling, S. C.: A Fluxgate Magnetometer for Space Application, *J. Spacecraft and Rockets*, **1**, 175, March 1964.
- 13-40. Ludwig, G. H.: The NASA Program for Particles and Fields Research in Space, *NASA TN D-1173*, 1962.
- 13-41. Ludwig, G. H. and McDonald, F. B.: Cosmic Ray Experiments for Explorer XII and the OGO, in *Space Research III*, W. Priester, ed., Interscience Publishers, New York, 1963.
- 13-42. Manring, E. R.: Interplanetary Matter, in *Advances in Space Science and Technology*, **3**, F. I. Ordway, ed., Academic Press, New York, 1961.
- 13-43. Manring, E. R.: Micrometeorite Measurements from 1958 Alpha and Gamma Satellites, *Planetary and Space Science*, **1**, 27, 1959.
- 13-44. Matthews, H. F. and Erickson, M. D.: The NASA Advanced Pioneer Mission, *SAE Paper*, 1964.
- 13-45. McDonald, F. B. and Webber, W. R.: Cerenkov-Scintillation Counter

- Measurements of the Light, Medium, and Heavy Nuclei in the Primary Cosmic Radiation from Sunspot Minimum to Sunspot Maximum, *J. Geophys. Res.*, **67**, 2119, June 1962.
- 13-46. Ness, N. F.: Satellite Measurements of the Geomagnetic Field, *NASA Report*, 1964.
- 13-47. O'Brien, B. J.: Review of Studies of Trapped Radiation with Satellite Borne Apparatus, *Space Science Rev.*, **1**, 415, 1962.
- 13-48. Perl, M. L.: The Status of the Scintillation Counter, *IRE Trans.*, **NS-9**, 236, June 1962.
- 13-49. Reagan, J. B. and Smith, R. V.: Instrumentation for Space Radiation Measurements, *IEEE Trans.*, **NS-10**, 172, Jan. 1963.
- 13-50. Roberts, A.: Progress in Spark Chamber Technology, *Nucleonics*, **22**, 68, May 1964.
- 13-51. Ruddock, K. A.: Optically Pumped Rubidium Vapor Magnetometer for Space Experiments, in *Space Research II*, H. C. van de Hulst, C. de Jager, and A. F. Moore, eds., Interscience Publishers, New York, 1961.
- 13-52. Schearer, L. D., Colegrove, F. D., and Walters, G. K.: Optically Pumped Nuclear Magnetometer, *Rev. Sci. Inst.*, **34**, 1363, Dec. 1963.
- 13-53. Serbu, G. P., Bourdeau, R. E., and Donley, J. L.: Electron Temperature Measurements on the Explorer VIII Satellite, *J. Geophys. Res.*, **66**, 4313, 1961.
- 13-54. Slocum, R. E. and Reilly, F. N.: Low Field Helium Magnetometer for Space Applications, *IEEE Trans.*, **NS-10**, 165, Jan. 1963.
- 13-55. Smith, R. V., Reagan, J. B., and Alber, R. A.: Use of Scintillation Detectors for Space Radiation Measurements, *IRE Trans.*, **NS-9**, 386, June 1962.
- 13-56. Sonnett, C. P. *et al.*: A Radial Rocket Survey of the Distant Geomagnetic Field, *J. Geophys. Res.*, **65**, 55, Jan. 1960.
- 13-57. Sonett, C. P.: Experimental Physics Using Space Vehicles, in *Advances in Space Science*, **2**, F. I. Ordway, III, ed., Academic Press, New York, 1960.
- 13-58. Wilkinson, D. H.: The Phoswitch—A Multiple Phosphor, *Rev. Sci. Inst.*, **23**, 414, Aug. 1952.
- 13-59. Wyckoff, R. C., ed.: Scientific Experiments for Mariner R-1 and R-2, Jet Propulsion Laboratory, *TR-315*, 1962.

#### 14. Instruments for Measuring Planetary Atmospheres

- 14-1. Barath, F. T.: Microwave Radiometer Development for Mariner Venus 1964, Jet Propulsion Laboratory, *SPS 37-23*, **4**, 258, 1963.
- 14-2. Barath, F. T. *et al.*: Mariner 2 Microwave Radiometer Experiment and Results, *Astrophys. J.*, **69**, 49, Feb. 1964.
- 14-3. Barrett, A. H. and Lilley, E.: Mariner-2 Microwave Observations of Venus, *Sky and Telescope*, **25**, 1, April 1963.
- 14-4. Bourdeau, R. E.: Space Flight Studies of the Ionosphere, in *Proceedings of the NASA-University Conference on the Science and Technology of Space Exploration*, **1**, 115, Government Printing Office, Washington, 1962.
- 14-5. Bowman, L., Josias, C., and Marshall, J. H.: Gas Chromatograph Instrumentation Development, Jet Propulsion Laboratory, *SPS 37-20*, **4**, 169, 1963.

- 14-6. Bull, H. T.: Planetary Interferometer, Jet Propulsion Laboratory, *SPS 37-23*, 4, 254, 1963.
- 14-7. Chaney, L. W. and Loh, L. T.: An Infrared Interference Spectrometer—Its Evaluation, Test, and Calibration, *NASA CR-61*, 1964.
- 14-8. Chase, S. C. and Neugebauer, G.: The Mariner 2 Infrared Radiometer Experiment, *J. Geophys. Res.*, 68, 6157, Nov. 15, 1963.
- 14-9. Chleck, D., Maehl, R., and Cucchiara, O.: Kryptonates: Kr<sup>85</sup> Becomes a Universal Tracer, *Nucleonics*, 21, 53, July 1963.
- 14-10. Chleck, D. and Cucchiara, O.: Radioactive Kryptonates—III. Applications, *J. Appl. Rad. and Isotopes*, 14, 599, 1963.
- 14-11. de Vaucouleurs, G.: Planetary Observations from Space Probes and Orbiters, in *Space Age Astronomy*, A. J. Deutsch and W. B. Klemperer, eds., Academic Press, New York, 1962.
- 14-12. Fastie, W. G.: Instrumentation for Far Ultraviolet Rocket Spectrophotometry, *NASA TN D-2250*, 1964.
- 14-13. Flattau, T. and Donegan, R.: Final Report for Study of Topside Sounder for Mars and Venus Ionosphere from Mariner Spacecraft, *NASA CR 52731*, 1963.
- 14-14. Gibson, H. and Nicholls, M. J.: A Study of the Radio-Frequency Probe Technique for Plasma Electron Density Measurements, *Brit. J. Appl. Phys.*, 14, 870, Dec. 1963.
- 14-15. Hanel, R. A. *et al.*: Experiments from a Small Probe Which Enters the Atmosphere of Mars, *NASA TN D-1899*, 1963.
- 14-16. Hanel, R. A.: Exploration of the Atmosphere of Venus by a Simple Capsule, *NASA TN D-1909*, 1964.
- 14-17. Hanel, R. A.: Low Resolution Radiometer, *ARS J.*, 31, 246, Feb. 1961.
- 14-18. Herzog, R. F. K. *et al.*: Determination of Atmospheric Parameters by the Use of Rocket-Borne Mass Spectrometers, *NASA CR-9*, 1963.
- 14-19. Jackson, J. E., Knecht, R. W., and Russell, S.: First Topside Soundings of the Ionosphere, *NASA TN D-1538*, 1963.
- 14-20. Jenkins, F. A. and White, H. E.: *Fundamentals of Optics*, McGraw-Hill Book Co., New York, 1950.
- 14-21. Karmen, A. and Bowman, R. L.: *Gas Chromatography*, Academic Press, New York, 1962.
- 14-22. Marshall, J. H. and Franzgrote, E. J.: Analysis of the Martian Atmosphere by Alpha Particle Bombardment, Jet Propulsion Laboratory, *SPS 37-26*, 4, 148, 1964.
- 14-23. Narcisi, R. S. *et al.*: Calibration of a Flyable Mass Spectrometer for N and O Atom Sensitivity, in *Space Research III*, W. Priester, ed., Interscience Publishers, New York, 1963.
- 14-24. Newton, G. P. *et al.*: Response of Modified Redhead Magnetron and Bayard-Alpert Vacuum Gauges aboard Explorer XVII, *NASA TN D-2146*, 1964.
- 14-25. Nier, A. O. *et al.*: Neutral Composition of the Atmosphere in the 100-to-200-Kilometer Range, *J. Geophys. Res.*, 69, 979, March 1, 1964.
- 14-26. Paul, W., Reinhard, H. P., and von Zahn, W.: Das Elektrische Massenspektrometer als Massenspektrometer und Isotopentrenner, *Zeit. f. Phys.*, 152, 143, 1958.
- 14-27. Rea, D. G.: Molecular Spectroscopy of Planetary Atmospheres, *Space Science Rev.*, 1, 159, Oct. 1962.

- 14-28. Rea, D. G. and Welch, W. J.: The Reflection and Emission of Electromagnetic Radiation by Planetary Surfaces and Clouds, *Space Science Rev.*, **2**, 558, Oct. 1963.
- 14-29. Richter, E. W., Robichaud, A. W., and Williams, T. S.: Multichannel Millimeter Radiometer for Deep Space, in *1962 Proceedings, National Aerospace Electronic Conference*, 1962.
- 14-30. Schaefer, E. J. and Nichols, M. H.: Neutral Composition Obtained from a Rocket-Borne Mass Spectrometer, in *Space Research IV*, P. Muller, ed., Interscience Publishers, New York, 1964.
- 14-31. Schaefer, E. J. and Nichols, M. H.: Mass Spectrometer for Upper Air Measurements, *ARS J.*, **31**, 1773, Dec. 1961.
- 14-32. Seiff, A.: Some Possibilities for Determining the Characteristics of the Atmospheres of Mars and Venus from Gas-Dynamic Behavior of a Probe Vehicle, *NASA TN D-1770*, 1963.
- 14-33. Spencer, N. W. and Reber, C. A.: A Mass Spectrometer for an Aeronomy Satellite, in *Space Research III*, W. Priester, ed., Interscience Publishers, New York, 1963.
- 14-34. Taylor, H. A., Brinton, H. C., and Smith, C. R.: Instrumentation for Atmospheric Composition Measurements, Instrument Society of America, *Proceedings of the 1962 National Aerospace Symposium*, 1962.
- 15. Instruments for Analyzing a Planet's Crust**
- 15-1. Adamski, D. F.: The Lunar Seismograph Experiment: Ranger 3, 4, 5, Jet Propulsion Laboratory, *TR 32-272*, 1962.
- 15-2. Anonymous: Scientific Experiments for Ranger 3, 4, and 5, Jet Propulsion Laboratory, *TR 32-199 (Rev.)*, 1962.
- 15-3. Anonymous: Final Technical Report on Feasibility Study of Drilling a Hole on the Moon, *AD-258 661*, 1960.
- 15-4. Arnold, J. R.: Gamma Ray Spectroscopy of the Moon's Surface, *Proc. Lunar and Planetary Expl. Coll.*, **I**, no. 3, Oct. 1958.
- 15-5. Bollin, E. M.: Lunar Surface and Subsurface Magnetic Susceptibility Instrumentation, *IRE Trans.*, **I-11**, 102, Dec. 1962. Also issued as *JPL TR 32-343*, 1962.
- 15-6. Burns, E. A. and Lyon, R. J. P.: Instrumentation for a Mineralogical Satellite, *Proceedings of the XIIIth. International Astronautical Congress*, in preparation.
- 15-7. Burns, E. A. and Lyon, R. J. P.: Feasibility of Remote Compositional Mapping of the Lunar Surface. Effects of Surface Roughness, *NASA CR 50544*, 1963.
- 15-8. Cameron, R. E.: The Role of Soil Science in Space Exploration, *Space Science Rev.*, **2**, 297, Aug. 1963.
- 15-9. Canup, R. E. *et al.*: Surveyor Geophysical Instrument, Interim Report, *NASA CR 52133*, 1962.
- 15-10. Eimer, M.: Photography of the Moon from Space Probes, Jet Propulsion Laboratory, *TR 32-347*, 1963.
- 15-11. Eimer, M.: Measuring Lunar Properties from a Soft-Lander, *Astronautics*, **7**, 30, July 1962.
- 15-12. Franzgrote, E.: Compositional Analysis by Alpha Scattering, Jet Propulsion Laboratory, *SPS 37-20*, **4**, 186, 1963.

- 15-13. Green, J. and Van Vopik, J. R.: The Role of Geology in Lunar Exploration, in *Advances in Space Science and Technology*, 3, F. I. Ordway, ed., Academic Press, New York, 1961.
- 15-14. Heiles, C. E. and Drake, F. D.: The Polarization and Intensity of Thermal Radiation from a Planetary Surface, *Icarus*, 2, 281, Nov. 1963.
- 15-15. Kovach, R. L. and Press, F.: Lunar Seismology, Jet Propulsion Laboratory, *TR 32-328*, 1962.
- 15-16. Kovach, R. L., Press, F., and Lehner, F.: Seismic Exploration of the Moon, *AIAA Preprint 63-255*, 1963.
- 15-17. Leary, F.: Television from Space, *Space/Aeronautics*, 41, 70, March 1964.
- 15-18. Lehner, F. E. *et al.*: A Seismograph for Lunar Experiments, *J. Geophys. Res.*, 67, 4779, Nov. 1962.
- 15-19. Lyon, R. J. P.: Evaluation of Infrared Spectrophotometry for Compositional Analysis of Lunar and Planetary Soils, *NASA TN D-1871*, 1963.
- 15-20. Lyon, R. J. P. and Burns, E. A.: Infrared Spectral Analysis of the Lunar Surface from an Orbiting Spacecraft, Proceedings of the Second Symposium on Remote Sensing of Environments.
- 15-21. Martina, E. F.: Neutron-Gamma Ray Instrumentation Experiment for Lunar Surface Composition Analysis, Aerospace Corp., *TDR-930(2260-31) TR-1*, 1962.
- 15-22. Martina, E. F. and Schrader, C. D.: Analysis of the Moon's Surface by Nuclear Reactions, University of California, *UCRL-5916*, 1960.
- 15-23. McCarthy, J. L., Beswick, A. G., and Brooke, G. W.: Application of Penetrometers to the Study of Physical Properties of Lunar and Planetary Surfaces, *NASA TN D-2413*, 1964.
- 15-24. Mesner, M. H. and Staniszewski, J. R.: Television Cameras for Space Exploration, *Astronautics*, 5, 36, May 1960.
- 15-25. Metzger, A. E. *et al.*: Ranger Gamma Ray Spectrometer, *Nucleonics*, 20, 64, Oct. 1962.
- 15-26. Metzger, A. E.: Electron-Excited X-ray Fluorescence for Lunar Surface Analysis—Analytical Studies, Jet Propulsion Laboratory, *SPS 37-26*, 4, 143, 1964.
- 15-27. Metzger, A. E.: Some Calculations Bearing on the Use of Neutron Activation for Remote Compositional Analysis, Jet Propulsion Laboratory, *TR 32-186*, 1962.
- 15-28. Miller, D. C. and Handee, C. F.: X-ray Analysis of the Lunar Surface, *ARS Paper 61-109-1803*, 1961.
- 15-29. Monaghan, R. *et al.*: Instrumentation for Nuclear Analysis of the Lunar Surface, *IEEE Trans.*, NS-10, 183, Jan. 1963.
- 15-30. Murphy, C. B.: Differential Thermal Analysis, *Modern Plastics*, Aug. 1960.
- 15-31. Nash, D. B.: X-ray Diffraction Studies on Silicate Rock Glasses, Jet Propulsion Laboratory, *SPS 37-20*, 4, 1963.
- 15-32. Oyama, V. I., Vango, S. P., and Wilson, E. M.: Application of Gas Chromatography to the Analyses of Organics, Water, and Adsorbed Gases in the Lunar Crust, *ARS J.*, 32, 354, March 1962, also issued as *JPL TR 32-107*, 1961.
- 15-33. Peckham, V. A. and Dallas, J. P.: Development of a Lunar Rock Drill and Subsurface Sampling System, *IEEE Trans.*, AS-2, 388, April 1964.

- 15-34. Press, F., Buwalda, P., and Neugebauer, M.: A Lunar Seismic Experiment, *J. Geophys. Res.*, **65**, 3097, 1960.
- 15-35. Schrader, C. D. and Stinner, R. J.: Remote Analysis of Surfaces by Neutron-Gamma Ray Inelastic Scattering Technique, *J. Geophys. Res.*, **66**, 1951, 1961.
- 15-36. Schrader, C. D. *et al.*: Neutron-Gamma Ray Instrumentation for Lunar Surface Composition Analysis, *ARS J.*, **32**, 631, April 1962.
- 15-37. Schrader, C. D.: Analyzing the Moon's Surface, *Nucleonics*, **20**, 67, Oct. 1962.
- 15-38. Speed, R. C. *et al.*: Geological Exploration of the Moon and Planets, in *Proceedings of the NASA-University Conference on the Science and Technology of Space Exploration*, Government Printing Office, Washington, 1962.
- 15-39. Thorman, H. C.: Review of Techniques for Measuring Rock and Soil Strength Properties at the Surface of the Moon, *SAE Paper 632C*, 1963.
- 15-40. Trombka, J. I. and Metzger, A. E.: Neutron Methods for Lunar and Planetary Compositional Studies, in *Analysis Instrumentation—1963*, L. Fowler, R. D. Eanes, T. J. Kehoe, eds., Plenum Press, New York, 1963.
- 15-41. Trombka, J. and Metzger, A.: The Use of Neutron Activation for Lunar and Planetary Surface Compositional Studies, Jet Propulsion Laboratory, *SPS 37-20*, **4**, 190, 1963.
- 15-42. Turkevich, A.: Chemical Analysis of Surfaces by Use of Large-Angle Scattering of Heavy Charged Particles, *Science*, **134**, 672, Sept. 8, 1961.
- 15-43. Van Dilla, M. A. *et al.*: Lunar Composition by Scintillation Spectroscopy, *IRE Trans.*, **NS-9**, 405, June 1962.
- 15-44. Wilhite, W. F.: The Development of the Surveyor Gas Chromatograph, Jet Propulsion Laboratory, *TR 32-425*, 1963.
- 15-45. Wilhite, W. F. and Burnell, M. R.: The Lunar Gas Chromatograph: Design Problems and Solutions, in *Analysis Instrumentation—1963*, L. Fowler, R. D. Eanes, T. J. Kehoe, eds., Plenum Press, New York, 1963.
- 16. Instruments for Detecting Life**
- 16-1. Anonymous: The Search for Extraterrestrial Life, *NASA EP-10*, 1963.
- 16-2. Blei, I.: Detection of Extraterrestrial Life: Method II: Optical Rotary Dispersion, *NASA N62-16489*, 1962.
- 16-3. Briggs, M. H.: Automated Life-Detection Devices, *Spaceflight*, **5**, 128, July 1963.
- 16-4. Cameron, A. G. W., ed.: *Interstellar Communication*, W. A. Benjamin, New York, 1963.
- 16-5. Eskind, N.: Sample Collection for Mars Biological Experiments, Jet Propulsion Laboratory, *SPS 37-23*, **4**, 275, 1963.
- 16-6. Green, V. W. *et al.*: Microscopic System for Mars Study Program, *NASA CR 51538*, 1962.
- 16-7. Heim, A. H.: Radioisotopic Metabolic Detection of Possible Martian Life Forms, *Proc. Lunar and Planetary Exploration Coll.*, **III**, no. 2, 37, May 5, 1963.
- 16-8. Lederberg, J. and Sagan, C.: Microenvironments for Life on Mars, *Proc. Nat'l. Acad. Sci.*, **48**, 1473, 1962.
- 16-9. Lederberg, J.: Exobiology: Experimental Approaches to Life Beyond the Earth, in *Science in Space*, L. V. Berkner and H. Odishaw, eds., McGraw-Hill Book Co., New York, 1961.



- 16-10. Levin, G. V. and Carriker, A. W.: Life on Mars?, *Nucleonics*, **20**, 71, Oct. 1962.
- 16-11. Levin, G. V. *et al*: Gulliver: A Quest for Life on Mars, *Science*, **138**, 114, Oct. 12, 1962.
- 16-12. Levinthal, E.: Payload to Mars, *Stanford Today*, Winter, 1963.
- 16-13. Oparin, A.: The Origin of Life in Space, *Space Science Rev.*, **3**, 5, July 1964.
- 16-14. Oyama, V. I.: Mars Biological Analysis by Gas Chromatography, *Proc. Lunar and Planetary Exploration Coll., III*, no. 2, 29, May 1963.
- 16-15. Rea, D. G., Belsky, T., and Calvin, M.: Interpretation of the 3- to 4-Micron Infrared Spectrum of Mars, *Science*, **141**, 923, Sept. 6, 1963.
- 16-16. Rho, J. H.: Fluorometric Measurements of Growth: II. Fluorescence as a Measure of Bacterial Growth of Proteins, Jet Propulsion Laboratory, *SPS 37-25*, **4**, 243, 1963.
- 16-17. Sinton, W. M.: Spectroscopic Evidence for Vegetation on Mars, *Astrophys. J.*, **126**, 233, Sept. 1957.
- 16-18. Sinton, W. M.: Further Evidence of Vegetation on Mars, *Science*, **130**, 1237, Nov. 6, 1959.
- 16-19. Soffen, G. A.: Simple Vidicon Microscopy, *Proc. Lunar and Planetary Exploration Coll., III*, no. 2, 47, May 1963.
- 16-20. Stuart, J. L.: Extraterrestrial Biological Instrumentation Problems, *Proc. San Diego Symp. for Biomedical Eng.*, 1963.
- 16-21. Stuart, J. L.: Instrumentation Requirements for Life Detection Systems, paper presented at the First Rocky Mountain Bioengineering Symposium, 1964.
- 16-22. Tuttle, S. B.: Lightweight Sample Collector for Exobiology Experiments, Jet Propulsion Laboratory, *SPS 37-24*, **4**, 220, 1963.
- 16-23. Vishniac, W.: Extraterrestrial Biology, *Aerospace Medicine*, **31**, 678, 1960.
- 16-24. Weston, C. R.: Principles of Optical Measurements Applied to Biological Growth in the Wolf Trap, paper presented at the First Rocky Mountain Bioengineering Symposium, 1964.
- 16-25. Young, R. S.: Exobiology, in *Proceedings of the NASA-University Conference on the Science and Technology of Space Exploration*, **1**, 423, Government Printing Office, Washington, 1962.

## 17. Instruments Used on Solar, Cometary, and Asteroidal Probes

- 17-1. Beller, W.: Scientists Plan Missions to Comets, *Missiles & Rockets*, **12**, 22, May 6, 1963.
- 17-2. Benton, R.: Exploring the Comets, *Spaceflight*, **6**, 110, July 1964.
- 17-3. Donn, B.: Coma Formation and an Artificial Comet Experiment, *Astronomical J.*, **66**, 282, Sept. 1961.
- 17-4. Goldberg, L. and Dyer, E. R.: The Sun, in *Science in Space*, L. V. Berkner and H. Odishaw, eds., McGraw-Hill Book Co., New York, 1961.
- 17-5. Lair, J. C.: The Mission to a Comet, Space Technology Laboratory, *9844-0023-MU-RO1, AD 265 306*, 1961.
- 17-6. Newburn, R. L.: The Exploration of Mercury, the Asteroids, the Major Planets and their Satellite Systems, and Pluto, in *Advances in Space Science and Technology*, **3**, F. I. Ordway, ed., Academic Press, New York, 1961.

- 17-7. Space Technology Laboratory: Comet Intercept Study—Final Report, *8668-6002-RU-000*, 1963.
- 17-8. Swings, P.: Recent Progress in Cometary Spectroscopy, *AFCLR-64-227*, *AD 430 639*, 1963.
- 17-9. Swings, P.: Possible Contributions of Space Experiments to Cometary Physics, Smithsonian Astrophysical Observatory, *Rpt. 111, N63-14253*, 1962.
- 17-10. Swings, P.: Objectives of Space Investigation of Comets, in *Space Age Astronomy*, A. J. Deutsch and W. B. Klemperer, eds., Academic Press, New York, 1962.

# INDEX

- ABL, 502  
Accelerometers, in guidance and control, 224-227  
    history of, 14  
    integrating, 227  
Acoustic transmission line, in atmospheric research, 418-420  
Activation analysis, 382, 429, 443, 456-459  
Adaptive control, 107  
    (See also Automata)  
Advanced Pioneer (see Solar probe)  
Aerobee sounding rocket, 9, 405  
Aeronomy, instruments used in, 381-426  
Aerosol microscope, 492, 493  
Alpha scattering experiment, 382, 402, 443  
    in atmospheric analysis, 415-417  
    in crustal analysis, 447-449  
Amino acids, detection of, 478, 486  
Anemometers, 383, 424  
Antennas, Earth-based, 92, 94, 97, 99, 150  
    Mariner-2, 192  
    spacecraft, 94  
Apollo Program, 178  
ARIS ships, 147, 148  
Asteroids, description of, 30, 31  
    probes to the, 273-275  
    instruments on, 503, 504, 507  
Astrodynamics (see Space mechanics)  
Astronomical Unit, measurement of, 12, 20, 379, 380  
Atlas, 17  
Atlas-Agena, characteristics, 172  
Atlas-Centaur, characteristics, 173  
Atmospheres, planetary, description of, 27-31  
    instruments for measuring, 381-426  
    questions about, 5  
    sample collection in, 400, 401  
Atmospheric braking, 62, 63  
    (See also Drag bodies, Reentry)  
Atomic clock experiments, 21  
Attitude control, comparison of techniques for, 212-214  
    coordinate systems for, 77  
    equations for, 77  
    history of, 11  
    sensors for, 123  
    spin stabilization in, 213  
Attitude-control subsystem, definition of, 76  
    design of, 210-215  
    effect on antenna beamwidth, 95  
    functions of, 39, 210  
    interfaces, 75, 211  
    Mariner-2, 214, 215  
    momentum requirements of, 211  
Automata, 4, 15, 18, 34, 108, 109  
    theory of, 123-126  
Automated Biological Laboratory, 502  
Automatic checkout, 140-142  
    (See also Checkout)  
Batteries, 202  
Beacons, 112  
Bennett tube (see Radio frequency mass spectrometer)  
Biological contamination, 46  
    (See also Sterilization)  
Bioluminescence, in life detection, 480, 485, 498  
Bistatic radar, 383, 440, 441  
    in atmospheric research, 421  
    in planetary surface study, 440, 441  
Block allocation of payload space, 292  
Blockhouse, 144, 145  
Bottomside sounders, 383, 420, 428  
Brahe, Tycho, 11  
Braking ellipses, 63  
    (See also Atmospheric braking, Reentry)  
British Interplanetary Society, 10, 11  
Bubble chamber, 315, 348  
Bumper Project, 16  
Cadmium-sulfide cell, 314, 323-325, 375  
Capacitor micrometeoroid detector, 364, 370, 371  
Cape Canaveral (see Cape Kennedy)  
Cape Kennedy, 16, 144-148  
Celestial mechanics, history, 4, 43  
    (See also Space mechanics)  
Cerenkov detector, 314, 322, 323  
Channel multiplier, 314, 319, 320  
Characteristic velocity, definition, 58  
Checkout, automatic, 140-142  
    history, 15  
    operations during, 137-141  
Chemiluminescence, in atmospheric research, 417

- Chromatography (*see* Gas chromatographs, Paper chromatography)
- Clairaut, A. C., 11, 12
- Clock experiments, 21
- Clock, spacecraft, 122
- Cloud chamber, 315, 347, 348
- Cognitive devices (*see* Adaptive control, Automata)
- Comets, description of, 32  
   probes to, 270, 272  
   instruments for, 506  
   velocity requirements for, 66, 75
- Commands, flow paths of, 122, 123
- Communication, antenna for, 92, 94  
   bandwidth considerations in, 83  
   data processing, 81, 100, 101  
   frequency selection in, 94  
   history of, 12  
   improvements in, 97  
   information carriers, 85, 86  
   information theory in, 83  
   lasers in, 86  
   matched receivers in, 84  
   modulation in, 87  
   multiplexing in, 90  
   noise in, 83, 91, 92  
   phase-lock approach in, 82  
   redundancy in, 84
- Communication subsystem, constraints in design of, 92-96  
   design, 187-194  
   engineering trade-offs in, 82  
   functions of, 39  
   integration, 189-194  
   interfaces, 80, 95, 188  
   for Mariner 2, 82, 83, 191  
   sterilization of, 9  
   typical block diagram, 81
- Computer, in attitude control, 76, 78
- Computer subsystem, design, 230-232  
   functions of, 39, 223  
   interfaces, 231  
   for Mariner 2, 232, 233
- Congreve, W., 15, 157
- Control (*see* Guidance and control)
- Cosmic dust (*see* Micrometeoroids)
- Cosmic rays, characteristics of, 23-25, 312  
   Forbush decrease of, 24, 25  
   (*See also* Radiation detectors)
- Cost, as a performance factor, 38  
   of launch vehicles, 158-160
- Countdown sequence, 139
- Crocco orbit, 47, 53
- Crustal research instruments, 427-476
- Curved-surface plasma analyzers, 349-356
- Data compression, 84, 100, 440
- Data processing, 81, 100, 101, 290
- Data selection, 85
- Dating, isotopic, 382, 443, 463, 464
- Deep Space Net, 129  
   (*See also* DSIF)
- Deep Space Instrumentation Facility (*see* DSIF)
- Deimos, 30
- Densitometers, gas, 382, 402, 417-420  
   surface, 429, 443, 459-461
- Differential thermal analysis, 382, 443, 461, 462
- Discoverer Program, 318
- Drag bodies, 383, 423, 425, 426
- Drills, 475
- DSIF, 79, 127  
   antennas, 99, 150  
   description of, 146-153  
   frequencies used in, 93  
   site locations, 93, 97, 150  
   in tracking, 112, 114, 149  
   accuracy, 114  
   (*See also* SFOF)
- DSN (*see* DSIF)
- Earth, atmospheric windows, 8  
   magnetic field, 21-23  
   magnetopause, 22
- Eastern Test Range, 16, 146-148  
   (*See also* Cape Kennedy)
- EGO, mass spectrometer, 411  
   positron detector, 342-344
- Einstein, A., 20
- Electric-conductivity meter, 383, 465, 467
- Electric propulsion, advantages of, 51  
   in attitude control, 212  
   in interplanetary flight, 209, 210  
   space mechanics, 49
- Electrostatic plasma analyzers, 348-362
- Emulsion, 315, 347
- Engineering instruments, description of, 241-243  
   functions of, 39  
   on IMP, 243
- Environmental-control subsystem, 122  
   description of, 216-223  
   functions of, 39  
   interfaces, 217
- Environmental simulation, 130-132
- Esnault-Pelterie, R., 12
- ETR (*see* Eastern Test Range)
- Experiment, definition of, 289  
   list, 283-285  
   selection of, 292-295

- Explorer S-46, electron spectrometer, 335, 336
- Explorer 6, cosmic-ray telescope, 318  
magnetometer, 300
- Explorer 8, micrometeoroid detector, 375  
planar plasma probes, 357-359
- Explorer 10, Faraday-cup probe, 359, 360  
magnetometer, 298, 309
- Explorer 12, cadmium-sulfide cell, 324  
cosmic-ray telescope, 318  
plasma analyzer, 354
- Explorer 13, micrometeoroid detector, 374
- Explorer 16, micrometeoroid detectors, 372-375
- Explorer 18 (*see* IMP)
- Extraterrestrial life (*see* Life, extraterrestrial)
- Facilities, 127-153  
functions of, 39  
history, 15  
launch, 141-148  
testing, 130-136  
tracking, 148-153  
(*See also* DSIF)
- Faraday-cup plasma probes, 349, 356-361
- Flux, definition of, 313
- Fluxgate magnetometers, 299-305  
on IMP, 286, 302  
on Mariner 2, 286, 302-304  
on Pioneer 6, 286, 302, 304, 305
- Forbush decrease, 24, 331
- Foucault, J. B. L., 14
- Galle, J. G., 11
- Gamma-ray spectrometers, 452-454
- Gamma-ray telescopes, 334, 342, 343
- Gas chromatographs, in atmospheric analysis, 411-415  
in crustal analysis, 444-447  
in life detection, 445, 480, 485, 487  
principles of, 382, 402, 411, 412, 443  
Surveyor prototype, 444-447
- Gas densitometer, 382, 402, 417, 418
- Gas jets, in attitude control, 212
- Gauss, J. K. F., 11
- Geiger-Mueller counter, in Gulliver life detector, 495  
on IMP, 286  
with ionization chamber, 337-342  
in magnetic spectrometers, 335, 336  
on Mariner 2, 286  
on Mariner 4, 286, 327, 328  
on Pioneer 5, 286, 329  
in X-ray diffractometer, 455  
in X-ray spectrometer, 452
- Geodetic satellite, 383, 465, 475, 476
- Geophysical instruments, 464-476  
table of, 465
- Goddard, R. H., 9-12, 15-17, 110
- Goldstone site (*see* DSIF)
- Gravimeter, 383, 465, 475
- Gravitation, experiments in, 21, 378  
red shift due to, 21, 378
- Greenhouse model of Venusian atmosphere, 29
- Ground-support equipment, at launch site, 137-145  
history of, 15  
(*See also* Facilities)
- Guidance and control, aiming plot, 117  
closed-loop, 108, 109  
compared with navigation, 106  
feedback in, 108  
history of, 14  
at launch, 109, 110  
learning circuits in, 123-126  
midcourse, 107, 109  
open-loop, 108, 109  
planetary capture, 119, 120  
planetary descent, 121  
precursor, 120  
principles of, 105-126  
sources of trajectory error in, 52  
spacecraft clock in, 122  
terminal, 110, 117, 118  
trajectory accuracy in, 52  
(*See also* Automata, DSIF, Navigation, Tracking)
- Guidance-and-control subsystem, design, 223-230  
functions of, 39, 106, 108, 109  
interfaces, 106
- Gulliver, in life detection, 493-497
- Gyroscope, in attitude control, 76  
invention of, 14  
in trajectory guidance and control, 110, 111, 224-227  
types, 224, 225
- Heat transfer analysis on spacecraft, 216-221
- Helium magnetometers, 299, 309-312  
on Mariner 3 and Mariner 4, 287, 310, 311
- Hertz, H., 12
- History of space probes, 7-18
- Hohmann, W., 11
- Hohmann transfer orbit, 47, 56
- Horizon scanners, 228-230

- IAF, 8  
 ICBM, 14, 16, 17, 157  
 IGY, 9, 17  
 IMP, characteristics, 23, 248, 249  
   drawing, 252  
   engineering instrument list, 243  
   magnetometer, 286, 298, 302, 309  
   photographs of, 253, 254  
   plasma probe, 286, 349, 354, 359  
   radiation detectors, 286, 314, 315, 319  
     327, 330, 337, 340, 341  
   scientific instrument list, 286  
 Inertia wheels, in attitude control, 212  
 Inertial sensors (*see* Accelerometers, Gyroscope)  
 Information theory, 83  
 Injun satellite, 324, 326  
 Instruments (*see* Engineering instruments, Scientific instruments)  
 Integration, spacecraft, 36-39, 178-180, 288  
 Interfaces, definition of, 37, 179  
   problems, 13, 36, 176, 180, 288  
   specifications, 180  
 Interferometers, in scientific research, 386, 398, 399, 428, 429  
   in tracking, 112-114  
 International Astronautical Federation, 8  
 International Geophysical Year, 9, 17  
 Interplanetary gas, 20, 26  
 Interplanetary magnetic field, 23  
 Interplanetary Monitoring Platform (*see* IMP)  
 Interplanetary probes, characteristics of specific, 245-255  
 Interstellar probes, 34, 273-275  
   velocity requirements for, 66  
 Ion propulsion, 209-210  
   (*See also* Electric propulsion)  
 Ionization chamber, Neher type, 318, 330, 337, 340  
   principles of operation, 314, 316, 318, 319  
   used with Geiger-Mueller counters, 337-342  
 Ionospheric instruments, 420-422  
 Isotope interchange experiment, in life detection, 481, 485  
 J-Band life-detection experiment (*see* Stain experiments)  
 Jodrell Bank, 13, 17, 20  
 Juno II launch vehicle, 17  
 Jupiter, description, 30  
   flight windows, 67  
   magnetic field, 23  
   probes to, 274, 275  
   radiation belts, 23  
 Kepler, J., 11  
 Kryptonate experiment in atmospheric research, 382, 402, 415-417  
 Lagrange, J. L., 11  
 Landing capsules, 239, 240  
 Landing techniques, 239-241  
 Langmuir probes, 383, 420  
 Laplace, P. S. de, 11, 12  
 Laser, in communication, 86  
 Lasswitz, K., 9  
 Launch guidance, 109, 110  
 Launch operations, 137-148  
 Launch pad, 143, 144  
 Launch ranges, 145-148  
   (*See also* Cape Kennedy)  
 Launch vehicles, 154-175  
   characteristics, table of, 172-174  
   costs, 158-161  
   design of, 171  
   functions of, 39  
   interfaces of, 155  
   propulsive functions, 55  
   recovery of, 159  
   reliability of, 158  
   staging of, 161  
 Launch windows, 49, 61  
   planetary, table of, 67  
 Life detection, 477-502  
   instruments, table of, 480  
   nature of problem, 477-483  
   (*See also* Life, extraterrestrial)  
 Life, extraterrestrial, communication with, 34  
   condition for existence of, 33  
   existence of, 32-34  
   properties of, 482  
 Light-flash micrometeoroid detector, 364, 371, 372  
 Light-transmission micrometeoroid detector, 364, 374, 375  
 Limb-diffraction experiment, 383, 422, 428  
   on Mariner 4, 287, 422  
 Locomotion, on planetary surfaces, 206-209  
 Louvers, in spacecraft thermal control, 219-221  
 Lunar probes (*see* Ranger Program, Surveyor Program)  
 Lunik, ion traps, 361  
 Magnetic cleanliness, 222, 223, 298  
 Magnetic fields, of Earth, 21

- instruments for measuring, 297-311  
 measurable parameters of, 296  
 of the Moon, 23  
 of Venus, 21  
 (*See also* Magnetometers)
- Mneagtic-induction meters, 383, 465-467
- Magnetometers, design, 297-311, 465, 475, 506  
 fluxgate, 299-305  
 helium, 299, 309-312  
 on Mariner 2, 286, 302-304  
 on Mariner 3 and Mariner 4, 287, 310, 311  
 on Pioneer 6, 286, 304, 305  
 proton-precession, 299, 305, 306  
 rubidium-vapor, 299, 306-309  
 search-coil, 298-301
- Magnetopause, 22
- Marconi, G., 12
- Mariner 1, 257, 262  
 (*See also* Mariner 2)
- Mariner 2, aiming plot for, 117  
 antennas, 192  
 ascent trajectory, 146  
 attitude-control subsystem, 214, 215  
 Central Computer and Sequencer, 232, 233  
 characteristics, 258, 259  
 communication subsystem, block diagram, 191  
 performance, 82  
 data automation, 191  
 data encoder, 193  
 infrared radiometer, 389-392  
 infrared spectrometer (proposed), 396, 397  
 instrument list, 286  
 ionization chamber, 286, 318, 319  
 load profile, 195  
 louver temperature control, 220, 221  
 magnetometers, 286, 302-304  
 magnetic-field measurements, 22  
 micrometeoroid detector, 286, 364, 366-368  
 microwave radiometer, 286, 387-389  
 midcourse maneuver, 77, 112, 117  
 midcourse propulsion subsystem, 205, 206  
 plasma probe, 286, 349, 355-357  
 measurements during flight, 24  
 photograph of, 262  
 power supply, 198  
 radiation detectors, 286, 314, 315, 337  
 solar panels, 200  
 solar simulation for, 132  
 structure, 234, 235  
 word structure, 84
- Mariner 3, 263-265  
 ultraviolet photometer, 393-395  
 (*See also* Mariner 4)
- Mariner 4, 264  
 characteristics, 260, 261  
 cosmic-ray telescope, 287, 331, 332  
 instrument list, 287  
 magnetometer, 287, 310-312  
 micrometeoroid detector, 287, 364, 368, 369  
 photographs of, 264, 265  
 plasma probe, 287, 349  
 radiation detectors, 287, 314, 315, 319, 326, 327, 337, 342  
 radio propagation experiment, 287, 422  
 television experiment, 287, 437-440
- Mars, atmosphere of, 29  
 canals, 29, 30  
 description of, 29  
 flight windows, 67  
 flyby-probe velocity requirements, 68-71  
 life on, 30, 33  
 questions about, 29  
 satellites of, 30
- Mars scanner, for detection of micro-environments, 431-433, 482
- Mass spectrometer, in atmospheric research, 348, 401-411, 506  
 in crustal analysis, 443, 444  
 double-focusing, 403-407  
 in life detection, 480, 481, 485-487  
 list of types, 403  
 principles, 382  
 quadrupole, 403, 407-409  
 radio-frequency, 403, 410, 411  
 simple, 403-407  
 time-of-flight, 403, 409, 410
- Materials, in spacecraft structures, 236, 237
- Maxwell, J. C., 12
- Mercury, description of, 28  
 flight windows, 67  
 perihelion, rotation of, 20  
 probe, 274, 275
- Mercury Project, 16
- Metabolism detector, 479, 481, 486, 493-498  
 (*See also* Gulliver)
- Meteoroid protection, 237, 238  
 (*See also* Micrometeoroids)
- Meteorological instruments, 423, 424
- Microenvironments for life, detection of, 431, 482  
 (*See also* Mars scanner)

- Microlock, 16
- Micrometeoroid detectors, calibration, 363, 367  
 design, 362-377  
 on Explorer 16, 372-375  
 on Mariner 2, 286, 366-368  
 on Mariner 4, 287, 368, 369  
 on Pioneer 5, 286, 365  
 table of types, 364, 376
- Micrometeoroids, damage from, 237, 238  
 description, 26, 27  
 instruments for measuring, 362-367  
 mass distribution, 27  
 measurable parameters, 296
- Microscope, aerosol, 492, 493  
 petrographic, 382, 428, 443, 462, 463
- Midcourse correction, definition of, 62  
 geometry of, 116  
 for Mariner 2, 117  
 timing of, 113  
 typical sequence, 112
- Midcourse guidance, 107, 109
- Mineral identification, from infrared spectra, 433-435
- Minitrack, history, 16
- Minivator (*see* Multivator)
- Missions, for space probes, delineation, 46
- Modulation, in communications, 82, 87  
 comparison of different types, 89  
 importance in tracking, 89  
 PCM, 82, 88  
 phase-lock, 82, 88, 89
- Moon, magnetic field, 23
- MOUSE, 9
- Multiplexing of instruments, 90
- Multivator, in life detection, 486, 493, 497-502
- Navigation, celestial, 112, 113, 115  
 definition of, 106  
 history of, 14
- Neptune, description of, 30  
 discovery of, 11
- Neutron activation analysis, 382, 429, 443, 456-459
- Neutron detectors, 315, 334, 336, 337
- Neutron inelastic scattering experiment, 443, 456, 459
- Newton, I., 11, 12, 20
- Noise, in communication, 83, 91, 92  
 cosmic, 93
- Nova launch vehicle, 174
- Nuclear abundance detector, 315, 343-345
- Nuclear rockets, 51, 157  
 characteristics of, 162-164  
 principles of, 168-170
- OAO, 26, 503  
 ultraviolet spectrometer, 399
- Oberth, H., 9, 11, 12
- Objectives of space-probe research, 3-6
- OGO, 36, 343
- Optical pumping, (*see* Helium magnetometer, Rubidium-vapor magnetometer)
- Optical-rotary-dispersion experiment, in life detection, 478, 481, 486, 491, 498
- Optical sensors, 226-230
- Orbital assembly, 162
- Orbiting Astronomical Observatory (*see* OAO)
- Orbiting Geophysical Observatory (*see* OGO)
- Orbiting Solar Observatory (*see* OSO)
- Organized elements in meteorites, 479, 492
- OSO, 26, 32, 270
- Out-of-ecliptic probes, 65, 253, 254, 274, 275
- Ozma, Project, 34  
 (*See also* Radio listening experiments)
- Panspermia, 5, 33, 487, 507
- Paper chromatography, in life detection, 487
- Parity bit, 84
- Parking orbit, 56
- Paul Massenfilter (*see* Quadrupole mass spectrometer)
- Peenemunde, 16
- Penetrometers, 468-470
- Peptide-bond detection, in life detection, 487-489
- Performance, measures of, 38, 289
- Petrographic microscope, 382, 428, 443, 462, 463
- pH measurement, in life detection, 480, 485, 489, 490, 498  
 (*See also* Wolf Trap)
- Phase lock, in communication, 82, 88, 89
- Phobos, 30
- Phosphatase reaction, in life detection, 498-500
- Phoswich, 330, 333, 334, 342
- Photometer, 382-395, 428-435, 505  
 infrared, 430-435  
 principles of, 382-385, 428-430  
 ultraviolet, 386  
 for Mariner 3, 393-395
- X-ray, 386  
 (*See also* Mars scanner)



- Piezoelectric ballistic pendulum, in micrometeoroid detection, 364, 369, 370
- Piezoelectric microphone, in micrometeoroid detection, 364-369  
 calibration of, 367  
 on IMP, 286  
 on Mariner 2, 286, 364, 366-368  
 on Mariner 4, 287, 364, 368, 369  
 on Pioneer 5, 286, 367
- Pioneer Program, 10, 18, 300
- Pioneer 1, 17
- Pioneer 5, characteristics, 246, 247  
 instrument list, 286  
 magnetometer, 286, 300, 301  
   results from, 22  
 micrometeoroid detector, 286, 367  
 photograph of, 245  
 proportional counter telescope, 286, 318, 319  
 radiation detectors, 286, 314, 315, 328, 337
- Pioneer 6, characteristics of, 250, 251  
 cosmic-ray telescope, 286, 331  
 drawing, 255  
 instrument list, 286, 287  
 magnetometer, 286, 302-304  
 photograph of, 256  
 plasma probe, 286, 349-354, 359  
 radiation detectors, 286, 314, 315, 327  
 radio propagation experiment, 287, 360, 361, 378
- Planar plasma probes, 349, 356-361
- Planets, descriptions of, 28  
 launch windows, 67  
 mass measurements, 20  
 questions about, 5
- Plasma, description of, 23, 24  
 instruments, 348-362, 506  
 measurable properties, 296  
 (*See also* Solar wind)
- Plasma probes (*see* Curved-surface plasma analyzers, Faraday-cup plasma probes)
- Pluto, description of, 28, 31  
 discovery of, 11  
 origin of, 53
- Polarimeters, 382, 384, 385, 400, 428, 506
- Positron detector, 342, 343
- Post-Saturn launch vehicle, 174
- Powered descent, 64
- Power-supply subsystem, description, 194-203  
 functions of, 39  
 interfaces, 95, 199  
 on Mariner 2, block diagram, 198  
 load profile, 195  
 solar panels, 200  
 radioisotopic power, 201-203, 221, 222, 453
- Pressure gauges, 383, 424
- Pressurized-can micrometeoroid detector, 364, 372, 373
- Private-A rocket, 16
- Proof-test spacecraft model, 135
- Proportional counter, 314, 316-319, 452  
 on Pioneer 5, 286, 318, 319
- Propulsion, chemical, 162-168  
 comparison of types, 51  
 ion, 44, 209, 210  
 nuclear, 162-164, 168-170  
 surface, 206-209
- Propulsion subsystem, design, 203-210  
 functions of, 39, 46, 53, 212  
 on Mariner 2, 205, 206  
 surface, 206-209
- Proteins, detection of, 478, 487-489
- Proton-precession magnetometer, 299, 305, 306
- Quadrupole mass spectrometer, 403, 407-409
- Radar, bistatic, 383, 421, 440, 441  
 in guidance and control, 111, 112, 118, 121, 229, 230  
 history of, 14  
 in tracking, 148  
 in scientific measurement, 382, 428, 430
- Radar astronomy, in measurement of the A.U., 20
- Radiation, description, 23-27
- Radiation damage, 221, 222
- Radiation detectors, descriptions, 311-348  
 list of major types, 283
- Radio astronomy, 13
- Radio-frequency mass spectrometer, 357
- Radio interferometer, 112
- Radio listening experiments, 485  
 (*See also* Ozma, Project)
- Radioisotopic power, 201-203, 221, 222, 453
- Radiometer, Dicke, 388  
 infrared, 386, 389-392  
   on Mariner 2, 286, 386-392  
 microwave, 386-389, 428  
   on Mariner 2, 286, 386-389  
 principles of, 382-395, 428, 429  
 Suomi, 391
- Radio propagation experiments, 378, 506

- on Mariner 4, 287, 422
- on Pioneer 6, 287, 360, 361, 378
- (See also Limb diffraction experiments)
- Ram spectrometer, 382, 402, 417, 423, 429
- Ranger Program, 12, 18, 178, 318, 326, 354, 372, 430
  - gamma-ray spectrometer, 452-454
  - seismometer, 472, 473
- Recoverable launch vehicles, 159, 161, 170
- Redox-potential experiment, in life detection, 480, 485, 498
- Redstone launch vehicle, 17
- Reentry, corridors, 62, 119, 238
  - heating, 62, 63, 238-240
  - structures, 238-240
- Relativity, time dilation in, 21, 378
  - in space mechanics, 53
  - test of General Theory, 20, 21, 378
- Reliability, of communication subsystem, 96
  - confidence levels, 184
  - importance of, 34, 38, 176, 177, 504
  - requirements for various missions, 96, 180
  - theory, 181-184
  - typical mortality curve, 181
  - of typical spacecraft, 184-187
- Rendezvous, 64
- Resonance orbits (see Crocco orbit)
- Retarding-potential plasma probe (see Faraday-cup plasma probes)
- Rocket engines, in attitude control, 212
  - chemical, 164-168
  - description, 162-164
  - in launch vehicles, 172-174
  - nuclear, 157, 162-164, 168-170
  - in on-board propulsion, 203-210
  - table of major types, 164
- Rockets, history of, 17
  - table of major U.S. launch vehicles, 172-174
- Rubidium-vapor magnetometer, 299, 306-309
  - on IMP, 286, 309
- Russian 1961 Venus probe, 256, 257
  - ion trap, 361
- Rutherford, E., 415
- Rutherford experiment, in surface analysis, 382, 402, 415-417
- Sample collectors, atmospheric, 400, 401
  - biological, 482, 483, 489, 492, 495, 498
  - crustal, 440-442, 462, 470, 471
- Satellites, history of, 9, 10
  - (See also Explorer, OAO, OGO, OSO)
  - Saturn launch vehicles, 30, 31
  - Saturn 1, characteristics, 172
  - Saturn 1B, characteristics, 173
  - Saturn 5, characteristics, 173
  - Schuler, M., 14
  - Scientific-instruments, calibration, 289
    - definition of, 289
    - dynamic range, 290
    - evaluation of, 293
    - flexibility requirement, 291
    - functions of, 39
    - integration, 288-292
    - interfaces, 288
    - list of types, 283-285
    - scheduling of development, 291, 292
    - selection of, 292-295
    - specifications for, 292
  - Scintillation chamber, 315, 347
  - Scintillation detectors, 314, 320-322, 453, 458
    - (See also Nuclear abundance detector, Positron detector, Telescopes)
  - Search-coil magnetometer, 298-301
    - on Pioneer 5, 286, 301
  - Seismometers, 383, 465, 471-475
  - Sensor, definition, 289
  - Sferics detector, 422
  - SFOF, 127, 149
    - commands, flow of, 122
    - description, 97, 101-104, 152, 153
    - functions of, 153
  - Simple composition detectors, 415-417
  - Simulation, of the space environment, 130, 131
  - SNAP Program, 201-203, 222
  - Soil-mechanics experiments, 383, 465, 468-471
  - Solar cells, 197-203, 325
  - Solar cosmic rays, 25
  - Solar flares, 24, 25
  - Solar probes, 65, 269-271, 504, 507
    - instruments for, 505
  - Solar wind, 22-24, 312
    - effect on comets, 32
    - (See also Plasma)
  - Solid-state detectors, 314, 325-328
  - Sounding rockets, 9
  - Space chambers, 132, 133, 136
  - Space dynamics (see Space mechanics)
  - Space Flight Operations Facility (see SFOF)
  - Space mechanics, 43-78
    - accuracy of trajectories, 52
    - characteristic velocity, 59
    - of cometary probes, 66, 75
    - definition, 43

- effects on spacecraft design, 44  
 feasibility calculations, 47  
 ground rules, 45  
 history of, 11  
 Hohmann transfer ellipse, 47, 56  
 impulsive thrusts in, 49  
 interstellar, 66  
 isochrone diagram, 61  
 isoerg diagram, 60  
 for launch vehicles, 54  
 launch windows, 49, 61  
 low-thrust, 49  
 maps, for interplanetary trips, 61, 68-75  
 midcourse corrections, 49  
 optimization techniques, 52  
 for out-of-ecliptic probes, 65  
 powered descent, 64  
 reentry, 62  
 relativistic, 53  
 rendezvous, 64  
 for solar probes, 65  
 Space probes, characteristics of major types, 244-280  
   definition of, 3  
   design of, 176-243  
   generalized, 39  
   objectives of, 3  
   priority of, 4  
   versus manned spacecraft, 3  
   (See also IMP, Mariner 2, Mariner 4, Pioneer 5, Pioneer 6, Voyager)  
 Space Sciences Steering Committee, 294, 295  
 Spark chamber, 315, 345-347  
 Specific impulse, 162, 163  
 Spectrometers, Ebert configuration, 396, 400  
   gamma-ray, 315, 452-454  
   infrared, 382, 396-398, 430-435, 480, 484  
   magnetic particle, 315, 335-337  
   principles of, 382-385, 395-400, 428-430, 505, 506  
   ram, 382, 402, 417-423  
   ultraviolet, 399-400  
   X-ray, 443, 449-452  
   (See also Mass spectrometer)  
 Spectrophotometer, 384, 385, 395-400, 428-435  
   ultraviolet, in life detection, 480, 485-489  
 Speed-of-sound experiment, in atmospheric research, 382, 402, 418-420  
   in crustal research, 475  
 Spherical ion traps, 349, 361, 362  
 Spin stabilization, 213  
 Sputnik 3, ion trap, 361  
 Stain experiments, in life detection, 480, 485, 490, 491  
 Star trackers, design of, 226, 228  
   geometry for, 115  
 Sterilization, 4, 33, 96, 478, 483  
   criterion, 483  
 Structural subsystem, design, 232, 234-241  
   functions of, 39  
   materials for, 236, 237  
 Subsurface sondes, 383, 465, 475  
 Sun, description, 32  
   (See also Solar flares, Solar probes, Solar wind)  
 Suomi radiometer, 391  
 Surface propulsion, 206-209  
 Surveyor Program, 10, 12, 18, 178, 430, 464  
   gas chromatograph, 444-447, 487  
   magnetic-inductance meter, 467, 468  
   neutron-activation-analysis experiment, 457  
   reliability study, 183-185  
   seismometer, 472-474  
   soil-mechanics experiments, 468-471  
   television camera, 440  
   thermal-diffusivity meter, 467, 468  
   X-ray diffractometer, 455, 456  
   X-ray spectrometer, 452  
 Telescopes, radiation, description of, 314, 328-335  
   on Explorer 12, 332, 333  
   on IMP, 286  
   list of types, 330  
   on Mariner 4, 287, 331, 332  
   on Pioneer 5, 286, 318, 319  
   on Pioneer 6, 286, 331  
   (See also Nuclear abundance detector, Phoswich, Positron detector)  
 Television, 382  
   in life detection, 480, 484, 485  
   on Mariner 4, 287, 437-440  
   in planetary reconnaissance, 428, 430-440  
   (See also Vidicon)  
 Telstar 1, radiation detectors, 325, 326  
 Terminal guidance, 110, 117, 118  
 Testing, 128-136  
   history of, 15  
 Thermal control of spacecraft, 216-221  
 Thermal-diffusivity meter, 383, 465, 467, 468  
 Thermal photography, 382, 428, 430  
 Thermal protection, during reentry, 238-240

- Thermometers, 383, 424  
 Thor-Able I, 17  
     characteristics, 172  
 Thor-Agena, characteristics, 172  
 Time dilation, 53  
 Time-of-flight micrometeoroid experiments, 364, 375-377  
 Titan 2, characteristics, 172  
 Titan 3, characteristics, 173  
 Topside sounders, 383, 421, 428  
 Touchdown-dynamics experiments, 468-471  
 Tracking, compatibility with communication subsystem, 82, 89  
     in guidance and control, 111, 112  
     in measurement of the A.U., 20  
     radar characteristics, 148  
     use of interferometry in, 112, 414  
     (See also DSIF, Minitrack)  
 Trajectories, interplanetary, accuracy of, 52  
     calculational techniques, 48  
     ground rules for, 45  
     launch-window table, 67  
     maps of velocity requirements, 68-74  
 Transponder, 112  
 Trapped radiation, description, 22, 312  
     (See also Radiation detectors)  
 Triton, 31  
 Turbidity experiment, in life detection, 480, 485, 489, 490, 498  
     (See also Wolf Trap)  
 Uranus, 30, 31  
 Van Allen belts, 22, 324  
     (See also Trapped radiation)  
 Vanguard Program, 9, 16  
 Vanguard 3, micrometeoroid detector, 372, 373  
 Venus, description of, 28, 29  
     flight windows, 67  
     isochrone diagram, 61  
     isoerg diagram, 60  
     magnetic field, 23  
 Venus probes, flight windows, 67  
     flyby velocity requirements, 73, 74  
     (See also Mariner 2)  
 Verein fur Raumschiffahrt, 15  
 Verne, J., 16  
 Vidicon, 462, 484, 506  
     principles, 435-440, 480  
 Viking rocket, 7, 9  
 von Pirquet, G., 11  
 Voyager Program, 18  
 Voyager spacecraft, 265-269  
 V-2 rocket, 7, 8, 14, 16, 17, 157, 162  
 WAC Corporal rocket, 16  
 Western Test Range, 16, 146-148  
 Wiener, N., 15  
 White Sands, 7, 16  
 Wire-grid micrometeoroid detector, 364, 373, 374  
 Wolf Trap, in life detection, 489, 490, 497  
     (See also pH measurement, Turbidity experiment)  
 WTR (see Western Test Range)  
 X-ray diffractometer, 382, 429, 443, 454-456  
 X-ray fluorescence spectrometer, 449-452  
 Zeeman effect, 23, 296, 298, 305, 306



# Date Due

<del>APR 1 1978</del>	<del>APR 10 1985</del>	
	APR 10 1985	
<del>APR 14 1976</del>		
	<del>APR 14 1976</del>	
<del>APR 18 1986</del>		
	APR 18 1986	
APR 1 1986		
	APR 11 1986	
	JAN 26 1987	
	OCT 17 1992	
APR 25 1989		
	OCT 15 1992	
	MAR 17 1987	
	MAR 06 1997	

 bd

CAT. NO. 23 233

PRINTED IN U.S.A.

TL 790 .C67  
Corliss, William R.  
Space probes and planetary exp

010101 000



0 1163 0058666 0  
TRENT UNIVERSITY

TL790 .C67

RECON  
REC

Corliss, William R

Space probes and planetary  
exploration.

DATE

ISSUED TO

48953

TL  
790  
C67

**48953**  
Corliss, William R  
Space probes and planetary  
exploration

Trent  
University

